KfK 4399
Dezember 1988

# Gas-Liquid Flow in Dividing Tee-Junctions with a Horizontal Inlet and Different Branch Orientations and Diameters

J. Reimann, H. J. Brinkmann, R. Domański
Institut für Reaktorbauelemente

Kernforschungszentrum Karlsruhe

KERNFORSCHUNGSZENTRUM KARLSRUHE
INSTITUT FÜR REAKTORBAUELEMENTE

KfK 4399

# Gas-Liquid Flow in Dividing Tee-Junctions with a Horizontal Inlet and Different Branch Orientations and Diameters

J. Reimann, H.J. Brinkmann and R. Domański *

*Technical University of Warsaw, Poland, presently at KfK



Kernforschungszentrum Karlsruhe GmbH, Karlsruhe

Kernforschungszentrum Karlsruhe GmbH
Postfach 3640, 7500 Karlsruhe 1

ISSN 0303-4003

## ABSTRACT

An extensive data base is presented, summarizing previous and new experiments, on the phase redistribution and pressure differences for a gas-liquid mixture flowing through the horizontal inlet pipe (diameter $D_1 = 50$ mm) of a Tee-junction. Branch to inlet diameter ratios of $D_3/D_1 = 1; 0.52; 0.2;$ and 0.08 were investigated. The branch orientation was horizontal, vertical upward or vertical downward. Mostly air-water experiments were performed with pressures between 0.4 and 1 MPa. Experiments with steam-water flows at pressures between 1.5 and 10 MPa were performed for $D_3/D_1 = 1$ and a horizontal branch.

The results on phase redistribution and pressure drop are compared with other experimental data and model predictions, published previously by various authors.

There are clear trends in the experimental data on phase redistribution: For the upward branch, the branch quality $x_3$ is the highest, for the downward branch the lowest for constant inlet conditions. With decreasing branch diameter, in general, the branch quality increases for the same branch mass flow rate. This tendency can be reversed for $D_3/D_1 << 1$ due to the effect of local phase distribution in the inlet pipe and for $D_3/D_1 \approx 1$ and inclined branch due to flow reversal effects in the branch pipe.

Presently, phase redistribution is mostly modeled in a very simplistic way without taking into account local phase distribution in the inlet pipe. Most models are fitted with experimental data from a small parameter range and a horizontal branch. Therefore, the models should only be applied with care for other inlet conditions and diameter ratios. Most of the models are not applicable for other branch directions.

The data base for Tee-junctions pressure differences is much more limited. Most experiments were performed with a horizontal branch and $D_3/D_1 = 1$. Previously published models often include assumptions which are not yet verified experimentally. A comparison of different models with results for $D_3/D_1 = 0.52$ and 1 is presented. Again no model gives satisfactory results for abitrary conditions.

The large amount of experimental data given in this report is expected to be a good data base for further model development.

# GAS-FLÜSSIGKEITS-STRÖMUNG IN T-STÜCKEN MIT HORIZONTALEM EINLAUF UND VERSCHIEDENEN ABZWEIGRICHTUNGEN UND -DURCHMESSERN

## ZUSAMMENFASSUNG:

Der Bericht enthält eine umfassende Datensammlung über die Phasenumverteilung und Druckdifferenzen bei der Strömung eines Gas-Flüssigkeits-Gemisches durch ein T-Stück. Frühere und neue Experimente werden in dem Bericht zusammengefaßt. Es wurden T-Stücke mit horizontalem Zuströmrohr ($D_1 = 50$ mm) untersucht und Abzweig- zu Einlaufdurchmesser von $D_3/D_1 = 1$; 0,52; 0.2 und 0,08. Die Abzweigrichtungen waren horizontal, senkrecht nach oben oder senkrecht nach unten. Ein Großteil der Versuche wurde mit Luft-Wasser-Strömung durchgeführt mit Drücken zwischen 0,4 und 1 MPa. Die Experimente mit Dampf-Wasser-Strömung erfolgten bei Drücken zwischen 1,5 und 10 MPa, horizontaler Abzweigrichtung und $D_3/D_1$.

Die experimentellen Ergebnisse über Phasenumverteilung und Druckverlust werden mit anderen experimentellen Daten verglichen sowie Rechenmodellen von verschiedenen Autoren.

In bezug auf die Phasenumverteilung ergeben sich folgende Tendenzen: Der Abzweigdampfgehalt $x_3$ ist am höchsten für den nach oben gerichteten Abzweig und am kleinsten für die Neigung nach unten. Für abnehmenden Abzweigdurchmesser nimmt der Abzweigdampfgehalt im allgemeinen ab bei gleichem Abzweigmassenstrom. Diese Tendenz kann sich umkehren; bei $D_3/D_1 << 1$ bedingt durch die lokale Phasenverteilung im Einlauf; bei $D_3/D_1 \approx 1$ und geneigten Abzweigen aufgrund von Rückströmeffekten im Abzweig.

Gegenwärtig wird die Phasenumverteilung in sehr vereinfachter Form rechnerisch modelliert, ohne die lokale Phasenverteilung im Einlaufrohr zu berücksichtigen. Die meisten Modelle werden mit experimentellen Ergebnissen aus einem kleinen Parameterbereich und horizontalem Abzweig angepaßt. Die Modelle sollten deshalb nur mit Vorsicht für andere Einlaufbedingungen und Durchmesserverhältnisse verwendet werden. Die Modelle können nicht die Phasenumverteilung für andere Abzweigrichtungen beschreiben.

Die Datenmenge über T-Stück-Druckdifferenzen ist sehr viel begrenzter. Die meisten Experimente wurden mit horizontalem Abzweig und $D_3/D_1 = 1$ durchgeführt. Die bisherigen Rechenmodelle beinhalten oft Annahmen, die experimentell nicht verifiziert sind. Der Bericht enthält einen Vergleich verschiedener Modelle mit Ergebnissen für $D_3/D_1 = 0{,}52$ und 1. Wiederum ist kein Modell in der Lage, für beliebige Bedingungen die Messungen mit zufriedenstellender Genauigkeit zu beschreiben.

Die große Auswahl der in diesem Bericht aufgeführten experimentellen Ergebnisse sollte eine gute Grundlage darstellen für zukünftige Arbeiten zur Modellierung der Strömungsvorgänge in T-Stücken.

TABLE OF CONTENT

# LIST OF FIGURES

## Nomenclature

| | | | |
|---|---|---|---|
| A | pipe cross section | K | correction factor |
| a | factor | K* | momentum correction factor |
| b | exponent | $\dot{m}$ | mass flow rate |
| C | contraction coefficient | p | pressure |
| C | constant | R | density ratio $\rho_L/\rho_G$ |
| C* | Chisholm Parameter | Re | Reynolds number |
| D | pipe diameter | S | slip (velocity ratio $u_G/u_L$) |
| E | entrainment fraction | T | temperature |
| Fr | Froude Number | $\dot{V}$ | volumetric flow rate |
| G | mass flux | v | superficial velocity |
| g | acceleration due to gravity | u | phase velocity |
| h | interface level | x | flow quality |
| K | loss coefficient | y | length coordinate |

Indices

| | | | |
|---|---|---|---|
| 1 | inlet pipe | HM | Homogeneous Model |
| 2 | run pipe | HLM | Hwang Lahey Model |
| 3 | branch pipe | i | current index |
| b | entrainment beginning | irr | irreversibel |
| BSM | Ballyk-Shoukri Model | L | liquid phase |
| C | position of vena contracta | m | momentum |
| CM | Chisholm Model | max | maximum |
| $C_0$ | parameter used in HLM | mod | model |
| cal | calculated | pr | predicted |
| crit | critical flow | rev | reversibel |
| e | energy | RSM | Reimann Seeger Model |
| exp | experimental | sG | superficial gas |
| G | gas phase | sL | superficial liquid |
| h | homogeneous | | |

Greek Symbols

| | | | |
|---|---|---|---|
| $\alpha$ | void fraction | $\rho$ | density |
| $\Delta p$ | pressure difference | $\Phi$ | angle between branch and vertical |
| $\mu$ | dynamic viscosity | $\phi$ | branch two-phase loss multiplier |
| $\mu$ | exponent | $\sigma$ | surface tension |
| $\chi$ | isotropic expansion coefficient | $\Theta$ | angle of "zone of influence" |
| $\nu$ | kinematic viscosity | | |

# 1. INTRODUCTION

Two-phase flow through Tee-junctions has gained increasing interest in the last years due to the technical applications in piping networks of chemical and power plants and oil-gas transport. For many years, the main interest was focussed on loss-of-coolant accidents in nucelar reactor safety analysis. Presently, with the use of two-phase flow pipelines this case becomes of increasing importance in the field of oil-gas transport.

When a two-phase mixture is divided in a Tee-junction, the branch and run qualities $x_3$ and $x_2$ in general differ from the inlet quality $x_1$. Up to now, no physical model exists to describe this phase redistribution and the associated pressure differences between inlet and branch, $\Delta p_{1\text{-}3}$, and inlet and run $\Delta p_{1\text{-}2}$, as a function of the mass flow rate ratio $\dot{m}_3/\dot{m}_1$ for abitrary values of the inlet quantities (pressure $p_1$, mass flux $G_1$ and quality $x_1$ or superficial liquid and gas velocity $v_{sL}$ and $v_{sG}$), branch to inlet pipe diameter ratio $D_3/D_1$, angle $\phi$ between the branch pipe and the vertical and angle between branch and inlet pipe.

The phase redistribution is influenced by three effects:

(1) The different local momentum fluxes of the phases in the inlet pipe: if the local phase velocities are about equal, then the lighter phase preferentially enters the branch.
(2) The gravity force in the inlet pipe which determines the phase and momentum flux distribution (flow regime) in the pipe cross section. For horizontal inlet pipes, the heavier phase is concentrated in the lower portion of the pipe and, therefore, enters favourably a branch inclined in the downward direction.
(3) The gravity force in the branch: for inclined branches flow reversal of one phase can occur.

In the following, this report will concentrate on a horizontal inlet (and run) pipe and an angle between inlet pipe and branch of 90° (Tee-junction).

The difficulties to model the phase redistribution are made clear in Fig. 1.1a (from Reimann et al. /1/), containing the distribution of the void fraction along the vertical diameter y, in the horizontal inlet pipe for different values of the inlet superficial gas velocity $v_{sG}$ and a constant inlet superficial liquid velocity $v_{sL}$. These values are on a vertical line in a flow regime map with coordinates as used

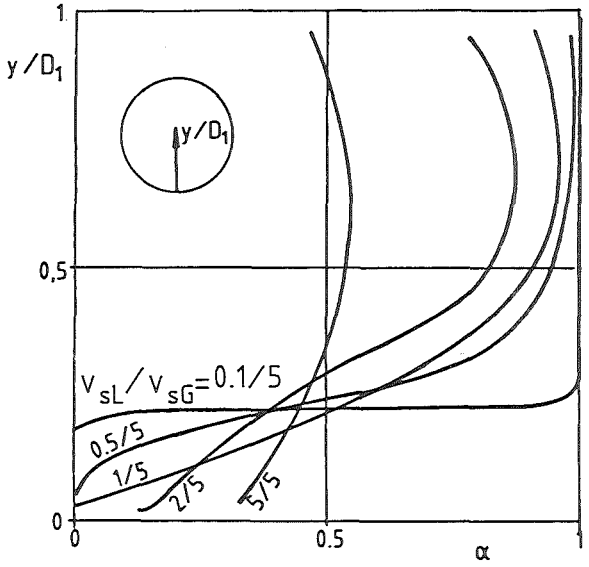


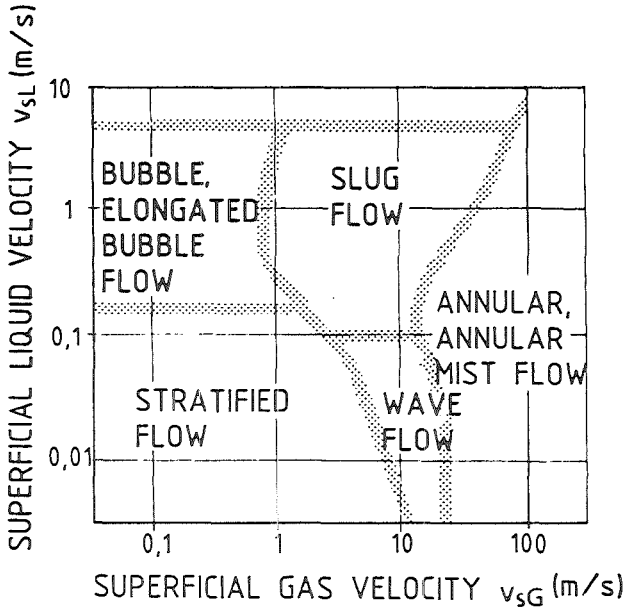


Fig. 1.1 Vertical Void Fraction Distributions in Horizontal Inlet Pipe (from /1/) and Flow Pattern Map; from /2./

in Fig. 1.1b (from Mandhane et al. /2/) and belong to different characteristic flow pattern regimes.

It is noted for further discussions that the flow regime boundaries are no sharp curves but rather transition zones. The boundaries are dependent on fluid properties and pipe diameter, see e.g. Taitel and Dukler /3/ and different values are given by different authors. The boundaries given by Mandhane et al. are rather characteristic for air-water flow at nearly atmospheric pressures and pipe diameters of $D_1 \approx 50$ mm. At higher pressures, as always used in the present experiments, the boundary between slug flow and annular flow shifts to smaller values of $v_{sG}$, compare Reimann et al. /4/. Therefore, test points with $v_{sG} = 10$ m/s and 20 m/s are rather attributed to the annular flow regime than to the slug flow regime.

For a downward orientated branch, the local distribution in the region close to the normalized distance $y/D_1 = 0$ is of interest, for the upward branch the value close to $y/D_1 = 1$. For fairly axisymmetric distributions (superficial liquid velocity $v_{sL} = 4$ m/s, dispersed bubble flow pattern, see Fig. 1.1b), the distributions close to the wall are about the same for all three branch locations. For the other examples shown in Fig. 1.1a, the phase distributions are dominated by stratification due to gravity.

For $v_{sL} = 0.1$ m/s a stratified wavy flow occurs in the inlet pipe; for $v_{sL} = 0.5$, 1 and 2 m/s a slug flow occurs. For the horizontal branch the values at $y/D_1 = 0.5$ should then be characteristic, however, taking into account that for slug flow in general a liquid film exists at the wall.

An annular void fraction profile (not shown in Fig. 1.1a) is characterized by an excentric liquid film at the wall which is thin at the top of the pipe and thick at the bottom of the pipe. The gas core contains droplets, the droplet concentration decreases with increasing $y/D_1$.

In general, the phase distributions are not known. The measurement of the momentum flux distribution is even more complicated. Figure 1.1a illustrates that the branch orientation is of strong influence on the phase redistribution. This influence increases with decreasing ratio $D_3/D_1$ because the smaller $D_3/D_1$ the more local is the portion of the cross section where the mixture is taken off into the branch.

These introductory remarks illustrate that the influence of the inlet parameters are very complex. Presently, the parameter range has not been covered sufficiently by experiments. Table I gives a brief overview on previous experiments with a horizontal inlet pipe (Refs. /5/ to /37/), without attempting to be complete. The branch orientation is defined by the angle $\phi$, starting with $\phi = 0^{\circ}$ for the upward branch. Figure 1.2 shows the range of investigated inlet conditions in terms of superficial velocities in a flow regime map. Table I depicts that most of the experiments were performed with air-water flow and nearly atmospheric pressures which often restricts the $\dot{m}_3/\dot{m}_1$ range to values considerably smaller than one. With high system pressure, there is only one set of experiments with $D_3/D_1 = 1$ and two sets with $D_3/D_1 << 1$, however, limited to stratified flow. Further experiments are highly desirable because high pressures are typical for applications both in steam-water systems and oil-gas transport. Table I.1 also shows that branch directions others than horizontal were also investigated very marginally.

Besides the horizontal inlet pipe there is considerable work with a vertical inlet pipe. There are many common features, especially if the flow patterns are not dominated by stratification due to gravity. Therefore, the reader is referred to the work from e.g. Zetzmann /38/, Honan and Lahey /39/ which also include experiments with angles of 45° and 135° between branch and inlet pipe ("Wyes"). Most of the work by Azzopardi et al. /40/ refers to vertical inlet pipes, too.

Presently, the largest parameter range has been investigated in the Two-Phase Test Facility of the Nuclear Research Centre Karlsruhe (KfK). This report contains detailed information on all experimental data (about 2800 measurement points) with the 50 mm diameter inlet pipe, both the previous results (Refs. /21/ to /27/) and the new data, which only partially were published up to now (Refs. /28/ to /30/). This large amount of experimental results is expected to be a good data base for further model development. The results with the 204 mm diameter inlet pipe concentrating on stratified flow and small branches (Refs. /14/ to /20/) were presented in detail by Smoglie /18/.

In Sections 2 and 3, the previously performed experiments on phase redistribution and pressure drop and the state of the art of corresponding models are briefly reviewed. In Sections 5 and 6, the new experimental results (concentrating on $D_3/D_1 < 1$) are presented and compared with previous data and models.

| Authors | Geometry | | | | | Flow Parameters | | | | | | | | | Measurement | | |
|---|---|---|---|---|---|---|---|---|---|---|---|---|---|---|---|---|---|
| | $D_1$ (mm) | $D_3/D_1$ (1) | branch angle $\phi(0)$ $0^{(1)}$ | $90^{(2)}$ | $180^{(3)}$ | fluid a-w[4] | system s-w[3] | flow patterns d[6] | i[7] | a[8] | s[9] | $G_1$ range ($kg(m^2s)$ | $x_1$ range (%) | $p_1$ (MPa) | $\dot{m}_3/\dot{m}_1$ range (1) | phase red-distr. | press. drop |
| Tsuyama & Taga /5/, 1959 | 23.4 | 1 | | | | | | | x | | | 50-1000 | 0.1-12 | ≈ 0.15 | 0-0.9 | x | x |
| Fouda & Rhodes /6/, 1975 | 51 | 0.5 | x | | | x | | | | x | | 360-684 | 35-67 | ≈ 0.15? | small? | x | x |
| Collier /7/, 1976 | 38,1 | 0.66 | | x | | x | | | | x | x | 136 | 2-50 | ≈ 0.25 | 0-0.95 | x | |
| Hong /8/, 1978 | 9.5 | 1 | x[10] | x | x | | | | | x | x | 2.3-47 | 0.25-1 | ≈ 0.15 | 0-1 | x | |
| Whalley & Azzopardi /9,10/, 1980,82 | 31.8 | 0.4 | x[10] | x | x | x | | | | x | | 152 | 56 | ≈ 0.25 | 0-0.4 | x | |
| Henry /11/, 1981 | 100 | 0.2 | | x | | x | | | | x | | 200-850 | 5-50 | ≈ 0.15 | 0-0.06 | x | |
| Saba & Lahey /12,13/, 1982,84 | 38.1 | 1 | | x | | x | | | x | | | 1350-2700 | 0.1-1 | ≈ 0.1 | 0.3,0.5,0.7 | x | x |
| KfK-experiments: Reimann, Smoglie et al. /14-20/, 1982-86 | 204 | 0.03 | | | | | | | | | | liquid | | | | | |
| | " | 0.04 | x | x | x | x | | | | | x | level $h/D_1$: | 0-1 | 0.4 | 0-$\dot{m}_{3crit}/\dot{m}_1$ | x | x |
| | " | 0.06 | | | | | | | | | | | | | | | |
| | " | 0.10 | | | | | | | | | | | | | | | |
| KfK-experiments: Seeger, Reimann et al. /21-27/, 1981-86 | 50 | 1 | x | x | x | x | | x | x | x | | 500-7500 | 0.2-33 | 0.4-1 | 0-1 | x | x |
| | " | 1 | | x | | | x | | x | x | | 900-2000 | 3-35 | 2.5-10 | 0-1 | x | x |
| KfK-experiments: "new" KfK-results /28-30/, 1986-87 | 50 | 0.08 | | | | | | | | | | | | | | | |
| | " | 0.2 | x | x | x | x | | x | x | x | x | 130-6130 | 0.4-77 | 0.4-1 | 0-$\dot{m}_{3crit}/\dot{m}_1$ | x | x |
| | " | 0.52 | | | | | | | | | | | | | | | |
| | " | 1 | | x | | | | | | x | x | 50-1340 | 7-77 | 0.7 | 0-1 | x | x |
| Katsaounis /31,32/, 1985,87 | 45;203 | 0.4 | x | | | x | | | x | | x | 30-1700 | 0-0.16 | ≈ 0.15 | 0-1 | x | x |
| Maciaszek & Memponteil /36/, 1986 | 135 | 0.15 | x | x | x | | x | | | | x | $h/D_1$ = | 0-1 | 2 | 0-$\dot{m}_{3crit}/\dot{m}_1$ | x | x |
| Shoham et al. /33/, 1987 | 51 | 1 | | x | | x | | | | x | x | 19-230 | 22-98 | 0.3 | 0-1 | x | |
| Ballyk & Shoukri /34/, 1987 | 25.6 | 0.5;1 | | x | | | x | | | x | | 400-1200 | 2-15 | 0.01-0.1 | 0-1 | x | x |
| Hwang & Lahey /35/, 1987 | 38 | 1 | | x[11] | | x | | | | | | 1350-2700 | 0.2-0.4 | ≈ 0.15 | 0-0.35 | x | x |
| Anderson /37/, 1987 | 323 | 0.1 | | x | | x | | | | | x | $h/D_1$ = | 0-1 | 4-6 | 0-$\dot{m}_{3crit}/\dot{m}_1$ | x | x |

(1) upward branch
(2) horizontal branch
(3) downward branch
(4) air-water
(5) steam-water
(6) dispersed bubble
(7) intermittent (slug, elongated bubble)
(8) annular
(9) stratified
(10) further angles $\phi$ investigated
(11) besides "Tee" also "WYE" (45° and 135°) investigated

Table I.1: Tee-junction Experiments with a Horizontal Inlet Pipe

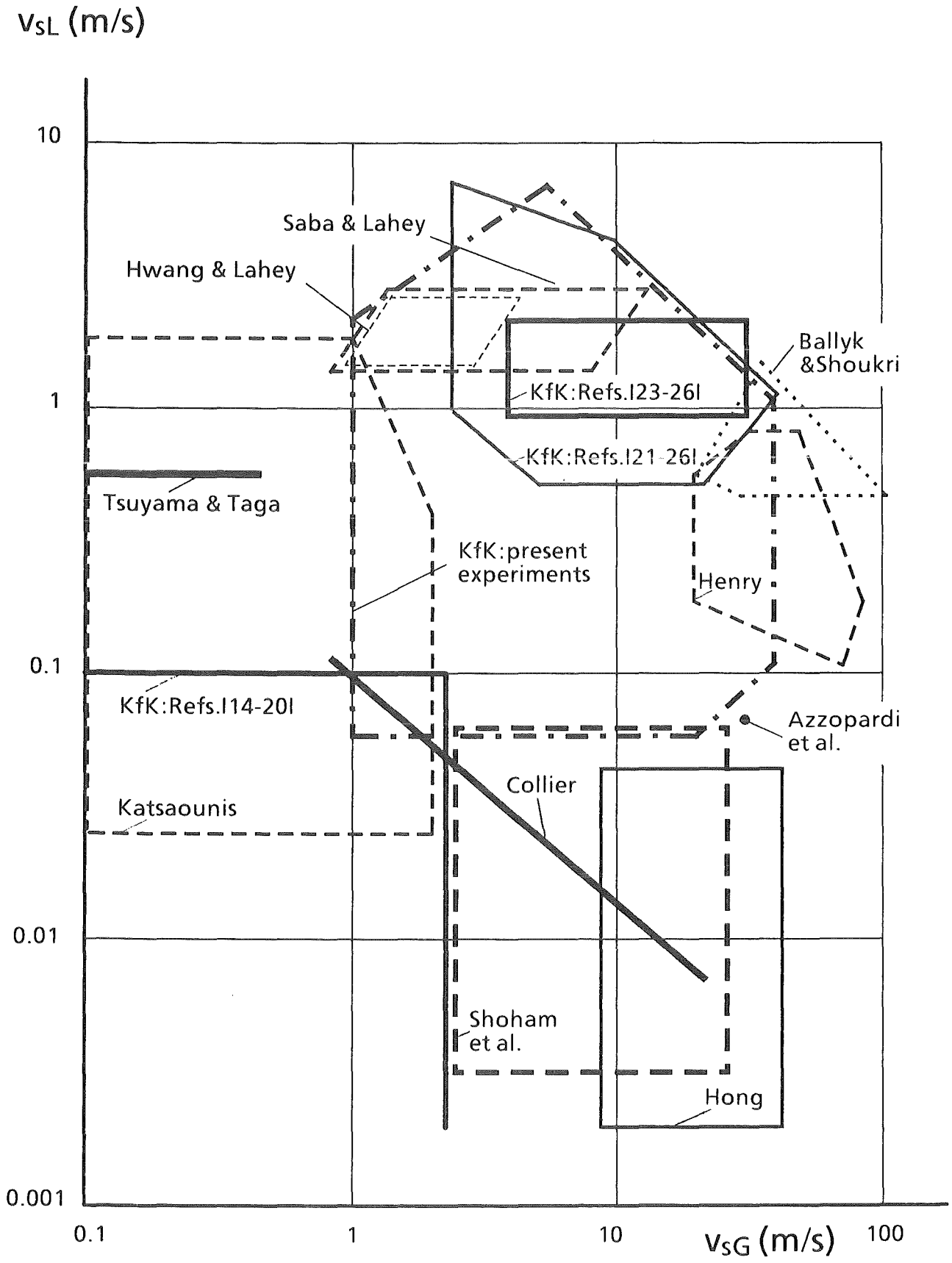


Fig. 1.2 Flow Parameter Range of Tee-junction Experiments with Horizontal Inlet Pipes.

## 2. SUMMARY OF PREVIOUS WORK ON PHASE REDISTRIBUTION

### 2.1 General Remarks and Tendencies

The approaches to describe phase redistribution can be subdivided into three categories (compare Lahey /41/): Completely empirical approaches; mechanistic (fluid mechanics based) models; and phenomenological flow regime based models. None of these have general applicability, but since the last two are more physically based, they provide better insight into the fundamental mechanisms involved.

Figure 2.1 represents schematically the phase redistribution which is plotted in two different ways: Plot a) shows the quality ratio from branch and inlet $x_3/x_1$ versus the mass flow rate ratio $\dot{m}_3/\dot{m}_1$, also termed mass split. Plot b) shows the gas mass flow ratio $\dot{m}_{3G}/\dot{m}_{1G}$ as a function of the liquid mass flow ratio $\dot{m}_{3L}/\dot{m}_{1L}$. Using the first method, the curve for equal phase redistribution ($x_3/x_1 = 1$) is a horizontal straight line. Of special interest is the curve which is obtained if the branch acts as a perfect gas separator: This curve is termed total phase separation curve and consists of two branches: starting from $\dot{m}_3/\dot{m}_1 = 0$, at first only gas is withdrawn into the branch ($x_3 = 1$) up to a value of the mass split where all gas is entering the branch. Increasing the mass split can be only achieved by an

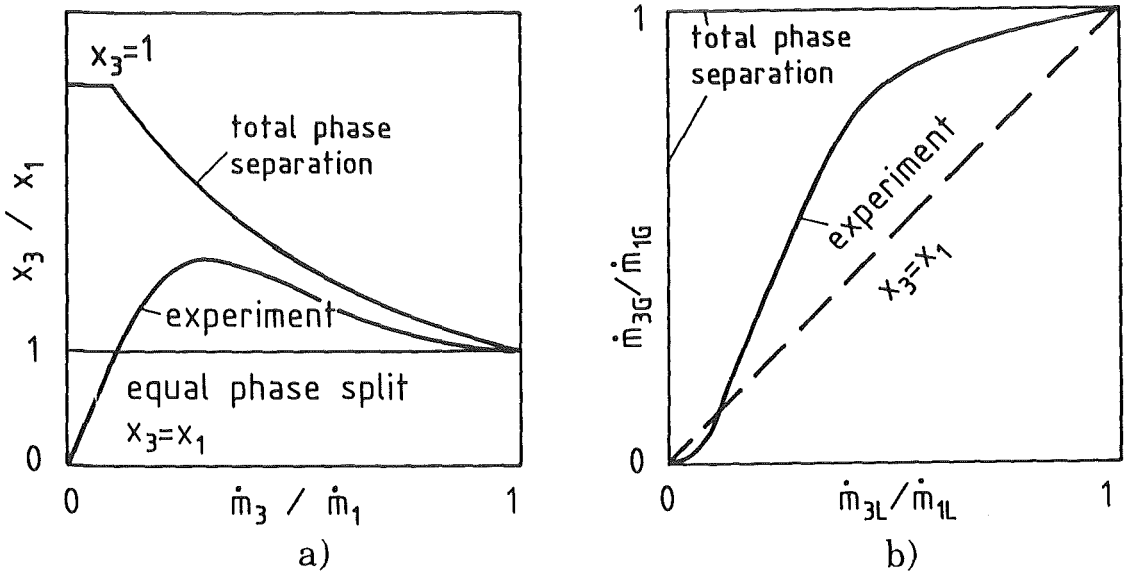


Fig. 2.1 Schematical Graph of Different Representations of Phase Redistribution.

intake of liquid. This curve for total branch separation (condition: run quality $x_2 = 0$) is then given by

$$x_3/x_1 = (\dot{m}_3/\dot{m}_1)^{-1} \qquad (2.1)$$

The first part of the curve is restricted to very low values of $\dot{m}_3/\dot{m}_1$ and the experimental results are mostly far below this curve. Therefore, this part is in general not shown in the graphs. For high mass split ratios, however, the experimental results can be very close to the curve of total phase separation.

Using the presentation $\dot{m}_{3G}/\dot{m}_{1G} = f(\dot{m}_{3L}/\dot{m}_{1L})$, again the curves for equal and total phase redistribution can be easily plotted. In the subsequent sections, the first way of data presentation is preferred because the phase redistribution curve exhibits often a characteristic maximum $(x_3/x_1)_{max}$ whose value can not be seen quantitatively in the latter diagramm.

Of course, the data can be easily cross-plotted. Due to the fact that in literature also the second way of presentation was used frequently , in this section both kinds of graphs are shown.

The Figs. 2.2 and 2.3 contain results for different branch orientations $\phi$. Figure 2.2a, (from Seeger /24/) shows typical results for an inlet superficial liquid velocity of $v_{sL} = 2$ m/s with a slug flow pattern in the inlet pipe. The same results are cross-plotted in Fig. 2.3; this figure additionally contains results for dispersed bubble flow in the inlet pipe ($v_{sL} = 4$ m/s). For the horizontal branch ($\phi = 90°$), $x_3/x_1$ is smaller than one for very small values of $\dot{m}_3/\dot{m}_1$ due to the fact that mainly the mixture close to the wall, characterized by a high liquid fraction, enters the branch. With increasing $\dot{m}_3/\dot{m}_1$, increasingly gas is deflected into the branch; $x_3/x_1$ reaches values considerably above one. A further increase of $\dot{m}_3/\dot{m}_1$ is reached by increasing mainly the liquid flow rate. Therefore, $x_3/x_1$ decreases until the value $x_3/x_1 = 1$ is reached for $\dot{m}_3/\dot{m}_1 = 1$. For $v_{sL} = 2$ m/s and $\dot{m}_3/\dot{m}_1 > 0.4$ the phase redistribution curve is very close to the curve of total phase separation. This tendency is not so much expressed for dispersed bubble flow.

For the upward branch ($\phi = 0°$), as expected, $x_3/x_1$ is closer to the curve of total phase separation. At very small values of $\dot{m}_3/\dot{m}_1$ only gas is extracted into the branch and $x_3$ becomes unity.

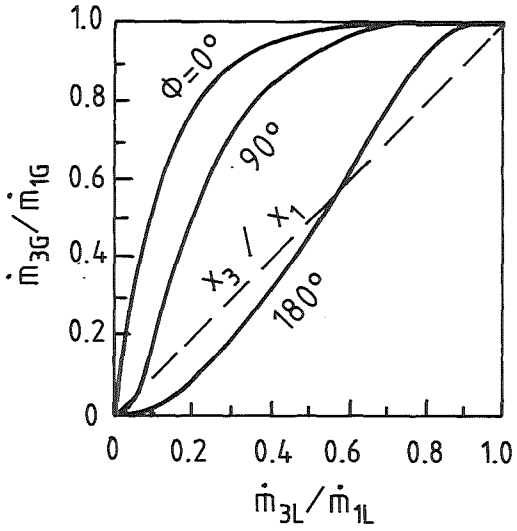


a) slug flow data;
from Seeger /24/.

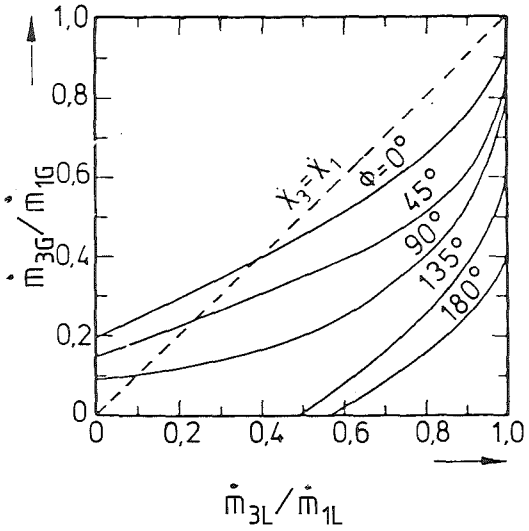


b) annular flow data;
from Hong /8/.

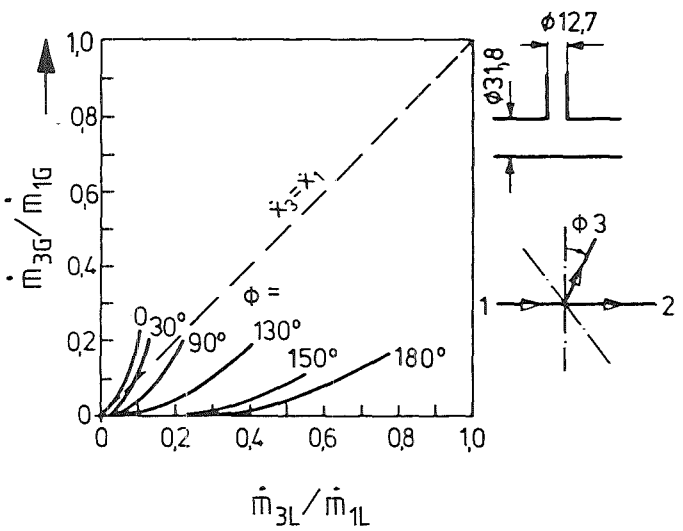


c) annular flow data;
from Azzopardi and Whalley /10/.

Fig. 2.2 Influence of Branch Orientation; Results from /8,10,24/.

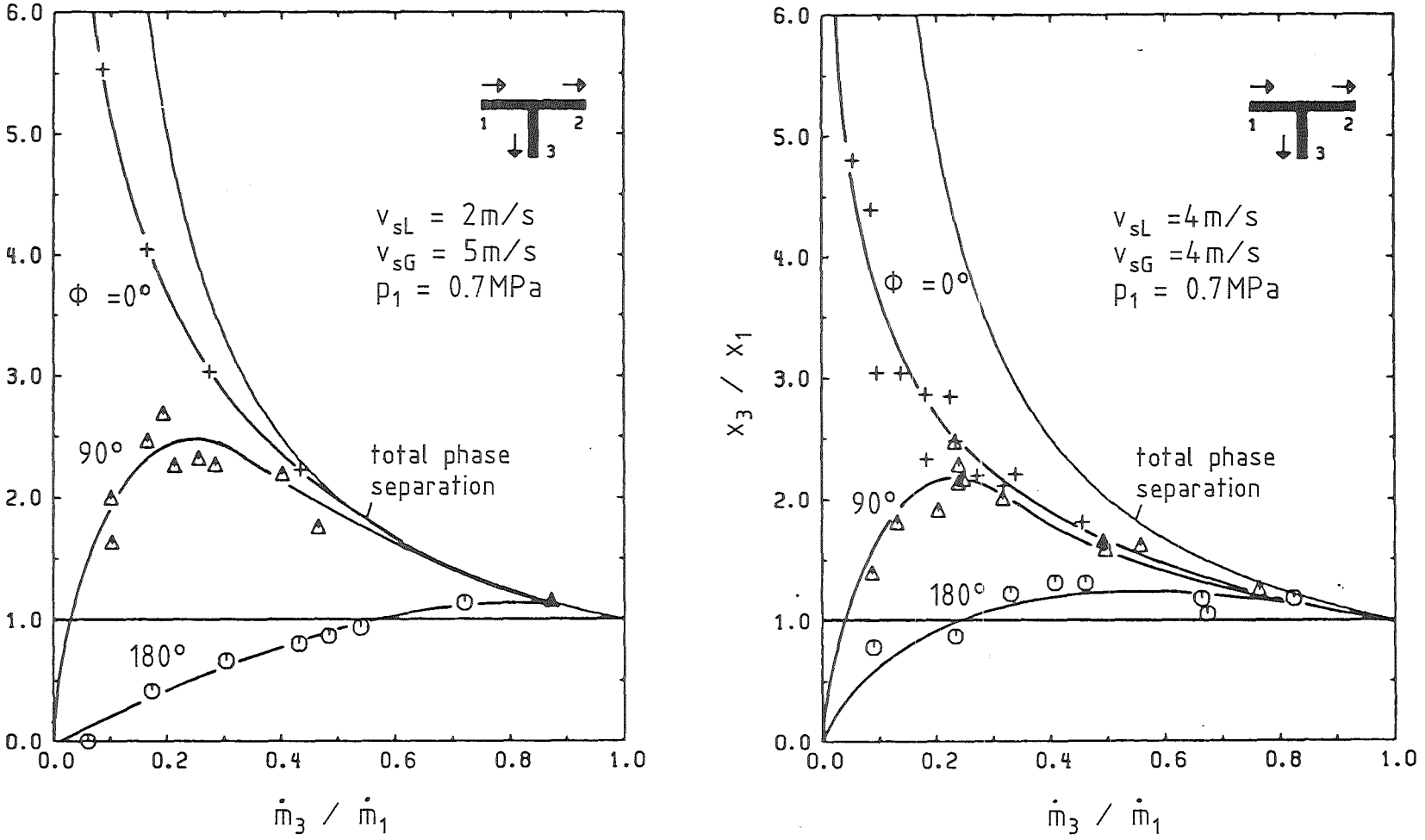


Fig. 2.3 Influence of Branch Orientation. Results from /26/.

For the downward branch ($\phi = 180°$), the split ratio range with $x_3/x_1 < 1$ is much larger. However, depending on the inlet conditions, $x_3/x_1$ can also become larger than one. Here, the influence of the different momentum fluxes on the redistribution exceeds the influence of the gravity force.

The influence of the branch orientation will be discussed in much more details in the following.

The Figs. 2.2b and 2.2c (taken from Katsaounis /32/) contain results from Hong /8/ and Azzopardi and Whalley /10/ for a much lower inlet superficial liquid velocity $v_{sL} = 0.05$ m/s and a flow pattern in the transition from wavy to annular flow. The results are quite different from those for high values of $v_{sL}$ (high inlet mass fluxes). However, the results from the latter authors also differ although the inlet flow conditions were very similar. This has to be attributed to the effect of different inlet diameters $D_1$ and diameter ratios $D_3/D_1$; again, details will be discussed in the following.

## 2.2 Horizontal Branch ($\phi = 90°$)

### 2.2.1 Annular Flow

This flow regime was the objective of numerous investigations (compare Table I). However, the data base is still insufficient to develop a phase redistribution model which is valid for the total range of flow parameters in this flow regime. This is due to the fact that for horizontal pipes the flow pattern is in general not axisymmetric. The lower the gas flow rate the more liquid concentrates at the bottom of the pipe, and droplet entrainment mostly starts from the gas-liquid interface in the lower portion of the pipe. This phase stratification should effect the most the branch flow for diameter ratios $D_3/D_1 << 1$ because the liquid flowing at the bottom of the pipe cannot be withdrawn as easily as for $D_3/D_1 = 1$.

Results for $D_3/D_1 = 1$ covering the total mass split ratio range are presented in Fig. 2.4, containing data from Hong /8/ and Shoham et al. /33/ for experiments carried out with small inlet superficial liquid velocities and low inlet mass fluxes, respectively.

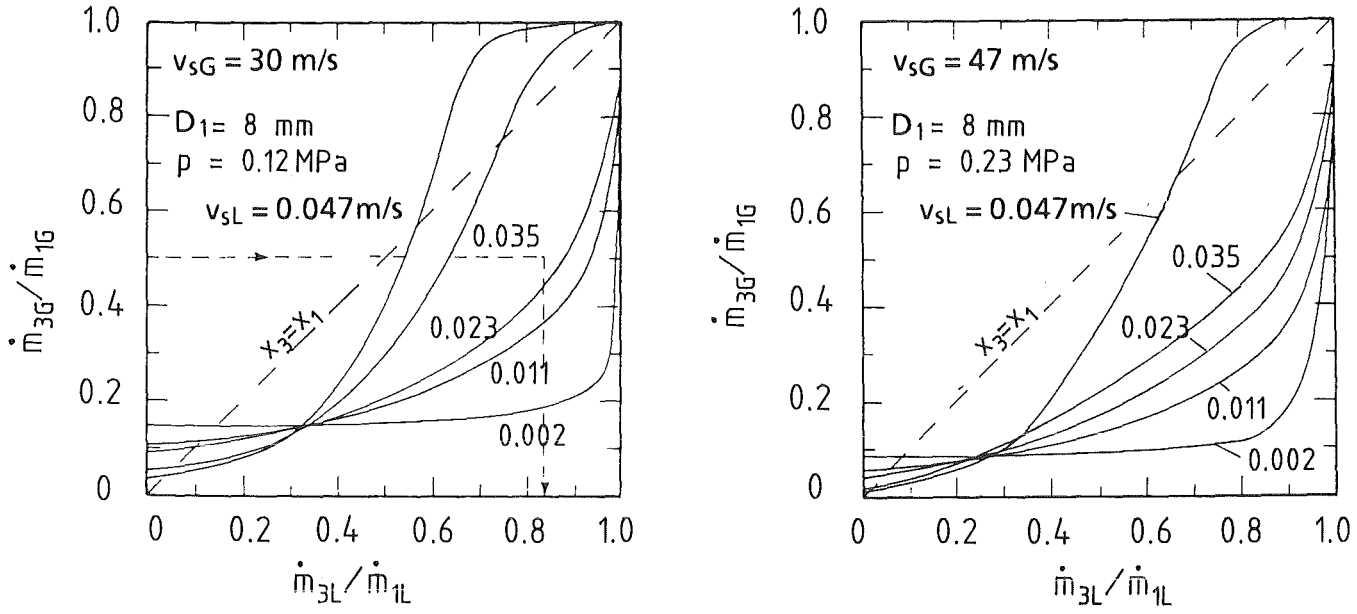


Experimental results from Hong

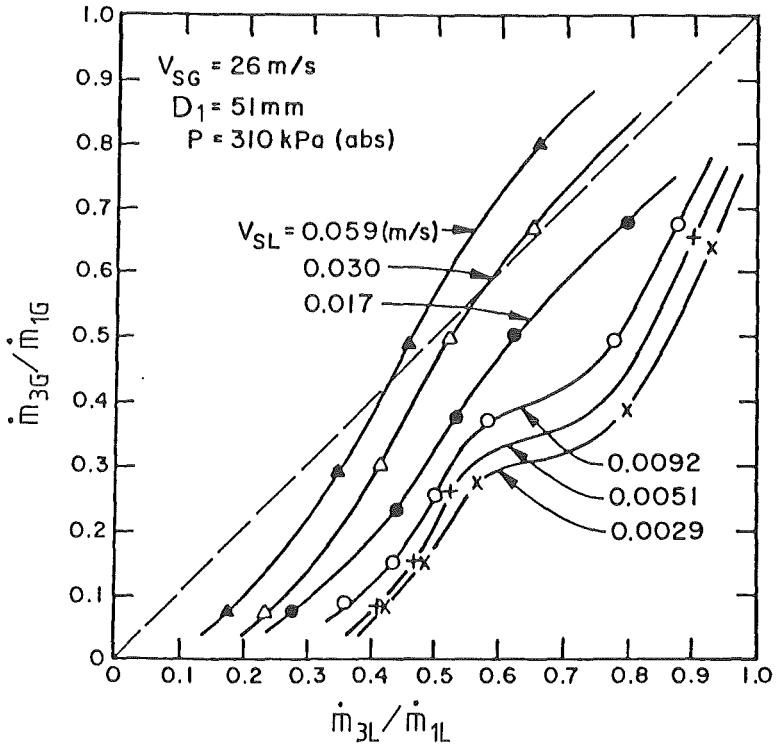


c) Experimental results from Shoham et al.

Fig. 2.4 Annular Flow Data: Low Mass Fluxes, $\phi = 90°$, $D_3/D_1 = 1$; Results from /8,33/.

Most of the data are located below the diagonal representing the curve $x_3 = x_1$ which means that the liquid phase tends to flow preferentially into the branch. For the lowest values of $v_{sL}$ and high values of the mass split the total liquid inventory is diverted into the branch and gas is still flowing into the run. This tendency is very untypical and is explained by the very small velocity of the thin film (without considerable droplet entrainment). Therefore, the liquid momentum flux is much smaller than the gas momentum flux and the liquid "creeps" into the branch. At the lowest branch flow rates, ($\dot{m}_{3l}/\dot{m}_{1L} \approx 0$), the results obtained by Hong indicate that only gas enters the branch, whereas the results from Shoham et al. show that liquid is withdrawn at first. The latter result makes sense if it is assumed that at first the liquid film is withdrawn into the branch. The contrary result is assumed to be caused by the fact that this liquid is not transported through the branch but flows back into the run. This effect was observed by the present authors if the "horizontal" branch was inclined upwards by some degrees. Another reason could be a vertical pipe section downstream of the throttle valve at the end of the horizontal branch.

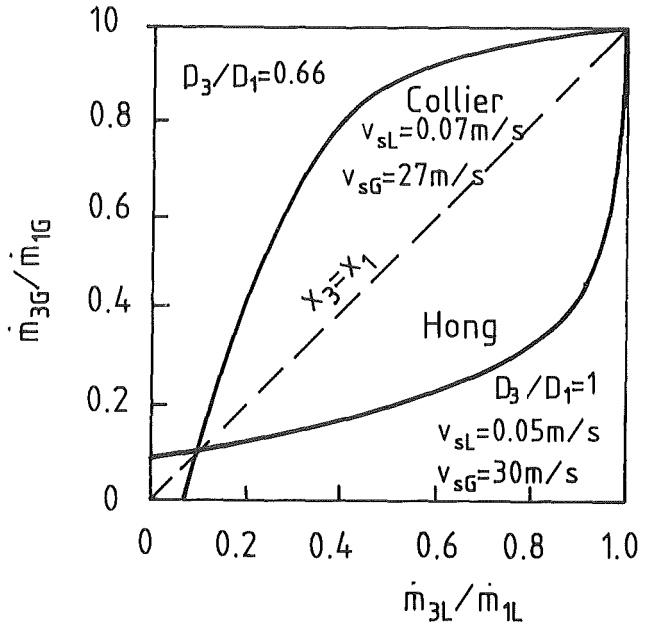


Fig. 2.5 Annular Flow Data: Low Mass Fluxes, $\phi = 90°$, $D_3/D_1 = 0.66, 1$; Results from /7,8/.

Both figures reflect the tendency that with increasing inlet superficial liquid velocity the gas intake increases and at the highest values gas preferentially enters the branch at high mass split ratios.

Figure 2.5 contains results for different values of $D_3/D_1$ but very similar inlet conditions. In the experiments presented by Collier /7/ for $D_3/D_1 = 0.66$ gas flows preferentially in the branch. In contrast, Hong measured for $D_3/D_1 = 1$ a very high liquid intake. This difference cannot be explained by the different diameter ratio alone, because the influence of $D_3/D_1$ should be much smaller, compare Section 5.

Results for higher inlet superficial liquid velocities and higher inlet mass fluxes, respectively, are shown in Fig. 2.6. The low pressure steam-water data from Ballyk and Shoukri /34/ (Fig. 2.6a) are characterized by a larger $(x_3/x_1)_{max}$ compared to Seeger's /24/ air-water results obtained at higher pressures (Fig. 2.6b). Figure 2.6a contains also predictions with the model from Seeger et al. /26/, described in detail in Section 2.2.5, and the model from Azzopardi and Whalley /9,10/, presented later in this section. The first model predicts the experiments reasonably well. The dependency of the redistribution curve on the inlet superficial liquid velocity $v_{sL}$ for $v_{sG}$ = const. was very small for the investigated parameter range.

In Fig. 2.2c the data from Azzopardi and Whalley for $D_3/D_1 = 0.4$ are presented. The investigated split ratio was $\dot{m}_3/\dot{m}_1 << 1$. For the horizontal branch ($\phi = 90°$), the results agree qualitatively with the data obtained by Shoham et al. /33/ (Fig. 2.4c), obtained with $D_3/D_1 = 1$.

An open question is the quantitative influence of system pressure (density ratio). Qualitatively, it is expected that with increasing pressure the phase redistribution becomes smaller. This tendency is shown in Figs. 2.6a and 2.6b. Figure 2.7 (from Seeger /24/) shows data with a large pressure variation for constant values of $v_{sL}$ and $v_{sG}$. The pressure influence is relatively small .(Note that for p = 0.4 MPa the test point is in the transition zone between annular and slug flow whereas at higher pressures the boundary to the slug flow regime has shifted to smaller values of $v_{sG}$, see Reimann et al. /4/). Again, it is evident that much more work is needed to investigate the pressure influence.

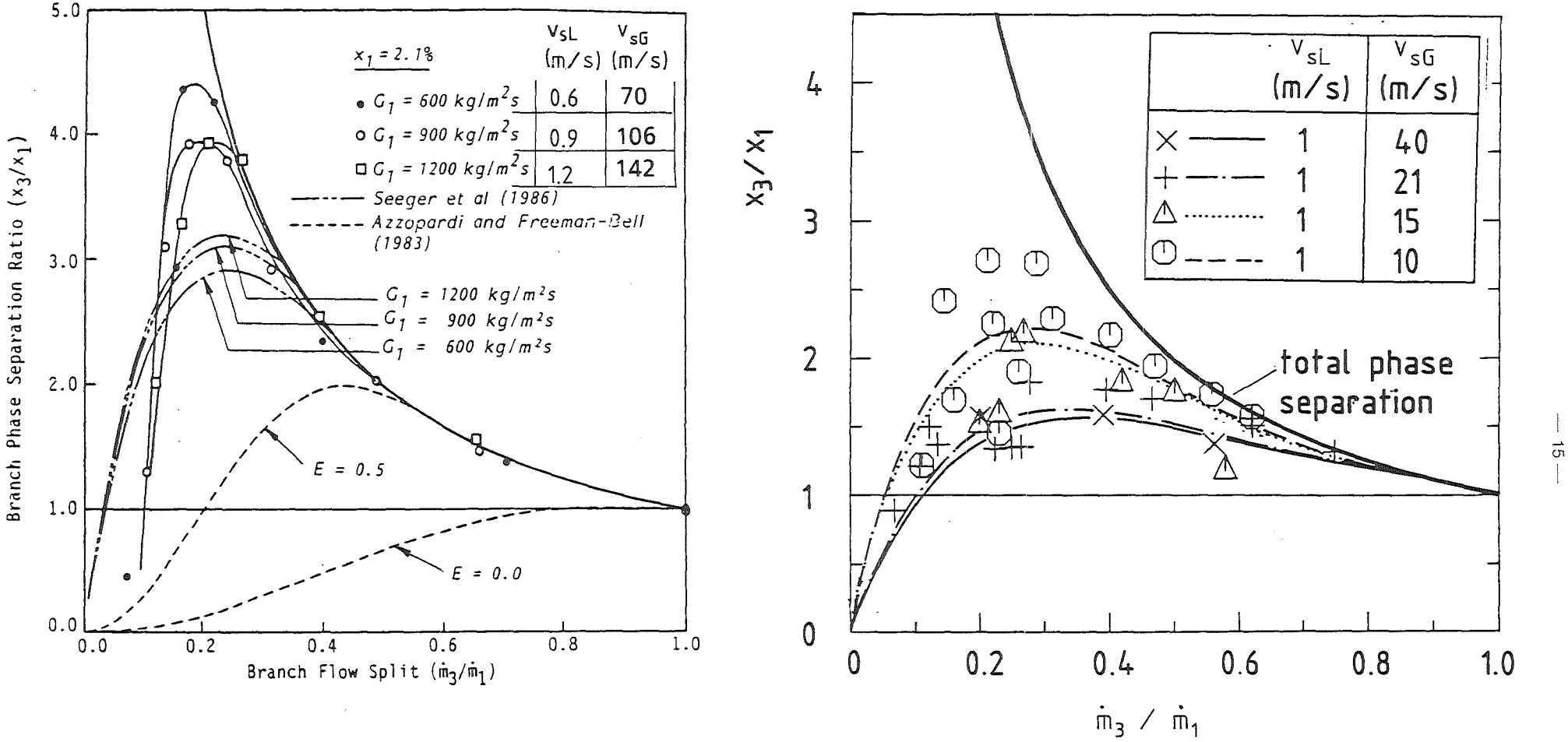


Fig.2.6 Annular Flow Data: High Mass Fluxes, $\phi = 90°$, $D_3/D_1 = 1$; Results from /24,34/.

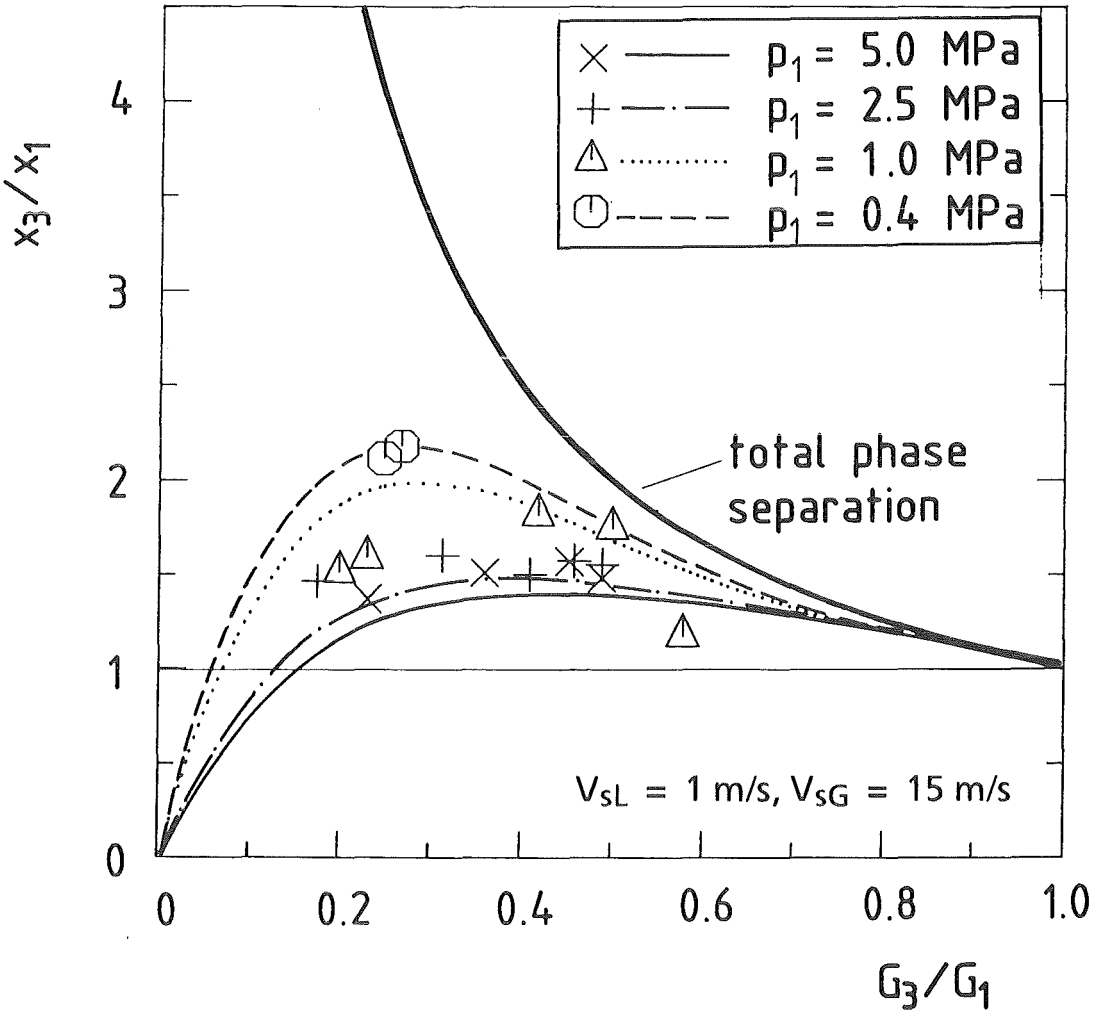


Fig. 2.7 Annular Flow Data: Pressure Influence, p = 0.4-5 MPa, $\phi = 90°$, $D_3/D_1 = 1$; from /24/.

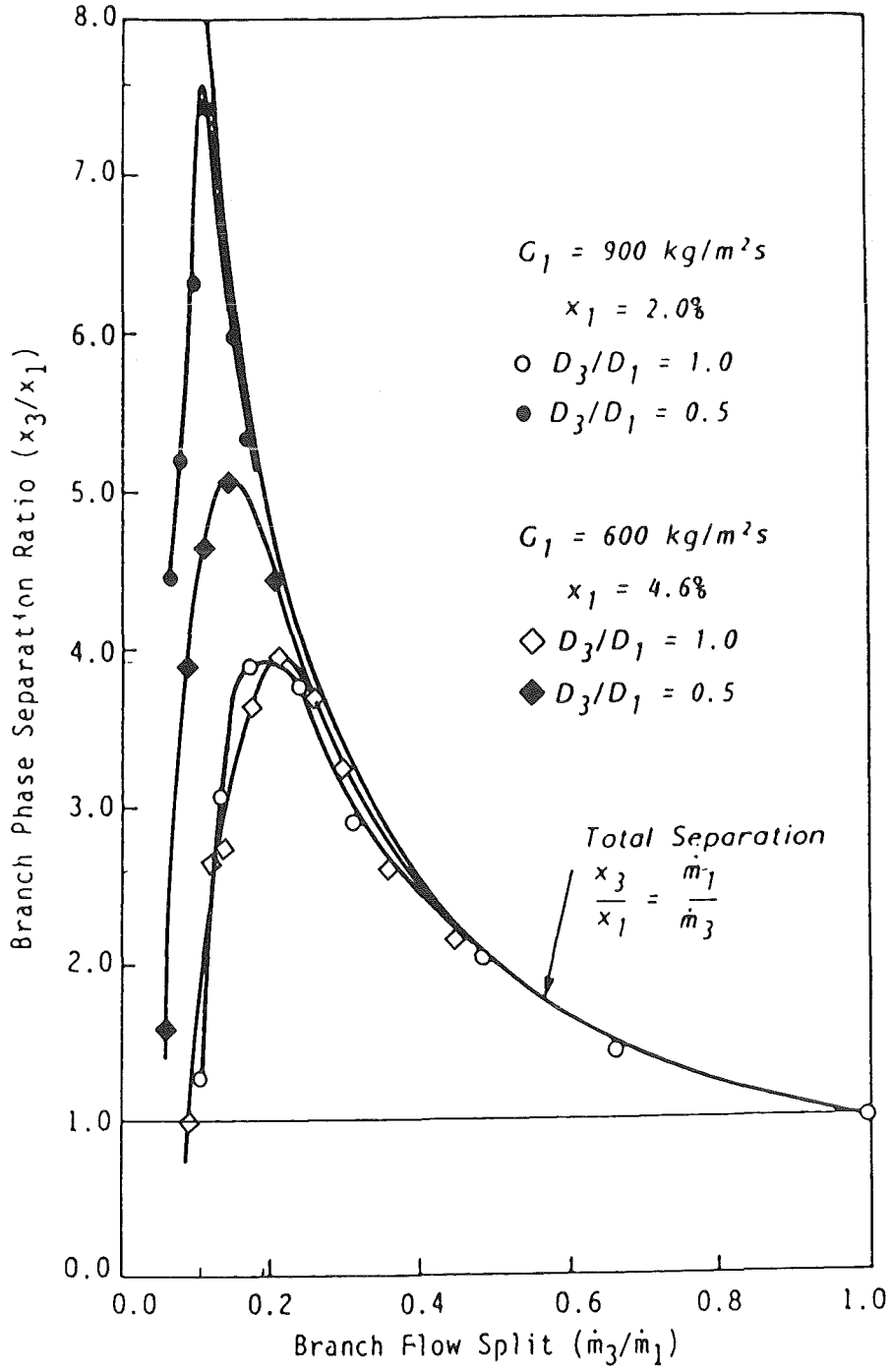


Fig. 2.8 Diameter Ratio Influence on Phase Redistribution: Annular Flow, $\phi = 90°$, $D_3/D_1 = 0.5$ and 1; from /34/.

Another point of discussion is the influence of the diameter ratio. Figure 2.8 contains results from Ballyk and Shoukri /34/ for $D_3/D_1 = 0.5$ and 1. With decreasing $D_3/D_1$ the phase separation increases, details will be discussed in Section 5.1.2. This tendency can be also observed in Fig. 2.5. To take into account the diameter ratio, Azzopardi /40/ proposed a correction factor K ,given below. However, the present data base is insufficient to describe the parameter range where this factor can be applied.

To describe the phase redistribution for the low range of $\dot{m}_3/\dot{m}_1$ and annular flow, Azzopardi and Whalley assumed a "zone of influence" from which the liquid film and gas were withdrawn. The rest of the liquid film and gas, and all the entrained liquid droplets, were assumed to be unaffected, and exited the test section through the run of the tee. They further reasoned that the affected region could be characterized by an angle $\Theta$, shown schematically in Fig. 2.9. Note that if $D_3 = D_1 = D_2$, the liquid extracted was (originally) assumed to be that part of the liquid film within the sector defined by the angle $\Theta$, while the vapor removed was assumed to be that in the shaded area. That is, the "zone of influence" (ZOI) for vapor extraction was defined by the area between the conduit wall and the chord subtended by the angle $\ominus$.

The resulting equations are:

$$x_3/x_1 = (\dot{m}_1/\dot{m}_3)(\ominus - \sin\ominus)/(2\pi), \tag{2.2}$$

with

$$\ominus = (2/K)(\dot{m}_3/\dot{m}_1)(1-x_3)/((1-x_1)(1-E)), \tag{2.3}$$

where K takes into account the diameter ratio

$$K = 1.2(D_3/D_1)^{0.4} \tag{2.4}$$

and E is the ratio of liquid droplets in the gas core to the total inlet liquid flow rate. This entrainment fraction E is not generally known for horizontal flow; in Fig. 2.6a, E was taken as a parameter.

This model does not predict satisfactorily the data from Ballyk et al. /34/ shown in Fig. 2.6a. This is due to the fact that the model uses implicitly the assumption that the momentum flux of the liquid film is in the order of the gas momentum flux. This is only true for very thin films (very small inlet liquid mass flow rate,

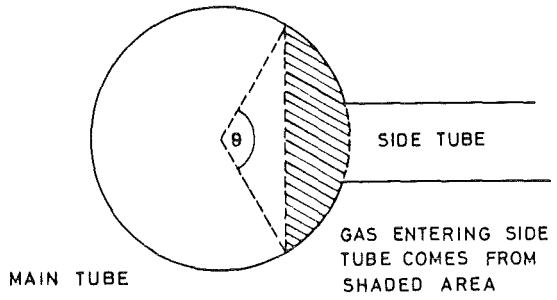


$$\frac{\text{SHADED AREA}}{\text{TOTAL CROSS SECTIONAL AREA OF MAIN TUBE}} = \frac{\theta - \sin\theta}{2\pi}$$

Fig. 2.9 Flow Geometry Used in Annular Flow Model from Azzopardi and Whalley /9,10/.

respectively inlet superficial liquid velocity in the order of $v_{sL} = 0.05$ m/s). The values of the experiments shown in Fig. 2.6 are considerably higher and, therefore, the assumptions are no longer valid. A parameter range was not given, where the model given above is valid.

More recently, Shoham et al. /33/ presented a model which has some common features with the model presented above. The model is based on equal zones of influence for both phases, a constant film thickness and no droplet entrainment in the gas core. The model predicted quite well experiments from the authors, also performed at very low superficial liquid velocities. Again, this model is not expected to describe annular flow data at high superficial liquid velocities. Comparisons with more appropriate data will be given in Section 5.3.

Seeger et al. /26/ proposed a relationship which is not tailored to a specific flow regime. However, annular flow data obtained at high liquid velocities $v_{sL}$ were also included to develop the correlation, compare Section 2.2.5. Some results were already presented in Fig. 2.6, more comparisons will be shown in Section 5.

Henry /11/ developed a correlation which fitted his data for $\dot{m}_3/\dot{m}_1 \leq 0.06$ and $D_3/D_1 = 0.2$ both for annular and stratified wavy flow. Due to the very small

parameter range investigated, these correlations are not presented here; the reader is referred to /11/.

### 2.2.2 Smooth Stratified, Stratified-Wavy Flow

Experiments in the stratified flow regime performed with $D_3/D_1 = 1$ by Hong and Shoham et al. are shown in Fig. 2.10. For stratified-wavy flow (Fig. 2.10b and 2.10c), no liquid flows into the branch at low mass splits for all inlet conditions. The liquid enters the branch only after a higher portion of the gas is diverted into the branch. Thus it seems that there is a trend of a branch gas fraction threshold needed to initiate diversion of the liquid phase into the branch. For example, when $v_{sL} = 0.0029$ m/s, this threshold is approximately $\dot{m}_{3G}/\dot{m}_{1G} = 0.23$, as shown in Fig. 2.10b. If the branch gas fraction intake is below 23 %, no liquid will enter the branch. The gas phase threshold decreases as the liquid phase flow rate increases. For $v_{sL} = 0.059$ m/sec, the threshold is about $\dot{m}_{3G} = \dot{m}_{1G}$.

Analyzing the liquid phase route preference, the following is observed: At low liquid flow rates, i.e., $v_{sL} = 0.0029$ and 0.0051 m/s, the liquid phase preferentially flows into the branch. For the lowest liquid flow rate of $v_{sL} = 0.0029$ m/s, when 60 % of the gas flow rate is diverted into the branch, all the liquid phase is diverted into the branch and the run receives only air. At an intermediate liquid flow rate of $v_{sL} = 0.0092$ m/s, the results closely follow the equal splitting line, as the gas phase and the liquid phase split evenly through the branch. At higher liquid flow rates, however, the route selectivity of the liquid phase changes, and it tends to flow preferentially into the run. For the highest liquid flow rate of $v_{sL} = 0.059$ m/s, when all the gas phase is diverted into the branch, only 50 % of the liquid flows into the branch.

Stratified smooth splitting ratios are given in Fig. 2.10a. The average superficial gas velocity during these runs was $v_{sG} = 2.5$ m/s. The liquid superficial velocities were the same as in the stratified wavy flow case.

One can immediately observe that for all inlet liquid flow rates in stratified smooth flow, the gas preferentially flows into the branch since all the splitting curves are located above the equal splitting line. The threshold needed to start liquid flow into the branch is higher than during stratified wavy flow conditions. For the lowest liquid flow rate, i.e. $v_{sL} = 0.0029$ m/s, the threshold is above 50 %,

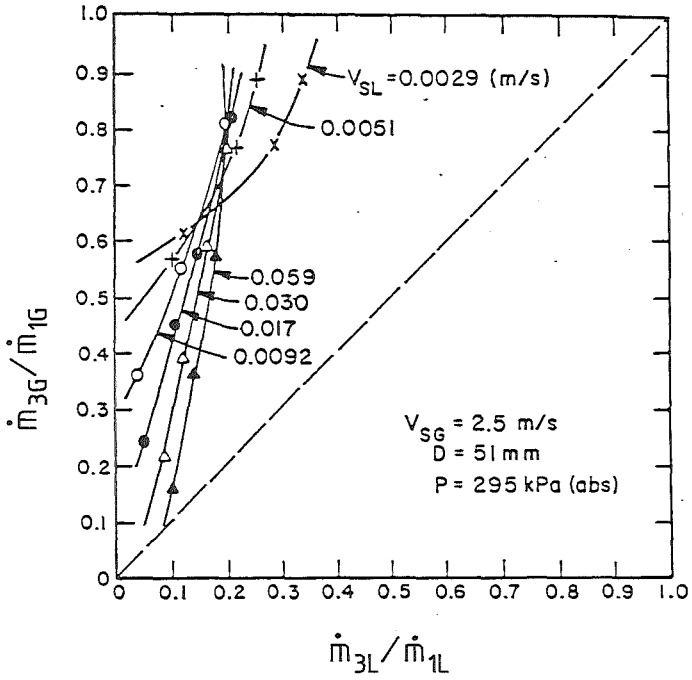


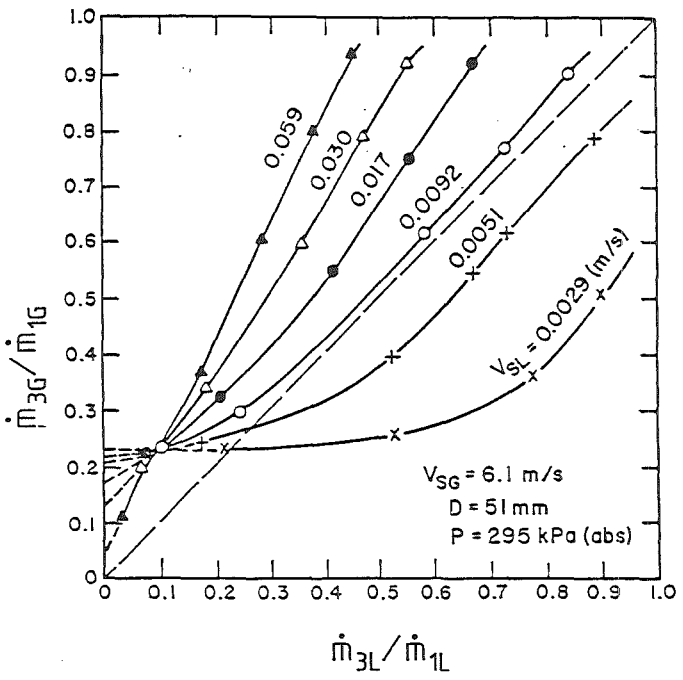


a), b) Results from Shoham et al.

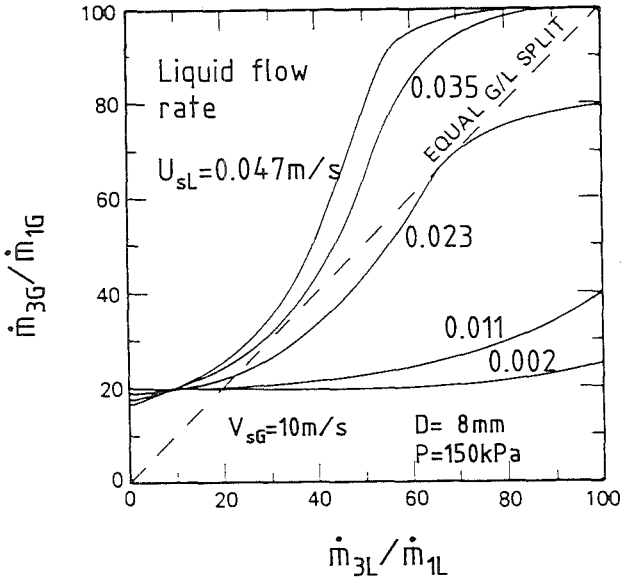


c) Results from Hong

Fig. 2.10 Stratified Flow Data: $\phi = 90°$, $D_3/D_1 = 1$; Results from /8,33/.

and decreases rapidly as the liquid flow rate increases. At the highest liquid flow rate of $v_{sL} = 0.059$ m/s, liquid starts to flow into the branch for even zero branch gas fraction intake.

Typical of flow splitting during stratified smooth flow is the steep slope exhibited by the splitting curves. This indicates strong preference of the liquid phase to flow straight into the run. For all the experiments, when the total gas flow rate is diverted into the branch, only 30 % to 40 % of the liquid phase flows into the branch. Shoham et al. also developed a model for stratified flow which, however, it does not predict the measurement as well as the annular flow model; for details see /33/.

Collier /7/ also presented results from experiments mostly performed in the stratified flow regime, however, for $D_3/D_1 = 0.66$, as shown in Fig. 2.11. With increasing $v_{sL}$ the gas fraction increases which is in agreement with the tendency also seen in Fig. 2.10. At very low branch flow rates, the curves have a different tendency and do not start with only gas flow into the branch. This is somewhat surprising because the liquid level is expected to be below the branch entrance.

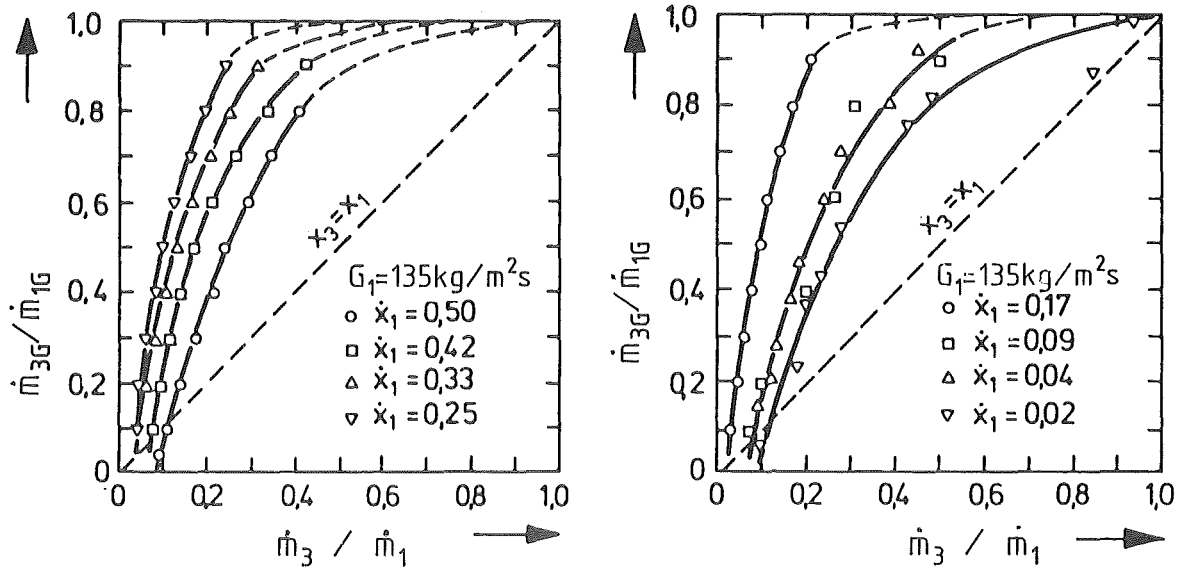


Fig. 2.11 Stratified and Annular Flow Data: $\phi = 90^{o}$, $D_3/D_1 = 0.66$; from /7/.

Smoglie and Reimann (Refs. /16/ - /20/) investigated stratified smooth air-water flow for diameter ratios $D_3/D_1 << 1$. If the gas liquid interface is high above or below the branch entrance, only liquid or gas can enter the branch. The beginning of gas entrainment (g.e.) for the liquid level above the branch or liquid entrainment (l.e.) for a liquid level below the branch was described in the following way:

$$K = h_b (g \rho_b (\rho_L - \rho_G))^{0.2} m_{3b}^{-0.4}, \tag{2.5}$$

with

$$K = 0.69 \text{ for l.e. and } K = 0.75 \text{ for g.e.}$$

$h_b$ is the interface level for entrainment beginning, g is the acceleration due to gravity, $\rho_b$ and $\dot{m}_b$ are the density and mass flow rate of the continuous phase at entrainment beginning. It is interesting to note that Eq. (2.5) does not contain explicitly the branch diameter. The validity of Eq. (2.5) is restricted to values $h_b/D_3 > 1$.

For small diameter ratios $D_3/D_1$ the single phase branch mass flow rate can be determined by

$$m_{3b} = \zeta \varepsilon A_3 (\rho_b \Delta p_{1-3})^{0.5}, \tag{2.6}$$

where $\zeta$ is the flow coefficient and $\varepsilon$ the gas expansion coefficient (if $\rho_b = \rho_L$: $\varepsilon = 1$). $A_3$ is the branch cross section and $\Delta p_{1-3}$ the branch pressure drop.

For interface levels $|h| < h_b$ a two-phase mixture enters the branch; the branch quality $x_3$ was described by

$$x_{3pr} = \left[ \frac{1.15}{1 + (\rho_L/\rho_G)^{0.5}} \right]^{\left(1 + C\frac{h}{h_b}\right)} \left[ 1 - \frac{1}{2}\frac{h}{h_b}\left(1 + \frac{h}{h_b}\right)\left(\frac{1.15}{1 + (\rho_L/\rho_G)^{0.5}}\right)^{\left(1 - \frac{h}{h_b}\right)} \right]^{0.5} \tag{2.7}$$

where

$C = 1$ for l.e. $(h/h_b \leq 0)$

$C = 1.09$ for g.e. $(h/h_b > 0)$

Here, h is positive for gas entrainment and negative for liquid entrainment. Figure 2.12 shows the experimental results.

The results for the branch mass flow rate are shown in Fig. 2.13. The experiments were fitted by single curves by normalizing $\dot{m}_3$ with $\dot{m}_{3b}$. The different values of $\dot{m}_{3b}$ for l.e. and g.e. are the reason for the discontinuity at $h = 0$.

High pressure stratified steam-water experiments with $D_3/D_1 << 1$ were performed by Maciaszek and Memponteil /35/ and Anderson /36/. Following the procedure proposed in Refs. /14-20/, the first authors proposed correlations which are in close agreement with the relationships given above. Anderson also compared his high pressure data with the correlation given above (which was deduced from low pressure air-water experiments) and found an excellent agreement as shown in Fig. 2.14.

### 2.2.3 Dispersed Bubble Flow

The dispersed bubble flow pattern should be best suited for a rigorous modeling of the phase redistribution using balance equations and closure laws. This is due to the fairly well defined inlet pipe conditions (axisymmetric void fraction and momentum distribution) and due to the fact that the interaction of the bubbles with the surrounding liquid appears to be relatively simple to take into account by a corresponding closure law. For simplicity, a two-dimensional flow is assumed and the aim is to calculate the stagnation streamlines, different for the two phases, which divide those zones of the inlet cross section where the flows enter the branch from the other zones where the flows stream into the run.

Such a rigorous attempt to model phase redistribution (pressure drop not included) was made recently by Lemmonier and Hervieu /42/. Their model is based on a two-dimensional approach and hence, uses local equations. The first step consists in modelling the single-phase flow in the Tee-junction. The free streamline theory is used to predict the flow of the continuous phase. The two recirculation zones which are present in this configuration are predicted by the model. Then the location of a gas bubble results from the single-phase flow field. Finally, the trajectories of gas bubbles are calculated and used to predict the redistribution properties of the Tee-junction.

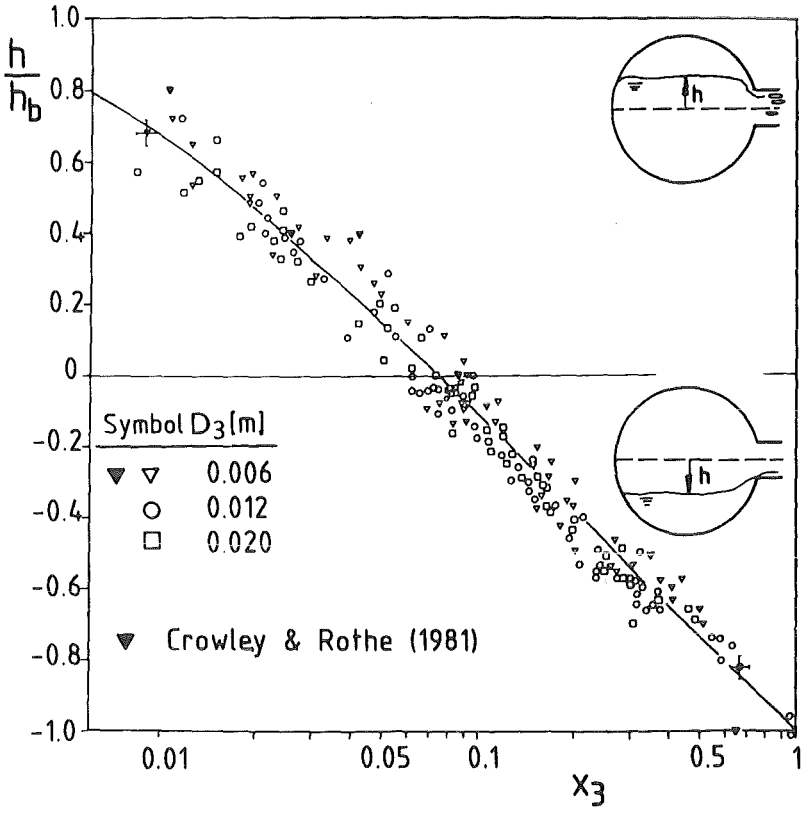


Fig. 2.12 Stratified Flow Data: Branch Quality $x_3$, $\phi = 90°$, $D_3/D_1 << 1$; from /20/.

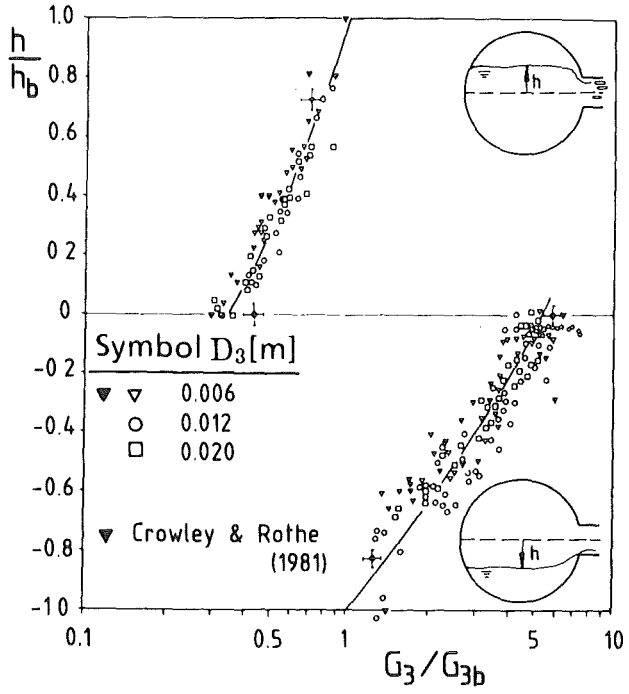


Fig. 2.13 Stratified Flow Data: Branch Mass Flux $G_3$, $\phi = 90°$, $D_3/D_1 << 1$; from /20/.

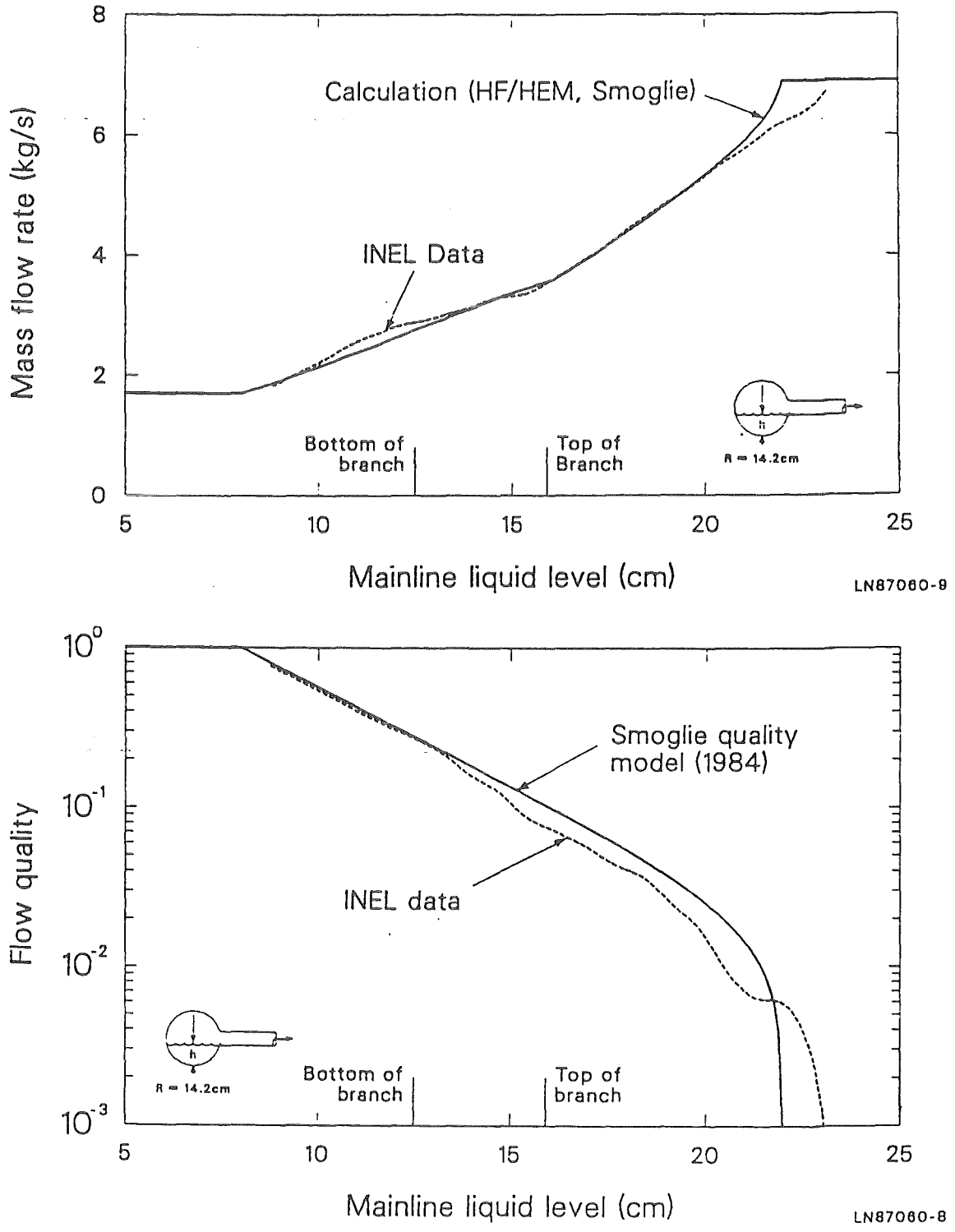


Fig. 2.14 Stratified Flow Data: Branch Mass Flux and Quality, High Pressure Steam-water Flow, $\phi = 90^{o}$, $D_3/D_1 = 0.1$; from /36/.

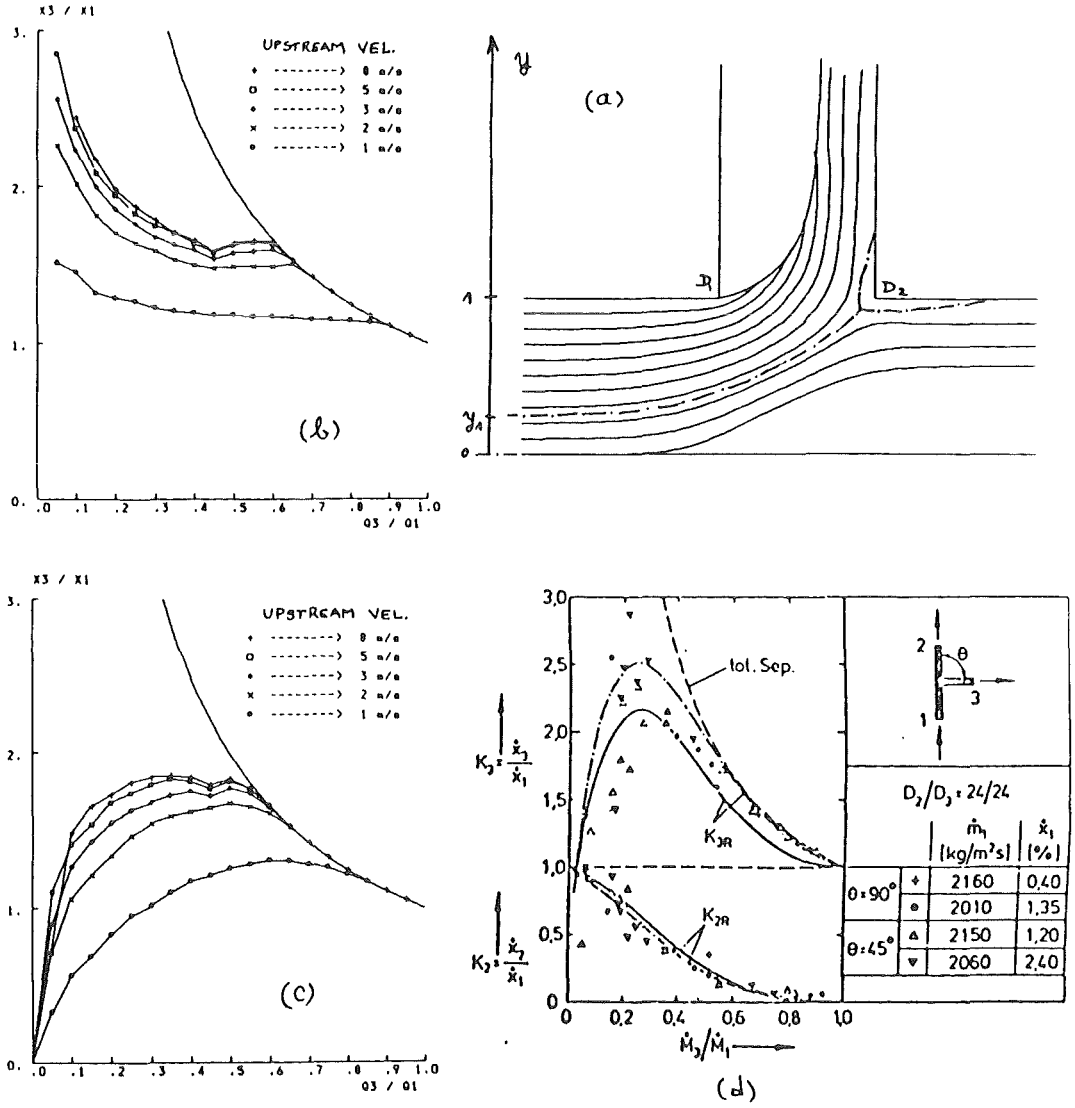


Separation efficiency prediction. (a) Control volume used in the mass balance ( eq. 59). Separation curves calculated with different void profiles with the upstream velocity as a parameter. (b) flat void profile . (c) parabolic void profile. (d) Zetzmann data (1970) is reproduced to exhibit the characteristic shape of the separation curve.

Fig. 2.15 Dispersed Bubble Flow Data: Calculated Phase Redistribution, $\phi = 90°$; from /42/.

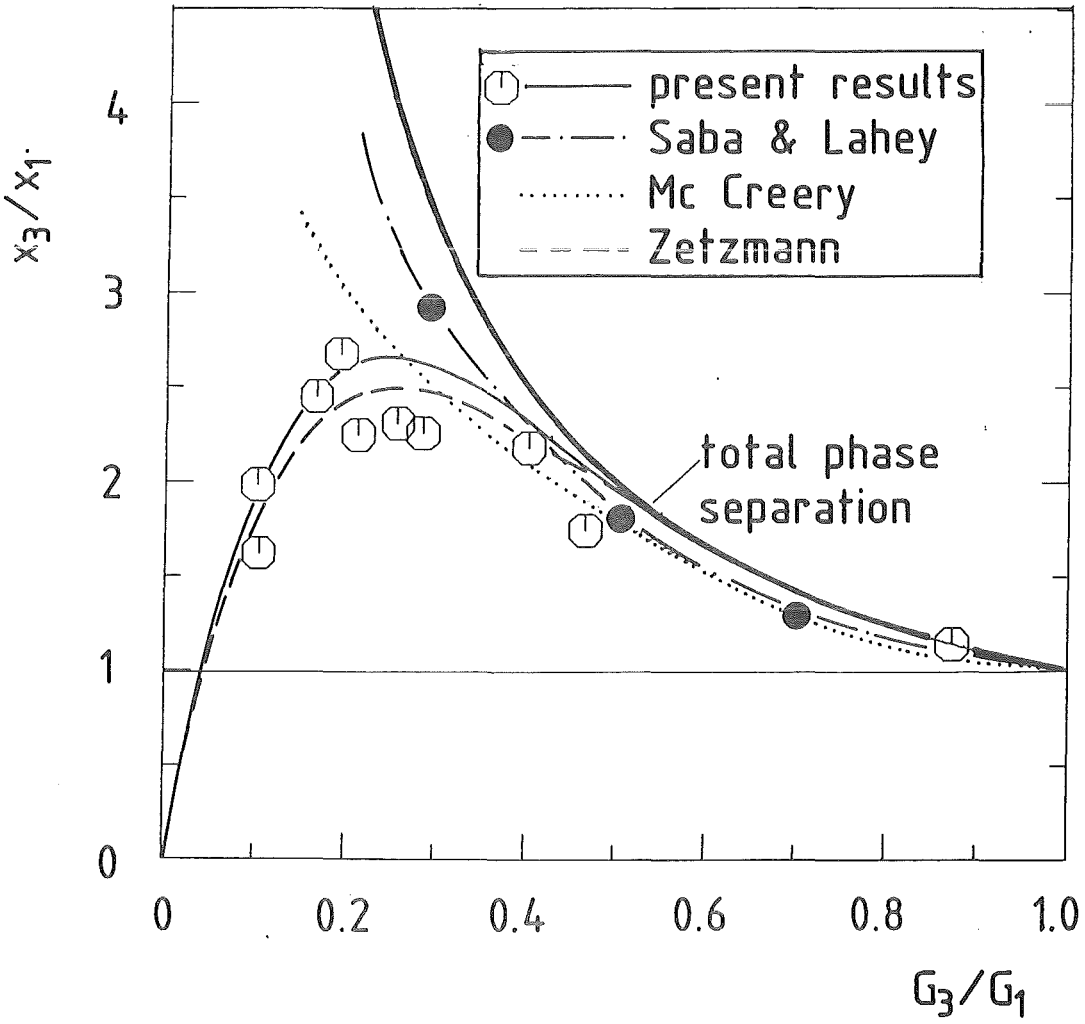


Fig. 2.16 Slug Flow Data: $\phi = 90°$, $D_3/D_1 = 1$; Results from /12,24/.

The model predicts curves of the type shown in Fig. 2.15 which are qualitatively in good agreement with experimental results from Seeger /24/ shown in Fig. 5b. Further work is in progress to obtain better quantitative agreement.

McCreary /43/ also attempted to use a simple modeling approach for dispersed flow. However, he clearly stated that the interaction laws to close the model were not fruitful. He then proceeded in a rather empirical way; his final relationships are given in Section 2.2.5.

### 2.2.4 Slug Flow

Figure 2.16 shows for $D_3/D_1 = 1$ typical results for inlet condition in the slug flow regime. The curves from Seeger /24/ exhibit the typical maximum whereas the experiments from Saba and Lahey /13/ do not show this maximum due to the limitation in the split ratio to $\dot{m}_3/\dot{m}_1 \leq = 0.3$. It is interesting to note that the

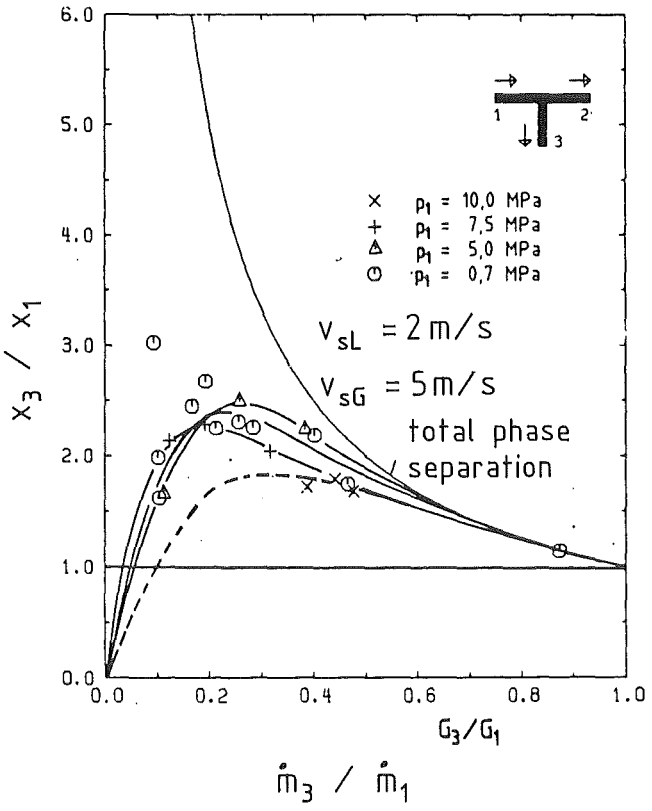


Fig. 2.17 Slug Flow Data: Pressure Influence p = 0.7-10 MPa, $\phi = 90°$, $D_3/D_1$; from /24/.

experiments from Zetzmann /38/ with a vertical upward flow in the inlet pipe are very close to the results for the horizontal branch, compare Section 5.12. More data from /27/ for $D_3/D_1 = 1$ are presented in Section 2.1.5.

Figure 2.17 (from /24/) contains results for a wide pressure range. Again, the phase redistribution decreases with increasing pressure, however, the pressure influence is very small.

### 2.2.5 Non Flow Regime Specific Models

Models described in this section are not flow regime based but rather try to predict the phase redistribution for a wider parameter range by using a mechanistic approach (Saba and Lahey /13/) or a highly empirical approach (Seeger et al. /26/). The model proposed by McCreery /43/ lies in between. All models are fitted with experiments with $D_3/D_1 = 1$ and conditions mostly in the slug flow regime and the transition zones to the neighbouring flow regimes. This fact should be considered by applying these models.

Saba and Lahey proposed a complete calculation scheme for both phase redistribution and pressure drop in the Tee junction. For eight parameters of interest (three mass fluxes and qualities, two pressure drops), where three parameters are specified, five equations are needed. The selected equations are: two mass balances (one for each phase), two momentum equations for the mixture and the gas momentum balance for the branch. The way, the last equation is derived, gives rise to substantial criticism (e.g. see Lemonnier and Hervieu /42/). This equation is used to fit the authors' data from the slug flow regime. The model calculates a curve which is quite close to the curve of total phase separation (Eq. (2.1)), as shown in Fig. 2.18. The characteristical maximum and the decrease of $x_3/x_1$ at low split ratios is, therefore, not obtained. Similar results, however, with a much simpler calculation procedure are obtained with the model of McCreery, presented in the following.

McCreery started with the two-dimensional balance equations for mass and momentum for each phase using an expression for the interfacial friction. As mentioned, this procedure was not successful and, therefore, friction was taken into account in a more heuristic way by using modified densities $\rho^*_G$ and $\rho^*_L$, given below. The relationships for these densities were developed using the

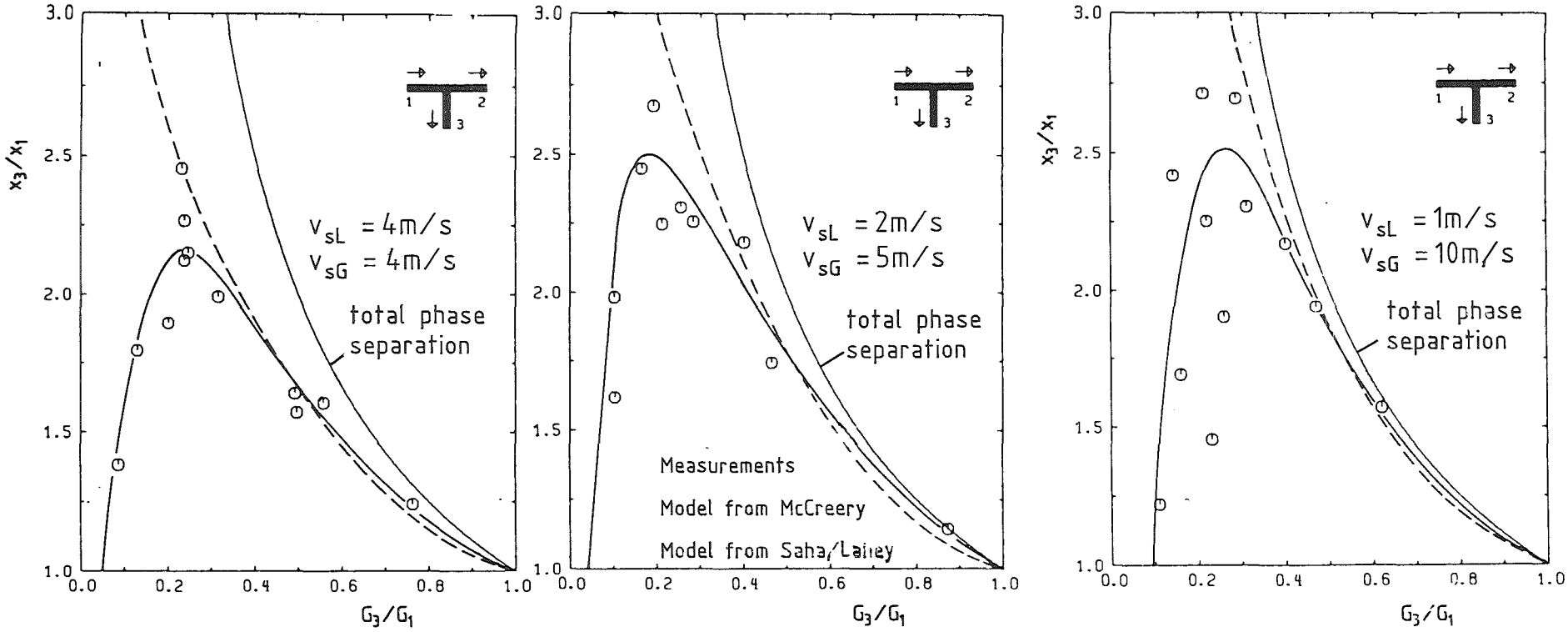


Fig. 2.18 Comparison between Experimental and Calculated Data: $\phi = 90°$, $D_3/D_1 = 1$; Results from /13,24,43/.

experimental results from Honan and Lahey /39/ for a vertical inlet pipe and the first results from air-water experiments obtained by Reimann et al. /21/. The final relationships are:

The homogeneous branch void fraction $\alpha_{3h}$ is given by

$$\alpha_{3h} = 1 - (\rho_L^*/\rho_G^*)^{1.5}(1-\alpha_{1h}) \tag{2.8}$$

where $\alpha_{1h}$ is the homogeneous inlet void fraction defined by

$$\alpha_{1h} = (1+(\rho_G/\rho_L)(1-x_1)/x_1)^{-1} \tag{2.9}$$

and $\rho_L^*$ and $\rho_G^*$ are modified densities given by

$$\rho_L^* = \rho_L - \alpha_{1h}^{\eta}(\rho_L - \rho_G) \tag{2.10}$$

$$\rho_G^* = \rho_G + (1-\alpha_h)^{\eta}(\rho_l - \rho_G) \tag{2.11}$$

The exponent $\eta$ is given by

$$\eta = 1.15(1\text{-}\dot{m}_3/\dot{m}_1)^{0.096} \text{ for } \dot{m}_3/\dot{m}_1 \leq 0.7 \tag{2.12}$$

and

$$\eta = 1 + 0.14(1\text{-}\dot{m}_3/\dot{m}_1) \text{ for } \dot{m}_3/\dot{m}_1 > 0.7 \tag{2.13}$$

As mentioned, this model describes only the right part of the phase redistribution curve, as seen in Fig. 2.18, however, with a quite good accuracy. (The experimental data shown in this figure were not available when McCreery developed his model).

Seeger et al. /26/ used the following expression for the phase redistribution to fit their air-water and steam-water data

$$x_3/x_1 = 5(\dot{m}_3/\dot{m}_1)\text{-}6(\dot{m}_3/\dot{m}_1)^2 + 2(\dot{m}_3/\dot{m}_1)^3 + a\,(\dot{m}_3/\dot{m}_1)(1\text{-}\dot{m}_3/\dot{m}_1)^b \tag{2.14}$$

where the factor a determines the height of the maximum value of $x_3/x_1$ and b has a value of b = 4. The idea underlined was that $(x_3/x_1)_{max}$ is a function of the ratio of the momentum fluxes in the inlet pipe $(\rho u_1^2)_G/(\rho u_1^2)_L = (\rho_G/\rho_L)S_1^2$ where $S_1$ is the slip in the inlet pipe.

If $(x_3/x_1)_{max}$ is plotted as a function of $(\rho_G/\rho_L)S_1^2$ (see Fig. 2.19), the experimental points (except those in the dispersed bubble flow regime) can be fitted by a straight line in a double-logarithmic plot given by:

$$(x_3/x_1)_{max} = ((\rho_G/\rho_L)S_1^2)^{-0.26} \tag{2.15}$$

The factor a was determined to

$$a = 13.9((\rho_G/\rho_L))S_1^2)^{-0.26} \tag{2.16}$$

The following parameter range was used to develop Eqs. (2.15)-(2.16):

$$0.9 \leq = v_{sL} \leq = 2.2 \text{ m/s}$$
$$4 \leq = v_{sG} \leq = 40 \text{ m/s}$$

For dispersed bubble flow ($v_{sL} \geq 4$ m/s) the factor a was determined to a = 14.6.

The slip $S_1$ in the inlet pipe was calculated using the correlation proposed by Rouhani /54/:

$$S_1 = \rho_L((1 + 0.12(1-x_1))/\rho_{h1} + W_{rel}/(G_1 - x_1/\rho_G)/(1-x_1), \tag{2.17}$$

where

$$\rho_{h1} = (x_1/\rho_G + (1-x_1)/\rho_L)^{-1}, \tag{2.18}$$

and

$$W_{rel} = (1.18/\rho_L^{0.5})(g\sigma(\rho_L-\rho_G))^{0.25} \tag{2.19}$$

and $\sigma$ is the surface tension.

A correlation which predicts a curve similar to Eq. (2.14) was given by Zetzmann /38/ based on experiments with a vertical inlet pipe. Due to the small parameter range investigated, this correlation is not dependent on the inlet conditions.

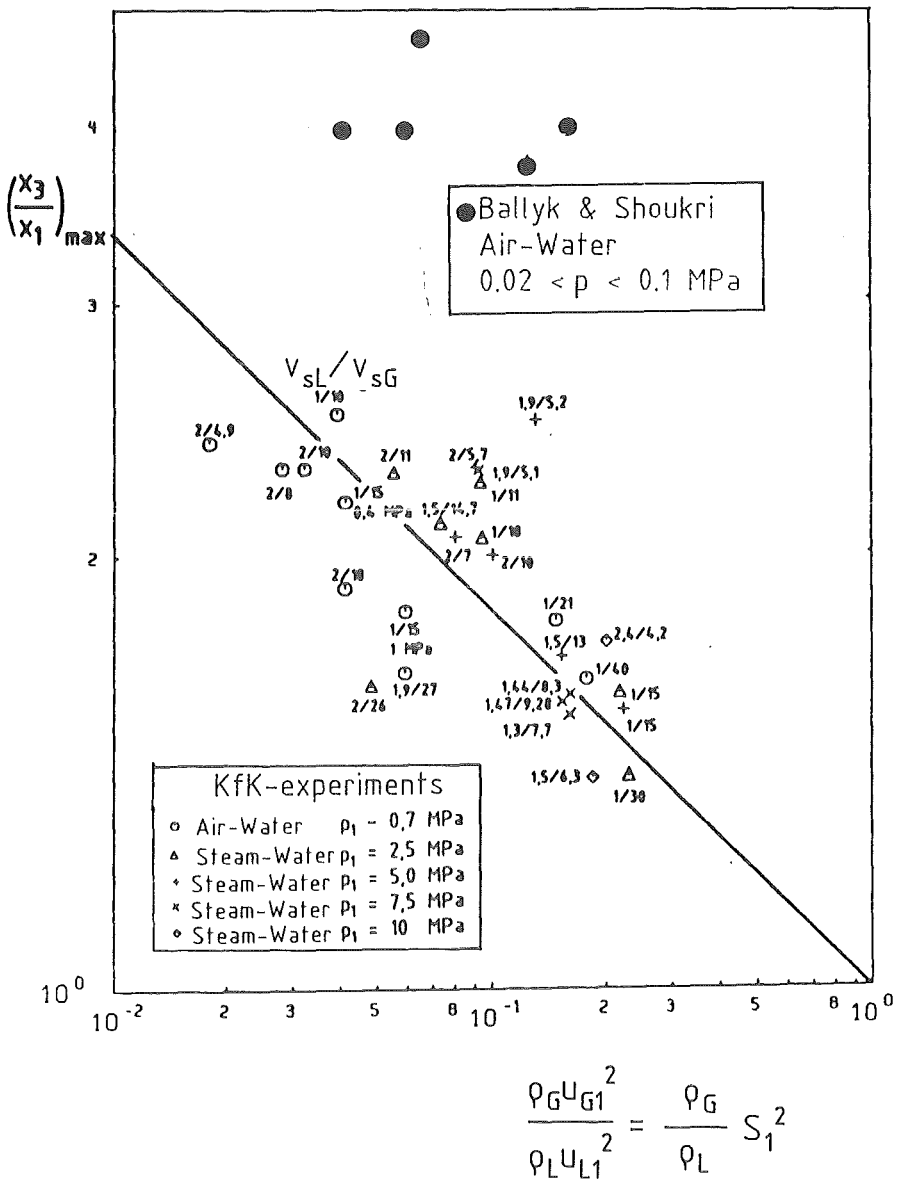


Fig. 2.19 Dependence of Phase Redistribution Maximum; from /26/.

Figure 2.19 contains also results from Ballyk and Shoukri /34/, more details in Section 5.12.

## 2.3 Upward Branch ($\phi = 0^{o}$)

### 2.3.1 General Tendencies

As shown in Table I.1, the data base for upward branches is much smaller than for horizontal branches. The gas intake is expected to be larger compared to the horizontal branch because phase separation is enforced by the impact of the gravity force. This impact can be divided into three effects:

a) Work has to be done to lift a liquid particle from a lower level on the streamline in the inlet pipe to the higher position at the branch entrance. This gravity effect is probably small compared to the next effect.

b) The void fraction is higher in the upper part of the inlet pipe cross section. The degree of this phase separation in the inlet pipe, and with this the effect of branch orientation, becomes smaller with increasing momentum fluxes in the inlet pipe. Phase separation is expected to be even more expressed for a smaller value of $D_3/D_1$ because the fluid entering the smaller branch is taken more locally from the upper portion of the pipe. As will be discussed in detail later , this tendency can be different for very small values of $D_3/D_1$ if the branch diameter is in the order of the thickness of the liquid film at the top of the pipe.

c) Phase separation in the branch itself: For very small branch valve openings ($\dot{m}_3/\dot{m}_1 \approx 0$), a gas liquid mixture enters the branch. However, the drag force on the liquid phase is too small to transport the liquid film or droplets further downstream. Flow reversal of the liquid phase occurs and the liquid enters the run and only gas leaves the branch pipe.

This phenomenon of flow reversal in the branch entrance and the transport of the liquid into the run was illustrated in detail by Seeger et al. /25/. The following relationship was recommended to describe the maximum branch mass flux with $x_3 = 1$:

$$G_{3max,\,x=1} = A\ 0.23(gD(\rho_L-\rho_G)\rho_G)^{0.5}, \qquad (2.20)$$

where A = 0.5 for inlet conditions in the dispersed bubble flow regime and A = 1 for other inlet conditions. Relationships similar to Eq. (2.20) were used to describe the transition between different flow regimes in vertical upward flow, see Wallis /44/.

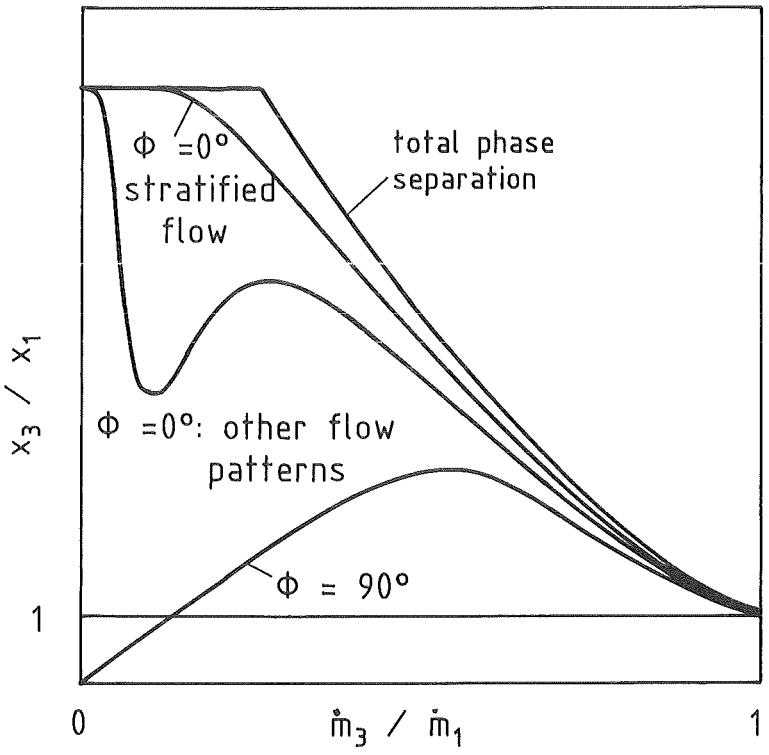


Fig. 2.20 Characteristical Differences of Phase Redistribution for Upward ($\phi = 0^{\circ}$) and Horizontal Branch ($\phi = 90^{\circ}$), $D_3/D_1 = 1$.

The influence of flow reversal exists only in a very small range of $\dot{m}_3/\dot{m}_1$ which is often not covered by the measurement system. If for example an air-water flow is assumed with $v_{sG} = 10$ m/s, $v_{sL} = 2$ m/s, $p_1 = 0.7$ MPa and $D_3 < D_1 = 1$, then the maximum mass split ratio where liquid cannot be transported through the branch is $\dot{m}_3/\dot{m}_1 = 0.007$.

Figure 2.20 shows schematically characteristic differences of the phase redistribution for the upward and horizontal branch for $D_3/D_1 = 1$. At high splits the curve for the upward branch is even closer to the curve of total phase separation. At very low values of $\dot{m}_3$ the branch quality $x_3$ goes to unity and with this $x_3/x_1$ obtains the maximum value. The question is if a further maximum

exists at $\dot{m}_3 >> 0$ as typically observed for the horizontal branch. This is expected for flow patterns which are not domintated by stratification. For stratified flow, a decrease of $x_3/x_1$ is expected for increasing branch flow rate up to $\dot{m}_3/\dot{m}_1 = 1$.

For $D_3/D_1 < 1$ flow reversal effects are shifted to even lower values of $\dot{m}_3/\dot{m}_1$ and the existence of a maximum at $\dot{m}_3 >> 0$ is more probable; more details in Section 5.

### 2.3.2 Specific Flow Regimes

Experiments with annular flow at low mass fluxes, performed by Hong /8/ and Azzopardi /10/ were shown in Fig. 4 b) and c). Hong measured the total split curve and obtained very high gas intakes for low values of $\dot{m}_3/\dot{m}_1$ (about 20 % of the total gas flow enters the branch unless a measurable amount of liquid is entrained). This is in contrast to the previous discussions and to the results from Azzopardi who observed a much higher liquid fraction at $\dot{m}_3/\dot{m}_1 \approx 0$. The experiments differ by the diameter ratio, however, it is believed that this is not the reason for the large difference. More experiments are required to clearify this situation.

Experiments with much higher mass flow rates in the slug flow, annular flow and dispersed bubble flow regime were performed at KfK (Refs. /21-26/) with $D_3/D_1 = 1$. Results are shown in Figs. 2.2a, 2.3 and 2.21. A maximum at $\dot{m}_3/\dot{m}_1 >> 0$ was not measured. However, such a maximum could exist at values $\dot{m}_3/\dot{m}_1$ below the measurement range ($\dot{m}_3/\dot{m}_1 \geq 0.1$). There is the tendency that the phase redistribution becomes smaller with increasing $v_{sL}$. Further experiments are required for a wider inlet parameter range and lower values of $\dot{m}_3/\dot{m}_1$.

Up to now, no physically based models exist taking into account the specific features of the flow phenomena in the upward branch. As a rule of thumb, the following relationship was recommended by Seeger et al. /26/:

$$x_3/x_1 = (\dot{m}_3/\dot{m}_1)^{-0.8}, \qquad (2.21)$$

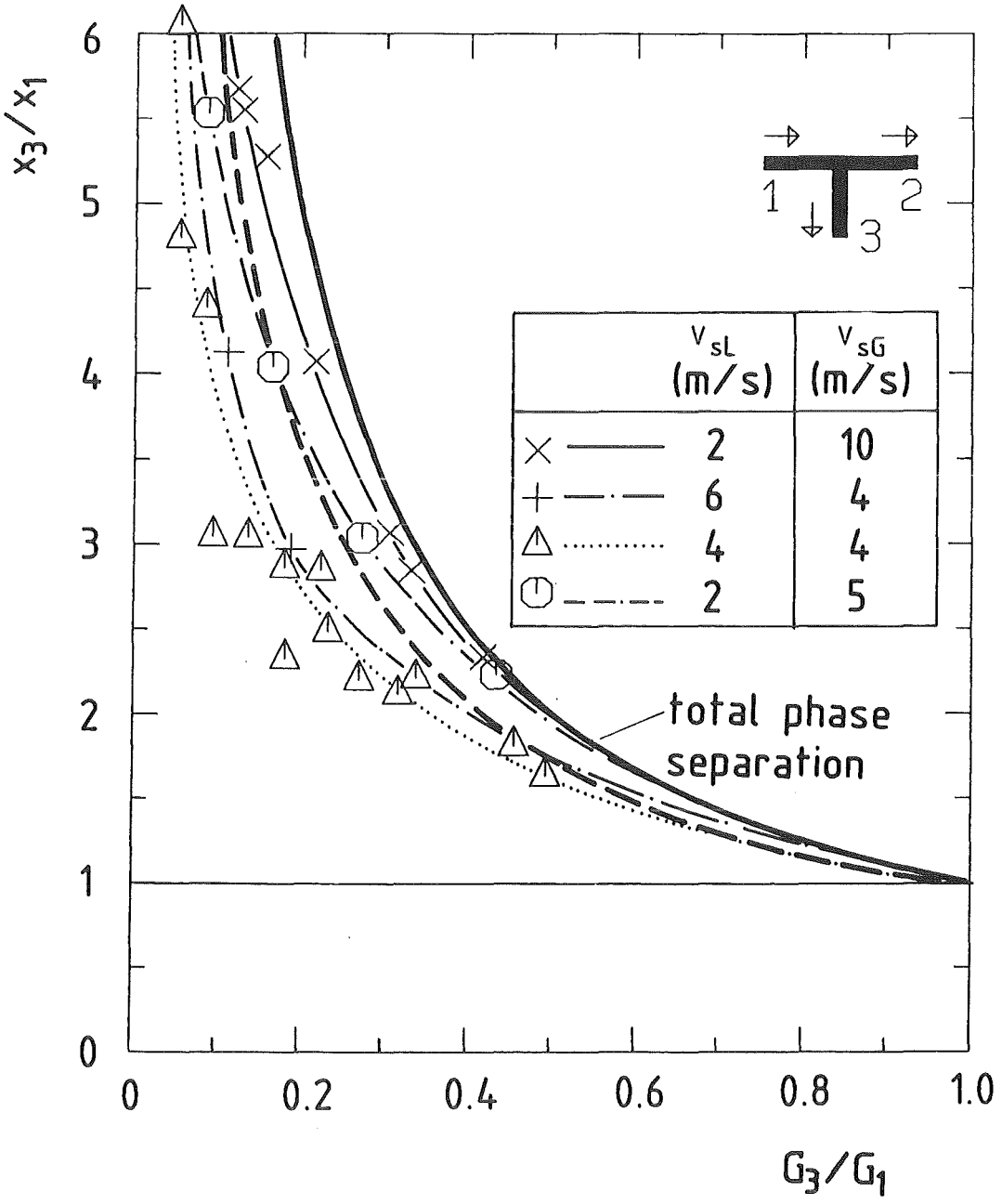


Fig. 2.21 Phase Redistribution for Upward Branch ($\phi = 0^{\circ}$), $D_3/D_1 = 1$; from /26/.

based on experiments with $D_3/D_1 = 1$ and the inlet conditions investigated in /26/. The use of Eq. (2.21) should be restricted to $\dot{m}_3/\dot{m}_1 > 0.15$.

Phase redistribution for $D_3/D_1 << 1$ in the smooth stratified flow regime was investigated in Refs. /16/ to /20/. The beginning of droplet entrainment is described by Eq. (2.5) using a value of $K = 1.67$. The branch quality was described with the following correlation

$$x_3 = 1 - \left(\frac{1.15}{1 + (\rho_L/\rho_G)^{0.5}}\right)^{\left(2\frac{h}{h_b}\right)} \left[ 1 - \frac{1}{2}\frac{h}{h_b}\left(1 + \frac{h}{h_b}\right)\left(\frac{1.15}{1 + (\rho_L/\rho_G)^{0.5}}\right)^{\left(1-\frac{h}{h_b}\right)}\right]^{0.5} \qquad (2.22)$$

Figure 2.22 (from Smoglie and Reimann /20/) shows the experimental results. The branch quality is very close to 100 % as far as stratified flow exists in the inlet pipe. This is due to the strong vorticity of the gas flow near the branch entrance which accelerates the droplets in the radial direction so that only a small portion can enter the branch.

Experiments with $D_3/D_1 = 0.3$ in the elongated bubble and stratified flow regime were performed by Katsaounis /31,32/. In all experiments the phase distribution curve was very close to the curve for total phase separation within the experimental error. Figure 2.23 (from /32/) illustrates the flow mechanisms for the geometry investigated.

## 2.4 Downward Branch ($\phi = 180°$)

The data base for this branch direction is even smaller than for the upward branch. For this flow direction the effect of the different inlet momentum fluxes (which favours in general the gas phase to enter the branch) competes with the effect of the gravity force which favours the liquid phase to enter the branch.

Compared to the flow reversal effect in the upward branch there is a similar effect in the downward branch. At small branch mass flux ratios liquid with some bubbles enters the branch. A part of the bubbles (or all of them) can rise in the recirculation zone for very small mass flux ratios and enter the run. This three-dimensional flow effect is explained in more detail in /25/.

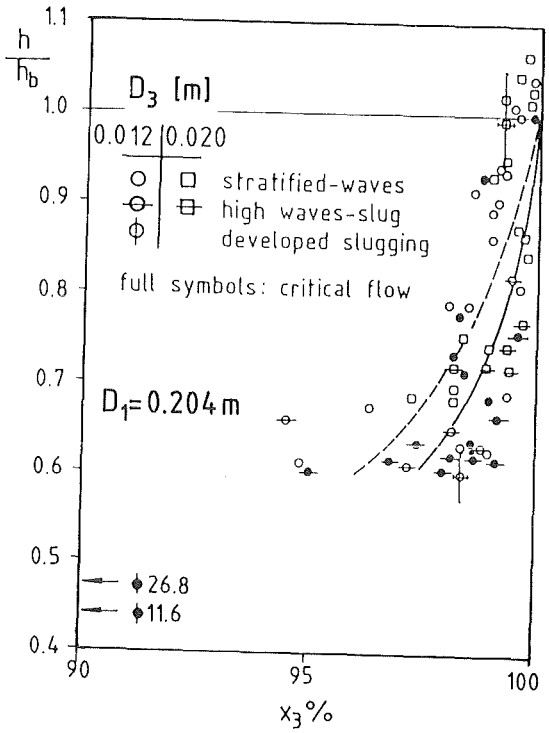


Fig. 2.2 2 Stratified Flow Data: Branch Quality $x_3$, $\phi = 0^o$, $D_3/D_1 << 1$; from /20/.

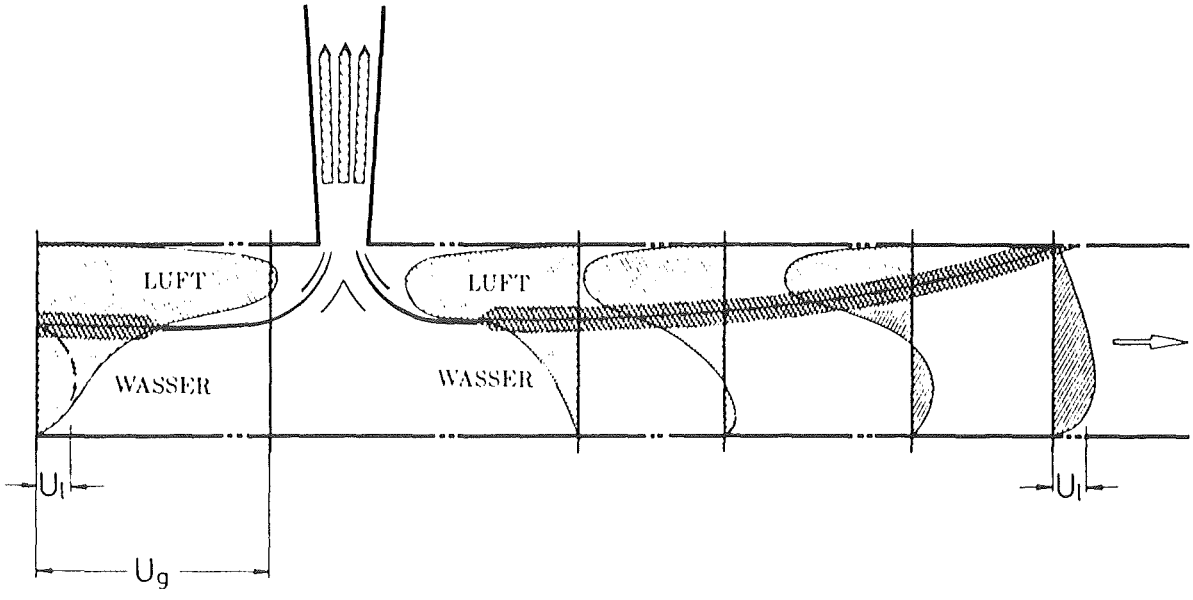


Fig. 2.23 Flow Mechanisms for Stratified Flow and Upward Branch; from /32/.

Prior to the KfK-experiments, there were some single measurement points in the annular flow regime from Hong /8/ and Azzopardi and Whalley /10/, see Fig. 2.2b and 2.2c. In both experiments a considerable amount of liquid could be withdrawn before gas started to enter the branch.

A wider range of inlet conditions with test points in the dispersed bubble, slug and annular-flow-regime was investigated in the KfK-experiments with $D_3/D_1 = 1$ (Refs. /21/ to /26/). Figure 2.24 from /26/ shows typical results for a constant superficial liquid velocity $v_{sL} = 1$ m/s and a constant superficial gas velocity $v_{sG} = 5$ m/s. The lower the inlet velocities the larger is the phase stratification and the more expressed is the tendency that liquid favourably enters the branch. With increasing pressure difference between inlet and branch (that is with increasing split ratio $\dot{m}_3/\dot{m}_1$) gas is increasingly favoured to enter the branch. For inlet flow patterns which are not dominated by stratification due to gravity the ratio $x_3/x_1$ becomes also larger than one for higher values of $\dot{m}_3/\dot{m}_1$.

To fit the experimental data, a first empirical approach was presented in /26/: Again, a relationship equivalent to Eq. (2.14) was used. The exponent b was expressed as a function of the liquid mass flux:

$$b = 3 + 2.2 \tanh(0.5(G_{1L} - 3000)), \tag{2.23}$$

whereas the factor a is dependent on both the liquid and gas mass flux as shown in Fig. 2.25.

In order to determine the maximum mass flux $G_3$ where $x_3$ is still zero, the following relationship was proposed:

$$G_{3\,max,x=0} = 0.52\rho_L^{0.5}(\sigma g(\rho_L-\rho_G))^{0.25}. \tag{2.24}$$

This is similar to the relationship for the rise velocity of bubbles given by Wallis /44/. The final correlation for the phase distribution for the downward branch is then given by

$$x_3/x_1 = 5\eta - 6\eta^2 + 2\eta^3 + a\eta(1-\eta)^b, \tag{2.25}$$

where

$$\eta = (G_3/G_1 - G_{3max,x=0}/G_1)/(1-G_{3max,x=0}/G_1). \tag{2.26}$$

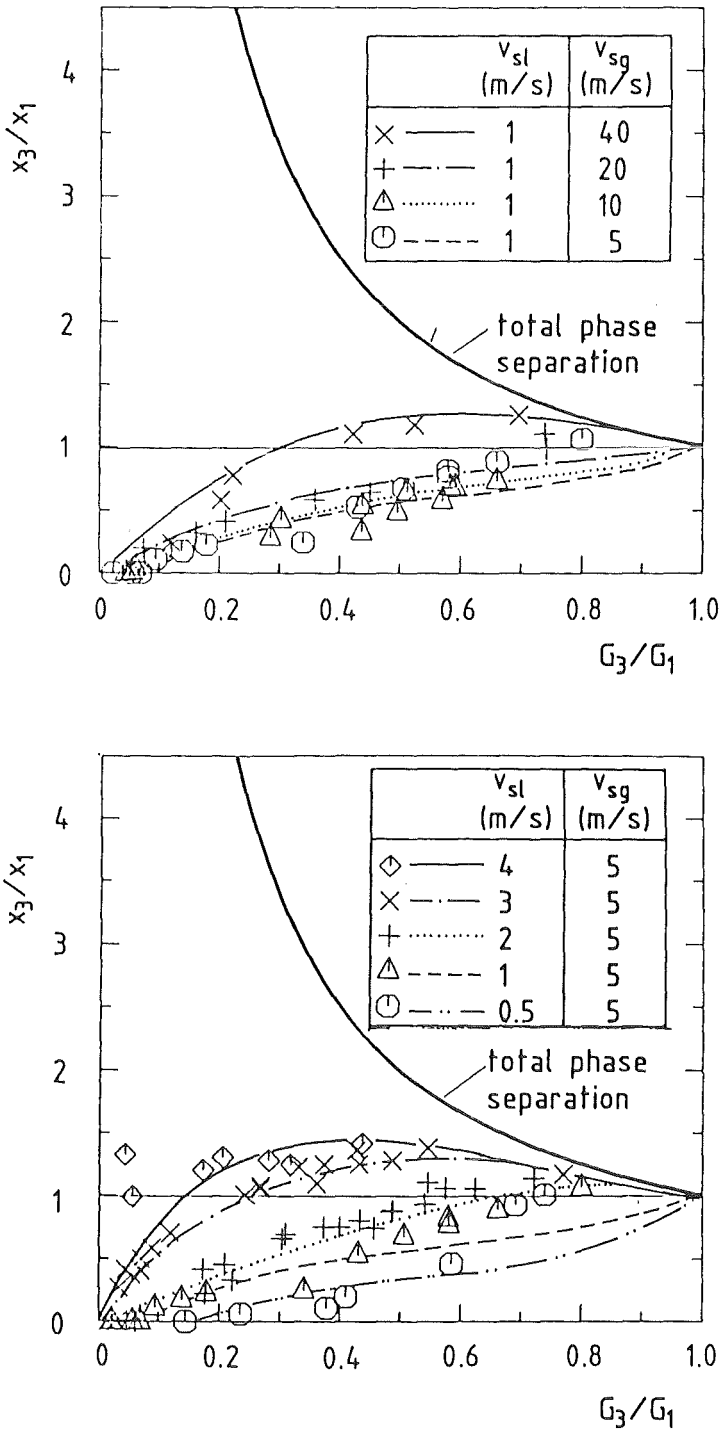


Fig. 2.24 Phase Redistribution for Downward Flow ($\phi = 180^{o}$), $D_3/D_1 = 1$; from /26/.

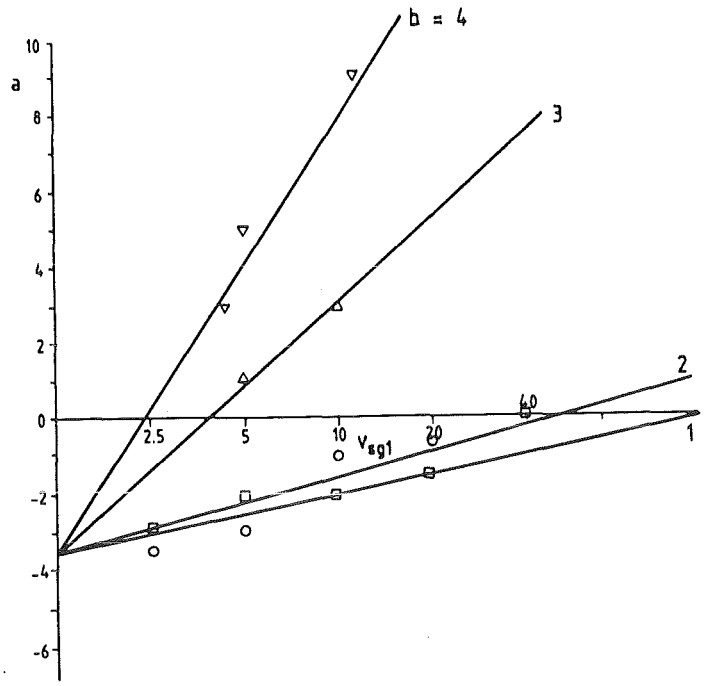


Fig. 2.25 Dependence of Factor a on Liquid and Gas Mass Flux, from /26/.

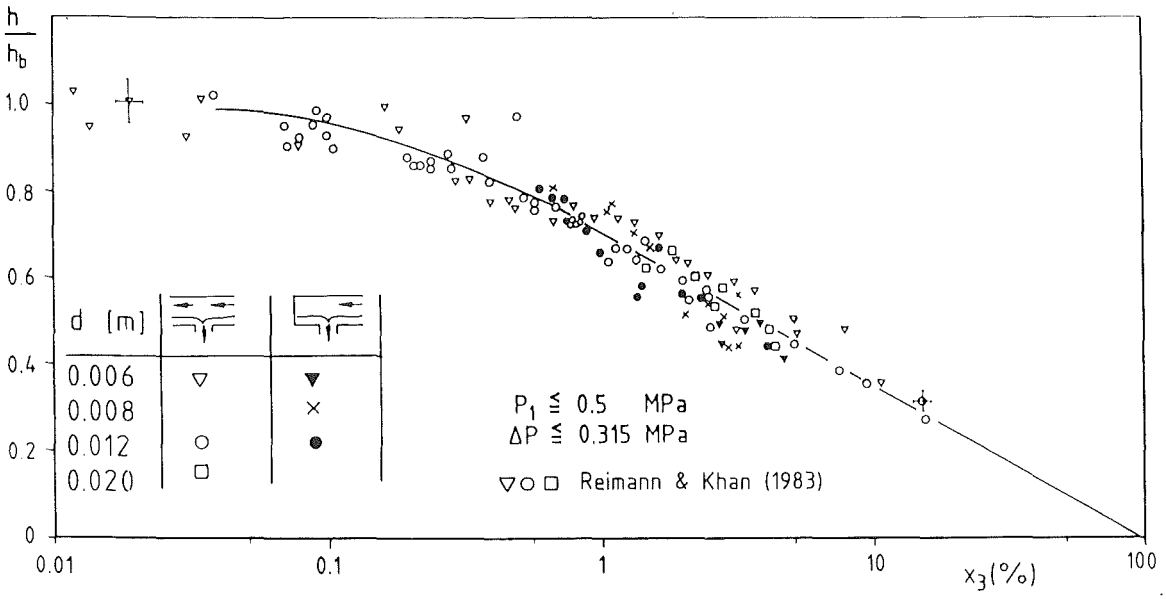


Fig. 2.26 Stratified Flow Data: Branch Quality $x_3$, $\phi = 180°$, $D_3/D_1$; from /20/.

Again Eq.(2.25) is not valid at high pressures ($p \approx p_{crit}$). The exponent b is given by Eq. (2.23) and a is taken from Fig. 2.25. The curves plotted in Fig. 2.24 were calculated in this way.

Experiments with $D_3/D_1 << 1$ in the smooth stratified flow regime are described in Refs. /14/ to /20/. The flow entering the branch had a high vorticity if the branch liquid mass flow rate $\dot{m}_{3L}$ was about the inlet liquid mass flow rate $\dot{m}_{1L}$ (stagnant liquid in the run, $\dot{m}_{2L} \approx 0$). The flow close to the branch was vortex free for $\dot{m}_{2L} > 0$, for details see e.g. /20/.

The beginning of gas entrainment is described by Eq. (2.5) with K = 2 for vortex flow and K = 1.17 for vortex-free flow.

The branch quality is calculated according to:

$$x_3 = = \left(\frac{1.15}{1 + (\rho_L/\rho_G)^{0.5}}\right)^{\left(2.5\frac{h}{h_b}\right)} \left[ 1 - \frac{1}{2}\frac{h}{h_b}\left(1 + \frac{h}{h_b}\right)\left(\frac{1.15}{1 + (\rho_L/\rho_G)^{0.5}}\right)^{\left(1-\frac{h}{h_b}\right)}\right]^{0.5} \qquad (2.27)$$

Figure 2.26 shows the branch quality. Different symbols are used to distinguish between experiments with superimposed velocities ($\dot{m}_{2L} > 0$) and those without.

# 3. SUMMARY OF PREVIOUS WORK ON PRESSURE DROP IN TEE-JUNCTIONS

## 3.1 General Remarks

When a flow is divided in a Tee-junction, the deceleration of the fluid causes a reversible pressure rise in the run and in the branch due to the Bernoulli effect. However, mostly the reversible pressure rise in the branch is smaller than the irreversible pressure drop; therefore, the resultant pressure difference $\Delta p_{1-3}$ between inlet and branch is equivalent to a pressure drop and has a positive sign, whereas in the run the irreversible pressure drop is considerably smaller and therefore $\Delta p_{1-2}$ typically has a negative sign, characterizing a pressure rise (the subscripts 1, 2, or 3 refer to the inlet, run, or branch conditions).

Only a few two-phase experiments were performed previously with elaborate differential pressure measurements along the axis of the inlet, branch, and run of the pipe which properly separate the Tee-junction pressure differences from the frictional and gravitational pressure differences.

Figure 3.1 (from Reimann and Seeger /27/) gives an example for measured pressure gradients and the extrapolated pressure differences.

Up to now no pressure drop model for two-phase flow in Tee-junctions has proved to give satisfactory results for arbitrary flow parameters. This might not be surprising if one considers that i) the interest in this subject is relatively new and ii) the flow mechanisms involved are very complex and, at present, poorly understood. Even for the much simpler case of frictional pressure drop in straight pipes, no unique correlation had been developed after more than four decades of extensive work which gives satisfactory results for the total parameter range of flow conditions.

The different methods suggested in literature for two-phase Tee-junctions pressure drop are, in general, direct extensions of the methods used in single-phase flow. These are based on a simple momentum or energy balance on the junctions as a control volume, compare e.g. Collier /45/. The generally accepted procedure is to use the loss coefficients, determined in single-phase flow, in two-phase flow. In single phase flow, there is a separation stream-line which separates that part of the inlet flow which enters the branch from that one which flows into the run. In two-phase flow the separation stream lines are different for

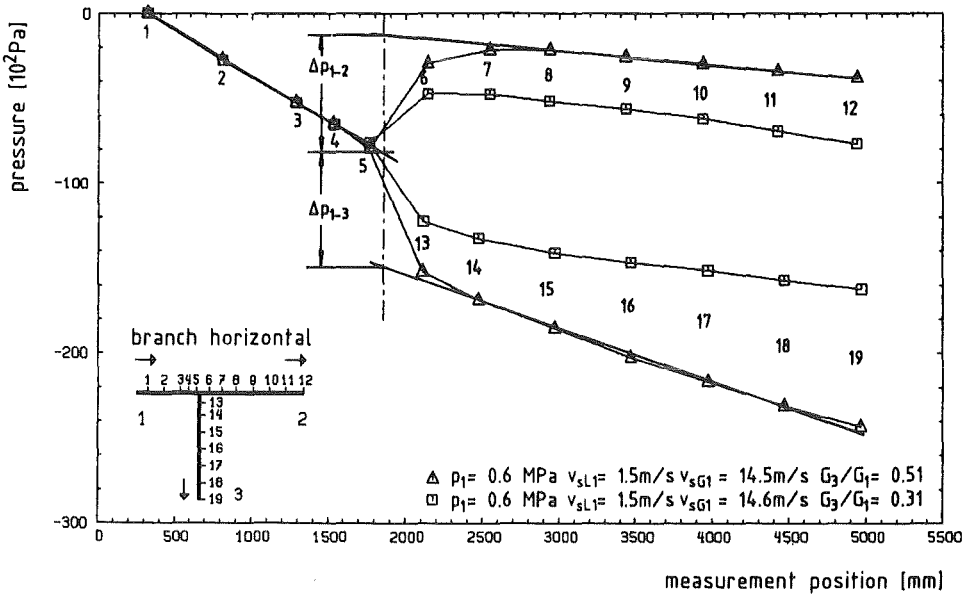


Fig. 3.1 Measured Axial Pressure in a Piping System with a Horizontal Tee-Junction; from /27/.

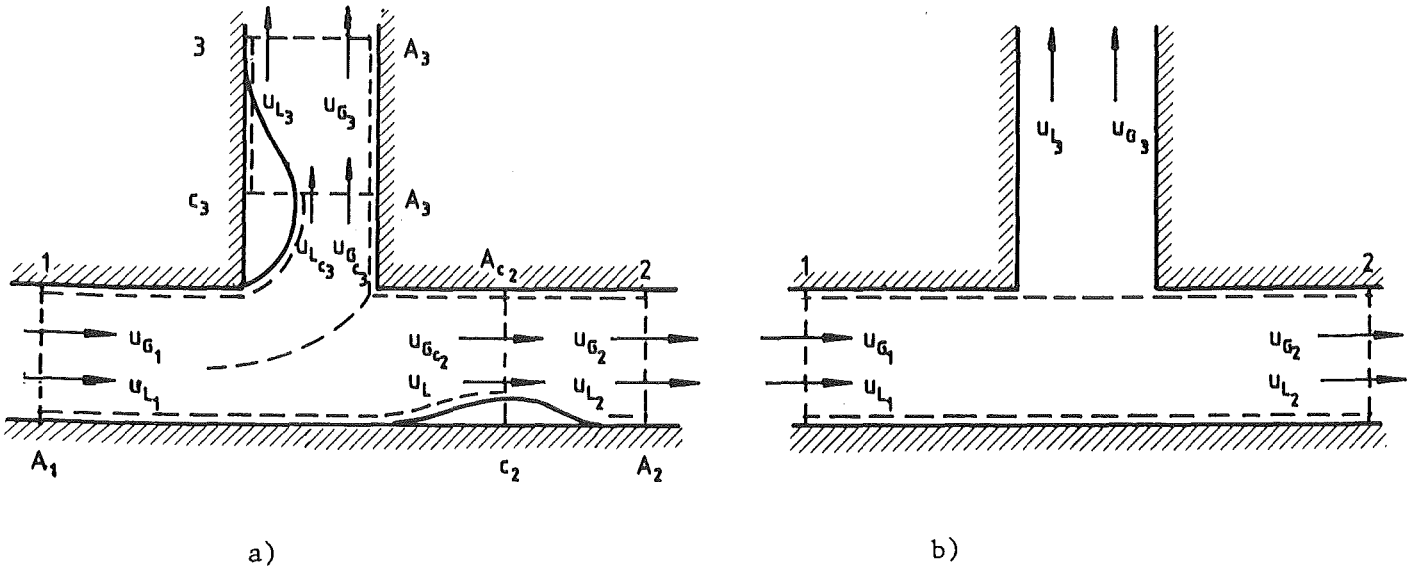


Fig. 3.2 Control Volumes for Tee-junction Flow.

the two phases which means that there is a strong interaction of the phases near the branch entrance. This phase interaction is not only limited to the region upstream of the branch entrance but also occurs immediately downstream both in the branch and the run. Here, recirculation zones exist and the local flow mechanisms are far from being understood. If the branch direction deviates from the horizontal, flow reversal effects in the branch complicate this situation even more. The influence of these phase interactions on Tee-junction pressure drop can be very different for different inlet flow patterns and all models developed up to now are fitted somehow to a limited range of flow parameters and care should be taken to use these models in a different parameter range.

If the momentum or energy balances for each phase are formulated for the Tee-junction as a control volume, expressions are derived which contain the quality x and cross section averaged void fraction $\alpha$, respectively, slip S in all three cross sections (see Section 3.2). The void fraction and slip, respectively, is dependent on the phase interactions discussed above and is not known a priori in the vicinity of the branch entrance.

To develop a mechanistic model the local phase interaction has to be modeled. A first attempt in this direction was presented by Saba and Lahey /12/.

An improvement of current understanding would be achieved by detailed measurements of the local void and phase velocity distributions. This cannot be achieved presently due to the lack of appropriate measurement techniques. A first step in this direction was made by Ballyk and Shoukri /34/ who measured the cross section averaged void fraction in several cross sections close to the branch entrance. Much more measurements are needed to develop void fraction and slip correlations, respectively. Similar measurements were performed by Honan and Lahey /39/ for a vertical inlet pipe.

Up to now, the unknown void fraction or slip is calculated by using correlations for well developed two-phase flow taken from literature or by the assumptions of homogeneity ($S \equiv 1$). Some models use both homogeneous and non-homogeneous assumptions and the choice has been influenced probably by sensitivity calculations to fit a given data set.

## 3.2 Single-Phase Flow

Using an energy balance, the pressure differences $\Delta p_{1\text{-}2}$ and $\Delta p_{1\text{-}3}$ are written as a sum consisting of the reversible pressure increase and the irreversible pressure drop (see e.g. Miller /46/):

$$\Delta p_{1-i} = (\Delta p_{1-i})_{rev} + (\Delta p_{1-i})_{irr}, \tag{3.1}$$

with i = 2 for the run and i = 3 for the branch, where

$$(\Delta p_{1-i})_{rev} = \frac{1}{2}\left(\frac{G_i^2}{\rho_i} - \frac{G_i^2}{\rho_1}\right), \tag{3.2}$$

and

$$(\Delta p_{1-i})_{irr} = K_{1i}\left(\frac{G_i^2}{2\rho_{1_i}}\right), \tag{3.3}$$

where $\rho$ is the fluid density, $K_{12}$ and $K_{13}$ are loss coefficients from single phase flow depending on the mass flux ratio $G_3/G_1$ which corresponds to the volume flow rate ratio $\dot{V}_3/\dot{V}_1$.

Another method to model the pressure difference $\Delta p_{1\text{-}3}$ is to split it into a reversible pressure difference $\Delta p_{1\text{-}c3}$ between inlet 1 and the throat of the vena contracta $C_3$ and a pressure difference $\Delta p_{c3\text{-}3}$ between $C_3$ and a position 3 downstream in the branch, modeled according to a sudden expansion (compare Fig. 3.2a). Therefore we get

$$\Delta p_{1-C3} = \frac{1}{2}\left(\frac{G_{C3}^2}{\rho_{C3}} - \frac{G_1^2}{\rho_1}\right) \tag{3.4}$$

and

$$\Delta p_{C3-3} = \frac{G_3^2}{\rho_3} - \frac{G_3 G_{C3}}{\rho_3}. \tag{3.5}$$

By eliminating $G_{c3}$ using the relationship for the conservation of mass and by introducing a contraction coefficient $C_3 = A_c/A$, where A is the total cross section, we obtain for $\rho_{c3} = \rho_3$,

$$\Delta p_{1-3} = \frac{1}{2}\left(\frac{G_3^2}{\rho_3} - \frac{G_1^2}{\rho_1}\right) + \left(\frac{1}{C_3} - 1\right)^2 \frac{G_3^2}{2\rho_3}. \tag{3.6}$$

Comparing (3.1) - (3.3) with (3.6) the results in the following relationship between $C_3$ and $K_{13}$:

$$C_3 = \left(1 + \left(\frac{\rho_3}{\rho_1}\right)^{0.5} \frac{G_1}{G_3} K_{13}^{0.5}\right)^{-1}. \tag{3.7a}$$

Eliminating the mass flux by the volume flow rate $\dot{V}$, $C_3$ becomes

$$C_3 = \left(1 + \left(\frac{\rho_1}{\rho_3}\right)^{0.5} \cdot \frac{A_3 \dot{V}_1}{A_1 \dot{V}_3} K_{13}^{0.5}\right)^{-1}, \tag{3.7b}$$

where A is the cross sectional area.

For incompressible flow $\rho_1$ is equal to $\rho_3$. A comparison of $C_3$, determined from two-dimensional potential theory (compare, e.g. Sallet and Popp /47/)) and the right side of (3.7), using experimental results for $K_{13}$ shows good agreement. Therefore, this procedure for modeling the pressure drop seems to be physically reasonable and will be applied later.

If in an analogous way the pressure difference $\Delta p_{1\text{-}2}$ is modeled, relationships identical to (3.6) and (3.7) are obtained except that the index 3 is replaced by the index 2. The existence of a vena contracta in the run (compare Fig. 3.2a) is impressively shown in the textbook of Hackeschmidt /48/.

The modeling $\Delta p_{1\text{-}3}$ with an energy balance, as shown above, is generally accepted too for two-phase flow (see Section 3.3.1). To describe $\Delta p_{1\text{-}2}$, however, often an axial momentum balance (compare e.g. Collier /45/) is preferred which results in the following expression for the control volume shown in Fig. 3.2b:

$$\Delta p_{1-2} = (G_2^2/\rho_2 - G_1^2/\rho_1) \tag{3.8}$$

Experimental observations show that the pressure rise usually differs from the value calculated from Eq. (3.8) because the direction of the leaving stream is not exactly at right angle to the main stream. Equation (3.8) is then modified to

$$\Delta p_{1-2} = K^*_{12}(G_2^2/\rho_2 - G_1^2/\rho_1), \tag{3.9}$$

where $K_{12}^*$ is a momentum correction factor usually less than unity.

The factor $K_{12}^*$ can be determined for a given $K_{12}$ or vice versa, using Eqs. (3.1) - (3.3) and Eq. (3.9).

Figure 3.3 shows values for $K_{13}$ from Miller /46/ for Tee-junctions with different diameter ratios. Figure 3.4a shows results for $D_3/D_1 = 1$ from Miller /46/, Saba and Lahey /13/, Ballyk and Shoukri /34/, Hwang and Lahey /35/ and Seeger et al. /26/. The KfK-data agree well with the results from Ballyk and Shoukri and Miller. The relationships for the KfK results are given in Section 6.1.

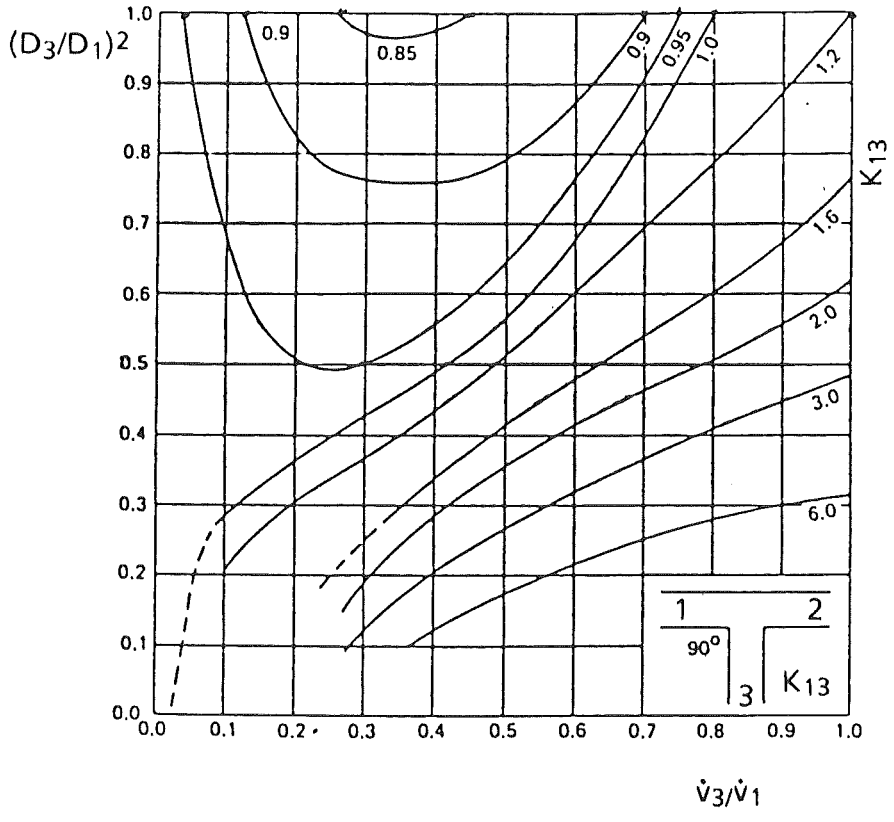


Fig. 3.3 Loss Coefficient $K_{13}$ for Tee-junctions with Different Diameter Ratios; from Miller /46/.

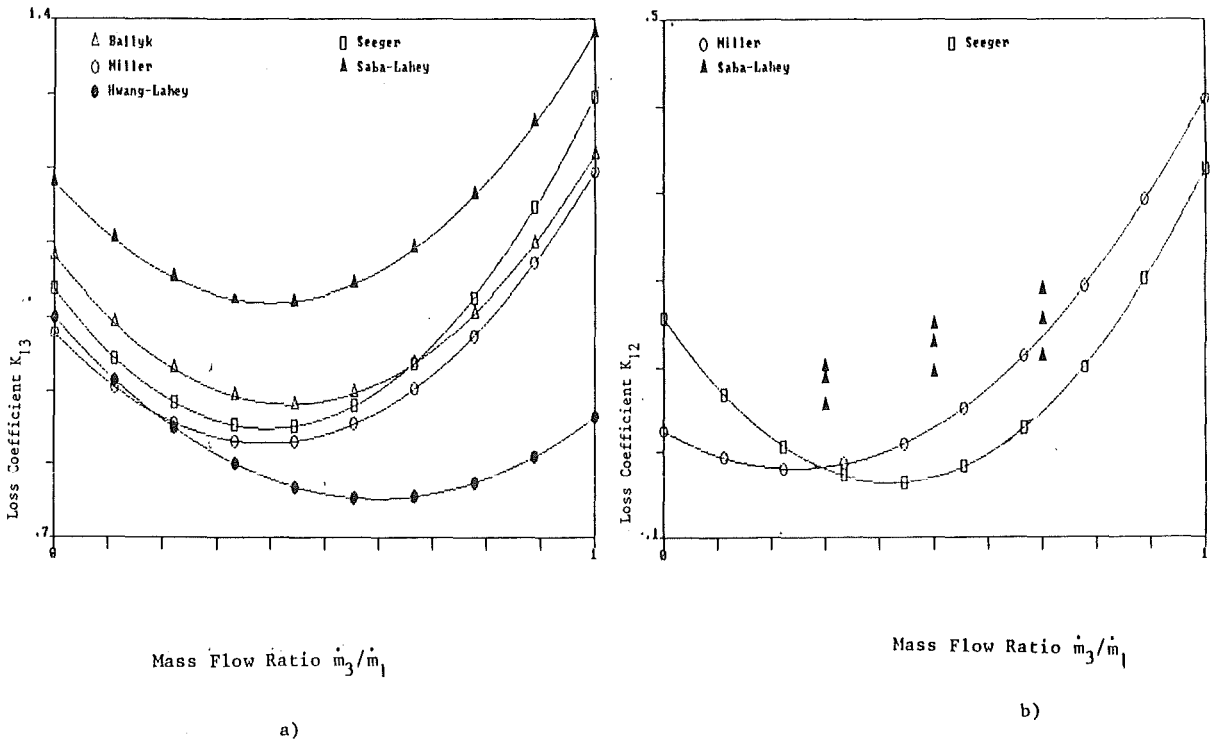


Fig. 3.4 Comparison of Pressure Loss Coefficients $K_{13}$ and $K_{12}$ for $D_3/D_1 = 1$ Measured in Single-phase Flow

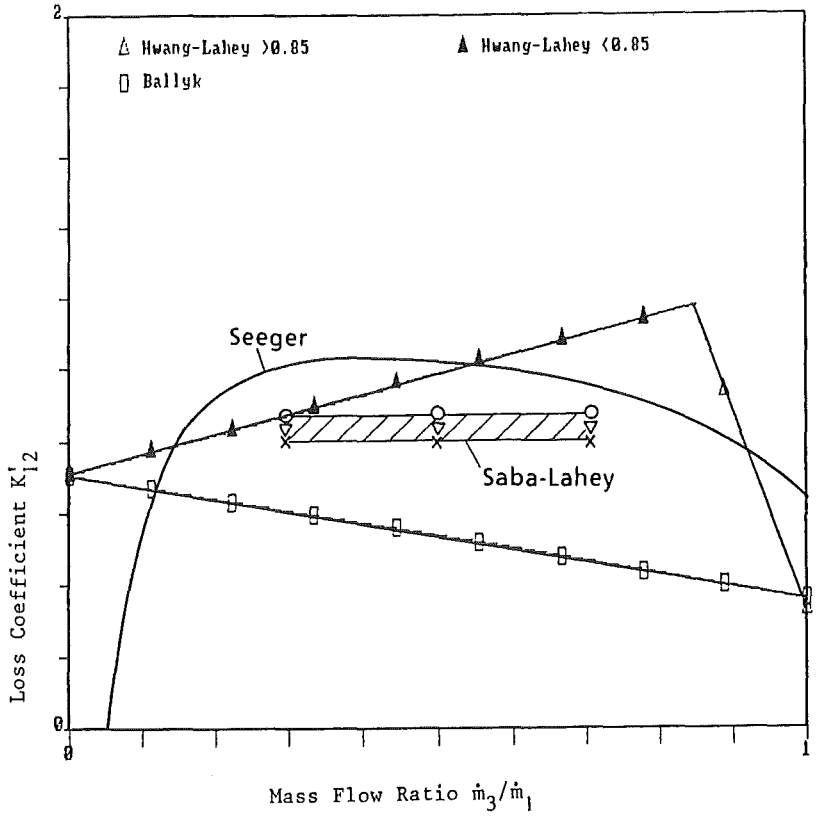


Fig. 3.5 Comparison of Pressure Loss Coefficients $K_{12}'$ for $D_3/D_1 = 1$ Measured in Single-phase Flow

Figure 3.4b shows the results for $K_{12}$ from different authors /12, 35, 46/. Again the KfK-data agree quite well with other work. In Fig. 3.5 the results for $K_{12}$* are shown.The $K_{12}$* relationships from Lahey et al. /12, 35/ have been divided by 2 because a different definition of Eq. (3.9) was used (factor 0.5 on right hand side). If $K_{12}$ goes to a value above zero for small values of $\dot{m}_3/\dot{m}_1$, then $K_{12}$* goes to negative values which is not physically meaningful. The differences in the curves for $K_{12}$ or $K_{12}$* are much more pronounced than for $K_{13}$ due to the much smaller irreversible pressure losses which have to be measured. The difficulty to model the two-phase pressure difference $\Delta p_{1\text{-}2}$ will be even more pronounced.

## 3.3 Two-Phase Flow

### 3.3.1 Relationships for $\Delta p_{1\text{-}3}$

#### 3.3.1.1 Homogeneous Model (HM)

For two-phase flow, Eq. (3.1) can be written as

$$\Delta p_{1-3} = (\Delta p_{1-3})_{rev} + K_{13} \frac{G_1^2}{2\rho_{L1}} \varphi \,, \tag{3.10}$$

where $\varphi$ is the branch two-phase loss multiplier. The assumption of homogeneous flow in the cross sections 1,2,3 gives the following expression for the reversible pressure difference $(\Delta p_{1\text{-}3})_{rev}$:

$$(\Delta p_{1-3})_{rev} = \frac{\rho_{h3}}{2}\left( (\frac{G_3}{\rho_{h3}})^2 - (\frac{G_1}{\rho_{h1}})^2 \right), \tag{3.11}$$

with the homogeneous density $\rho_{hi}$ given by

$$\rho_{hi} = (x_i/\rho_G + (1\text{-}x_i)/\rho_L)^{-1}. \tag{3.12}$$

and the two-phase loss multiplier becomes

$$\varphi_{1IM} = \rho_{L1}/\rho_{h1}. \tag{3.13}$$

$K_{13}$ is taken from single-phase flow measurements as a function of the mass flow rate ratio $\dot{m}_3/\dot{m}_1$.

### 3.3.1.2 Chisholm Model (CM)

Fitzsimmons /51/ performed steam-water experiments with a horizontal Tee-junction with inlet mass fluxes $1000 < G_1 < 5000$ kg/m$^2$s. However, only the mass flux ratio $G_3/G_1$ equal to unity was investigated.

Chisholm /52/ analyzed these data and proposed the use of Eq. (3.11) and the following two-phase loss multiplier

$$\varphi_{CM} = (1-x_1)^2 \left(1 + \frac{C^*_{1-3}}{X_{tt}} + \frac{1}{X^2_{tt}}\right), \tag{3.14}$$

with

$$\frac{1}{X_{tt}} = \left(\frac{x_1}{1-x_1}\right)\left(\frac{\rho_L}{\rho_G}\right)^{0.5} \tag{3.15}$$

and

$$C^*_{1-3} = \left(1 + 0.75\left(\frac{\rho_L - \rho_G}{\rho_L}\right)^{0.5}\right)\left(\left(\frac{\rho_L}{\rho_G}\right)^{0.5} + \left(\frac{\rho_G}{\rho_L}\right)^{0.5}\right) \tag{3.16}$$

### 3.3.1.3 Reimann Seeger Model (RSM)

Reimann and Seeger /22,26/ started with equations corresponding to Eqs. (3.4) to (3.7), written for the single phases. After expressing the void fraction $\alpha$ by

$$\alpha = \left(1 + (S/R)(1-x)/x\right)^{-1} \tag{3.17}$$

where R is the density ratio $\rho_L/\rho_G$ and S is the slip, the following expression for the reversible pressure difference $(\Delta p_{1\text{-}3})_{rev}$ was obtained:

$$(\Delta p_{1-3})_{rev} = \frac{\rho_{h3}}{2\rho_1^2}\left\{G_3^2\left(x_3 R + S_3(1-x_3)\right)^2\left(x_3 + \frac{1-x_3}{S_3^2}\right) - G_1^2\left(x_1 R + S_1(1-x_1)\right)^2\left(x_3 + \frac{1-x_3}{S_1^2}\right)\right\}, \tag{3.18}$$

which can be rewritten as:

$$(\Delta p_{1-3})_{rev} = \frac{\rho_{h3}}{2}\left[\left(\frac{G_3}{\rho_{e3}}\right)^2 - \left(\frac{G_1}{\rho_{*1}}\right)^2\right], \tag{3.19}$$

where $\rho_{ei}$, the so called energy density at station i, is given by

$$\rho_{ei} = \left[\frac{x_i^3}{\alpha_i^2 \rho_G^2} + \frac{(1-x_i)^3}{(1-\alpha_i)^2 \rho_L^2}\right]^{-0.5}, \tag{3.20}$$

and the density $\rho_{*1}$ is given from

$$\rho_{*1} = \left[\frac{(1-x_1)^2(1-x_3)}{(1-x_1)^2 \rho_L^2} + \frac{x_1^2 x_3}{x_1^2 \rho_G^2}\right]^{-0.5}. \tag{3.21}$$

It is worth to note that the expression for $(\Delta p_{1\text{-}3})_{rev}$ according to Eq. (3.18) differs from the expression given by Saba and Lahey /12/ (compare Section 3.3.1.4). Equations (3.18) - (3.21) were also used in the work published recently by Ballyk and Shoukri /34/.

The total pressure drop $\Delta p_{1\text{-}3}$ was given by

$$\Delta p_{1-3} = \frac{\rho_{h3}}{2\rho_L}\left\{\frac{G_3^2}{C_3^2}\left(x_3 R + S_{C3}(1-x_3)\right)^2\left(x_3 + \frac{1-x_3}{S_{C3}^2}\right) - G_1^2\left(x_1 R + S_1(1-x_1)\right)^2\left(x_3 + \frac{1-x_3}{S_1^2}\right)\right\}$$

$$+ \frac{G_3^2}{\rho_L}\left\{\left(x_3 R + S_3(1-x_3)\right) - \frac{1}{C_3}\left(x_3 R + S_{C3}(1-x_3)\right)\left(x_3 + \frac{1-x_3}{S_{C3}}\right)\right\}, \tag{3.22}$$

where corresponding to Eq. (3.7) the contraction coefficient $C_3$ is defined as

$$C_3 = \left(1 + \left(\frac{\rho_{h3}}{\rho_{h1}}\right)^{0.5}\frac{G_1}{G_3}K_{13}^{0.5}\right)^{-1}. \tag{3.23}$$

It is noteworthy that Eq. (3.22) reduces to the homogeneous model HM (Eqs. (3.10)-(3.13)) for $S_1 = S_{C3} = S_3 = 1$.

The corresponding expressions for the pressure difference $\Delta p_{1-2}$ are obtained by replacing the index 3 by index 2, see Section 3.2.3.

The Eqs. (3.18) and (3.19) contain the slip $S_1$, $S_{C3}$ and $S_3$ as parameters. Due to the lack of knowledge, several assuptions were varied for the slip at the different positions. Finally, very rigid assumptions were made including homogeneity in all cross sections. For this homogeneous model again Eq. (3.11) is used for $(\Delta p_{1-3})_{rev}$ but the following two-phase multiplier was obtained:

$$\varphi_{RMS} = \rho_{L1}\rho_{h3}/\rho_{h1}^2 \tag{3.24}$$

It should be mentioned that this homogeneous model, termed RSM, is different from the expressions obtained from the "full" RMS (Eq. 3.22)) using $S_i = 1$.

The loss coefficient $K_{13}$ is again taken from single phase flow measurements. It was recommended to evaluate $K_{13}$ as a function of the volume flow rate ratio $\dot{V}_3/\dot{V}_1$ instead of $K_{13} = f(G_3/G_1)$. This difference is in general not very significant as will be demonstrated in Section 6.

The main difference between the HM and the RSM is the factor $\rho_{h3}/\rho_{h1}$. The two models become equal for $G_3/G_1 = 1$.

Another correction factor K was suggested for the use of the previously presented homogeneous models (HM, CM, RSM). This factor K was determined from the KfK measurements with $D_3/D_1 = 1$ and $G_3/G_1 = 1$ (full flow branch points). For these test points, $(\Delta p_{1-3})_{rev}$ according to Eq. (3.11) is zero and $(\Delta p_{1-3})_{irr}$ has a maximum. Figure 3.6 (from /27/) shows that the model predictions deviate from the measurements, however, the deviations are fairly independent on inlet mass flux $G_1$ and quality $x_1$. To compensate these deviations, the following relationship is proposed:

$$\Delta p_{1-3} = (\Delta p_{1-3})_{rev} + K(\Delta p_{1-3})_{irr}, \tag{3.25}$$

with K = 1.34 for the HM and RSM and K = 0.85 for the CM.

Much more experiments with $G_3/G_1 = 1$ are required to determine the parameter range where Eq. (3.18) can be used. The KfK-experiments (Refs. /21-27/) and the experiments performed by Lahey et al. /12,24/ are characterized by relatively

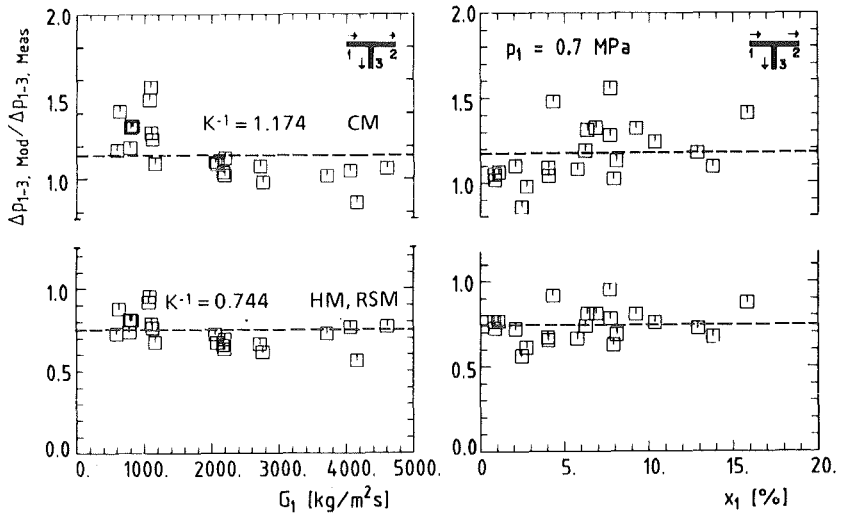


Fig. 3.6 Ratio of Predicted to Measured Branch Pressure Drop for $G_3/G_1 = 1$, Horizontal Branch and Air-water Flow; from /27/.

high mass fluxes. No measurements with $G_3/G_1 = 1$ were performed in the latter experiments. Analyzing the early data from Fitzsimmons /51/, performed at high mass fluxes, showed that the HM also predicted values about 30 % too low. The new data from Ballyk and Shoukri /34/ for lower mass fluxes and annular flow indicate that all homogeneous models fail, as shown in Section 3.3.1.7.

### 3.3.1.4 Hwang Lahey Model (HLM)

The pressure drop $\Delta p_{1-3}$ for separated flow was given by Saba and Lahey /12/ to

$$\Delta p_{1-3} = \frac{\rho_{h3}}{2}\left(\frac{G_3^2}{\rho_{e3}^2} - \frac{G_1^2}{\rho_{e1}^2}\right) + K_{13}\frac{G_1^2}{2\rho_L}\varphi, \tag{3.26}$$

where the energy density is used at the cross sections 1 and 3.

Hwang and Lahey /35/ found in their study that homogeneous flow could be assumed downstream of the junction, that is $\rho_{e3} = \rho_{h3}$. Among the models for $\varphi$, the

authors stated that the RSM did the best job of correlating their data. Therefore, Eq. (3.24) is recommended.

The void fracton $\alpha_1$ in the equation of the energy density $\rho_{e1}$ was eliminated using Eq. (3.17). An empirical correlation was used for the slip $S_1$, based on their results and KfK-data /26/, given by

$$S_1 = C_o + (C_o - 1)\frac{\rho_L}{\rho_G}\frac{x_1}{1-x_1}, \tag{3.27}$$

with

$$C_o = 1.1 - 0.1(\rho_L/\rho_G)^{-0.0001(\rho_L/\rho_G)}. \tag{3.28}$$

3.3.1.5 Ballyk Shoukri Model (BSM)

As mentioned, Ballyk and Shoukri /34/ use the relationship as given in Eq. (3.19) for $(\Delta p_{1\text{-}3})_{rev}$. The following relationship is proposed for the total pressure drop:

$$\Delta p_{1-3} = \frac{\rho_{h3}}{2}\left|\frac{G_3^2}{(\rho_{e3})^2} - \frac{G_1^2}{(\rho_{*1})^2}\right| + K_{1-3}\frac{\rho_{h3}}{2}\frac{G_1^2}{(\rho_{*1})^2}\varphi^*, \tag{3.29}$$

where $\rho_{*1}$ is given by Eq. (3.21).

Comparing Eq. (3.10) with Eq. (3.29) the two-phase loss multiplier is then given by

$$\varphi_{BSM} = \varphi^* \rho_{L1}\rho_{h3}/\rho_{*1}^2, \tag{3.30}$$

where the following empirical correlation was recommended for $\varphi^*$ to fit their low-pressure steam-water annular flow data:

$$\varphi^* = -1.47 + 24.61\frac{\dot{m}_3}{\dot{m}_1} - 20.33\left(\frac{\dot{m}_3}{\dot{m}_1}\right)^2 + 3.24\left(\frac{\dot{m}_3}{\dot{m}_1}\right)^3 \quad (D_3/D_1 = 1.0, \dot{m}_3/\dot{m} > 0.1),$$

$$\varphi^* = -18.06 + 328.88\left(\frac{\dot{m}_3}{\dot{m}_1}\right) - 300.8\left(\frac{\dot{m}_3}{\dot{m}_1}\right)^2 \quad (D_3/D_1 = 0.5, \dot{m}_3/\dot{m}_1 < .2). \tag{3.31}$$

It has to be pointed out that this model is based on measured void fractions. Due to the fact that in no other Tee-junction experiments with a horizontal inlet pipe

void fractions were measured, it is not possible to compare directly this model with other data.

### 3.3.1.6 Other Models

The models discussed up to now are characteristical for large diameter ratios. For small diameter ratios $D_3/D_1$, the pressure drop can be modeled according to the flow through orifices or nozzles, compare e.g. Fouda and Rhodes /6/. Again these correlations should not be used outside the investigated parameter range. This is also true for Katsaounis ' /32/ model based on his experiments with very low inlet velocities and an upward branch. This model did not predict satisfactorily other data and, therefore, will not be discussed further.

### 3.3.1.7 Comparison of Predicted and Measured Values for $\Delta p_{1\text{-}3}$

The Figs. 3.7-3.11 show the ratio of predicted pressure drop $\Delta p_{1\text{-}3,mod}$ to measured pressure drop $\Delta p_{1\text{-}3,meas.}$ as a function of the split ratio $G_3/G_1$, using the KfK-data (Refs. /21-27/). For these data, Eq. 3.25 is used in combination with the corresponding two-phase loss multipliers. Parameters in the figures are the inlet superficial velocities $v_{sG}$ and $v_{sL}$. Figure 3.7 contains the results for air water flow and the horizontal branch.

The results of the HM and CM are very similar: the models predict well the experimental results in the range of $0.6 < G_3/G_1 < 1$, but overpredict the experiments at lower values of $G_3/G_1$. This tendency does not change significantly if the dependence $K_{13} = f(\dot{V}_3/\dot{V}_1)$ is used instead of $K_{13} = f(G_3/G_1)$. The RSM predicts the measurements much better in the lower range of the mass flux ratio.

Figure 3.8 shows the comparison with the steam-water experiments. Again the HM and CM models deviate strongly for $G_3/G_1 < 0.6$. The RSM starts to deviate at considerably lower mass flux ratios ($G_3/G_1 < 0.3$). A systematic dependence on system parameters can not be seen clearly.

Figure 3.9 contains air-water data for the downward branch. The RSM is superior in the total rang of $G_3/G_1$.

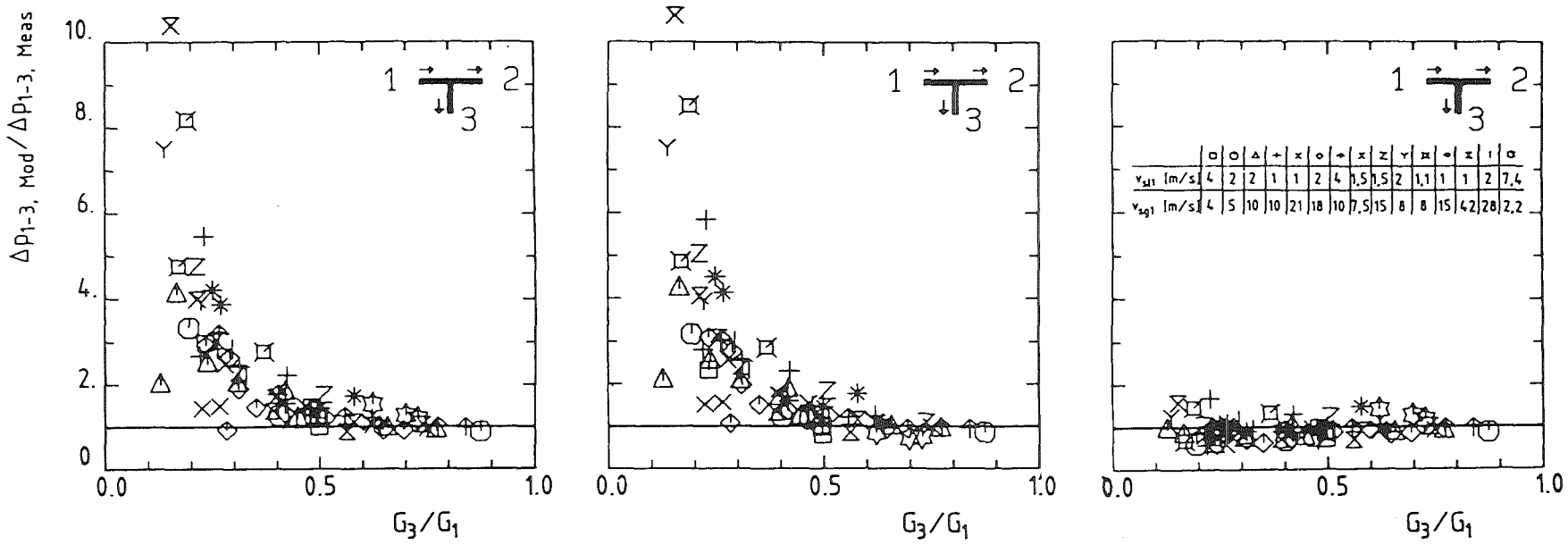


Fig. 3.7 Ratio of Predicted to Measured Branch Pressure Drop for Horizontal Branch and Air-water Flow; from /27/.

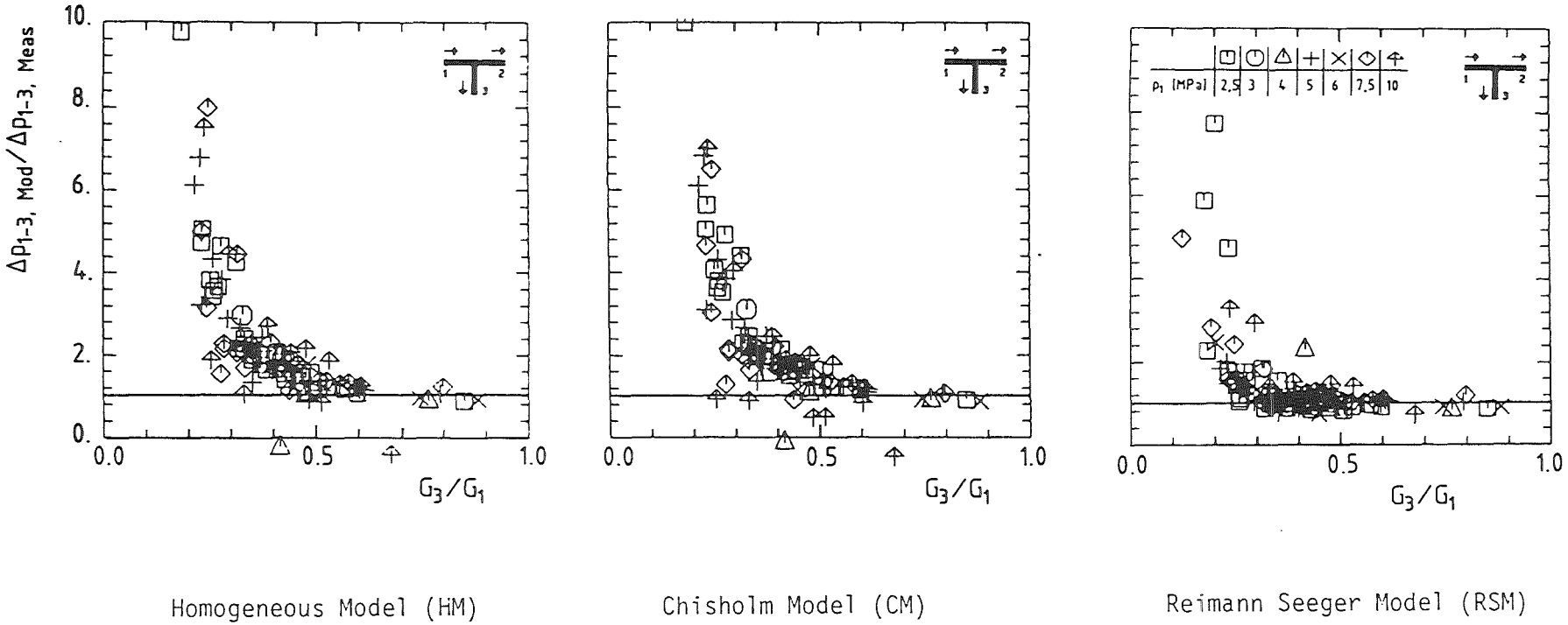


Fig. 3.8 Ratio of Predicted to Measured Branch Pressure Drop for Horizontal Branch and Air-water Flow, Steam-water Flow, from /27/.

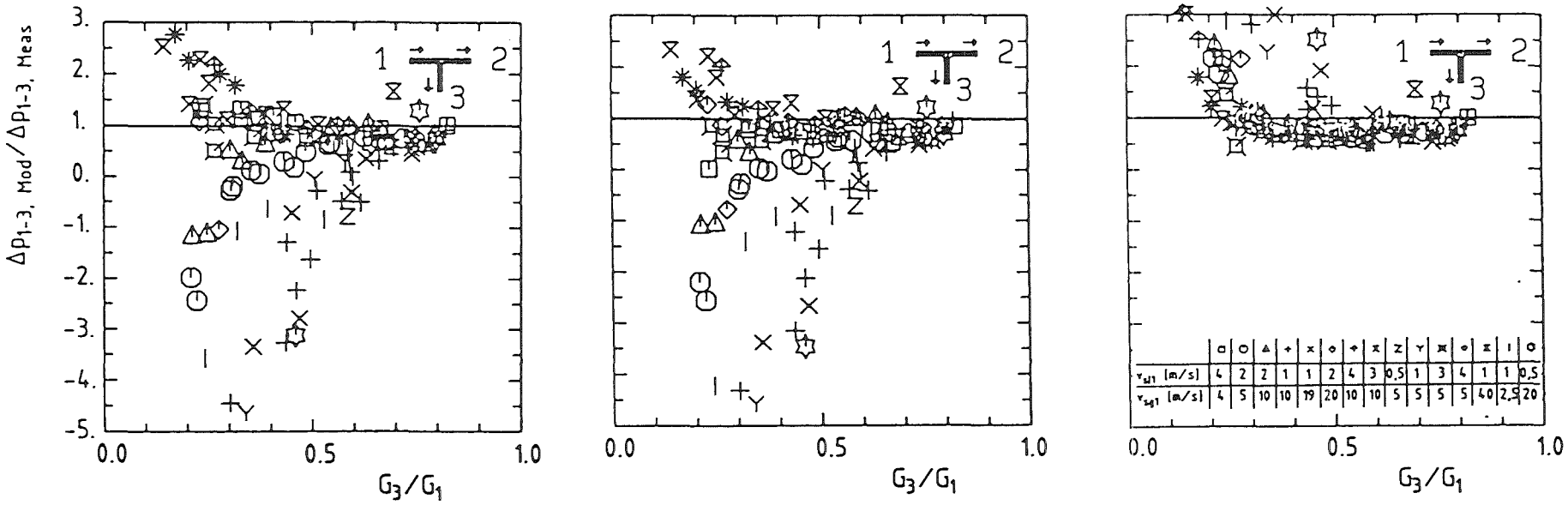


Fig. 3.9 Ratio of Predicted to Measured Branch Pressure Drop for Downward Branch and Air-water Flow; from /27/.

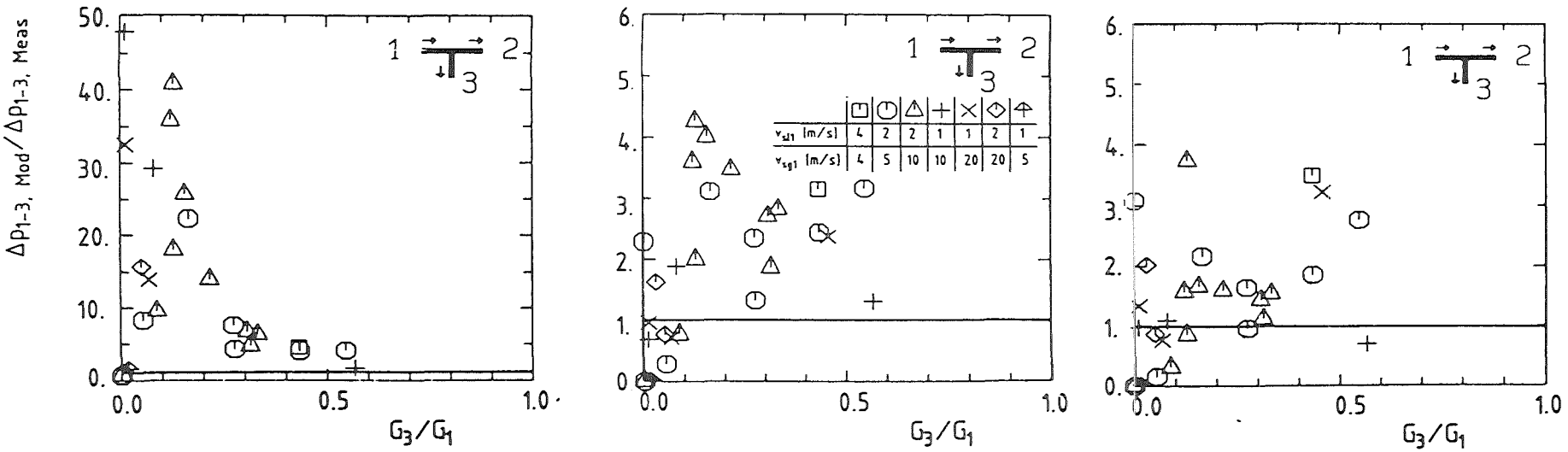


Homogeneous Model (HM)

Reimann Seeger Model (RSM):
$S_1 = S_3 = 1$

Reimann Seeger Model (RSM):
$S_1 = 1, S_3 > 1$

Fig. 3.10 Ratio of Predicted to Measured Branch Pressure Drop for Upward Branch and Air-water flow; from /27/.

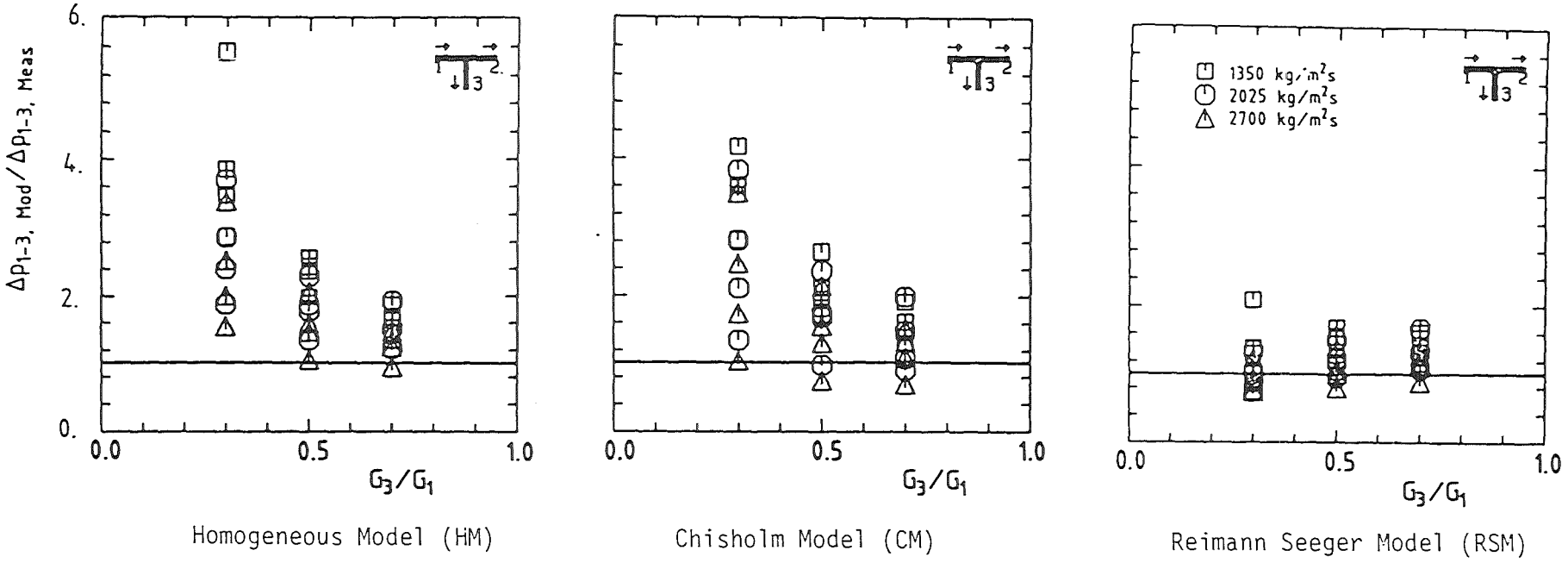


Fig. 3.11 Ratio of Predicted to Measured Branch Pressure Drop for Horizontal Branch and Air-water Flow for Experiments from Saba and Lahey /12/; from /27/.

For the upward branch (Fig. 3.10), all models fail; the CM (not shown) gives values similar to the HM. The deviations given by the RSM model are smallest (note the different scales of the ordinate). The failure of the models can be explained by the separation effects in the branch which increase with decreasing branch mass flux $G_3$. The length to diameter ratio $L/D_3$ of about 50 was probably not large enough to obtain a well-developed two-phase flow which is required to determine $\Delta p_{1\text{-}3}$.

Figure 3.11 compares the results of the models with the experimental data from Saba and Lahey /12/. Two-phase flow measurements at $G_3/G_1 = 1$ were not performed. Therefore, the correction factor K from the present experiments was used. The RSM model gives the best mean value and the lowest data scatter. If a correction factor $K = 1$ is taken, the agreement is not improved.

Figure 3.12 shows a comparison between the RSM and the HLM for the KfK air-water data with the horizontal branch. The HLM predicts values very close to the RSM (for the other experiments too). This is not surprising due to the fact that the HLM differs only by the energy density $\rho_{e3}$ and Eqs. (3.27) and (3.28) always give values for the slip $S_1$ very close to one for the investigated inlet conditions. Therefore, $\rho_{e3}$ becomes very close to $\rho_{h3}$. It should be mentioned that the correlation developed by Rouhani /54/ (Section 3.3.2) predicts much larger slip values for the same parameter range.

Figure 3.13 from Hwang and Lahey /35/ shows a comparison of the HLM with their data and the KfK-data for the horizontal branch. More than 95 % of the measured values were predicted within a band width of 30 %. From the considerations given above it is supposed that the RSM predicts the experimental data from /34/ with about the same accuracy.

Figures 3.14 and 3.15 (from Ballyk and Shoukri /34/) show a comparison of measured and calculated values of the two-phase flow multiplier $\varphi_{RSM}$ according to Eqs. (3.10) and (3.24). The RSM deviates significantly at high split ratios due to the fact that the assumption of homgeneity is not justified for the parameter range investigated. However, it is interesting to note that the differences decrease with increasing inlet quality $x_1$ and mass flux $G_1$ because the flow becomes more homogeneous. The values of the homogeneous two-phase flow multiplier $\varphi_{HM}$ are independent of $\dot{m}_3/\dot{m}_1 = 1$.

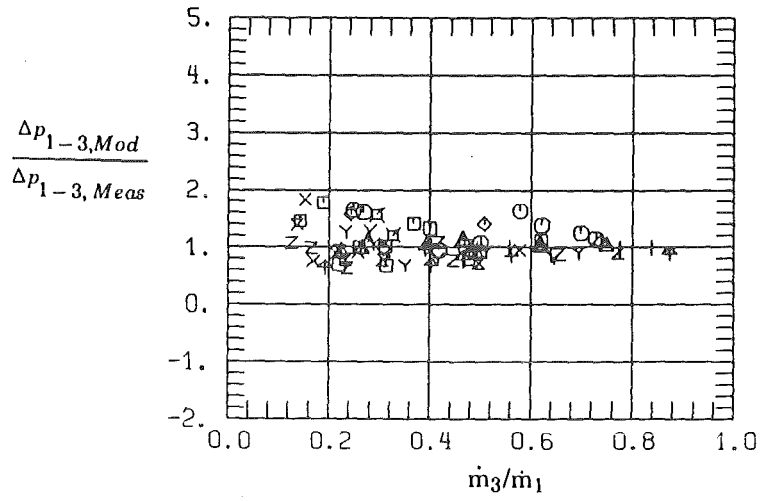


Hwang Lahey Model (HLM)

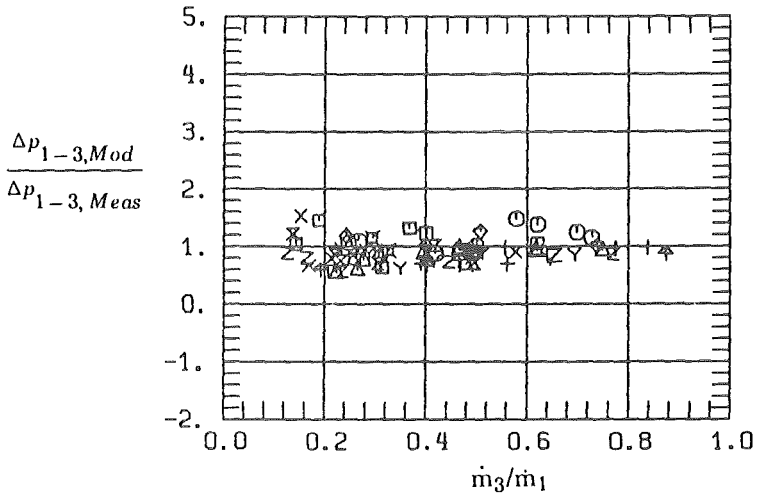


RSM

Fig. 3.12 Ratio of Predicted to Measured Branch Pressure Drop for Horizontal Branch and Air-water Flow.

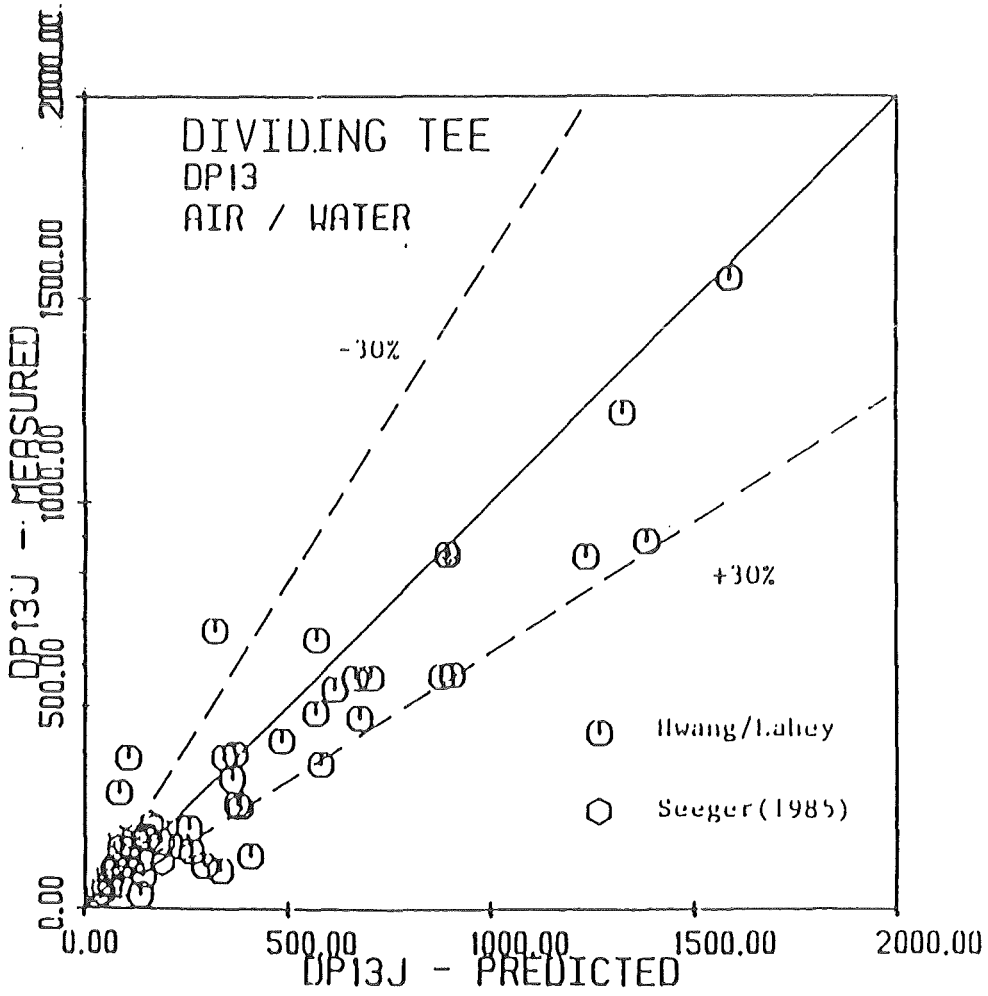


Fig. 3.13 Predicted vs. Measured Branch Pressure Drop According to Hwang and Lahey /35/; from /35/.

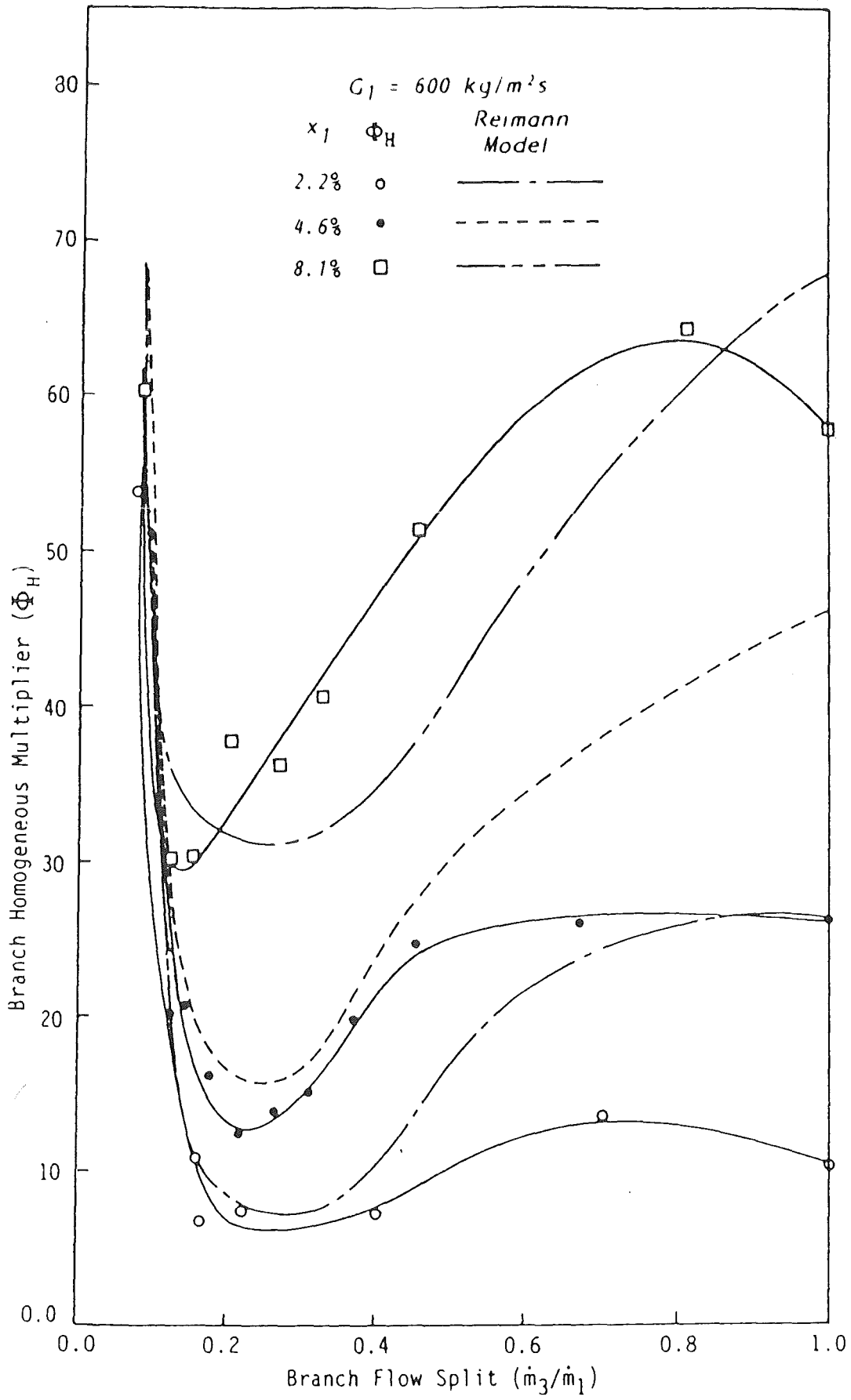


Fig. 3.14 Homogeneous Two-phase Multiplier vs. Flow Split for Experiments from Ballyk and Shoukri, Effect of Inlet Quality; from /34/.

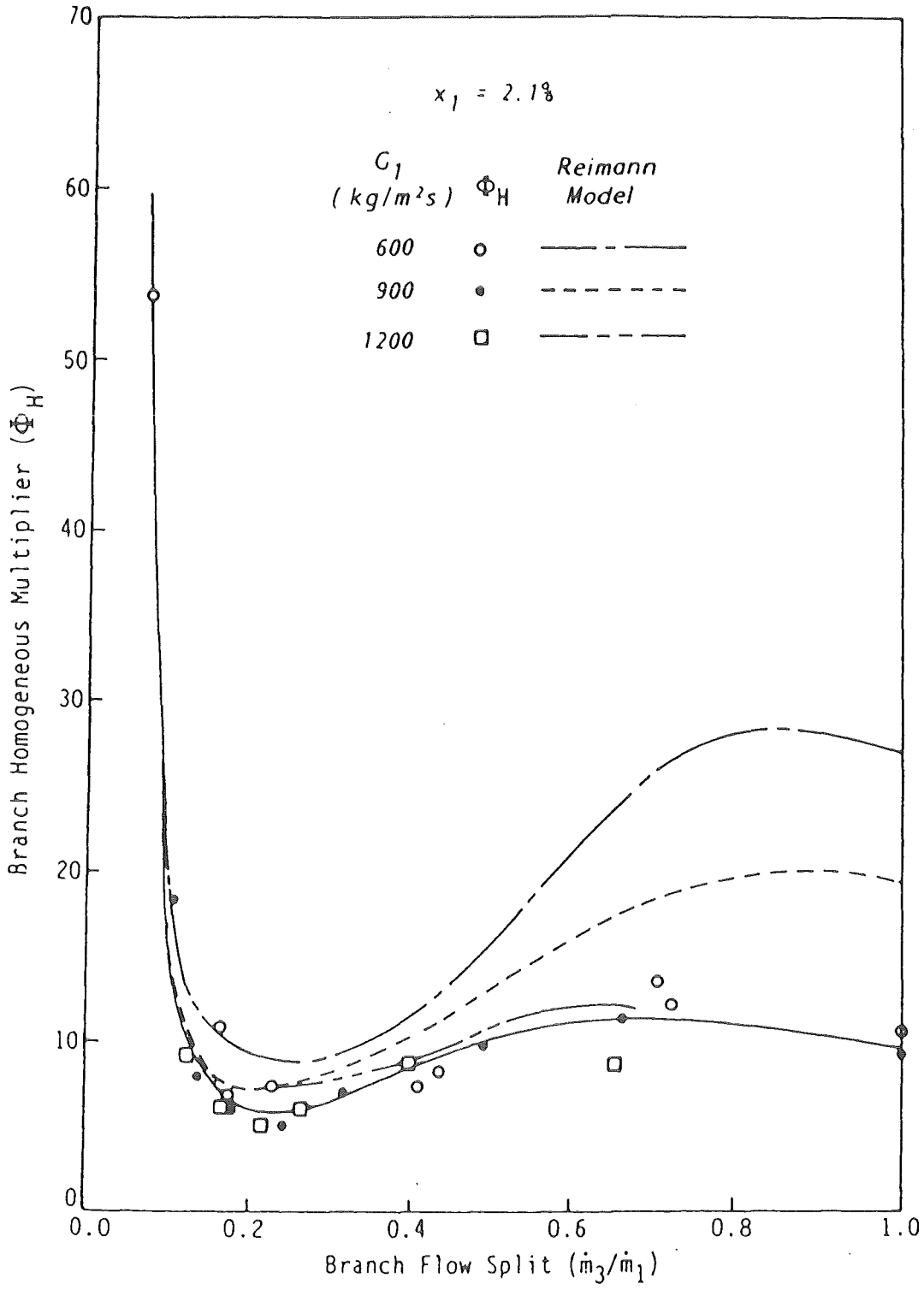


Fig. 3.15 Homogeneous Two-phase Multiplier vs. Flow Split for Experiments from Ballyk and Shoukri, Effect of Inlet Mass Flux; from /34/.

Figure 3.16 shows the fit of the data from Ballyk and Shoukri with their relationship according to Eqs. (3.29) to (3.31). A questionable point in this model is that although different relationships are used for the loss coefficient $K_{13}$ for the different diameters and measured values were available for the void fractions, the experiments cannot be described with a unique function of $\varphi^*$, compare Eq. (3.31).

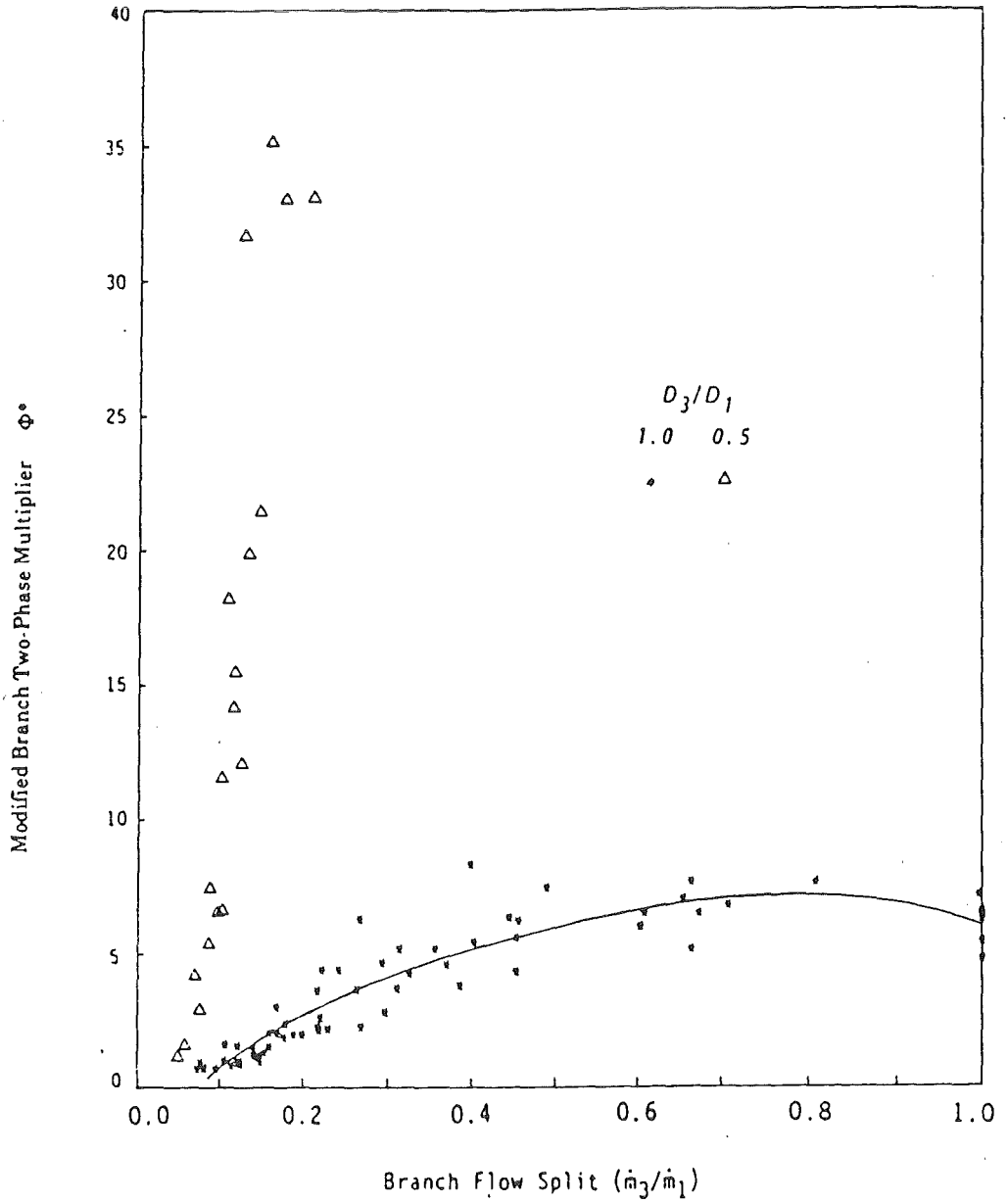


Fig. 3.16 Modified Branch Two-phase Multiplier According to Ballyk and Shoukri /34/.

### 3.3.2 Relationship for $\Delta p_{1\text{-}2}$

#### 3.3.2.1 Models Based on a Momentum Balance

Formulating Eq. (3.9) for separate flow, the following relationship is obtained

$$\Delta p_{1-2} = K^*_{12} \left| \left( \frac{G_2^2}{\rho_{m2}} \right) - \left( \frac{G_1^2}{\rho_{m1}} \right) \right|, \tag{3.32}$$

where the momentum correction factor $K_{12}^*$ is determined from single-phase data and $\rho_m$ is the momentum density given by

$$\rho_{mi} = \left( \frac{x_i^2}{\alpha_i \rho_G} + \frac{(1-x_i)^2}{1-\alpha_i} \frac{1}{\rho_L} \right)^{-1}. \tag{3.33}$$

Using homogeneous assumptions, the pressure rise due to momentum changes takes the form

$$\Delta p_{1-2} = K^*_{12} \left( \frac{G_2^2}{\rho_{h2}} - \frac{G_1^2}{\rho_{h1}} \right). \tag{3.34}$$

Equations (3.32) - (3.34) were already used in the early work of Madden and St. Pierre /53/ and Fouda and Rhodes /6/ and more recently by Lahey et al. /12,14,35/ and Ballyk and Shoukri /34/. As already mentioned in Section 3.2, Lahey et al. use a factor 0.5 on the right hand side of Eqs. (3.32) and (3.34) which is, however, compensated by the function used for $K^*_{12}$.

The Expressions (3.32) - (3.33) are termed in the following the Separated Flow Momentum Balance Model (SMM), whereas Expression (3.34) is called the Homogeneous Momentum Balance Model (HMM). Numerous variations exist, e.g. by assuming a homogeneous flow in one station or by determining the void fraction with different void fraction (or slip) correlations.

#### 3.3.2.2 Model Based on an Energy and Momentum Balance

To describe $\Delta p_{1\text{-}3}$, Reimann and Seeger /22,26/ use the same procedure as for modeling $\Delta p_{1\text{-}3}$. As outlined in Section 3.2, $\Delta p_{1\text{-}2}$ is split into a reversible pressure difference (given by an energy balance) between inlet, 1, and throat of the vena

contracta, $C_2$, and a pressure difference between vena contracta and a position downstream in the run, 2, described with a momentum balance. Relationships similar to Eq. (3.22) - (3.23) are obtained including the slips at the positions 1, $C_2$ and 2. Visual observations indicated that the flow at the vena contracta is well mixed. Therefore $\rho_{c2} = 1$ was assumed. Due to the much smaller pressure differences between inlet and run compared to inlet and branch, further assumptions of homogeneity were not recommended. Instead, it was suggested to use Rouhani's slip correlation given by Eqs. (2.17)-(2.19). The model (termed RSM) is then given by:

$$\Delta p_{1-2} = \frac{\rho_{h2}}{2\rho_L^2}\left\{\frac{G_2^2}{C_2^2}[x_2R+(1-x_2)]^2 - G_1^2[x_1R+S_1(1-x_1)]^2\left(x_2+\frac{1-x_2}{S_1^2}\right)\right\}$$

$$+\frac{G_2^2}{\rho_L}\left\{[x_2R+S_2(1-x_2)]\left(x_2+\frac{1-x_2}{S_2}\right)-\frac{1}{C_2}[x_2R+(1-x_2)]\right\}, \qquad (3.35)$$

with

$$C_2=\left(1+\left(\frac{\rho_{h2}}{\rho_{h1}}\right)^{0.5}\cdot\frac{G_1}{G_2}\sqrt{K_{12}}\right), \qquad (3.36)$$

where $K_{12}$ is taken from single phase flow measurements. If $K_{12}$ becomes less than zero, $K_{12}$ has to be set $K=0$.

### 3.3.2.3 Comparison of Predicted and Measured Values for $\Delta p_{1-2}$

In Figs. 3.17-3.20 the KfK experiments (Refs. /21-26/) are compared with the HMM, the SMM and the RSM. For the SMM, the void fraction was eliminated by Eq. (3.17) and the slip was calculated with the Rouhani correlation.

For horizontal branch and air-water flow (Fig. 3.17), the HMM gives values which are generally too high and scatter most. The two other models agree better with the measurements.

For steam-water flow (Fig. 3.18) the HMM predicts slightly high values; the RSM gives a better mean value but the scatter is still great. The SMM produces the lowest scattering and a good mean value.

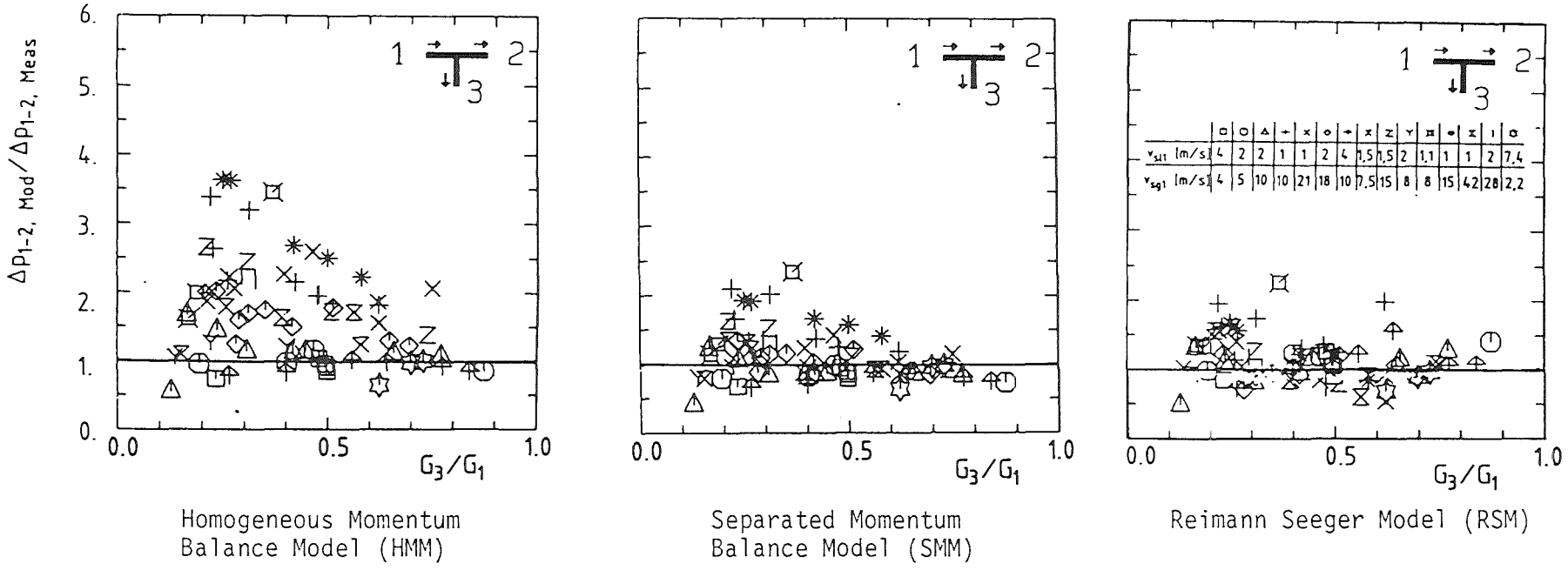


Fig. 3.17 Ratio of Predicted to Measured Run Pressure Difference for Horizontal Branch and Air-water Flow ($\rho_1 \approx 0.7$ MPa); from /27/.

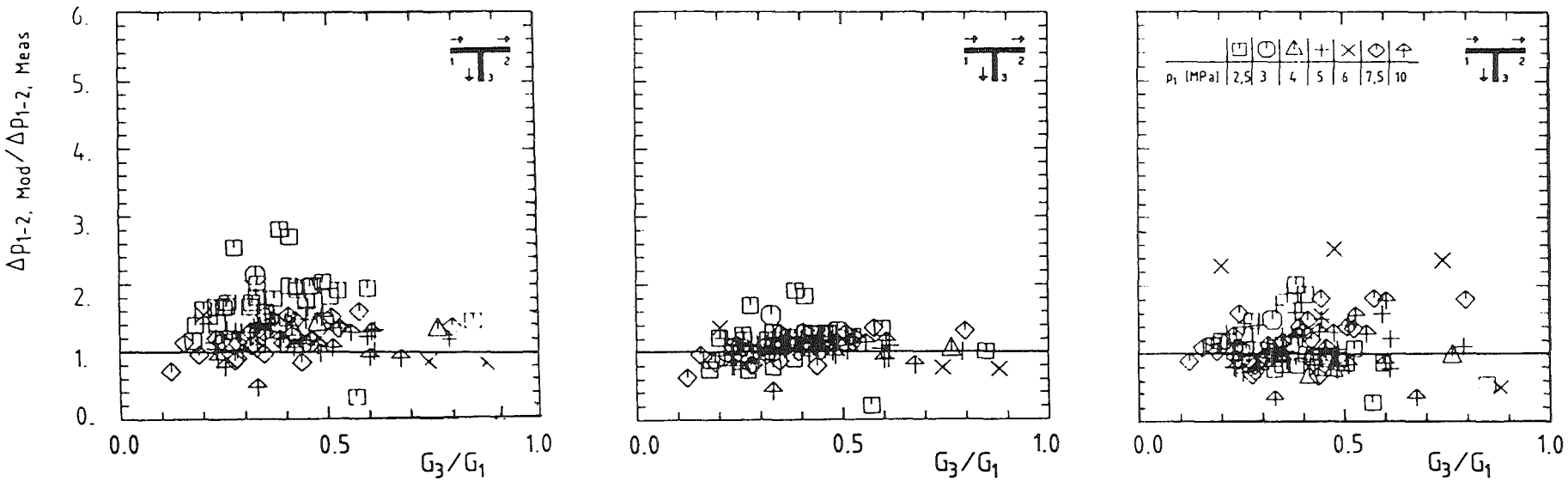


Fig. 3.18 Ratio of Predicted to Measured Run Pressure Difference for Horizontal Branch and Steam-water Flow ($2.5 < \rho_1 < 10$ MPa); from /27/.

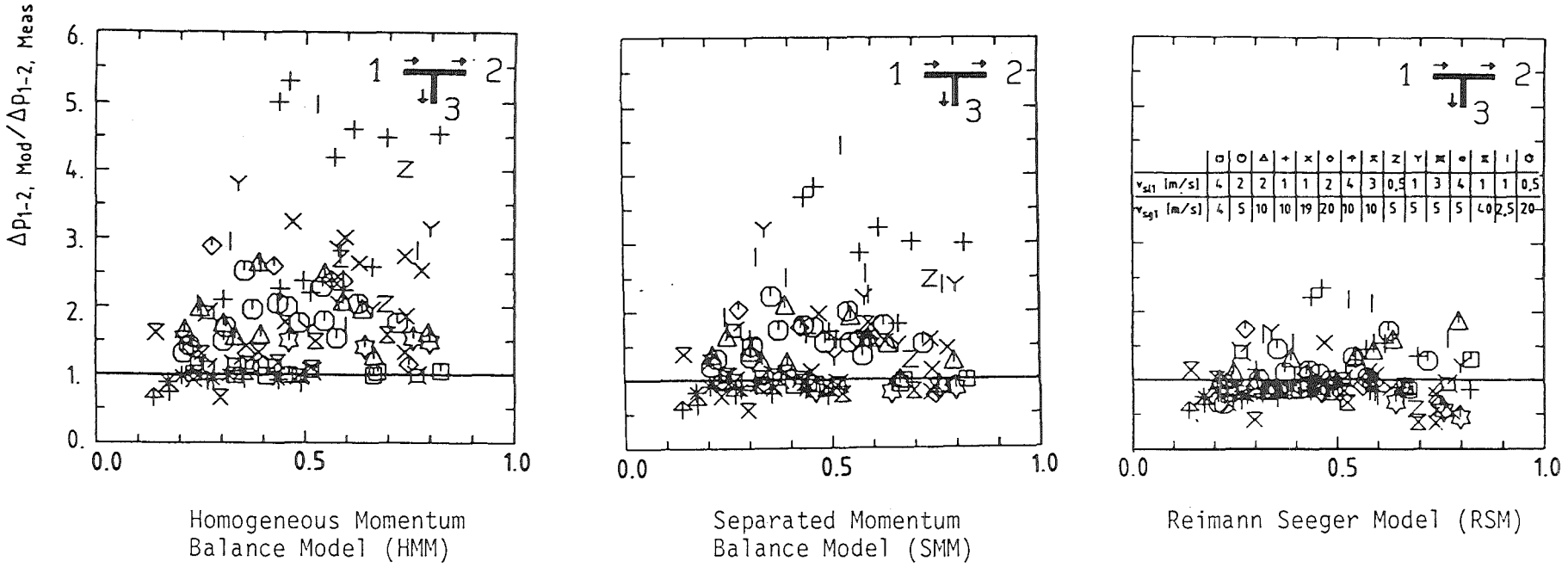


Fig. 3.19 Ratio of Predicted to Measured Run Pressure Difference for Downward Branch and Air-water Flow ($\rho_1 \approx 0.7$ MPa); from /27/.

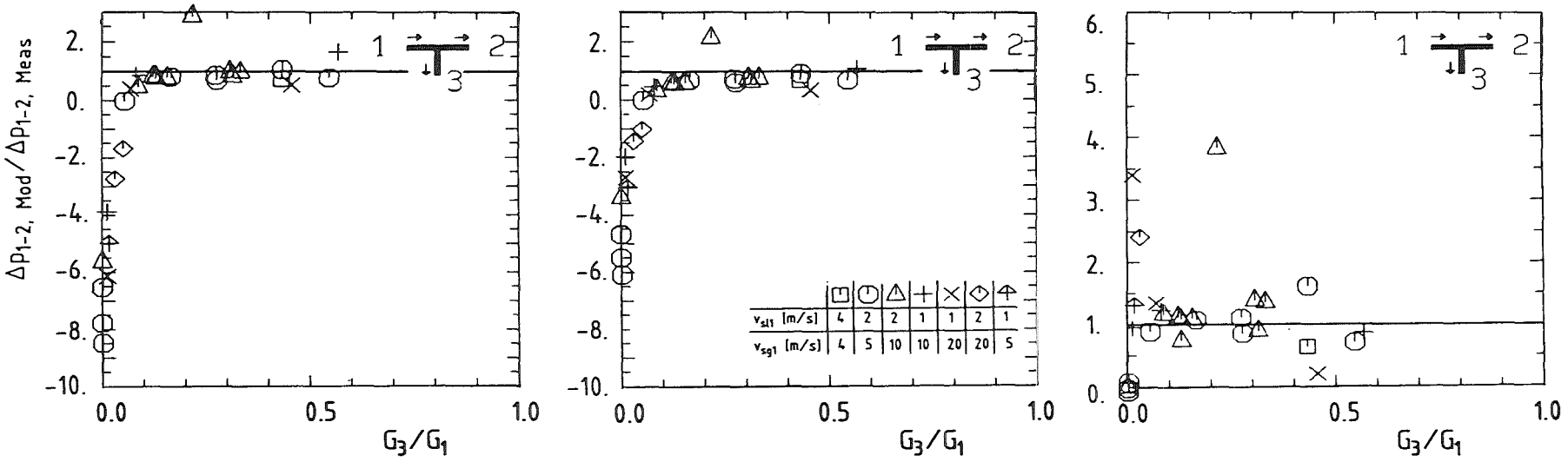


Homogeneous Momentum Balance Model (HMM)

Separated Momentum Balance Model (SMM)

Reimann Seeger Model (RSM)

Fig. 3.20 Ratio of Predicted to Measured Run Pressure Difference for Upward Branch and Air-water Flow ($\rho_1 \approx 0.7$ MPa); from /27/.

For air-water flow and the downward orientated branch (Fig. 3.19), the RSM has the highest accuracy.

The air-water experiments with the upward branch (Fig. 3.20) are predicted by all models with about the same accuracy for $G_3/G > 0.15$. With this branch orientation some of the experiments were performed at very low values of $G_3/G_1$. Here the RSM is superior to the other models.

Figure 3.21 shows for comparison corresponding graphs based on the experimental data of Saba and Lahey /12/. The RSM gives in general high values with a relatively large scatter. The SMM produces a small scatter but the values are generally too low. The HMM fits best their data and, therefore, this model was recommended by Saba and Lahey.

In a later work, Hwang and Lahey /35/ recommended the SMM but assumed homogeneous flow in the run, thus $\rho_{m2} = \rho_{h2}$. The momentum density $\rho_{m1}$ was determined using Eqs. (3.27)-(3.28). Figure 3.22 shows a good agreement between predicted and measured data from own experiments and KfK-results with the horizontal Tee-junction /26/. More than 95 % of the data were predicted within $\pm 25$ %.

Fouda and Rhodes /6/ also used the HMM and SMM to predict their annular flow experiments with an upward branch and $D_3/D_1 = 1$. The HMM resulted in values which are a factor of two too high (assuming the same $K_{12}^*$ in single and two-phase flow). The SMM predicted values which were only about 30 % too high. Therefore, the data were fitted with a momentum correction factor $K_{12}^*$ which was about 30 % lower than for single phase flow.

The annular flow data from Ballyk and Shoukri /34/ were highly overpredicted by the HMM with a large data scatter. Figure 3.23 from /34/ contains the results obtained with the SMM using measured void fractions to determine the momentum densities. The measured momentum correction factor $K_{12}^*$ is plotted as a function of split ratio. The data scatter rather around a value of 1 than around the curve of $K_{12}^*$ for single-phase flow. If $K_{12}^*$ is taken from single-phase flow, as usual, then the ratio of predicted to measured $\Delta p_{1\text{-}2}$ is given by the ratio of single-phase to two-phase flow $K_{12}^*$ values. These results are shown in Fig. 3.24. The agreement is not satisfactory. Figure 3.25 shows the comparison between the

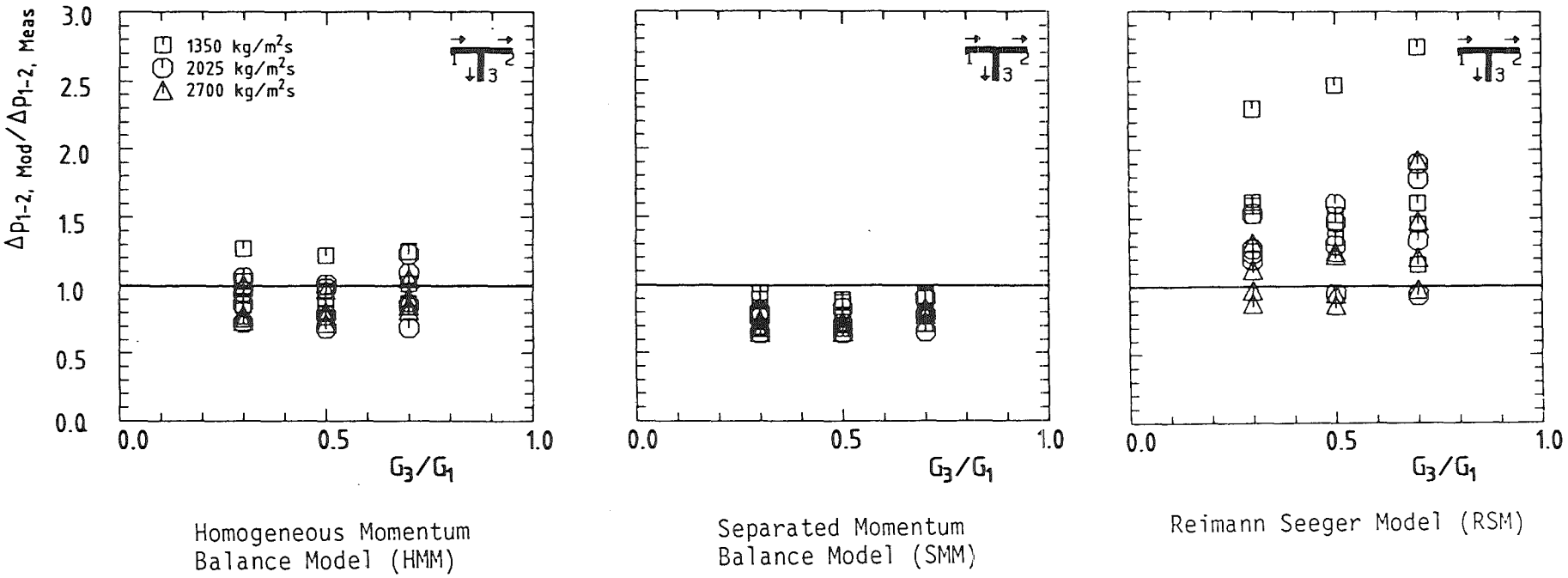


Fig. 3.21 Ratio of Predicted to Measured Run Pressure Difference for Horizontal Branch and Air-water Flow for Experiments from Saba and Lahey /12/; from /27/.

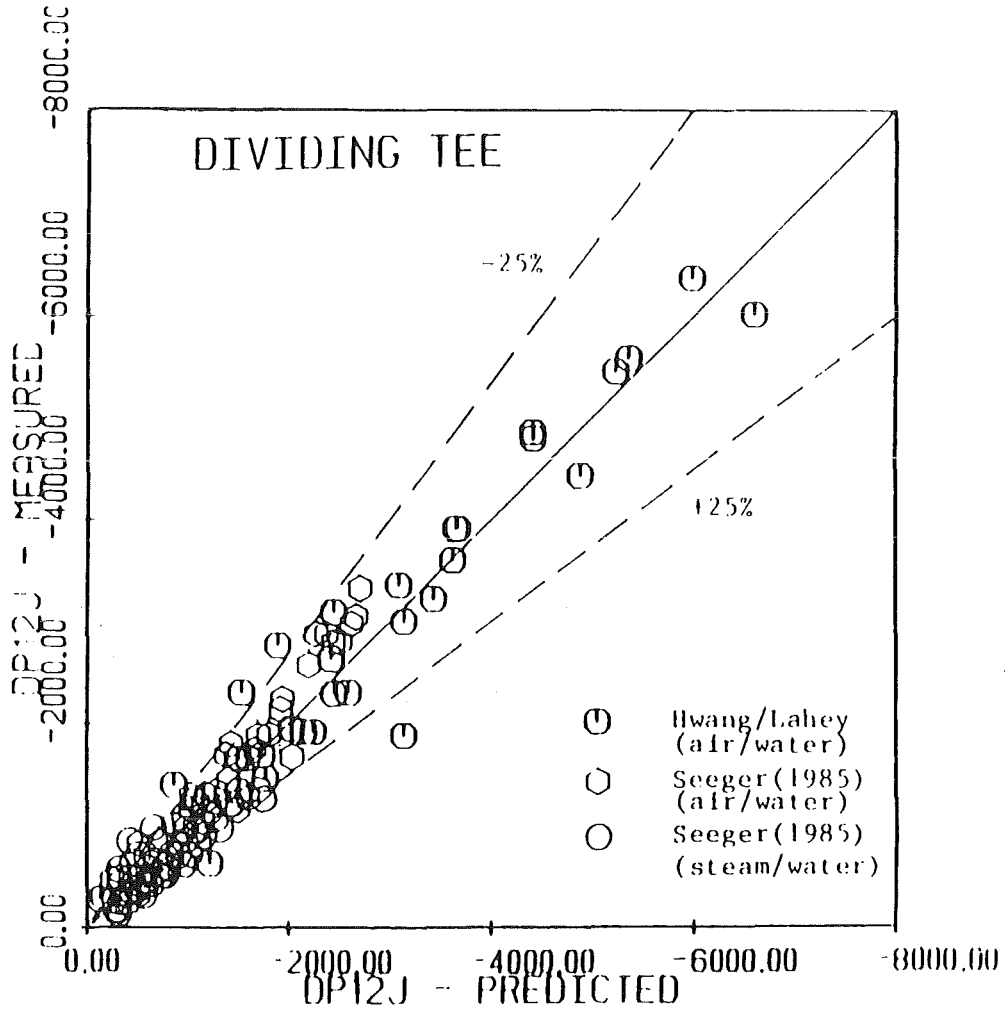


Fig. 3.22 Predicted vs. Measured Run Pressure Difference According to Hwang and Lahey /35/; from /35/.

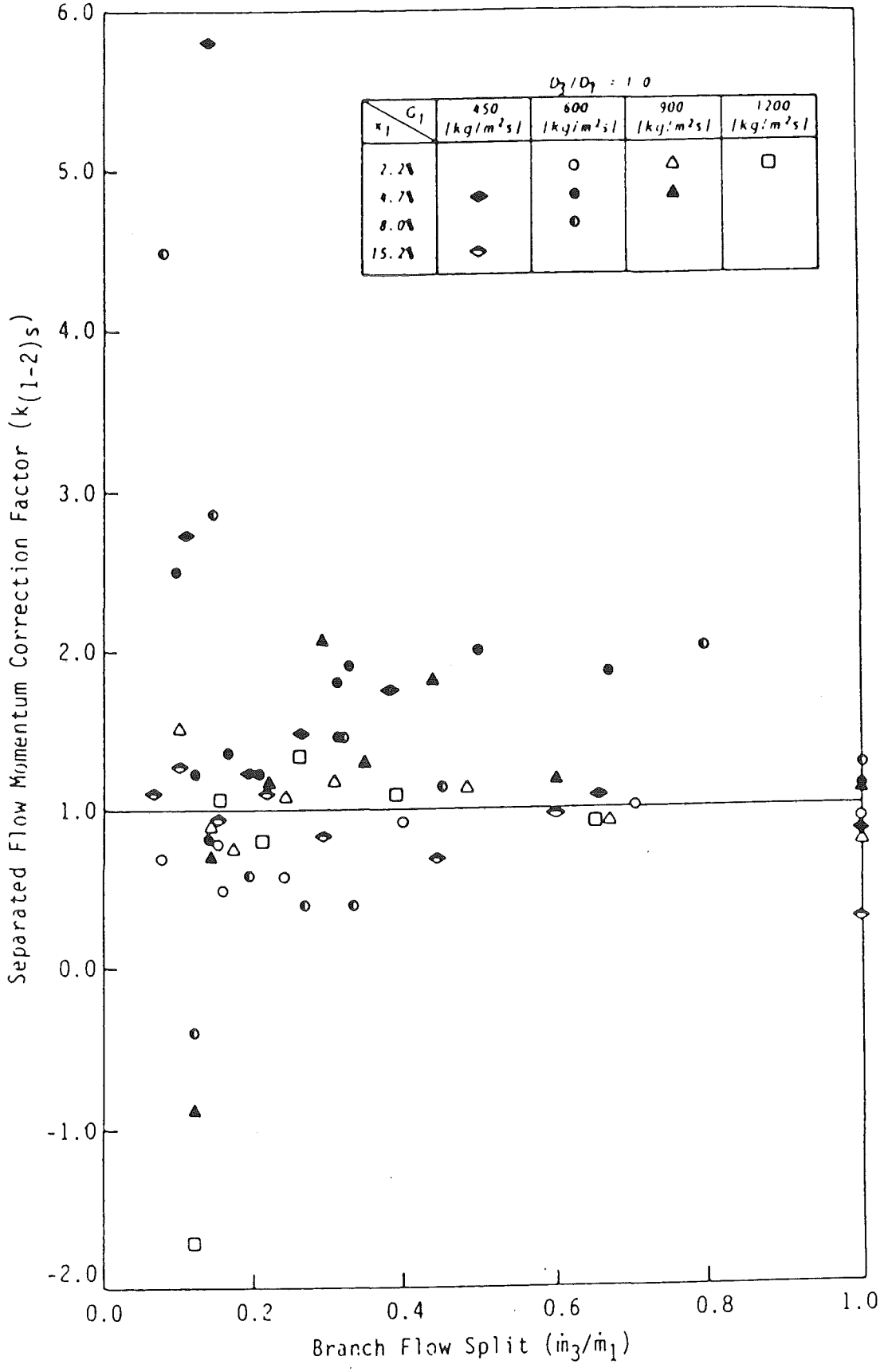


Fig. 3.23 Separated Flow Momentum Correction Factor vs. Flow Split for $D_3/D_1 = 1$; from Ballyk and Shoukri /34/.

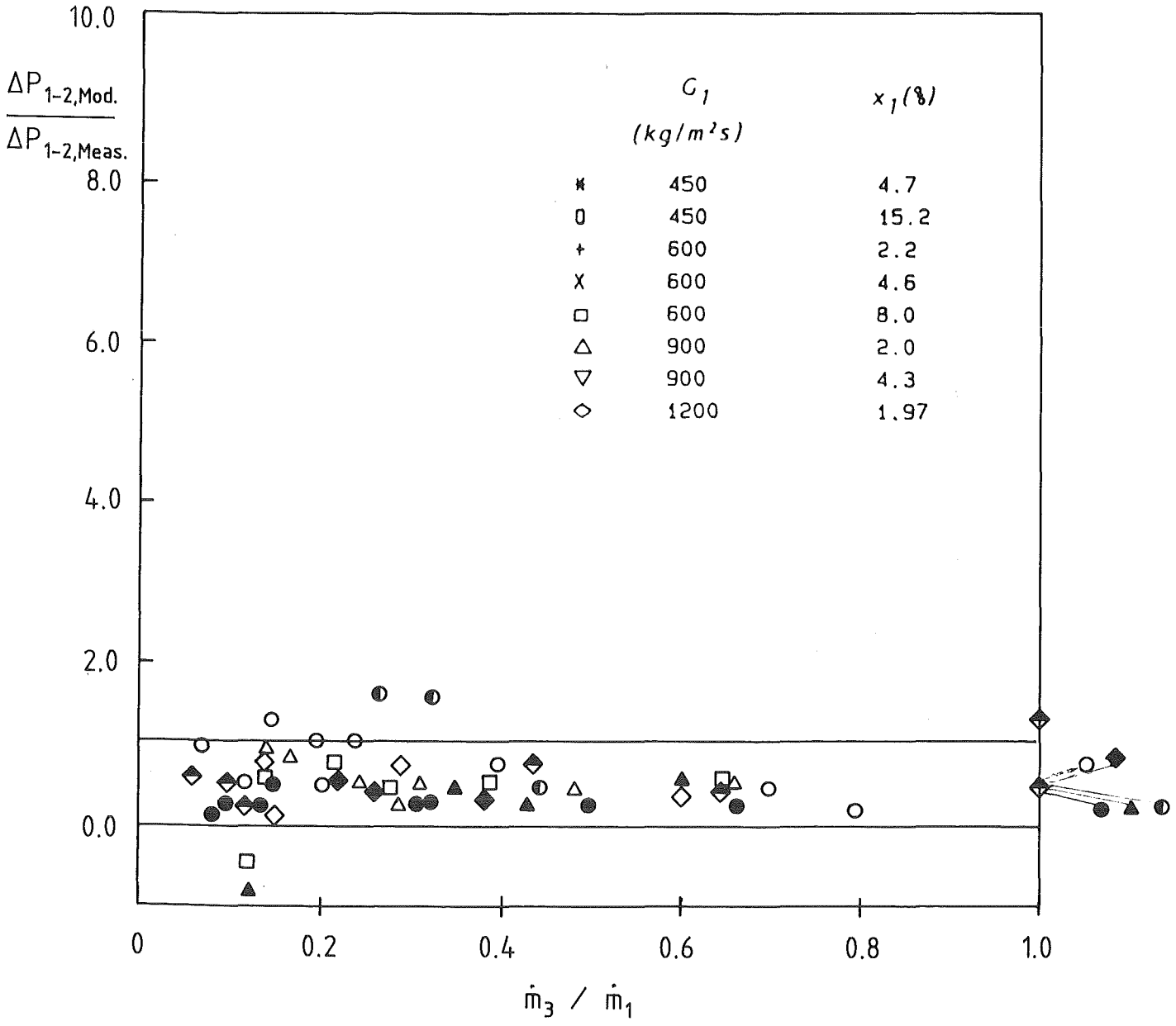


Fig. 3.24 Ratio of Predicted to Measured Run Pressure Difference According to Ballyk and Shoukri; from /34/.

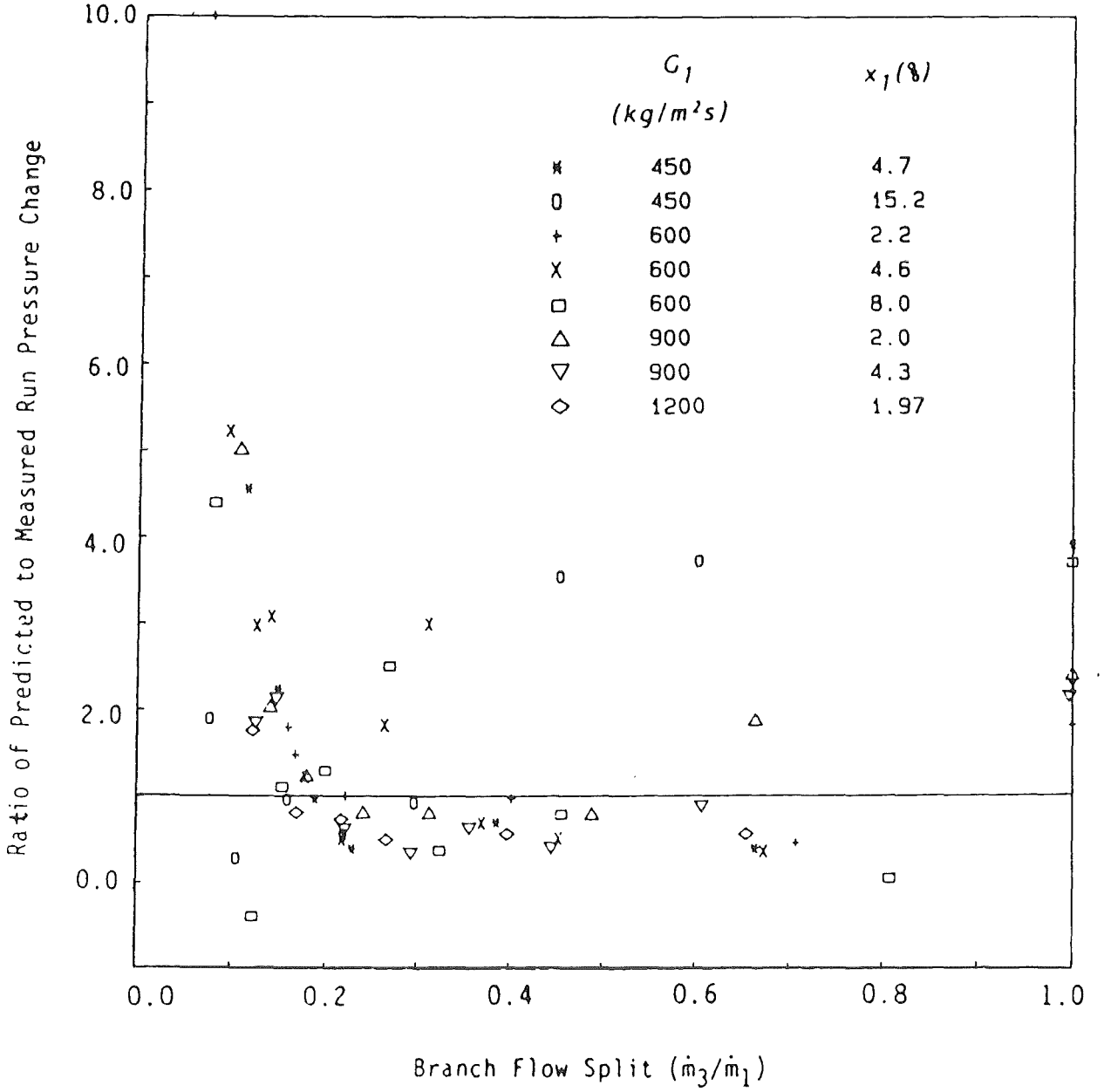


Fig. 3.25 Ratio of Predicted to Measured Run Pressure Difference According to Reimann Seeger Model; from /34/.

RSM and Ballyk and Shoukri's data, using also measured values for the void fraction. Again the agreement is not satisfactory.

Summarizing Section 3, it can be said that, presently, we are far from having generally applicable correlations for $\Delta p_{1\text{-}2}$ and $\Delta p_{1\text{-}3}$. However, an increasing number of results from different experimental facilities have been published recently. Experimental results should be fed into a data bank and each model should be tested with all data. In respect to future measurements, it is highly desirable to have more information on void and momentum distribution near the Tee-junction. A first step in this direction is the measurement of the cross-section averaged void fraction (compare /34/) at different axial positions for a wide range of inlet parameters and split ratios. These measurements would give insight in the deviation from undisturbed pipe flow approaching the Tee-junction and clearify the validity of different assuption concerning non-homogeneity.

# 4. TEST FACILITY AND TEST PROCEDURE

## 4.1 Test Loops

The test facility, described in detail by John & Reimann /4.1/, consists of two loops connected with the same mixing chamber and test section. The air-water system shown in Fig. 4.1 is supplied by a high volume water pump and four air compressors providing a maximum mass flow rate of 30 kg/s of water and 1 kg/s of air at a system pressure of 4 bar. The operating pressure can be increased to about 1 MPa at reduced maximum flow rates. After leaving the test section and the Tee-junction measurement system, the air-water mixture is separated, the air is exhausted to the atmosphere and the liquid is recirculated.

The steam-water loop is shown in Fig. 4.2. The steam-water mixture is supplied by two boilers with a maximum flow rate of about 5 kg/s. The quality can be varied between 0 and 1. The maximum pressure is 15 MPa. Two methods of operation are possible. In the first, one boiler is used to supply the slightly superheated steam, the other the slightly subcooled water. In the second, either one or two boilers can be used to supply slightly subcooled water at high pressure and a two-phase mixture is produced by flashing in the mixing chamber. At the end of the measurement set-up, the steam water flow is condensed and fed back to the boilers.

Mass flow rates are measured in single-phase condition prior to mixing. In the air-water loop, there are two measurement stations both in the air and water supply lines. Both the "NW 100" orifices are fixed whereas in the "NW 50" stations three exchangable orifices with different ranges are used. The steam-water flow rates are measured by means of two measurement sections in each supply line.

Figure 4.3 shows the mixing chamber. Mixing of the phases is accomplished by means of a perforated tube. This tube has a wall thickness of 3 mm and contains about 600 drilled holes (diameter 2 mm) which are inclined slightly in the direction of the flow. For some tests, these holes are partly closed by a sleeve to make sure that even at low volumetric flows the pressure drop across the holes is high enough to ensure stable behaviour of the mixing chamber. There are two methods of operating the mixing chambers: In the first method, gas flows through the center pipe and water is injected from the outer annulus. In the second method, the mixing chamber is revolved by 180°, so that water flows through the center pipe and gas is injected into the water from the outer annulus. The first

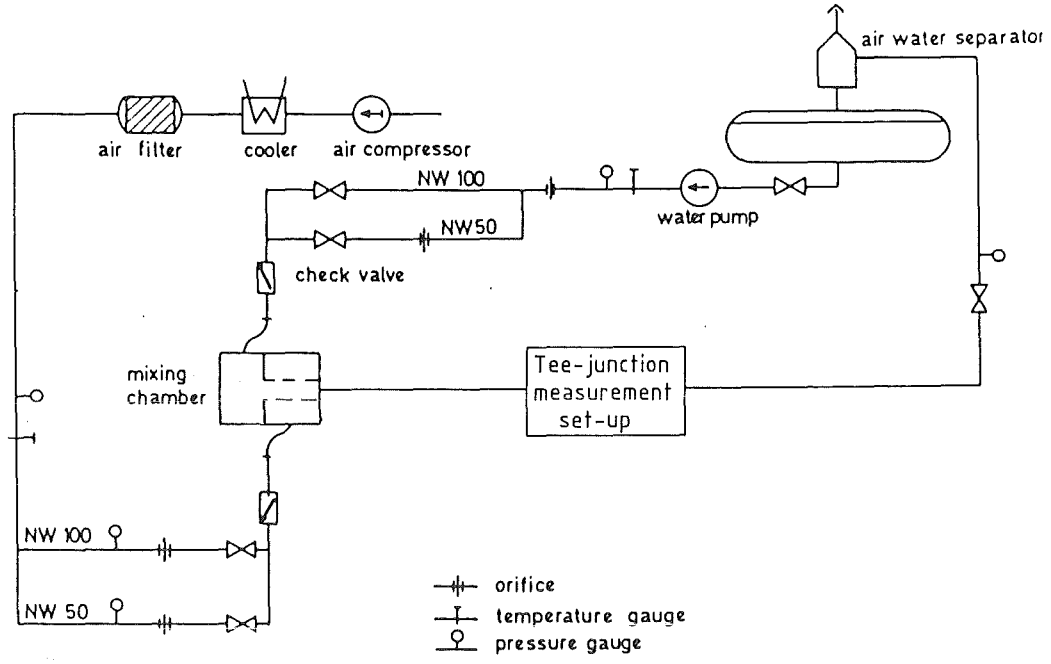


Fig. 4.1 Two-phase Air-water Loop.

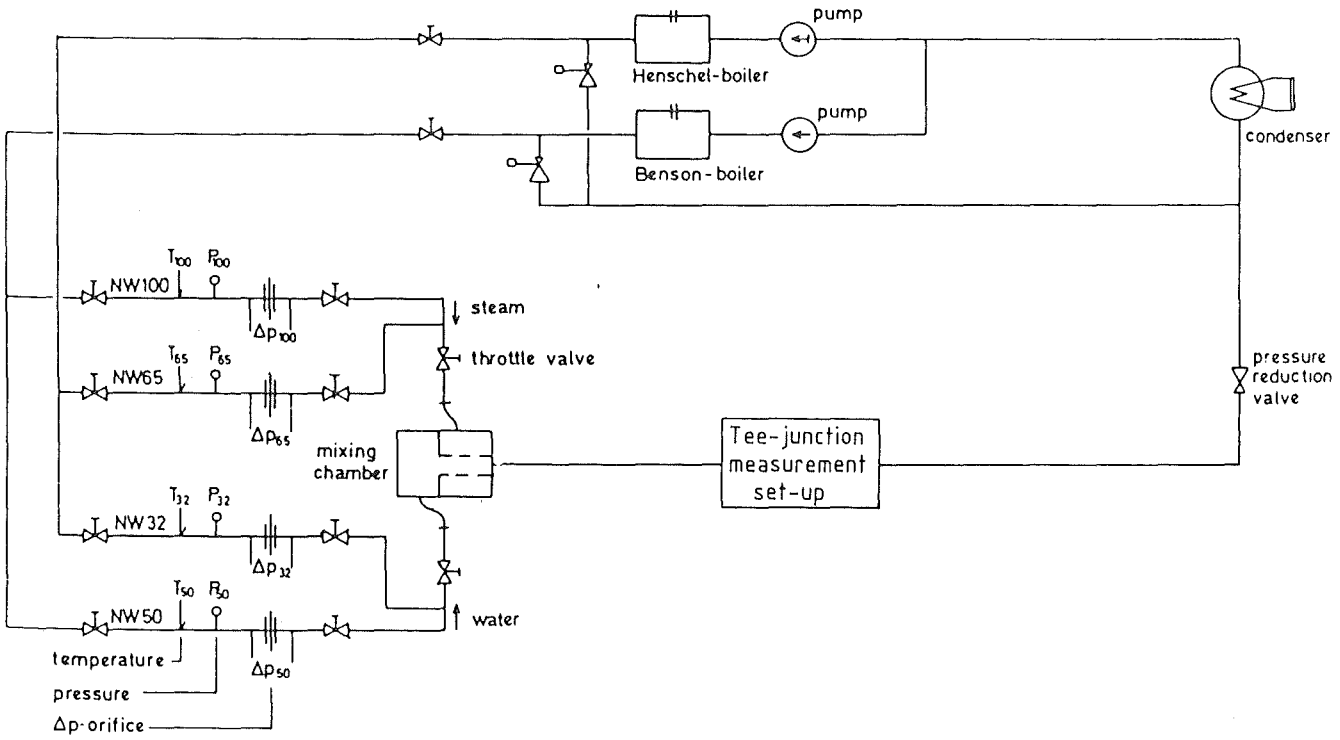


Fig. 4.2 Two-phase Steam-water Loop.

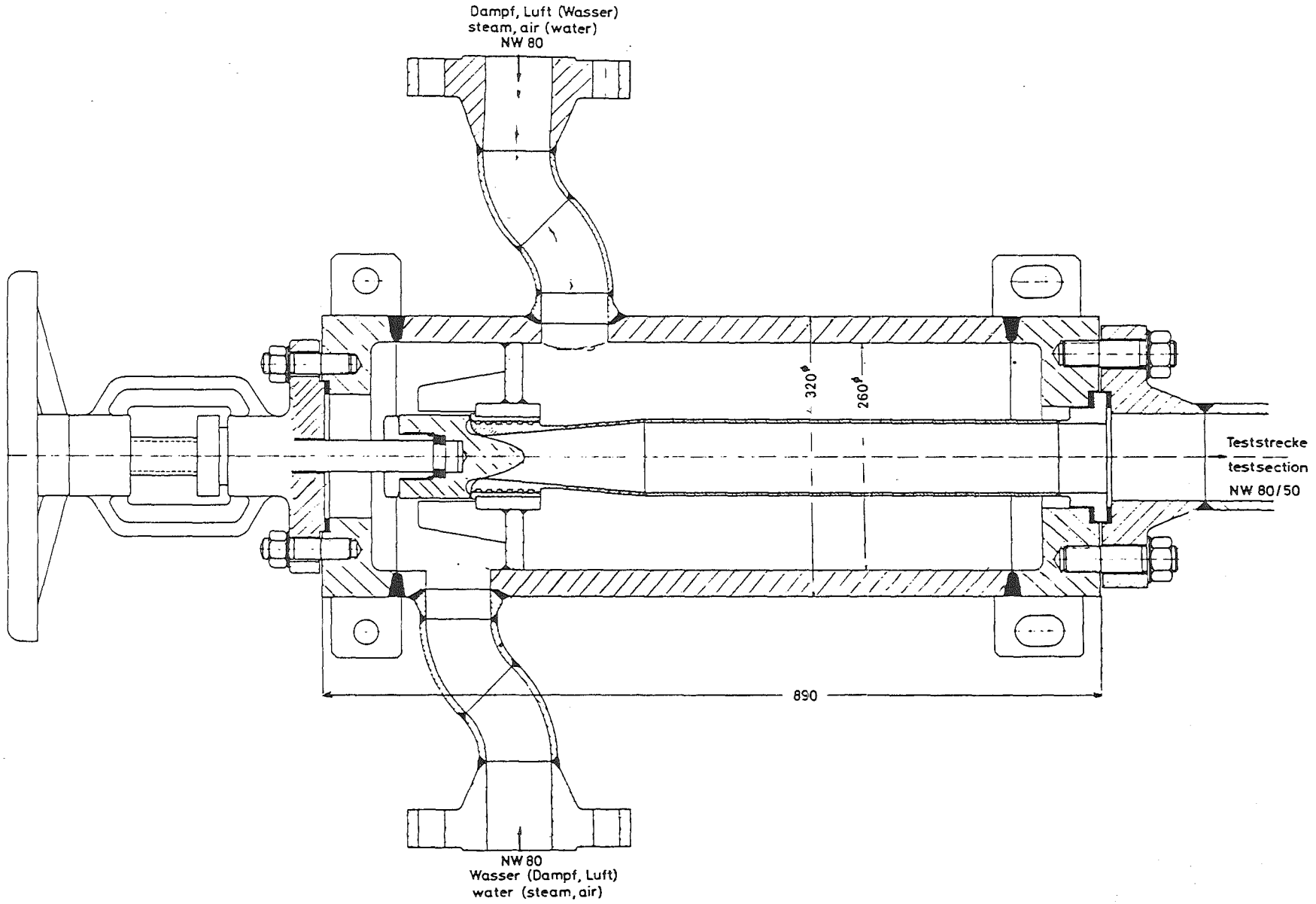


Fig. 4.3 Mixing Chamber.

method of operation may be used with other inserts for special purposes. For example, another insert is available to promote the development of annular mist flow in the test section. For the tests described in this report the second method of operation was always used. For steam-water experiments this method geometry promotes the reaching of thermal equilibrium.

## 4.2 Test Sections

The test section consisted of the horizontal inlet pipe (length about 2 m) between the mixing chamber and the Tee-junction, followed by the horizontal run of 3 m length and the branch pipe. The branch pipe was installed either horizontally, vertically upward or downward; the corresponding lengths were 3.1, 2.1, or 0.76 m. The horizontal pipe had an inner diameter of 50 mm; the piping material was carbon steel. For flow visualization studies, the Tee-junction and adjacent pipes were made of plexiglas.

Four different branch diameters were used: $D_3$ = 50, 26, 10, and 4.3 mm. The 50 mm and 26 mm diameter branch pipes had sharp edged entrances; the positions of the pressure taps to measure the pressure gradients are shown in Fig. 4.4 together with the locations of the pressure taps in the inlet and run pipe.

The branch geometries for the other diameter branch pipes are shown in Fig. 4.5. The 10 mm branch had a length of 360 mm and was connected downstream with a 50 mm diameter pipe. The branch entrance was sharp edged, the location of the pressure taps are shown in the figure. The 4.2 mm diameter branch was of a nozzle type geometry with a 4 mm inlet radius and a subsequent length of 17 mm with $D_3$ = 4.2 mm. There was a pressure tap 3 mm upstream of the branch exit to measure the pressure difference between inlet and branch.

The pressure taps had diameters of 2.5 mm and were located at the pipe bottom for the horizontal pipes. To avoid air entrapment, all lines were water purged periodically. The pressure differences could be measured with four parallel differential pressure transducers (Rosemount) with maximum measurement ranges of p = 0.12, 0.3, 0.75 and 3.7 kPa, for details see Seeger /23/.

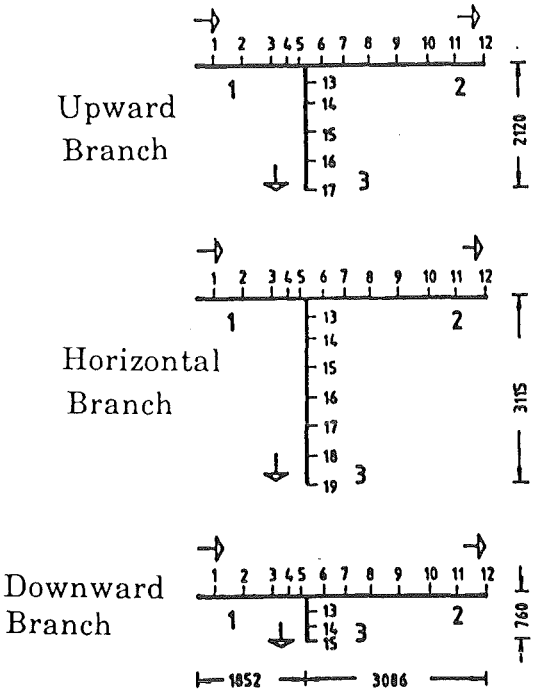


Fig. 4.4 Test Section Dimensions for $D_1 = D_2 = D_3 = 50$ mm and Pressure Measurement Locations.

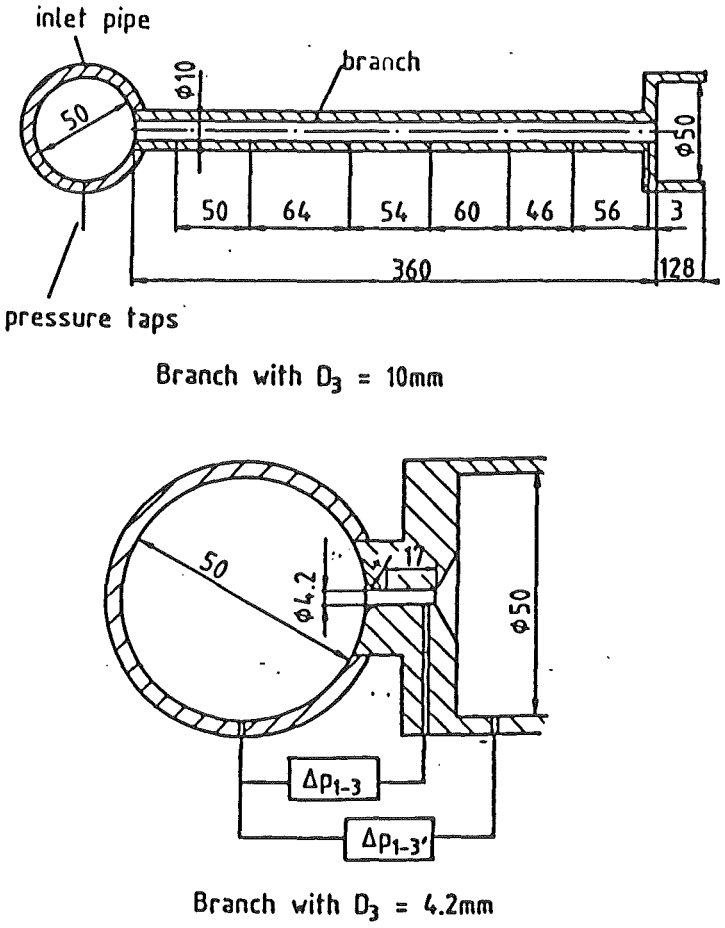


Fig. 4.5 Schematical Sketch of Branches with $D_3 = 10$ mm and $D_3 = 4.2$ mm

## 4.3 Branch and Run Measurement System

Figure 4.6 shows that particular part of the test facility which was specially built for the Tee-junction experiments with the larger branch diameters ($D_3$ = 26 and 50 mm): the flow is divided in the Tee-junction by means of the branch valve and the run valve. The branch valve is operated by hand, the run valve is an automatic control valve which keeps the pressure in the test section at a given value. The mixtures are throttled in the valves to a maximum pressure of 0.5 MPa and flow to specially designed separators. The water exits from the bottom, and the air or steam from the top of these vessels. Due to the wide range of mass flow rates ($0.024 < \dot{m}_L < 30$ kg/s, $0.001 < \dot{m}_G < 3$ kg/s) three measurement sections are installed for the gas phase and four for the liquid phase. These sections are equipped with variable throttle meters (Durchflußmeßgerät CD, Fa. Caldyn, Ettlingen, FRG), which are calibrated for three different throttle positions. For steam-water experiments the measurement sections can be cooled or heated to guarantee single-phase conditions.

Further downstream, the single-phase flow again enters a mixing chamber followed by an automatic control valve to keep the pressure in the separator system at a given value. The mixtures of the run and branch finally join and flow to the steam condenser or air-water separator.

The optimum operating behaviour of the run and branch separators is of great importance. On the one hand, the gas-liquid interface (and with this the vessel diameter) has to be large at large volume flow rates to prevent gas or liquid entrainment. On the other hand, measurement errors occur if the height of the interface in the separator is not constant. For a large vessel diameter, very small changes of the interface level cause considerable errors in case of low volume flow rates. Therefore, the separators used have different cross sections and a height of more than 7 m, as shown in Fig. 4.7. Depending on the flow rates, the interface was set to a level where entrainment did not occur but good level control was possible.

For the experiments with $D_3$ = 10 and 4.2 mm an additional separator was positioned in the branch piping between branch test section and the system described above. This separator with a relative small size (300 mm vessel diameter and 1.5 m height) was used for measurements at very low branch flow rates where the values were no longer in a favourable measurement range of the

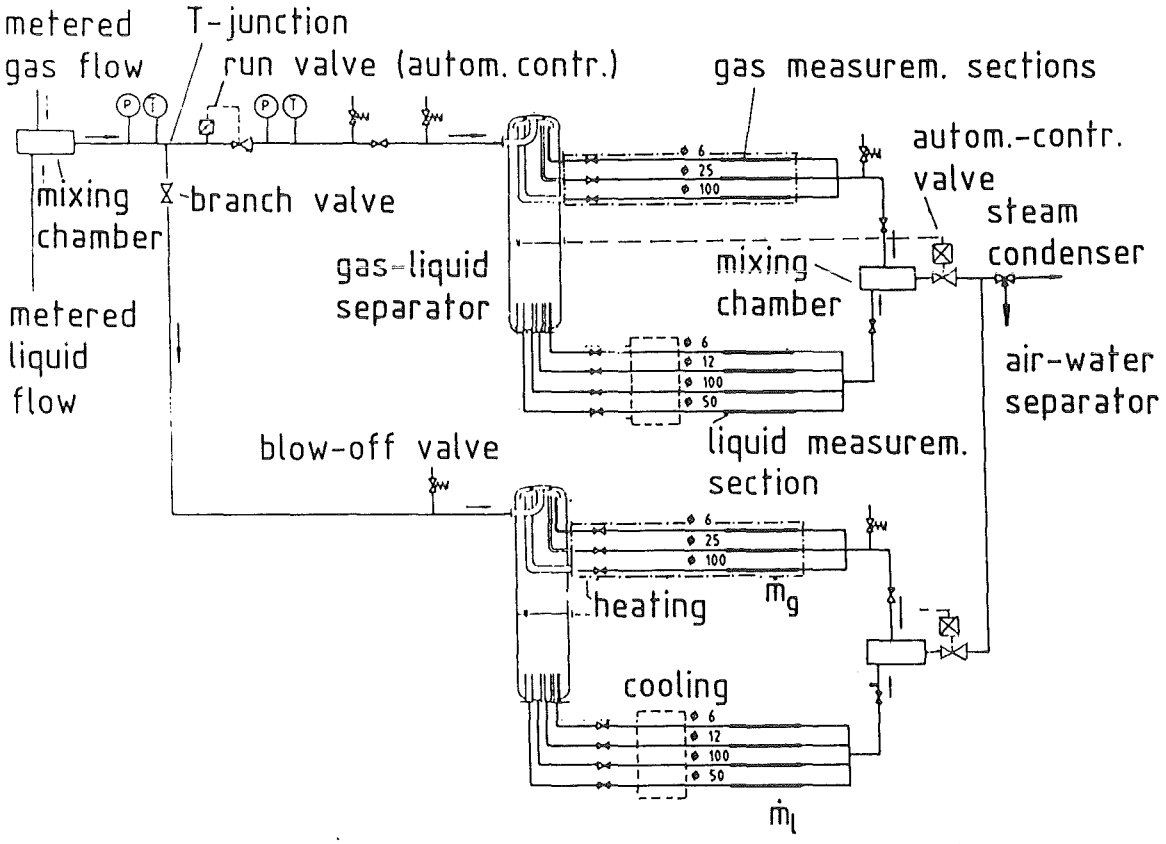


Fig. 4.6 Tee-junction Measurement Set-up.

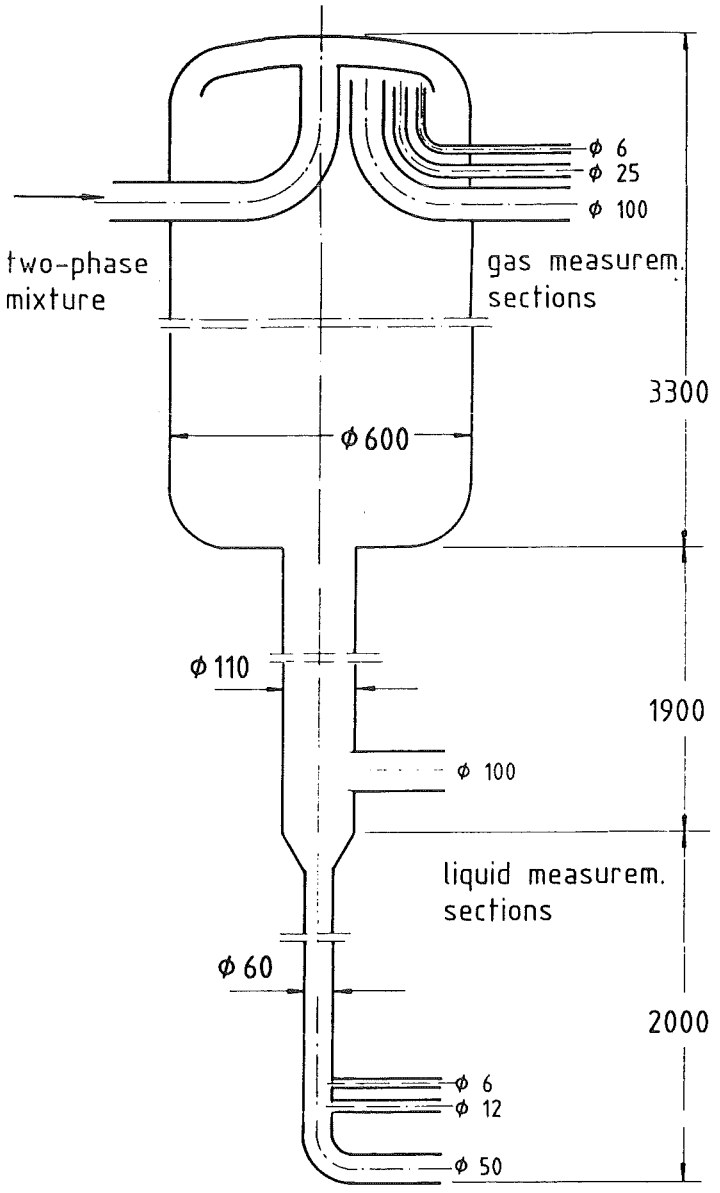


Fig. 4.7 Gas-liquid Separator

large system or when it was just much less time consuming to use this system. The gas flow rates were measured by rotameters or using the measurement stations of the large system.

The liquid flow rate could be measured by sampling the water for a given period of time keeping the liquid level in the separator constant. For very low water flow rates through the branch the valve in the water line was closed and the increase of the liquid level after a certain period of time was measured.
This separator was also installed when the experiments with the 26 mm branch diameter were performed and the very last experiments with the 50 mm diameter branch (repetition of previous experiments (Refs. /21/ to /26/) and extension of test matrix). Here again this separator was very convenient for very small branch flow rates. At higher flow rates the two-phase mixture went through the separator vessel and was separated in the large separator.

## 4.4 Test Procedure

The complexity of the system required exceptionally high service to perform the experiments. For selected flow conditions in the inlet (pressure $p_1$, mass flow rate $\dot{m}_1$, quality $x_1$) the split ratio $\dot{m}_3/\dot{m}_1$ was varied between zero (closed branch valve) and unity (closed run valve). Up to ten split points were established. For each split point appropriate measurement sections had to be chosen and the interface level (measured by differential pressure transducers) had to be selected and controlled. When the total system was stabilized, which in some cases took several hours, the measurements started. The data were directly processed by a PDP 11/40 computer. These data included temperature, absolute and differential pressure readings in the inlet, branch and run measurement sections, and the differential pressure measurements in the test section. A computer program was set up which also took into account heat losses and flashing due to throttling of steam-water flow. The output values were mass fluxes and qualities for the inlet, branch and run related to the system pressure in the test section.

The measurements of the mass flow rates both in the inlet, branch and run give valuable information on the measurement accuracy because the sum of the branch and run mass flow rates should be equal to the inlet values. However, this measurement of the mass balance only makes sense if the branch and run mass flow rates are of comparable size. For small branch rates, it is much more

important to have a high accuracy of the branch flow rate measurements and the run flow values can be calculated by the difference between inlet and branch values.

The procedure which includes the measurements of all flow rates is very time and man-power consuming, as mentioned above. Therefore, it was only applied in the previous and new experiments with $D_3 = 50$ mm and in the experiments with $D_3 = 26$ mm with higher branch mass flow rates. In the other experiments only the inlet and branch flow rates were measured. In order to proof the measurement accuracy many additional measurements were performed with the run valve closed where the branch flow rates are equal to the inlet flow rates. Redistribution data were only accepted if the agreement was good (see Section 4.7).

## 4.5 Measurement Accuracy

An error analysis for the single-phase mass flow rates in the inlet (for details see John and Reimann /55/) resulted in typical values of $\Delta\dot{m}/\dot{m} = 2.5$ %. For the measurement of the branch and run flow rates again great care was taken to ensure a high accuracy, as mentioned above. Therefore, as a conservative value, again a typical error of $\Delta\dot{m}/\dot{m} = 2.5$ % is assumed. Using the procedure of error calculation this results in an error of $\Delta(x_3/x_1)/(x_3/x_1) = 5$ % and $\Delta(\dot{m}_3/\dot{m}_1)/(\dot{m}_3/\dot{m}_1) = 3.5$ %. To check this accuracy, a lot of additional experiments with a closed run valve were performed (full branch flow experiments) and split experiments were not started unless this accuracy was reached. When the flow rates in both the run, inlet and branch were measured the sum of the branch and run single-phase flow rates had to agree within $\pm 3$ % with the inlet values.

Looking at the redistribution data, the data scatter at small branch flow rates is sometimes significantly higher than predicted above. This is attributed to changes of the interface levels in the separators (pressure fluctuations in the system, changing inlet conditions, etc.). Although great care was taken to minimize these effects, e.g. by special designs, compare Fig. 4.7, these effects could not be always eliminated.

## 4.6 Test Matrix and Measured Quantities

Figure 4.8 shows the test matrix of the experiments with $D_3 = 50$ mm. The results from these experiments were mostly already published previously (Refs. /21-26/). There are some new air-water experiments with this branch diameter and a horizontal branch as indicated in Fig. 4.8. These experiments extend the previous investigated parameter range to lower values of the inlet superficial velocities and should be well suited for comparisons with results and models from Shoham et al. /33/ and Azzopardi and Whalley /9,10/.

Figure 4.9 shows the test matrix of the experiments with $D_3 = 26$, 10 and 4.2 mm. The results from these experiments were only partly published (Refs. /28-30/). However, these publications do not include any detailed data tables.

All significant measured data are given as tables in the appendix. These tables content the quantities defining the inlet conditions $v_{sL}$, $v_{sG}$, $p_1$; for convenience also $\dot{m}_1$, $x_1$; the branch measurements $\dot{m}_3$, $x_3$, the ratio $x_3/x_1$; the run quantities $\dot{m}_2$, $x_2$ and the pressure differences $\Delta p_{1\text{-}3}$ and $\Delta p_{1\text{-}2}$. The given value for $\Delta p_{1\text{-}2}$ is the run pressure difference, extrapolated from measured pressure gradients in the inlet and run pipe. These values become very small (in the order of some mbars) for inlet conditions with a small frictional pressure gradient (small superficial velocities) and for small mass flow ratios $\dot{m}_3/\dot{m}_1$. In these cases the values can become very inaccurate and are, therefore, not included in the tables. Small mass flow ratios $\dot{m}_3/\dot{m}_1$ always occured for small diameter ratios (especially $D_3/D_1 = 0.08$). For $D_3/D_1 = 0.52$, there are also less values for $\Delta p_{1\text{-}2}$ than for $\Delta p_{1\text{-}3}$ because the data scatter was large and therefore the data were not reliable.

For the branches with $D_3 = 50$ and 26 mm, the given values for $\Delta p_{1\text{-}3}$ is the extrapolated value from the measured pressure gradients in the inlet and branch pipe. For the nozzle-type branch with a diameter of 4.2 mm, the given branch pressure drop $\Delta p_{1\text{-}3}$ was measured between the locations shown in Fig. 4.2. For the branch with $D_3 = 10$ mm, the given values for $\Delta p_{1\text{-}3}$ corresponds to the pressure differences measured between the inlet pipe and the first pressure tap downstream of the branch entrance, compare Fig. 4.5.

Due to the concentration on phase redistribution, often pressure differences were not measured at all as seen in the tables.

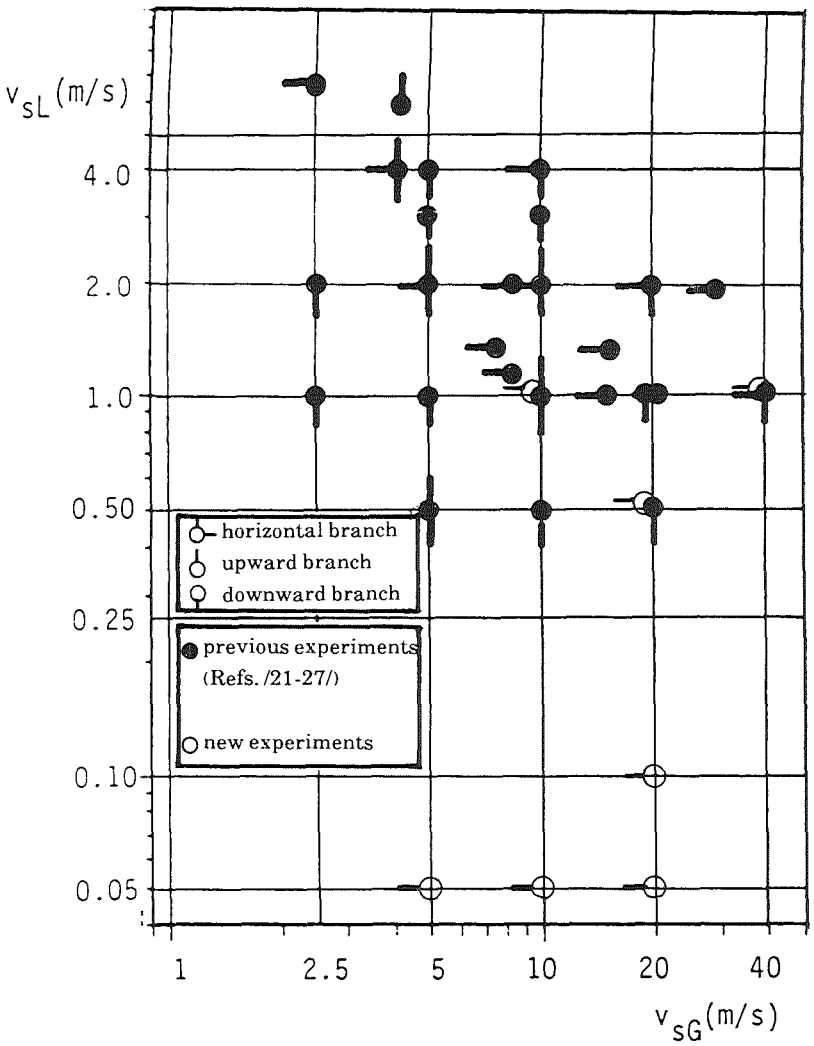


air-water experiments

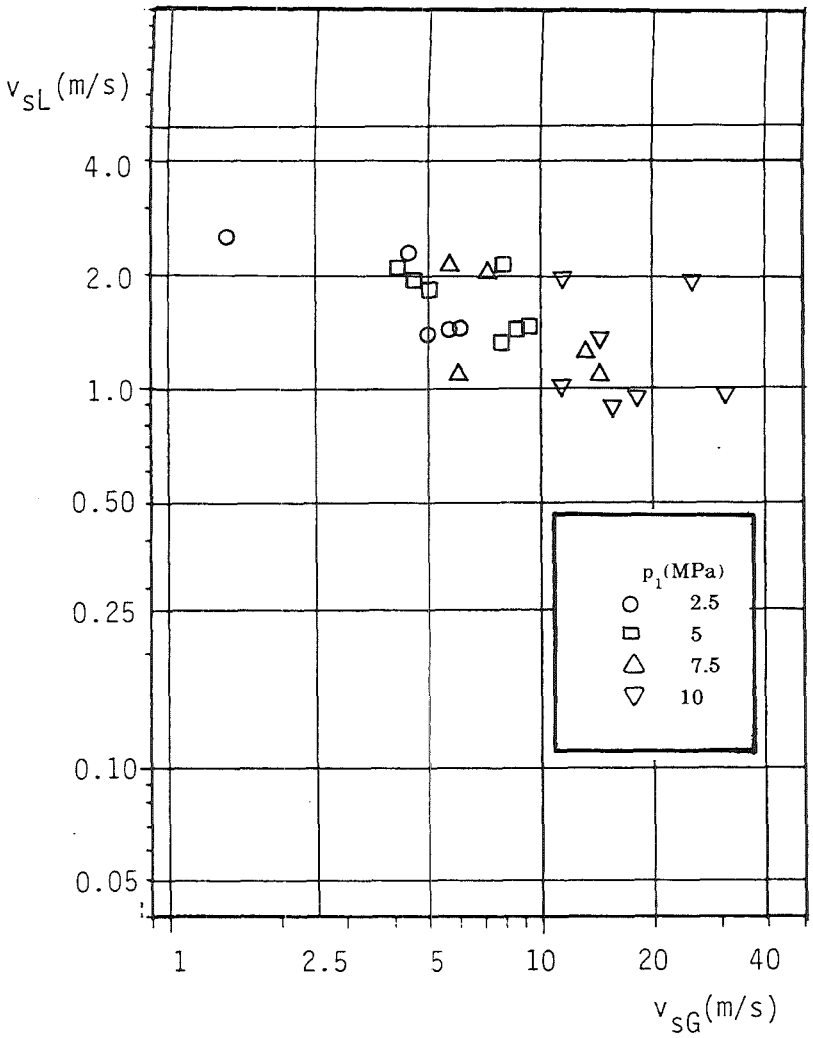


steam-water experiments (Refs /23-27/)
(horizontal branch)

Fig. 4.8 Test Matrix for Air-Water and Steam-Water Experiments with $D_3/D_1 = 1$.

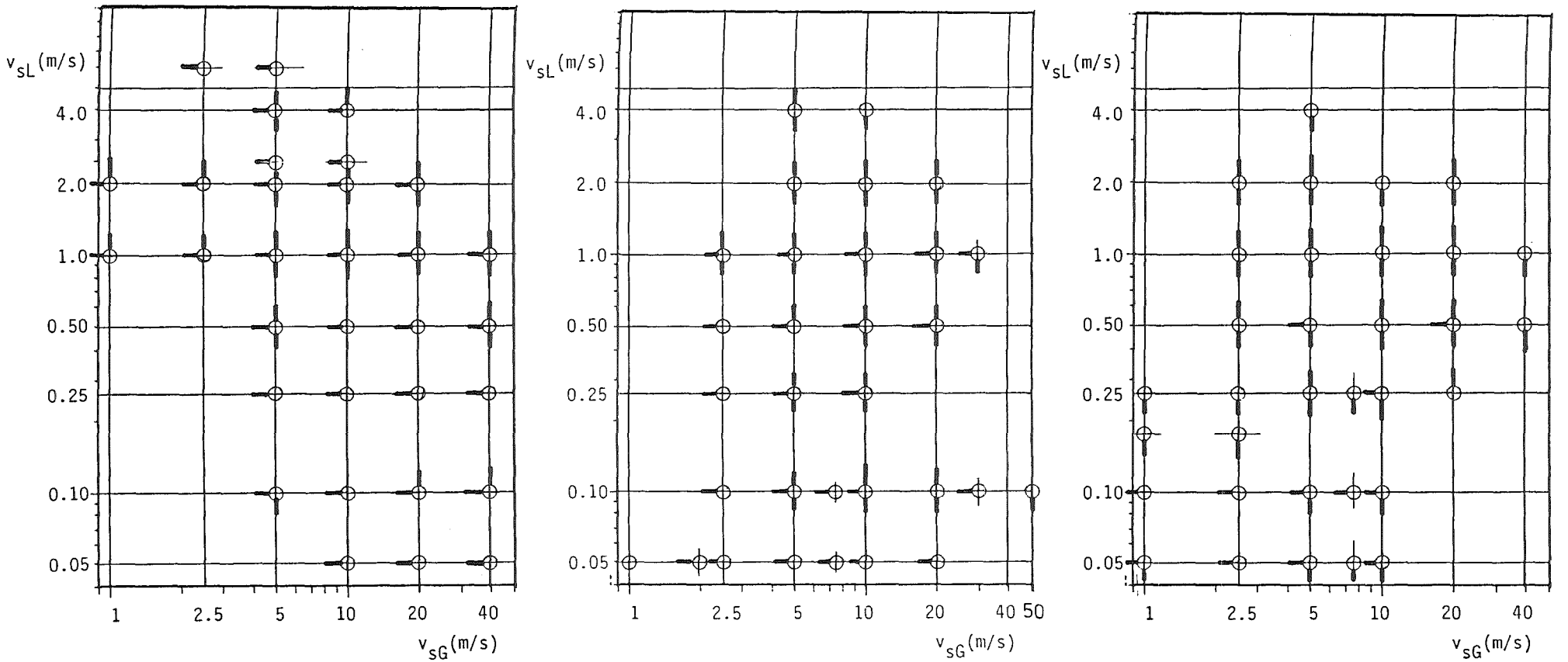


$D_3/D_1$ = 26/50 = 0.52

$D_3/D_1$ = 10/50 = 0.2

$D_3/D_1$ = 4.2/50 = 0.084

Fig. 4.9 Test Matrix for Air-water Experiments with $D_3/D_1$ = 0.52, 0.2 and 0.08.

In Section 6, only pressure measurements for $D_3 = 50$ and 26 mm will be discussed. If there will be interest in further details of the other data, the authors of this report should be contacted.

In Section 5, only some typical examples of the phase redistribution data will be presented. Further analyses can be performed using the data sets given in the appendix.

# 5. NEW RESULTS FOR PHASE REDISTRIBUTION AND COMPARISON WITH RELATED WORK

## 5.1 Phase Redistribution for $D_3/D_1 = 0.52$

### 5.1.1 Experimental Results

Compared to the previous experiments with $D_3/D_1 = 1$ (Refs. /21-26/), the test matrix for $D_3/D_1 = 0.52$ included test points at lower superficial liquid velocities with flow patterns in the stratified flow regime. Additionally, the range of branch mass flow rate was extended to lower values.

In Fig. 5.1 the branch quality $x_3$ is plotted as a function of the branch mass flow rate $\dot{m}_3$ for the horizontal branch direction. Parameter is the inlet superficial liquid velocity $v_{sL}$. The superficial gas velocity $v_{sG}$ is kept constant, $v_{sG} = 5$ m/s. For $v_{sL} = 0.1$ m/s a stratified wavy flow exists in the inlet pipe; the interface level is slightly below the branch entrance. Therefore, for very low pressure differences between inlet and branch only gas is entering the branch and $x_3$ becomes about unity. With increasing pressure difference, liquid is increasingly withdrawn into the branch and $x_3$ becomes smaller. The flow patterns with $0.25 \leq v_{sL} \leq 2$m/s belong to the slug flow regime, for $v_{sL} = 4$ m/s the flow pattern is already typical for dispersed bubble flow. These curves exhibit a characteristic maximum, as observed for $D_3/D_1 = 1$.

In the following figures the quality ratio $x_3/x_1$ is plotted as a function of the split ratio $\dot{m}_3/\dot{m}_1$. Figure 5.2a contains the results for the same experiments as shown in Fig. 5.1. For stratified flow, the maximum quality ratio $(x_3/x_1)_{max} = 1/x_1$ is reached at very small values of $\dot{m}_3/\dot{m}_1$. For the other inlet conditions, $(x_3/x_1)_{max}$ occurs at split values of $\dot{m}_3/\dot{m}_1 \approx 0.2$. The values of $(x_3/x_1)_{max}$ do not differ very much. For $v_{sL} \geq 0.5$ m/s, there is the tendency that the phase redistribution decreases with increasing inlet mass flow rate and superficial liquid velocity $v_{sL}$, respectively.

Figure 5.2b contains results for a significantly higher superficial gas velocity, $v_{sG} = 40$ m/s. A marked maximum is only observed for the inlet condition with annular flow close to the transition to slug flow, $v_{sL} = 1$ m/s. For the other measurements with annular flow and low liquid inputs, the maximum becomes very flat and $(x_3/x_1)_{max}$ is very close to one.

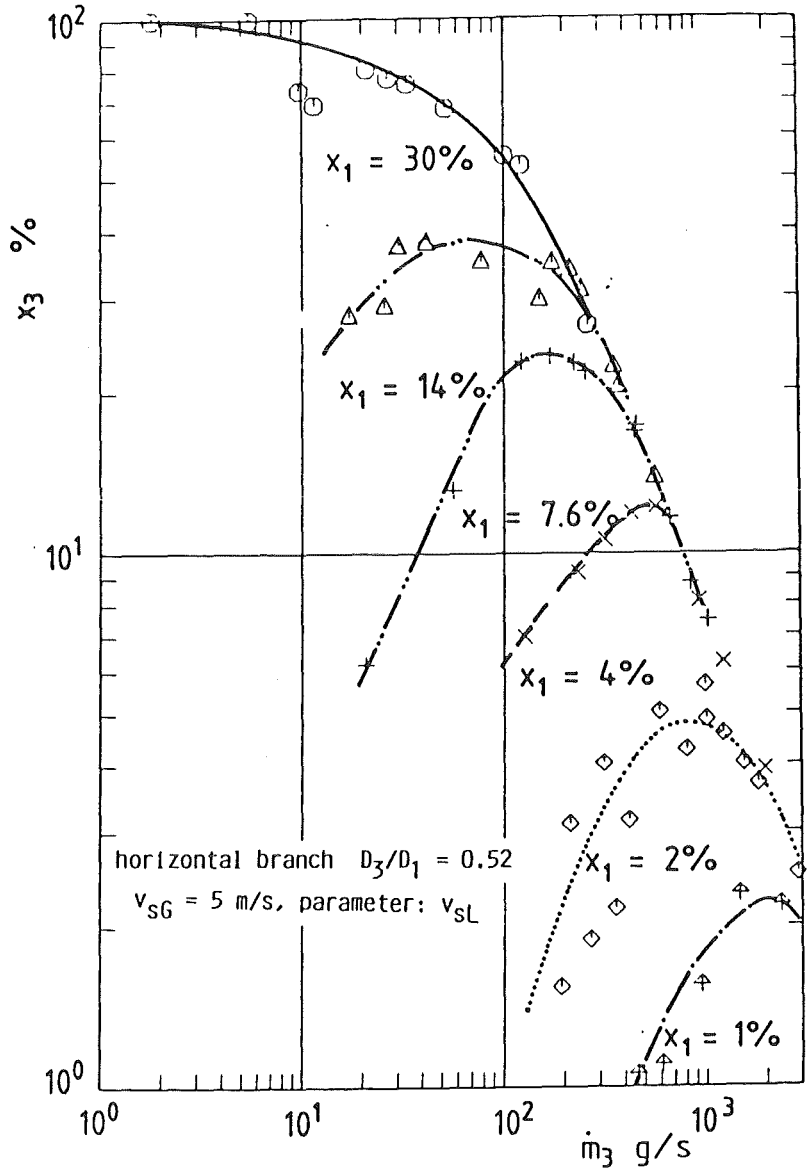


Symbols: $v_{sL}$ = 0.1 m/s: ○ ; 0.25 m/s: △ ; 0.5 m/s: +
$v_{sL}$ = 1.0 m/s: × ; 2.0 m/s: ◇ ; 4.0 m/s: ✦

Fig. 5.1 Branch Quality $x_3$ vs. Branch Mass Flow Rate $\dot{m}_3$ for Horizontal Branch, $v_{sG}$ = 5 m/s, $p_1$ = 0.7 MPa, $D_3/D_1$ = 0.52.

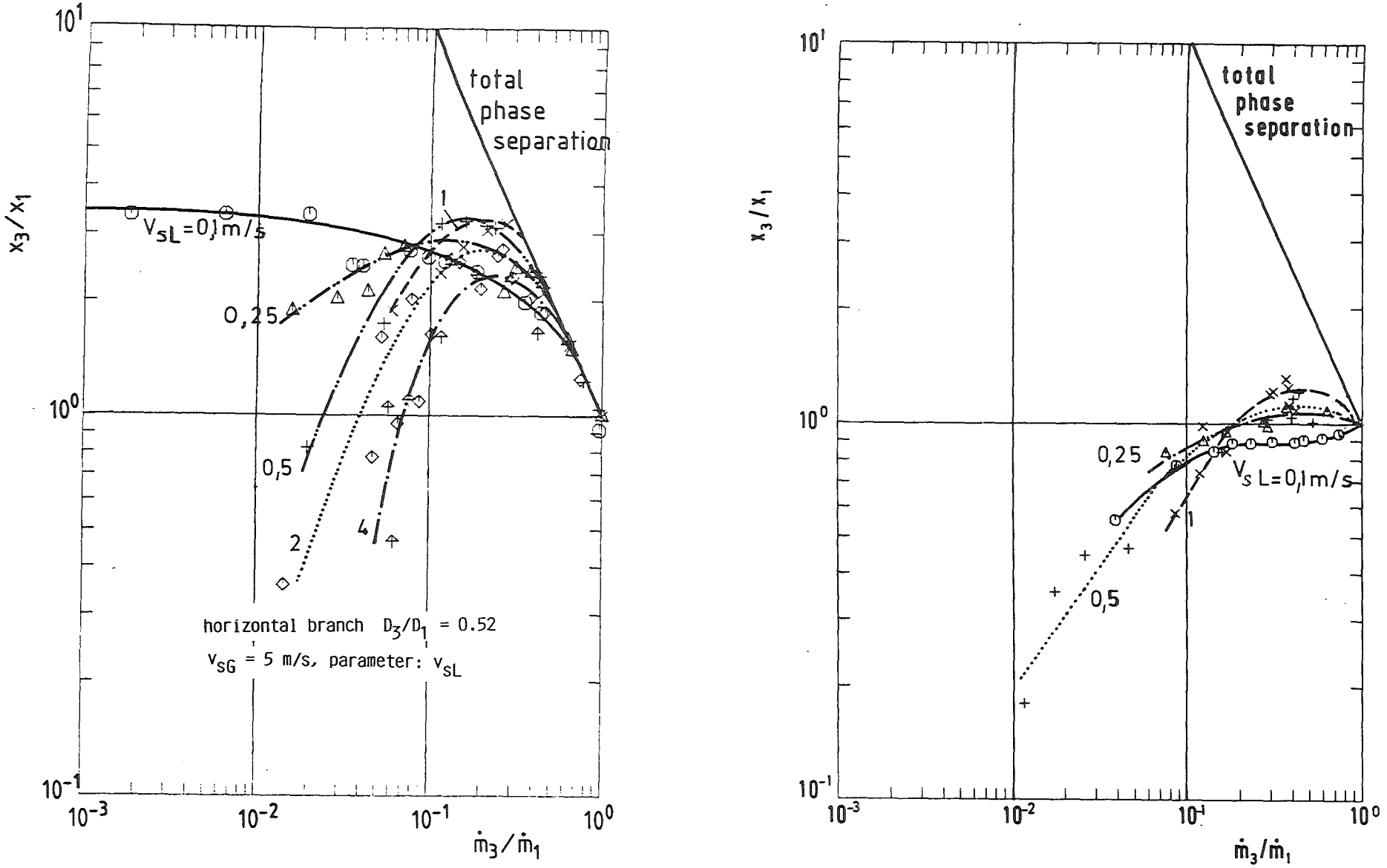


Fig. 5.2 Quality Ratio $x_3/x_1$ vs. Mass Flow Rate Ratio $\dot{m}_3/\dot{m}_1$ for Horizontal Branch, $v_{sG}$ = const., $p_1$ = 0.7 MPa, $D_3/D_1$ = 0.52

Figure 5.3 contains results for $v_{sL}$ = const. and different values of $v_{sG}$. This corresponds to a horizontal line in the flow map. The results shown in Fig. 5.3a mostly belong to the slug flow regime starting close to the elongated bubble regime ($v_{sG}$ = 1 m/s) until the transition to annular flow ($v_{sG} \approx$ 10 - 20 m/s). The test point with $v_{sG}$ = 40 m/s is attributed to the annular flow regime. The maximum values $(x_3/x_1)_{max}$ exhibit larger differences than for $v_{sG}$ = const. For $v_{sG} \geq$2.5 m/s the value decreases with increasing $v_{sG}$.

For the upward branch and $D_3/D_1$ = 1, no maximum value of the quality ratio $(x_3/x_1)_{max}$ was observed for $\dot{m}_3/\dot{m}_1 >> 0$. This could be attributed to the fact that the investigated $\dot{m}_3/\dot{m}_1$ range was limited to $\dot{m}_3/\dot{m}_1 \geq 0.1$, compare Section 2.3.2. For $D_3/D_1$ = 0.52 the measurement range was extended to lower values and a wider range of inlet parameters was investigated. Figure 5.4 contains the results for the same test conditions as investigated in Figs. 5.2b and 5.3b. The curves exhibit a maximum with, in general, higher values compared to the horizontal branch. This maximum is more dependent on $\dot{m}_3/\dot{m}_1$ and often occurs at values $m_3/\dot{m}_1 < 0.1$. For dispersed bubble flow (Fig. 5.4a), the curve is, as expected, close to the curve for the horizontal branch because this flow pattern is characterized by a rather axysimmetric phase and momentum distribution. The same is true for the test points in the annular flow regime (Fig. 5.5b) with the superficial gas velocity $v_{sG}$ = 40 m/s.

Figure 5.5 contains the corresponding results for the downward branch. For small superficial velocities (stratification dominated flow patterns) the branch quality $x_3$ increases strongly with increasing $\dot{m}_3/\dot{m}_1$ until $x_3/x_1$ = 1 is reached for $\dot{m}_3/\dot{m}_1$ = 1. With increasing liquid and gas inputs the quality ratio $x_3/x_1$ can exceed one and, therefore, a maximum occurs. Again, the curve for dispersed bubble flow is close to the curve for the horizontal branch.

For $D_3/D_1$ = 1 and the horizontal branch, the maximum quality ratio $(x_3/x_1)_{max}$ was plotted versus the momentum ratio $(\rho_G/\rho_L)S_1^2$ and the data were fitted by a straight curve using a double logarithm plot (compare Section 2.2.5). Figure 5.6 shows the corresponding presentation for $D_3/D_1$ = 0.52, for details see Table V.I. The different system pressures are characterized by different symbols. For inlet conditions with $0.1 < v_{sL}(m/s) < 4$, the results are fitted again by a straight line given by:

$$(x_3/x_1)_{max} = (\rho_G/\rho_L)S_1^2)^{-0.31}, \qquad (5.1)$$

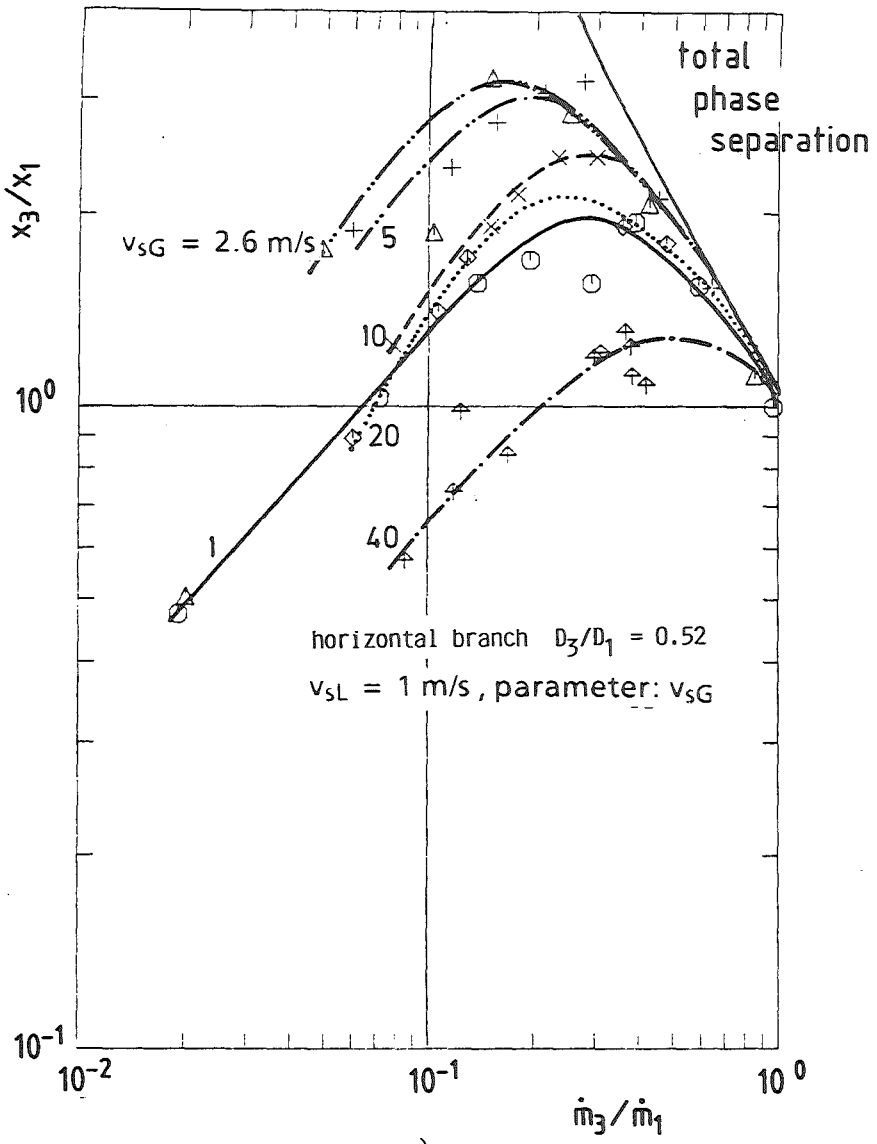


a)

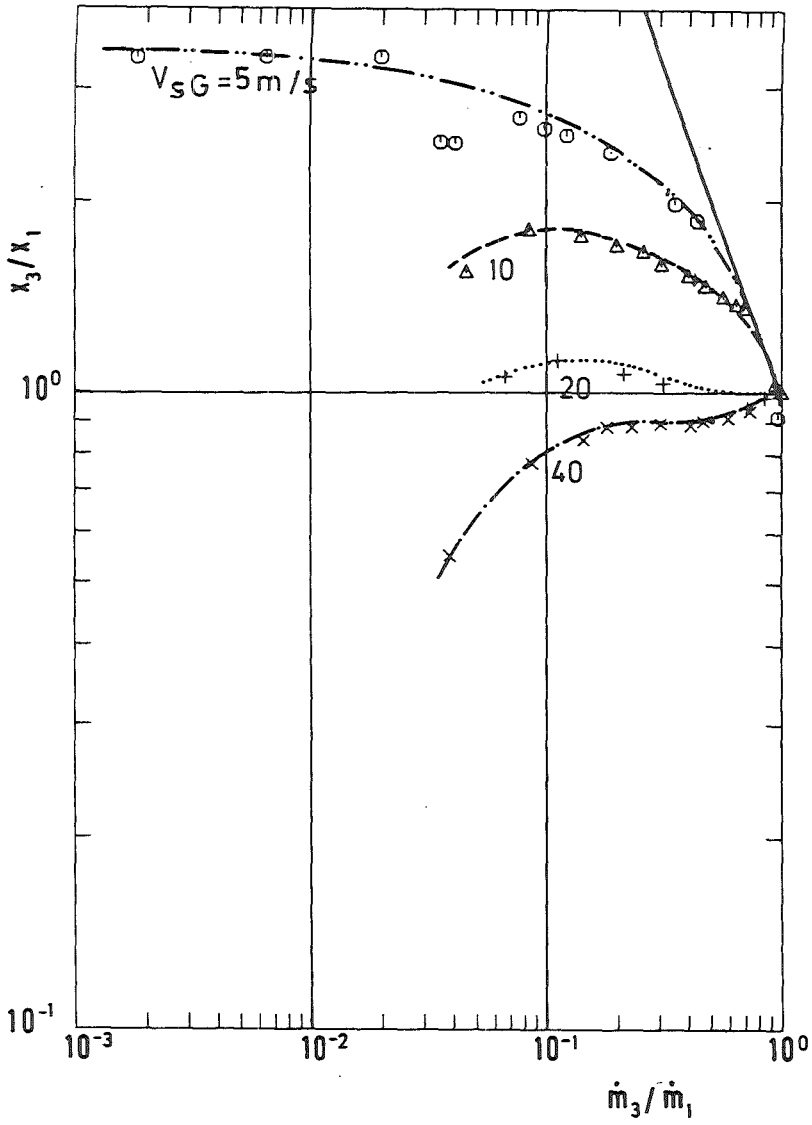


b)

Fig. 5.3 Quality Ratio $x_3/x_1$ vs. Mass Flow Rate Ratio $\dot{m}_3/\dot{m}_1$ for $v_{sL}$ = const., $p_1$ = 0.7 MPa, $D_3/D_1$ = 0.52, Horizontal Branch.

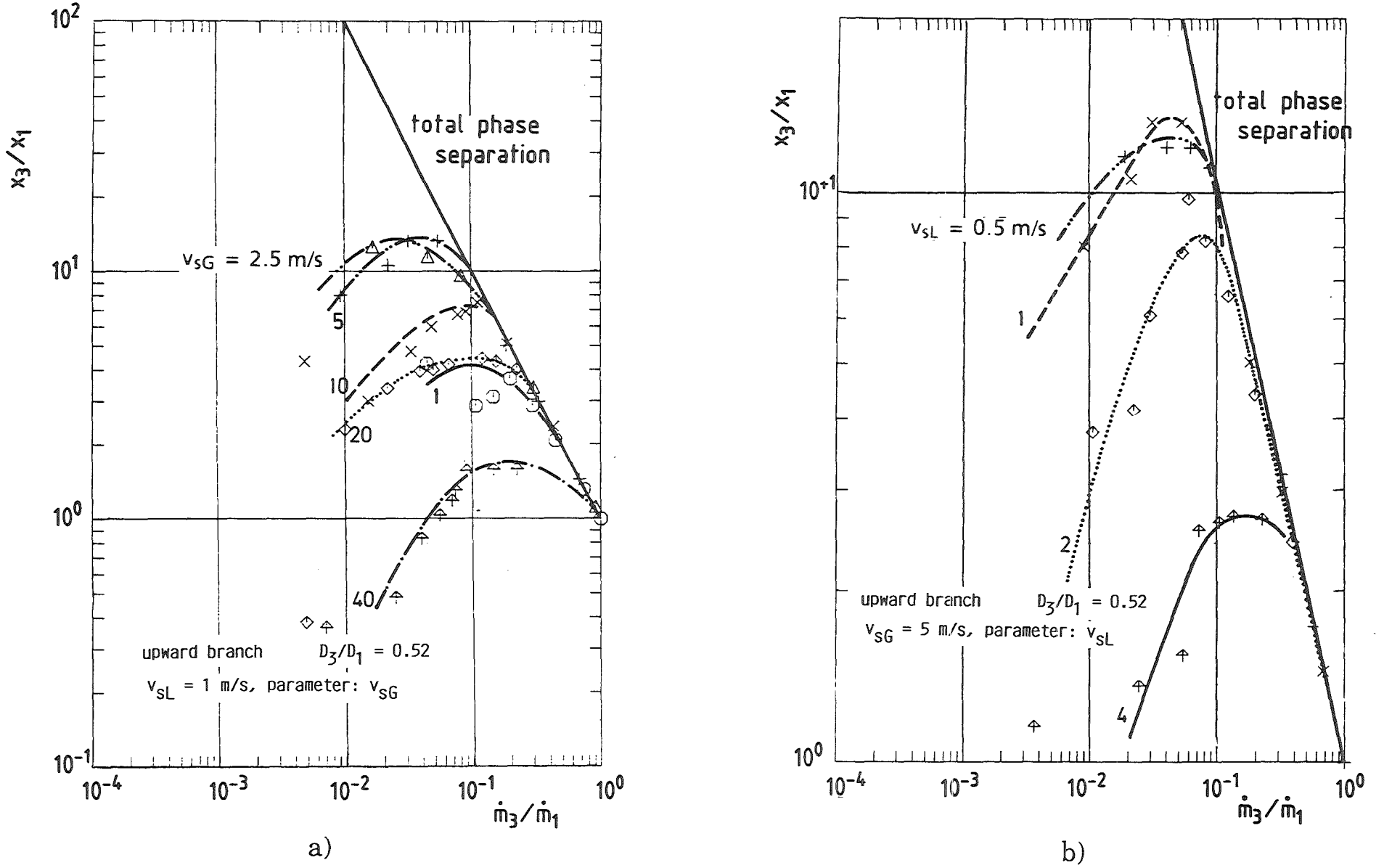


Fig. 5.4 Quality Ratio $x_3/x_1$ vs. Mass Flow Rate Ratio $\dot{m}_3/\dot{m}_1$ for $v_{sG}$ = const. and $v_{sL}$ = const., $p_1$ = 0.7 MPa, $D_3/D_1$ = 0.52, Upward Branch.

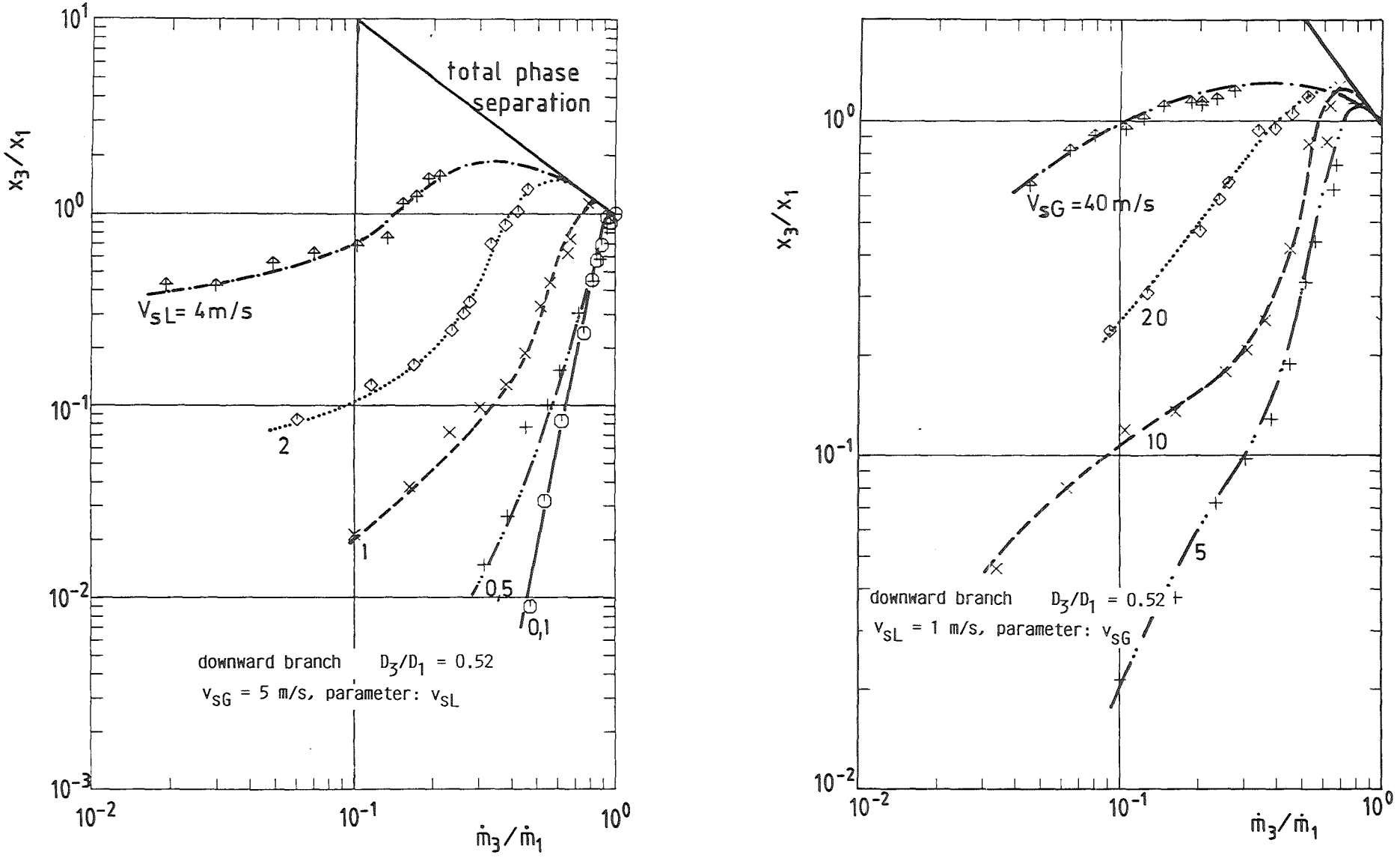


Fig. 5.5 Quality Ratio $x_3/x_1$ vs. Mass Flow Rate Ratio $\dot{m}_3/\dot{m}_1$ for $v_{sG}$ = const. and $v_{sL}$ = const., $p_1$ = 0.7 MPa, $D_3/D_1$ = 0.52, Downward Branch.

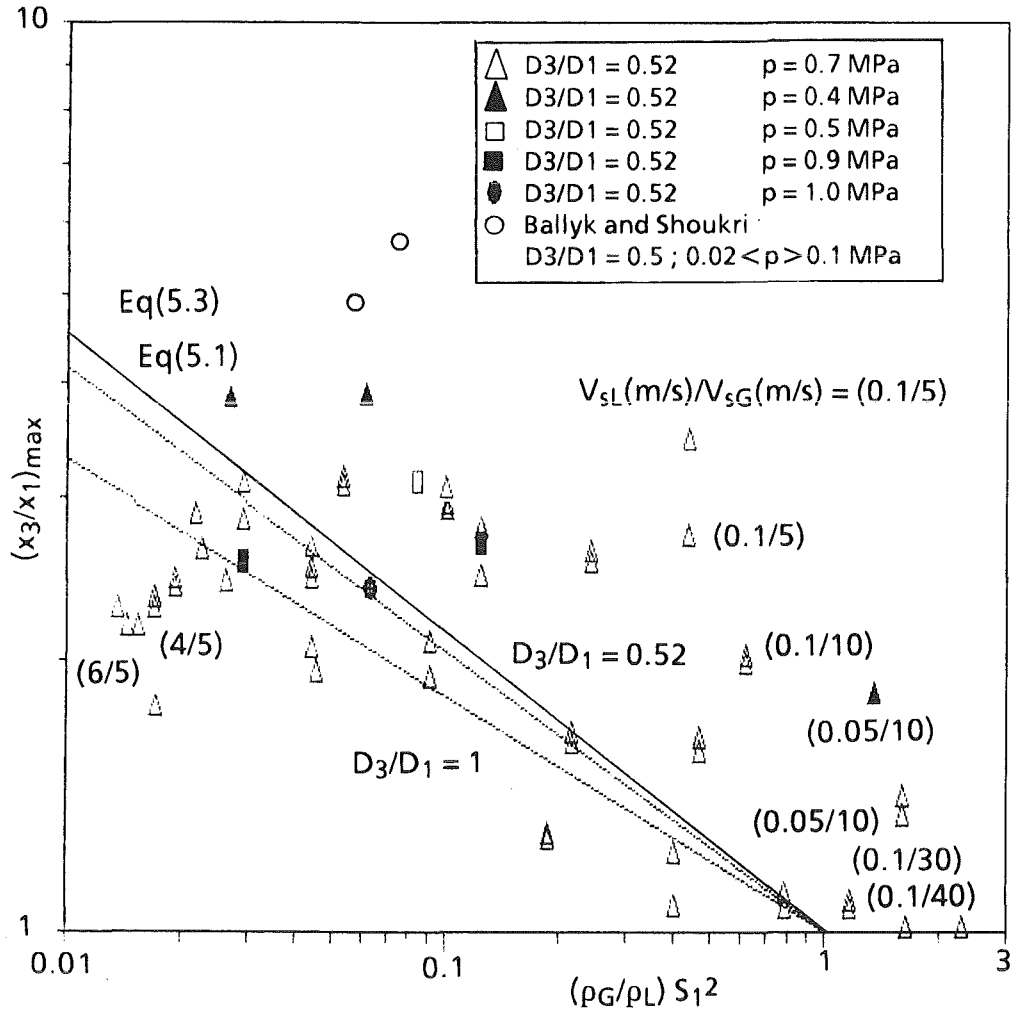


Fig. 5.6 Phase Redistribution Maximum for $D_3/D_1 = 0.52$ and Horizontal Branch

where the slip $S_1$ is calculated again with Rouhani's correlation (Eqs. (2.17)-(2.19).

The parameter range for which Eq. (5.1) is recommended, excludes inlet conditions with dispersed bubble flow, stratified-wavy and annular flow with low mass fluxes, corresponding to low superficial liquid velocities $v_{sL} < 0.1$ m/s. In Fig. 5.6, test points with these flow patterns are characterized by the ratio of the superficial velocities given beside the symbol. For dispersed bubble flow, $(x_3/x_1)_{max}$ is slightly above two as for $D_3/D_1 = 1$, see /26/. For the test points with stratified-wavy flow investigated in this study, the interface level was below the branch pipe entrance. Therefore, $(x_3/x_1)_{max}$ becomes $1/x_1$ for small mass splits, as mentioned previously. For annular flow with low mass fluxes, $(x_3/x_1)_{max}$ is about one.

Figure 5.7 shows $(x_3/x_1)_{max}$ for the upward branch, see also Table VII. Excluding again the above mentioned inlet conditions, the following relationship is proposed:

$$(x_3/x_1)_{max} = ((\rho_G/\rho_L)S_1^2)^{-0.56}. \qquad (5.2)$$

5.1.2 Influence of Diameter Ratio for $0.5 < D_3/D_1 \leq 1$

The diameter effect on the phase redistribution can be explained with the zone of influence (compare Lahey /41/), already introduced by Azzopardi and Whalley /10/: There is a zone of influence in the inlet pipe which increases with increasing transverse pressure difference between inlet pipe and branch entrance. When the branch diameter is reduced, the pressure difference between inlet and branch must be increased to extract the same mass flow rate $\dot{m}_3$ and with this the zone of influence is increased as shown schematically in Fig. 5.8. Due to the increase of void fraction with distance from the pipe wall, a larger portion of two-phase mixture with a higher void fraction is affected by the branch. The gas phase in general has a lower momentum flux than the liquid and is more easily deflected into the branch and, therefore, the phase redistribution increases with decreasing diameter.

This observation was confirmed by Zetzmann's experiments /38/ with a vertical inlet pipe, an example is shown in Fig. 5.9. The maximum quality ratio $(x_3/x_1)_{max}$ increased by a factor of 1.30 going from $D_3/D_1 = 1$ to $D_3/D_1 = 0.5$. Zetzmann

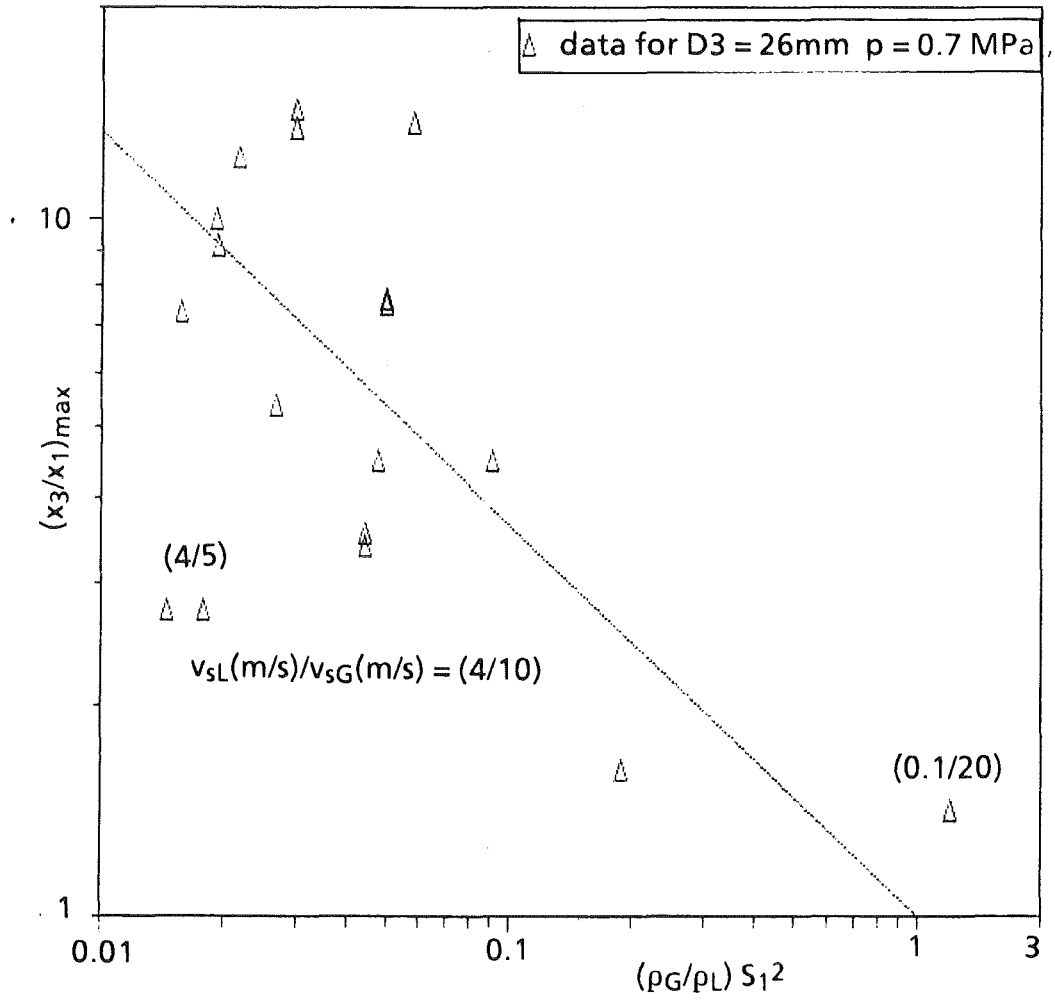


Fig. 5.7 Phase Redistribution Maximum for $D_3/D_1 = 0.52$ and Upward Branch

| p (bar) | $x_1$ (1) | $S_1$ (1) | $v_{SL}$ (m/s) | $v_{SG}$ (m/s) | $(\rho_G/\rho_L)S_1^2$ (1) | $(x_3/x_1)_{max}$ (1) |
|---|---|---|---|---|---|---|
| 4.0000 | 0.0830 | 3.5813 | 0.5000 | 10.0000 | 0.0614 | 3.8600 |
| 5.0000 | 0.1120 | 3.7474 | 0.5000 | 10.0000 | 0.0840 | 3.1300 |
| 7.0000 | 0.1380 | 3.4698 | 0.5000 | 10.0000 | 0.1008 | 2.9300 |
| 9.0000 | 0.1710 | 3.3935 | 0.5000 | 10.0000 | 0.1240 | 2.6900 |
| 4.0000 | 0.0420 | 2.3615 | 1.0100 | 10.0000 | 0.0267 | 3.8100 |
| 7.0000 | 0.0700 | 2.3036 | 1.0300 | 10.0000 | 0.0444 | 2.4300 |
| 10.0000 | 0.1000 | 2.3053 | 1.0000 | 9.9000 | 0.0636 | 2.4000 |
| 4.0000 | 0.4750 | 16.8038 | 0.0500 | 9.9000 | 1.3508 | 1.8100 |
| 7.0000 | 0.6260 | 13.8525 | 0.0500 | 10.3000 | 1.6064 | 1.3300 |
| 4.0000 | 0.6450 | 21.0159 | 0.0500 | 19.9000 | 2.1128 | 1.1000 |
| 7.0000 | 0.8240 | 16.5390 | 0.0500 | 29.8000 | 2.2900 | 0.9800 |
| 7.0000 | 0.2910 | 7.1987 | 0.1000 | 5.0000 | 0.4338 | 3.4300 |
| 7.0000 | 0.4000 | 8.5861 | 0.1000 | 9.9000 | 0.6172 | 2.0000 |
| 7.0000 | 0.6180 | 11.7989 | 0.1000 | 20.3000 | 1.1654 | 1.0700 |
| 7.0000 | 0.7680 | 13.9618 | 0.1000 | 40.3000 | 1.6319 | 1.0000 |
| 7.0000 | 0.0040 | 1.2755 | 1.9800 | 1.0000 | 0.0136 | 2.2500 |
| 7.0000 | 0.0100 | 1.3603 | 1.9900 | 2.5000 | 0.0155 | 2.1500 |
| 7.0000 | 0.0210 | 1.5162 | 2.0000 | 5.0000 | 0.0192 | 2.3800 |
| 7.0000 | 0.0390 | 1.7719 | 2.0000 | 10.0000 | 0.0263 | 2.4100 |
| 7.0000 | 0.0780 | 2.3264 | 2.0000 | 20.1000 | 0.0453 | 1.9100 |
| 7.0000 | 0.0080 | 1.4290 | 1.0000 | 1.0000 | 0.0171 | 1.7500 |
| 7.0000 | 0.0210 | 1.6138 | 1.0000 | 2.6000 | 0.0218 | 2.8500 |
| 7.0000 | 0.0390 | 1.8714 | 0.9900 | 5.0000 | 0.0293 | 2.8200 |
| 7.0000 | 0.0700 | 2.3036 | 1.0300 | 10.0000 | 0.0444 | 2.5000 |
| 7.0000 | 0.1400 | 3.3080 | 0.9800 | 20.0000 | 0.0916 | 2.0700 |
| 7.0000 | 0.2400 | 4.7232 | 1.0100 | 39.5000 | 0.1868 | 1.2700 |
| 7.0000 | 0.6180 | 11.7989 | 0.1000 | 20.3000 | 1.1654 | 1.0500 |
| 7.0000 | 0.3920 | 7.4571 | 0.2500 | 20.3000 | 0.4655 | 1.6200 |
| 7.0000 | 0.2500 | 5.0638 | 0.5000 | 20.0000 | 0.2147 | 1.6000 |
| 7.0000 | 0.1400 | 3.3080 | 0.9800 | 20.0000 | 0.0916 | 1.8900 |
| 7.0000 | 0.0760 | 2.2978 | 2.0000 | 20.1000 | 0.0442 | 2.0400 |
| 7.0000 | 0.6260 | 13.8525 | 0.0500 | 10.3000 | 1.6064 | 1.3900 |
| 7.0000 | 0.4000 | 8.5861 | 0.1000 | 9.9000 | 0.6172 | 1.9500 |
| 7.0000 | 0.2430 | 5.3713 | 0.2400 | 10.0000 | 0.2415 | 2.5300 |
| 7.0000 | 0.1380 | 3.4698 | 0.5000 | 10.0000 | 0.1008 | 3.0400 |
| 7.0000 | 0.0700 | 2.3036 | 1.0300 | 10.0000 | 0.0444 | 2.6400 |
| 9.0000 | 0.0390 | 1.6465 | 2.0000 | 10.0000 | 0.0292 | 2.5600 |
| 7.0000 | 0.0320 | 1.6520 | 2.5300 | 10.1000 | 0.0228 | 2.6200 |
| 7.0000 | 0.0180 | 1.4238 | 4.0700 | 9.6000 | 0.0170 | 2.2500 |
| 7.0000 | 0.7680 | 13.9618 | 0.1000 | 40.3000 | 1.6319 | 0.9200 |
| 7.0000 | 0.5500 | 9.6898 | 0.2500 | 39.1000 | 0.7860 | 1.0900 |
| 7.0000 | 0.3810 | 6.9084 | 0.5100 | 40.2000 | 0.3995 | 1.0550 |
| 7.0000 | 0.2400 | 4.7232 | 1.0100 | 39.5000 | 0.1868 | 1.2500 |
| 7.0000 | 0.0720 | 2.5249 | 0.5100 | 5.0000 | 0.0534 | 3.0600 |
| 7.0000 | 0.1380 | 3.4698 | 0.5000 | 10.0000 | 0.1008 | 2.8900 |
| 7.0000 | 0.2500 | 5.0638 | 0.5000 | 20.0000 | 0.2147 | 1.6400 |
| 7.0000 | 0.3810 | 6.9084 | 0.5100 | 40.2000 | 0.3995 | 1.2070 |
| 7.0000 | 0.1370 | 3.8430 | 0.2500 | 5.0000 | 0.1236 | 2.7700 |
| 7.0000 | 0.2430 | 5.3713 | 0.2400 | 10.0000 | 0.2415 | 2.5900 |
| 7.0000 | 0.3920 | 7.4571 | 0.2500 | 20.3000 | 0.4655 | 1.5600 |
| 7.0000 | 0.5500 | 9.6898 | 0.2500 | 39.1000 | 0.7860 | 1.0500 |
| 7.0000 | 0.2910 | 7.1987 | 0.1000 | 5.0000 | 0.4338 | 2.7100 |
| 7.0000 | 0.1370 | 3.8430 | 0.2500 | 5.0000 | 0.1236 | 2.4500 |
| 7.0000 | 0.0720 | 2.5249 | 0.5100 | 5.0000 | 0.0534 | 3.1300 |
| 7.0000 | 0.0390 | 1.8714 | 0.9900 | 5.0000 | 0.0293 | 3.0700 |
| 7.0000 | 0.0210 | 1.5162 | 2.0000 | 5.0000 | 0.0192 | 2.4300 |
| 7.0000 | 0.0160 | 1.4249 | 2.5200 | 5.0000 | 0.0170 | 2.3100 |
| 7.0000 | 0.0100 | 1.3107 | 4.0200 | 5.1000 | 0.0144 | 2.1500 |
| 7.0000 | 0.0080 | 1.2672 | 5.8400 | 5.3000 | 0.0134 | 2.1900 |

Table V.I Maximum Quality Ratio for Horizontal Branch (Air-water Flow, $D_3/D_1 = 0.52$)

| p (bar) | $x_1$ (1) | $S_1$ (1) | $v_{SL}$ (m/s) | $v_{SG}$ (m/s) | $(\rho_G/\rho_L)S_1^2$ (1) | $(x_3/x_1)_{max}$ (1) |
|---|---|---|---|---|---|---|
| 7.0000 | 0.0104 | 1.3649 | 2.0000 | 2.5000 | 0.0156 | 7.2000 |
| 7.0000 | 0.0205 | 1.5091 | 2.0000 | 5.0000 | 0.0191 | 9.8000 |
| 7.0000 | 0.0400 | 1.7855 | 2.0100 | 10.0000 | 0.0267 | 5.3000 |
| 7.0000 | 0.0762 | 2.3001 | 2.0100 | 19.8000 | 0.0443 | 3.3500 |
| 7.0000 | 0.6261 | 11.9727 | 0.1000 | 20.0000 | 1.2000 | 1.4000 |
| 7.0000 | 0.1398 | 3.2972 | 1.0300 | 20.0000 | 0.0910 | 4.4000 |
| 7.0000 | 0.0762 | 2.3001 | 2.0100 | 19.8000 | 0.0443 | 3.5000 |
| 7.0000 | 0.0787 | 2.6290 | 0.5000 | 5.1000 | 0.0579 | 13.5000 |
| 7.0000 | 0.0402 | 1.8864 | 1.0000 | 5.0000 | 0.0298 | 14.0000 |
| 7.0000 | 0.0209 | 1.5148 | 2.0000 | 5.1000 | 0.0192 | 9.0000 |
| 7.0000 | 0.0105 | 1.3170 | 4.0400 | 5.1000 | 0.0145 | 2.7000 |
| 7.0000 | 0.0205 | 1.8068 | 1.0000 | 2.5000 | 0.0216 | 12.0000 |
| 7.0000 | 0.0402 | 1.8864 | 1.0000 | 5.0000 | 0.0298 | 13.2000 |
| 7.0000 | 0.0787 | 2.4358 | 0.9900 | 10.1000 | 0.0497 | 7.5000 |
| 7.0000 | 0.0759 | 2.3880 | 1.0300 | 10.1000 | 0.0477 | 4.4000 |
| 7.0000 | 0.2416 | 4.7442 | 1.0300 | 39.2000 | 0.1884 | 1.6000 |
| 7.0000 | 0.0787 | 2.4358 | 0.9900 | 10.1000 | 0.0497 | 7.4000 |
| 7.0000 | 0.0400 | 1.7855 | 2.0100 | 10.0000 | 0.0267 | 5.3000 |
| 7.0000 | 0.0204 | 1.4586 | 4.0200 | 10.0000 | 0.0178 | 2.7000 |

Table V.II Maximum Quality Ratio for Upward Branch
(Air-water Flow, $D_3/D_1 = 0.52$)

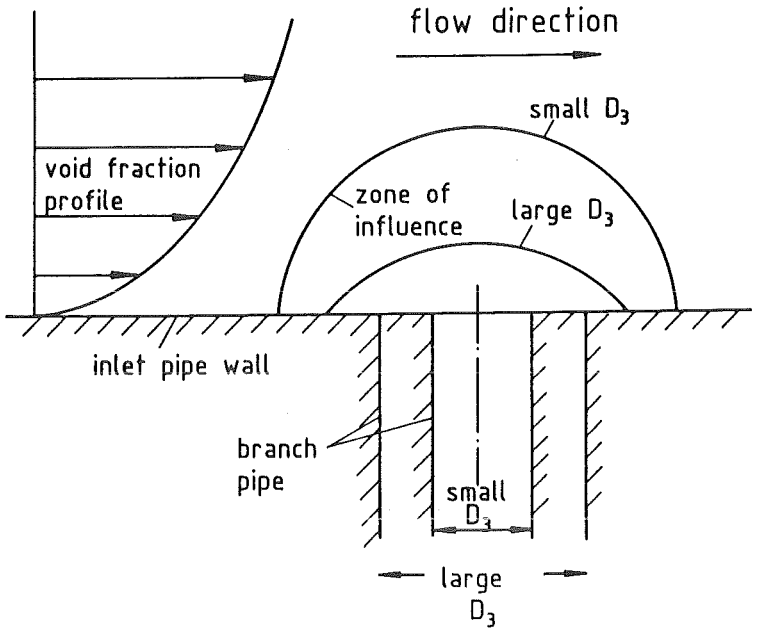


Fig. 5.8 Diameter Effect on Phase Redistribution.

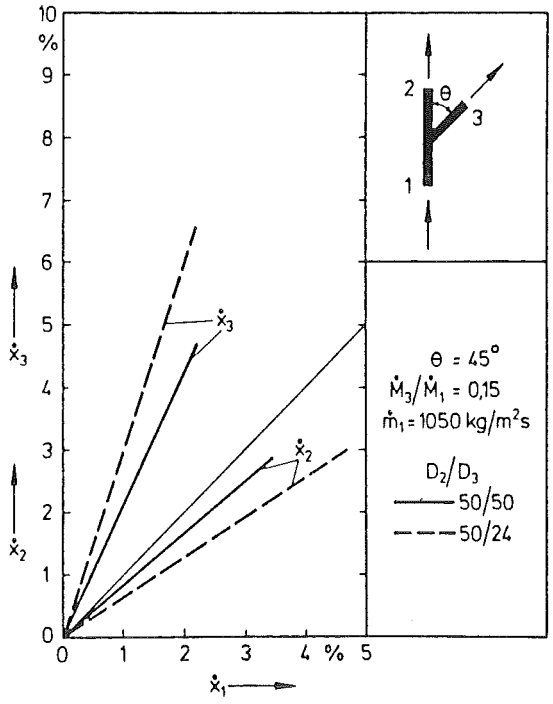


Fig. 5.9 Branch and Run Quality as a Function of Inlet Quality and Diameter Ratio (from /38/)

assumed that $x_3/x_1$ is proportional to a factor a' and different values were given for $D_3/D_1 = 1$ and $D_3/D_1 = 0.48$. However, only for the value given for $D_3/D_1 = 1$, the redistribution curve $x_3/x_1$ goes to one for $\dot{m}_3/\dot{m}_1 \rightarrow 1$. The maximum quality ratio increased by a factor of 1.33, going from $D_3/D_1 = 1$ to $D_3/D_1 = 0.48$. A factor of 1.34 is obtained using Azzopardi's relationship (Eq. (24)) where $x_3/x_1$ is proportional to $(D_1/D_3)^{0.4}$.

Fig. 5.6 contains also the values from Ballyk and Shoukri /34/ for their low pressure steam-water annular flow experiments with $D_3/D_1 = 0.5$. Similar to the results for $D_3/D_1 = 1$, their values are considerably higher than those from the present experiments. Azzopardi's and Zetzmann's relationships are independent on inlet mass flux, respectively momentum flux ratio. Taking into account the present results, the following relationship is finally proposed for the maximum quality ratio

$$(x_3/x_1)_{max} = \left( (\rho_G/\rho_L) S_1^2 \right)^{-0.26 (D_1/D_3)^{0.4}} \quad (5.3)$$

Again, the use of Eq. (5.3) should be limited for the parameter range $0.1 < v_{sL}(m/s) < 4$.

For the total phase redistribution curve, again Eq. (2.14) is suggested with the factor a given by

$$a = 13.9 \left( \left( (\rho_G/\rho_L) S_1^2 \right)^{0.26 (D_1/D_3)^{0.4}} - 1 \right). \quad (5.4)$$

## 5.2 Phase Redistribution for $D_3/D_1 = 0.2$ and 0.08

### 5.2.1 Experimental Results

For small values of $D_3/D_1$, the upper value of the achievable mass flow rate ratio $\dot{m}_3/\dot{m}_1$ is limited by critical flow (choked flow) in the branch, that is $\dot{m}_{3max} = \dot{m}_{3crit}$. In most of the experiments, $\dot{m}_{3max}$ was smaller than that value $\dot{m}_3$ which belongs to the maximum quality ratio $(x_3/x_1)_{max}$. This complicates the comparison with the results for larger diameter ratios.

The smaller the diameter ratio the more the local phase and momentum distribution in the inlet pipe dominates the withdrawl of the phases into the branch.

The Figs. 5.10 and 5.11 show the quality ratio $x_3/x_1$ for different branch directions and diameter ratios with the superficial velocities as parameters. Additonally, some results are presented in a plot with $x_3$ as the ordinate (Figs. 5.12 - 5.15).

For the upward branch and $D_3/D_1 = 0.2$ (Fig. 5.10) the characteristic maximum is clearly seen for $v_{sG} = 5$ m/s and $v_{sL} = 1$ and 2 m/s. For $D_3/D_1 = 0.08$ (Fig. 5.11), $x_3/x_1$ become relatively independent on $\dot{m}_3/\dot{m}_1$. However, the values are lower than those for $D_3/D_1 = 0.2$ if the curves would be extrapolated for the same values of $\dot{m}_3/\dot{m}_1$. At low superficial liquid velocities and decreasing $\dot{m}_3/\dot{m}_1$, a value is reached which corresponds to value close to $x_3 = 100$ %, see e.g. Fig. 5.12. This tendency is also seen in Fig. 5.14 for both the upward and the horizontal branch and stratified or annular flow in the inlet pipe.

For the horizontal branch the data shown in Fig. 5.10 scatter considerably. In general, the dependency of $x_3/x_1$ on $\dot{m}_3/\dot{m}_1$ is generally small. For stratification dominated flow patterns again $x_3$ can be very close to 100 %, see Fig. 5.12 and 5.14.

For the downward flow, a strong increase of $x_3/x_1$ with increasing $\dot{m}_3/\dot{m}_1$ is observed, compare Figs. 5.11 and 5.12. The dependency of $x_3/x_1$ on $\dot{m}_3/\dot{m}_1$ becomes smaller with increasing $v_{sG}$ and $v_{sL}$ (see Figs. 5.14 - 5.15).

### 5.2.2 Influence of Diameter Ratio

Figure 5.16 contains results for a test point with $v_{sL} = 2$ m/s, $v_{sG} = 10$ m/s (slug flow, transition to annular flow in inlet pipe). The following typical tendencies can be observed:

For the horizontal and downward branch, the quality ratio $x_3/x_1$ increases with decreasing diameter ratio $D_3/D_1$ for a given mass split $\dot{m}_3/\dot{m}_1$. This can be explained with the different sizes of the zone of influence, compare Section 5.1.2.

For the upward branch, $x_3/x_1$ for $D_3/D_1 = 1$ was larger than for $D_3/D_1 = 0.5$ at low mass flow rates. This effect was explained by flow reversal in the large branch pipe. The same tendency is observed, however, comparing the data for small diameter ratios. The unexpected behaviour of the data for $D_3/D_1 = 0.08$ is explained in the following way: After the passage of a slug a thick liquid film

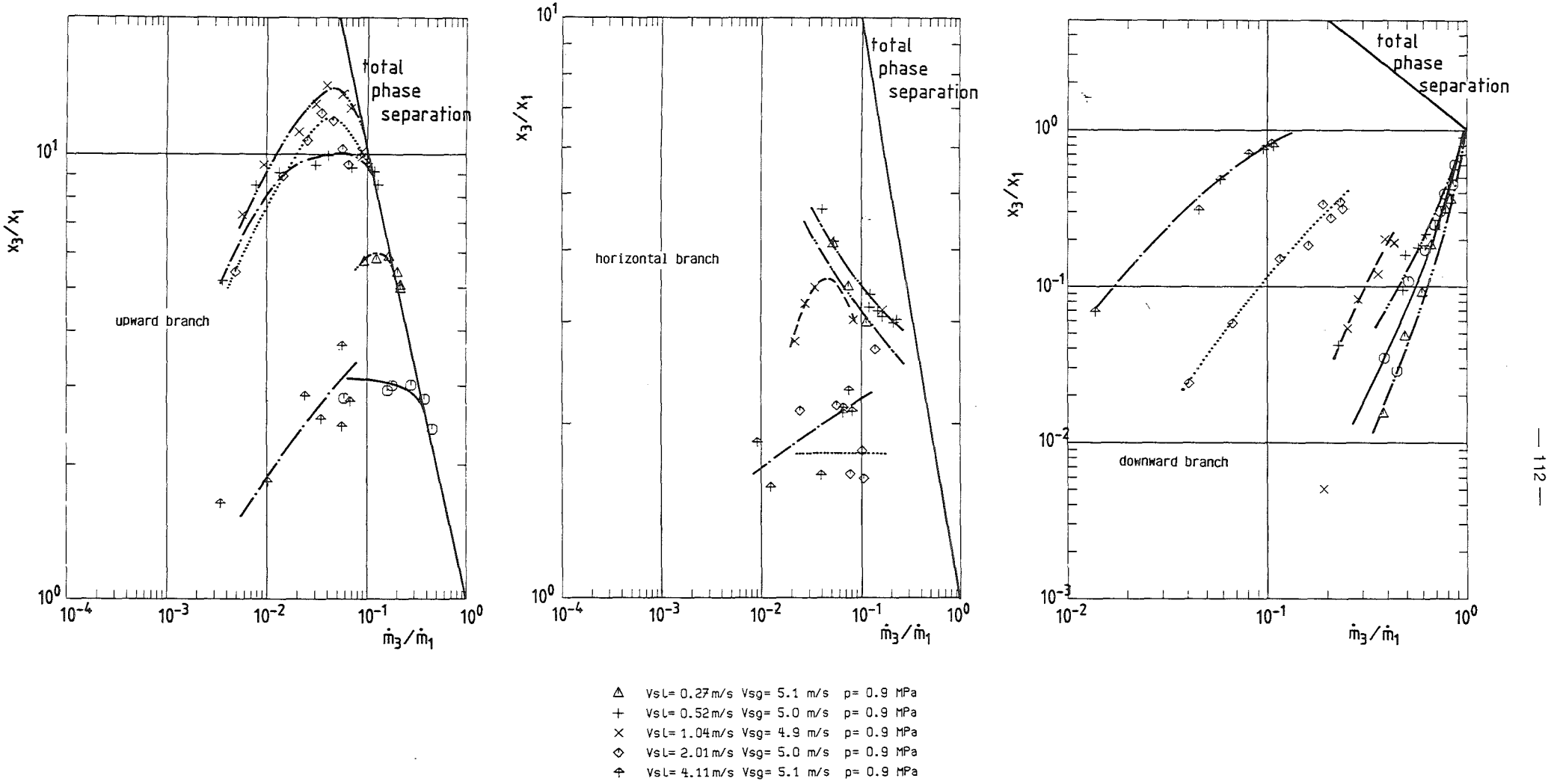


Fig. 5.10 Quality Ratio $x_3/x_1$ vs. Mass Flow Rate Ratio $\dot{m}_3/\dot{m}_1$ for $v_{sG} = 5$ m/s, $p_1 = 0.9$ MPa and $D_3/D_1 = 0.2$

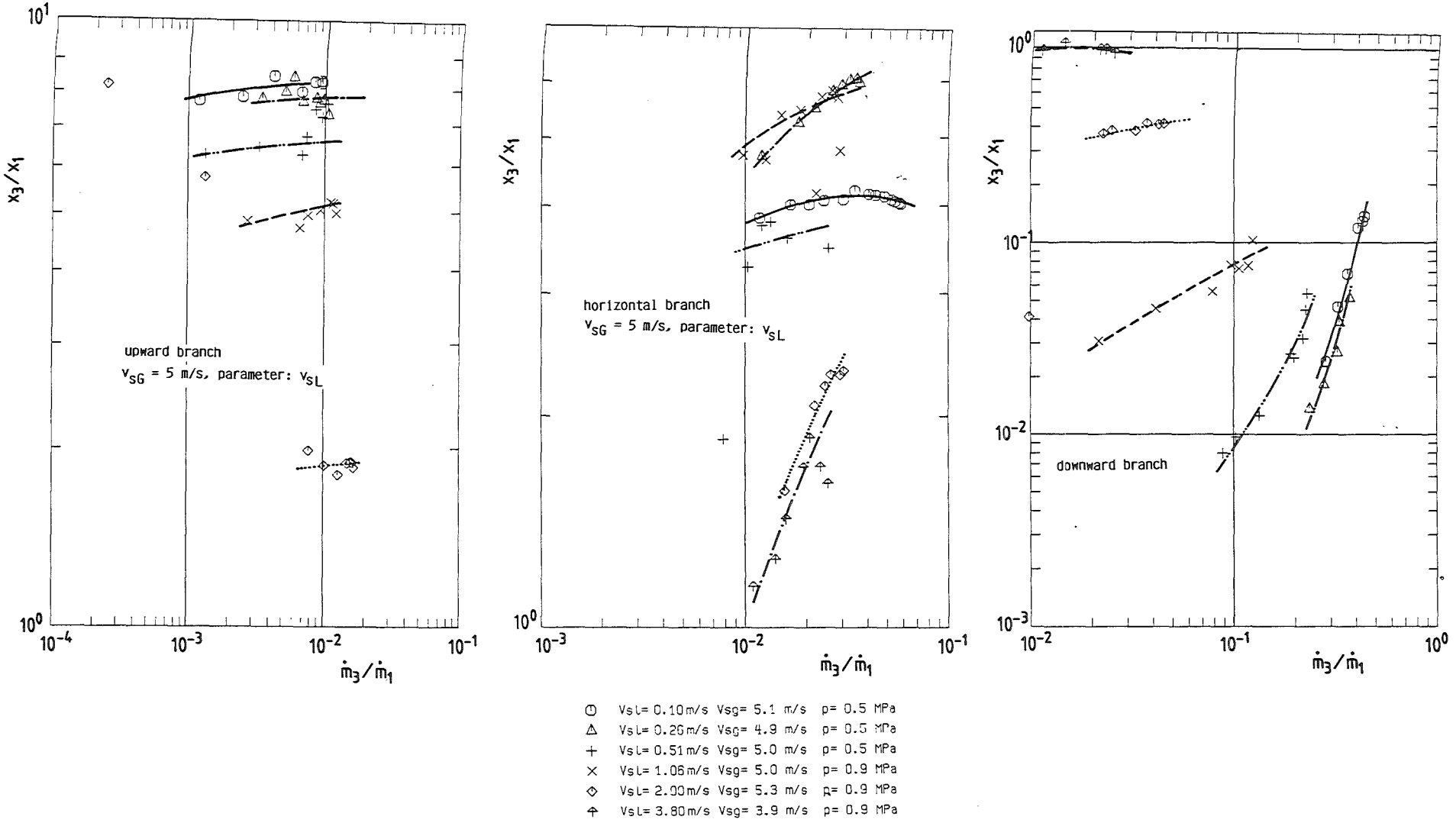


Fig. 5.11 Quality Ratio $x_3/x_1$ vs. Mass Flow Rate Ratio $\dot{m}_3/\dot{m}_1$ for $v_{sG} = 5$ m/s, $p_1 = 0.5$ MPa and $D_3/D_1 = 0.084$

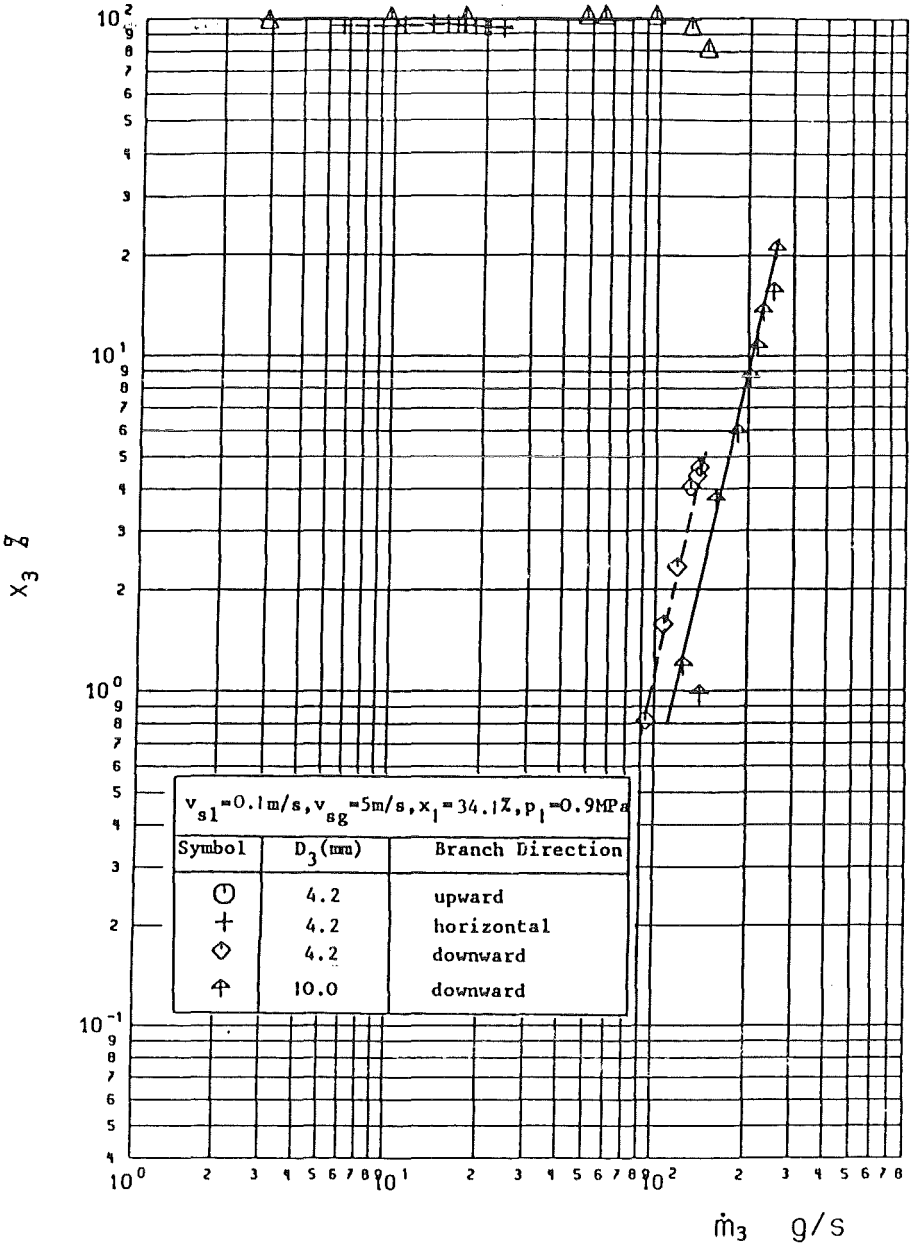


Fig. 5.12 Branch Quality $x_3$ for $v_{sL}$ = 0.1 m/s, $v_{sG}$ = 5 m/s, $D_3/D_1$ = 0.08 and $D_3/D_1$ = 0.2

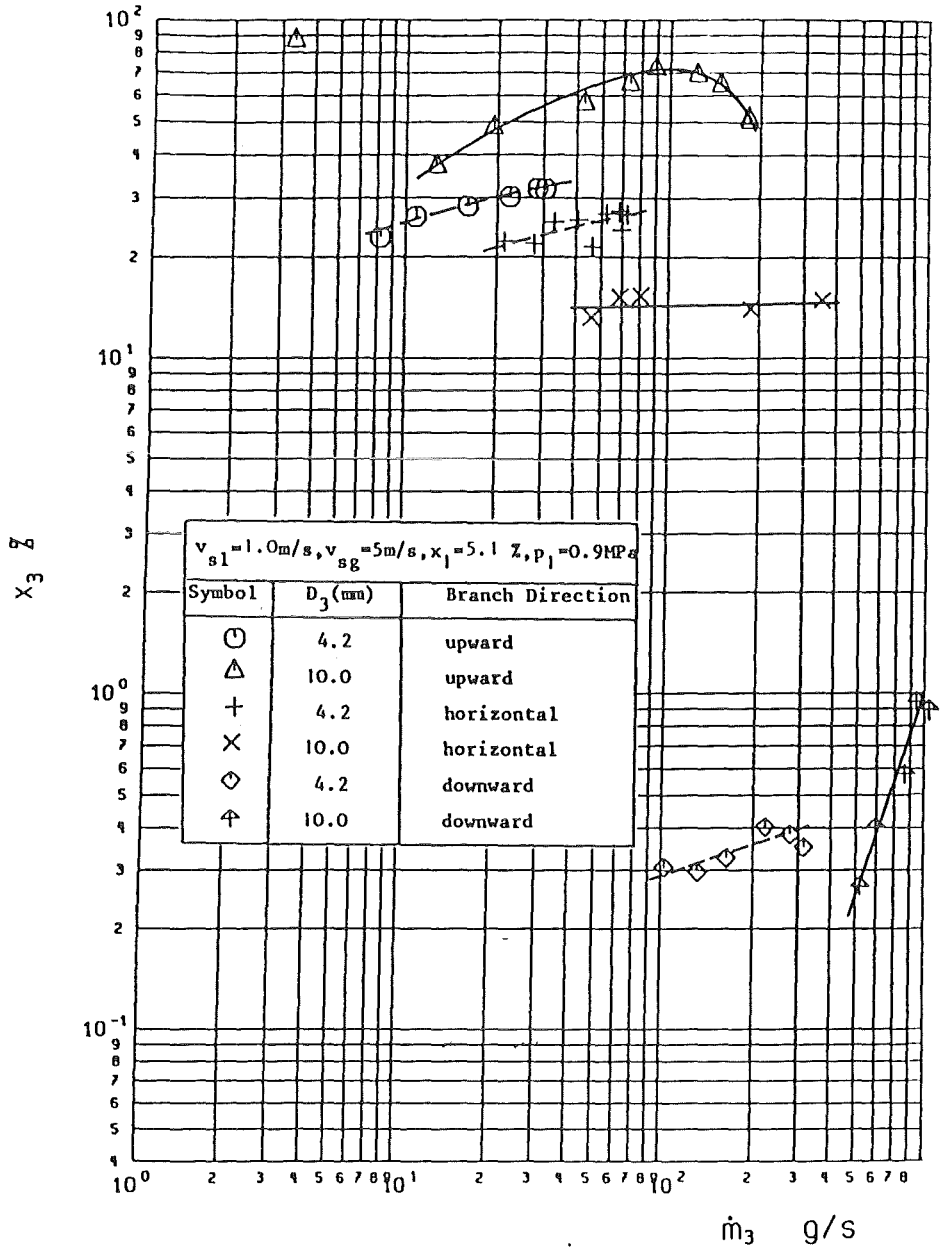


Fig. 5.13 Branch Quality $x_3$ for $v_{sL}$ = 1 m/s, $v_{sG}$ = 5 m/s, $D_3/D_1$ = 0.08 and $D_3/D_1$ = 0.2

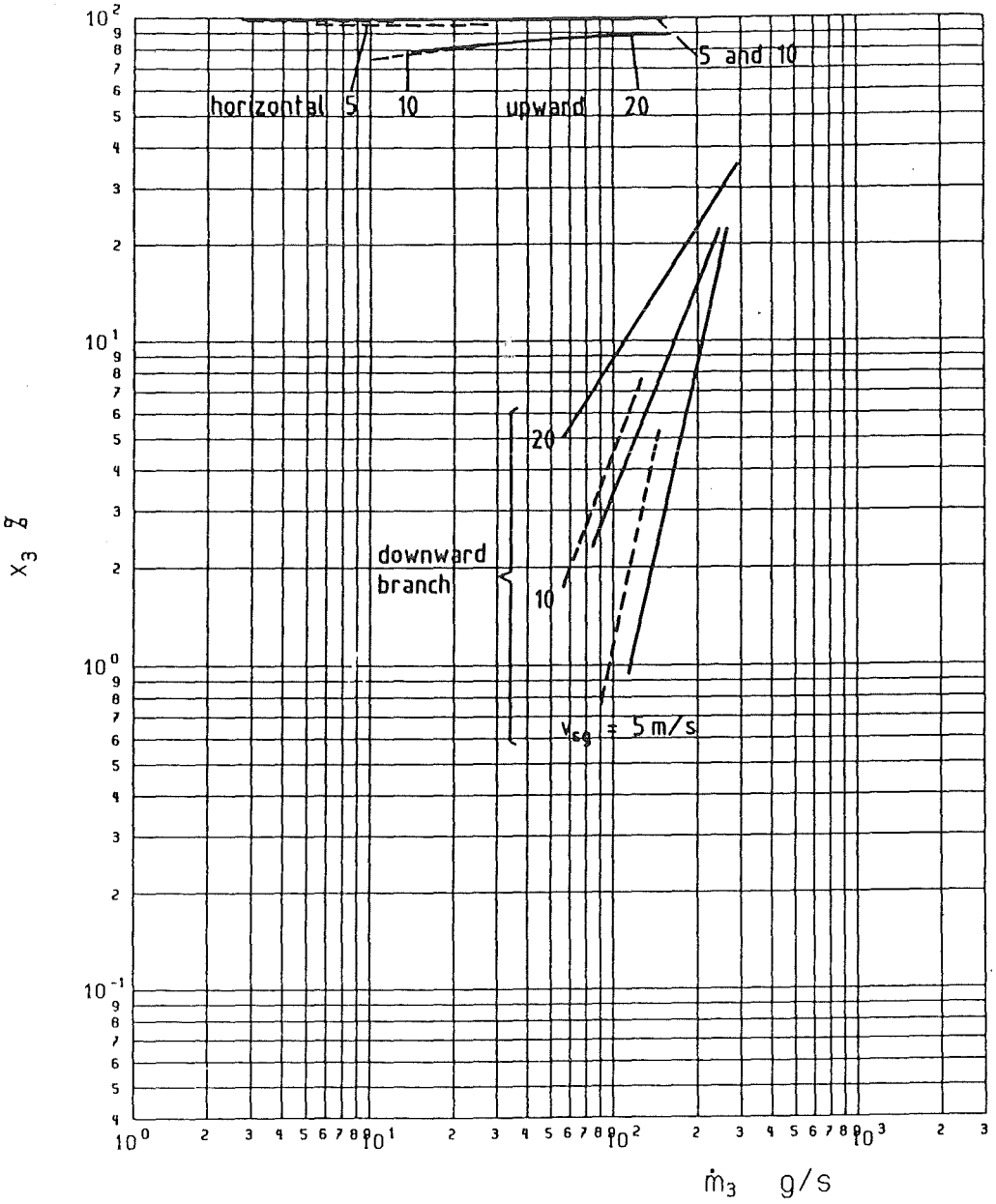


Fig. 5.14 Branch Quality $x_3$ for $v_{sL} = 0.1$ m/s, $v_{sG} = 5;10;20$ m/s, $D_3/D_1 = 0.08$ and $D_3/D_1 = 0.2$

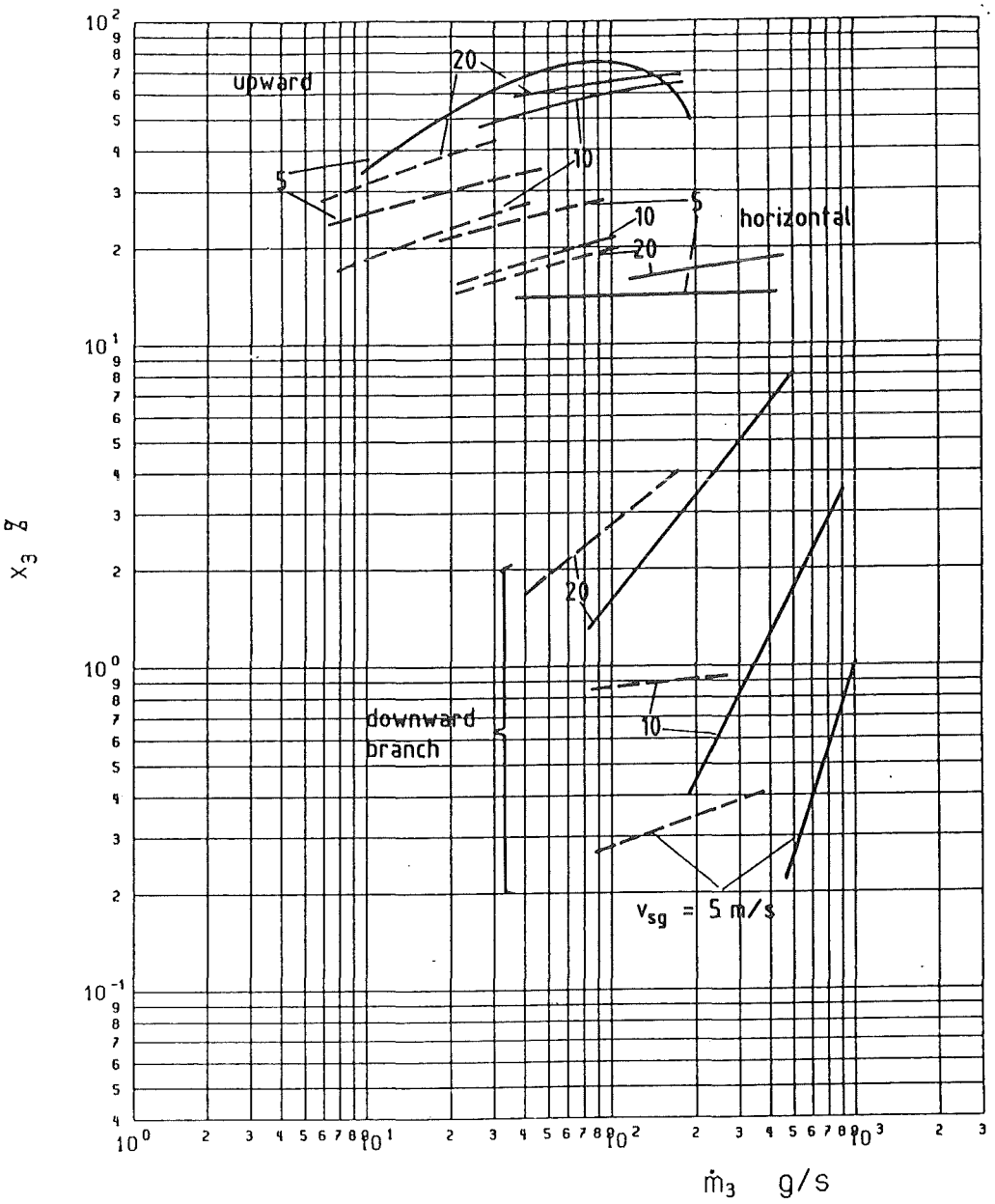


Fig. 5.15 Branch Quality $x_3$ for $v_{sL}$ = 1 m/s, $v_{sG}$ = 5;10;20 m/s, $D_3/D_1$ = 0.08 and $D_3/D_1$ = 0.2

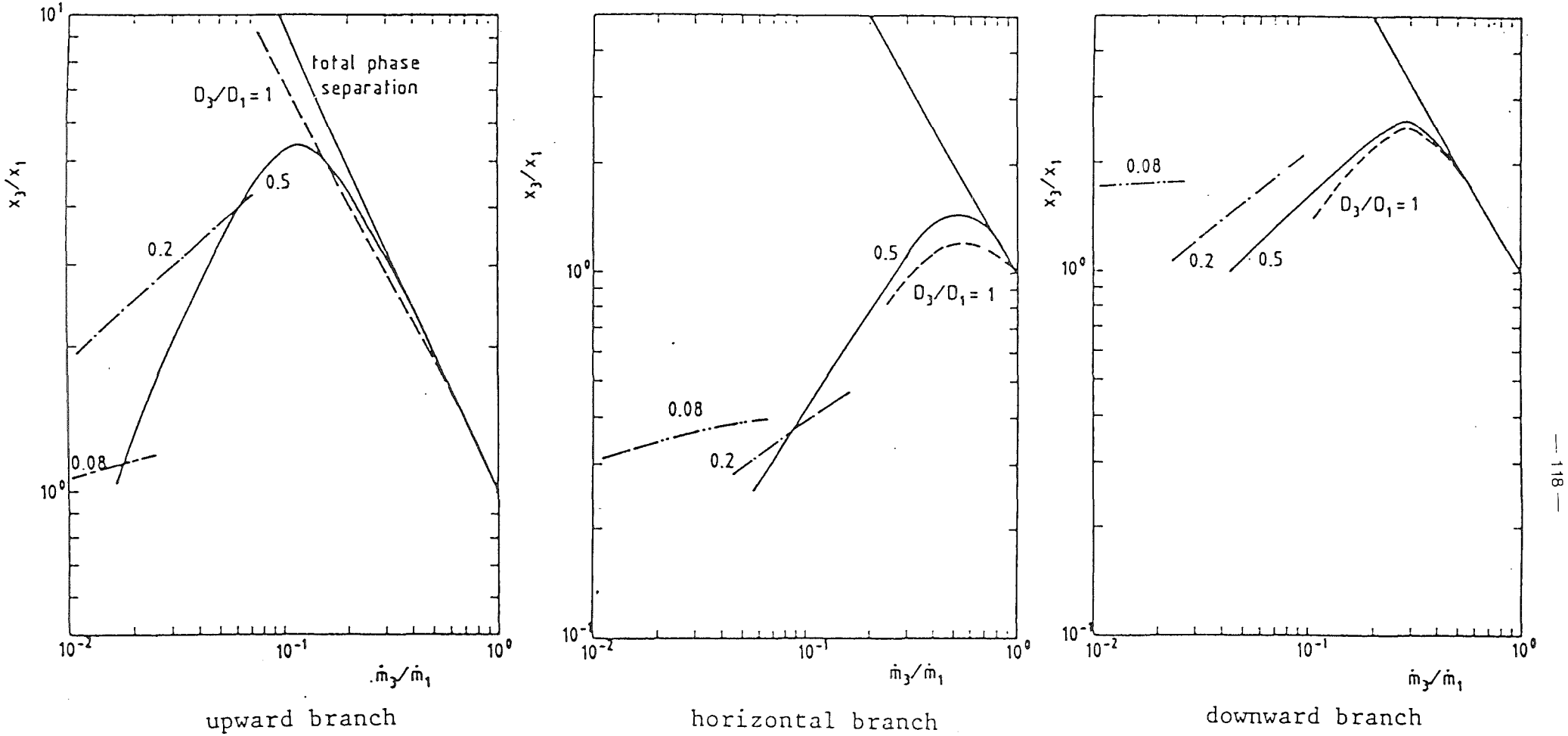


Fig. 5.16 Phase Redistribution for Different Diameter Ratios ($v_{sL}$ = 2 m/s, $v_{sG}$ = 10 m/s, p = 0.7 MPa)

occurs at the wall which gradually drains down. Often this film still exists at the top of the pipe when the next slug arrives. The tickness of this film is no longer small compared to the 4.2 mm branch diameter and the liquid portion extracted into the small branch is therefore larger than for the larger branch.

The tendency that $x_3/x_1$ for $D_3/D_1 = 0.08$ is smaller than for $D_3/D_1 = 0.2$ exists also for other test points in the slug flow regime, compare Fig. 5.15.

For stratified flow patterns without a significant liquid film at the top of the pipe, the branch diameter influence should disappear for small values of $D_3/D_1$, compare 5.2.4.

### 5.2.3 Discussion of Data with Critical Mass Flux

For the data with $D_3/D_1 \geq 0.5$ the characteristic maximum of the quality ratio was very useful to generalize phase redistribution tendencies. For small diameter ratios this maximum in general is not reached because of the limitation of $\dot{m}_3/\dot{m}_1$ due to critical branch flow, as mentioned earlier. However, these critical mass flux data are also very useful to demonstrate general trends.

Figure 5.17 shows these critical branch mass flow rates $\dot{m}_{3crit}$ with the corresponding branch quality $x_3$ as ordinate. The figure also contains the curves for the critical mass flow rate $\dot{m}_{3crit}$ calculated with the homogeneous equilibrium model (compare e.g. Wallis /44/), without taking into account friction effects:

$$\dot{m}_{3crit} = A \frac{\left| 2(1-x_3)p_1(1-p_3/p_1)/\rho_1 + 2(\chi/(\chi-1))x_3 p_1 (1-p_3/p_1^{(\chi-1)/\chi})/\rho_{g1} \right|^{0.5}}{(1-x_3)/\rho_1 + x(p_3/p_1)^{-(1/\chi)}/\rho_{g1}} \quad (5.4)$$

where $A_3$ is the cross section at the branch exit, $\chi$ the isentropic exponent of the gas ($\chi = 1.4$ for air), the index 1 refers to the stagnation conditions in the inlet pipe and the index 3 refers to the critical conditions at the branch exit.

The data for $D_3 = 4.2$ mm are well fitted by the calculated curve except for the vertical upward branch at high qualities. The reason for this are perhaps significant pressure losses due to the phase redistribution in the inlet pipe.

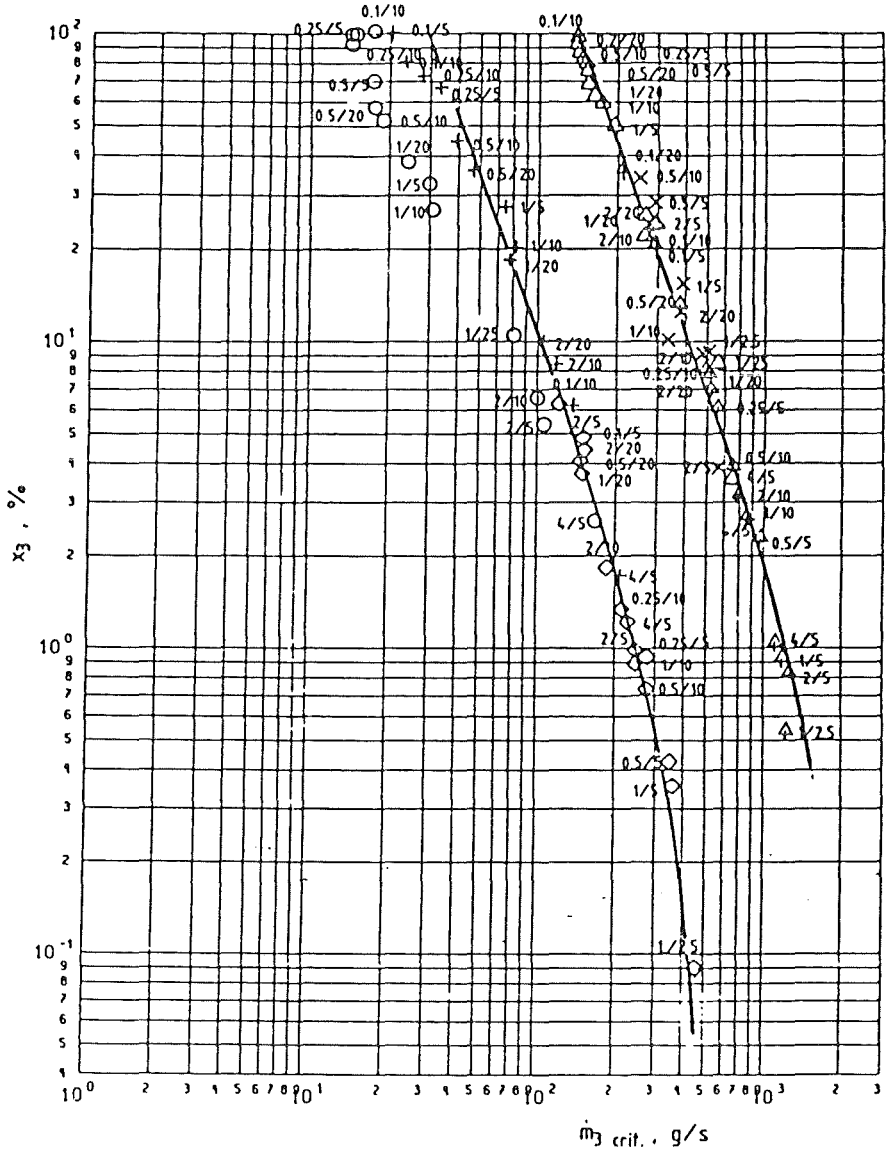


Fig. 5.17 Branch Quality $x_3$ for Critical Mass Flow Rates, $D_3/D_1 = 0.2$ and 0.084.

To fit the data for $D_3 = 10$ mm, Eq. (5.4) was multiplied by a factor of 0.7.This factor takes into account entrance losses due to the sharp-edged entrance and frictional losses in the pipe. The agreement is quite good for all data.

Figure 5.18 shows the branch quality $x_3$ for the critical mass flow data and $D_3 = 10$ mm as a function of the inlet superficial liquid velocity $v_{sL}$. The parameter is the inlet superficial gas velocity $v_{sG}$. The curves can differ more than an order of magnitude for a constant branch orientation. For the upward branch the results for all superficial gas velocities are very close together and up to a superficial liquid velocity of $v_{sL} \approx 0.5$ m/s very close to $x_3 = 1$. The largest dependency exists for the downward branch. The dependency on the superficial liquid velocity becomes smaller if the ratio $x_3/x_1$ is used instead of $x_3$ as shown in Fig. 5.19. For the upward branch larger differences exist between the different curves compared to Fig. 5.18. However, both for high and low values of $v_{sl}$ the curves tend to go to $x_3/x_1 \rightarrow 1$. This tendency also exists for the downward branch, however exhibiting a minimum at $v_{sL} \approx 1$ m/s instead of a maximum for the upward branch. For the downward branch the dependency on $v_{sG}$ is also reduced if $x_3/x_1$ is used as a variable.

For the horizontal branch the values do not show a distinct maximum or minimum and are in general the closest to unity.

The results for $D_3 = 4.2$ mm, Fig. 5.20, exhibit similar tendencies as for $D_3 = 10$ mm, except for the downward branch where the dependency of $x_3/x_1$ on $v_{sL}$ is more expressed.

### 5.2.4 Pressure Dependency of the Phase Redistribution

Phase redistribution is already very difficult to describe for a constant system pressure. The problem becomes even more complicated if the system pressure (or the fluid properties) are changed.

Figs. 5.21 - 5.23 contain some results for $p = 0.5$ and 0.9 MPa for all three branch orientations and $D = 10$ mm. Both $x_3$ and $x_3/x_1$ are plotted as a function of $\dot{m}_3$. The branch quality $x_3$ for the higher system pressure is always higher for the same inlet superficial velocities, which is not surprising, because the density change (a factor of 1.8 from $p_1 = 0.5$ to 0.9 MPa) is expected to have a strong influence. If the

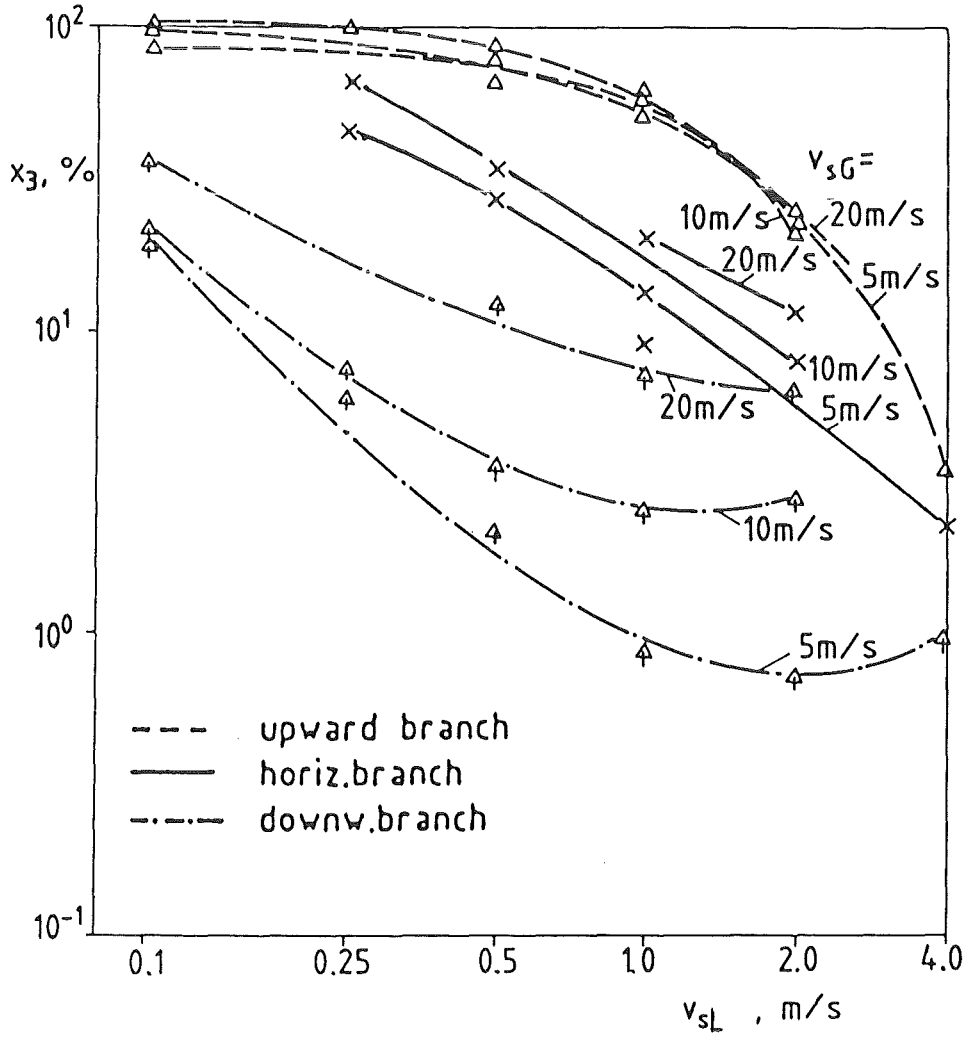


Fig. 5.18 Branch Quality $x_3$ for Critical Mass Flow Rates as Function of $v_{sL}$, $D_1 = 0.2$, $p_1 = 0.9$ MPa.

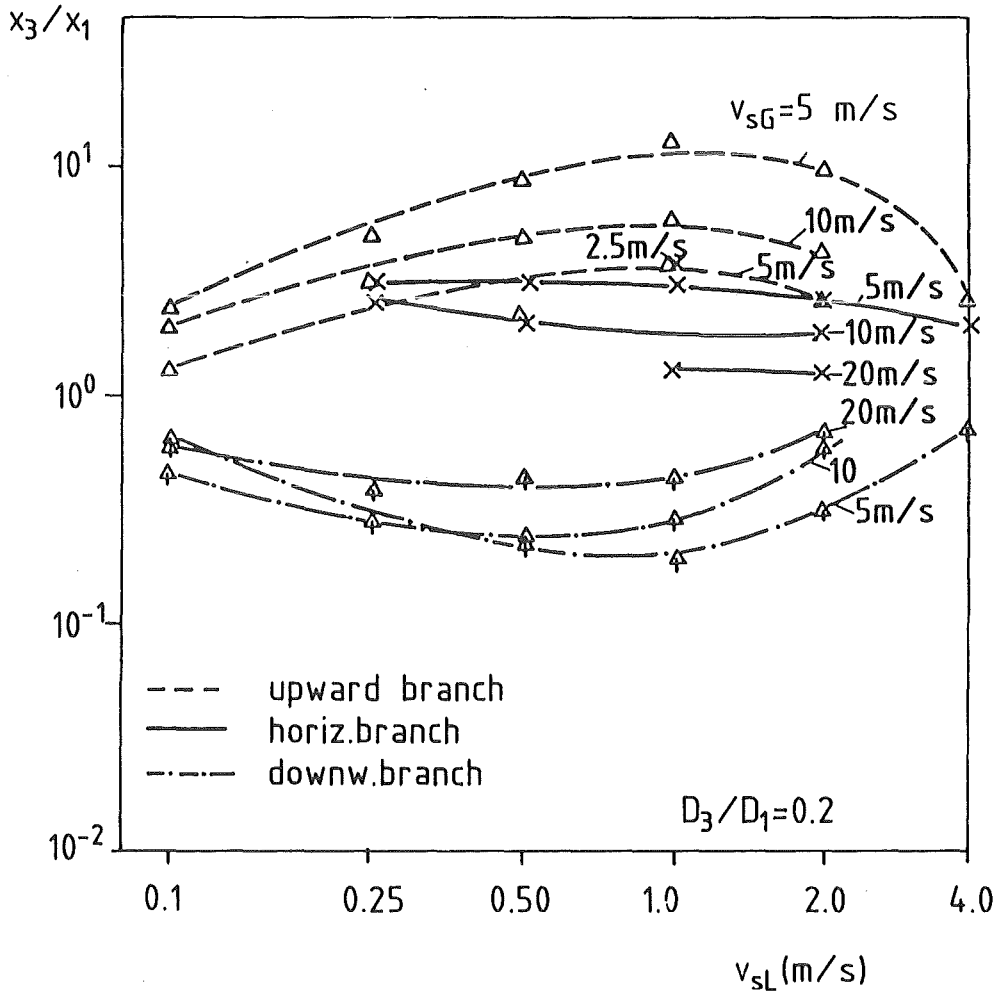


Fig. 5.19 Ratio $x_3/x_1$ for Critical Mass Flow Rates as a Function of Inlet Superficial Liquid Velocity $v_{sL}$; $D_3/D_1$ = O.O84.

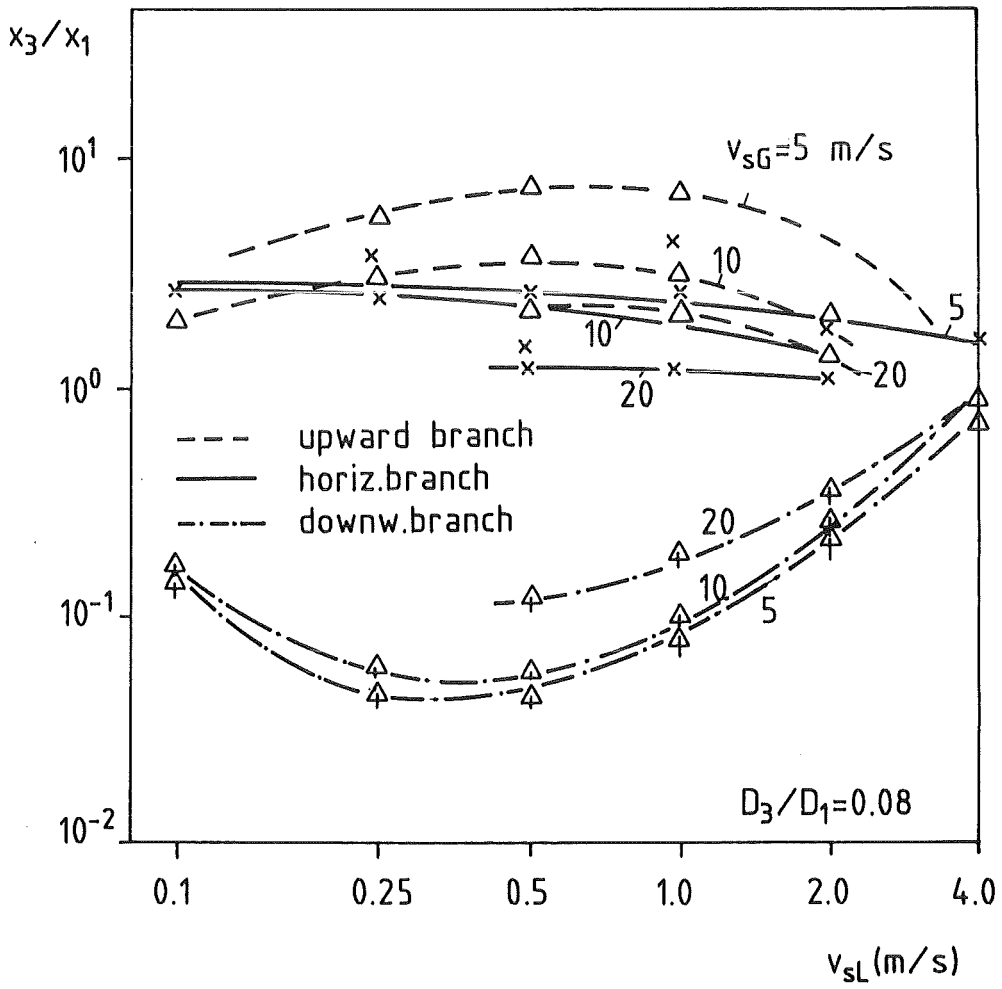


Fig. 5.20 Ratio $x_3/x_1$ for Critical Mass Flow Rates as a Function of Inlet Superficial Liquid Velocity $v_{sL}$; $D_3/D_1$ = O.2.

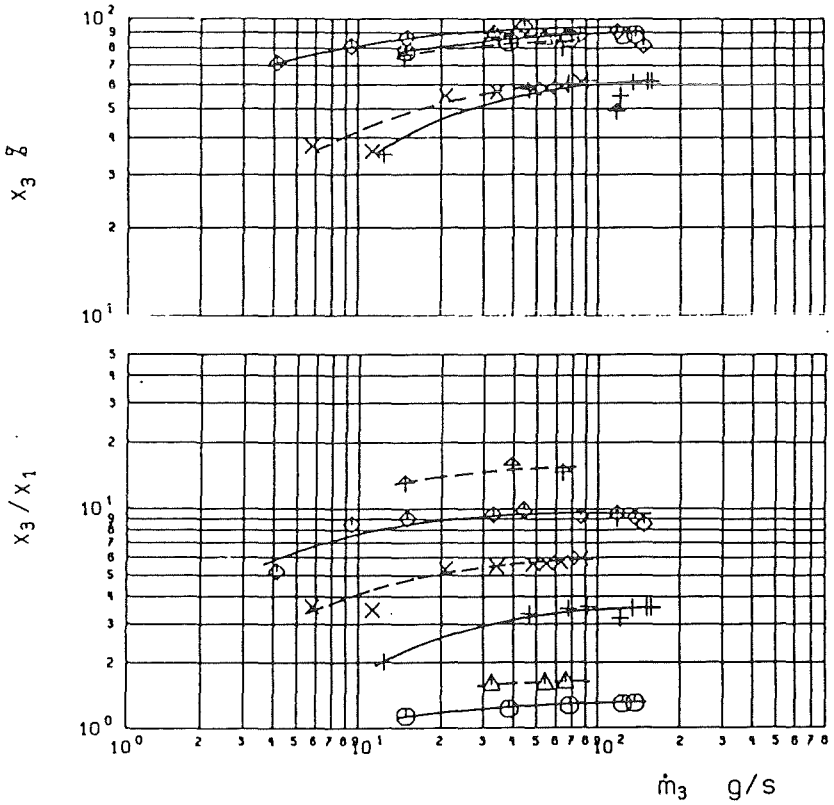


Fig. 5.21 Influence of System Pressure: Upward Branch, $D_3/D_1 = 0.2$.

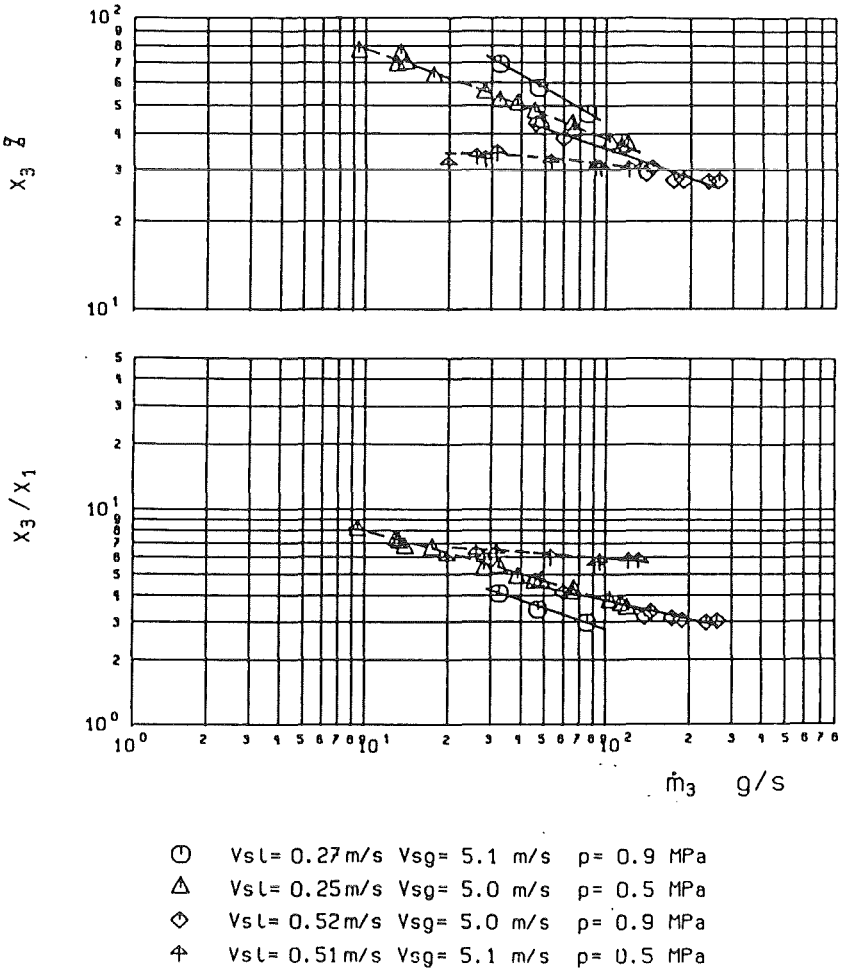


Fig. 5.22 Influence of System Pressure: Horizontal Branch, $D_3/D_1 = 0.2$.

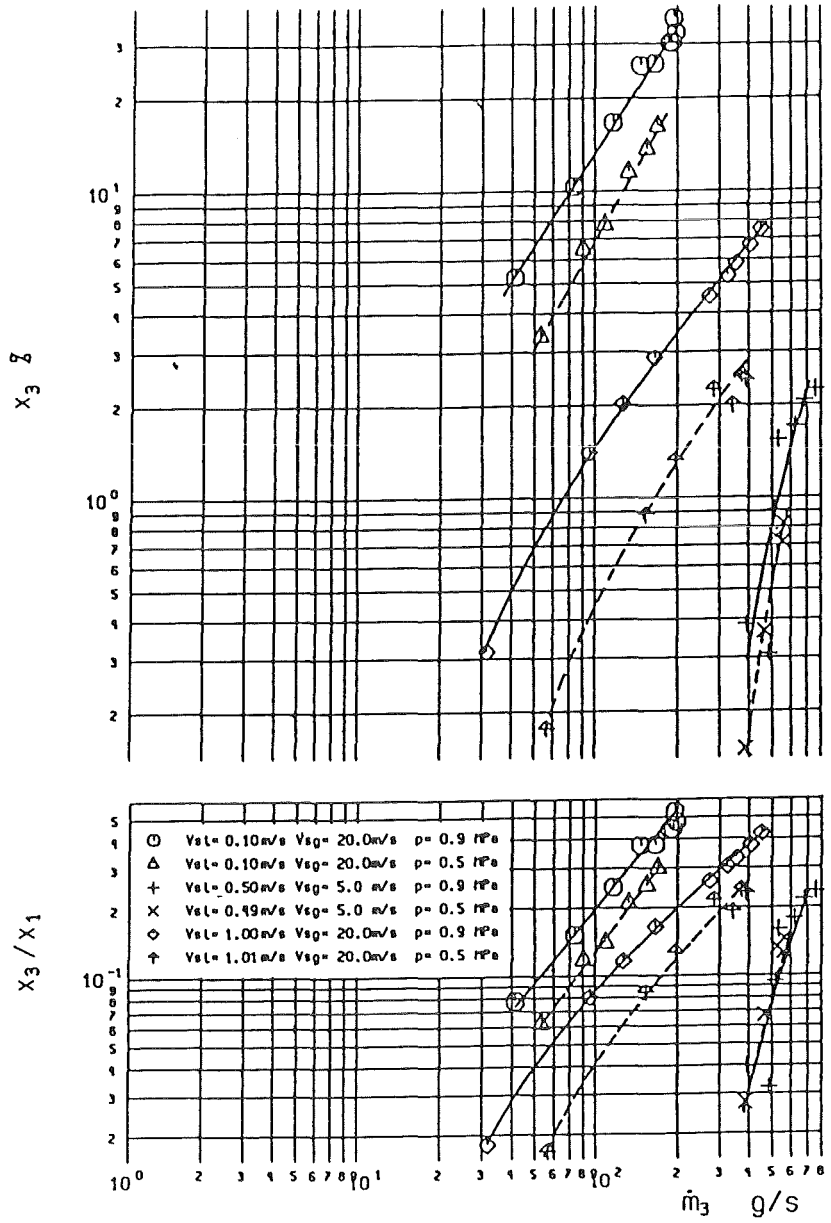


Fig. 5.23 Influence of System Pressure: Downward Branch, $D_3/D_1 = 0.2$.

ratio of the volume flow rates of the single phases into the branch would be independent of pressure, the difference should be about a factor of 1.8. However, if the ratio $x_3/x_1$ is plotted, then both curves should agree. The lower parts of the plots show that this is evidently not the case. For the upward and horizontal branch the data from the lower pressures are now higher, which indicates that the pressure influence is smaller than the gas density ratio. However, for the downward branch the ratio $x_3/x_1$ is still larger for the higher pressure which means that the pressure influence is even larger.

For $D_3/D_1 \leq 0.5$, the pressure influence was described in terms of the momentum ratio $(\rho_G/\rho_L)S^2_1$, where the slip was evaluated with cross section averaged quantities. For small branch diameters the description with local values should be more adquate. However, these local values are not known. Therefore, in a first attempt again Eq. ( 2.15) could be used. The data base given in the Appendix should be suited for further modelling attempts.

### 5.2.5 Phase Redistribution for Stratified Flow

In the following, the model given by Smoglie and Reimann /16-19/ for ideally stratified flow (see Section 2) is applied for some test points with $v_{sL} \geq 0.05$ m/s. In contrast to the model assumptions, a wavy flow existed in the experiments.

For the upward branch, the interface level was always too low to obtain liquid entrainment and the model predicts $x_3 = 1$.

With the horizontal branch additional experiments were performed where the interface level was measured with a traversing impedance-Pitot-tube probe. Figure 5.24 shows a comparison between measured and calculated values branch qualities. The gas-liquid interface is below the pipe axis in this experiment. At very low differential pressures, (low branch mass flow rates $\dot{m}_3$), the model predicts a single-phase gas flow into the branch. In practice, there is some droplet entrainment above the wavy interface and the measurements are slightly below $x_3 = 100$ %. With increasing mass flow rate, a point is reached where due to the lower local pressure at the interface, the interface level is raised and liquid from the interface is sucked into the branch. Further increase of the pressure difference increases considerably the liquid fraction and the branch quality increases. The liquid entrainment into the 10 mm diameter branch starts at a

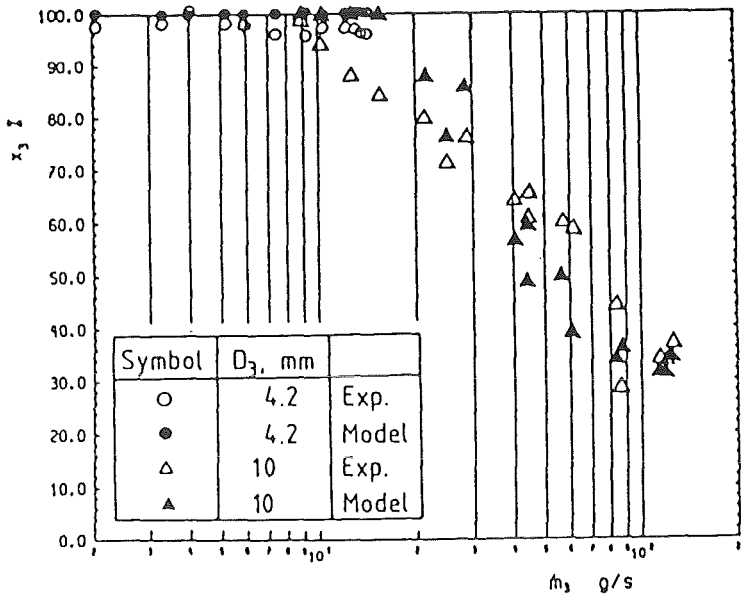


Fig. 5.24 Experimental and Calculated Branch Qualities for Horizontal Branch ($v_{sL}$ = O.O5 m/s, $v_{sG}$ = 8.O m/s, $p_1$ = 0.5 MPa).

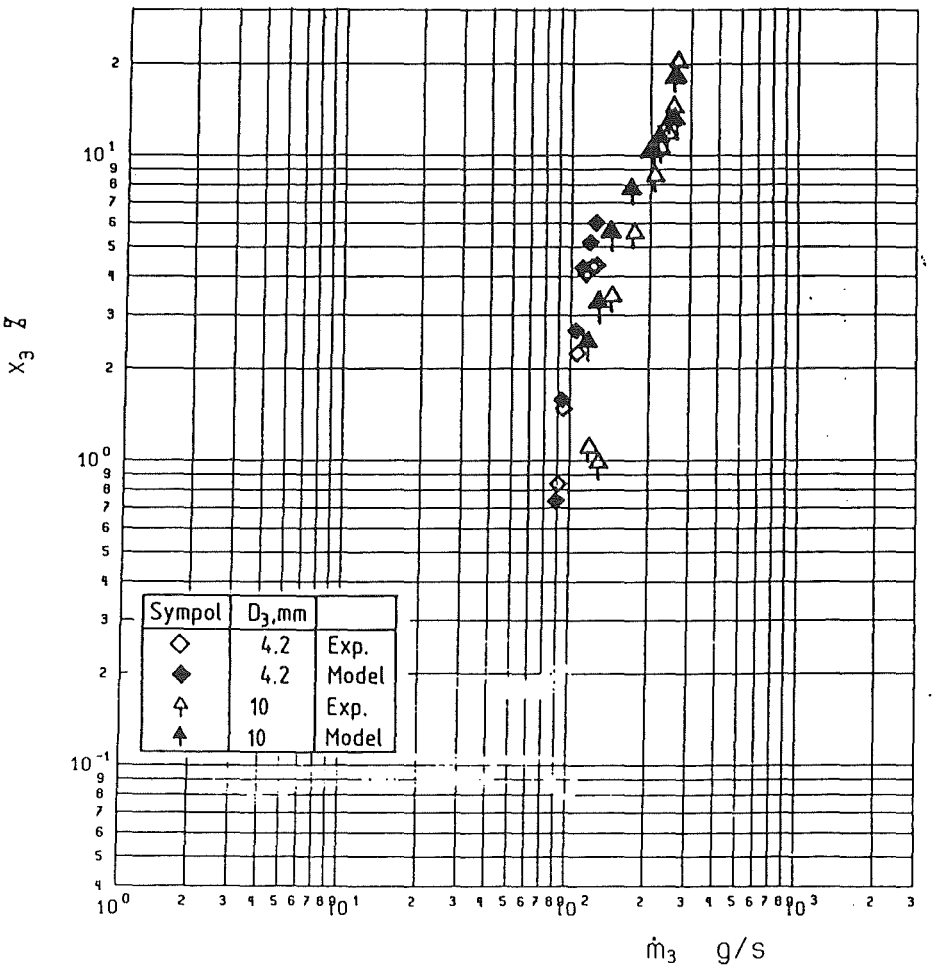


Fig. 5.25 Experimental and Calculated Branch Qualities for Downward Branch ($v_{sL}$ = O.1 m/s, $v_{sG}$ = O.5 m/s, $p_1$ = O.9 MPa).

lower mass flow rate than predicted. This is due to the fact that the distance between interface and the lowest point of the horizontal branch is smaller than the distance between interface and pipe axis which is used in the calculation. In general, the agreement is quite good.

Figure 5.25 compares the results for the downward branch. For this example the interface level was not measured but calculated with Rouhani's slip correlation (Eqs. (2.17)-(2.19)) in combination with Eq. (3.17), assuming ideally stratified flow.

Again, the agreement is very satisfactory for this example. In general, deviations from the ideal stratified flow (waves, air entrainment in liquid layer etc.) have a strong influence on the entrainment process. Further work to model these processes is required to obtain a good accuracy for a wider range of input values.

## 5.3 New Results on Phase Redistribution for $D_3/D_1 = 1$

The previously investigated test matrix (Refs. /21/-/27/) was restricted to relatively high values of $v_{sL}$, compare Fig. 4.8. New experiments were performed with inlet conditions at very low mass fluxes. These data can be compared with results from Hong /8/ and Shoham et al. /33/.

Additionally, two test runs with higher mass fluxes ($v_{sL} = 1$ m/s) were performed, as shown in Fig. 5.26. The agreement with previous results is good, compare Fig. 2.6b.

Figure 5.27 contains the results for the low inlet mass fluxes. For $v_{sL} = 0.05$ m/s and $v_{sG} = 5$ m/s a stratified wavy flow occurs in the inlet pipe. At $v_{sG} = 20$ m/s the flow pattern belongs to the wavy-annular flow regime. For $v_{sL} = 0.5$ m/s and $v_{sG} = 20$ m/s, the flow pattern is in the transition region from slug to annular flow.

For $v_{sL} = \text{const} = 0.05$ m/s the quality ratio $x_3/x_1$ is very close to one and the dependency of $x_3/x_1$ on mass split is small. With increasing $v_{sG}$, the quality ratio decreases. For $v_{sG} = \text{const} = 20$ m/s and wavy annular flow, again the quality ratio is very close to one.

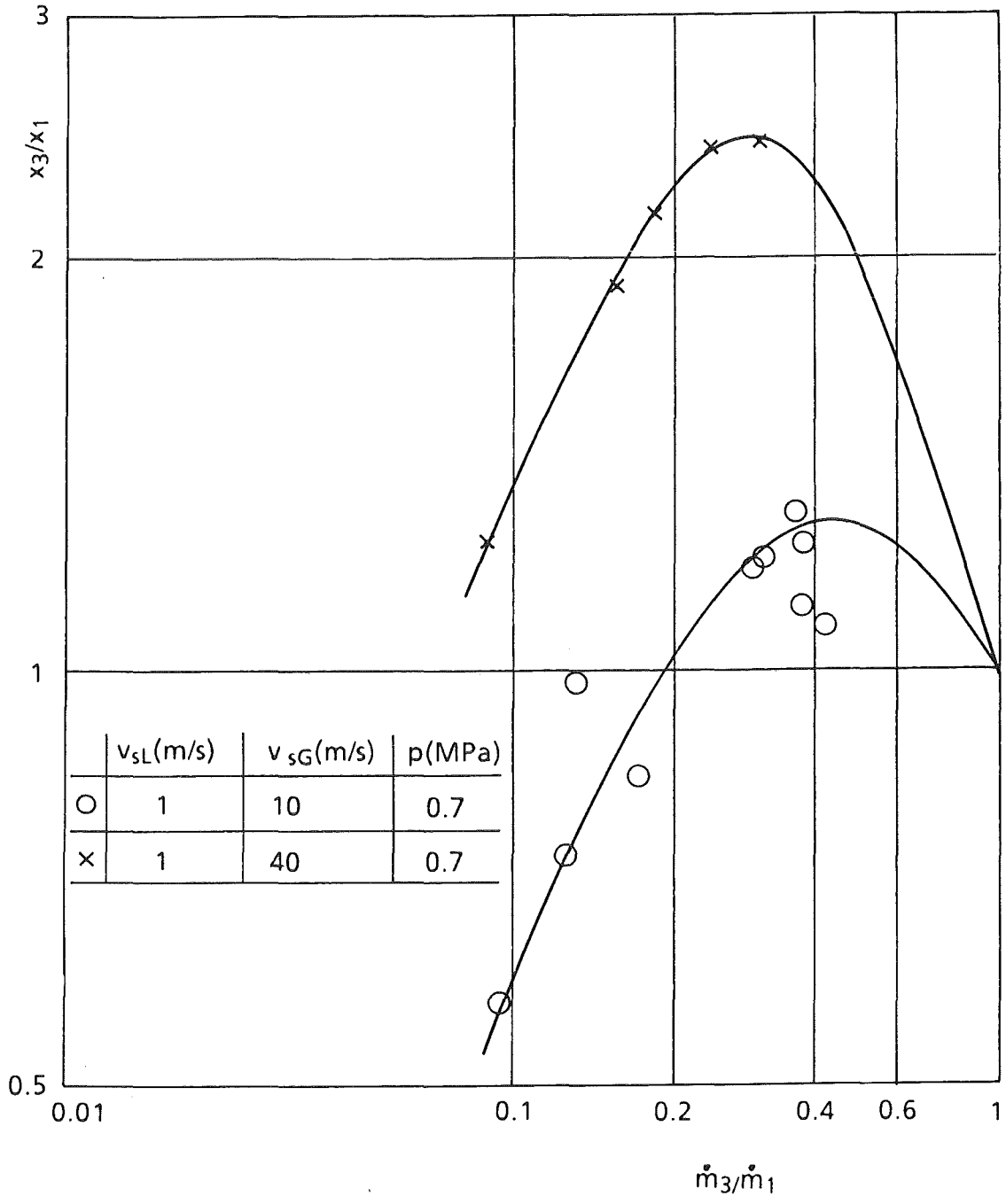


Fig. 5.26 Present Air-water Data for $D_3/D_1 = 1$ and $p_1 = 0.7$ MPa: $v_{sL} = \text{const} = 1$ m/s

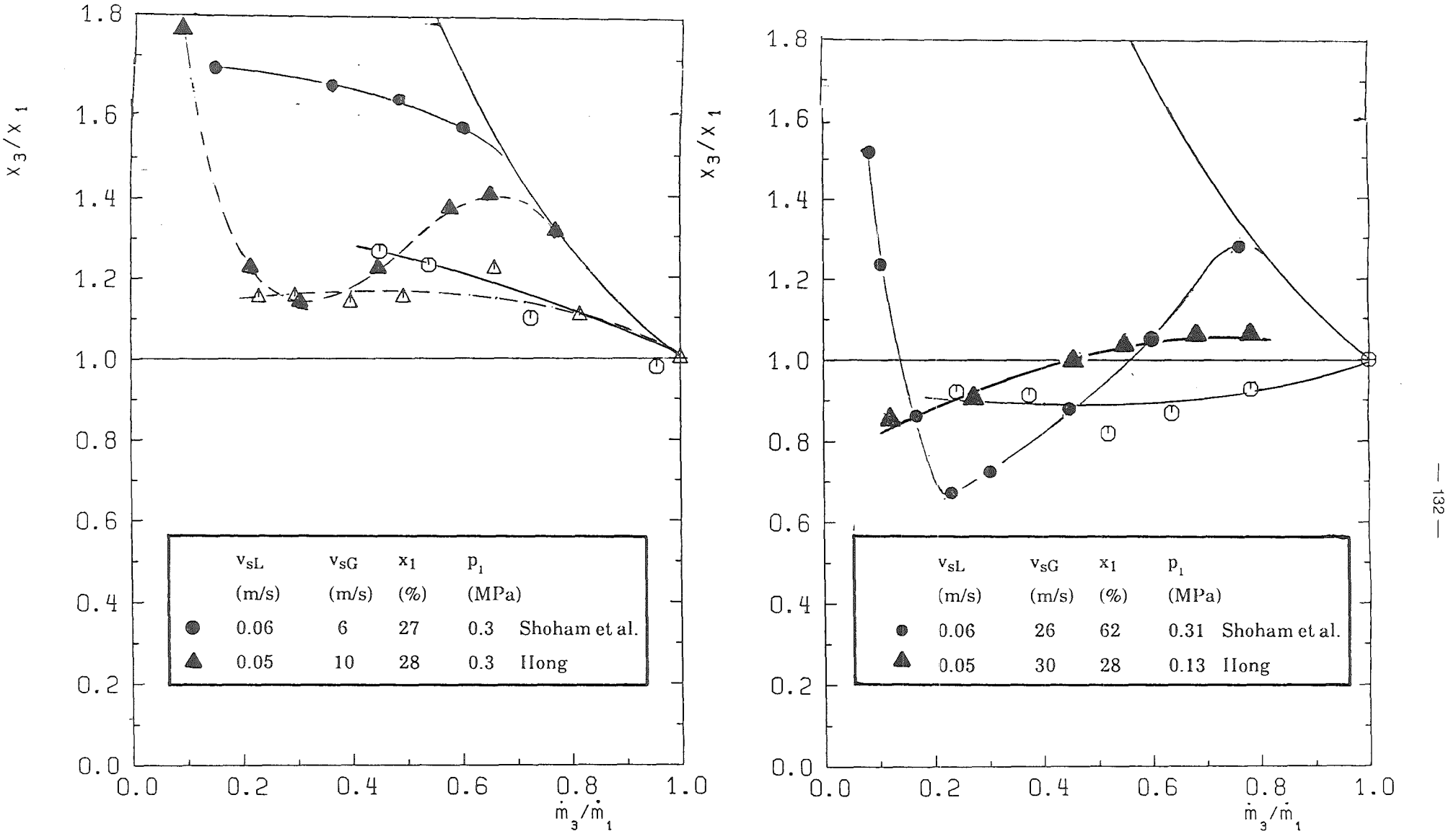


○ VsL=0.05 m/s VsG= 4.9 m/s x= 44.5% $p_1$ = 0.7 MPa
△ VsL=0.05 m/s VsG= 10.0m/s x= 62.4% $p_1$ = 0.7 MPa

○ VsL=0.05 m/s VsG= 20.4m/s x= 76.3% $p_1$ = 0.7 MPa

Fig. 5.27 Comparison of Low Mass Flux Data ($D_3/D_1 = 1$) with other Experiments from Shoham and Brill /33/ and Hong /8/

Figure 5.27 shows also a comparison with other work obtained at significantly lower pressures. For the inlet condition with stratified-wavy flow the quality ratio measured by Shoham et al. is significantly larger compared to the present results. The measured quality ratios from Hong for $v_{sL} = 0.05$ m/s and $v_{sG} = 10$ m/s are also generally higher. However the curve depicts a well defined minimum at split ratios of $\approx 0.2$ which was not observed by other authors.

For the test point in the wavy-annular flow regime (right hand side of Fig. 5.28) Shoham's results are slightly higher than the present results. The results from Hong again are characterized by a curve with a minimum.

One reason for the higher quality ratios obtained by the other workers could be the lower system pressure in these experiments. Figure 5.28 contains a comparison between the present experimental results for annular flow and predictions from the models proposed by Shoham et al. and Azzopardi and Whalley /10/.

The model from Shoham and Brill, which does not take into account droplet entrainment in the gas core, predicts higher values than Azzopardi's model with $E = 0$. With increasing droplet entrainment, Azzopardi's model predicts increasing values of $x_3/x_1$. The experimental quality ratios are mostly lower than the model predictions.

Figure 5.29 shows experimental results for stratified-wavy flow and predictions from the corresponding model from Shoham and Brill. At high mass splits the agreement is fairly good. At low mass splits and $v_{sG} = 10$ m/s, the measured quality ratios are significantly lower. A reason for this is the wavy interface and the beginning droplet entrainment which is not taken into account in the model.

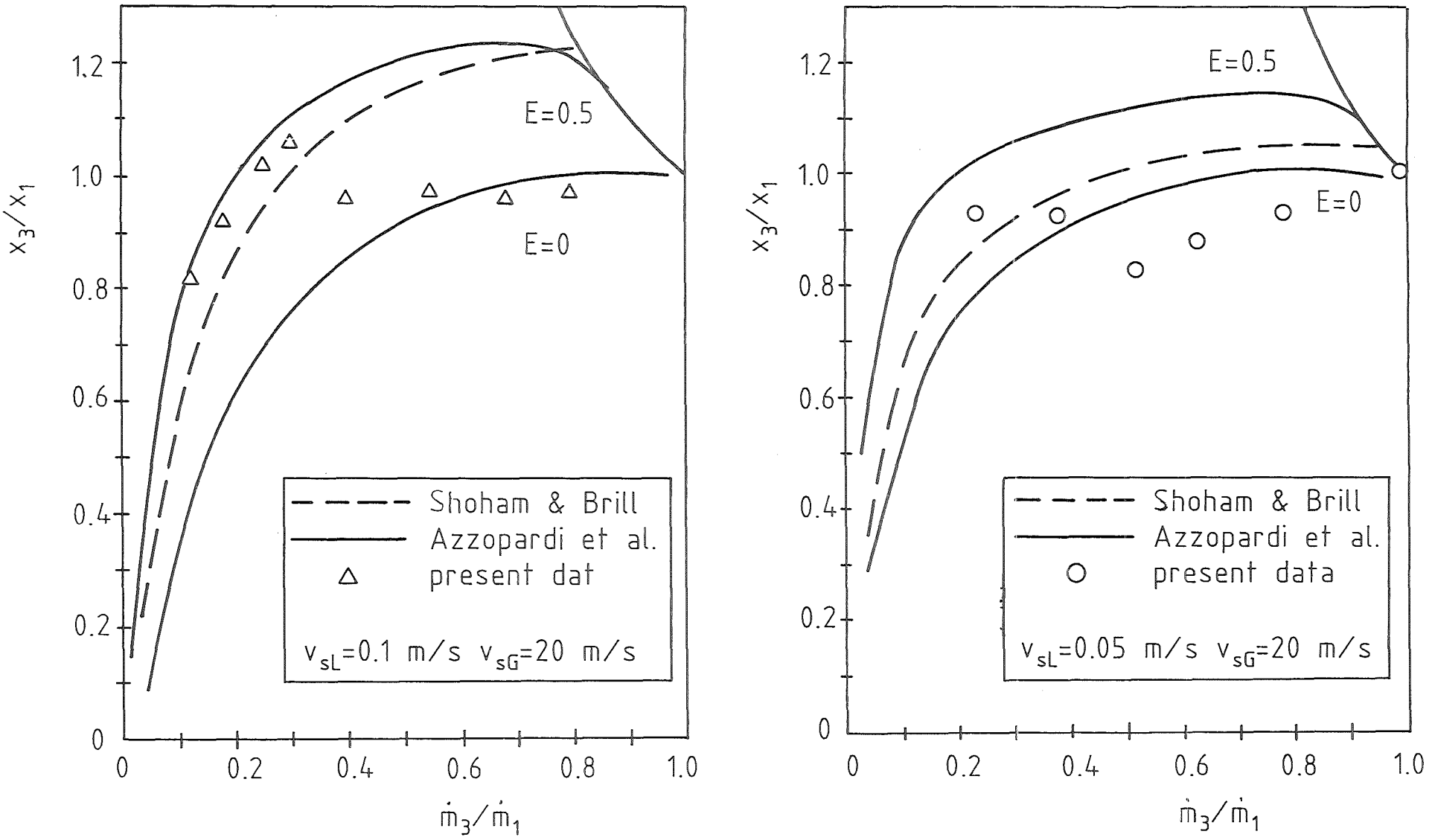


Fig. 5.28 Comparisons between Experimental Results and Model Predictions for Annular Air-water Flow ($p = 0.7$ MPa, $D_3/D_1 = 1$)

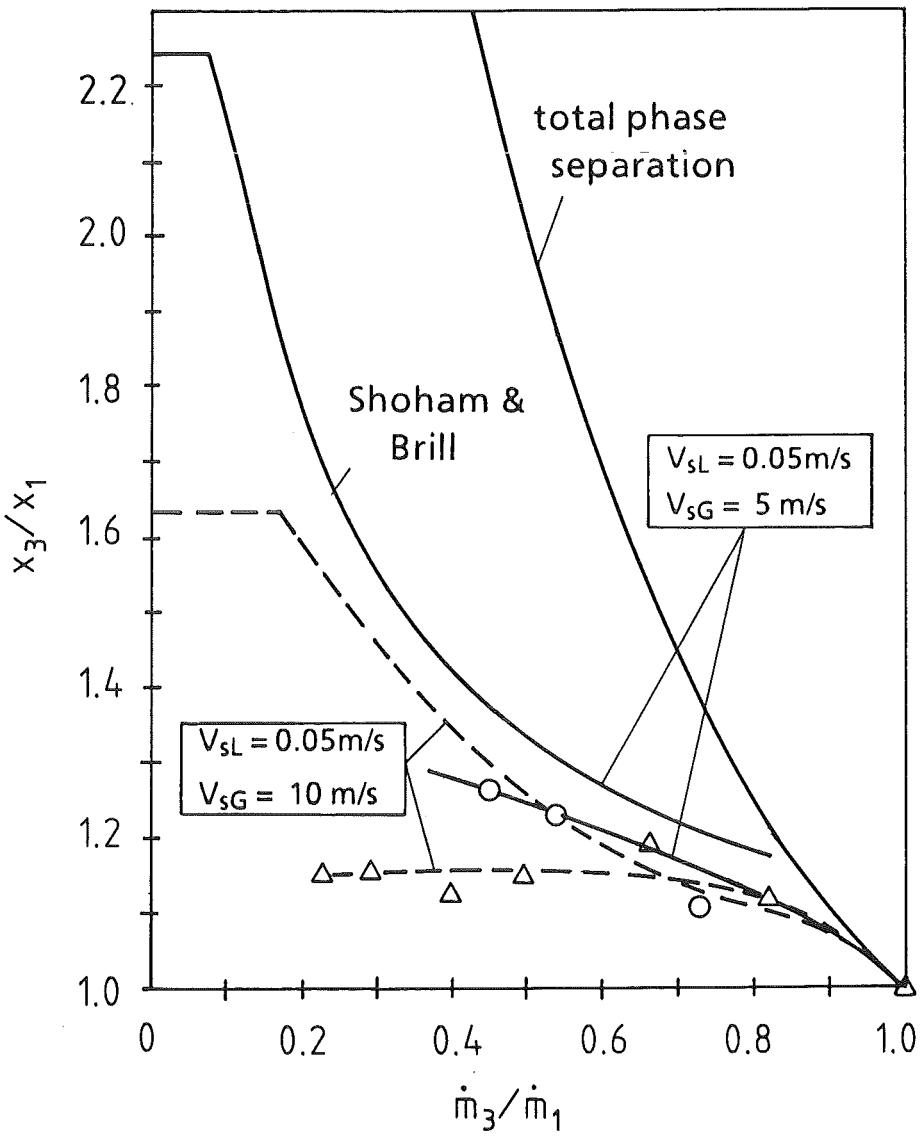


Fig. 5.29 Comparison between Experimental Results and Shoham and Brill Model for Stratified-Wavy Flow (Air-water Flow, p = 0.7 MPa)

# 6. NEW RESULTS ON TEE-JUNCTION PRESSURE DIFFERENCES AND DISCUSSION WITH PREVIOUS RESULTS

## 6.1 Single-phase Flow

To determine the loss coefficients $K_{13}$ and $K_{12}$ for the diameter ratio $D_3/D_1 = 0.52$, single-phase water experiments were performed with inlet water velocities between 1.7 and 8.7 m/s. The Figs. 6.1 and 6.2 show the axial pressure distributions in the inlet, run and branch pipes for different water inlet velocities and different mass splits. The characteristic pressure drop in the branch and pressure increase in the run is clearly seen. The pressure drops become constant after at a certain distance downstream of the Tee-junction. This means that there is no longer any influence from the Tee-junction. As outlined before, the Tee-junction pressure difference $\Delta p_{1\text{-}3}$ and $\Delta p_{1\text{-}2}$ were obtained by extrapolating the pressure gradients for well developed frictional flow to the Tee-junction entrance, compare also Fig. 3.1.

The Figs. 6.3 and 6.4 shows the calculated loss coefficients $K_{13}$ and $K_{12}$, using Eqs. (3.1)-(3.3). Again the experimental results curves agree well with the relationship suggested by Miller /46/. The present results were fitted using the method of least squares by:

$$K_{13} = 1.1477 - 2.02045(\dot{m}_3/\dot{m}_1) + 9.1725(\dot{m}_3/\dot{m}_1)^2, \qquad (6.1a)$$

$$K_{12} = -0.0138 - 0.03915(\dot{m}_3/\dot{m}_1) + 0.3922(\dot{m}_3/\dot{m}_1)^2. \qquad (6.1b)$$

For the experiments with $D_3/D_1 = 1$, the loss coefficients were taken from previous experiments (Ref. /24/), given by

$$K_{13} = 1.0369 - 0.9546(m_3/\dot{m}_1) + 1.2123(\dot{m}_3/\dot{m}_1)^2, \qquad (6.2a)$$

$$K_{12} = 0.1571 - 0.9197(\dot{m}_3/\dot{m}_1) + 1.09(\dot{m}_3/\dot{m}_1)^2. \qquad (6.2b)$$

For single-phase flow, the mass flow rate ratio $\dot{m}_3/\dot{m}_1$ is equal to the volume flow rate ratio $\dot{V}_3/\dot{V}_1$. Therefore, Eqs. (6.1) and (6.2) do not change if $\dot{m}_3/\dot{m}_1$ is replaced by $\dot{V}_3/\dot{V}_1$.

The data scatter in Fig. 6.3 is considerably smaller than in Fig. 6.4. This is due to the fact that the branch pressure drop is in general much larger than the run

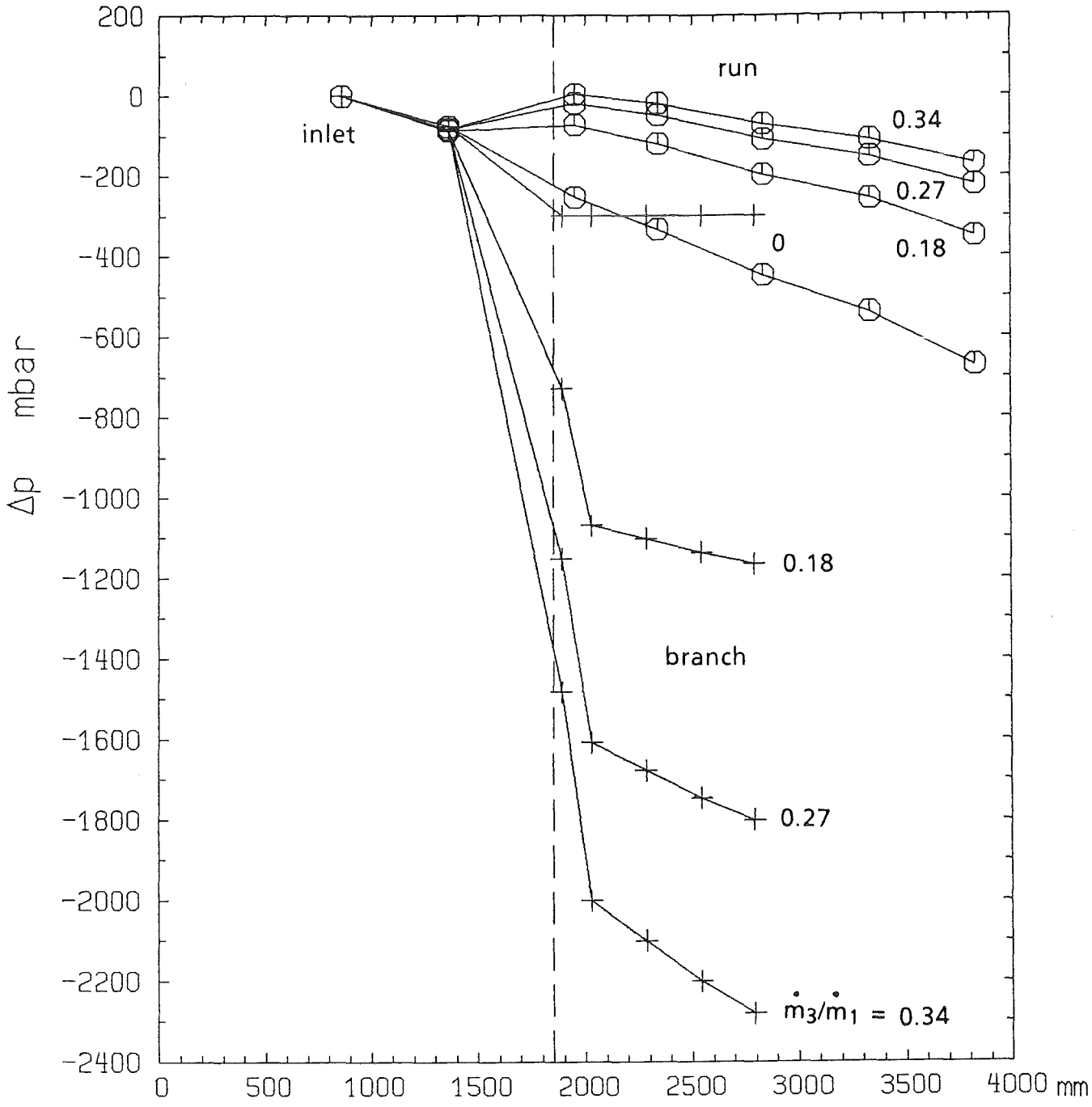


Fig. 6.1 Axial Pressure Distribution in Tee-junction with $D_3/D_1 = 0.52$: Water Flow, $v_{sL} = 8.5$ m/s

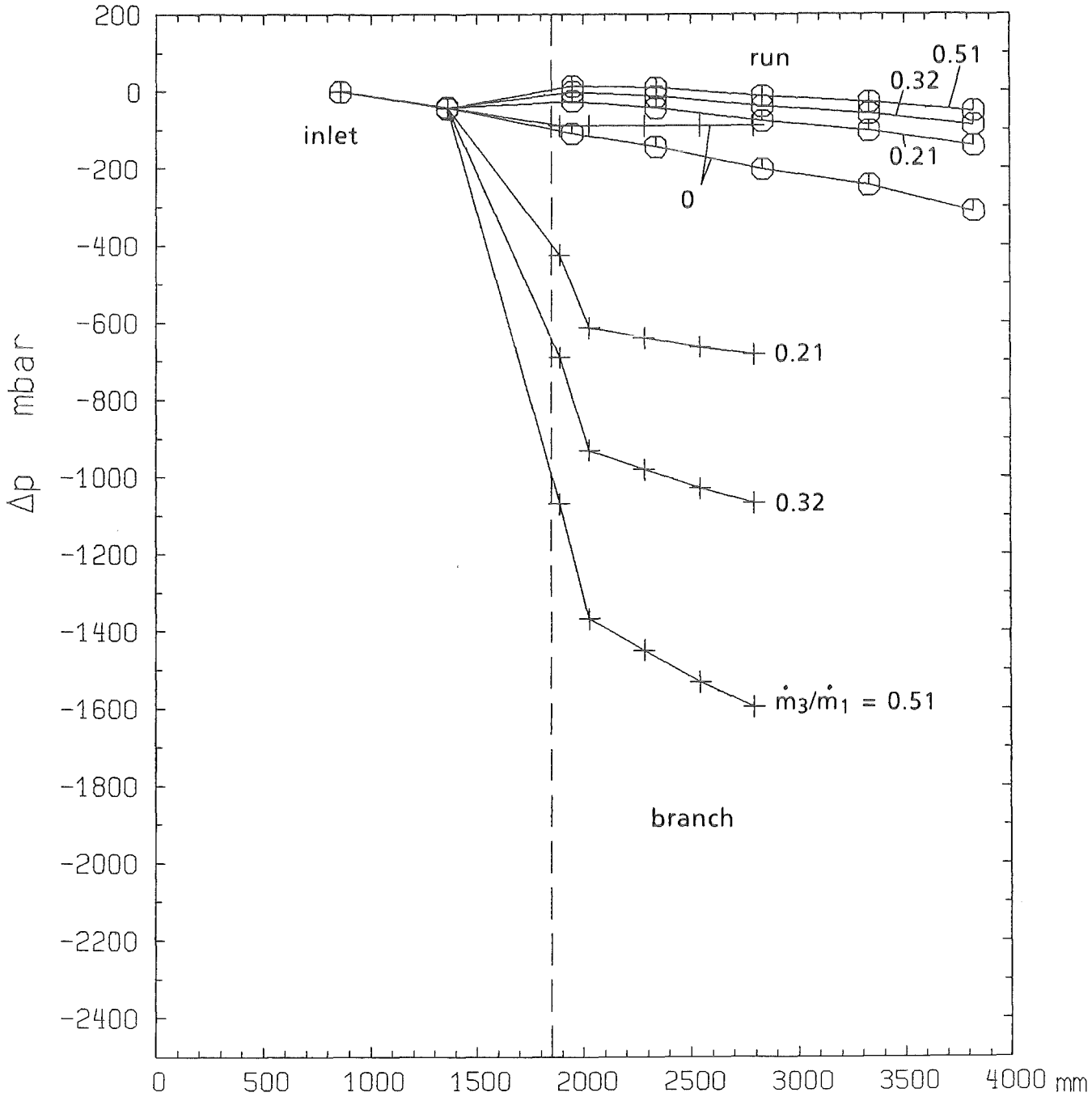


Fig. 6.2 Axial Pressure Distribution in Tee-junction with $D_3/D_1 = 0.52$: Water Flow, $v_{sL} = 6$ m/s

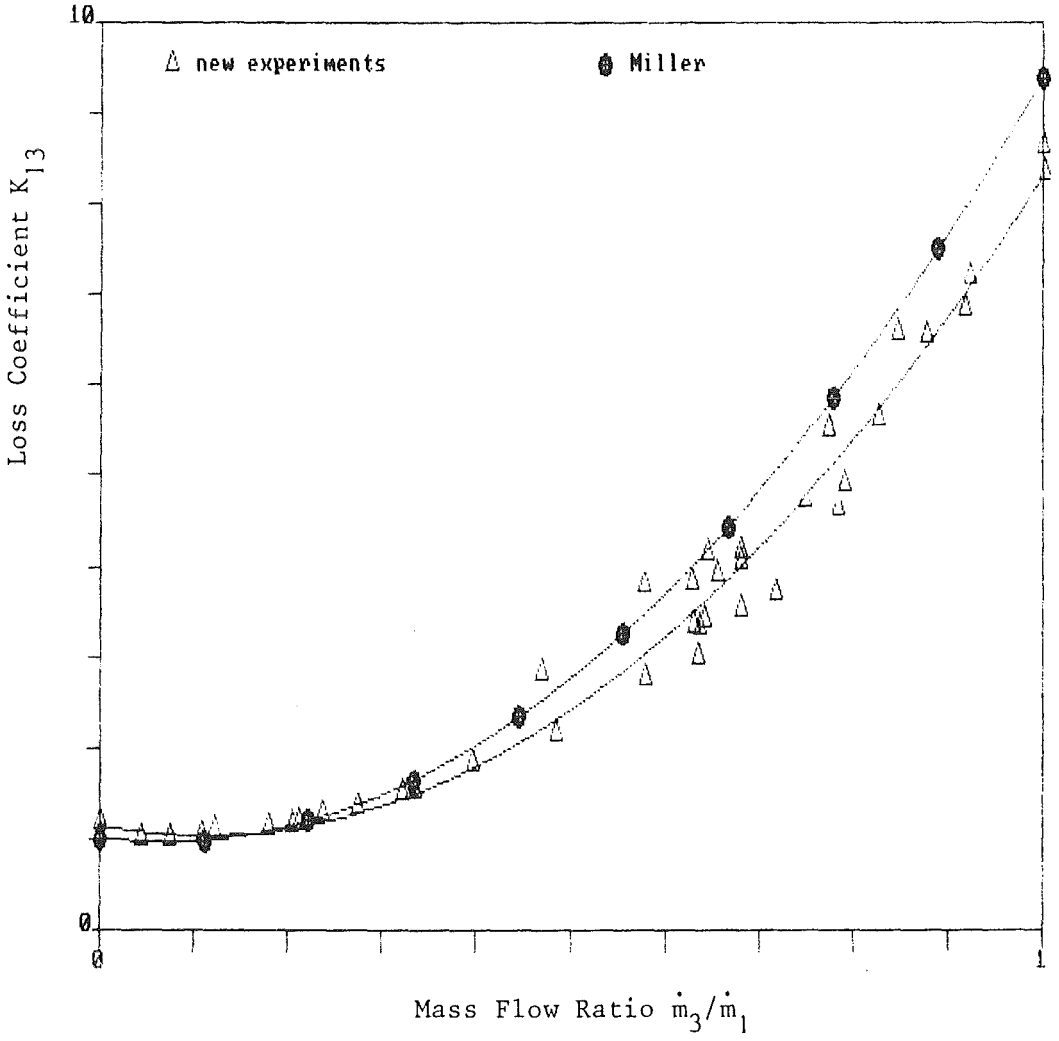


Fig. 6.3 Loss Coefficient $K_{13}$ for Tee-junction with $D_3/D_1 = 0.52$

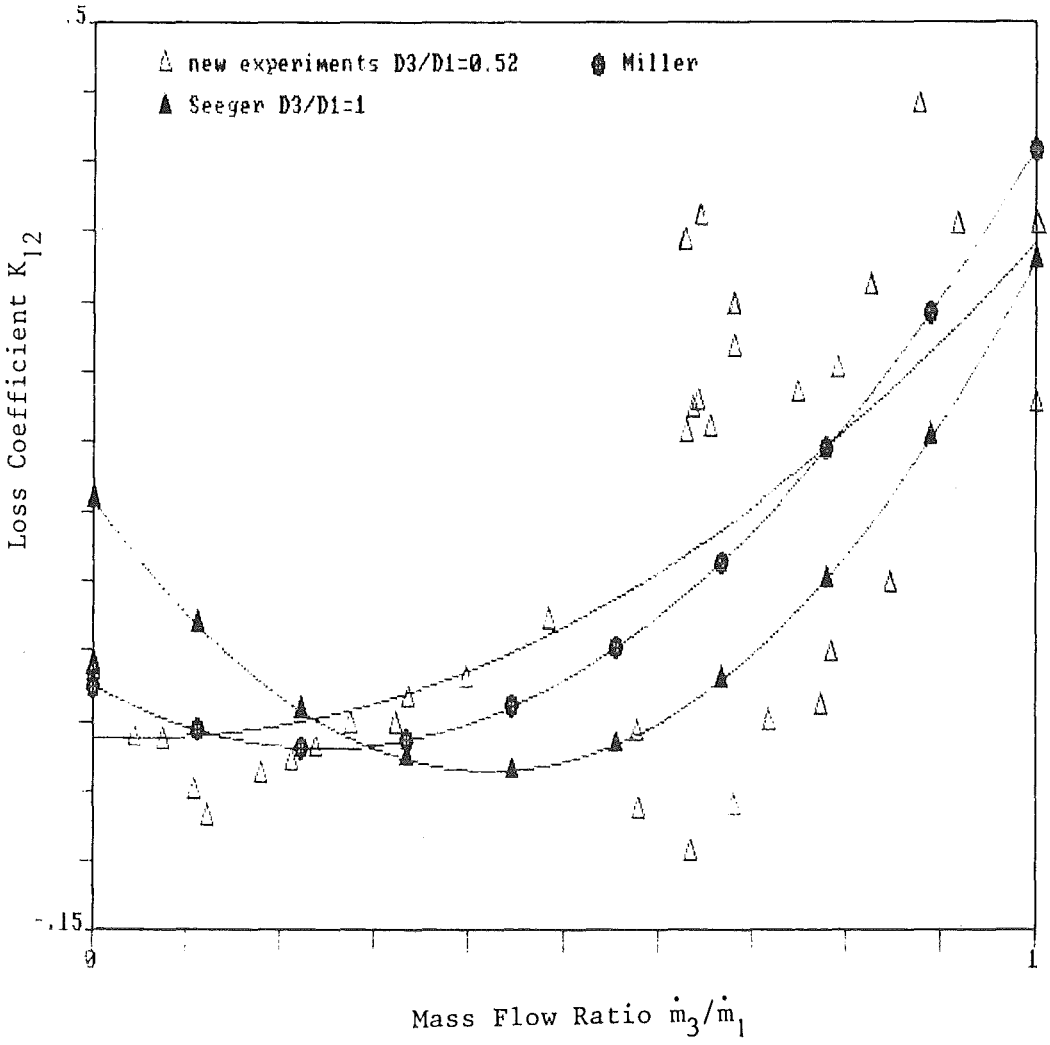


Fig. 6.4 Loss Coefficient $K_{12}$ for Tee-junction with $D_3/D_1 = 0.52$

pressure increase. Therefore, small changes in the frictional pressure drop, e.g. by deposition of corrosion products do not influence severely the determination of $K_{13}$. This is very different for $K_{12}$ due to the small pressure difference to be measured. The data scatter in Fig. 6.4 is larger than in previous experiments with $D_3/D_1 = 1$ (Refs. /20-27/). The reason for this could not be clearified. Therefore, the $\Delta p_{1\text{-}2}$ measurements both in single-phase and two-phase flow have a higher uncertainty and the following discussions concentrate on the branch pressure drop. (Fortunately, the branch pressure drop is in general much more important for technical applications).

The problem of accurate $\Delta p_{1\text{-}2}$ measurements is not characteristic to the present experimental conditions, but rather a general problem in all Tee-junction investigations. An indication for this is, that very different expressions for $K_{12}$* were proposed by Saba and Lahey /12 / and later by Hwang and Lahey /35/ using the same test section.

## 6.2 Two-phase Flow

Figures 6.5-6.7 show some examples for the axial pressure differences for different inlet conditions and Tee-junction diameters; parameter is again the mass split.

The general formulation of Tee-junction pressure drop results in expressions which contain the slip at different locations. The slips are not measured but have to be evaluated with more or less arbitrary assumptions. These assumptions cover the range of $S = 1$ (homogeneous flow) up to values of $S >> 1$ predicted by some correlations found in literature for well developed two-phase flow. In the following, the convenient assumption of homogeneity will be discussed in more detail. For model evaluation with $S > 1$, Rouhani's correlation (Eqs. (2.17)-(2.19)) will be used again which was recommended in a review paper for horizontal two-phase flow by Friedel /56/. The data base for upward and downward two-phase flow is much more limited. For simplicity, again Rouhani's correlation will be used, being aware that this is not the optimal choice. In future analyses, further correlations should be used.

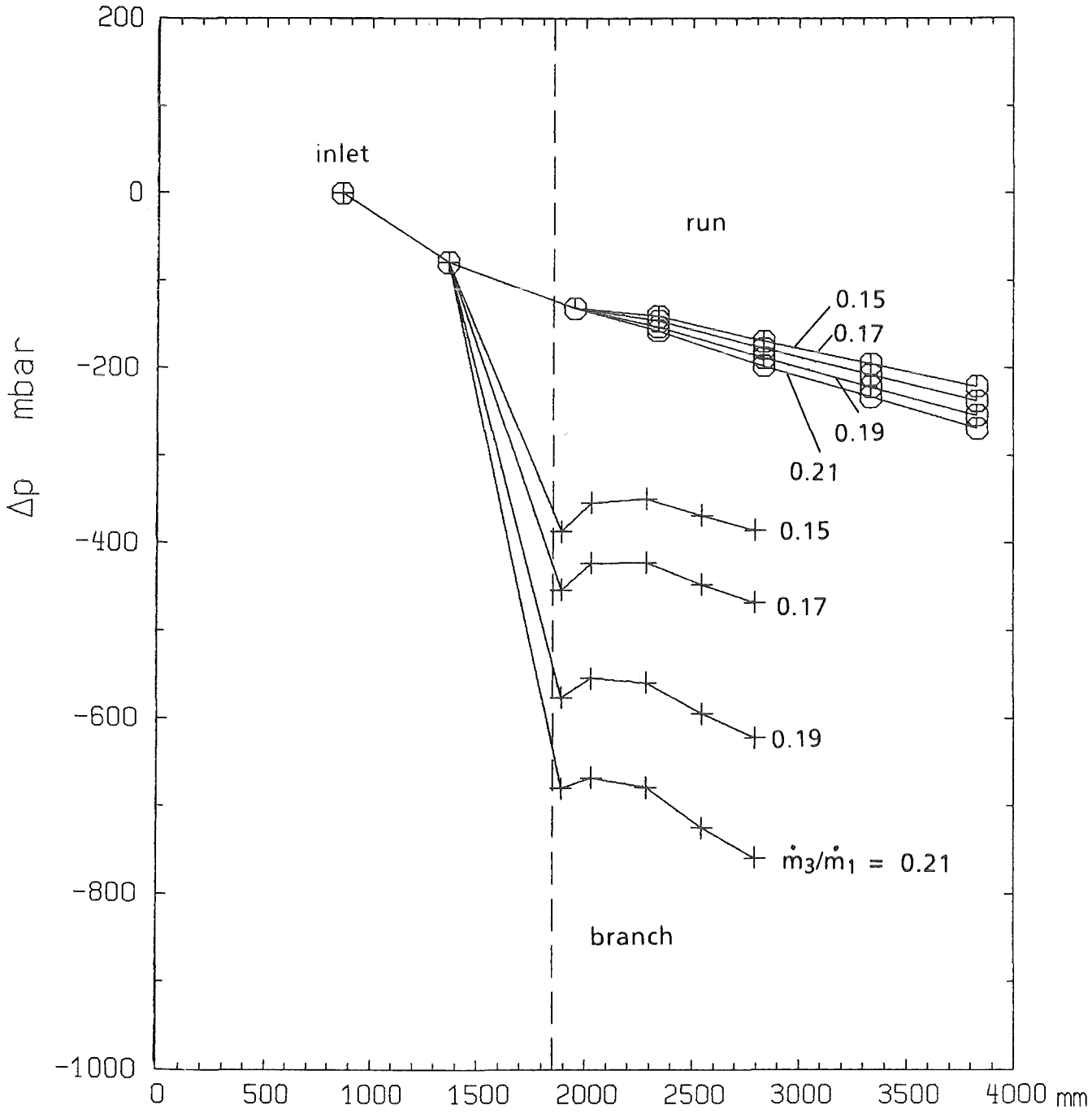


Fig. 6.5 Axial Pressure Distribution in Tee-junction with $D_3/D_1 = 0.52$: Air-water Flow, $v_{sL} = 4$ m/s, $v_{sG} = 5$ m/s, $p_1 = 0.7$ MPa, Downward Branch

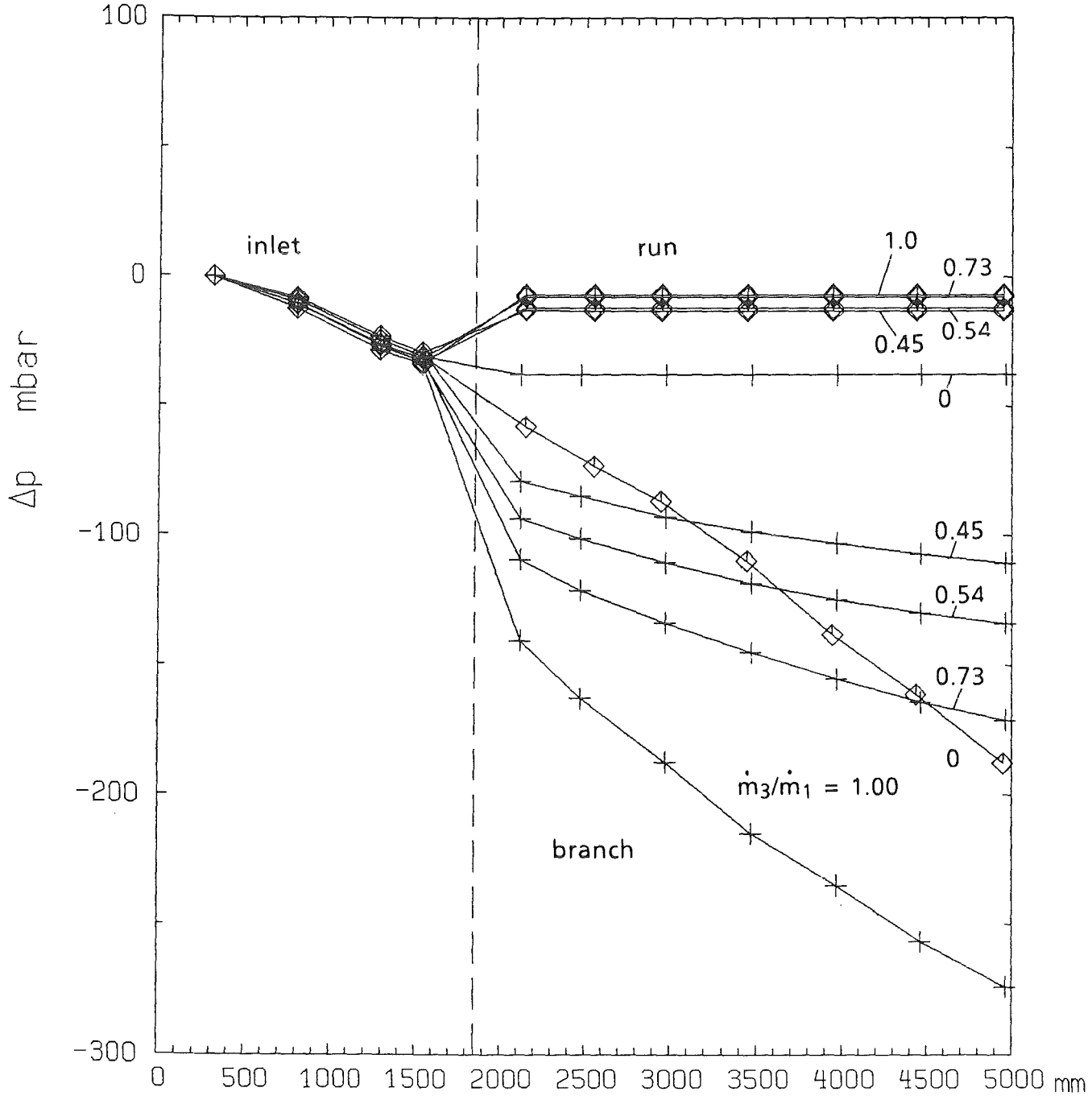


Fig. 6.6 Axial Pressure Distribution in Tee-junction with $D_3/D_1 = 1$: Air-water Flow, $v_{sL} = 1$ m/s, $v_{sG} = 10$ m/s, $p_1 = 0.7$ MPa, Horizontal Branch

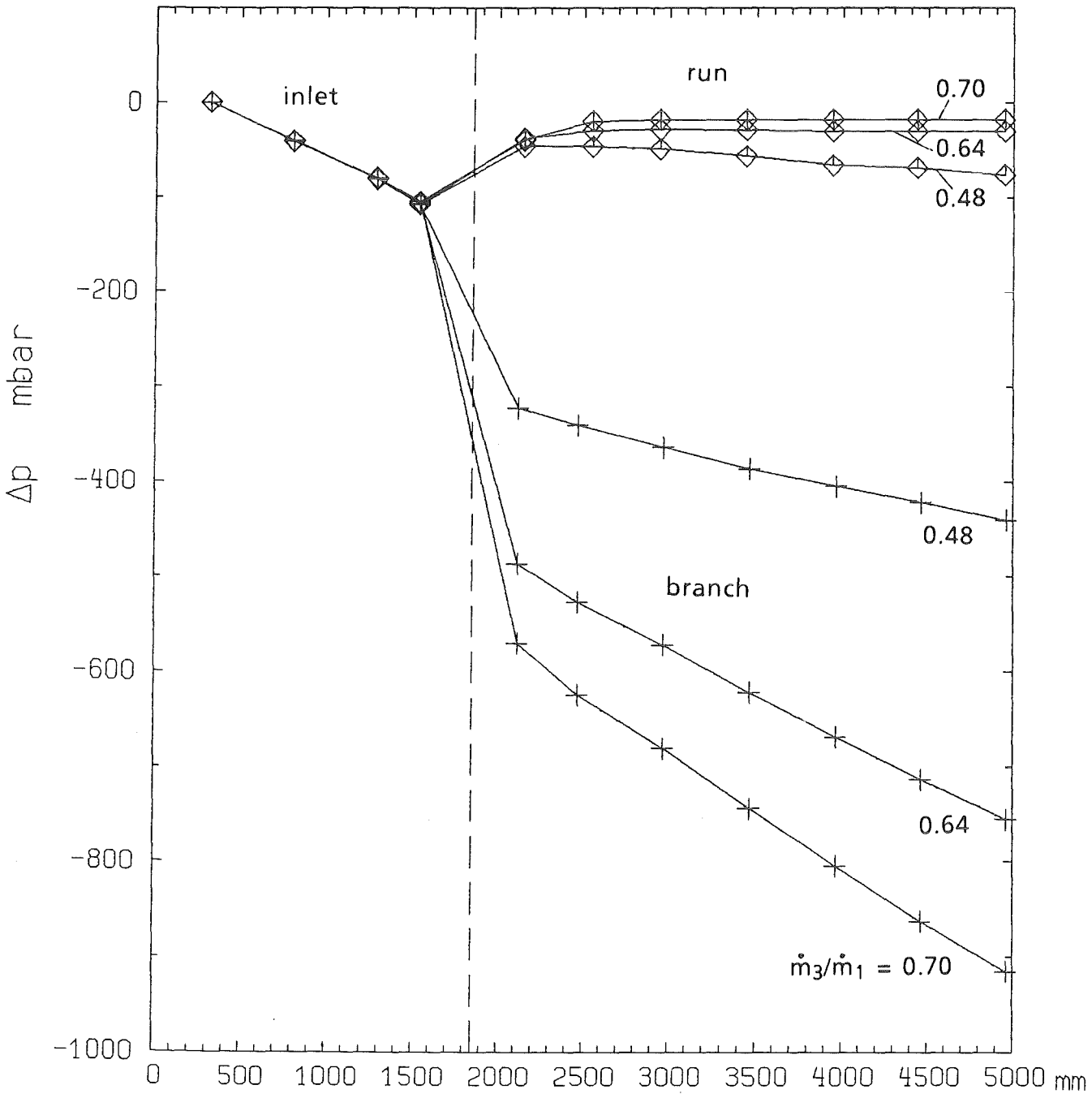


Fig. 6.7 Axial Pressure Distribution in Tee-junction with $D_3/D_1 = 0.52$: Air-water Flow, $v_{sL} = 1$ m/s, $v_{sG} = 40$ m/s, $p_1 = 0.7$ MPa, Horizontal Branch

### 6.2.1 Branch Pressure Drop

#### 6.2.1.1 Homogeneous Models

First, the measurements are compared with models of the following type (compare Section 3.3.1):

$$\Delta p_{1-3} = \frac{\rho_{h3}}{2}\left(\left(\frac{G_3}{\rho_{h3}}\right)^2 - \left(\frac{G_1}{\rho_{h1}}\right)^2\right) + K \cdot K_{13} \cdot \frac{G_1^2}{2\rho_{L1}} \cdot \varphi \quad , \tag{6.3}$$

where the first terms on the right hand side is the reversible pressure difference, defined with homogeneous densities. The two-phase loss multiplier $\varphi$ is evaluated again according to Eq. (3.13) (Homogeneous Model = HM), Eqs. (3.14)-(3.16) (Chisholm Model = CM), and Eq. (3.24) (Reimann Seeger Model = RSM).

K is a correction factor, introduced in Section 3.3.1.3. The loss coefficient $K_{13}$ is determined from the single-phase flow measurements in two ways:

a) $K_{13} = f(\dot{m}_3(\dot{m}_1)$. In this case Eq. (6.1) is directly applied.

b) $K_{13} = f(\dot{V}_3/\dot{V}_1)$. In this case $\dot{m}_3/\dot{m}_1$ is replaced in Eq. (6.1) by $\dot{V}_3/\dot{V}_1$, using

$$\dot{V}_3/\dot{V}_1 = (\dot{m}_3/\dot{m}_1)(\rho_{h1}/\rho_{h3}). \tag{6.4}$$

The Figs. (6.8)-(6.10) show for K = 1 the ratio of predicted to measured pressure drop $\Delta p_{1\text{-}3,Mod}/\Delta p_{1\text{-}3,Meas}$ as a function of the mass split for different branch orientations.

Starting the discussion with the results obtained with $K_{13} = f(\dot{m}_3/\dot{m}_1)$, the following tendencies are observed:

- Horizontal and upward branch: The pressure drop ratio is fairly constant for a wide range of mass splits ($0.2 < \dot{m}_3/\dot{m}_1 \leq 1$). In this range, the accuracy of the models is about the same for the upward branch. The CM has a smaller accuracy for the horizontal branch. At lower values of $\dot{m}_3/\dot{m}_1$, the results scatter considerably for the HM and CM. There is the tendency to overpredict the measurements with decreasing $\dot{m}_3/\dot{m}_1$, except for test points with $v_{sl.} = 0.05$ m/s (Fig. 6.8), where the tendency is reversed. The RMS tends to

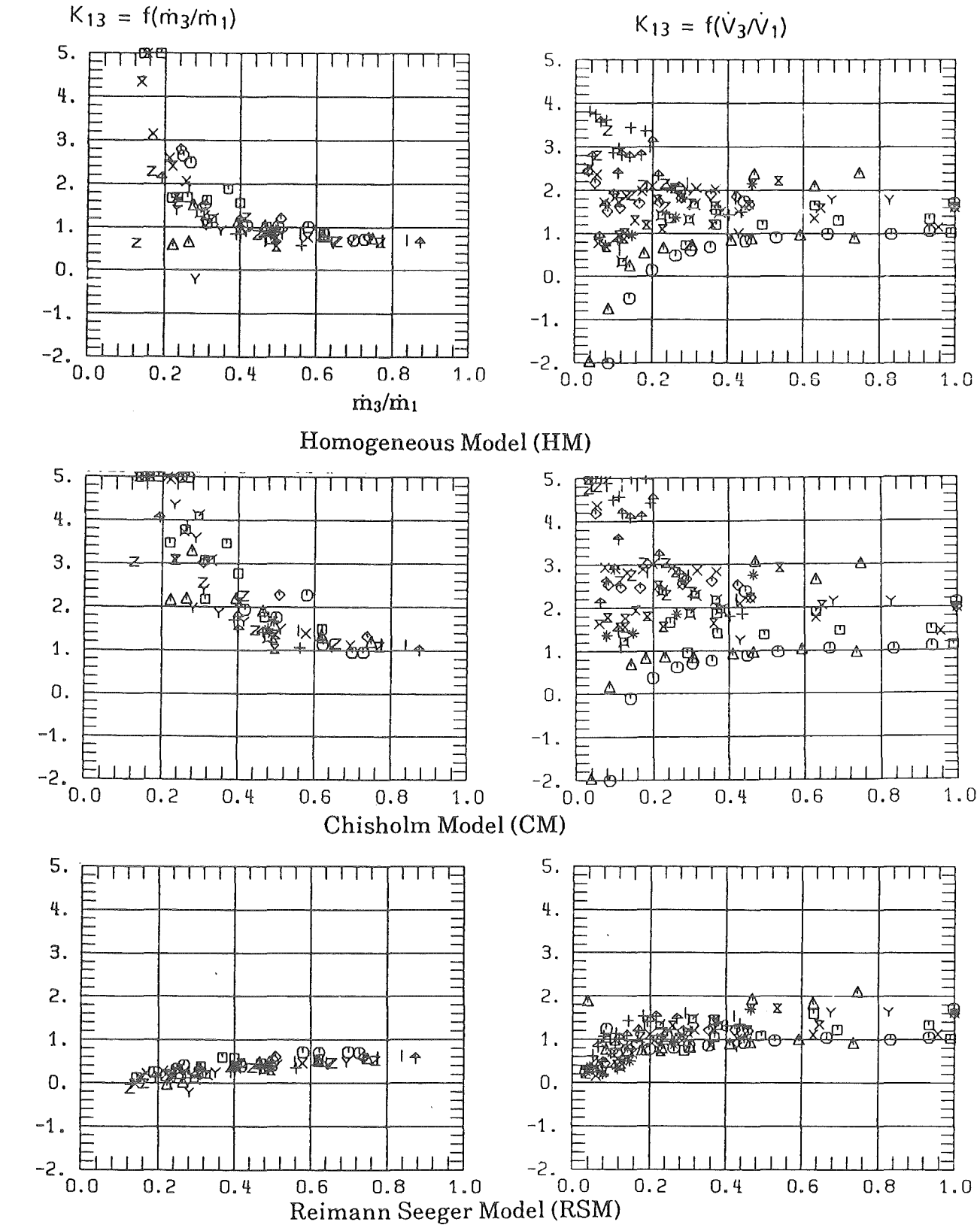


Fig. 6.8 Ratio of Predicted to Measured Branch Pressure Drop for Horizontal Branch with $D_3/D_1 = 0.52$ (Homogeneous Models, $K = 1$)

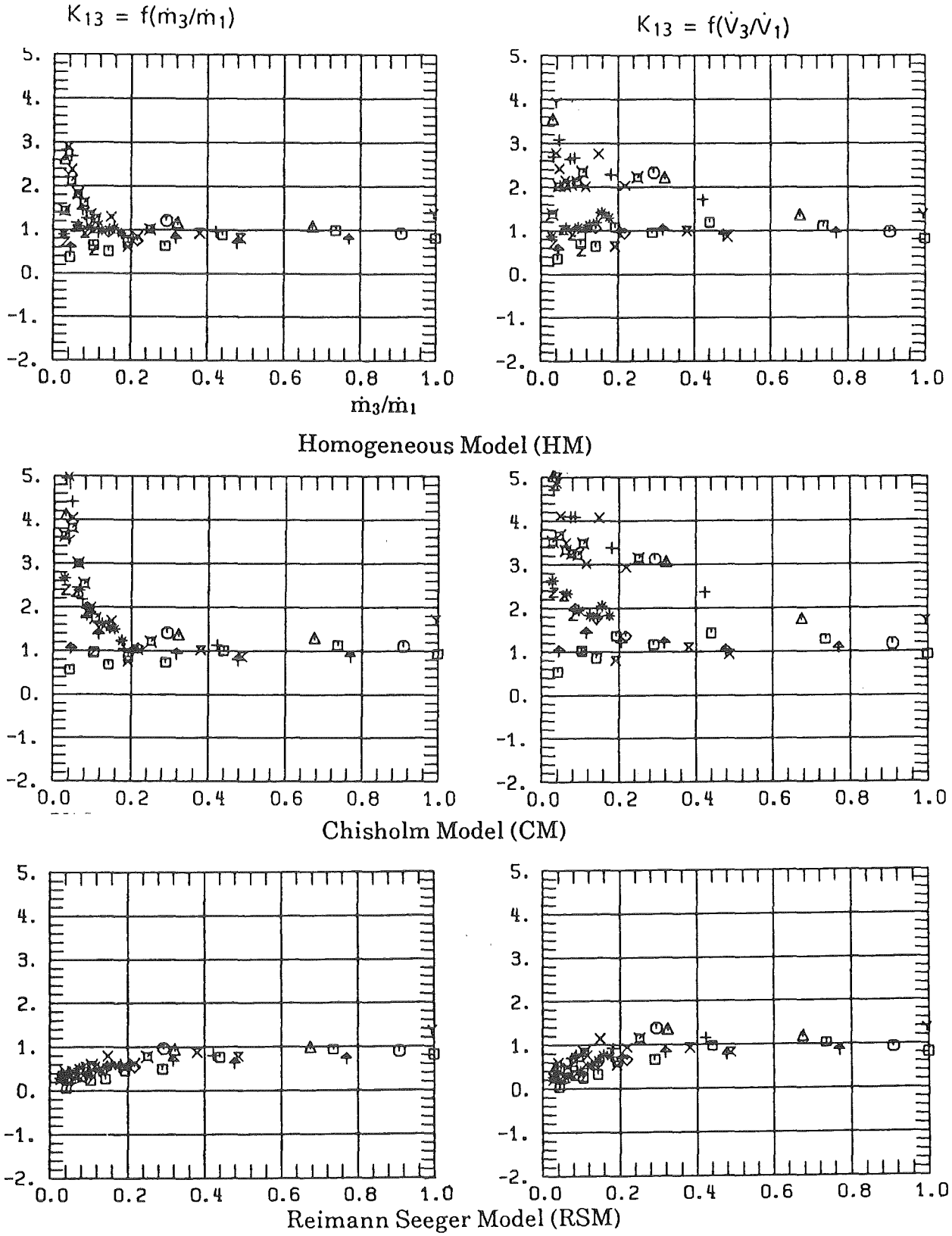


Fig. 6.9 Ratio of Predicted to Measured Branch Pressure Drop for Upward Branch with $D_3/D_1 = 0.52$ (Homogeneous Models, $K = 1$)

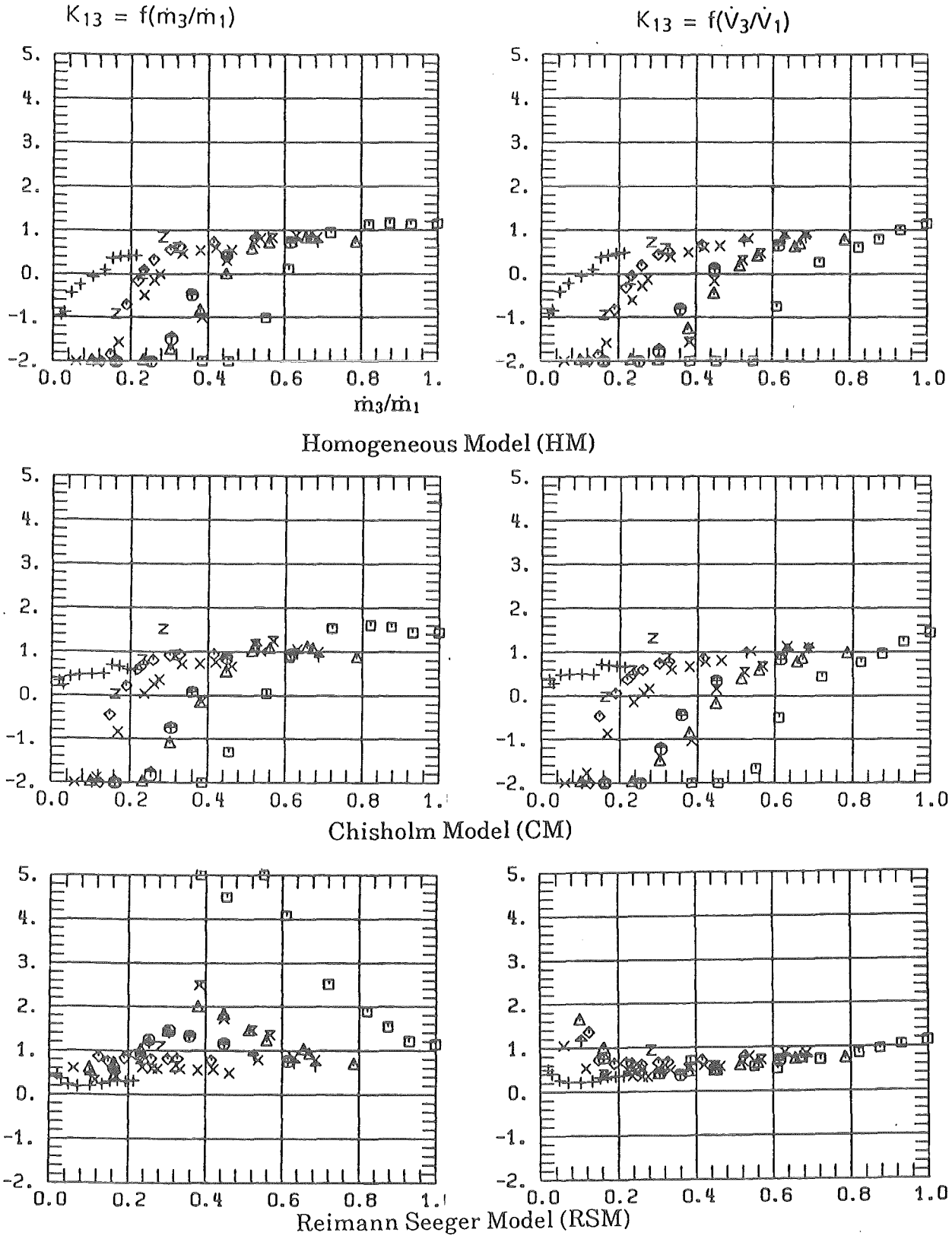


Fig. 6.10 Ratio of Predicted to Measured Branch Pressure Drop for Downward Branch with $D_3/D_1 = 0.52$ (Homogeneous Models, $K = 1$)

underpredict the measurements for decreasing $\dot{m}_3/\dot{m}_1$. However, the data scatter is considerably smaller than for the other models.

- Downward branch: Looking at test series with constant inlet values (equal symbols), the model predicts quite well the pressure drop for the high values of the mass split. With decreasing $\dot{m}_3/\dot{m}_1$, the pressure drop ratio becomes too small for the HM and CM and too high for the RSM.

A comparison between $K_{13} = f(\dot{m}_3/\dot{m}_1)$ and $K_{13} = f(\dot{V}_3/\dot{V}_1)$ reveals that there is no improvement for the HM and CM using $K_{13} = f(\dot{V}_3/V_1)$. For the RSM, the accuracy is about the same for the horizontal branch and slightly improved for the upward branch. For the downward branch, the data scatter is significantly reduced for a wide range of $\dot{m}_3/\dot{m}_1$.

In previous investigations with $D_3/D_1 = 1$, the correction factor K was chosen in such a way to fit the data for $(\Delta p_{1\text{-}3})_{rev} = 0$ which occurs at $\dot{m}_3/\dot{m}_1 = G_3/G_1 = 1$. These factors were determined previously /22/ to $K = 1.34$ for the HM and RSM and $K = 0.74$ for the CM. Figures 6.11-6.13 show the corresponding results for $D_3/D_1 = 0.52$:

For the horizontal branch and high mass splits, the accuracy decreases somewhat compared to $K = 1$ (Figure 6.8). At low mass splits, the pressure ratio is lifted to higher values for the RSM and the accuracy increases.

The RMS is remarkably improved for the upward branch (compare Figs. 6.9 and 6.12), for the downward branch the RMS is improved for the bulk of the data using $K_{13} = f(\dot{V}_3/\dot{V}_1)$. However, a part of the pressure ratios deviate significantly.

A comparison between the present data for $D_3/D_1 = 0.52$ and the previous ones with $D_3/D_1 = 1$ (using $K \neq 1$, as given above) shows the following tendencies, compare Figs. 3.7-3.9 and 6.11-6.13:

Horizontal Branch: For $D_3/D_1 = 1$, the HM and CM start to deviate already at higher mass splits. At low mass splits, these models also overpredict generally the measurements. The RSM has about the same accuracy for mass splits greater than 0.1. For $D_3/D_1 = 0.52$ the tendencies are similar.

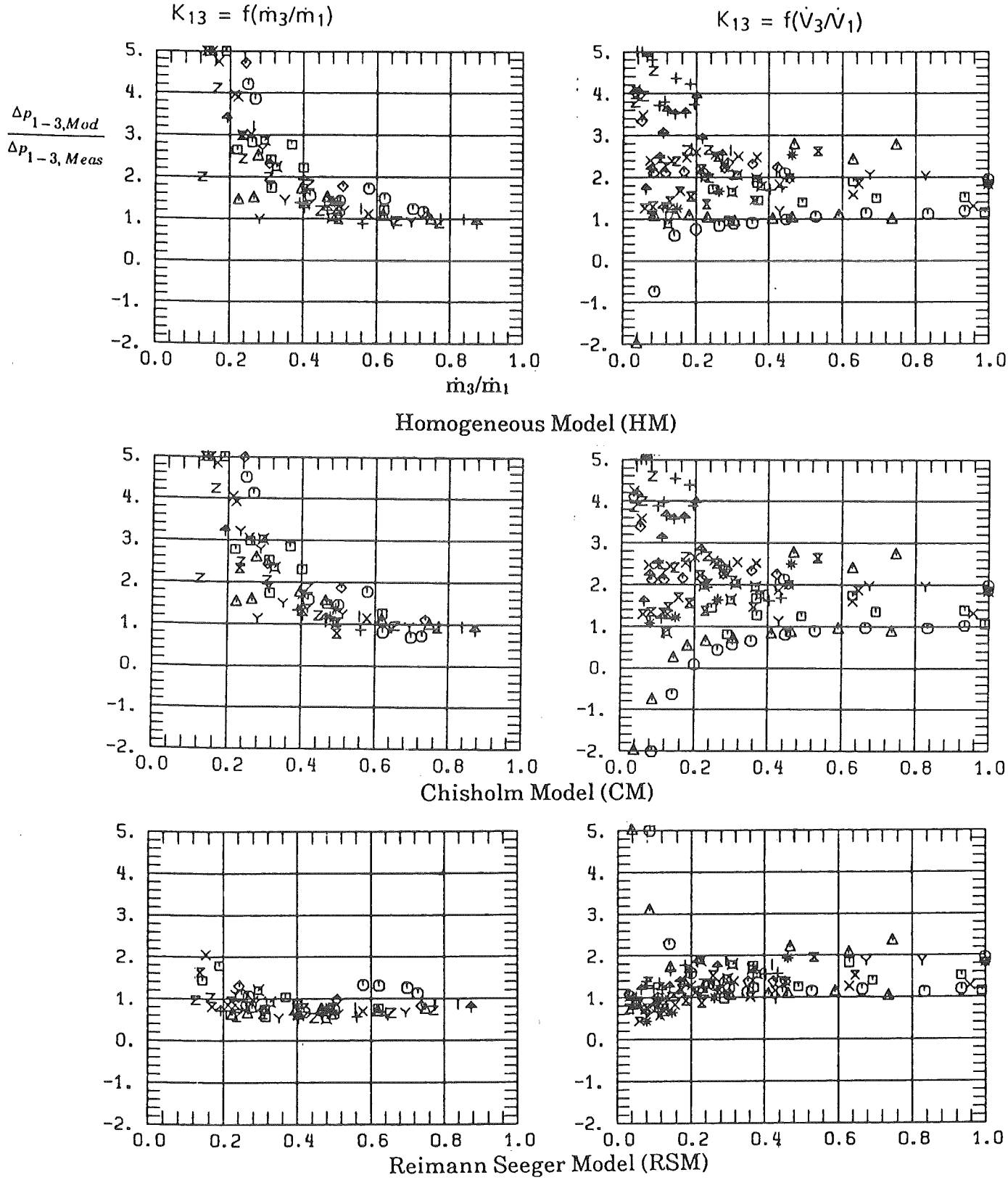


Fig. 6.11 Ratio of Predicted to Measured Branch Pressure Drop for Horizontal Branch with $D_3/D_1 = 0.52$ (Homogeneous Models, $K \neq 1$)

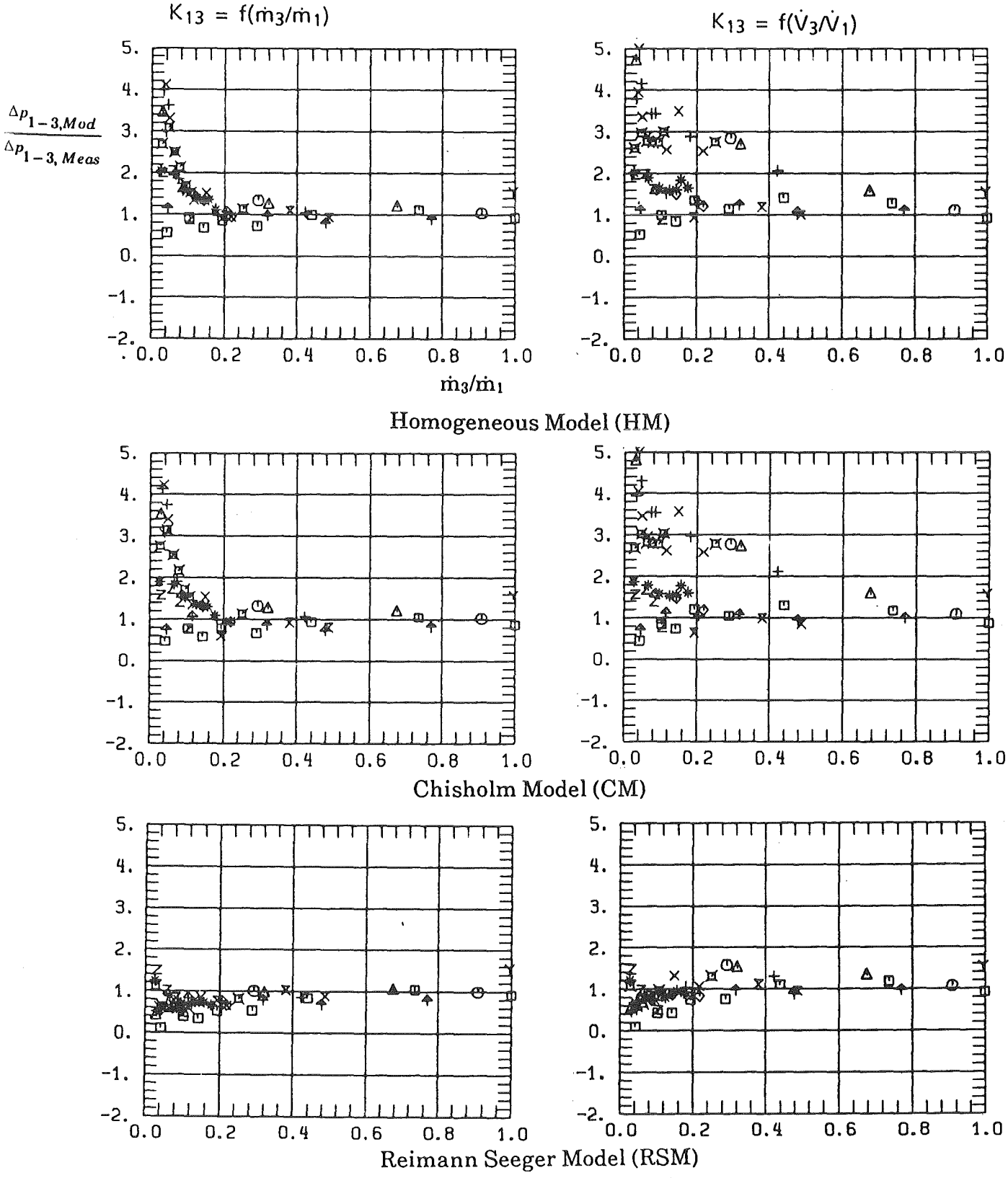


Fig. 6.12 Ratio of Predicted to Measured Branch Pressure Drop for Upward Branch with $D_3/D_1 = 0.52$ (Homogeneous Models, $K \neq 1$)

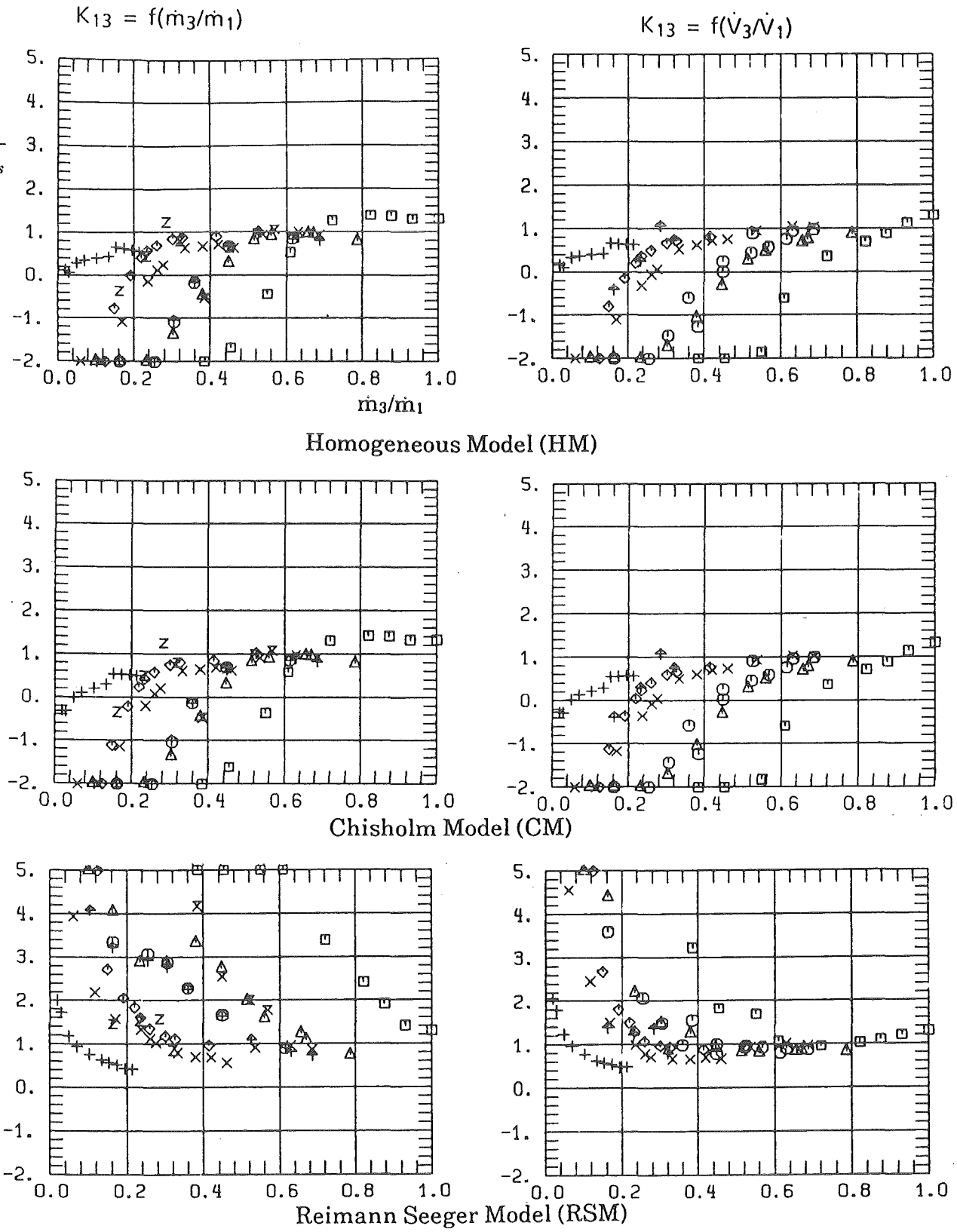


Fig. 6.13 Ratio of Predicted to Measured Branch Pressure Drop for Downward Branch with $D_3/D_1 = 0.52$ (Homogeneous Models, $K \neq 1$)

Upward Branch: For $D_3/D_1 = 1$ all models failed. The present results for $D_3/D_1 = 0.52$ are much more favourable: using the RMS there is a high accuracy for a wide mass split range. The reason for this is that

i) for the same value of $\dot{m}_3/\dot{m}_1$, the branch mass flux $G_3$ for $D_3/D_1 = 0.52$ is larger by a factor of about four which reduces phase separation effects in the branch.
ii) for the same branch pipe length, the diameter ratio is larger by a factor of two which is favourable to reach a well developed two-phase flow which is required for the determination of the measured Tee-junction pressure drop.

Downward Flow: Again the tendencies are very similar for $D_3/D_1 = 0.52$. The reason for the increasing deviation with decreasing mass split for given inlet conditions is not clear. Flow reversal effects in the branch are expected to be of less importance than for the upward branch. On the other hand, the branch pipe length was the smallest for the downward direction, compare Section 4.

Table VI.I summarizes the results showing the mean values of the pressure drop ratio and the corresponding standard deviations. The calculations were performed with results with $\dot{m}_3/\dot{m}_1 > 0.027$. The lower values were not included because measurement errors can become significant in this range and might be responsible for the big data scatter. For Table VI.I, 125 test points were used for the horizontal branch with $D_3/D_1 = 0.52$ and 57 and 76 test points, respectively, for the upward and downward branch, respectively. Using the previous results with $D_3/D_1 = 1$ and the horizontal branch, 78 test points were used. The framed numbers characterize the best results for each branch direction. These values are always connected with the RMS. The RMS with $K = 1.34$ and $K_{13} = f(\dot{V}_3/\dot{V}_1)$ has the highest overall accuracy. Therefore, this combination is generally recommended.

Figure 6.14 contains the new results for the horizonal branch with $D_3/D_1 = 1$, performed at much lower mass fluxes compared to the previous experiments. The data scatter at low mass split is larger for all models. The general remarks, given above, however, apply also to these data.

In order to improve further the model accuracy, correction functions could be evaluated, for instance, as a function of mass split. The RSM would be suited best because the data scattering is the smallest. However, such a procedure is questionable, as these functions will be different for different branch orientations

| | | $D_3/D_1 = 0.52$ | | | | | | | |
|---|---|---|---|---|---|---|---|---|---|
| | | K = 1 | | | | K = 1.34 (HM, RSM); 0.85 (CM) | | | |
| | | $K_{13} = f(m_3/m_1)$ | | $K_{13} = f(V_3/V_1)$ | | $K_{13} = f(m_3/m_1)$ | | $K_{13} = f(V_3/V_1)$ | |
| | | $\frac{\Delta p_{1\text{-}3\,mod}}{\Delta p_{1\text{-}3meas}}$ | σ | $\frac{\Delta p_{1\text{-}3\,mod}}{\Delta p_{1\text{-}3meas}}$ | σ | $\frac{\Delta p_{1\text{-}3\,mod}}{\Delta p_{1\text{-}3meas}}$ | σ | $\frac{\Delta p_{1\text{-}3\,mod}}{\Delta p_{1\text{-}3meas}}$ | σ |
|  | HM | 1.10 | 1.05 | 1.56 | 1.17 | 1.60 | 1.04 | 2.12 | 1.17 |
| | CM | 1.75 | 1.43 | 2.37 | 1.58 | 1.48 | 1.35 | 2.01 | 1.50 |
| | RSM | 0.85 | 0.35 | 1.00 | 0.42 | 1.17 | 0.79 | 1.37 | 0.83 |
|  | HM | 1.17 | 0.60 | 1.54 | 0.82 | 1.60 | 0.87 | 2.10 | 1.06 |
| | CM | 1.84 | 1.14 | 2.42 | 1.36 | 1.55 | 0.93 | 2.05 | 1.16 |
| | RSM | 0.54 | 0.25 | 0.65 | 0.33 | 0.75 | 0.26 | 0.900 | 0.300 |
|  | HM | -0.80 | 2.43 | -0.95 | 2.39 | -0.41 | 2.23 | -0.61 | 2.18 |
| | CM | -0.19 | 2.10 | -0.43 | 2.04 | -0.44 | 2.23 | -0.65 | 2.18 |
| | RSM | 1.12 | 1.05 | 0.62 | 0.26 | 2.17 | 1.80 | 1.50 | 1.25 |
| | | $D_3/D_1 = 1$ | | | | | | | |
|  | HM | 1.37 | 1.09 | 1.42 | 0.92 | 2.23 | 1.78 | 2.32 | 1.53 |
| | CM | 2.82 | 2.36 | 2.93 | 2.06 | 2.27 | 1.87 | 2.32 | 1.62 |
| | RSM | 2.34 | 0.20 | 0.40 | 0.30 | 0.85 | 0.29 | 0.92 | 0.22 |

## Table VI.I Branch Pressure Drop: Mean Values

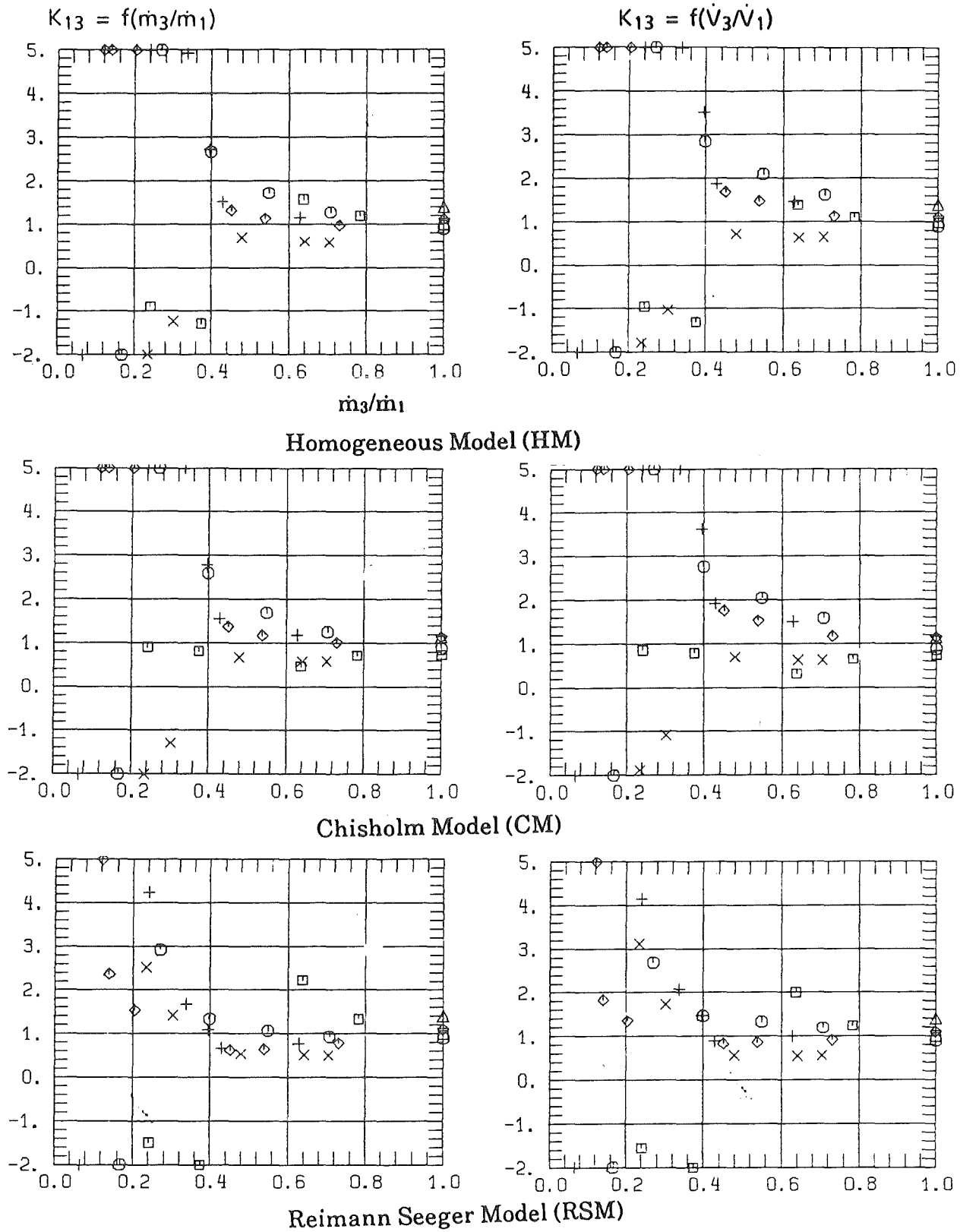


Fig. 6.14 Ratio of Predicted to Measured Branch Pressure Drop for Horizontal Branch with $D_3/D_1 = 1$ (Homogeneous Models, $K \neq 1$)

and diameter ratios. The range of applicability is then probably very restricted. Therefore, this procedure is not elaborated in the following.

In the following, some interesting conclusions can be drawn by determining the correction factor K for each test point in such a way, that the pressure drop ratio becomes unity. The Figs. 6.15-6.17 show the corresponding results, again evaluating the models with $K_{13}=f(\dot{m}_3/\dot{m}_1)$ and $K_{13}=f(\dot{V}_3/\dot{V}_1)$. The values scatter considerably which means that neither the assumption of a constant value is an appropriate choice nor the assumption of $K=f(\dot{m}_3/\dot{m}_1)$ or $K=f(\dot{V}_3/\dot{V}_1)$. However, these figures are well suited to show the consequence of the assumption of a homogeneous reversible pressure difference, compare Eq. (6.3). For $D_3/D_1=0.52$ and single-phase flow, $(\Delta p_{1\text{-}3})_{rev}$ is negative (pressure increase) for $\dot{m}_3/\dot{m}_1<0.27$ and becomes a pressure drop for $\dot{m}_3/\dot{m}_1>0.27$. A calculated value of $K=0$ means that there is no irreversible pressure loss at all, which is physically not meaningful. The other conclusion is that the evaluation of $(\Delta p_{1\text{-}3})_{rev}$ with homogeneous densities results in too high values. Therefore, in the following, models will be analysed with nonhomogeneous formulations.

### 6.2.1.2 Nonhomogeneous Models

The reversible pressure difference $(\Delta p_{1\text{-}3})_{rev}$ was given by Saba and Lahey /12/ in terms of the energy densities $\rho_{e1}$ and $\rho_{e3}$ (Eq. 3.20) and by Reimann and Seeger /27/ in terms of the energy density $\rho_{e3}$ and a density $\rho_{*1}$ defined by Eq. (3.21). In the following Rouhani's slip correlation is used to evaluate both $S_1$ and $S_3$.

Hwang and Lahey /35/ suggested to determine $(\Delta p_{1\text{-}3})_{rev}$ with the homogeneous density in the branch ($\rho_{e3}=\rho_{h3}$) and the energy density in the inlet. A slip correlation was proposed which predicts slip values very close to unity (Eqs. (3.27)-(3.28)). With this $\rho_{e1}$ also becomes quite close to $\rho_{h1}$.

Figure 6.18 shows a comparison between different formulations of $(\Delta p_{1\text{-}3})_{rev}$. For convenience, the expressions are summarized below:

a)
$$(\Delta p_{1-3})_{rev}=\frac{\rho_{h3}}{2}\left(\left(\frac{G_3}{\rho_{h3}}\right)^2-\left(\frac{G_1}{\rho_{h1}}\right)^2\right), \tag{6.5}$$

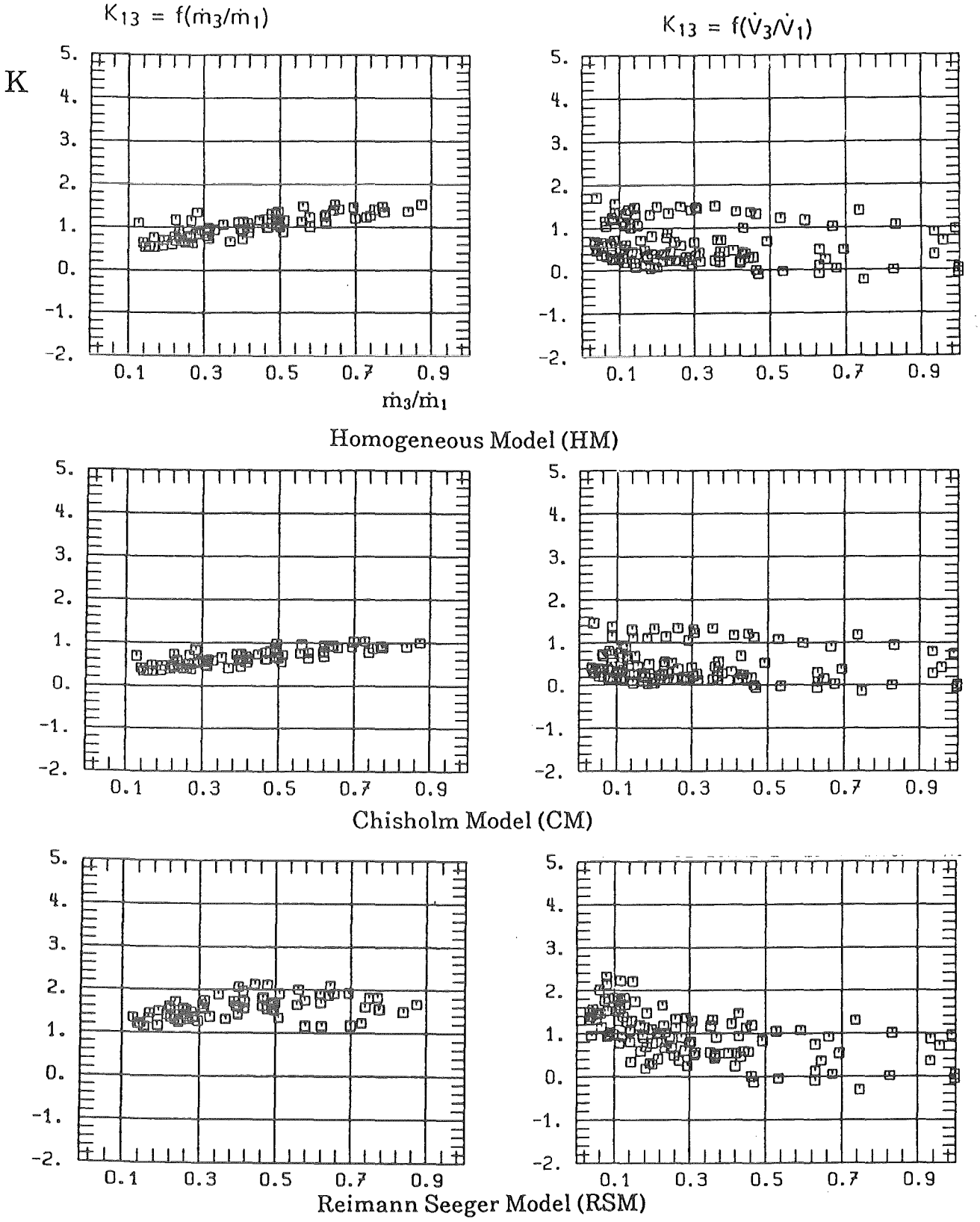


Fig. 6.15 Correction Factor K (Homogeneous Models) for Horizontal Branch

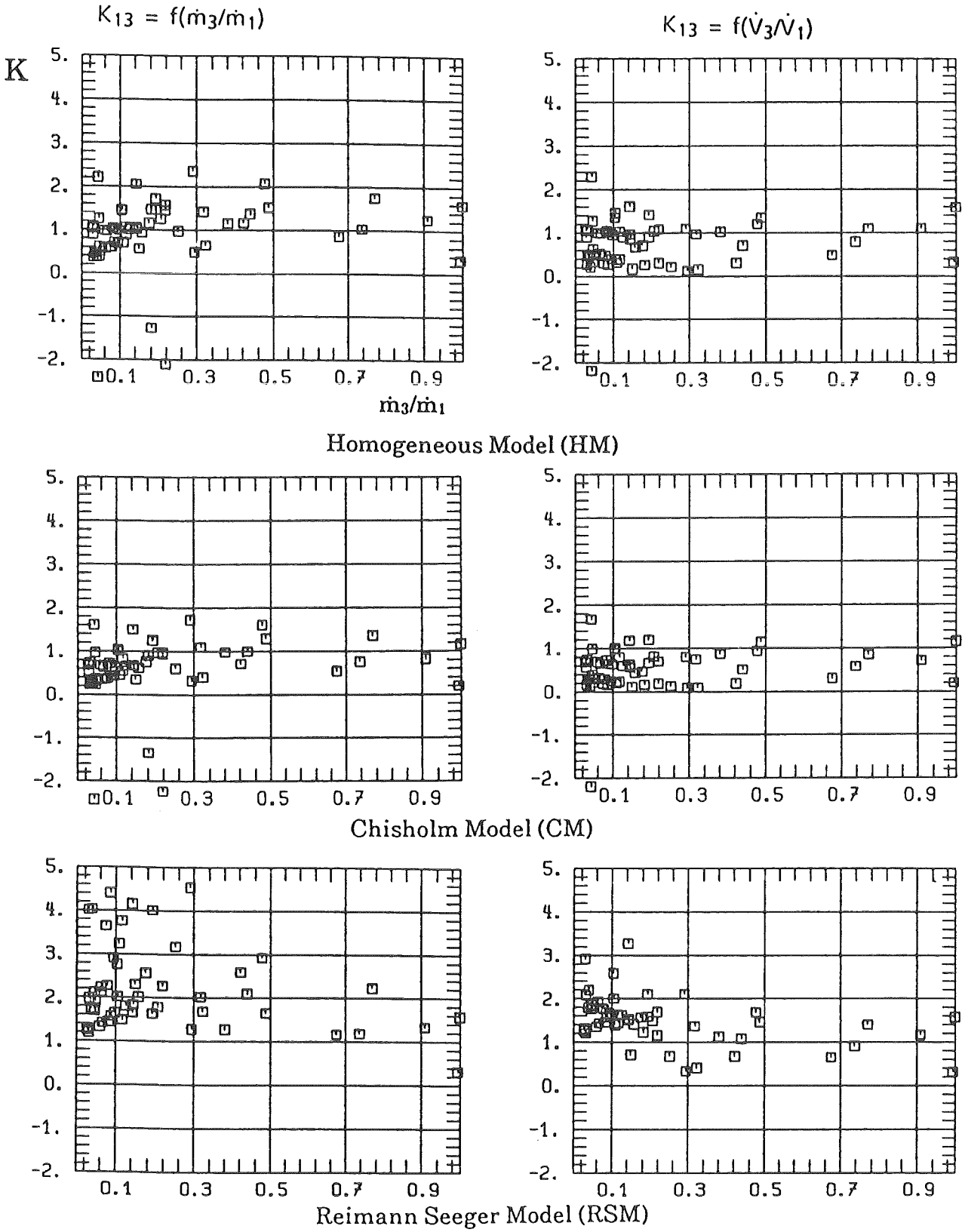


Fig. 6.16 Correction Factor K (Homogeneous Models) for Upward Branch

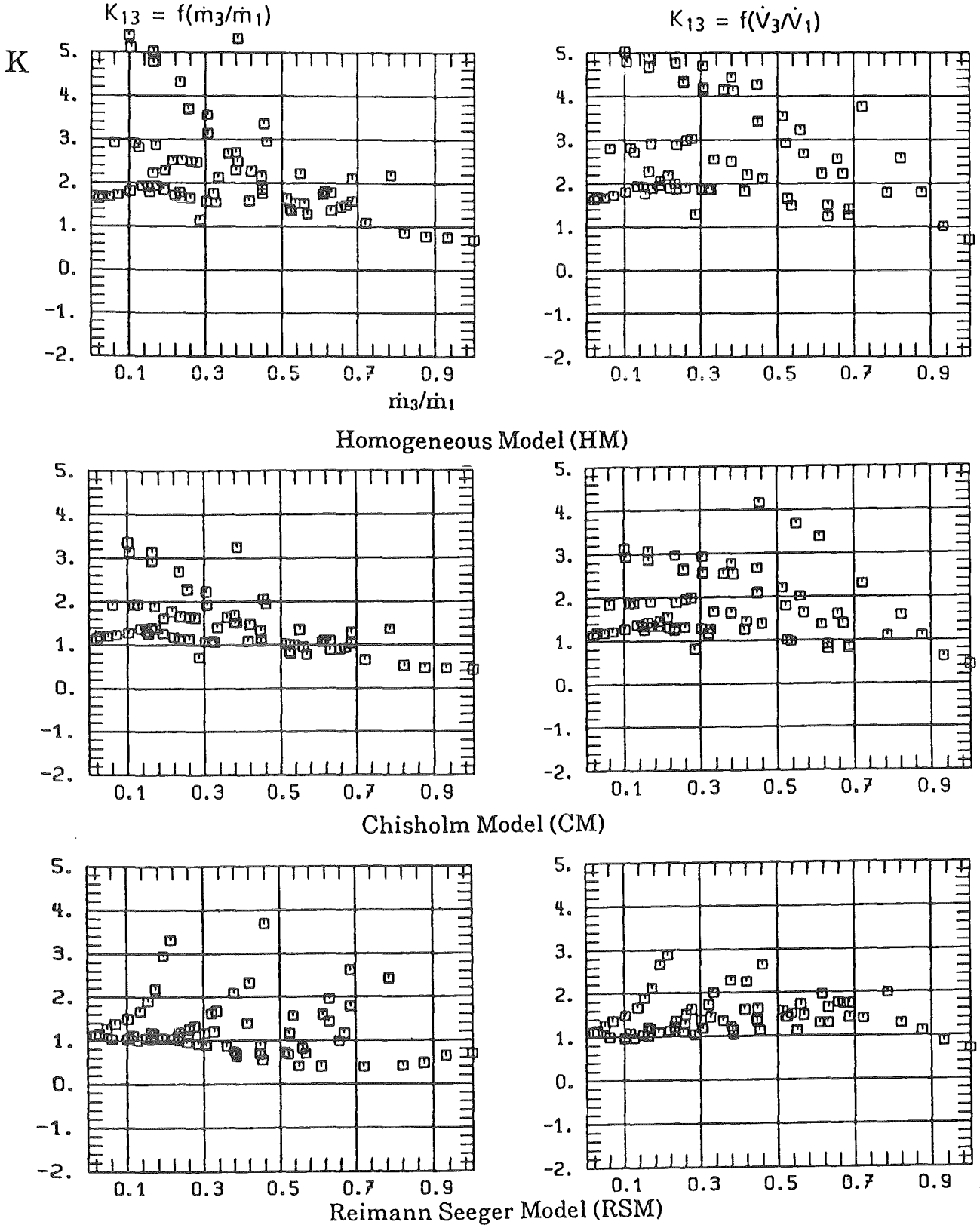


Fig. 6.17 Correction Factor K (Homogeneous Models) for Downward Branch

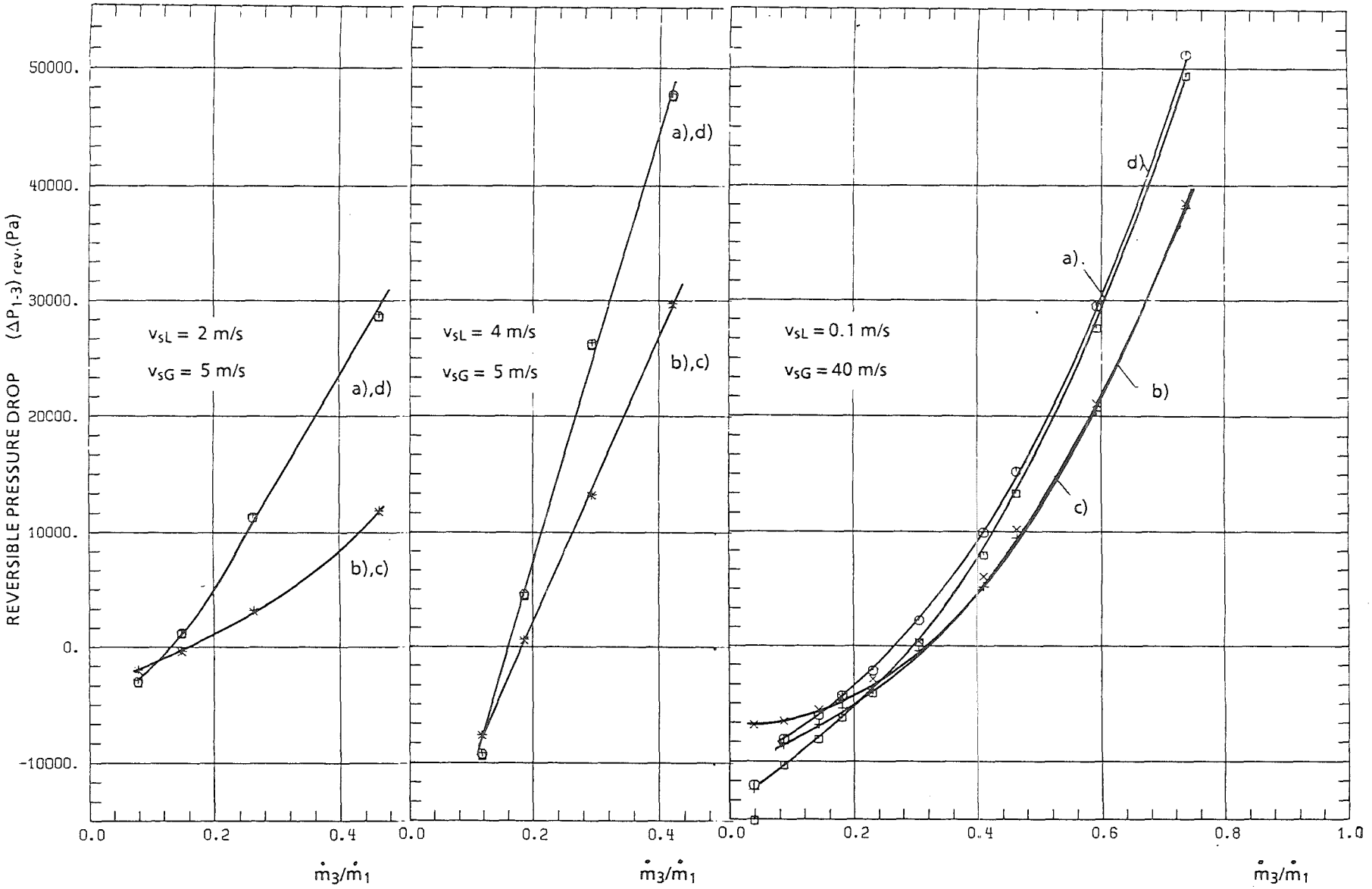


Fig. 6.18 Calculated Reversible Branch Pressure Difference $(\Delta p_{1\text{-}3})_{rev}$ for Characteristic Inlet Conditions (Data for Horizontal Branch)

b)
$$(\Delta p_{1-3})_{rev} = \frac{\rho_{h3}}{2}\left(\frac{G_3^2}{\rho_{e3}^2} - \frac{G_1^2}{\rho_{e1}^2}\right), \tag{6.6}$$

with $S_1$, $S_3$ from Eqs. (2.17)-(2.19)

c)
$$(\Delta p_{1-3})_{rev} = \frac{\rho_{h3}}{2}\left|\left(\frac{G_3}{\rho_{e3}}\right)^2 - \left(\frac{G_1}{\rho_{*1}}\right)^2\right|, \tag{6.7}$$

with $S_1$, $S_3$ from Eqs. (2.17)-(2.19).

d)
$$(\Delta p_{1-3})_{rev} = \frac{\rho_{h3}}{2}\left((\frac{G_3}{\rho_{h3}})^2 - (\frac{G_1}{\rho_{h1}})^2\right), \tag{6.8}$$

with $S_1$ from Eqs. (3.27)-(3.28).

The comparison is performed for a test point in the slug flow regime ($v_{sL}=2$ m/s, $v_{sG}=5$ m/s), the dispersed bubble flow regime ($v_{sL}=4$ m/s, $v_{sG}=5$ m/s) and the annular flow regime ($v_{sL}=0.1$ m/s, $v_{sG}=40$ m/s).

As expected, $(\Delta p_{1\text{-}3})_{rev}$ according to Hwang and Lahey (expression d)) becomes quite close to the homogeneous expression. A minor difference is only observed for $v_{sL}=0.1$ m/s and $v_{sG}=40$ m/s where high slip values occur. (According to Rouhani $S_1 \approx 13$). On the other hand the expressions b) and c) result also in very similar values; again differences can be only seen for highly separated flow. The nonhomogeneous expressions predict lower values for large mass splits which should improve the prediction of the total pressure drop.

Finally, a comparison is performed for the total pressure drop $\Delta p_{1\text{-}3}$ using the different expressions for $(\Delta p_{1\text{-}3})_{rev}$. In Eqs. (6.9) and (6.10), Eq. (6.6) is used in combination with $\varphi_{HM}$ and $\varphi_{RSM}$, respectively, for evaluation of $(\Delta p_{1\text{-}3})_{irr}$. In Eq. (6.11), Eq. (6.7) is used togehter with $\varphi_{RSM}$, and Eq. (6.12) represents again the nonhomogeneous RSM:

The HLM uses as two-phase flow multiplier $\varphi_{RSM}$. Due to the fact that this model predicts very similar values for $(\Delta p_{1\text{-}3})_{rev}$ as for the homogeneous model, the HLM should become very close to the homogeneous RSM. This is again confirmed in Fig. 6.19, compare also Fig. 3.12. Therefore, this model is no longer used for comparison in the following.

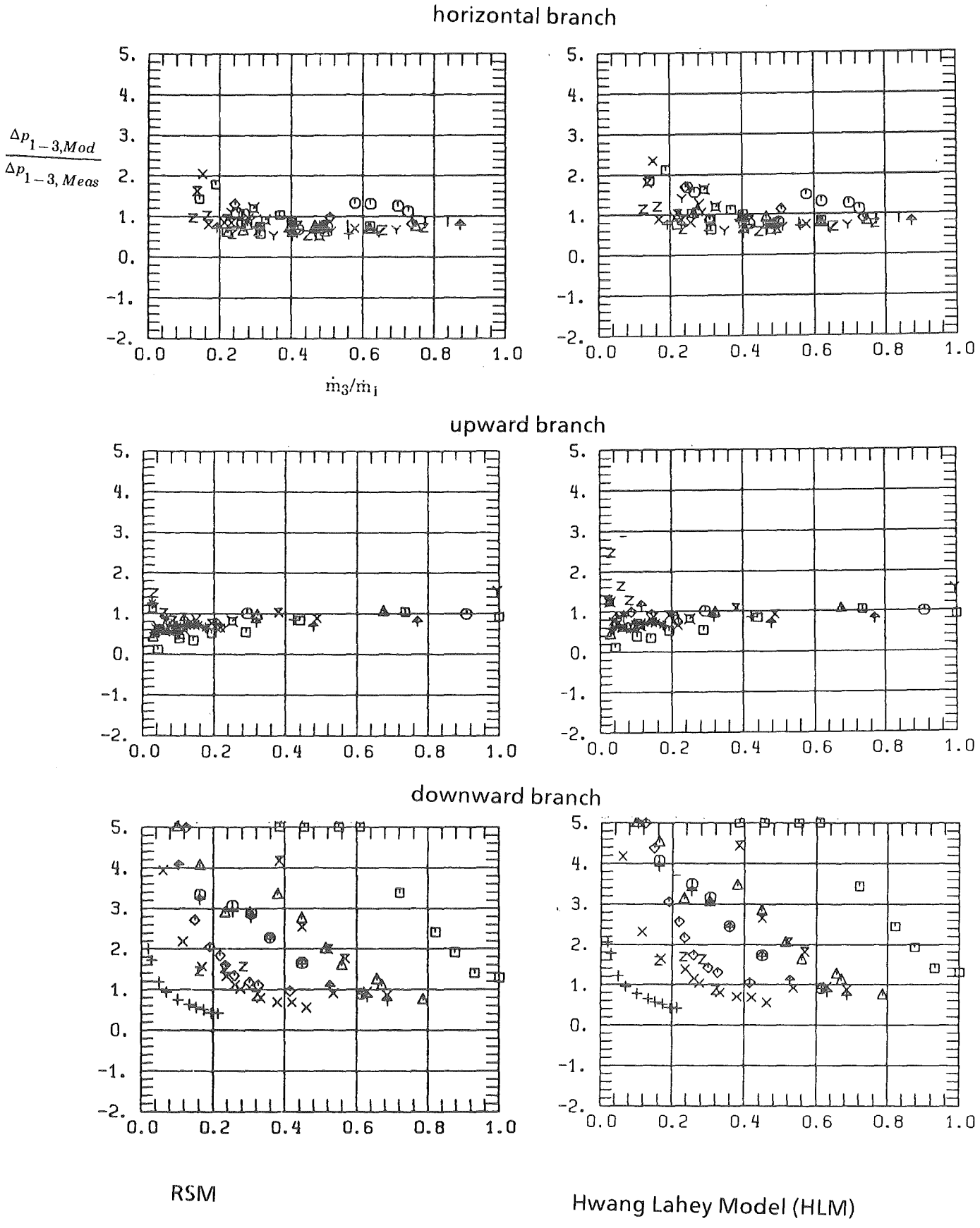


Fig. 6.19 Comparison between HLM and RSM for Different Branch Orientations, ($D_3/D_1 = 0.52$, $K \neq 1$, $K_{13} = f(\dot{m}_3/\dot{m}_1)$)

$$(\Delta p_{1-3}) = \frac{\rho_{h3}}{2}\left(\frac{G_3^2}{\rho_{e3}^2} - \frac{G_1^2}{\rho_{e1}^2}\right) + K_{13}\frac{G_1^2}{\rho_{h_1}}, \tag{6.9}$$

$$(\Delta p_{1-3}) = \frac{\rho_{h3}}{2}\left(\frac{G_3^2}{\rho_{e3}^2} - \frac{G_1^2}{\rho_{e1}^2}\right) + K_{13}\frac{G_1\rho_{h3}}{\rho_{h_1^2}}, \tag{6.10}$$

$$(\Delta p_{1-3}) = \frac{\rho_{h3}}{2}\left|\left(\frac{G_3}{\rho_{e3}}\right)^2 - \left(\frac{G_1}{\rho_{*1}}\right)^2\right| + K_{13}\frac{G_1\rho_{h3}}{\rho_{h_1^2}}, \tag{6.11}$$

$$\Delta p_{1-3} = \frac{\rho_{h3}}{2\rho_L}\left\{\frac{G_3^2}{C_3^2}\left(x_3R + S_{C3}(1-x_3)\right)^2\left(x_3 + \frac{1-x_3}{S_{C3}^2}\right) - G_1^2\left(x_1R + S_1(1-x_1)\right)^2\left(x_3 + \frac{1-x_3}{S_1^2}\right)\right\}$$

$$+ \frac{G_3^2}{\rho_L}\left\{\left(x_3R + S_3(1-x_3)\right) - \frac{1}{C_3}\left(x_3R + S_{C3}(1-x_3)\right)\left(x_3 + \frac{1-x_3}{S_{C3}}\right)\right\}. \tag{6.12}$$

The Figs. 6.20 - 6.22 show the results using Eqs. (6.9)-(6.12): For the horizontal branch, the nonhomogeneous model have a higher accuracy at higher mass splits, compare Figs. 6.8 and 6.20. The best result for the total measurement range is obtained with Eq. (6.10) using $K_{13} = f(\dot{V}_3/\dot{V}_1)$.

For the upward and downward branch, the accuracy is decreased due to a stronger underprediction of the measurements.

Figure 6.23 shows the influence of different assumptions concerning $(\Delta p_{1-3})_{rev}$ using $\varphi_{HM}$ and $\varphi_{RSM}$ as two-phase flow multipliers (horizontal branch, $K_{13} = f(\dot{m}_3/\dot{m}_1)$). For $S_1 = S_{1,Rouh}$ and $S_3 = 1$ the accuracy of the RSM is improved at low mass splits.

The general formulation of the RSM contains as a parameter also the slip $S_{C3}$ at the vena contracta. Assumptions for $S_{C3}$ range from $S_{C3} = 1$ up to $S_{C3} = (\rho_L/\rho_G)^{0.5}$. The latter expression is obtained for ideally separated phases. (Due to centrifugal forces, the phases can separate significantly between branch inlet and vena contracta). To use an intermediate value, $S_{C3}$ was calculated again with Rouhani's correlation. Figure 6.24 shows some parameter variations. Without going into detail, it can be concluded that no significant improvements are obtained compared to the results discussed above.

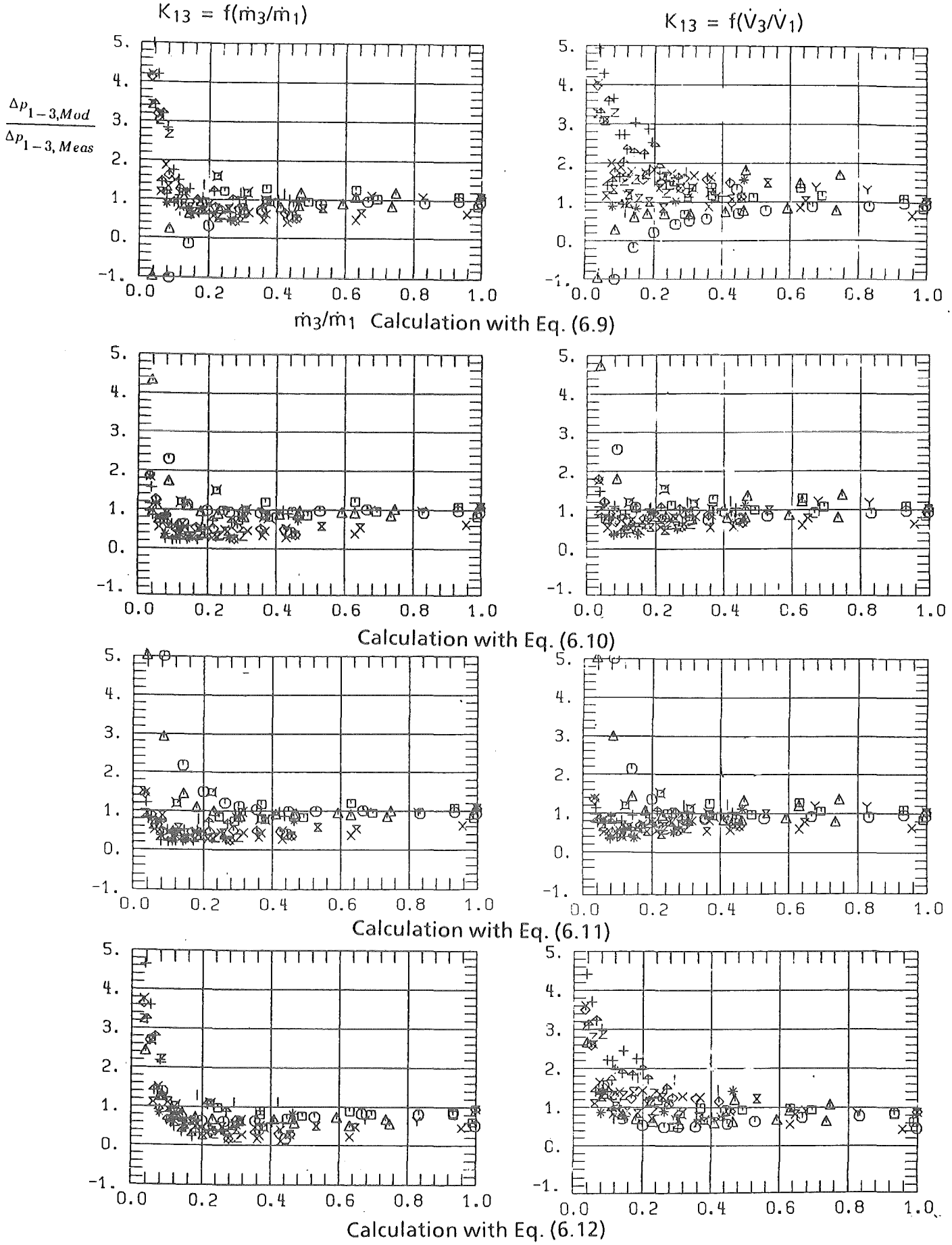


Fig. 6.20 Ratio of Predicted to Measured Branch Pressure Drop for Horizontal Branch with $D_3/D_1 = 0.52$ (Nonhomogeneous Models)

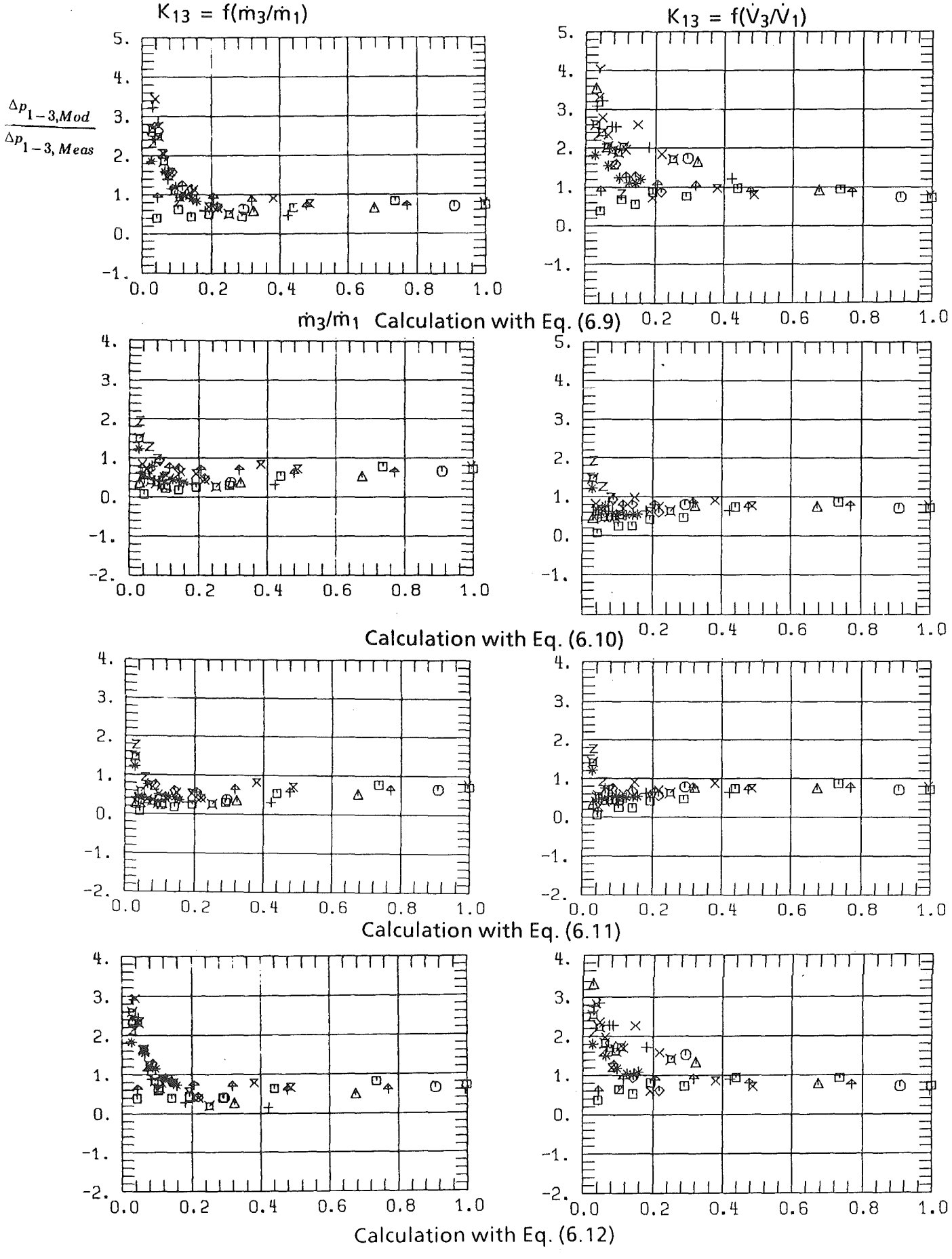


Fig. 6.21 Ratio of Predicted to Measured Branch Pressure Drop for Upward Branch with $D_3/D_1 = 0.52$ (Nonhomogeneous Models)

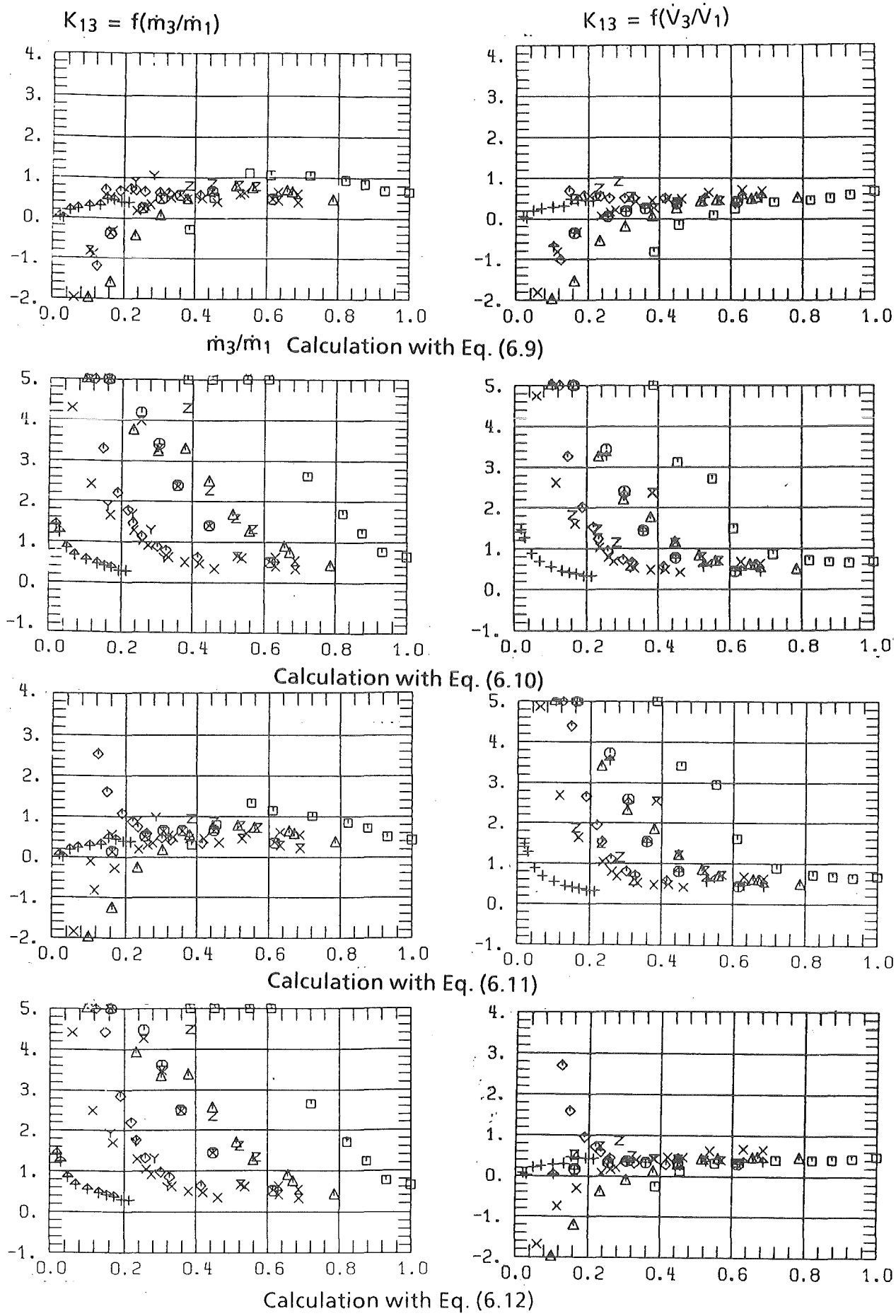


Fig. 6.22 Ratio of Predicted to Measured Branch Pressure Drop for Downward Branch with $D_3/D_1 = 0.52$ (Nonhomogeneous Models)

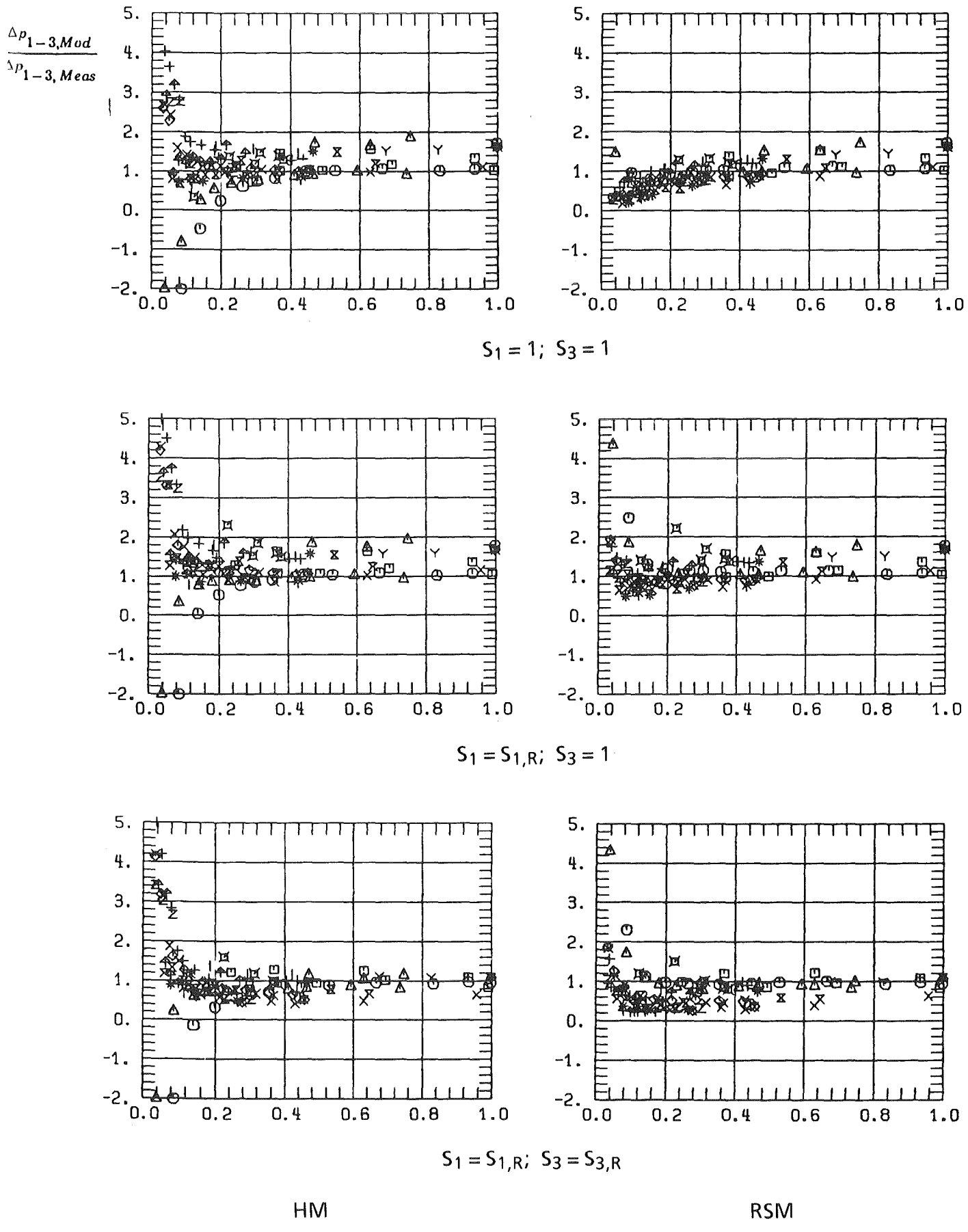


Fig. 6.23 Comparison of HM and RSM with Different Assumptions for $S_1$ and $S_3$ (Horizontal Branch, $D_3/D_1 = 0.52$)

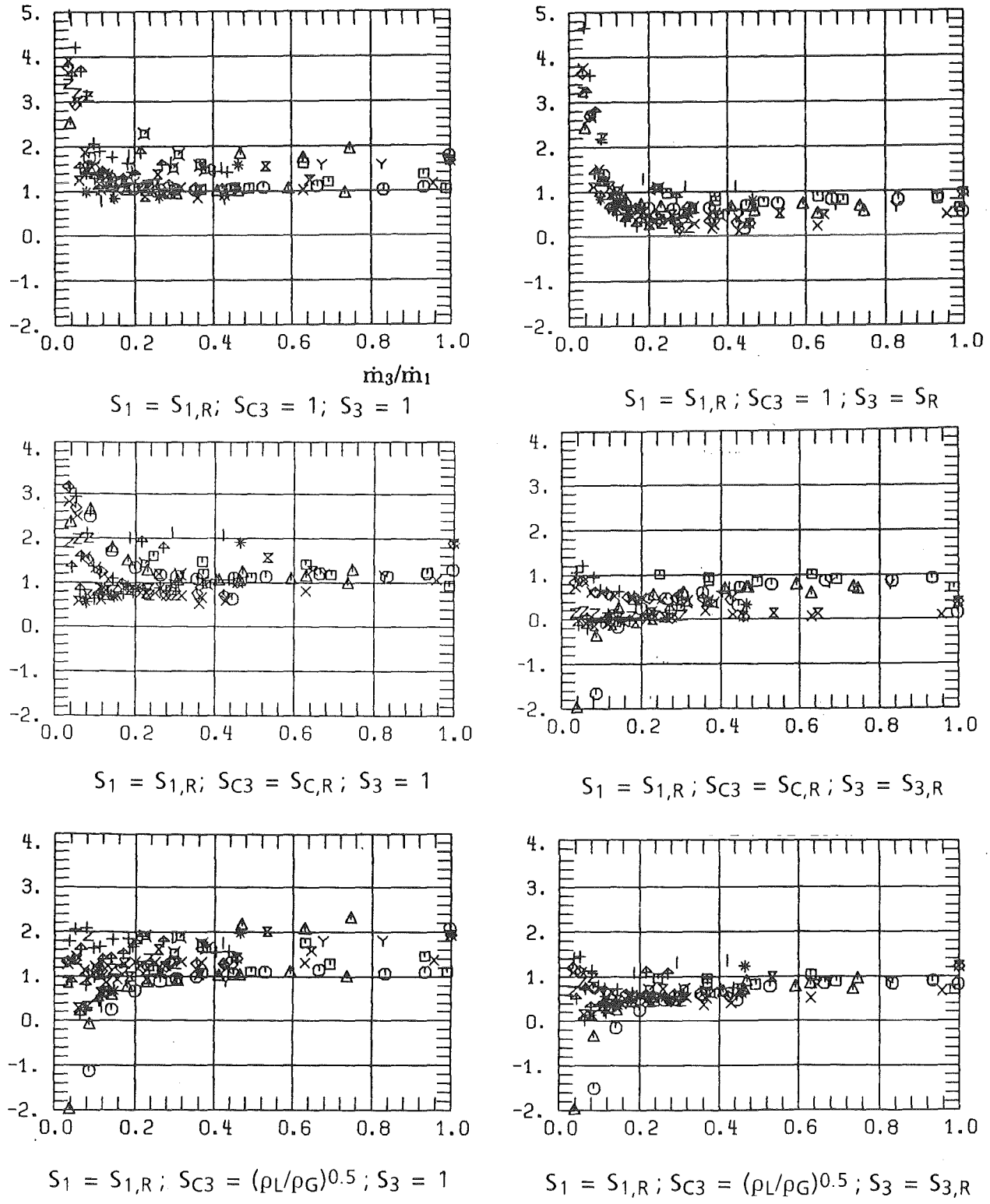


Fig. 6.24 Full RSM: Different Assumptions for $S_1$, $S_{C3}$ and $S_3$ (Horizontal Branch, $D_3/D_1 = 0.52$, $K_{13} = f(\dot{m}_3/\dot{m}_1)$

The Figs. 6.25 and 6.26 show examples of corresponding results for the previous experiments with $D_3/D_1 = 1$ and the horizontal branch. Again, improvements may be obtained for a special configuration or a limited flow parameter range but a general improvement is not achieved.

Summarizing the results for $D_3/D_1 = 0.52$ and 1, the following statements can be made:

- The best results were obtained with the homogeneous RMS using $K_{13} = f(\dot{V}_3/\dot{V}_1)$ and $K = 1.36$.
- The introduction of nonhomogeneity did not generally improve the models. Nevertheless, the authors think that improvements can only be achieved by taking into account nonhomogeneities. However, much more work is required to understand the fundamental processes.

### 6.2.2 Run Pressure Difference

#### 6.2.2.1 Models Used for Comparison

As outlined in Section 3.3.2 the models are based on either
- a momentum balance
or
- an energy and momentum balance.

Both types can be formulated using homogeneous or nonhomogeneous flow assumptions.

Assuming homogeneous flow, two models are considered:

a) the Homogeneous Momentum Balance Model (HMM) given by Eq. (3.3.4),
b) the Homogeneous Model (HM), which is the reduced form of the RSM (Eqs. (3.35)-(3.36)) by setting $S_1 = 1$ and $S_2 = 1$.

Three nonhomogeneous models are used for comparison:

c) the Separated Momentum Balance Model (SMM) according to Eqs. (3.32)-(3.33),
d) the RSM according to Eqs. (3.35)-(3.36),

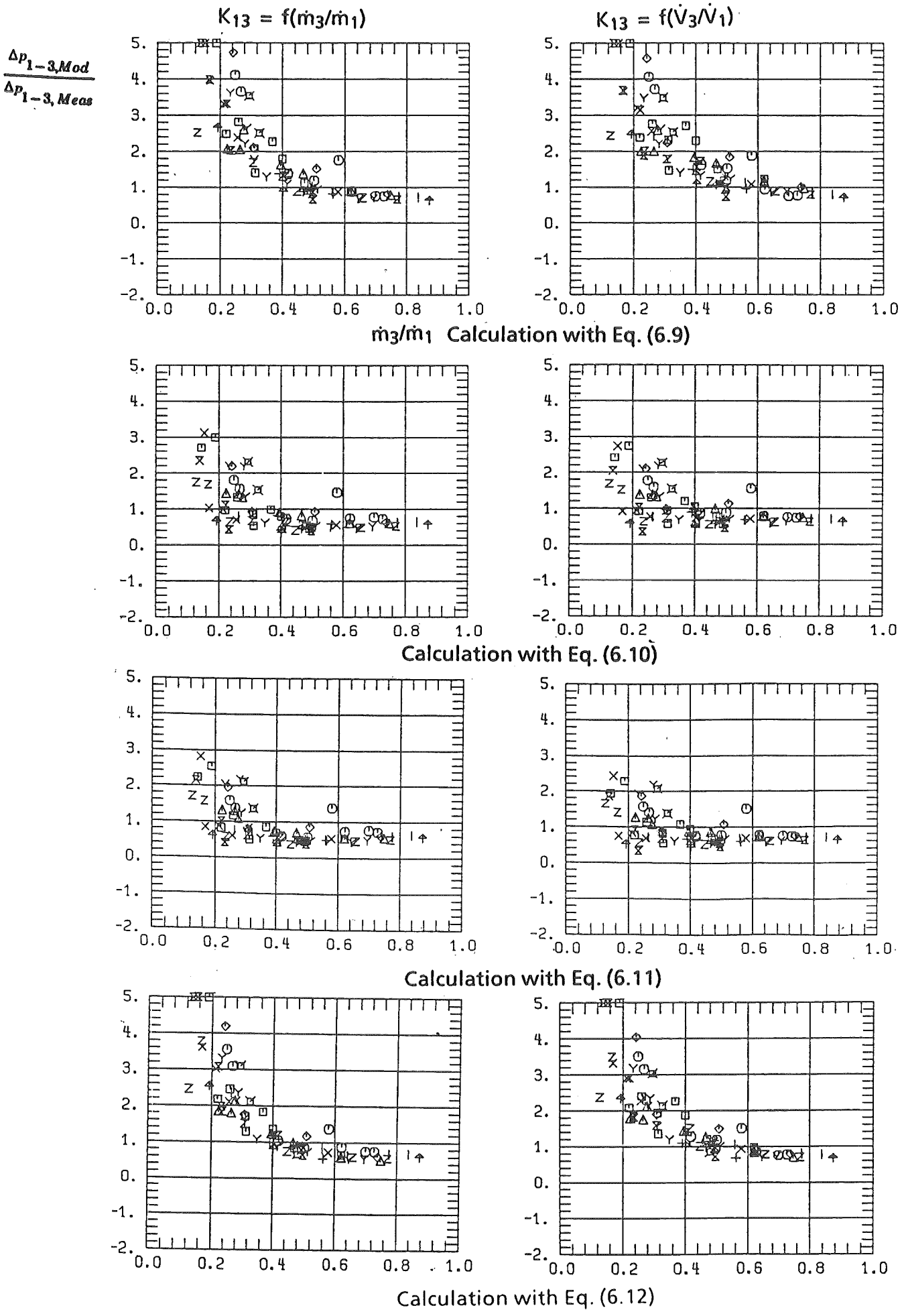


Fig. 6.25 Comparison of Nonhomogeneous Models for the Horizontal Branch with $D_3/D_1 = 1$: $S_1 = S_{1,R}$, $S_3 = S_{3,R}$, $S_{C3} = 1$

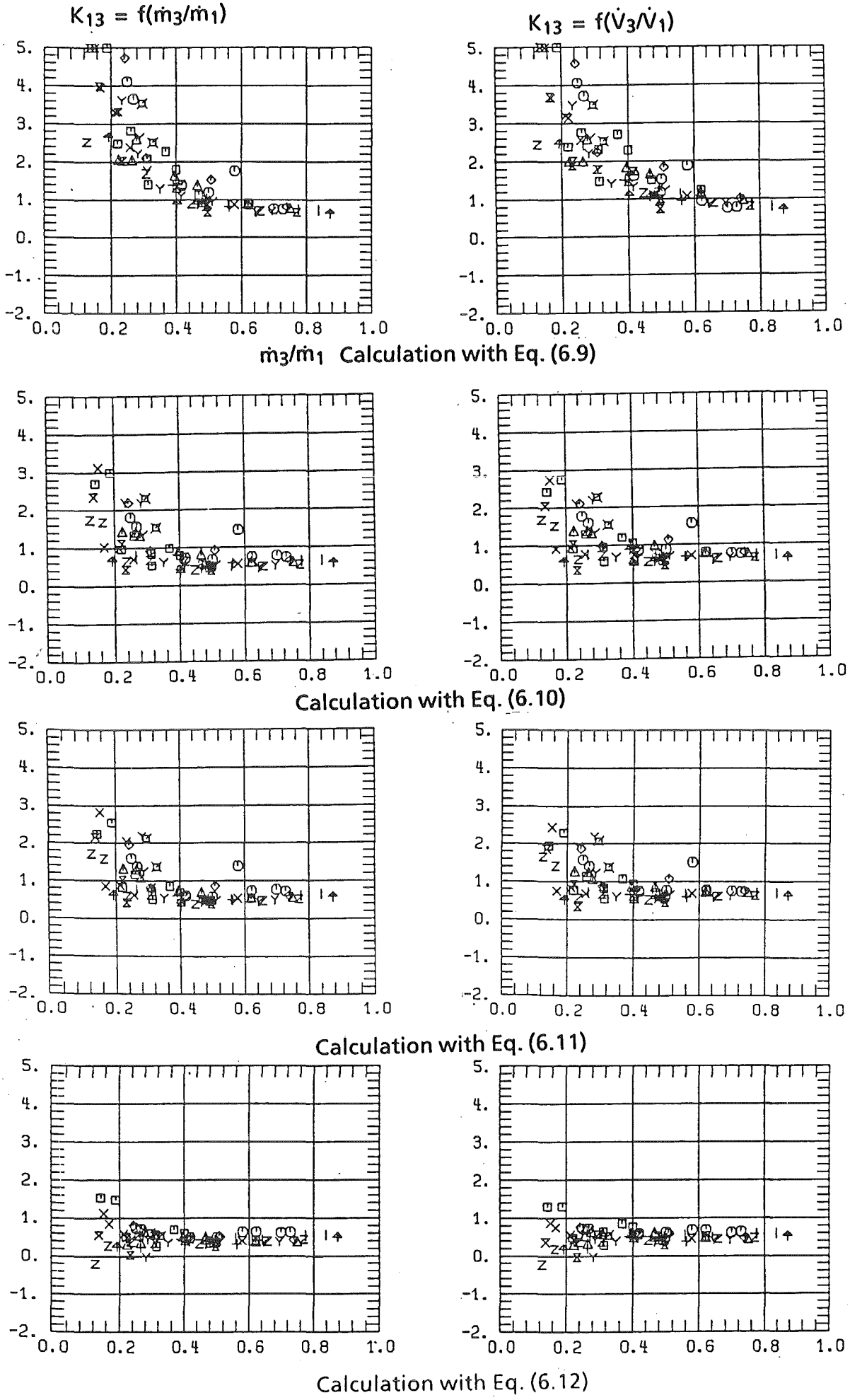


Fig. 6.26 Comparison of Nonhomogeneous Models for the Horizontal Branch with $D_3/D_1 = 1$: $S_1 = S_{1,R}$, $S_3 = S_{3,R}$, $S_{C3} = (\rho_I/\rho_G)^{0.5}$

e) the Hwang-Lahey Model (HLM) which is based on the SMM but uses the assumption $\rho_{m2} = \rho_{h2}$. The slip in the inlet pipe is determined with Eqs. (3.27)-(3.28).

Using the SMM and RSM, the slip is determined with Rouhani's relationship (Eqs. (2.17)-(2.19)).

6.2.2.2 Comparison of New Experiments with $D_3/D_1 = 1$

Figure 6.27 contains the ratio of predicted to measured pressure difference as a function of the mass flux ratio $G_3/G_1$ for the present experiments with $D_3/D_1 = 1$, using $K_{12} = f(\dot{m}_3/\dot{m}_1)$, according to Eq. (6.2b). As mentioned before, these new experiments extend the previously investigated parameter range to lower superficial inlet water velocities.

The homogeneous models are not suited to predict the measurements. Concerning the nonhomogeneous models, the SMM has the highest accuracy, followed by the RSM. The HLM does not predict satisfactorily the results.

The results shown in Fig. 6.27 were evaluated using the loss coefficient $K_{12}$ from previous measurements. This coefficient differs from the relationship used in the present experiments with $D_3/D_1 = 0.52$, see Fig. 3.4. According to Miller /46/, the relationship for $K_{12}$ should be independent on $D_3/D_1$. In order to determine the sensitivity of different $K_{12}$ relationships, Eq. (6.1b) was also used for the model predictions of the new experiments. Figure 6.28 shows that there is no remarkable change in the data for the model with the highest accuracy: the SMM. The same is true when $K_{12} = f(\dot{V}_3, \dot{V}_1)$ is used instead of $K_{12} = f(\dot{m}_3/\dot{m}_1)$, as shown in Fig. 6.29. The RMS is more sensitive to changes in $K_{12}$ but no clear improvement is obtained by using e.g. $K_{12} = f(\dot{V}_3/\dot{V}_1)$. The other models are not improved either.

6.2.2.3 Comparison of Experiments with $D_3/D_1 = 0.52$

The Figs. 6.30 and 6.31 contain the results for the horizontal branch. Compared to the branch pressure drop results, the scatter is much larger. Many points are outside of the ordinate interval given in the figures. Again the SMM has the highest accuracy, followed by the RSM with $K_{12} = f(\dot{m}_3/\dot{m}_1)$. Again the SMM is

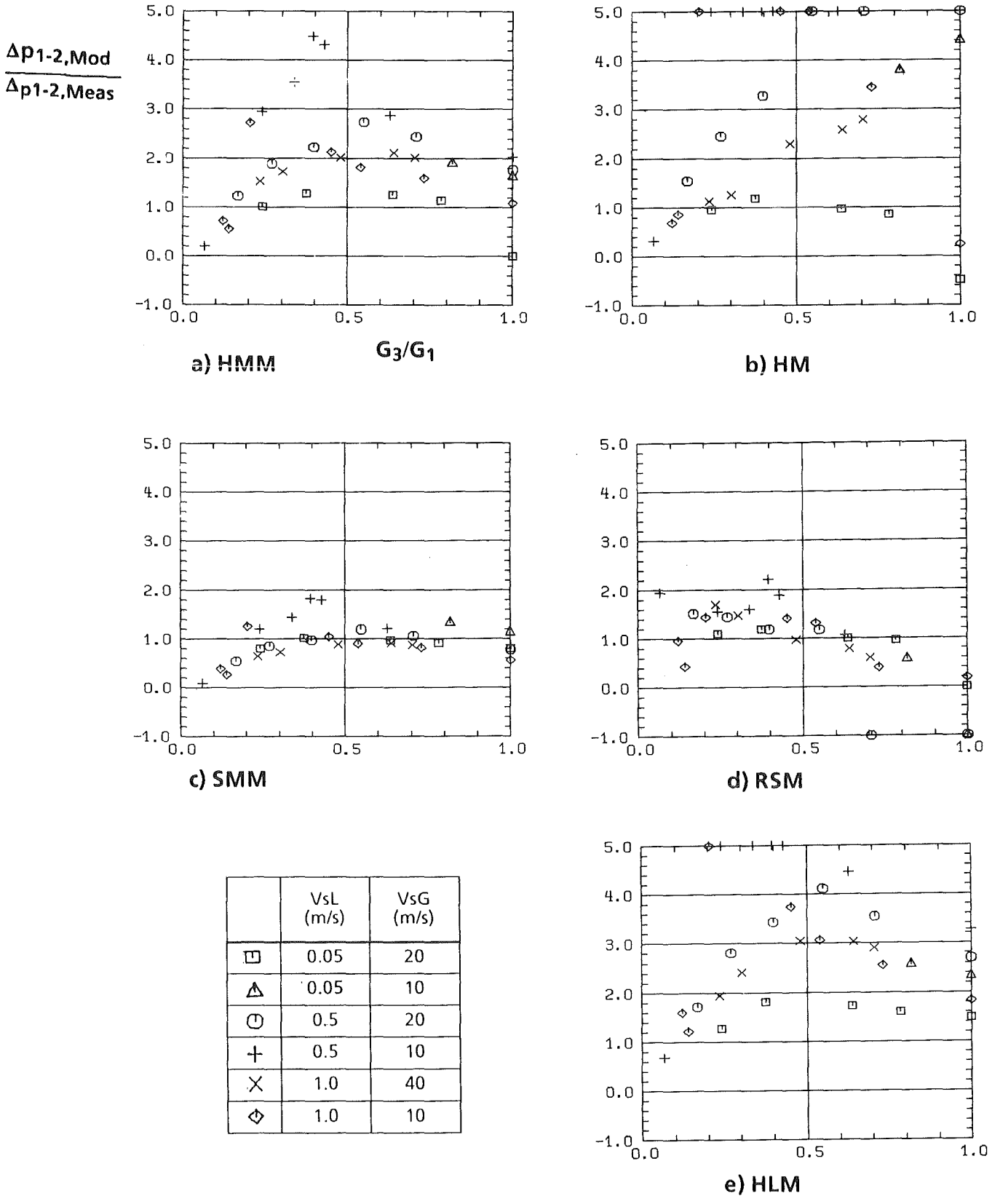


| | VsL (m/s) | VsG (m/s) |
|---|---|---|
| □ | 0.05 | 20 |
| △ | 0.05 | 10 |
| ○ | 0.5 | 20 |
| + | 0.5 | 10 |
| × | 1.0 | 40 |
| ◇ | 1.0 | 10 |

Fig. 6.27 Ratio of Predicted to Measured Run Pressure Difference for Horizontal Branch with $D_3/D_1 = 1$ (New Experiments): $K_{12} = f(\dot{m}_3/\dot{m}_1)$ according to Eq. (6.2b)

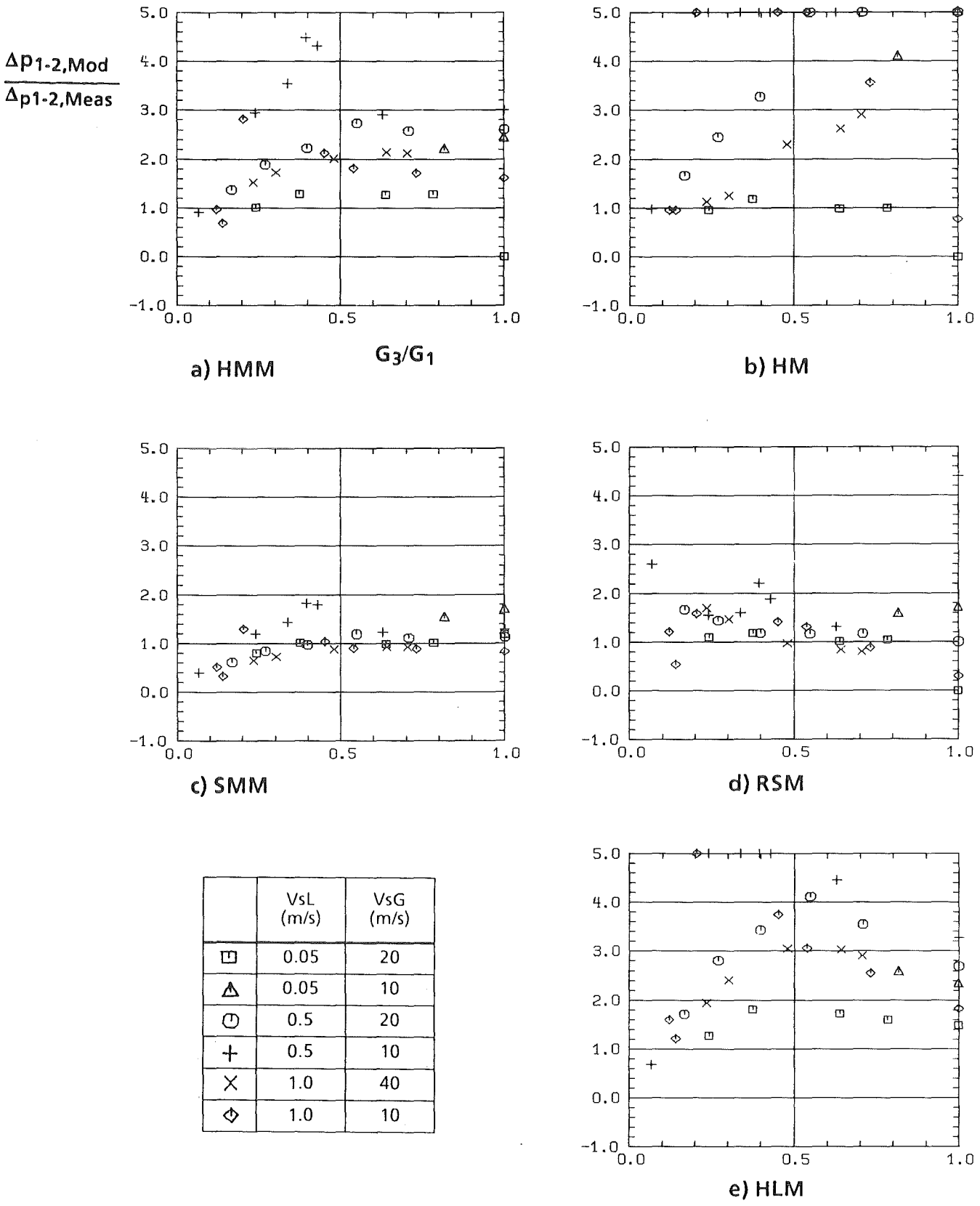


Fig. 6.28 Ratio of Predicted to Measured Run Pressure Difference for Horizontal Branch with $D_3/D_1 = 1$ (New Experiments): $K_{12} = f(\dot{m}_3/\dot{m}_1)$ according to Eq. (6.1b)

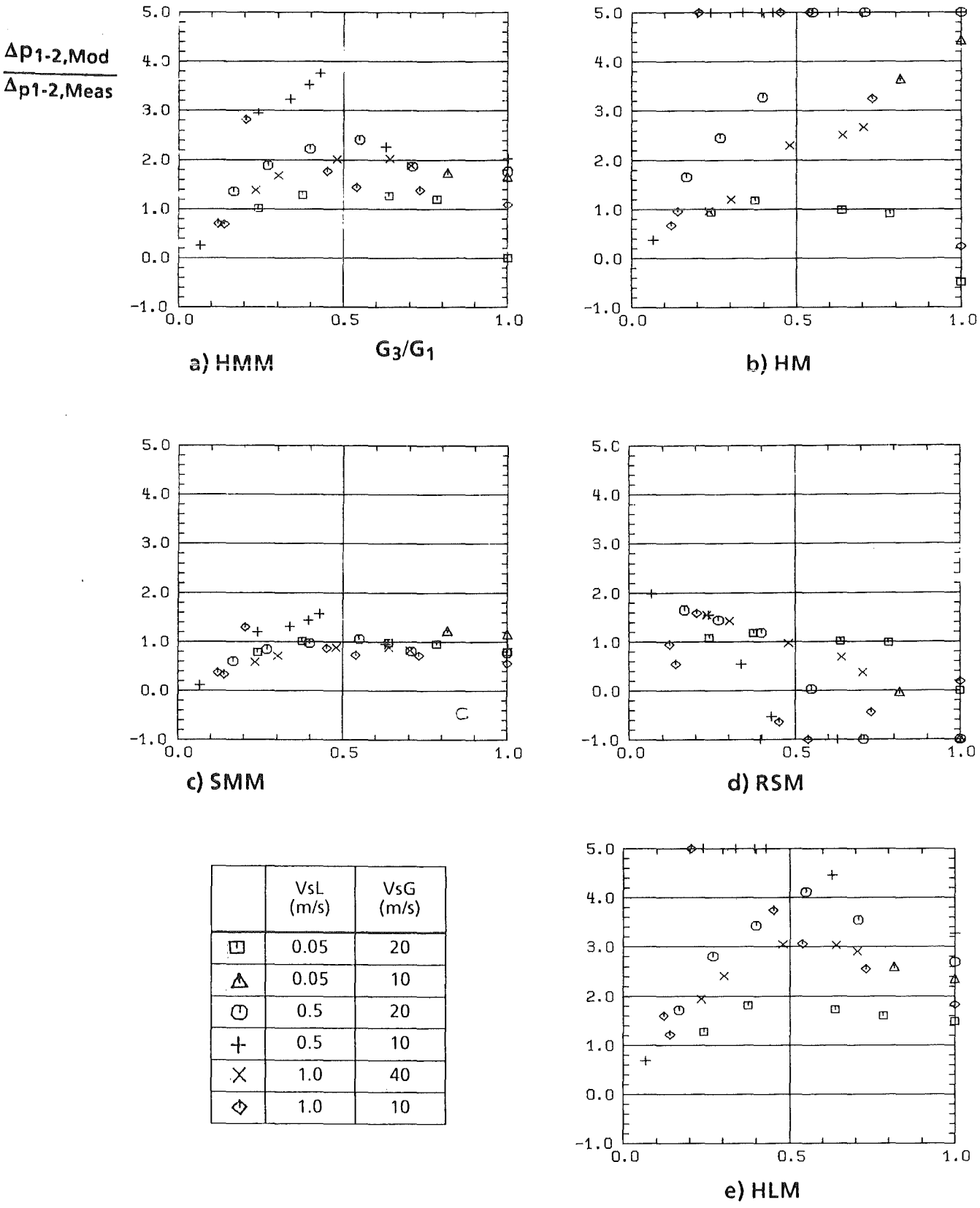


Fig. 6.29 Ratio of Predicted to Measured Run Pressure Difference for Horizontal Branch with $D_3/D_1 = 1$ (New Experiments): $K_{12} = f(V_3/V_1)$ according to Eq. (6.2b)

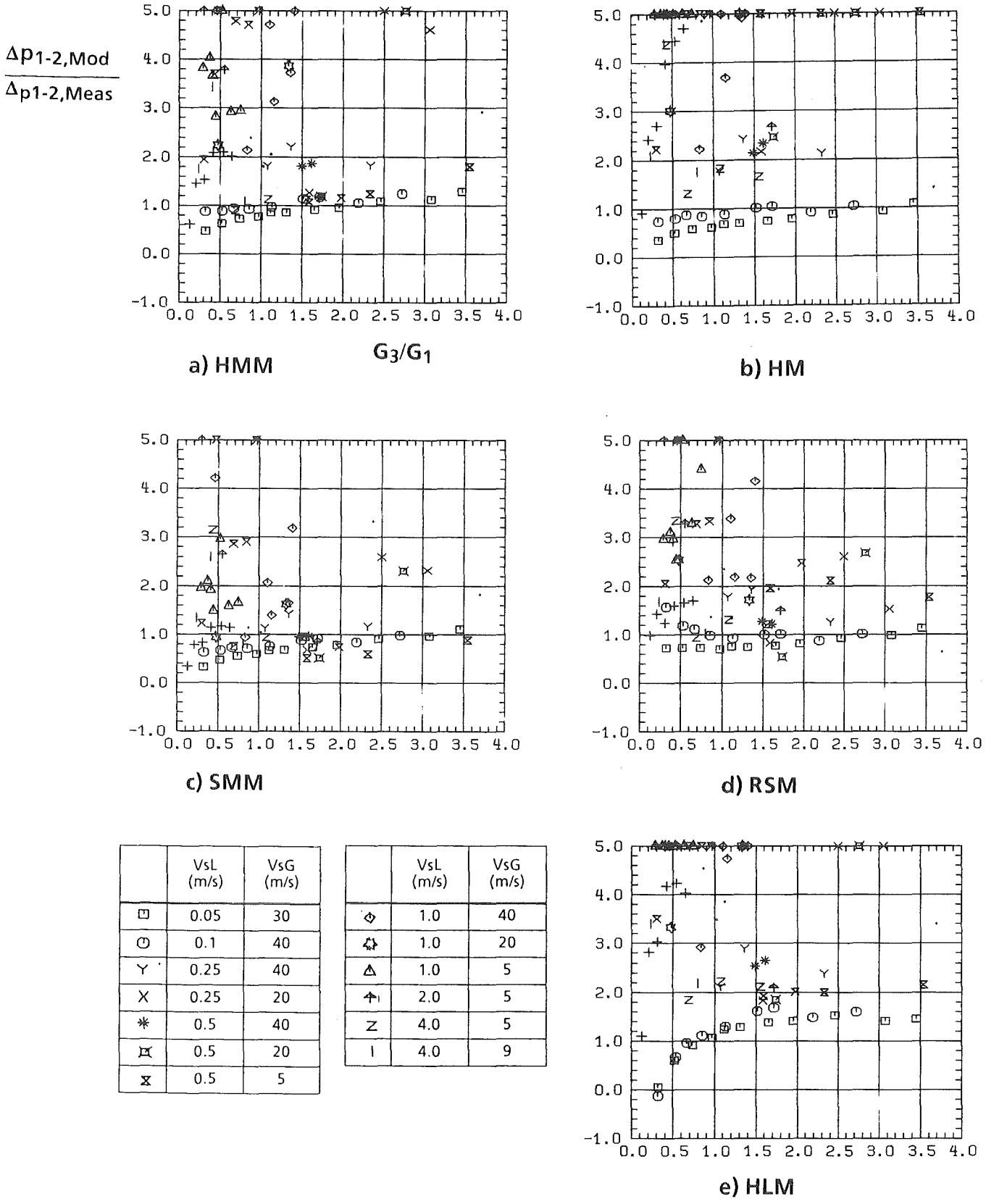


| | VsL (m/s) | VsG (m/s) |
|---|---|---|
| □ | 0.05 | 30 |
| ○ | 0.1 | 40 |
| Y | 0.25 | 40 |
| X | 0.25 | 20 |
| ✳ | 0.5 | 40 |
| ⊠ | 0.5 | 20 |
| ⧖ | 0.5 | 5 |

| | VsL (m/s) | VsG (m/s) |
|---|---|---|
| ◇ | 1.0 | 40 |
| ☆ | 1.0 | 20 |
| △ | 1.0 | 5 |
| + | 2.0 | 5 |
| Z | 4.0 | 5 |
| I | 4.0 | 9 |

Fig. 6.30 Ratio of Predicted to Measured Run Pressure Difference for Horizontal Branch with $D_3/D_1 = 0.52$ (New Experiments): $K_{12} = f(\dot{m}_3/\dot{m}_1)$ according to Eq. (6.2b)

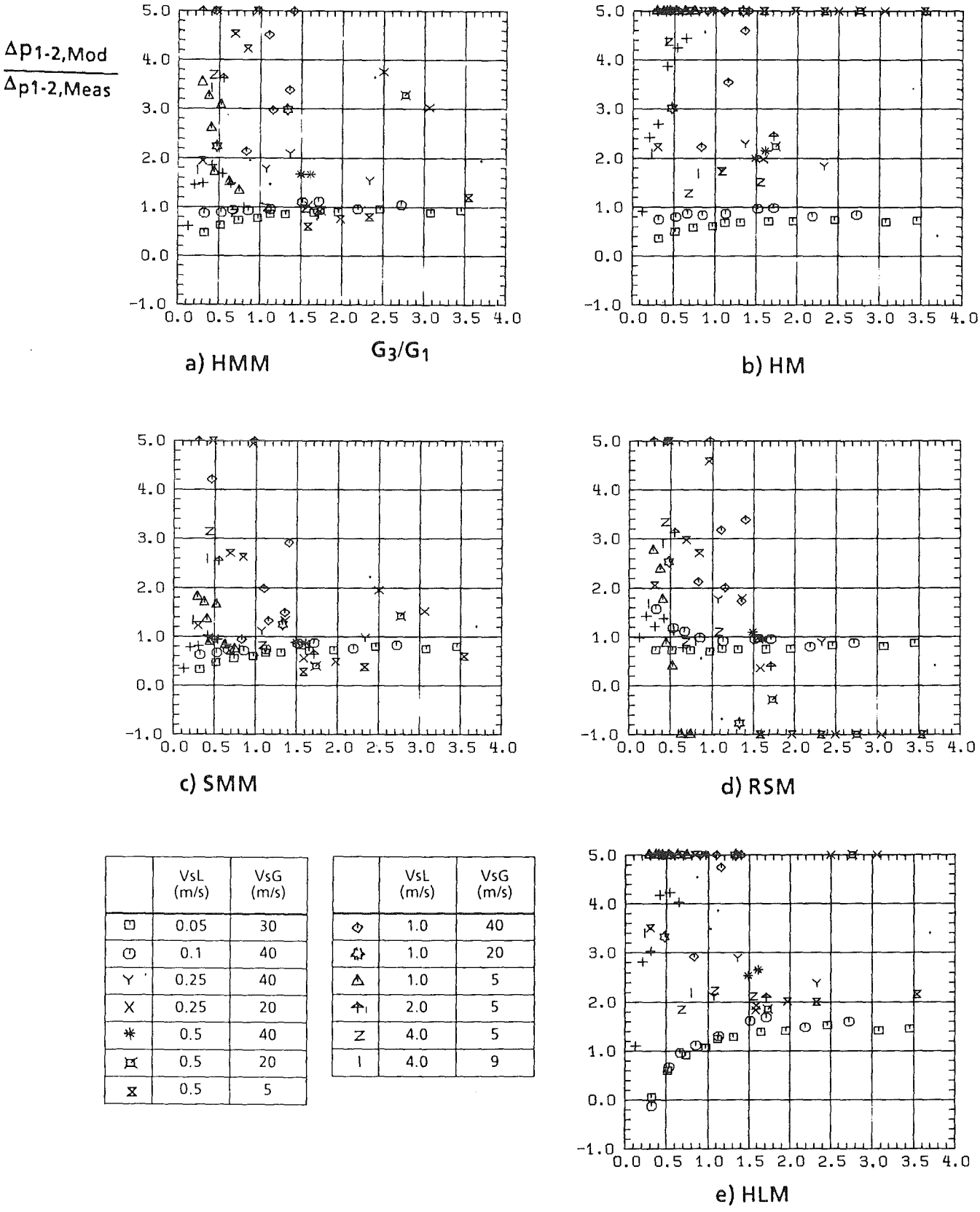


| | VsL (m/s) | VsG (m/s) |
|---|---|---|
| □ | 0.05 | 30 |
| ○ | 0.1 | 40 |
| Y | 0.25 | 40 |
| X | 0.25 | 20 |
| ✳ | 0.5 | 40 |
| ⌑ | 0.5 | 20 |
| ⧖ | 0.5 | 5 |

| | VsL (m/s) | VsG (m/s) |
|---|---|---|
| ◇ | 1.0 | 40 |
| ⛢ | 1.0 | 20 |
| △ | 1.0 | 5 |
| ⛢ | 2.0 | 5 |
| Z | 4.0 | 5 |
| I | 4.0 | 9 |

Fig. 6.31 Ratio of Predicted to Measured Run Pressure Difference for Horizontal Branch with $D_3/D_1 = 0.52$ (New Experiments): $K_{12} = f(V_3/V_1)$ according to Eq. (6.2b)

not sensitive if $K_{13}=f(\dot{V}_3/\dot{V}_1)$ is used instead of $K_{12}=f(\dot{m}_3/\dot{m}_1)$, in contrast to the RSM. An interesting fact is that for annular flow at low mass fluxes (square and circle symbols) the accuracy is the highest. Even the homogeneous models are satisfactory in this case although values larger than 10 are calculated for $S_1$ and $S_2$.

Summarizing the results for $\Delta p_{1-2}$ it can be concluded that

- for the horizontal branch with $D_3/D_1=1$ and 0.52 the SMM had the highest accuracy.
- Similar comparisons should be performed with the data for the upward and downward branch.
- More detailed analyses are required to investigate the influence of the slip in the different locations on the $\Delta p_{12}$ prediction.

## 7. CONCLUSIONS

An extensive experimental data base on Tee-junction phase redistribution and pressure drop is presented in this report. Only a small part of the results has been sufficiently analysed. Therefore, this data base should be very fruitful for further detailed discussions and comparisons with further investigations on two-phase Tee-junction flow.

The present models for phase redistribution and pressure drop are very simplistic. Further attempts should try to incorporate the distribution of local quantities (void fractions, phase velocities) in axial and radial directions. Much more detailed experimental investigations are required to understand the local phenomena.

REFERENCES

/1/ Reimann, J., John, H., Müller, S.: Impedance Probe for Detecting Flow Regime and Measuring the Phase Distribution in Horizontal Air-Water- and Steam-Water Flow; Two-Phase Flow Instrumentation Review Group Meeting, Troy, New York, March 13-14, 1978

/2/ Mandhane, J.M., Gregory, G.A., Aziz, K.: A Flow Pattern Map for Gas-Liquid Flow in Horizontal Pipes, Int. J. Multiphase Flow, 1, p. 537, 1974

/3/ Taitel, Y., Dukler, A.E.: A Model for Predicting Flow Regime Transitions in Horizontal and Near Horizontal Gas-Liquid Flow, A.I.Ch.E. Journal, 22, no. 1, p. 47, 1976

/4/ Reimann, J., John, H., Seeger, W.: Transition from Slug to Annular Flow in Horizontal Air-water and Steam Water Flow. KfK 3189, No.v 1981

/5/ Tsuyama, M., Taga, M.: On the Flow of the Air-Water Mixture in the Branch Pipe, Bull. JSME, Vol. 2, No. 5, 151-156, 1959

/6/ Fouda, E.A., Rhodes, E.: Two-Phase Annular Flow Stream Division in Simple Tee, Trans. Instn. Chem. Engrs., Vol. 52, 354-360, 1974

/7/ Collier, J.G.: Single-phase and two-phase flow behavior in primary circuit components, Proc. NATO Advanced Institute on Two-phase Flow and Heat Transfer, Vol. 1, pp. 313-365, Hemisphere Corp. 1976

/8/ Hong, K.C.: Two-Phase Flow Splitting at a Pipe Tee, J. Petr. Technol., 290 - 296, 1978

/9/ Whalley, P.B., Azzopardi, B.J.: Two-Phase Flow in a T-Junction, UKAEA Report AERE-R 9699, 1980

/10/ Azzopardi, B.J., Whalley, P.B.: The Effect of Flow Pattern on Two-Phase Flow in a T-Junction. Int. J. Multiphase Flow, Vol. 8, No. 5, pp. 491-507, 1982

/11/ Henry, J.A.R.: Dividing Annular Flow in a Horizontal Tee. Int. J. Multiphase Flow, Vol. 7, pp. 343-355, 1981

/12/ Saba, N., Lahey, R.T.: Phase Separation Phenomena in Branching Conduits. NUREG/CR-2590, 1982

/13/ Saba, N., Lahey, R.T.: Phase Separation Phenomena in Branching Conduits. Int. J. Multiphase Flow, Vol. 10, pp. 1-20, 1984

/14/ Reimann, J., Khan, M.: Flow Through a Small Pipe at the Bottom of a Large Pipe with Stratified Flow; Annual Meeting of the European Two-Phase Flow Group, Paris la Defense, June 2-4, 1982.

/15/ Reimann, J., Khan, M.: Flow Through a Small Break at the Bottom of a Large Pipe with Stratified Flow. Second International Topical Meeting on Nuclear Reactor Thermohydraulics, Jan. 11-14, 1983, Santa Barbara, California

/16/ Reimann, J., Smoglie, C.: Flow Through a Small Pipe at the Top of a Large Pipe with Stratified Flow. Annual Meeting of the European Two-Phase Flow Group, Zürich, Switzerland, June 14-16, 1983

/17/ Smoglie, C., Reimann, J.: Two-Phase Flow Through a Horizontal Branch in a Pipe with Stratified Flow. Jahrestagung Kerntechnik, Frankfurt, 22.-24. Mai, pp. 73-76, 1984, ISSN 0720 - 9207

/18/ Smoglie, C.: Zweiphasenströmungen durch kleine Abzweige in einem horizontalen Rohr mit geschichteter Gas-Flüssigkeits-Strömung; Dissertation, Universität Karlsruhe, 1984, KfK 3862

/19/ Smoglie, C., Reimann, J., Müller, U.: Two-Phase Flow Through Small breakes in a Horizontal Pipe with Stratified Flow; Chiu, Chong (Hrsg.), Proc. of Third Internat. Topical Meeting, Newport, R.I., October 15-18, 1985, ANS, 1985. - Vol. 2, p.13/A.1-A.8

/20/ Smoglie, C., Reimann, J., Two-Phase Flow Through Small Branches in a Horizontal Pipe with Stratified Flow; Int. Journal of Multiphase Flow, Vol. 12(1986), pp. 609-26

/21/ Reimann, J., John, H. Seeger, W.: Gemeinsamer Versuchsstand zum Testen und Kalibrieren verschiedener Zweiphasen-Massenstrom-Meßverfahren, Projekt Nukleare Sicherheit, Jahresbericht 1980, KfK 2950, pp. 4100/75-4100/115, 1981

/22/ Reimann, J., Seeger, W.: Two-Phase Pressure Drop in a Dividing T-Junction. The mechanics of Gas Liquid Flow Systems, Euromech Colloquium 176, Villard de Lans, France, Sept. 21-23, 1983

/23/ Reimann, J., Seeger, W.: Pressure Drop of Air-Water and Steam-Water Flow in a Dividing T-Junction. European Two-Phase Flow Group Meeting, Rome. Italy, June 19-21, 1984.

/24/ Seeger, W.: Untersuchungen zum Druckabfall und zur Massenstromumverteilung von Zweiphasenströmungen in rechtwinkligen Rohrverzweigungen. KfK 3876, März 1985

/25/ Seeger, W., Reimann, J., Müller, U.: Phase Separation in a T-Junction with a Horizontal Inlet. 2nd Int. Conference on Multi Phase Flow, London, GB, June 19-21, 1985

/26/ Seeger, W., Reimann, J., Müller, U.: Two-Phase Flow in a T-Junction with a Horizontal Inlet. Part I: Phase Separation. Int. Journal of Multiphase Flow, Vol. 12, No. 4, pp. 575-585, 1986

/27/ Reimann, J., Seeger, W.: Two-Phase Flow in a T-Junction with a Horizontal Inlet. Part II: Pressure Differences. Int. Journal of Multiphase Flow, Vol. 12, No. 4, pp. 587-608, 1986

/28/ Reimann, J., Brinkmann, H.J. Bopp, W.: Two-Phase Flow in T-Junctions with Small Branches, European Two-Phase Flow Meeting, München, June 10-13, 1986

/29/ Domanski, R., Reimann, J., Müller, U.: Phase Redistribution and Pressure Drop in T-Junctions with Different Diameter Ratios. European Two-Phase Flow Meeting, Trondheim, Norway, 1-4 June, 1987

/30/ Reimann, J., Domanski, R.: Two-Phase Flow Through Dividing T-Junctions with Different Diameter Ratios. AIChE Annual Meeting, New York, Nov. 15-20, 1987

/31/ /Katsaounis, A., Schultheiß, G.F.: Diverging Two-Phase Flow Pattern in a T-Junction and their Influence on the Form-Resistance Pressure Drop, 23rd ASME/AIChE Nat. Heat Transfer Conf., Denver, 1985

/32/ Katsaounis, A.: Zweiphasige Strömungsformen und Druckabfall in horizontalen T-Rohrverbindungen mit vertikalem Abzweig (Abschlußbericht). GKSS 87/E/12, 1987

/33/ Shoham, O., Brill, J.P., Taitel, Y.: Two-Phase Flow Splitting in a Tee Junction - Experiment and Modeling. Submitted to AIChe Journal

/34/ Ballyk, J.D., Shoukri, M.: Steam-Water Annular Flow in a Horizontal Dividing T-Junction. McMaster University, Mech.Eng.Dept.; Thermofluids Research Report No. ME/87/TF/RI, Hamilton, Canada, 1987

/35/ Hwang, S.T., Lahey, R.T.: A Study on Single and Two-Phase Pressure Drop in Branching Conduits. AIChE Annual Meeting, New York, Nov. 15-20, 1987

/36/ Maciaszek, T., Memponteil, A.: Experimental Study on Phase Separation in a Tee Junction for Steam Water Stratified Inlet Flow. European Two-Phase Flow Group Meeting, Munich, June 10-13, 1986

/37/ Anderson, J.L.: Entrainment and Pull-Through Phenomena at a Tee-junction. AIChE Annual Meeting, New York City, Nov. 15-20, 1987

/38/ Zetzmann, K.: Phasenseparation und Druckabfall in zweiphasig durchströmten vertikalen Rohrabzweigungen. Disseration, Universität Hannover, 1982

/39/ Honan, T.J., Lahey, R.T.: The Measurement of Phase Separation in Wyes and Tees, Nuclear Engineering and Design 64, pp.93 - 102, 1981

/40/ Azzopardi, B.J.: The Effect of the Side Arm Diameter on the Two-PhaseFlow Split at a "T" Junction. Int. J. Multiphase Flow, Vol. 10, No. 4, pp. 509-512, 1984

/41/ Lahey, R.T.: Current Understanding of Phase Separation Mechanisms in Branching Components. Nucl.Eng. and Design 95, pp. 145-161, 1986

/42/ Lemonnier, H., Hervieu, E.: Single-Phase and Two-Phase Flow in a Tee Junction: a Theoretical Study. European Two-Phase Flow Meeting, Trondheim, Norway, June 1-4, 1987

/43/ McCreery, G.: A Correlation for Phase Separation in a Tee. Multiphase Flows and Heat Transfer III, Part B: Applications (Ed. by Veziroglu and Bergles), Elsevier, Amsterdam, 1984

/44/ Wallis, G.B.: One-dimensional Two-Phase Flow. McGraw Hill, New York, 1969

/45/ Collier, J.G.: Single-phase and two-phase flow behavior in primary circuit components. Proc. NATO Advanced Institute on Two-phase Flow and Heat Transfer, Vol. 1, pp. 313-365. Hemisphere Corp., 1976

/46/ Miller, D.S.: Internal flow, a guide to losses in pipe and duct systems. BHRA, Cranfield, Bedford, UK, 1971

/47/ Sallet, D.W., Popp, M.: Experimental investigation of one- and two-phase flow through a tee-junction; physical modelling of multiphase flow. Coventry, England, 19-21 April 1983

/48/ Hackeschmidt, M.: Grundlagen der Strömungstechnik. VEB Deutscher Verlag für Grundstoffindustrie, Leipzig, DDR, 1970

/49/ Vogel, G.: Untersuchungen über den Verlust in rechtwinkligen Rohrverzweigungen. Heft 2, pp. 61-64. Mitteilung des hydr. Inst. der T.H. München, 1928

/50/ Gardel, A.: Les pertes de charges dans les écoulements au travers de branchements en té. Bull. Tech. Suisse Romande 9, 122-130; 10, 143-148, 1957

/51/ Fitzsimmons, D.E.: Two-phase pressure drop in piping components. HW 80970 REV1, General Electric Hanford Laboratoires, Richland, Washington, 1964

/52/ Chisholm, D.: Pressure losses in bends and tees during steam-water flow. NEL Report 318, National Engineering Lab., Glasgow, Scotland, 1967

/53/ Madden, J.M., St. Pierre, C.S.: Proc. Instn. mech. Engrs, 184/3C, 175, 1969/70

/54/ Rouhani, Z.: Modified correlations for void and two-phase pressure drop. AE-RTV-841, 1969

/55/ John, H., Reimann, J.: Gemeinsamer Versuchsstand zum Testen und Kalibirieren verschiedener Zweiphasen-Massenstrommeßverfahren. Anlagenbeschreibung KfK 2731B, Febr. 1979

/56/ Friedel, L.: Druckabfall bei der Strömung von Gas/Dampf- Flüssigkeits-gemischen in Rohren. Chem. Ing. Technik 50, Nr. 3, p. 167, 1978

# APPENDIX. Experimental Data

Table D.3: Air-Water Flow Data (Refs /21/ - /27/): $D_3/D_1$ = 1, Horizontal Branch($\Phi$ = 90°).

Table D.4: Air-Water Flow Data (Refs /21/ - /27/): $D_3/D_1$ = 1, Upward Branch ($\Phi$ = 0°).

Table D.5: Air-Water Flow Data (Refs /21/ - /27/): $D_3/D_1$ = 1, Downward Branch ($\Phi$ = 180°).

Table D.6: Steam-Water Flow Data (Refs /21/ - /27/): $D_3/D_1$ = 1, Horizontal Branch($\Phi$ = 90°).

Table D.7: Present Air-Water Flow Data: $D_3/D_1$ = 1, Horizontal Branch ($\Phi$ = 90°).

Table D.8: Present Air-Water Flow Data: $D_3/D_1$ = 0.52, Horizontal Branch ($\Phi$ = 90°).

Table D.9: Present Air-Water Flow Data: $D_3/D_1$ = 0.52, Upward Branch ($\Phi$ = 0°).

Table D.10: Present Air-Water Flow Data: $D_3/D_1$ = 0.52, Downward Branch ($\Phi$ = 180°).

Table D.11: Present Air-Water Flow Data: $D_3/D_1$ = 0.2, Horizontal Branch ($\Phi$ = 90°).

Table D.12: Present Air-Water Flow Data: $D_3/D_1$ = 0.2, Upward Branch ($\Phi$ = 0°).

Table D.13: Present Air-Water Flow Data: $D_3/D_1$ = 0.2, Downward Branch ($\Phi$ = 180°).

Table D.14: Present Air-Water Flow Data: $D_3/D_1$ = 0.084, Horizontal Branch ($\Phi$ = 90°).

Table D.15: Present Air-Water Flow Data: $D_3/D_1$ = 0.084, Upward Branch ($\Phi$ = 0°).

| RUN # | VsL1 (m/s) | VsG1 (m/s) | m1 (kg/s) | m2 (kg/s) | m3 (kg/s) | m3/m1 (-) | x1 (%) | x2 (%) | x3 (%) | x3 /x1 ( -) | p12 (Pa) | p13 (Pa) | T1 (K) | p1 (MPa) |
|---|---|---|---|---|---|---|---|---|---|---|---|---|---|---|
| 181.2 | 1.02 | 8.27 | 2.154 | 1.747 | 0.407 | 0.19 | 7.34 | 5.27 | 16.22 | 2.21 | -1217. | 499. | 299. | 0.833 |
| 182.0 | 1.07 | 8.19 | 2.245 | 1.419 | 0.826 | 0.37 | 7.04 | 2.33 | 15.13 | 2.15 | -1350. | 1751. | 299. | 0.843 |
| 33.1 | 1.00 | 9.92 | 2.113 | 0.802 | 1.311 | 0.62 | 7.61 | 0.49 | 11.96 | 1.57 | -3128. | 5570. | 290. | 0.686 |
| 32.1 | 1.03 | 9.90 | 2.180 | 1.500 | 0.680 | 0.31 | 7.46 | 3.10 | 17.09 | 2.29 | -1541. | 2253. | 290. | 0.696 |
| 69.0 | 1.02 | 9.59 | 2.142 | 1.669 | 0.472 | 0.22 | 7.22 | 4.66 | 16.28 | 2.25 | - 991. | 1793. | 300. | 0.707 |
| 101.1 | 1.05 | 10.48 | 2.217 | 1.175 | 1.041 | 0.47 | 7.59 | 1.26 | 14.73 | 1.94 | -3262. | 4655. | 293. | 0.686 |
| 101.2 | 1.05 | 10.42 | 2.215 | 1.328 | 0.887 | 0.40 | 7.50 | 1.63 | 16.28 | 2.17 | -2863. | 2869. | 295. | 0.686 |
| 101.6 | 1.04 | 10.69 | 2.199 | 1.883 | 0.316 | 0.14 | 7.69 | 5.86 | 18.60 | 2.42 | -1209. | 701. | 297. | 0.686 |
| 101.7 | 1.04 | 10.80 | 2.199 | 1.627 | 0.572 | 0.26 | 7.71 | 5.27 | 14.68 | 1.90 | -1905. | 1741. | 297. | 0.681 |
| 184.0 | 1.02 | 14.77 | 2.127 | 1.557 | 0.570 | 0.27 | 6.44 | 3.66 | 14.04 | 2.18 | -1649. | 1867. | 290. | 0.392 |
| 185.0 | 1.02 | 14.70 | 2.127 | 1.598 | 0.529 | 0.25 | 6.44 | 4.07 | 13.61 | 2.11 | -1492. | 1639. | 288. | 0.392 |
| 188.0 | 1.09 | 14.68 | 2.481 | 1.240 | 1.241 | 0.50 | 13.99 | 3.55 | 24.42 | 1.75 | -3836. | 6903. | 291. | 1.005 |
| 189.0 | 1.08 | 14.72 | 2.458 | 1.429 | 1.029 | 0.42 | 14.12 | 5.81 | 25.66 | 1.82 | -3296. | 5601. | 292. | 1.005 |
| 190.1 | 1.04 | 14.47 | 2.378 | 1.001 | 1.377 | 0.58 | 14.26 | 10.79 | 16.78 | 1.18 | -3718. | 3959. | 294. | 1.005 |
| 11.1 | 1.00 | 20.66 | 2.306 | 1.234 | 1.073 | 0.47 | 14.96 | 5.81 | 25.47 | 1.70 | -4529. | 7700. | 287. | 0.700 |
| 12.1 | 1.03 | 20.70 | 2.363 | 1.430 | 0.933 | 0.39 | 14.48 | 7.21 | 25.61 | 1.77 | -4961. | 6422. | 290. | 0.700 |
| 34.1 | 1.06 | 21.56 | 2.416 | 0.607 | 1.809 | 0.75 | 13.81 | 0.98 | 18.11 | 1.31 | -6176. | 18914. | 292. | 0.660 |
| 33.5 | 1.02 | 20.81 | 2.323 | 0.885 | 1.437 | 0.62 | 14.10 | 1.42 | 21.91 | 1.55 | -6763. | 13792. | 292. | 0.671 |
| 80.0 | 1.03 | 21.75 | 2.350 | 1.727 | 0.623 | 0.26 | 14.26 | 12.43 | 19.31 | 1.35 | -3311. | 4716. | 305. | 0.686 |
| 34.5 | 1.04 | 21.90 | 2.364 | 1.709 | 0.655 | 0.28 | 14.12 | 9.66 | 25.75 | 1.82 | -4384. | 4108. | 295. | 0.657 |
| 79.0 | 1.01 | 21.42 | 2.321 | 1.801 | 0.520 | 0.22 | 14.52 | 13.11 | 19.42 | 1.34 | -2966. | 4578. | 305. | 0.701 |
| 102.1 | 1.05 | 21.60 | 2.386 | 0.905 | 1.482 | 0.62 | 14.21 | 2.45 | 21.39 | 1.51 | -8517. | 14833. | 295. | 0.676 |
| 94.1 | 1.08 | 41.85 | 2.866 | 1.745 | 1.120 | 0.39 | 26.21 | 16.37 | 41.53 | 1.58 | -15636. | 16848. | 297. | 0.777 |
| 94.5 | 1.09 | 41.61 | 2.876 | 1.261 | 1.615 | 0.56 | 25.79 | 13.43 | 35.45 | 1.37 | -16848. | 31281. | 299. | 0.777 |
| 183.0 | 1.50 | 8.05 | 3.096 | 2.573 | 0.523 | 0.17 | 4.94 | 2.88 | 15.11 | 3.06 | -2305. | 1479. | 300. | 0.833 |
| 167.0 | 1.43 | 7.05 | 2.917 | 2.471 | 0.446 | 0.15 | 4.11 | 3.12 | 9.64 | 2.34 | -2099. | 494. | 288. | 0.715 |
| 169.0 | 1.52 | 7.38 | 3.090 | 2.433 | 0.658 | 0.21 | 3.94 | 2.18 | 10.49 | 2.66 | -2230. | 1546. | 288. | 0.695 |
| 170.0 | 1.54 | 7.37 | 3.140 | 2.332 | 0.808 | 0.26 | 3.89 | 1.42 | 11.01 | 2.83 | -3005. | 2211. | 288. | 0.696 |
| 171.0 | 1.50 | 8.08 | 3.067 | 1.293 | 1.774 | 0.58 | 4.04 | 1.24 | 6.09 | 1.51 | -5718. | 6506. | 293. | 0.657 |
| 174.0 | 1.49 | 15.29 | 3.136 | 2.474 | 0.762 | 0.21 | 6.88 | 5.21 | 13.21 | 1.92 | -2570. | 2079. | 288. | 0.600 |

Table D.3: Air-Water Flow Data (Refs /21/ - /27/): $D_3/D_1$ = 1, Horizontal Branch($\Phi$ = 90°).

| RUN # | VsL1 (m/s) | VsG1 (m/s) | m1 (kg/s) | m2 (kg/s) | m3 (kg/s) | m3/m1 (-) | x1 (%) | x2 (%) | x3 (%) | x3 /x1 ( -) | p12 (Pa) | p13 (Pa) | T1 (K) | p1 (MPa) |
|---|---|---|---|---|---|---|---|---|---|---|---|---|---|---|
| 175.0 | 1.46 | 15.20 | 3.081 | 2.132 | 0.949 | 0.31 | 6.96 | 3.61 | 14.48 | 2.08 | -3987. | 4678. | 289. | 0.600 |
| 176.0 | 1.45 | 15.11 | 3.063 | 1.507 | 1.556 | 0.51 | 6.96 | 2.72 | 11.08 | 1.59 | -6812. | 6545. | 289. | 0.600 |
| 177.0 | 1.47 | 14.98 | 3.087 | 0.808 | 2.279 | 0.74 | 6.85 | 1.08 | 8.90 | 1.30 | -8405. | 15131. | 293. | 0.600 |
| 23.3 | 2.00 | 1.17 | 3.942 | 2.362 | 1.580 | 0.40 | 0.49 | 0.01 | 1.20 | 2.45 | -2437. | 1213. | 292. | 0.700 |
| 24.1 | 1.95 | 5.00 | 3.894 | 0.493 | 3.401 | 0.87 | 2.04 | 0.03 | 2.33 | 1.14 | -6527. | 11342. | 296. | 0.686 |
| 24.0 | 1.97 | 4.80 | 3.940 | 2.104 | 1.836 | 0.47 | 2.01 | 0.70 | 3.51 | 1.74 | -5207. | 4667. | 292. | 0.706 |
| 44.0 | 2.03 | 4.99 | 4.059 | 2.425 | 1.634 | 0.40 | 2.02 | 0.41 | 4.41 | 2.18 | -6652. | 5150. | 296. | 0.710 |
| 24.6 | 1.97 | 4.75 | 3.927 | 3.172 | 0.755 | 0.19 | 1.98 | 1.19 | 5.29 | 2.68 | -3477. | 1634. | 296. | 0.706 |
| 178.0 | 1.95 | 7.69 | 3.979 | 2.379 | 1.600 | 0.40 | 3.95 | 1.47 | 7.62 | 1.93 | -7017. | 4840. | 296. | 0.882 |
| 179.0 | 1.99 | 7.95 | 4.051 | 3.153 | 0.898 | 0.22 | 3.92 | 2.51 | 8.91 | 2.27 | -4555. | 2066. | 297. | 0.867 |
| 180.0 | 1.96 | 7.88 | 3.997 | 3.449 | 0.548 | 0.14 | 3.90 | 3.19 | 8.39 | 2.15 | -2757. | 1018. | 298. | 0.862 |
| 19.0 | 2.19 | 11.01 | 4.452 | 1.022 | 3.430 | 0.77 | 3.73 | 0.29 | 4.76 | 1.27 | -12537. | 21375. | 289. | 0.637 |
| 19.1 | 2.02 | 9.87 | 4.106 | 1.411 | 2.696 | 0.66 | 3.88 | 0.64 | 5.58 | 1.44 | -10555. | 14508. | 289. | 0.681 |
| 39.5 | 1.98 | 9.87 | 4.042 | 2.239 | 1.803 | 0.45 | 3.87 | 0.72 | 7.79 | 2.01 | -10213. | 9913. | 296. | 0.686 |
| 39.1 | 1.98 | 9.85 | 4.037 | 3.083 | 0.953 | 0.24 | 3.90 | 2.07 | 9.83 | 2.52 | -5474. | 4315. | 293. | 0.684 |
| 38.1 | 2.01 | 9.96 | 4.089 | 3.572 | 0.516 | 0.13 | 3.84 | 3.68 | 4.94 | 1.29 | -4552. | 2923. | 296. | 0.681 |
| 100.4 | 2.05 | 10.47 | 4.177 | 2.897 | 1.281 | 0.31 | 3.98 | 2.05 | 8.33 | 2.09 | -8701. | 5375. | 296. | 0.686 |
| 100.1 | 2.08 | 10.67 | 4.231 | 2.466 | 1.765 | 0.42 | 3.96 | 1.16 | 7.88 | 1.99 | -11100. | 6888. | 295. | 0.676 |
| 18.1 | 2.06 | 10.40 | 4.206 | 3.511 | 0.695 | 0.17 | 4.07 | 3.34 | 7.76 | 1.91 | -2971. | 2347. | 295. | 0.686 |
| 35.7 | 2.08 | 17.00 | 4.415 | 2.580 | 1.835 | 0.42 | 7.69 | 2.60 | 14.85 | 1.93 | -13087. | 14718. | 294. | 0.857 |
| 40.4 | 2.04 | 18.14 | 4.344 | 2.824 | 1.520 | 0.35 | 8.09 | 4.18 | 15.35 | 1.90 | -10390. | 12560. | 298. | 0.843 |
| 90.0 | 2.11 | 17.87 | 4.430 | 1.357 | 3.074 | 0.69 | 6.65 | 1.08 | 9.11 | 1.37 | -17225. | 28788. | 301. | 0.725 |
| 90.6 | 2.12 | 16.19 | 4.436 | 3.159 | 1.278 | 0.29 | 6.37 | 4.53 | 10.93 | 1.71 | -8363. | 5299. | 296. | 0.755 |
| 90.3 | 2.10 | 17.81 | 4.408 | 3.166 | 1.242 | 0.28 | 6.66 | 6.65 | 6.70 | 1.01 | -9035. | 5587. | 301. | 0.725 |
| 41.1 | 2.00 | 19.03 | 4.269 | 3.273 | 0.996 | 0.23 | 8.39 | 7.18 | 12.40 | 1.48 | -5432. | 4312. | 296. | 0.800 |
| 35.1 | 1.98 | 16.15 | 4.232 | 2.919 | 1.313 | 0.31 | 8.08 | 5.53 | 13.79 | 1.71 | -8338. | 7544. | 292. | 0.900 |
| 35.4 | 2.04 | 16.11 | 4.337 | 1.537 | 2.800 | 0.65 | 7.86 | 1.58 | 11.31 | 1.44 | -15372. | 25464. | 293. | 0.900 |
| 40.0 | 2.02 | 17.49 | 4.296 | 2.096 | 2.199 | 0.51 | 7.89 | 1.78 | 13.71 | 1.74 | -11655. | 17733. | 298. | 0.843 |
| 91.1 | 1.86 | 27.71 | 4.151 | 2.165 | 1.987 | 0.48 | 12.26 | 4.85 | 20.33 | 1.66 | -14836. | 27432. | 296. | 0.794 |
| 92.1 | 1.86 | 27.46 | 4.141 | 2.788 | 1.353 | 0.33 | 12.05 | 9.08 | 18.18 | 1.51 | -9841. | 8640. | 299. | 0.794 |

Table D.3 (cont.): Air-Water Flow Data (Refs /21/ - /27/): $D_3/D_1$ = 1, Horizontal Branch($\Phi$ = 90°).

| RUN # | VsL1 (m/s) | VsG1 (m/s) | m1 (kg/s) | m2 (kg/s) | m3 (kg/s) | m3/m1 (-) | x1 (%) | x2 (%) | x3 (%) | x3 /x1 ( -) | p12 (Pa) | p13 (Pa) | T1 (K) | p1 (MPa) |
|---|---|---|---|---|---|---|---|---|---|---|---|---|---|---|
| 93.1 | 1.88 | 27.07 | 4.167 | 2.939 | 1.228 | 0.29 | 11.83 | 9.80 | 16.70 | 1.41 | -8380. | 5927. | 299. | 0.794 |
| 20.9 | 2.68 | 10.23 | 5.388 | 2.782 | 2.661 | 0.48 | 2.68 | 0.75 | 4.75 | 1.77 | -14821. | 10590. | 293. | 0.686 |
| 15.1 | 3.68 | 2.69 | 7.279 | 3.794 | 3.485 | 0.48 | 0.87 | 0.23 | 1.57 | 1.80 | -13240. | 8487. | 289. | 0.600 |
| 26.2 | 4.00 | 4.11 | 7.897 | 4.008 | 3.889 | 0.49 | 0.82 | 0.31 | 1.35 | 1.64 | -14634. | 9524. | 293. | 0.676 |
| 29.1 | 4.00 | 3.99 | 7.890 | 6.055 | 1.834 | 0.23 | 0.81 | 0.46 | 2.00 | 2.46 | -11665. | 3735. | 292. | 0.686 |
| 56.1 | 4.01 | 4.05 | 7.930 | 3.994 | 3.936 | 0.50 | 0.84 | 0.40 | 1.28 | 1.53 | -16775. | 11501. | 297. | 0.686 |
| 15.11 | 4.70 | 5.15 | 9.316 | 4.690 | 4.626 | 0.50 | 1.04 | 0.39 | 1.69 | 1.63 | -21397. | 13102. | 289. | 0.800 |
| 37.3 | 4.29 | 10.54 | 8.605 | 3.093 | 5.512 | 0.64 | 2.37 | 0.27 | 3.55 | 1.50 | -30710. | 35582. | 292. | 0.825 |
| 37.6 | 4.38 | 10.77 | 8.789 | 3.887 | 4.902 | 0.56 | 2.34 | 0.39 | 3.89 | 1.66 | -31860. | 26155. | 292. | 0.813 |
| 89.4 | 4.40 | 10.02 | 8.814 | 1.970 | 6.844 | 0.78 | 2.14 | 0.60 | 2.59 | 1.21 | -31720. | 39983. | 301. | 0.800 |
| 88.1 | 3.97 | 9.63 | 7.903 | 5.809 | 2.092 | 0.26 | 1.78 | 1.02 | 3.90 | 2.19 | -22224. | 6437. | 303. | 0.647 |
| 88.4 | 3.94 | 9.62 | 7.843 | 4.702 | 3.141 | 0.40 | 1.78 | 0.43 | 3.79 | 2.14 | -28496. | 13408. | 306. | 0.647 |
| 89.1 | 4.39 | 10.24 | 8.785 | 1.417 | 7.367 | 0.84 | 2.12 | 0.60 | 2.42 | 1.14 | -31851. | 44009. | 301. | 0.800 |
| 89.4 | 4.41 | 10.48 | 8.829 | 1.994 | 6.835 | 0.77 | 2.13 | 0.58 | 2.59 | 1.21 | -31720. | 39983. | 301. | 0.790 |
| 87.1 | 3.67 | 16.22 | 8.003 | 5.492 | 2.511 | 0.31 | 2.86 | 1.47 | 5.92 | 2.07 | -36295. | 17281. | 303. | 0.686 |
| 98.8 | 7.27 | 2.26 | 14.283 | 3.886 | 10.397 | 0.73 | 0.26 | 0.22 | 0.28 | 1.07 | -30450. | 26300. | 295. | 0.700 |
| 99.1 | 7.42 | 2.04 | 14.580 | 5.512 | 9.068 | 0.62 | 0.23 | 0.11 | 0.31 | 1.33 | -48100. | 16870. | 294. | 0.700 |
| 99.4 | 7.52 | 2.06 | 14.767 | 4.447 | 10.320 | 0.70 | 0.23 | 0.25 | 0.22 | 0.96 | -32300. | 22400. | 294. | 0.700 |
| 32.3 | 1.04 | 10.01 | 2.191 | 0.970 | 1.221 | 0.56 | 7.41 | 0.54 | 12.86 | 1.74 | - | - | 294. | 0.695 |
| 72.0 | 1.03 | 9.73 | 2.163 | 1.543 | 0.620 | 0.29 | 7.18 | 2.29 | 19.36 | 2.69 | - | - | 307. | 0.715 |
| 73.0 | 1.02 | 9.67 | 2.145 | 1.650 | 0.494 | 0.23 | 7.21 | 6.23 | 10.48 | 1.45 | - | - | 307. | 0.715 |
| 71.0 | 1.02 | 9.55 | 2.157 | 1.701 | 0.456 | 0.21 | 7.19 | 3.88 | 19.50 | 2.71 | - | - | 302. | 0.715 |
| 70.0 | 1.00 | 9.14 | 2.117 | 1.779 | 0.339 | 0.16 | 7.19 | 6.24 | 12.18 | 1.69 | - | - | 300. | 0.730 |
| 101.8 | 1.05 | 10.69 | 2.224 | 1.980 | 0.244 | 0.11 | 7.60 | 7.39 | 9.27 | 1.22 | - | - | 297. | 0.686 |
| 186.0 | 1.03 | 14.73 | 2.364 | 1.890 | 0.474 | 0.20 | 14.76 | 12.86 | 22.36 | 1.51 | - | - | 289. | 1.000 |
| 187.0 | 1.10 | 15.07 | 2.508 | 1.930 | 0.578 | 0.23 | 14.00 | 11.50 | 22.32 | 1.59 | - | - | 291. | 0.990 |
| 78.0 | 1.02 | 21.10 | 2.323 | 2.010 | 0.313 | 0.13 | 14.32 | 13.49 | 19.62 | 1.37 | - | - | 305. | 0.701 |
| 76.0 | 1.01 | 20.83 | 2.308 | 2.062 | 0.246 | 0.11 | 14.44 | 14.07 | 17.52 | 1.21 | - | - | 298. | 0.696 |
| 77.0 | 1.02 | 21.53 | 2.330 | 2.173 | 0.157 | 0.07 | 14.33 | 14.44 | 12.76 | 0.89 | - | - | 303. | 0.686 |
| 9.1 | 1.02 | 21.74 | 2.336 | 2.051 | 0.286 | 0.12 | 14.90 | 13.86 | 22.35 | 1.50 | - | - | 289. | 0.676 |

Table D.3 (cont.): Air-Water Flow Data (Refs /21/ - /27/): $D_3/D_1$ = 1, Horizontal Branch($\Phi$ = 90°).

| RUN # | VsL1 (m/s) | VsG1 (m/s) | m1 (kg/s) | m2 (kg/s) | m3 (kg/s) | m3/m1 (-) | x1 (%) | x2 (%) | x3 (%) | x3 /x1 ( -) | p12 (Pa) | p13 (Pa) | T1 (K) | p1 (MPa) |
|---|---|---|---|---|---|---|---|---|---|---|---|---|---|---|
| 9.5 | 1.02 | 20.84 | 2.338 | 1.753 | 0.585 | 0.25 | 14.59 | 12.90 | 19.69 | 1.35 | - | - | 291. | 0.696 |
| 12.1 | 1.03 | 20.70 | 2.363 | 1.430 | 0.933 | 0.39 | 14.48 | 7.21 | 25.61 | 1.77 | - | - | 290. | 0.700 |
| 94.8 | 1.07 | 42.19 | 2.837 | 2.265 | 0.572 | 0.20 | 26.02 | 22.25 | 40.94 | 1.57 | - | - | 299. | 0.764 |
| 45.0 | 2.03 | 4.87 | 4.055 | 2.901 | 1.154 | 0.28 | 2.00 | 1.00 | 4.52 | 2.26 | - | - | 292. | 0.710 |
| 49.0 | 2.05 | 4.98 | 4.093 | 3.043 | 1.050 | 0.26 | 2.00 | 1.10 | 4.62 | 2.31 | - | - | 298. | 0.715 |
| 46.0 | 2.03 | 5.05 | 4.066 | 3.199 | 0.866 | 0.21 | 2.03 | 1.35 | 4.57 | 2.25 | - | - | 295. | 0.705 |
| 42.0 | 2.04 | 4.87 | 4.075 | 3.400 | 0.675 | 0.17 | 2.02 | 1.44 | 4.96 | 2.45 | - | - | 291. | 0.720 |
| 47.0 | 2.01 | 4.95 | 4.024 | 3.614 | 0.410 | 0.10 | 2.02 | 1.80 | 4.01 | 1.98 | - | - | 297. | 0.713 |
| 48.0 | 2.05 | 5.00 | 4.091 | 3.668 | 0.422 | 0.10 | 2.02 | 1.88 | 3.27 | 1.62 | - | - | 294. | 0.710 |
| 43.0 | 2.02 | 4.88 | 4.038 | 3.664 | 0.374 | 0.09 | 2.05 | 1.62 | 6.19 | 3.02 | - | - | 291. | 0.720 |
| 38.1 | 1.98 | 9.97 | 4.032 | 3.334 | 0.698 | 0.17 | 3.88 | 2.68 | 9.57 | 2.47 | - | - | 297. | 0.680 |
| 18.1 | 2.07 | 10.51 | 4.213 | 3.517 | 0.697 | 0.17 | 3.99 | 3.25 | 7.76 | 1.94 | - | - | 295. | 0.690 |
| 38.0 | 1.98 | 9.91 | 4.043 | 3.711 | 0.332 | 0.08 | 3.88 | 3.91 | 3.65 | 0.94 | - | - | 295. | 0.681 |
| 35.0 | 2.05 | 16.77 | 4.345 | 1.536 | 2.809 | 0.65 | 7.74 | 1.19 | 11.31 | 1.46 | - | - | 293. | 0.857 |
| 40.0 | 2.02 | 17.49 | 4.296 | 2.096 | 2.199 | 0.51 | 7.89 | 1.78 | 13.71 | 1.74 | - | - | 298. | 0.843 |
| 35.0 | 1.99 | 16.68 | 4.239 | 2.923 | 1.316 | 0.31 | 7.96 | 5.33 | 13.79 | 1.73 | - | - | 292. | 0.862 |
| 41.0 | 2.00 | 18.37 | 4.276 | 3.280 | 0.996 | 0.23 | 8.25 | 7.08 | 12.11 | 1.47 | - | - | 297. | 0.833 |
| 41.1 | 2.07 | 18.17 | 4.403 | 3.869 | 0.534 | 0.12 | 7.93 | 7.78 | 8.97 | 1.13 | - | - | 297. | 0.833 |
| 28.0 | 4.11 | 4.05 | 8.108 | 1.917 | 6.191 | 0.76 | 0.79 | 0.18 | 0.98 | 1.24 | - | - | 296. | 0.686 |
| 27.0 | 4.15 | 3.96 | 8.181 | 3.615 | 4.566 | 0.56 | 0.78 | 0.18 | 1.25 | 1.61 | - | - | 296. | 0.696 |
| 56.0 | 4.03 | 4.19 | 7.944 | 4.001 | 3.944 | 0.50 | 0.81 | 0.36 | 1.28 | 1.57 | - | - | 297. | 0.670 |
| 55.0 | 4.09 | 4.24 | 8.069 | 5.515 | 2.554 | 0.32 | 0.80 | 0.44 | 1.60 | 1.99 | - | - | 301. | 0.674 |
| 54.0 | 4.08 | 4.23 | 8.049 | 6.057 | 1.991 | 0.25 | 0.81 | 0.50 | 1.73 | 2.15 | - | - | 300. | 0.671 |
| 50.0 | 4.04 | 4.05 | 7.975 | 6.072 | 1.903 | 0.24 | 0.79 | 0.51 | 1.67 | 2.12 | - | - | 300. | 0.681 |
| 51.0 | 4.04 | 4.11 | 7.967 | 6.352 | 1.615 | 0.20 | 0.79 | 0.61 | 1.50 | 1.90 | - | - | 301. | 0.676 |
| 52.0 | 4.02 | 4.03 | 7.933 | 6.896 | 1.038 | 0.13 | 0.81 | 0.72 | 1.46 | 1.79 | - | - | 295. | 0.690 |
| 53.0 | 4.04 | 4.25 | 7.980 | 7.289 | 0.691 | 0.09 | 0.81 | 0.79 | 1.13 | 1.38 | - | - | 298. | 0.666 |
| 96.1 | 3.95 | 4.08 | 7.807 | 6.020 | 1.787 | 0.23 | 0.85 | 0.50 | 2.00 | 2.37 | - | - | 298. | 0.705 |
| 58.0 | 4.37 | 10.31 | 8.759 | 7.474 | 1.285 | 0.15 | 2.28 | 2.03 | 3.77 | 1.65 | - | - | 297. | 0.840 |
| 59.0 | 4.45 | 10.25 | 8.913 | 7.996 | 0.918 | 0.10 | 2.18 | 2.10 | 2.84 | 1.30 | - | - | 301. | 0.833 |

Table D.3 (cont.): Air-Water Flow Data (Refs /21/ - /27/): $D_3/D_1$ = 1, Horizontal Branch($\Phi$ = 90°).

| RUN # | VsL1 (m/s) | VsG1 (m/s) | m1 (kg/s) | m2 (kg/s) | m3 (kg/s) | m3/m1 (-) | x1 (%) | x2 (%) | x3 (%) | x3 /x1 ( -) | p12 (Pa) | p13 (Pa) | T1 (K) | p1 (MPa) |
|---|---|---|---|---|---|---|---|---|---|---|---|---|---|---|
| 60.0 | 4.49 | 10.13 | 8.979 | 8.416 | 0.563 | 0.06 | 2.13 | 2.01 | 3.88 | 1.82 | - | - | 303. | 0.835 |
| 61.0 | 4.50 | 10.03 | 9.003 | 8.464 | 0.539 | 0.06 | 2.11 | 2.06 | 2.86 | 1.36 | - | - | 301. | 0.833 |
| 62.0 | 4.43 | 10.46 | 8.872 | 7.256 | 1.616 | 0.18 | 2.23 | 1.81 | 4.11 | 1.84 | - | - | 302. | 0.833 |
| 63.0 | 4.41 | 10.12 | 8.833 | 6.890 | 1.943 | 0.22 | 2.18 | 1.66 | 4.01 | 1.84 | - | - | 303. | 0.840 |
| 64.0 | 4.41 | 10.35 | 8.835 | 6.741 | 2.094 | 0.24 | 2.20 | 1.53 | 4.34 | 1.98 | - | - | 304. | 0.833 |
| 65.0 | 4.44 | 10.01 | 8.890 | 6.403 | 2.487 | 0.28 | 2.16 | 1.28 | 4.43 | 2.05 | - | - | 300. | 0.842 |
| 66.0 | 4.51 | 10.36 | 9.020 | 6.045 | 2.975 | 0.33 | 2.20 | 1.01 | 4.62 | 2.10 | - | - | 301. | 0.842 |
| 67.0 | 4.42 | 10.66 | 8.856 | 5.284 | 3.572 | 0.40 | 2.31 | 0.83 | 4.49 | 1.95 | - | - | 301. | 0.842 |
| 37.0 | 4.22 | 10.41 | 8.457 | 6.307 | 2.149 | 0.25 | 2.41 | 0.70 | 7.43 | 3.08 | - | - | 289. | 0.826 |
| 34.1 | 1.06 | 21.56 | 2.416 | 0.607 | 1.809 | 0.75 | 13.81 | 0.98 | 18.11 | 1.31 | - | - | 292. | 0.660 |
| 33.5 | 1.02 | 20.81 | 2.323 | 0.885 | 1.437 | 0.62 | 14.10 | 1.42 | 21.91 | 1.55 | - | - | 292. | 0.671 |
| 80.0 | 1.03 | 21.75 | 2.350 | 1.727 | 0.623 | 0.26 | 14.26 | 12.43 | 19.31 | 1.35 | - | - | 305. | 0.686 |
| 34.5 | 1.04 | 21.90 | 2.364 | 1.709 | 0.655 | 0.28 | 14.12 | 9.66 | 25.75 | 1.82 | - | - | 295. | 0.657 |
| 79.0 | 1.01 | 21.42 | 2.321 | 1.801 | 0.520 | 0.22 | 14.52 | 13.11 | 19.42 | 1.34 | - | - | 305. | 0.701 |
| 78.0 | 1.02 | 21.10 | 2.323 | 2.010 | 0.313 | 0.13 | 14.32 | 13.49 | 19.62 | 1.37 | - | - | 305. | 0.701 |
| 76.0 | 1.01 | 20.83 | 2.308 | 2.062 | 0.246 | 0.11 | 14.44 | 14.07 | 17.52 | 1.21 | - | - | 298. | 0.696 |
| 77.0 | 1.02 | 21.53 | 2.330 | 2.173 | 0.157 | 0.07 | 14.33 | 14.44 | 12.76 | 0.89 | - | - | 303. | 0.686 |
| 102.1 | 1.05 | 21.60 | 2.386 | 0.905 | 1.482 | 0.62 | 14.21 | 2.45 | 21.39 | 1.51 | - | - | 295. | 0.676 |
| 9.1 | 1.02 | 21.74 | 2.336 | 2.051 | 0.286 | 0.12 | 14.90 | 13.86 | 22.35 | 1.50 | - | - | 289. | 0.676 |
| 9.5 | 1.02 | 20.84 | 2.338 | 1.753 | 0.585 | 0.25 | 14.59 | 12.90 | 19.69 | 1.35 | - | - | 291. | 0.696 |
| 11.1 | 1.00 | 20.66 | 2.306 | 1.234 | 1.073 | 0.47 | 14.96 | 5.81 | 25.47 | 1.70 | - | - | 287. | 0.700 |
| 35.0 | 2.05 | 16.77 | 4.345 | 1.536 | 2.809 | 0.65 | 7.74 | 1.19 | 11.31 | 1.46 | - | - | 293. | 0.857 |
| 35.1 | 2.08 | 17.00 | 4.415 | 2.580 | 1.835 | 0.42 | 7.69 | 2.60 | 14.85 | 1.93 | - | - | 294. | 0.857 |
| 40.1 | 2.04 | 18.14 | 4.344 | 2.824 | 1.520 | 0.35 | 8.09 | 4.18 | 15.35 | 1.90 | - | - | 298. | 0.843 |
| 35.0 | 1.99 | 16.68 | 4.239 | 2.923 | 1.316 | 0.31 | 7.96 | 5.33 | 13.79 | 1.73 | - | - | 292. | 0.862 |
| 41.0 | 2.00 | 18.37 | 4.276 | 3.280 | 0.996 | 0.23 | 8.25 | 7.08 | 12.11 | 1.47 | - | - | 297. | 0.833 |
| 41.1 | 2.07 | 18.17 | 4.403 | 3.869 | 0.534 | 0.12 | 7.93 | 7.78 | 8.97 | 1.13 | - | - | 297. | 0.833 |
| 90.1 | 2.11 | 17.87 | 4.430 | 1.357 | 3.074 | 0.69 | 6.65 | 1.08 | 9.11 | 1.37 | - | - | 301. | 0.725 |
| 90.3 | 2.10 | 17.81 | 4.408 | 3.166 | 1.242 | 0.28 | 6.66 | 6.65 | 6.70 | 1.01 | - | - | 301. | 0.725 |
| 168.0 | 1.43 | 7.11 | 2.918 | 2.511 | 0.407 | 0.14 | 4.15 | 3.42 | 8.60 | 2.07 | - | - | 288. | 0.715 |

Table D.3 (cont.): Air-Water Flow Data (Refs /21/ - /27/): $D_3/D_1$ = 1, Horizontal Branch($\Phi$ = 90°).

| RUN # | VsL1 (m/s) | VsG1 (m/s) | m1 (kg/s) | m2 (kg/s) | m3 (kg/s) | m3/m1 (-) | x1 (%) | x2 (%) | x3 (%) | x3/x1 (-) | p12 (Pa) | p13 (Pa) | T1 (K) | p1 (MPa) |
|---|---|---|---|---|---|---|---|---|---|---|---|---|---|---|
| 3.0 | 3.89 | 4.34 | 7.709 | 4.375 | 3.334 | 0.43 | 1.06 | 0.78 | 1.44 | 1.35 | -17759. | 1905. | 295. | 0.8 |
| 41.0 | 1.99 | 3.70 | 3.979 | 3.321 | 0.658 | 0.17 | 1.75 | 0.27 | 6.97 | 3.98 | -4544. | 308. | 294. | 0.6 |
| 42.0 | 2.03 | 4.95 | 4.042 | 2.933 | 1.109 | 0.27 | 1.73 | 0.44 | 5.17 | 2.98 | -6706. | 907. | 295. | 0.6 |
| 43.0 | 1.93 | 4.77 | 3.849 | 2.184 | 1.665 | 0.43 | 1.75 | 0.14 | 3.86 | 2.21 | -6119. | 1614. | 299. | 0.6 |
| 224.0 | 1.81 | 4.67 | 3.604 | 3.600 | 0.004 | 0.00 | 1.83 | 1.70 | 100.00 | 54.65 | -2865. | 13662. | 289. | 0.6 |
| 224.1 | 1.81 | 4.60 | 3.604 | 3.600 | 0.004 | 0.00 | 1.80 | 1.70 | 100.00 | 55.54 | -2865. | 13662. | 289. | 0.6 |
| 225.0 | 1.81 | 4.66 | 3.612 | 3.605 | 0.007 | 0.00 | 1.82 | 1.63 | 100.00 | 55.00 | -2203. | 11269. | 291. | 0.6 |
| 236.0 | 2.03 | 4.99 | 4.043 | 1.833 | 2.210 | 0.55 | 1.74 | 0.73 | 2.58 | 1.48 | -8577. | 1480. | 292. | 0.6 |
| 237.0 | 2.03 | 5.01 | 4.043 | 2.923 | 1.120 | 0.28 | 1.75 | 0.51 | 4.97 | 2.84 | -8178. | 1568. | 298. | 0.6 |
| 238.0 | 2.06 | 5.02 | 4.118 | 3.893 | 0.225 | 0.05 | 1.72 | 0.74 | 18.67 | 10.85 | -5065. | 1150. | 298. | 0.6 |
| 239.0 | 2.02 | 5.44 | 4.038 | 4.033 | 0.005 | 0.00 | 1.90 | 1.80 | 100.00 | 52.69 | -3131. | 31. | 298. | 0.6 |
| 15.0 | 2.12 | 10.17 | 4.296 | 3.744 | 0.552 | 0.13 | 3.34 | 2.30 | 10.45 | 3.13 | -6115. | 316. | 297. | 0.6 |
| 16.0 | 2.03 | 10.23 | 4.114 | 3.582 | 0.532 | 0.13 | 3.51 | 1.19 | 19.14 | 5.45 | -8098. | 805. | 290. | 0.6 |
| 17.0 | 2.05 | 9.98 | 4.153 | 3.647 | 0.506 | 0.12 | 3.39 | 1.25 | 18.82 | 5.56 | -7351. | 405. | 291. | 0.6 |
| 18.0 | 2.06 | 9.99 | 4.173 | 3.518 | 0.655 | 0.16 | 3.38 | 0.76 | 17.40 | 5.16 | -10633. | 565. | 292. | 0.6 |
| 19.0 | 2.02 | 9.96 | 4.098 | 3.212 | 0.886 | 0.22 | 3.43 | 0.60 | 13.71 | 3.99 | -3484. | 962. | 293. | 0.6 |
| 20.0 | 2.01 | 9.90 | 4.085 | 2.726 | 1.359 | 0.33 | 3.42 | 0.37 | 9.54 | 2.79 | -12001. | 2015. | 294. | 0.6 |
| 21.0 | 2.02 | 9.90 | 4.098 | 2.841 | 1.257 | 0.31 | 3.41 | 0.37 | 10.26 | 3.01 | -11801. | 1931. | 295. | 0.6 |
| 214.0 | 2.28 | 9.49 | 4.600 | 3.157 | 1.443 | 0.31 | 2.91 | 0.71 | 7.72 | 2.66 | -15168. | 2879. | 301. | 0.6 |
| 233.0 | 1.96 | 9.83 | 3.985 | 3.982 | 0.003 | 0.00 | 3.48 | 3.42 | 100.00 | 28.71 | -4275. | 21766. | 296. | 0.6 |
| 234.0 | 1.86 | 9.82 | 3.787 | 3.453 | 0.336 | 0.09 | 3.66 | 0.73 | 32.95 | 9.28 | -8879. | 1418. | 296. | 0.6 |
| 231.0 | 1.03 | 11.75 | 2.148 | 1.974 | 0.174 | 0.08 | 6.43 | 2.38 | 52.41 | 8.15 | -2256. | 297. | 295. | 0.6 |
| 232.0 | 1.02 | 10.14 | 2.148 | 2.122 | 0.026 | 0.01 | 6.66 | 5.52 | 100.00 | 15.02 | -1288. | 154. | 295. | 0.6 |
| 239.0 | 1.06 | 9.81 | 2.209 | 0.956 | 1.253 | 0.57 | 6.27 | 1.74 | 9.72 | 1.55 | -3727. | 3956. | 293. | 0.6 |
| 243.0 | 1.06 | 19.90 | 2.350 | 1.278 | 1.072 | 0.46 | 11.95 | 21.10 | 1.11 | 0.09 | -13265. | 12651. | 296. | 0.6 |
| 244.0 | 1.03 | 19.81 | 2.301 | 2.141 | 0.160 | 0.07 | 12.15 | 8.91 | 56.12 | 4.61 | -3150. | 1008. | 296. | 0.6 |
| 245.0 | 1.03 | 19.63 | 2.299 | 2.270 | 0.027 | 0.01 | 12.05 | 10.99 | 100.00 | 8.30 | -1094. | 485. | 296. | 0.6 |
| 227.0 | 2.21 | 20.14 | 4.606 | 4.367 | 0.239 | 0.05 | 6.17 | 1.03 | 100.00 | 16.21 | -1361. | 2213. | 289. | 0.6 |
| 229.0 | 2.02 | 20.12 | 4.251 | 4.119 | 0.132 | 0.03 | 6.68 | 5.17 | 53.72 | 8.04 | -2583. | 493. | 292. | 0.6 |
| 240.0 | 0.91 | 4.99 | 1.862 | 1.830 | 0.032 | 0.02 | 3.78 | 2.10 | 100.00 | 26.42 | - 732. | 2467. | 299. | 0.6 |

Table D.4: Air-Water Flow Data (Refs /21/ - /27/): $D_3/D_1$ = 1, Upward Branch ($\Phi$ = 0°).

| RUN # | VsL1 (m/s) | VsG1 (m/s) | m1 (kg/s) | m2 (kg/s) | m3 (kg/s) | m3/m1 (-) | x1 (%) | x2 (%) | x3 (%) | x3/x1 (-) | p12 (Pa) | p13 (Pa) | T1 (K) | p1 (MPa) |
|---|---|---|---|---|---|---|---|---|---|---|---|---|---|---|
| 223. | 0.50 | 5.24 | 1.039 | 0.272 | 0.767 | 0.74 | 5.62 | 5.46 | 5.68 | 1.01 | - 326. | 1822. | 299. | 0.487 |
| 224. | 0.50 | 4.93 | 1.030 | 0.319 | 0.711 | 0.69 | 5.58 | 6.45 | 5.18 | 0.93 | - 590. | 1591. | 294. | 0.500 |
| 225. | 0.50 | 5.03 | 1.031 | 0.429 | 0.603 | 0.58 | 5.57 | 9.81 | 2.55 | 0.46 | - 383. | 1110. | 294. | 0.490 |
| 141. | 0.50 | 20.39 | 1.438 | 0.290 | 1.148 | 0.80 | 32.20 | 20.05 | 35.28 | 1.10 | -4400. | 12131. | 292. | 0.970 |
| 142. | 0.51 | 20.03 | 1.456 | 0.351 | 1.105 | 0.76 | 31.21 | 26.87 | 32.59 | 1.04 | -4282. | 5862. | 293. | 0.969 |
| 143. | 0.51 | 20.10 | 1.447 | 0.517 | 0.930 | 0.64 | 31.31 | 39.07 | 27.00 | 0.86 | -4436. | 5247. | 294. | 0.969 |
| 144. | 0.50 | 20.13 | 1.441 | 0.778 | 0.664 | 0.46 | 31.51 | 43.67 | 17.26 | 0.55 | -3192. | 1293. | 294. | 0.969 |
| 216. | 1.03 | 5.07 | 2.069 | 1.023 | 1.047 | 0.51 | 2.81 | 3.74 | 1.90 | 0.68 | -1384. | 1730. | 293. | 0.490 |
| 217. | 1.03 | 4.96 | 2.079 | 0.874 | 1.206 | 0.58 | 2.79 | 3.67 | 2.15 | 0.77 | -1230. | 2429. | 293. | 0.500 |
| 219. | 1.02 | 5.12 | 2.046 | 1.350 | 0.696 | 0.34 | 2.87 | 3.98 | 0.71 | 0.25 | - 376. | 1026. | 291. | 0.488 |
| 220. | 1.01 | 5.08 | 2.041 | 0.860 | 1.181 | 0.58 | 2.87 | 3.58 | 2.35 | 0.82 | - 890. | 3148. | 292. | 0.493 |
| 221. | 1.02 | 5.07 | 2.055 | 0.697 | 1.358 | 0.66 | 2.84 | 3.46 | 2.53 | 0.89 | -1366. | 3631. | 292. | 0.491 |
| 222. | 1.01 | 4.99 | 2.028 | 0.405 | 1.623 | 0.80 | 2.87 | 2.11 | 3.06 | 1.07 | - 836. | 4485. | 293. | 0.500 |
| 213. | 0.99 | 2.52 | 1.996 | 0.803 | 1.193 | 0.60 | 2.90 | 4.80 | 1.63 | 0.56 | - 793. | 1546. | 291. | 0.979 |
| 214. | 0.96 | 2.43 | 1.930 | 0.909 | 1.021 | 0.53 | 2.93 | 5.19 | 0.92 | 0.31 | - 227. | 1251. | 291. | 0.989 |
| 215. | 1.00 | 2.49 | 2.021 | 0.466 | 1.555 | 0.77 | 2.82 | 2.39 | 2.95 | 1.05 | - 545. | 3016. | 292. | 0.978 |
| 96. | 0.99 | 8.57 | 2.089 | 0.806 | 1.283 | 0.61 | 6.75 | 11.72 | 3.69 | 0.55 | - 899. | 2640. | 303. | 0.700 |
| 97. | 1.03 | 10.37 | 2.156 | 0.658 | 1.498 | 0.69 | 6.79 | 10.40 | 5.22 | 0.77 | -1119. | 4409. | 297. | 0.600 |
| 98. | 1.05 | 10.25 | 2.156 | 0.388 | 1.768 | 0.82 | 6.71 | 7.97 | 6.44 | 0.96 | -1111. | 7001. | 300. | 0.600 |
| 99. | 1.03 | 10.18 | 2.154 | 1.159 | 0.995 | 0.46 | 6.67 | 9.93 | 2.91 | 0.43 | - 684. | 2042. | 301. | 0.600 |
| 187. | 1.21 | 10.28 | 2.605 | 1.817 | 0.788 | 0.30 | 9.11 | 11.38 | 3.88 | 0.43 | -1540. | 1460. | 291. | 0.980 |
| 188. | 1.18 | 10.10 | 2.551 | 1.432 | 1.119 | 0.44 | 9.20 | 12.52 | 4.96 | 0.54 | -2010. | 2595. | 292. | 0.990 |
| 189. | 1.19 | 10.69 | 2.575 | 1.257 | 1.318 | 0.51 | 9.39 | 12.87 | 6.06 | 0.65 | -2517. | 3759. | 294. | 0.970 |
| 190. | 1.12 | 10.29 | 2.426 | 0.992 | 1.434 | 0.59 | 9.68 | 14.05 | 6.66 | 0.69 | -2423. | 4646. | 294. | 0.980 |
| 228. | 1.00 | 10.07 | 2.183 | 1.102 | 1.081 | 0.50 | 10.57 | 15.92 | 5.11 | 0.48 | -1693. | 2247. | 292. | 0.977 |
| 229. | 1.03 | 9.86 | 2.242 | 0.762 | 1.480 | 0.66 | 10.19 | 15.43 | 7.49 | 0.74 | -1941. | 5541. | 293. | 0.990 |
| 230. | 1.03 | 10.26 | 2.135 | 0.917 | 1.219 | 0.57 | 5.35 | 8.35 | 3.09 | 0.58 | -1085. | 3277. | 295. | 0.480 |
| 231. | 1.00 | 9.26 | 2.058 | 1.159 | 0.898 | 0.44 | 5.24 | 7.96 | 1.73 | 0.33 | - 608. | 2162. | 289. | 0.491 |
| 102. | 1.01 | 17.93 | 2.268 | 1.204 | 1.064 | 0.47 | 13.02 | 18.95 | 6.35 | 0.49 | -2189. | 2712. | 289. | 0.700 |
| 103. | 1.02 | 17.73 | 2.287 | 0.925 | 1.362 | 0.60 | 12.76 | 19.90 | 7.88 | 0.62 | -2812. | 4765. | 292. | 0.700 |

Table D.5: Air-Water Flow Data (Refs /21/ - /27/): $D_3/D_1$ = 1, Downward Branch ($\Phi$ = 180°).

| RUN # | VsL1 (m/s) | VsG1 (m/s) | m1 (kg/s) | m2 (kg/s) | m3 (kg/s) | m3/m1 (-) | x1 (%) | x2 (%) | x3 (%) | x3/x1 (-) | p12 (Pa) | p13 (Pa) | T1 (K) | p1 (MPa) |
|---|---|---|---|---|---|---|---|---|---|---|---|---|---|---|
| 104. | 1.04 | 17.77 | 2.338 | 0.522 | 1.816 | 0.78 | 12.57 | 13.99 | 12.22 | 0.97 | -4008. | 18799. | 294. | 0.700 |
| 105. | 1.04 | 17.80 | 2.338 | 0.617 | 1.721 | 0.74 | 12.53 | 18.66 | 10.42 | 0.83 | -3637. | 16659. | 295. | 0.700 |
| 106. | 1.04 | 17.85 | 2.338 | 0.872 | 1.466 | 0.63 | 12.57 | 18.34 | 9.23 | 0.73 | -3589. | 6787. | 296. | 0.700 |
| 131. | 0.94 | 20.70 | 2.322 | 1.490 | 0.832 | 0.36 | 20.43 | 25.16 | 11.95 | 0.59 | -4755. | 1725. | 292. | 0.976 |
| 132. | 1.08 | 19.95 | 2.566 | 0.672 | 1.895 | 0.74 | 17.81 | 12.22 | 19.79 | 1.11 | -9057. | 25673. | 292. | 0.977 |
| 133. | 1.05 | 19.33 | 2.494 | 0.644 | 1.850 | 0.74 | 17.94 | 18.31 | 17.81 | 0.99 | -5961. | 15693. | 289. | 0.975 |
| 134. | 1.08 | 19.41 | 2.558 | 1.404 | 1.154 | 0.45 | 17.46 | 22.52 | 11.29 | 0.65 | -4896. | 4251. | 291. | 0.977 |
| 139. | 1.01 | 40.53 | 2.627 | 1.252 | 1.377 | 0.52 | 24.57 | 19.62 | 29.02 | 1.18 | -15884. | 20875. | 297. | 0.690 |
| 140. | 1.01 | 40.61 | 2.623 | 0.796 | 1.827 | 0.70 | 24.46 | 9.91 | 30.79 | 1.26 | -16160. | 18200. | 297. | 0.686 |
| 207. | 1.94 | 2.59 | 3.866 | 2.344 | 1.523 | 0.39 | 1.55 | 2.14 | 0.66 | 0.42 | - 990. | 1750. | 292. | 0.987 |
| 208. | 1.97 | 2.63 | 3.908 | 2.657 | 1.251 | 0.32 | 1.56 | 2.04 | 0.53 | 0.34 | - 741. | 1642. | 292. | 0.986 |
| 209. | 1.97 | 2.73 | 3.909 | 2.962 | 0.947 | 0.24 | 1.58 | 1.98 | 0.35 | 0.22 | - 796. | 793. | 293. | 0.970 |
| 210. | 2.06 | 2.55 | 4.096 | 1.682 | 2.414 | 0.59 | 1.41 | 1.86 | 1.10 | 0.78 | -1608. | 4598. | 294. | 0.975 |
| 211. | 2.01 | 2.42 | 3.985 | 1.366 | 2.620 | 0.66 | 1.39 | 1.32 | 1.42 | 1.02 | -1722. | 5722. | 294. | 0.980 |
| 115. | 1.98 | 5.00 | 3.959 | 1.803 | 2.156 | 0.54 | 2.02 | 1.76 | 2.23 | 1.11 | -3280. | 5887. | 295. | 0.686 |
| 72. | 2.05 | 4.90 | 4.074 | 1.140 | 2.934 | 0.72 | 1.69 | 1.08 | 1.92 | 1.14 | -3600. | 9436. | 309. | 0.632 |
| 71. | 2.03 | 4.84 | 4.049 | 1.864 | 2.185 | 0.54 | 1.70 | 1.82 | 1.59 | 0.94 | -2468. | 4549. | 307. | 0.637 |
| 70. | 2.04 | 4.80 | 4.062 | 2.307 | 1.754 | 0.43 | 1.70 | 1.95 | 1.37 | 0.80 | -2361. | 3193. | 303. | 0.637 |
| 69. | 2.05 | 5.08 | 4.075 | 2.102 | 1.973 | 0.48 | 1.71 | 1.92 | 1.50 | 0.87 | -3115. | 3921. | 303. | 0.608 |
| 68. | 2.02 | 4.96 | 4.025 | 2.801 | 1.223 | 0.30 | 1.73 | 1.99 | 1.15 | 0.66 | -2324. | 2625. | 301. | 0.617 |
| 184. | 2.04 | 4.95 | 4.101 | 3.247 | 0.855 | 0.21 | 2.76 | 3.15 | 1.25 | 0.45 | -1664. | 1513. | 294. | 0.980 |
| 185. | 2.02 | 4.75 | 4.065 | 2.209 | 1.856 | 0.46 | 2.71 | 3.29 | 2.02 | 0.75 | -2445. | 3858. | 294. | 0.995 |
| 186. | 2.08 | 4.85 | 4.174 | 1.777 | 2.397 | 0 57 | 2.68 | 2.46 | 2.85 | 1.06 | -4020. | 6883. | 294. | 0.990 |
| 198. | 2.04 | 5.07 | 4.049 | 3.148 | 0.901 | 0.22 | 1.40 | 1.67 | 0.47 | 0.33 | -1598. | 2157. | 294. | 0.480 |
| 199. | 2.00 | 5.04 | 3.981 | 2.749 | 1.232 | 0.31 | 1.44 | 1.64 | 1.01 | 0.70 | -2117. | 2681. | 294. | 0.490 |
| 200. | 2.03 | 4.79 | 4.038 | 2.534 | 1.504 | 0.37 | 1.42 | 1.63 | 1.07 | 0.75 | -2159. | 3072. | 291. | 0.510 |
| 201. | 2.06 | 5.10 | 4.081 | 2.453 | 1.628 | 0.40 | 1.40 | 1.63 | 1.06 | 0.76 | -2127. | 3807. | 293. | 0.480 |
| 202. | 2.05 | 5.02 | 4.064 | 1.531 | 2.533 | 0.62 | 1.40 | 1.27 | 1.49 | 1.06 | -2806. | 6885. | 294. | 0.488 |
| 82. | 2.00 | 9.68 | 4.047 | 0.836 | 3.211 | 0.79 | 3.33 | 0.37 | 4.10 | 1.23 | -6682. | 19897. | 302. | 0.612 |
| 81. | 2.00 | 9.66 | 4.053 | 1.479 | 2.574 | 0.64 | 3.34 | 0.91 | 4.74 | 1.42 | -5877. | 12297. | 299. | 0.612 |

Table D.5 (cont.): Air-Water Flow Data (Refs /21/ - /27/): $D_3/D_1$ = 1, Downward Branch ($\Phi$ = 180°).

| RUN # | VsL1 (m/s) | VsG1 (m/s) | m1 (kg/s) | m2 (kg/s) | m3 (kg/s) | m3/m1 (-) | x1 (%) | x2 (%) | x3 (%) | x3/x1 (-) | p12 (Pa) | p13 (Pa) | T1 (K) | p1 (MPa) |
|---|---|---|---|---|---|---|---|---|---|---|---|---|---|---|
| 80. | 2.02 | 9.89 | 4.098 | 1.861 | 2.237 | 0.55 | 3.33 | 2.37 | 4.12 | 1.24 | -4416. | 9186. | 294. | 0.593 |
| 79. | 2.03 | 9.87 | 4.117 | 1.694 | 2.423 | 0.59 | 3.33 | 1.32 | 4.73 | 1.42 | -5704. | 12077. | 293. | 0.593 |
| 78. | 2.03 | 9.77 | 4.119 | 2.521 | 1.598 | 0.39 | 3.36 | 3.47 | 3.20 | 0.95 | -3111. | 4569. | 289. | 0.598 |
| 76. | 2.01 | 9.30 | 4.077 | 3.068 | 1.009 | 0.25 | 3.28 | 3.68 | 2.08 | 0.63 | -2312. | 2449. | 303. | 0.637 |
| 75. | 2.03 | 9.46 | 4.110 | 2.862 | 1.247 | 0.30 | 3.30 | 3.44 | 2.98 | 0.90 | -3644. | 3176. | 299. | 0.627 |
| 123. | 1.98 | 9.91 | 4.117 | 3.243 | 0.873 | 0.21 | 5.61 | 6.13 | 3.70 | 0.66 | -2489. | 1919. | 292. | 0.992 |
| 125. | 2.05 | 10.11 | 4.245 | 2.839 | 1.406 | 0.33 | 5.50 | 5.94 | 4.62 | 0.84 | -4754. | 3685. | 293. | 0.988 |
| 126. | 2.06 | 10.25 | 4.264 | 2.590 | 1.674 | 0.39 | 5.49 | 5.09 | 6.09 | 1.11 | -5938. | 6136. | 293. | 0.977 |
| 127. | 2.10 | 10.31 | 4.348 | 1.461 | 2.888 | 0.66 | 5.37 | 2.04 | 7.06 | 1.31 | -10233. | 15912. | 293. | 0.971 |
| 90. | 1.97 | 18.31 | 4.122 | 1.690 | 2.432 | 0.59 | 6.52 | 3.12 | 8.87 | 1.36 | -8332. | 19505. | 300. | 0.642 |
| 89. | 1.97 | 18.44 | 4.129 | 2.374 | 1.755 | 0.43 | 6.50 | 6.36 | 6.69 | 1.03 | -5945. | 8587. | 300. | 0.637 |
| 88. | 2.06 | 18.56 | 4.312 | 1.089 | 3.223 | 0.75 | 6.25 | 1.17 | 7.97 | 1.27 | -17939. | 35061. | 296. | 0.627 |
| 87. | 2.03 | 19.22 | 4.252 | 1.863 | 2.389 | 0.56 | 6.39 | 4.37 | 7.96 | 1.25 | -8550. | 16989. | 295. | 0.608 |
| 86. | 1.99 | 18.73 | 4.173 | 3.021 | 1.152 | 0.28 | 6.42 | 7.13 | 4.57 | 0.71 | -3390. | 3535. | 298. | 0.622 |
| 192. | 2.19 | 21.09 | 4.778 | 3.675 | 1.104 | 0.23 | 10.35 | 10.60 | 9.54 | 0.92 | -8080. | 3672. | 289. | 0.990 |
| 177. | 2.99 | 4.79 | 5.961 | 4.519 | 1.441 | 0.24 | 1.85 | 1.85 | 1.86 | 1.01 | -4380. | 1965. | 294. | 0.989 |
| 178. | 3.02 | 4.73 | 6.016 | 4.410 | 1.607 | 0.27 | 1.81 | 1.77 | 1.91 | 1.06 | -5222. | 3074. | 294. | 0.985 |
| 179. | 3.06 | 4.77 | 6.104 | 4.087 | 2.017 | 0.33 | 1.78 | 1.58 | 2.19 | 1.23 | -6540. | 4256. | 295. | 0.980 |
| 180. | 3.02 | 5.00 | 6.028 | 3.784 | 2.244 | 0.37 | 1.88 | 1.60 | 2.35 | 1.25 | -7442. | 4652. | 295. | 0.976 |
| 181. | 3.22 | 4.96 | 6.423 | 3.683 | 2.740 | 0.43 | 1.77 | 1.29 | 2.42 | 1.36 | -9051. | 8580. | 291. | 0.975 |
| 182. | 3.08 | 5.06 | 6.153 | 2.800 | 3.353 | 0.54 | 1.87 | 1.02 | 2.59 | 1.38 | -11388. | 12754. | 292. | 0.970 |
| 183. | 2.96 | 5.01 | 5.905 | 1.364 | 4.541 | 0.77 | 1.94 | 0.82 | 2.27 | 1.17 | -10567. | 21389. | 293. | 0.975 |
| 203. | 3.00 | 4.85 | 5.923 | 3.048 | 2.876 | 0.49 | 0.95 | 0.70 | 1.22 | 1.28 | -9823. | 9296. | 297. | 0.502 |
| 205. | 2.96 | 4.48 | 5.838 | 3.758 | 2.106 | 0.36 | 0.92 | 0.87 | 1.01 | 1.10 | -6061. | 4611. | 298. | 0.519 |
| 206. | 3.03 | 4.79 | 5.978 | 4.384 | 1.594 | 0.27 | 0.90 | 0.87 | 0.97 | 1.08 | -3036. | 6415. | 299. | 0.490 |
| 95. | 2.92 | 9.59 | 5.851 | 4.641 | 1.209 | 0.21 | 2.37 | 2.35 | 2.46 | 1.04 | -4480. | 3318. | 302. | 0.637 |
| 94. | 2.93 | 10.00 | 5.880 | 4.394 | 1.487 | 0.25 | 2.50 | 2.23 | 3.29 | 1.32 | -7432. | 4655. | 299. | 0.642 |
| 93. | 2.93 | 9.26 | 5.877 | 3.590 | 2.288 | 0.39 | 2.38 | 1.80 | 3.28 | 1.38 | -10148. | 8190. | 298. | 0.657 |
| 92. | 2.97 | 9.89 | 5.971 | 2.893 | 3.078 | 0.52 | 2.47 | 1.25 | 3.62 | 1.46 | -15859. | 14948. | 297. | 0.647 |
| 91. | 3.00 | 9.89 | 6.014 | 3.407 | 2.607 | 0.43 | 2.40 | 1.32 | 3.82 | 1.59 | -14049. | 10739. | 294. | 0.627 |

Table D.5 (cont.): Air-Water Flow Data (Refs /21/ - /27/): $D_3/D_1$ = 1, Downward Branch ($\Phi$ = 180°).

| RUN # | VsL1 (m/s) | VsG1 (m/s) | m1 (kg/s) | m2 (kg/s) | m3 (kg/s) | m3/m1 (-) | x1 (%) | x2 (%) | x3 (%) | x3/x1 (-) | p12 (Pa) | p13 (Pa) | T1 (K) | p1 (MPa) |
|---|---|---|---|---|---|---|---|---|---|---|---|---|---|---|
| 193. | 3.05 | 10.20 | 6.205 | 4.762 | 1.443 | 0.23 | 3.79 | 3.36 | 5.19 | 1.37 | -10531. | 4276. | 290. | 0.976 |
| 194. | 2.99 | 9.91 | 6.072 | 4.852 | 1.220 | 0.20 | 3.74 | 3.61 | 4.25 | 1.14 | -7607. | 2770. | 293. | 0.978 |
| 195. | 3.02 | 9.67 | 6.128 | 5.249 | 0.879 | 0.14 | 3.66 | 3.67 | 3.59 | 0.98 | -2677. | 1836. | 289. | 0.980 |
| 57. | 4.09 | 4.00 | 8.087 | 6.199 | 1.888 | 0.23 | 0.93 | 0.97 | 0.79 | 0.85 | -6640. | 2034. | 301. | 0.800 |
| 58. | 4.05 | 3.96 | 8.012 | 5.367 | 2.645 | 0.33 | 0.93 | 0.84 | 1.12 | 1.20 | -10235. | 4603. | 306. | 0.800 |
| 59. | 3.92 | 3.83 | 7.748 | 4.183 | 3.565 | 0.46 | 0.93 | 0.71 | 1.20 | 1.28 | -12190. | 7560. | 309. | 0.800 |
| 60. | 3.96 | 3.87 | 7.832 | 2.558 | 5.274 | 0.67 | 0.93 | 0.88 | 0.96 | 1.02 | -13260. | 17688. | 309. | 0.800 |
| 61. | 4.10 | 3.93 | 8.118 | 4.322 | 3.796 | 0.47 | 0.91 | 0.74 | 1.17 | 1.28 | -12226. | 6371. | 298. | 0.800 |
| 62. | 4.08 | 3.77 | 8.069 | 2.714 | 5.355 | 0.66 | 0.88 | 0.61 | 1.02 | 1.16 | -14240. | 13871. | 301. | 0.800 |
| 63. | 3.92 | 4.04 | 7.756 | 1.362 | 6.394 | 0.82 | 0.98 | 0.25 | 1.13 | 1.16 | -12473. | 19692. | 303. | 0.800 |
| 118. | 4.10 | 9.70 | 8.263 | 7.128 | 1.135 | 0.14 | 2.76 | 2.63 | 3.59 | 1.30 | -10168. | 2046. | 292. | 1.000 |
| 119. | 4.05 | 9.65 | 8.167 | 6.746 | 1.421 | 0.17 | 2.78 | 2.51 | 4.11 | 1.47 | -13031. | 2066. | 293. | 1.000 |
| 120. | 3.97 | 9.74 | 8.009 | 5.883 | 2.126 | 0.27 | 2.86 | 2.31 | 4.39 | 1.53 | -17295. | 7170. | 295. | 1.000 |
| 121. | 3.94 | 9.88 | 7.962 | 5.147 | 2.815 | 0.35 | 2.92 | 2.09 | 4.45 | 1.52 | -21842. | 13480. | 295. | 1.000 |
| 122. | 4.20 | 9.52 | 8.453 | 4.327 | 4.126 | 0.49 | 2.65 | 1.05 | 4.34 | 1.64 | -30794. | 26375. | 295. | 1.000 |
| 110. | 3.94 | 4.97 | 7.842 | 6.230 | 1.612 | 0.21 | 1.49 | 1.39 | 1.91 | 1.28 | -6981. | 3070. | 294. | 1.000 |
| 111. | 3.91 | 5.00 | 7.783 | 6.442 | 1.341 | 0.17 | 1.51 | 1.45 | 1.78 | 1.18 | -6051. | 2265. | 295. | 1.000 |
| 112. | 4.03 | 4.87 | 8.016 | 5.773 | 2.243 | 0.28 | 1.43 | 1.29 | 1.79 | 1.25 | -10364. | 3410. | 291. | 1.000 |
| 113. | 3.87 | 5.05 | 7.707 | 5.262 | 2.445 | 0.32 | 1.54 | 1.38 | 1.88 | 1.22 | -10443. | 3750. | 291. | 1.000 |
| 114. | 3.88 | 4.95 | 7.730 | 4.363 | 3.367 | 0.44 | 1.51 | 1.05 | 2.10 | 1.39 | -14790. | 11732. | 293. | 1.000 |
| 313. | 0.21 | 5.05 | 0.467 | 0.304 | 0.162 | 0.35 | 12.39 | 18.99 | 0.00 | 0.00 | - | - | 293. | 0.490 |
| 234. | 1.03 | 10.04 | 2.137 | 2.021 | 0.116 | 0.05 | 5.42 | 5.73 | 0.03 | 0.01 | - | - | 293. | 0.493 |
| 314. | 0.25 | 5.13 | 0.543 | 0.074 | 0.419 | 0.77 | 10.65 | 7.46 | 0.61 | 0.06 | - | - | 293. | 0.482 |
| 317. | 0.26 | 5.04 | 0.574 | 0.279 | 0.295 | 0.51 | 10.07 | 20.69 | 0.02 | 0.00 | - | - | 293. | 0.490 |
| 302. | 3.08 | 2.56 | 6.057 | 5.913 | 0.144 | 0.02 | 0.48 | 0.50 | 0.00 | 0.00 | - | - | 293. | 0.490 |
| 303. | 3.98 | 2.56 | 7.826 | 7.684 | 0.142 | 0.02 | 0.37 | 0.38 | 0.00 | 0.00 | - | - | 293. | 0.490 |
| 304. | 2.03 | 2.49 | 4.009 | 3.808 | 0.201 | 0.05 | 0.71 | 0.75 | 0.00 | 0.00 | - | - | 291. | 0.488 |
| 305. | 2.03 | 4.93 | 4.037 | 3.877 | 0.160 | 0.04 | 1.41 | 1.46 | 0.00 | 0.00 | - | - | 291. | 0.490 |
| 307. | 1.03 | 2.49 | 2.043 | 1.839 | 0.204 | 0.10 | 1.40 | 1.56 | 0.00 | 0.00 | - | - | 292. | 0.490 |
| 308. | 1.03 | 7.37 | 2.099 | 1.985 | 0.107 | 0.05 | 4.03 | 4.27 | 0.00 | 0.00 | - | - | 292. | 0.490 |

Table D.5 (cont.): Air-Water Flow Data (Refs /21/ - /27/): $D_3/D_1$ = 1, Downward Branch ($\Phi$ = 180°).

| RUN # | VsL1 (m/s) | VsG1 (m/s) | m1 (kg/s) | m2 (kg/s) | m3 (kg/s) | m3/m1 (-) | x1 (%) | x2 (%) | x3 (%) | x3/x1 (-) | p12 (Pa) | p13 (Pa) | T1 (K) | p1 (MPa) |
|---|---|---|---|---|---|---|---|---|---|---|---|---|---|---|
| 165. | 0.52 | 5.05 | 1.128 | 0.545 | 0.583 | 0.52 | 10.20 | 19.74 | 1.27 | 0.12 | - | - | 296. | 0.982 |
| 226. | 0.52 | 5.04 | 1.068 | 0.631 | 0.438 | 0.41 | 5.41 | 8.42 | 1.08 | 0.20 | - | - | 293. | 0.491 |
| 280. | 0.51 | 4.92 | 1.063 | 0.909 | 0.154 | 0.14 | 5.34 | 6.24 | 0.00 | 0.00 | - | - | 291. | 0.490 |
| 281. | 0.51 | 4.92 | 1.063 | 0.812 | 0.250 | 0.24 | 5.34 | 6.88 | 0.34 | 0.06 | - | - | 291. | 0.490 |
| 282. | 0.51 | 4.86 | 1.063 | 0.661 | 0.400 | 0.38 | 5.34 | 8.22 | 0.09 | 0.02 | - | - | 291. | 0.496 |
| 283. | 1.01 | 4.94 | 2.036 | 1.844 | 0.192 | 0.09 | 2.75 | 3.01 | 0.31 | 0.11 | - | - | 295. | 0.488 |
| 319. | 0.51 | 4.93 | 1.052 | 0.884 | 0.168 | 0.16 | 5.38 | 6.40 | 0.00 | 0.00 | - | - | 291. | 0.488 |
| 148. | 0.49 | 9.89 | 1.188 | 0.938 | 0.251 | 0.21 | 18.79 | 23.41 | 1.53 | 0.08 | - | - | 297. | 0.980 |
| 149. | 0.52 | 10.45 | 1.251 | 0.560 | 0.691 | 0.55 | 18.47 | 34.64 | 5.37 | 0.29 | - | - | 297. | 0.960 |
| 150. | 0.51 | 10.33 | 1.240 | 0.613 | 0.627 | 0.51 | 18.95 | 34.29 | 3.95 | 0.21 | - | - | 294. | 0.977 |
| 151. | 0.58 | 10.93 | 1.382 | 0.925 | 0.456 | 0.33 | 17.93 | 25.45 | 2.69 | 0.15 | - | - | 291. | 0.965 |
| 152. | 0.60 | 10.37 | 1.410 | 0.330 | 1.080 | 0.77 | 16.83 | 36.98 | 10.67 | 0.63 | - | - | 292. | 0.975 |
| 153. | 0.59 | 10.46 | 1.387 | 0.351 | 1.036 | 0.75 | 17.21 | 39.66 | 9.61 | 0.56 | - | - | 293. | 0.975 |
| 154. | 0.63 | 10.77 | 1.483 | 0.334 | 1.149 | 0.77 | 16.39 | 36.56 | 10.53 | 0.64 | - | - | 293. | 0.963 |
| 155. | 0.49 | 9.77 | 1.089 | 0.636 | 0.454 | 0.42 | 11.42 | 18.76 | 1.14 | 0.10 | - | - | 290. | 0.539 |
| 156. | 0.49 | 9.55 | 1.075 | 0.733 | 0.342 | 0.32 | 11.57 | 16.48 | 1.06 | 0.09 | - | - | 291. | 0.554 |
| 156. | 0.50 | 10.38 | 1.113 | 0.520 | 0.593 | 0.53 | 11.26 | 21.10 | 2.64 | 0.23 | - | - | 292. | 0.515 |
| 157. | 0.50 | 10.11 | 1.100 | 0.562 | 0.539 | 0.49 | 11.29 | 19.95 | 2.27 | 0.20 | - | - | 292. | 0.524 |
| 158. | 0.53 | 9.95 | 1.142 | 0.407 | 0.735 | 0.64 | 9.98 | 22.46 | 3.06 | 0.31 | - | - | 290. | 0.485 |
| 159. | 0.50 | 10.06 | 1.101 | 0.304 | 0.799 | 0.73 | 10.59 | 28.41 | 3.78 | 0.36 | - | - | 291. | 0.492 |
| 160. | 0.51 | 10.32 | 1.119 | 0.276 | 0.848 | 0.76 | 10.49 | 28.66 | 4.53 | 0.43 | - | - | 292. | 0.486 |
| 321. | 0.51 | 9.85 | 1.105 | 1.002 | 0.103 | 0.09 | 10.24 | 11.30 | 0.00 | 0.00 | - | - | 292. | 0.490 |
| 145. | 0.52 | 20.06 | 1.465 | 0.888 | 0.578 | 0.39 | 31.02 | 41.03 | 15.63 | 0.50 | - | - | 292. | 0.965 |
| 146. | 0.51 | 19.50 | 1.442 | 1.052 | 0.389 | 0.27 | 30.58 | 38.93 | 8.03 | 0.26 | - | - | 294. | 0.972 |
| 147. | 0.58 | 19.87 | 1.576 | 1.411 | 0.165 | 0.10 | 27.96 | 30.75 | 4.11 | 0.15 | - | - | 298. | 0.966 |
| 167. | 1.01 | 5.17 | 2.089 | 1.108 | 0.980 | 0.47 | 5.63 | 9.85 | 0.85 | 0.15 | - | - | 291. | 0.967 |
| 168. | 1.05 | 5.18 | 2.179 | 1.243 | 0.927 | 0.43 | 5.51 | 9.53 | 0.17 | 0.03 | - | - | 290. | 0.980 |
| 169. | 1.06 | 5.17 | 2.198 | 0.739 | 1.459 | 0.66 | 5.46 | 10.23 | 3.05 | 0.56 | - | - | 290. | 0.983 |
| 170. | 1.05 | 5.39 | 2.180 | 0.867 | 1.313 | 0.60 | 5.69 | 10.42 | 2.57 | 0.45 | - | - | 292. | 0.980 |
| 171. | 1.05 | 5.39 | 2.185 | 1.009 | 1.176 | 0.54 | 5.66 | 9.81 | 2.10 | 0.37 | - | - | 291. | 0.977 |

Table D.5 (cont.): Air-Water Flow Data (Refs /21/ - /27/): $D_3/D_1 = 1$, Downward Branch ($\Phi = 180°$).

| RUN # | VsL1 (m/s) | VsG1 (m/s) | m1 (kg/s) | m2 (kg/s) | m3 (kg/s) | m3/m1 (-) | x1 (%) | x2 (%) | x3 (%) | x3/x1 (-) | p12 (Pa) | p13 (Pa) | T1 (K) | p1 (MPa) |
|---|---|---|---|---|---|---|---|---|---|---|---|---|---|---|
| 172. | 1.01 | 5.19 | 2.101 | 0.372 | 1.729 | 0.82 | 5.71 | 12.68 | 4.20 | 0.74 | - | - | 292. | 0.986 |
| 173. | 1.01 | 5.16 | 2.089 | 0.433 | 1.656 | 0.79 | 5.71 | 10.93 | 4.34 | 0.76 | - | - | 294. | 0.991 |
| 218. | 0.98 | 4.92 | 1.981 | 1.130 | 0.850 | 0.43 | 2.93 | 3.96 | 1.55 | 0.53 | - | - | 291. | 0.501 |
| 275. | 0.98 | 5.02 | 1.984 | 1.871 | 0.113 | 0.06 | 2.88 | 3.06 | 0.00 | 0.00 | - | - | 295. | 0.490 |
| 284. | 1.01 | 5.00 | 2.034 | 1.988 | 0.047 | 0.02 | 2.79 | 2.85 | 0.00 | 0.00 | - | - | 295. | 0.487 |
| 283. | 1.01 | 4.99 | 2.037 | 1.845 | 0.192 | 0.09 | 2.78 | 3.04 | 0.31 | 0.11 | - | - | 295. | 0.488 |
| 278. | 0.99 | 5.07 | 1.989 | 1.713 | 0.276 | 0.14 | 2.87 | 3.26 | 0.50 | 0.18 | - | - | 295. | 0.485 |
| 277. | 0.99 | 4.98 | 1.990 | 1.634 | 0.356 | 0.18 | 2.86 | 3.35 | 0.65 | 0.23 | - | - | 295. | 0.492 |
| 306. | 1.04 | 4.97 | 2.096 | 1.950 | 0.146 | 0.07 | 2.71 | 2.91 | 0.00 | 0.00 | - | - | 291. | 0.486 |
| 212. | 0.94 | 2.50 | 1.898 | 1.139 | 0.759 | 0.40 | 3.09 | 4.76 | 0.59 | 0.19 | - | - | 286. | 0.982 |
| 237. | 0.99 | 2.51 | 1.965 | 1.903 | 0.062 | 0.03 | 1.47 | 1.51 | 0.00 | 0.00 | - | - | 292. | 0.490 |
| 238. | 1.03 | 2.55 | 2.037 | 1.878 | 0.159 | 0.08 | 1.37 | 1.49 | 0.00 | 0.00 | - | - | 293. | 0.470 |
| 239. | 0.98 | 2.44 | 1.940 | 1.663 | 0.276 | 0.14 | 1.49 | 1.74 | 0.03 | 0.02 | - | - | 293. | 0.507 |
| 240. | 1.00 | 2.58 | 1.993 | 1.500 | 0.494 | 0.25 | 1.46 | 1.76 | 0.56 | 0.38 | - | - | 293. | 0.485 |
| 241. | 1.00 | 2.56 | 1.991 | 1.275 | 0.716 | 0.36 | 1.48 | 1.79 | 0.92 | 0.62 | - | - | 292. | 0.490 |
| 242. | 1.06 | 2.57 | 2.113 | 1.005 | 1.108 | 0.52 | 1.39 | 1.23 | 1.53 | 1.10 | - | - | 294. | 0.490 |
| 243. | 1.02 | 2.58 | 2.028 | 0.928 | 1.100 | 0.54 | 1.44 | 1.28 | 1.58 | 1.10 | - | - | 290. | 0.480 |
| 244. | 1.04 | 2.55 | 2.060 | 0.731 | 1.328 | 0.65 | 1.41 | 1.08 | 1.58 | 1.13 | - | - | 292. | 0.485 |
| 245. | 1.02 | 2.53 | 2.018 | 0.549 | 1.468 | 0.73 | 1.44 | 1.14 | 1.55 | 1.08 | - | - | 293. | 0.490 |
| 270. | 1.00 | 2.42 | 1.991 | 1.806 | 0.185 | 0.09 | 1.40 | 1.54 | 0.00 | 0.00 | - | - | 292. | 0.490 |
| 271. | 0.99 | 2.42 | 1.972 | 1.749 | 0.223 | 0.11 | 1.41 | 1.58 | 0.03 | 0.02 | - | - | 292. | 0.490 |
| 272. | 1.00 | 2.43 | 1.982 | 1.663 | 0.319 | 0.16 | 1.40 | 1.62 | 0.24 | 0.17 | - | - | 294. | 0.490 |
| 273. | 1.00 | 2.42 | 1.978 | 1.274 | 0.704 | 0.36 | 1.39 | 1.98 | 0.33 | 0.24 | - | - | 295. | 0.490 |
| 274. | 1.00 | 2.42 | 1.978 | 1.388 | 0.590 | 0.30 | 1.39 | 1.86 | 0.29 | 0.21 | - | - | 295. | 0.490 |
| 307. | 1.03 | 2.49 | 2.043 | 1.839 | 0.204 | 0.10 | 1.40 | 1.56 | 0.00 | 0.00 | - | - | 292. | 0.490 |
| 227. | 1.00 | 9.94 | 2.191 | 1.580 | 0.626 | 0.29 | 10.41 | 13.28 | 2.93 | 0.28 | - | - | 292. | 0.979 |
| 285. | 1.02 | 9.87 | 2.115 | 2.019 | 0.096 | 0.05 | 5.31 | 5.56 | 0.00 | 0.00 | - | - | 295. | 0.490 |
| 286. | 0.99 | 9.83 | 2.051 | 1.925 | 0.125 | 0.06 | 5.45 | 5.80 | 0.21 | 0.04 | - | - | 295. | 0.490 |
| 310. | 1.03 | 9.96 | 2.130 | 2.015 | 0.108 | 0.05 | 5.39 | 5.70 | 0.00 | 0.00 | - | - | 291. | 0.490 |
| 311. | 1.03 | 9.96 | 2.130 | 0.000 | 2.130 | 1.00 | 5.39 | 0.00 | 5.39 | 1.00 | - | - | 291. | 0.490 |

Table D.5 (cont.): Air-Water Flow Data (Refs /21/ - /27/): $D_3/D_1 = 1$, Downward Branch ($\Phi = 180°$).

| RUN # | VsL1 (m/s) | VsG1 (m/s) | m1 (kg/s) | m2 (kg/s) | m3 (kg/s) | m3/m1 (-) | x1 (%) | x2 (%) | x3 (%) | x3/x1 (-) | p12 (Pa) | p13 (Pa) | T1 (K) | p1 (MPa) |
|---|---|---|---|---|---|---|---|---|---|---|---|---|---|---|
| 128. | 1.06 | 19.84 | 2.534 | 2.001 | 0.533 | 0.21 | 18.16 | 20.99 | 7.50 | 0.41 | - | - | 290. | 0.982 |
| 129. | 1.04 | 19.63 | 2.499 | 2.095 | 0.404 | 0.16 | 18.36 | 20.76 | 5.95 | 0.32 | - | - | 290. | 0.990 |
| 130. | 1.04 | 19.66 | 2.498 | 2.313 | 0.184 | 0.07 | 18.13 | 19.29 | 3.62 | 0.20 | - | - | 292. | 0.981 |
| 135. | 1.02 | 39.34 | 2.626 | 2.041 | 0.585 | 0.22 | 24.25 | 25.81 | 18.83 | 0.78 | - | - | 291. | 0.688 |
| 136. | 1.04 | 38.94 | 2.681 | 2.359 | 0.322 | 0.12 | 23.76 | 26.20 | 5.85 | 0.25 | - | - | 290. | 0.692 |
| 137. | 1.00 | 40.88 | 2.611 | 2.081 | 0.530 | 0.20 | 24.85 | 27.50 | 14.43 | 0.58 | - | - | 293. | 0.679 |
| 138. | 0.99 | 40.36 | 2.583 | 1.492 | 1.091 | 0.42 | 24.83 | 22.87 | 27.51 | 1.11 | - | - | 296. | 0.687 |
| 341. | 1.00 | 30.03 | 2.298 | 2.245 | 0.052 | 0.02 | 15.02 | 15.37 | 0.00 | 0.00 | - | - | 291. | 0.488 |
| 342. | 1.00 | 30.05 | 2.298 | 2.228 | 0.069 | 0.03 | 15.02 | 15.47 | 0.69 | 0.05 | - | - | 291. | 0.488 |
| 343. | 1.00 | 29.95 | 2.298 | 2.215 | 0.083 | 0.04 | 15.03 | 15.53 | 1.83 | 0.12 | - | - | 291. | 0.490 |
| 344. | 1.00 | 29.95 | 2.298 | 2.152 | 0.146 | 0.06 | 15.03 | 15.92 | 1.90 | 0.13 | - | - | 291. | 0.490 |
| 248. | 1.94 | 2.40 | 3.816 | 3.671 | 0.145 | 0.04 | 0.70 | 0.72 | 0.00 | 0.00 | - | - | 293. | 0.475 |
| 249. | 1.95 | 2.34 | 3.841 | 3.639 | 0.202 | 0.05 | 0.68 | 0.71 | 0.01 | 0.01 | - | - | 295. | 0.480 |
| 251. | 2.06 | 2.55 | 4.068 | 3.122 | 0.946 | 0.23 | 0.72 | 0.81 | 0.44 | 0.61 | - | - | 291. | 0.490 |
| 252. | 2.06 | 2.55 | 4.065 | 3.849 | 0.229 | 0.06 | 0.72 | 0.76 | 0.01 | 0.01 | - | - | 291. | 0.490 |
| 267. | 2.05 | 2.57 | 4.040 | 3.790 | 0.251 | 0.06 | 0.72 | 0.75 | 0.23 | 0.32 | - | - | 290. | 0.480 |
| 269. | 2.06 | 2.50 | 4.071 | 3.356 | 0.715 | 0.18 | 0.71 | 0.81 | 0.24 | 0.33 | - | - | 291. | 0.490 |
| 304. | 2.03 | 2.49 | 4.009 | 3.808 | 0.201 | 0.05 | 0.71 | 0.75 | 0.00 | 0.00 | - | - | 291. | 0.488 |
| 305. | 2.03 | 4.93 | 4.037 | 3.877 | 0.160 | 0.04 | 1.41 | 1.46 | 0.00 | 0.00 | - | - | 291. | 0.490 |
| 116. | 1.95 | 4.86 | 3.900 | 2.003 | 1.897 | 0.49 | 2.03 | 2.25 | 1.79 | 0.88 | - | - | 295. | 0.701 |
| 67. | 1.91 | 4.43 | 3.804 | 3.145 | 0.659 | 0.17 | 1.78 | 2.00 | 0.74 | 0.42 | - | - | 299. | 0.666 |
| 66. | 1.93 | 4.44 | 3.834 | 3.601 | 0.233 | 0.06 | 1.68 | 1.80 | 0.00 | 0.00 | - | - | 310. | 0.657 |
| 266. | 1.95 | 4.93 | 3.878 | 3.692 | 0.186 | 0.05 | 1.46 | 1.54 | 0.01 | 0.01 | - | - | 291. | 0.490 |
| 197. | 2.02 | 4.97 | 4.006 | 3.298 | 0.708 | 0.18 | 1.42 | 1.66 | 0.32 | 0.22 | - | - | 294. | 0.493 |
| 305. | 2.03 | 4.93 | 4.037 | 3.877 | 0.160 | 0.04 | 1.41 | 1.46 | 0.00 | 0.00 | - | - | 291. | 0.490 |
| 77. | 1.98 | 9.24 | 4.013 | 3.634 | 0.379 | 0.09 | 3.33 | 3.53 | 1.47 | 0.44 | - | - | 304. | 0.642 |
| 124. | 2.00 | 10.31 | 4.161 | 3.681 | 0.480 | 0.12 | 5.69 | 6.07 | 2.78 | 0.49 | - | - | 292. | 0.980 |
| 85. | 1.98 | 18.91 | 4.149 | 3.368 | 0.780 | 0.19 | 6.49 | 7.16 | 3.59 | 0.55 | - | - | 295. | 0.612 |
| 191. | 1.96 | 21.68 | 4.341 | 3.733 | 0.609 | 0.14 | 11.68 | 12.52 | 6.51 | 0.56 | - | - | 287. | 0.979 |
| 175. | 3.02 | 4.99 | 6.023 | 5.305 | 0.718 | 0.12 | 1.91 | 1.99 | 1.34 | 0.70 | - | - | 290. | 0.979 |

Table D.5 (cont.): Air-Water Flow Data (Refs /21/ - /27/): $D_3/D_1$ = 1, Downward Branch ($\Phi$ = 180°).

| RUN # | VsL1 (m/s) | VsG1 (m/s) | m1 (kg/s) | m2 (kg/s) | m3 (kg/s) | m3/m1 (-) | x1 (%) | x2 (%) | x3 (%) | x3/x1 (-) | p12 (Pa) | p13 (Pa) | T1 (K) | p1 (MPa) |
|---|---|---|---|---|---|---|---|---|---|---|---|---|---|---|
| 309. | 1.97 | 7.54 | 3.940 | 3.785 | 0.155 | 0.04 | 2.19 | 2.28 | 0.00 | 0.00 | - | - | 292. | 0.488 |
| 318. | 0.55 | 2.70 | 1.101 | 0.872 | 0.229 | 0.21 | 2.78 | 3.51 | 0.00 | 0.00 | - | - | 293. | 0.485 |
| 319. | 0.51 | 4.93 | 1.052 | 0.328 | 0.168 | 0.16 | 5.38 | 17.23 | 0.00 | 0.00 | - | - | 291. | 0.488 |
| 320. | 0.51 | 7.53 | 1.091 | 0.960 | 0.131 | 0.12 | 7.96 | 9.05 | 0.00 | 0.00 | - | - | 291. | 0.490 |
| 321. | 0.51 | 9.85 | 1.105 | 1.002 | 0.103 | 0.09 | 10.24 | 11.30 | 0.00 | 0.00 | - | - | 292. | 0.490 |
| 323. | 0.25 | 9.91 | 0.604 | 0.516 | 0.088 | 0.15 | 18.73 | 21.94 | 0.00 | 0.00 | - | - | 292. | 0.487 |
| 324. | 0.25 | 9.89 | 0.604 | 0.489 | 0.115 | 0.19 | 18.73 | 22.98 | 0.39 | 0.02 | - | - | 292. | 0.488 |
| 325. | 0.25 | 9.89 | 0.604 | 0.479 | 0.126 | 0.21 | 18.73 | 23.51 | 0.52 | 0.03 | - | - | 292. | 0.488 |
| 326. | 0.25 | 9.89 | 0.604 | 0.349 | 0.144 | 0.24 | 18.73 | 0.34 | 0.45 | 0.02 | - | - | 292. | 0.488 |
| 327. | 0.26 | 9.95 | 0.629 | 0.456 | 0.173 | 0.27 | 18.00 | 24.44 | 1.00 | 0.06 | - | - | 292. | 0.485 |
| 328. | 0.26 | 9.77 | 0.629 | 0.440 | 0.189 | 0.30 | 18.00 | 24.81 | 2.11 | 0.12 | - | - | 292. | 0.494 |
| 329. | 0.50 | 14.96 | 1.158 | 1.062 | 0.096 | 0.08 | 14.85 | 16.19 | 0.00 | 0.00 | - | - | 292. | 0.490 |
| 330. | 1.00 | 15.12 | 2.141 | 2.080 | 0.061 | 0.03 | 8.15 | 8.39 | 0.00 | 0.00 | - | - | 292. | 0.492 |
| 331. | 0.99 | 19.75 | 2.170 | 2.107 | 0.063 | 0.03 | 10.46 | 10.77 | 0.00 | 0.00 | - | - | 292. | 0.490 |
| 332. | 0.50 | 19.69 | 1.206 | 1.148 | 0.058 | 0.05 | 18.82 | 19.78 | 0.00 | 0.00 | - | - | 291. | 0.490 |
| 333. | 0.51 | 24.97 | 1.288 | 1.142 | 0.046 | 0.04 | 22.36 | 16.46 | 0.00 | 0.00 | - | - | 291. | 0.490 |
| 334. | 0.99 | 24.97 | 2.221 | 2.162 | 0.059 | 0.03 | 12.96 | 13.32 | 0.00 | 0.00 | - | - | 291. | 0.490 |
| 335. | 0.99 | 29.92 | 2.294 | 2.242 | 0.052 | 0.02 | 15.16 | 15.52 | 0.00 | 0.00 | - | - | 291. | 0.494 |
| 336. | 0.50 | 30.58 | 1.325 | 1.291 | 0.034 | 0.03 | 26.31 | 26.99 | 0.00 | 0.00 | - | - | 292. | 0.486 |
| 337. | 4.05 | 4.00 | 7.981 | 6.378 | 1.873 | 0.23 | 0.57 | 0.40 | 1.07 | 1.86 | - | - | 293. | 0.490 |
| 341. | 1.00 | 30.03 | 2.298 | 2.245 | 0.052 | 0.02 | 15.02 | 15.37 | 0.00 | 0.00 | - | - | 291. | 0.488 |
| 342. | 1.00 | 30.05 | 2.298 | 2.228 | 0.069 | 0.03 | 15.02 | 15.47 | 0.69 | 0.05 | - | - | 291. | 0.488 |
| 343. | 1.00 | 29.95 | 2.298 | 2.215 | 0.083 | 0.04 | 15.03 | 15.53 | 1.83 | 0.12 | - | - | 291. | 0.490 |
| 344. | 1.00 | 29.95 | 2.298 | 2.152 | 0.146 | 0.06 | 15.03 | 15.92 | 1.90 | 0.13 | - | - | 291. | 0.490 |
| 345. | 2.01 | 15.40 | 4.107 | 4.033 | 0.074 | 0.02 | 4.31 | 4.39 | 0.00 | 0.00 | - | - | 292. | 0.490 |
| 346. | 2.04 | 9.78 | 4.111 | 4.008 | 0.103 | 0.03 | 2.73 | 2.80 | 0.00 | 0.00 | - | - | 292. | 0.490 |
| 161. | 0.50 | 4.90 | 1.091 | 0.172 | 0.919 | 0.84 | 10.23 | 31.80 | 6.20 | 0.61 | - | - | 294. | 0.978 |
| 162. | 0.49 | 5.11 | 1.073 | 0.165 | 0.908 | 0.85 | 10.80 | 35.21 | 6.35 | 0.59 | - | - | 295. | 0.975 |
| 163. | 0.51 | 5.02 | 1.119 | 0.310 | 0.809 | 0.72 | 10.33 | 26.81 | 4.00 | 0.39 | - | - | 292. | 0.981 |
| 164. | 0.50 | 4.92 | 1.096 | 0.363 | 0.733 | 0.67 | 10.41 | 26.55 | 2.43 | 0.23 | - | - | 292. | 0.989 |

Table D.5 (cont.): Air-Water Flow Data (Refs /21/ - /27/): $D_3/D_1$ = 1, Downward Branch ($\Phi$ = 180°).

| RUN # | VsL1 (m/s) | VsG1 (m/s) | m1 (kg/s) | m2 (kg/s) | m3 (kg/s) | m3/m1 (-) | x1 (%) | x2 (%) | x3 (%) | x3/x1 (-) | p12 (Pa) | p13 (Pa) | T1 (K) | p1 (MPa) |
|---|---|---|---|---|---|---|---|---|---|---|---|---|---|---|
| 176. | 2.98 | 4.71 | 5.938 | 5.523 | 0.415 | 0.07 | 1.83 | 1.91 | 0.75 | 0.41 | - | - | 294. | 0.990 |
| 204. | 3.02 | 4.86 | 5.967 | 3.396 | 2.571 | 0.43 | 0.92 | 0.74 | 1.16 | 1.26 | - | - | 297. | 0.490 |
| 295. | 3.01 | 4.94 | 5.952 | 5.855 | 0.097 | 0.02 | 0.96 | 0.97 | 0.00 | 0.00 | - | - | 291. | 0.490 |
| 296. | 3.02 | 4.98 | 5.969 | 5.795 | 0.174 | 0.03 | 0.95 | 0.98 | 0.00 | 0.00 | - | - | 293. | 0.490 |
| 297. | 3.02 | 4.98 | 5.969 | 5.768 | 0.201 | 0.03 | 0.95 | 0.98 | 0.00 | 0.00 | - | - | 293. | 0.490 |
| 298. | 3.02 | 5.01 | 5.969 | 5.712 | 0.257 | 0.04 | 0.95 | 0.98 | 0.40 | 0.42 | - | - | 293. | 0.487 |
| 299. | 3.02 | 5.01 | 5.969 | 5.640 | 0.329 | 0.06 | 0.95 | 0.99 | 0.35 | 0.37 | - | - | 293. | 0.487 |
| 300. | 3.01 | 5.01 | 5.952 | 5.528 | 0.424 | 0.07 | 0.96 | 0.99 | 0.47 | 0.49 | - | - | 293. | 0.487 |
| 301. | 3.02 | 5.01 | 5.973 | 5.450 | 0.524 | 0.09 | 0.95 | 0.99 | 0.56 | 0.59 | - | - | 293. | 0.487 |

Table D.5 (cont.): Air-Water Flow Data (Refs /21/ - /27/): $D_3/D_1$ = 1, Downward Branch ($\Phi$ = 180°).

| RUN # | VsL1 (m/s) | VsG1 (m/s) | m1 (kg/s) | m2 (kg/s) | m3 (kg/s) | m3/m1 (-) | x1 (%) | x2 (%) | x3 (%) | x3/x1 (-) | p12 (Pa) | p13 (Pa) | T1 (K) | p1 (MPa) |
|---|---|---|---|---|---|---|---|---|---|---|---|---|---|---|
| 71.0 | 0.75 | 6.92 | 1.882 | 1.136 | 0.746 | 0.40 | 21.64 | 24.07 | 29.41 | 1.36 | -3304. | 4838. | 497. | 2.5 |
| 72.0 | 0.74 | 6.74 | 1.870 | 1.175 | 0.695 | 0.37 | 22.05 | 24.44 | 30.46 | 1.38 | -3268. | 4382. | 499. | 2.6 |
| 73.0 | 0.73 | 7.08 | 1.854 | 1.241 | 0.613 | 0.33 | 23.34 | 27.51 | 30.88 | 1.32 | -3114. | 3240. | 499. | 2.6 |
| 74.0 | 0.71 | 7.14 | 1.825 | 1.363 | 0.462 | 0.25 | 23.92 | 27.70 | 33.87 | 1.42 | -3078. | 1489. | 499. | 2.6 |
| 75.0 | 0.68 | 7.67 | 1.803 | 1.548 | 0.255 | 0.14 | 26.02 | 32.08 | 33.90 | 1.30 | -2390. | 389. | 500. | 2.6 |
| 10.0 | 1.34 | 10.30 | 3.258 | 2.640 | 0.618 | 0.19 | 19.34 | 25.90 | 17.30 | .894 | -5660. | 1669. | 499. | 2.6 |
| 11.0 | 1.30 | 10.92 | 3.218 | 2.304 | 0.914 | 0.28 | 20.75 | 28.82 | 19.62 | .945 | -8021. | 5565. | 499. | 2.6 |
| 12.0 | 1.40 | 9.78 | 3.340 | 1.722 | 1.618 | 0.48 | 17.90 | 25.01 | 20.09 | 1.12 | -8719. | 18213. | 500. | 2.6 |
| 13.0 | 1.40 | 10.26 | 3.371 | 1.047 | 2.324 | 0.69 | 18.61 | 52.12 | 17.73 | .953 | -11339. | 35424. | 499. | 2.6 |
| 120.0 | 0.76 | 8.43 | 2.029 | 1.170 | 0.859 | 0.42 | 26.40 | 24.35 | 40.44 | 1.53 | -5100. | 9992. | 501. | 2.7 |
| 121.0 | 0.77 | 8.34 | 2.031 | 1.276 | 0.755 | 0.37 | 26.09 | 26.60 | 41.84 | 1.60 | -4723. | 7517. | 501. | 2.7 |
| 122.0 | 0.77 | 8.13 | 2.029 | 1.331 | 0.698 | 0.34 | 25.46 | 24.29 | 41.35 | 1.62 | -4449. | 6689. | 501. | 2.7 |
| 123.0 | 0.78 | 7.97 | 2.027 | 1.487 | 0.540 | 0.27 | 24.96 | 25.02 | 43.35 | 1.74 | -3676. | 3894. | 501. | 2.7 |
| 124.0 | 0.77 | 8.33 | 2.036 | 1.739 | 0.297 | 0.15 | 25.98 | 28.88 | 47.89 | 1.84 | -3076. | 958. | 502. | 2.7 |
| 125.0 | 0.76 | 9.21 | 2.003 | 1.083 | 0.920 | 0.46 | 25.96 | 23.61 | 38.61 | 1.49 | -31328. | 11364. | 496. | 2.4 |
| 126.0 | 0.76 | 8.22 | 1.968 | 1.326 | 0.642 | 0.36 | 24.56 | 25.10 | 36.91 | 1.50 | -4817. | 6225. | 497. | 2.5 |
| 128.0 | 0.74 | 13.16 | 2.260 | 1.667 | 0.593 | 0.26 | 35.61 | 45.19 | 44.48 | 1.25 | -9417. | 5695. | 498. | 2.6 |
| 129.2 | 0.75 | 13.93 | 2.291 | 1.800 | 0.491 | 0.21 | 35.75 | 45.71 | 43.46 | 1.22 | -8522. | 3375. | 498. | 2.5 |
| 130.0 | 0.75 | 13.93 | 2.285 | 1.593 | 0.692 | 0.30 | 35.83 | 47.25 | 42.31 | 1.18 | -9211. | 8026. | 498. | 2.5 |
| 131.0 | 0.78 | 5.53 | 1.844 | 1.227 | 0.617 | 0.33 | 16.91 | 13.71 | 30.79 | 1.82 | -2008. | 4030. | 496. | 2.4 |
| 132.0 | 0.77 | 5.29 | 1.829 | 1.415 | 0.414 | 0.23 | 17.02 | 17.10 | 17.10 | 1.80 | -1511. | 1178. | 498. | 2.5 |
| 133.0 | 0.79 | 5.27 | 1.852 | 1.270 | 0.582 | 0.31 | 16.73 | 13.25 | 32.15 | 1.92 | -1887. | 3279. | 497. | 2.5 |
| 140.0 | 1.53 | 13.35 | 3.757 | 3.050 | 0.707 | 0.19 | 20.06 | 21.98 | 27.01 | 1.35 | -8500. | 4706. | 495. | 2.4 |
| 141.0 | 1.52 | 13.23 | 3.726 | 2.965 | 0.761 | 0.20 | 20.05 | 23.62 | 27.51 | 1.37 | -9251. | 5846. | 495. | 2.4 |
| 142.0 | 1.56 | 12.20 | 3.748 | 2.742 | 1.006 | 0.27 | 18.37 | 21.31 | 25.10 | 1.36 | -10136. | 10231. | 495. | 2.4 |
| 143.0 | 1.58 | 12.23 | 3.779 | 2.212 | 1.567 | 0.41 | 18.27 | 19.69 | 24.85 | 1.36 | -13587. | 24862. | 494. | 2.4 |
| 144.0 | 1.59 | 11.64 | 3.769 | 2.452 | 1.317 | 0.35 | 17.43 | 19.37 | 23.98 | 1.37 | -11197. | 16989. | 495. | 2.4 |
| 202.0 | 1.24 | 7.36 | 2.842 | 1.973 | 0.870 | 0.31 | 14.61 | 12.81 | 26.14 | 1.79 | -5907. | 7353. | 496. | 2.4 |
| 203.0 | 1.23 | 6.96 | 2.815 | 2.078 | 0.737 | 0.26 | 14.55 | 14.14 | 25.41 | 1.75 | -5154. | 5341. | 497. | 2.5 |

Table D.6: Steam-Water Flow Data (Refs /21/ - /27/): $D_3/D_1$ = 1, Horizontal Branch($\Phi$ = 90°).

| RUN # | VsL1 (m/s) | VsG1 (m/s) | m1 (kg/s) | m2 (kg/s) | m3 (kg/s) | m3/m1 (-) | x1 (%) | x2 (%) | x3 (%) | x3 /x1 ( -) | p12 (Pa) | p13 (Pa) | T1 (K) | p1 (MPa) |
|---|---|---|---|---|---|---|---|---|---|---|---|---|---|---|
| 198.0 | 1.09 | 5.51 | 2.779 | 2.078 | 0.701 | 0.25 | 23.20 | 24.92 | 39.84 | 1.72 | -5358. | 3389. | 537. | 5.0 |
| 200.0 | 1.10 | 5.74 | 2.811 | 2.022 | 0.789 | 0.28 | 23.54 | 25.50 | 38.48 | 1.63 | -5199. | 4302. | 537. | 4.9 |
| 201.0 | 1.09 | 5.72 | 2.797 | 1.738 | 1.059 | 0.38 | 23.59 | 23.29 | 37.55 | 1.59 | -6320. | 8642. | 536. | 4.9 |
| 28.0 | 1.03 | 1.25 | 2.187 | 1.439 | 0.748 | 0.34 | 8.05 | 5.93 | 16.23 | 2.02 | -1827. | 2126. | 549. | 6.0 |
| 34.0 | 1.02 | 1.37 | 2.187 | 1.382 | 0.805 | 0.37 | 8.96 | 3.96 | 20.09 | 2.24 | -4275. | 3508. | 550. | 6.1 |
| 35.0 | 1.45 | 1.80 | 3.112 | 2.631 | 0.481 | 0.15 | 8.43 | 5.66 | 32.30 | 3.83 | -2022. | 501. | 551. | 6.2 |
| 36.2 | 1.45 | 1.84 | 3.112 | 1.349 | 1.763 | 0.57 | 8.61 | 7.17 | 12.72 | 1.48 | -5461. | 7758. | 551. | 6.2 |
| 37.3 | 1.45 | 1.84 | 3.112 | 1.023 | 2.089 | 0.67 | 8.61 | 28.20 | 9.02 | 1.05 | -4921. | 8600. | 551. | 6.2 |
| 7.0 | 1.64 | 0.86 | 3.369 | 1.383 | 1.986 | 0.59 | 4.48 | 5.72 | 6.16 | 1.37 | -2387. | 4405. | 564. | 7.5 |
| 8.0 | 1.66 | 0.68 | 3.373 | 2.759 | 0.614 | 0.18 | 3.57 | 2.24 | 12.82 | 3.59 | -1814. | 410. | 564. | 7.5 |
| 9.0 | 1.60 | 1.10 | 3.322 | 2.245 | 1.077 | 0.32 | 5.67 | 8.46 | 6.66 | 1.17 | -3657. | 2002. | 562. | 7.3 |
| 63.0 | 1.40 | 2.08 | 3.103 | 2.366 | 0.737 | 0.24 | 11.84 | 10.48 | 27.30 | 2.31 | -3900. | 1212. | 563. | 7.3 |
| 64.0 | 1.45 | 1.79 | 3.152 | 2.705 | 0.447 | 0.14 | 10.02 | 10.45 | 26.16 | 2.61 | -2507. | 444. | 564. | 7.5 |
| 65.0 | 1.42 | 2.01 | 3.138 | 2.851 | 0.287 | 0.09 | 11.29 | 13.41 | 27.49 | 2.43 | -1863. | 265. | 564. | 7.5 |
| 83.0 | 1.10 | 3.61 | 2.785 | 2.045 | 0.740 | 0.27 | 22.84 | 25.33 | 38.98 | 1.71 | -3521. | 2858. | 564. | 7.5 |
| 84.0 | 1.14 | 3.65 | 2.883 | 1.767 | 1.116 | 0.39 | 22.34 | 19.04 | 39.42 | 1.76 | -4773. | 5984. | 564. | 7.5 |
| 94.0 | 1.08 | 3.19 | 2.685 | 2.370 | 0.315 | 0.12 | 20.94 | 26.27 | 34.64 | 1.65 | -1669. | 140. | 564. | 7.5 |
| 95.0 | 1.09 | 3.25 | 2.719 | 2.133 | 0.586 | 0.22 | 21.09 | 27.09 | 29.76 | 1.41 | -3312. | 1916. | 564. | 7.5 |
| 96.0 | 1.11 | 3.16 | 2.728 | 1.892 | 0.836 | 0.31 | 20.44 | 20.05 | 37.29 | 1.82 | -3531. | 3615. | 564. | 7.5 |
| 97.0 | 1.10 | 3.28 | 2.742 | 2.087 | 0.655 | 0.24 | 21.07 | 24.60 | 34.67 | 1.65 | -3404. | 2475. | 564. | 7.5 |
| 98.0 | 1.08 | 3.30 | 2.691 | 2.192 | 0.499 | 0.19 | 21.66 | 27.05 | 33.03 | 1.52 | -2863. | 1425. | 564. | 7.5 |
| 99.0 | 1.10 | 3.16 | 2.709 | 1.627 | 0.444 | 0.40 | 20.56 | 16.09 | 36.97 | 1.80 | -4558. | 5266. | 564. | 7.5 |
| 100.0 | 1.55 | 1.57 | 3.307 | 2.738 | 0.569 | 0.17 | 8.35 | 8.52 | 20.29 | 2.43 | -2310. | 902. | 564. | 7.5 |
| 101.0 | 1.50 | 1.94 | 3.279 | 2.586 | 0.693 | 0.21 | 10.44 | 13.08 | 16.46 | 1.57 | -3669. | 1668. | 564. | 7.5 |
| 102.0 | 1.52 | 1.78 | 3.301 | 2.444 | 0.857 | 0.26 | 9.52 | 8.93 | 19.96 | 2.09 | -4304. | 2299. | 564. | 7.5 |
| 103.0 | 1.54 | 1.77 | 3.322 | 2.349 | 0.973 | 0.29 | 9.42 | 6.55 | 22.07 | 2.34 | -4264. | 2413. | 564. | 7.5 |
| 104.0 | 1.55 | 1.69 | 3.336 | 2.224 | 1.112 | 0.33 | 8.92 | 4.06 | 21.75 | 2.43 | -4550. | 3215. | 564. | 7.5 |
| 155.0 | 1.47 | 2.62 | 3.336 | 2.464 | 0.872 | 0.26 | 13.85 | 14.23 | 26.38 | 1.90 | -5316. | 3444. | 564. | 7.5 |
| 156.0 | 1.53 | 1.65 | 3.297 | 2.280 | 1.017 | 0.31 | 8.81 | 6.60 | 19.26 | 2.19 | -3640. | 3078. | 564. | 7.5 |
| 157.0 | 1.57 | 1.50 | 3.346 | 2.526 | 0.820 | 0.25 | 7.90 | 8.79 | 14.36 | 1.82 | -3265. | 1825. | 564. | 7.5 |

Table D.6 (cont.): Steam-Water Flow Data (Refs /21/ - /27/): $D_3/D_1$ = 1, Horizontal Branch($\Phi$ = 90°).

| RUN # | VsL1 (m/s) | VsG1 (m/s) | m1 (kg/s) | m2 (kg/s) | m3 (kg/s) | m3/m1 (-) | x1 (%) | x2 (%) | x3 (%) | x3 /x1 ( -) | p12 (Pa) | p13 (Pa) | T1 (K) | p1 (MPa) |
|---|---|---|---|---|---|---|---|---|---|---|---|---|---|---|
| 204.0 | 1.22 | 9.93 | 2.805 | 2.206 | 0.599 | 0.21 | 14.53 | 14.51 | 27.00 | 1.86 | -4340. | 3145. | 498. | 2.5 |
| 205.0 | 1.59 | 5.52 | 3.440 | 2.708 | 0.732 | 0.21 | 9.43 | 8.93 | 18.56 | 1.97 | -4647. | 3429. | 497. | 2.5 |
| 206.0 | 1.60 | 5.70 | 3.479 | 2.899 | 0.580 | 0.17 | 9.64 | 10.33 | 16.99 | 1.76 | -3599. | 380. | 498. | 2.5 |
| 16.0 | 0.82 | 3.80 | 1.889 | 1.389 | 0.500 | 0.26 | 14.68 | 13.55 | 27.61 | 1.88 | -1668. | 1533. | 509. | 3.1 |
| 38.3 | 1.31 | 5.69 | 3.112 | 1.937 | 1.175 | 0.38 | 17.21 | 24.86 | 18.15 | 1.05 | -6442. | 7548. | 524. | 4.0 |
| 39.3 | 1.31 | 5.69 | 3.112 | 2.086 | 1.026 | 0.33 | 17.21 | 29.95 | 10.01 | 0.58 | -5290. | 3125. | 524. | 4.0 |
| 40.4 | 1.31 | 5.69 | 3.112 | 1.222 | 1.890 | 0.61 | 17.21 | 28.98 | 19.42 | 1.13 | -7688. | 18445. | 524. | 4.0 |
| 4.0 | 1.47 | 3.67 | 3.307 | 2.345 | 0.962 | 0.29 | 13.05 | 12.89 | 23.27 | 1.78 | -4767. | 3403. | 537. | 5.0 |
| 5.0 | 1.36 | 3.96 | 3.128 | 1.631 | 1.497 | 0.48 | 14.89 | 16.29 | 20.91 | 1.40 | -6216. | 8958. | 537. | 5.0 |
| 6.0 | 1.50 | 3.37 | 3.340 | 1.277 | 2.063 | 0.62 | 11.86 | 21.02 | 13.65 | 1.15 | -6153. | 11414. | 537. | 5.0 |
| 18.0 | 1.50 | 2.73 | 3.287 | 2.271 | 1.016 | 0.31 | 10.34 | 7.39 | 22.34 | 2.16 | -4546. | 4644. | 542. | 5.3 |
| 19.0 | 1.47 | 3.10 | 3.265 | 1.757 | 1.508 | 0.46 | 11.82 | 10.44 | 18.49 | 1.56 | -5972. | 7773. | 541. | 5.3 |
| 30.1 | 1.06 | 1.91 | 2.297 | 1.641 | 0.626 | 0.29 | 9.77 | 6.58 | 22.80 | 2.33 | -2135. | 1782. | 537. | 5.0 |
| 54.0 | 1.50 | 1.91 | 3.163 | 1.652 | 1.511 | 0.48 | 7.10 | 10.95 | 7.95 | 1.12 | -4497. | 4059. | 537. | 5.0 |
| 55.0 | 1.45 | 2.17 | 3.097 | 2.167 | 0.930 | 0.30 | 8.24 | 5.64 | 18.41 | 2.23 | -4062. | 3235. | 537. | 5.0 |
| 56.0 | 1.40 | 2.37 | 3.032 | 2.423 | 0.609 | 0.20 | 9.18 | 7.89 | 23.00 | 2.51 | -2918. | 1331. | 538. | 5.0 |
| 66.0 | 1.57 | 2.98 | 3.418 | 2.809 | 0.609 | 0.18 | 10.26 | 10.79 | 21.07 | 2.05 | -3756. | 1051. | 537. | 5.0 |
| 69.0 | 1.56 | 3.17 | 3.440 | 2.692 | 0.748 | 0.22 | 10.84 | 10.85 | 21.77 | 2.01 | -4180. | 1985. | 537. | 5.0 |
| 134.0 | 0.86 | 5.95 | 2.393 | 1.547 | 0.846 | 0.35 | 29.24 | 30.60 | 45.71 | 1.56 | -4879. | 6206. | 537. | 5.0 |
| 135.0 | 0.87 | 5.98 | 2.409 | 1.975 | 0.434 | 0.18 | 29.19 | 36.62 | 40.25 | 1.38 | -4174. | 2010. | 538. | 5.0 |
| 136.0 | 0.86 | 6.28 | 2.430 | 1.749 | 0.681 | 0.28 | 30.38 | 35.10 | 45.82 | 1.51 | -5258. | 4526. | 537. | 5.0 |
| 137.0 | 0.85 | 6.22 | 2.393 | 1.124 | 1.269 | 0.38 | 30.58 | 33.44 | 45.26 | 1.48 | -5472. | 7102. | 537. | 5.0 |
| 138.0 | 0.86 | 2.41 | 1.962 | 1.424 | 0.538 | 0.27 | 14.43 | 18.07 | 19.24 | 1.33 | -1768. | 1785. | 537. | 5.0 |
| 139.0 | 0.87 | 2.55 | 1.997 | 1.199 | 0.798 | 0.40 | 14.70 | 13.16 | 24.32 | 1.65 | -2375. | 3447. | 536. | 4.9 |
| 191.0 | 1.62 | 4.29 | 3.669 | 2.383 | 1.286 | 0.35 | 13.46 | 11.26 | 24.56 | 1.82 | -6957. | 7713. | 537. | 4.9 |
| 192.0 | 1.63 | 4.37 | 3.714 | 2.559 | 1.155 | 0.31 | 13.83 | 13.44 | 24.19 | 1.75 | -6812. | 6355. | 537. | 5.0 |
| 193.0 | 1.62 | 4.34 | 3.679 | 2.671 | 1.008 | 0.27 | 13.87 | 12.81 | 27.00 | 1.94 | -6597. | 5569. | 537. | 5.0 |
| 195.0 | 1.62 | 2.30 | 3.436 | 2.529 | 0.907 | 0.26 | 7.70 | 5.85 | 17.72 | 2.30 | -3790. | 3183. | 537. | 4.9 |
| 196.0 | 1.60 | 2.43 | 3.424 | 2.641 | 0.783 | 0.23 | 8.18 | 7.11 | 18.59 | 2.27 | -3748. | 2285. | 537. | 4.9 |
| 197.0 | 1.59 | 2.65 | 3.434 | 2.860 | 0.574 | 0.17 | 9.06 | 9.93 | 17.82 | 1.97 | -2534. | 1037. | 537. | 5.0 |

Table D.6 (cont.): Steam-Water Flow Data (Refs /21/ - /27/): $D_3/D_1$ = 1, Horizontal Branch($\Phi$ = 90°).

| RUN # | VsL1 (m/s) | VsG1 (m/s) | m1 (kg/s) | m2 (kg/s) | m3 (kg/s) | m3/m1 (-) | x1 (%) | x2 (%) | x3 (%) | x3 /x1 ( -) | p12 (Pa) | p13 (Pa) | T1 (K) | p1 (MPa) |
|---|---|---|---|---|---|---|---|---|---|---|---|---|---|---|
| 158.0 | 1.59 | 1.38 | 3.369 | 2.679 | 0.690 | 0.20 | 7.23 | 10.13 | 8.81 | 1.22 | -2858. | 1469. | 564. | 7.5 |
| 159.0 | 0.97 | 3.00 | 2.432 | 1.654 | 0.778 | 0.32 | 21.46 | 21.89 | 37.14 | 1.73 | -3078. | 2777. | 564. | 7.4 |
| 160.0 | 0.98 | 2.99 | 2.450 | 1.831 | 0.619 | 0.25 | 21.56 | 25.71 | 34.03 | 1.58 | -2802. | 2381. | 564. | 7.5 |
| 161.0 | 0.99 | 3.04 | 2.474 | 1.390 | 1.084 | 0.44 | 21.37 | 15.92 | 37.09 | 1.74 | -3361. | 5017. | 563. | 7.4 |
| 85.0 | 1.05 | 2.04 | 2.540 | 1.406 | 1.134 | 0.45 | 18.91 | 9.09 | 36.44 | 1.93 | -3279. | 4315. | 584. | 10.0 |
| 86.0 | 1.07 | 2.04 | 2.579 | 1.708 | 0.871 | 0.34 | 18.59 | 17.15 | 34.80 | 1.87 | -3314. | 2295. | 584. | 10.0 |
| 87.0 | 1.05 | 2.18 | 2.566 | 1.937 | 0.629 | 0.25 | 19.96 | 29.20 | 22.44 | 1.12 | -5753. | 1559. | 585. | 10.0 |
| 88.0 | 1.11 | 1.97 | 2.636 | 1.851 | 0.785 | 0.30 | 17.36 | 59.96 | 5.17 | 0.30 | -3842. | 5842. | 584. | 9.9 |
| 90.0 | 1.06 | 2.36 | 2.634 | 1.547 | 1.087 | 0.41 | 20.87 | 15.71 | 38.09 | 1.82 | -3718. | 4193. | 584. | 9.9 |
| 91.0 | 1.06 | 2.32 | 2.626 | 1.810 | 0.816 | 0.31 | 20.80 | 21.27 | 37.61 | 1.81 | -3843. | 2080. | 584. | 10.0 |
| 92.0 | 1.07 | 2.40 | 2.666 | 2.079 | 0.587 | 0.22 | 21.18 | 27.20 | 31.80 | 1.50 | -3060. | 692. | 584. | 10.0 |
| 93.0 | 1.10 | 2.19 | 2.668 | 2.200 | 0.468 | 0.18 | 19.35 | 22.94 | 36.67 | 1.90 | -2765. | 480. | 585. | 10.0 |
| 105.0 | 1.62 | 0.50 | 3.297 | 1.910 | 1.387 | 0.42 | 3.57 | 5.11 | 5.12 | 1.43 | -2924. | 2178. | 585. | 10.0 |
| 106.0 | 1.61 | 0.52 | 3.273 | 2.101 | 1.172 | 0.36 | 3.76 | 6.92 | 3.92 | 1.04 | -2309. | 1846. | 585. | 10.0 |
| 107.0 | 1.60 | 0.52 | 3.265 | 2.160 | 1.105 | 0.34 | 3.73 | 6.93 | 3.62 | 0.97 | -2383. | 1491. | 585. | 10.0 |
| 108.0 | 1.62 | 0.45 | 3.281 | 2.700 | 0.581 | 0.18 | 3.19 | 4.48 | 4.85 | 1.52 | -1789. | 744. | 585. | 10.0 |
| 162.0 | 1.53 | 1.14 | 3.281 | 2.257 | 1.024 | 0.31 | 8.45 | 5.54 | 20.07 | 2.38 | -4414. | 2565. | 586. | 10.3 |
| 163.0 | 1.68 | 1.56 | 3.669 | 2.656 | 1.013 | 0.28 | 10.18 | 8.76 | 23.06 | 2.26 | -4081. | 1948. | 586. | 10.2 |
| 164.0 | 1.66 | 1.59 | 3.628 | 2.392 | 1.236 | 0.34 | 10.34 | 6.44 | 23.28 | 2.25 | -5094. | 2820. | 586. | 10.0 |
| 165.0 | 1.04 | 1.84 | 2.470 | 1.506 | 0.964 | 0.39 | 17.54 | 10.43 | 35.76 | 2.04 | -2791. | 2335. | 586. | 10.0 |
| 300.0 | 1.07 | 2.04 | 2.579 | 1.708 | 0.871 | 0.34 | 18.59 | 17.15 | 34.80 | 1.87 | -3314. | 2295. | 584. | 10.0 |

Table D.6 (cont.): Steam-Water Flow Data (Refs /21/ - /27/): $D_3/D_1$ = 1, Horizontal Branch($\Phi$ = 90°).

| RUN | VsL1 (m/s) | VsG1 (m/s) | m1 (kg/s) | m2 (kg/s) | m3 (kg/s) | m3/m1 (-) | x1 (%) | x2 (%) | x3 (%) | x3/x1 (-) | p12 (Pa) | p13 (Pa) | T1 (K) | p1 (MPa) |
|---|---|---|---|---|---|---|---|---|---|---|---|---|---|---|
| 1360. | 0.05 | 4.91 | 0.171 | 0.007 | 0.164 | 0.96 | 44.48 | 65.96 | 43.51 | 0.98 | - | - | 303. | 0.686 |
| 1361. | 0.05 | 4.91 | 0.171 | 0.094 | 0.077 | 0.45 | 44.48 | 34.77 | 56.23 | 1.26 | - | - | 303. | 0.686 |
| 1362. | 0.05 | 4.91 | 0.171 | 0.078 | 0.093 | 0.54 | 44.48 | 32.35 | 54.74 | 1.23 | - | - | 303. | 0.686 |
| 1363. | 0.05 | 4.94 | 0.171 | 0.047 | 0.124 | 0.73 | 44.38 | 32.67 | 48.78 | 1.10 | - | - | 306. | 0.686 |
| 1345. | 0.05 | 9.96 | 0.256 | 0.000 | 0.256 | 1.00 | 62.43 | 28.60 | 62.44 | 1.00 | -152. | 852. | 293. | 0.686 |
| 1346. | 0.05 | 9.96 | 0.256 | 0.047 | 0.209 | 0.82 | 62.43 | 33.33 | 68.97 | 1.10 | -176. | 368. | 293. | 0.686 |
| 1347. | 0.05 | 10.04 | 0.257 | 0.087 | 0.170 | 0.66 | 62.61 | 35.82 | 76.32 | 1.22 | - | - | 293. | 0.686 |
| 1348. | 0.05 | 10.04 | 0.257 | 0.130 | 0.127 | 0.50 | 62.61 | 53.41 | 71.97 | 1.15 | - | - | 293. | 0.686 |
| 1349. | 0.05 | 10.04 | 0.257 | 0.154 | 0.103 | 0.40 | 62.61 | 56.89 | 71.21 | 1.14 | - | - | 293. | 0.686 |
| 1350. | 0.05 | 10.10 | 0.256 | 0.180 | 0.076 | 0.30 | 62.52 | 58.47 | 72.06 | 1.15 | - | - | 296. | 0.686 |
| 1351. | 0.05 | 10.10 | 0.256 | 0.197 | 0.059 | 0.23 | 62.52 | 59.66 | 72.00 | 1.15 | - | - | 296. | 0.686 |
| 1338. | 0.05 | 20.08 | 0.425 | 2.917 | 3.342 | 7.87 | 76.31 | 100.00 | 96.99 | 1.27 | -901. | 3730. | 291. | 0.686 |
| 1339. | 0.05 | 20.31 | 0.424 | 0.092 | 0.332 | 0.78 | 76.28 | 96.33 | 70.73 | 0.93 | -1034. | 1865. | 295. | 0.686 |
| 1340. | 0.05 | 20.45 | 0.424 | 0.154 | 0.271 | 0.64 | 76.28 | 93.90 | 66.28 | 0.87 | -882. | 1106. | 297. | 0.686 |
| 1341. | 0.05 | 20.45 | 0.424 | 0.204 | 0.221 | 0.52 | 76.28 | 91.17 | 62.53 | 0.82 | -682. | 603. | 297. | 0.686 |
| 1342. | 0.05 | 20.45 | 0.424 | 0.265 | 0.159 | 0.38 | 76.28 | 80.21 | 69.73 | 0.91 | 153. | 279. | 297. | 0.686 |
| 1343. | 0.05 | 20.45 | 0.424 | 0.322 | 0.103 | 0.24 | 76.28 | 78.18 | 70.31 | 0.92 | 59. | 233. | 297. | 0.686 |
| 1352. | 0.10 | 19.91 | 0.512 | 0.450 | 0.062 | 0.12 | 61.77 | 63.33 | 50.34 | 0.82 | 0. | 0. | 296. | 0.686 |
| 1353. | 0.10 | 19.91 | 0.512 | 0.420 | 0.091 | 0.18 | 61.77 | 62.79 | 57.08 | 0.92 | 0. | 0. | 296. | 0.686 |
| 1354. | 0.10 | 19.91 | 0.512 | 0.379 | 0.132 | 0.26 | 61.77 | 60.99 | 64.00 | 1.04 | 0. | 0. | 296. | 0.686 |
| 1355. | 0.10 | 19.91 | 0.512 | 0.352 | 0.160 | 0.31 | 61.77 | 59.72 | 66.27 | 1.07 | 0. | 0. | 296. | 0.686 |
| 1356. | 0.10 | 19.84 | 0.512 | 0.301 | 0.210 | 0.41 | 61.77 | 63.85 | 58.78 | 0.95 | 0. | 0. | 295. | 0.686 |
| 1357. | 0.10 | 20.06 | 0.515 | 0.230 | 0.285 | 0.55 | 62.02 | 64.20 | 60.27 | 0.97 | 0. | 0. | 295. | 0.686 |
| 1358. | 0.10 | 20.30 | 0.514 | 0.159 | 0.355 | 0.69 | 61.98 | 69.54 | 58.59 | 0.95 | 0. | 0. | 299. | 0.686 |
| 1359. | 0.10 | 20.30 | 0.514 | 0.101 | 0.414 | 0.80 | 61.98 | 72.40 | 59.44 | 0.96 | 0. | 0. | 299. | 0.686 |
| 1308. | 0.51 | 10.00 | 1.148 | 0.000 | 1.148 | 1.00 | 13.74 | 0.01 | 13.73 | 1.00 | -658. | 4541. | 298. | 0.686 |
| 1309. | 0.49 | 9.94 | 1.116 | 0.415 | 0.701 | 0.63 | 13.99 | 4.07 | 19.86 | 1.42 | -632. | 2928. | 299. | 0.686 |
| 1310. | 0.50 | 9.96 | 1.136 | 0.649 | 0.487 | 0.43 | 13.78 | 5.35 | 24.99 | 1.81 | -232. | 2156. | 299. | 0.686 |
| 1331. | 0.49 | 10.09 | 1.125 | 0.989 | 0.137 | 0.12 | 14.09 | 12.42 | 26.12 | 1.85 | 343. | 327. | 299. | 0.686 |
| 1332. | 0.49 | 10.09 | 1.125 | 1.050 | 0.075 | 0.07 | 14.09 | 13.93 | 16.22 | 1.15 | 621. | 266. | 299. | 0.686 |

Table D.7: Present Air-Water Flow Data: $D_3/D_1$ = 1, Horizontal Branch ($\Phi$ = 90°).

| RUN | VsL1 (m/s) | VsG1 (m/s) | m1 (kg/s) | m2 (kg/s) | m3 (kg/s) | m3/m1 (-) | x1 (%) | x2 (%) | x3 (%) | x3/x1 (-) | p12 (Pa) | p13 (Pa) | T1 (K) | p1 (MPa) |
|---|---|---|---|---|---|---|---|---|---|---|---|---|---|---|
| 1333. | 0.49 | 10.09 | 1.125 | 0.948 | 0.178 | 0.16 | 14.09 | 10.99 | 30.58 | 2.17 | 166. | 337. | 299. | 0.686 |
| 1334. | 0.50 | 10.09 | 1.130 | 0.858 | 0.272 | 0.24 | 14.03 | 8.44 | 31.66 | 2.26 | 0. | 509. | 299. | 0.686 |
| 1335. | 0.50 | 10.09 | 1.130 | 0.748 | 0.382 | 0.34 | 14.03 | 5.85 | 30.07 | 2.14 | -195. | 926. | 299. | 0.686 |
| 1336. | 0.50 | 10.16 | 1.130 | 0.683 | 0.447 | 0.40 | 14.03 | 3.64 | 29.92 | 2.13 | -247. | 1443. | 301. | 0.686 |
| 1325. | 0.50 | 20.06 | 1.291 | 0.000 | 1.291 | 1.00 | 24.65 | 9.05 | 24.65 | 1.00 | -1554. | 12585. | 296. | 0.686 |
| 1326. | 0.50 | 19.94 | 1.301 | 0.381 | 0.920 | 0.71 | 24.33 | 4.66 | 32.47 | 1.33 | -1567. | 6650. | 296. | 0.686 |
| 1327. | 0.50 | 19.94 | 1.301 | 0.586 | 0.714 | 0.55 | 24.33 | 11.94 | 34.51 | 1.42 | -1211. | 4219. | 296. | 0.686 |
| 1328. | 0.50 | 20.14 | 1.301 | 0.783 | 0.518 | 0.40 | 24.33 | 17.86 | 34.12 | 1.40 | -950. | 2594. | 299. | 0.686 |
| 1329. | 0.49 | 20.26 | 1.287 | 0.939 | 0.348 | 0.27 | 24.74 | 21.17 | 34.38 | 1.39 | -451. | 1542. | 299. | 0.686 |
| 1330. | 0.49 | 20.26 | 1.287 | 1.071 | 0.216 | 0.17 | 24.74 | 22.92 | 33.78 | 1.37 | 375. | 849. | 299. | 0.686 |
| 1312. | 1.00 | 10.09 | 2.115 | 0.000 | 2.115 | 1.00 | 7.40 | 16.54 | 7.40 | 1.00 | -2694. | 10661. | 303. | 0.686 |
| 1313. | 1.00 | 10.21 | 2.114 | 0.569 | 1.545 | 0.73 | 7.64 | 3.32 | 9.23 | 1.21 | -2400. | 7732. | 297. | 0.686 |
| 1314. | 1.00 | 10.21 | 2.114 | 0.974 | 1.139 | 0.54 | 7.64 | 1.97 | 12.49 | 1.63 | -2080. | 6035. | 297. | 0.686 |
| 1315. | 1.00 | 10.42 | 2.114 | 1.160 | 0.954 | 0.45 | 7.64 | 2.31 | 14.11 | 1.85 | -1646. | 4965. | 303. | 0.686 |
| 1321. | 1.01 | 10.26 | 2.143 | 1.883 | 0.260 | 0.12 | 7.52 | 7.56 | 7.21 | 0.96 | 1119. | 1059. | 299. | 0.686 |
| 1322. | 1.00 | 10.22 | 2.111 | 1.815 | 0.297 | 0.14 | 7.61 | 6.57 | 13.97 | 1.84 | -961. | 1248. | 299. | 0.686 |
| 1323. | 1.00 | 10.36 | 2.111 | 1.681 | 0.431 | 0.20 | 7.61 | 4.83 | 18.46 | 2.43 | 461. | 1693. | 303. | 0.686 |
| 1316. | 0.99 | 38.35 | 2.547 | 0.753 | 1.794 | 0.70 | 23.66 | 17.38 | 26.29 | 1.11 | -6491. | 46524. | 299. | 0.686 |
| 1317. | 0.99 | 38.35 | 2.547 | 0.915 | 1.633 | 0.64 | 23.66 | 19.59 | 25.94 | 1.10 | -6899. | 37976. | 299. | 0.686 |
| 1318. | 1.01 | 38.36 | 2.580 | 1.343 | 1.237 | 0.48 | 23.60 | 21.26 | 26.13 | 1.11 | -6103. | 21521. | 296. | 0.686 |
| 1319. | 1.02 | 38.15 | 2.607 | 1.996 | 0.611 | 0.23 | 23.31 | 25.73 | 15.41 | 0.66 | -517. | 5733. | 295. | 0.686 |
| 1320. | 1.02 | 38.15 | 2.607 | 1.818 | 0.789 | 0.30 | 23.31 | 26.66 | 15.59 | 0.67 | -1942. | 7674. | 295. | 0.686 |

Table D.7 (cont.): Present Air-Water Flow Data: $D_3/D_1$ = 1, Horizontal Branch ($\Phi$ = 90°).

| RUN # | VsL1 (m/s) | VsG1 (m/s) | m1 (kg/s) | m2 (kg/s) | m3 (kg/s) | m3/m1 (-) | x1 (%) | x2 (%) | x3 (%) | x3/x1 (-) | p12 (Pa) | p13 (Pa) | T1 (K) | p1 (MPa) |
|---|---|---|---|---|---|---|---|---|---|---|---|---|---|---|
| 1074. | 0.05 | 10.37 | 0.260 | 0.236 | 0.024 | 0.09 | 62.63 | 60.39 | 84.34 | 1.35 | -177. | -20. | 299. | 0.686 |
| 1075. | 0.05 | 10.37 | 0.260 | 0.219 | 0.041 | 0.16 | 62.63 | 58.28 | 85.62 | 1.37 | -233. | -247. | 299. | 0.686 |
| 1076. | 0.05 | 10.24 | 0.260 | 0.196 | 0.064 | 0.25 | 61.79 | 54.23 | 84.99 | 1.38 | -287. | 966. | 299. | 0.686 |
| 1077. | 0.05 | 10.24 | 0.260 | 0.164 | 0.096 | 0.37 | 61.79 | 51.27 | 79.68 | 1.29 | -407. | 2209. | 299. | 0.686 |
| 1078. | 0.05 | 10.24 | 0.260 | 0.132 | 0.128 | 0.49 | 61.79 | 48.23 | 75.81 | 1.23 | -416. | 3709. | 299. | 0.686 |
| 1079. | 0.05 | 10.24 | 0.260 | 0.080 | 0.180 | 0.69 | 61.79 | 41.90 | 70.61 | 1.14 | -319. | 6240. | 299. | 0.686 |
| 1080. | 0.05 | 10.24 | 0.260 | 0.017 | 0.243 | 0.93 | 61.79 | 62.11 | 61.77 | 1.00 | -408. | 9275. | 299. | 0.686 |
| 1081. | 0.05 | 10.24 | 0.260 | 0.003 | 0.258 | 0.99 | 61.79 | 68.70 | 61.72 | 1.00 | -351. | 13766. | 299. | 0.686 |
| 219. | 0.10 | 5.08 | 0.274 | 0.009 | 0.264 | 0.97 | 29.06 | 99.78 | 26.62 | 0.92 | -408. | 3850. | 300. | 0.686 |
| 220. | 0.10 | 5.11 | 0.281 | 0.158 | 0.123 | 0.44 | 28.43 | 9.30 | 52.98 | 1.86 | -502. | 2259. | 300. | 0.686 |
| 221. | 0.11 | 5.04 | 0.288 | 0.186 | 0.102 | 0.35 | 27.91 | 12.88 | 55.25 | 1.98 | -509. | 1760. | 295. | 0.686 |
| 222. | 0.10 | 5.00 | 0.280 | 0.228 | 0.053 | 0.19 | 28.45 | 19.40 | 67.70 | 2.38 | -436. | 578. | 295. | 0.686 |
| 223. | 0.10 | 5.06 | 0.285 | 0.273 | 0.012 | 0.04 | 27.94 | 26.20 | 68.85 | 2.46 | -459. | 167. | 299. | 0.686 |
| 397. | 0.10 | 5.03 | 0.275 | 0.275 | 0.001 | 0.00 | 29.70 | 29.57 | 99.80 | 3.36 | -1136. | 11. | 289. | 0.686 |
| 398. | 0.10 | 5.03 | 0.275 | 0.273 | 0.002 | 0.01 | 29.70 | 29.24 | 99.94 | 3.37 | -1096. | 16. | 289. | 0.686 |
| 399. | 0.10 | 5.03 | 0.275 | 0.270 | 0.005 | 0.02 | 29.70 | 28.28 | 99.98 | 3.37 | -1081. | 66. | 289. | 0.686 |
| 400. | 0.10 | 5.03 | 0.275 | 0.265 | 0.010 | 0.04 | 29.70 | 28.09 | 73.50 | 2.47 | -1104. | 108. | 289. | 0.686 |
| 401. | 0.10 | 5.03 | 0.275 | 0.254 | 0.021 | 0.08 | 29.70 | 25.50 | 80.24 | 2.70 | -1106. | 255. | 289. | 0.686 |
| 402. | 0.10 | 5.03 | 0.275 | 0.248 | 0.027 | 0.10 | 29.70 | 24.53 | 77.17 | 2.60 | -1010. | 415. | 289. | 0.686 |
| 403. | 0.10 | 5.03 | 0.275 | 0.241 | 0.034 | 0.12 | 29.70 | 23.36 | 75.23 | 2.53 | -1012. | 464. | 289. | 0.686 |
| 1188. | 0.12 | 9.83 | 0.389 | 0.001 | 0.388 | 1.00 | 39.97 | 42.00 | 39.97 | 1.00 | -90. | 16676. | 297. | 0.686 |
| 1189. | 0.12 | 9.83 | 0.383 | 0.023 | 0.360 | 0.94 | 40.62 | 21.75 | 41.83 | 1.03 | -82. | 12876. | 297. | 0.686 |
| 1190. | 0.10 | 9.83 | 0.352 | 0.109 | 0.243 | 0.69 | 44.21 | 9.00 | 59.92 | 1.36 | -37. | 10305. | 297. | 0.686 |
| 1191. | 0.10 | 9.83 | 0.352 | 0.126 | 0.226 | 0.64 | 44.21 | 14.88 | 60.63 | 1.37 | -43. | 8936. | 297. | 0.686 |
| 1192. | 0.10 | 9.83 | 0.352 | 0.153 | 0.199 | 0.57 | 44.21 | 20.66 | 62.29 | 1.41 | -45. | 7286. | 297. | 0.686 |
| 1193. | 0.10 | 9.83 | 0.352 | 0.185 | 0.167 | 0.47 | 44.21 | 25.53 | 64.91 | 1.47 | -49. | 5512. | 297. | 0.686 |
| 1194. | 0.10 | 9.83 | 0.352 | 0.210 | 0.141 | 0.40 | 44.21 | 28.68 | 67.33 | 1.52 | -47. | 4263. | 297. | 0.686 |
| 1195. | 0.10 | 9.80 | 0.357 | 0.341 | 0.016 | 0.05 | 43.39 | 42.26 | 67.05 | 1.55 | 145. | 284. | 297. | 0.686 |
| 1197. | 0.10 | 9.53 | 0.346 | 0.317 | 0.029 | 0.08 | 43.83 | 40.62 | 78.77 | 1.80 | 69. | 558. | 295. | 0.686 |
| 1198. | 0.10 | 10.12 | 0.357 | 0.307 | 0.050 | 0:14 | 45.18 | 39.56 | 79.63 | 1.76 | 2. | 998. | 295. | 0.686 |

Table D.8: Present Air-Water Flow Data: $D_3/D_1$ = 0.52, Horizontal Branch ($\Phi$ = 90°).

| RUN # | VsL1 (m/s) | VsG1 (m/s) | m1 (kg/s) | m2 (kg/s) | m3 (kg/s) | m3/m1 (-) | x1 (%) | x2 (%) | x3 (%) | x3/x1 (-) | p12 (Pa) | p13 (Pa) | T1 (K) | p1 (MPa) |
|---|---|---|---|---|---|---|---|---|---|---|---|---|---|---|
| 1199. | 0.10 | 10.12 | 0.357 | 0.286 | 0.071 | 0.20 | 45.18 | 37.36 | 76.83 | 1.70 | 3. | 1714. | 295. | 0.686 |
| 1200. | 0.10 | 10.12 | 0.357 | 0.264 | 0.092 | 0.26 | 45.18 | 34.73 | 75.12 | 1.66 | -3. | 2361. | 295. | 0.686 |
| 1201. | 0.10 | 10.12 | 0.357 | 0.247 | 0.110 | 0.31 | 45.18 | 33.34 | 71.80 | 1.59 | -21. | 3037. | 295. | 0.685 |
| 210. | 0.10 | 20.42 | 0.525 | 0.012 | 0.512 | 0.98 | 61.79 | 96.75 | 60.95 | 0.99 | -456. | 31388. | 296. | 0.686 |
| 211. | 0.10 | 20.12 | 0.520 | 0.081 | 0.439 | 0.84 | 61.42 | 66.61 | 60.45 | 0.98 | -550. | 21198. | 296. | 0.686 |
| 212. | 0.10 | 20.02 | 0.518 | 0.149 | 0.369 | 0.71 | 61.30 | 68.45 | 58.40 | 0.95 | -713. | 28444. | 296. | 0.686 |
| 213. | 0.10 | 20.40 | 0.525 | 0.361 | 0.164 | 0.31 | 61.65 | 60.65 | 63.85 | 1.04 | -581. | 7941. | 296. | 0.686 |
| 214. | 0.10 | 20.42 | 0.527 | 0.414 | 0.112 | 0.21 | 61.55 | 60.32 | 66.04 | 1.07 | -386. | 5078. | 296. | 0.686 |
| 215. | 0.10 | 20.42 | 0.527 | 0.468 | 0.058 | 0.11 | 61.55 | 60.59 | 69.23 | 1.12 | -157. | 2765. | 296. | 0.686 |
| 216. | 0.10 | 20.42 | 0.527 | 0.491 | 0.035 | 0.07 | 61.55 | 61.27 | 65.33 | 1.06 | 16. | 1832. | 296. | 0.686 |
| 1050. | 0.10 | 39.96 | 0.832 | 0.800 | 0.032 | 0.04 | 76.75 | 78.13 | 42.48 | 0.55 | -152. | 943. | 294. | 0.686 |
| 1051. | 0.10 | 40.43 | 0.831 | 0.759 | 0.072 | 0.09 | 76.72 | 78.37 | 59.40 | 0.77 | -1469. | 1714. | 298. | 0.686 |
| 1052. | 0.10 | 40.43 | 0.831 | 0.712 | 0.119 | 0.14 | 76.72 | 78.72 | 64.71 | 0.84 | -2372. | 3537. | 298. | 0.686 |
| 1053. | 0.10 | 40.43 | 0.831 | 0.681 | 0.150 | 0.18 | 76.72 | 78.66 | 67.92 | 0.89 | -2857. | 5561. | 298. | 0.686 |
| 1054. | 0.10 | 40.43 | 0.831 | 0.639 | 0.192 | 0.23 | 76.72 | 79.36 | 67.93 | 0.89 | -3595. | 8649. | 298. | 0.686 |
| 1055. | 0.10 | 40.43 | 0.831 | 0.576 | 0.254 | 0.31 | 76.72 | 80.26 | 68.70 | 0.90 | -4428. | 16179. | 298. | 0.686 |
| 1056. | 0.10 | 40.43 | 0.831 | 0.490 | 0.341 | 0.41 | 76.72 | 82.65 | 68.20 | 0.89 | -4735. | 27261. | 298. | 0.686 |
| 1057. | 0.10 | 40.43 | 0.831 | 0.446 | 0.385 | 0.46 | 76.72 | 83.12 | 69.31 | 0.90 | -5047. | 35013. | 298. | 0.686 |
| 1058. | 0.10 | 39.80 | 0.825 | 0.336 | 0.489 | 0.59 | 76.56 | 86.18 | 69.93 | 0.91 | -6445. | 54569. | 296. | 0.686 |
| 1059. | 0.10 | 39.80 | 0.825 | 0.218 | 0.607 | 0.74 | 76.56 | 89.62 | 71.87 | 0.94 | -6247. | 97353. | 296. | 0.686 |
| 88. | 0.25 | 4.96 | 0.566 | 0.001 | 0.565 | 1.00 | 13.73 | 9.09 | 13.74 | 1.00 | -430. | 8958. | 300. | 0.686 |
| 89. | 0.25 | 4.96 | 0.566 | 0.191 | 0.375 | 0.66 | 13.73 | 0.75 | 20.35 | 1.48 | -533. | 214. | 300. | 0.686 |
| 90. | 0.24 | 4.92 | 0.556 | 0.309 | 0.246 | 0.44 | 13.88 | 0.37 | 30.83 | 2.22 | -704. | 5117. | 300. | 0.686 |
| 194. | 0.25 | 4.99 | 0.567 | 0.212 | 0.355 | 0.63 | 13.96 | 0.30 | 22.12 | 1.58 | -822. | 5719. | 296. | 0.686 |
| 195. | 0.25 | 5.20 | 0.563 | 0.347 | 0.216 | 0.38 | 14.18 | 2.06 | 33.67 | 2.37 | -231. | 3557. | 298. | 0.668 |
| 196. | 0.25 | 5.09 | 0.562 | 0.385 | 0.176 | 0.31 | 14.23 | 4.91 | 34.61 | 2.43 | -222. | 2549. | 299. | 0.686 |
| 197. | 0.25 | 5.11 | 0.568 | 0.416 | 0.152 | 0.27 | 14.13 | 8.47 | 29.61 | 2.09 | -212. | 1466. | 299. | 0.686 |
| 198. | 0.25 | 5.13 | 0.566 | 0.535 | 0.031 | 0.05 | 14.20 | 12.87 | 37.34 | 2.63 | -630. | 314. | 300. | 0.686 |
| 321. | 0.26 | 4.97 | 0.594 | 0.592 | 0.002 | 0.00 | 13.70 | 13.52 | 55.57 | 4.06 | -1117. | 68. | 287. | 0.686 |
| 322. | 0.26 | 4.97 | 0.594 | 0.585 | 0.009 | 0.02 | 13.70 | 13.51 | 25.71 | 1.88 | -1096. | 118. | 287. | 0.686 |

Table D.8 (cont.): Present Air-Water Flow Data: $D_3/D_1$ = 0.52, Horizontal Branch ($\Phi$ = 90°).

| RUN # | VsL1 (m/s) | VsG1 (m/s) | m1 (kg/s) | m2 (kg/s) | m3 (kg/s) | m3/m1 (-) | x1 (%) | x2 (%) | x3 (%) | x3/x1 (-) | p12 (Pa) | p13 (Pa) | T1 (K) | p1 (MPa) |
|---|---|---|---|---|---|---|---|---|---|---|---|---|---|---|
| 323. | 0.26 | 4.97 | 0.594 | 0.577 | 0.017 | 0.03 | 13.70 | 13.28 | 27.68 | 2.02 | -1117. | 213. | 287. | 0.686 |
| 324. | 0.26 | 4.97 | 0.594 | 0.568 | 0.026 | 0.04 | 13.70 | 13.01 | 28.85 | 2.11 | -1015. | 246. | 287. | 0.686 |
| 325. | 0.26 | 4.97 | 0.594 | 0.552 | 0.042 | 0.07 | 13.70 | 11.85 | 37.82 | 2.76 | -1189. | 359. | 287. | 0.686 |
| 326. | 0.26 | 4.97 | 0.594 | 0.515 | 0.079 | 0.13 | 13.70 | 10.46 | 34.93 | 2.55 | -1217. | 921. | 287. | 0.686 |
| 1175. | 0.25 | 10.17 | 0.648 | 0.630 | 0.017 | 0.03 | 24.34 | 23.72 | 46.80 | 1.92 | 280. | 348. | 303. | 0.686 |
| 1176. | 0.25 | 9.97 | 0.635 | 0.607 | 0.027 | 0.04 | 24.34 | 22.90 | 56.15 | 2.31 | 220. | 537. | 303. | 0.686 |
| 1177. | 0.25 | 9.97 | 0.635 | 0.592 | 0.043 | 0.07 | 24.34 | 21.41 | 64.76 | 2.66 | 135. | 754. | 303. | 0.686 |
| 1178. | 0.25 | 9.97 | 0.635 | 0.573 | 0.062 | 0.10 | 24.34 | 20.24 | 62.38 | 2.56 | 50. | 1153. | 303. | 0.686 |
| 1179. | 0.25 | 9.97 | 0.635 | 0.555 | 0.080 | 0.13 | 24.34 | 18.56 | 64.52 | 2.65 | 1. | 1829. | 303. | 0.686 |
| 1180. | 0.25 | 9.97 | 0.635 | 0.533 | 0.102 | 0.16 | 24.34 | 17.39 | 60.73 | 2.49 | -3. | 2591. | 303. | 0.686 |
| 1181. | 0.25 | 9.97 | 0.635 | 0.500 | 0.135 | 0.21 | 24.34 | 15.04 | 58.83 | 2.42 | -35. | 3563. | 303. | 0.686 |
| 1182. | 0.25 | 9.97 | 0.635 | 0.474 | 0.160 | 0.25 | 24.34 | 13.45 | 56.54 | 2.32 | -60. | 4535. | 303. | 0.686 |
| 1183. | 0.24 | 10.02 | 0.623 | 0.446 | 0.177 | 0.28 | 24.92 | 13.05 | 54.85 | 2.20 | -61. | 5477. | 303. | 0.686 |
| 1184. | 0.24 | 10.02 | 0.623 | 0.384 | 0.239 | 0.38 | 24.92 | 8.43 | 51.48 | 2.07 | -51. | 8538. | 303. | 0.686 |
| 1185. | 0.24 | 10.02 | 0.625 | 0.331 | 0.295 | 0.47 | 24.83 | 3.87 | 48.35 | 1.95 | -33. | 11571. | 303. | 0.686 |
| 1186. | 0.24 | 10.02 | 0.625 | 0.289 | 0.337 | 0.54 | 24.83 | 1.56 | 44.79 | 1.80 | -19. | 15138. | 303. | 0.686 |
| 1187. | 0.24 | 10.02 | 0.625 | 0.000 | 0.625 | 1.00 | 24.83 | 11.56 | 24.84 | 1.00 | -186. | 25585. | 303. | 0.686 |
| 200. | 0.25 | 20.31 | 0.805 | 0.768 | 0.037 | 0.05 | 39.23 | 38.40 | 56.55 | 1.44 | 328. | 2172. | 302. | 0.686 |
| 201. | 0.25 | 20.24 | 0.813 | 0.738 | 0.074 | 0.09 | 38.87 | 36.61 | 61.30 | 1.58 | 0. | 3424. | 301. | 0.686 |
| 202. | 0.25 | 20.69 | 0.818 | 0.710 | 0.107 | 0.13 | 39.23 | 35.91 | 61.25 | 1.56 | -635. | 5010. | 303. | 0.686 |
| 203. | 0.25 | 20.66 | 0.812 | 0.660 | 0.151 | 0.19 | 39.47 | 34.48 | 61.25 | 1.55 | -485. | 7125. | 303. | 0.686 |
| 111. | 0.25 | 20.18 | 0.810 | 0.463 | 0.348 | 0.43 | 39.38 | 24.97 | 58.58 | 1.49 | -1690. | 30074. | 297. | 0.686 |
| 110. | 0.25 | 19.94 | 0.809 | 0.263 | 0.546 | 0.68 | 39.26 | 20.17 | 48.43 | 1.23 | -55. | 26254. | 295. | 0.686 |
| 109. | 0.27 | 19.99 | 0.837 | 0.145 | 0.692 | 0.83 | 38.02 | 1.29 | 45.74 | 1.20 | -702. | 39596. | 295. | 0.686 |
| 95. | 0.26 | 38.12 | 1.112 | 0.789 | 0.322 | 0.29 | 54.96 | 55.61 | 53.37 | 0.97 | 1088. | 25937. | 291. | 0.681 |
| 96. | 0.26 | 38.01 | 1.112 | 0.702 | 0.410 | 0.37 | 54.41 | 51.42 | 59.55 | 1.09 | -404. | 23276. | 293. | 0.681 |
| 97. | 0.26 | 37.83 | 1.114 | 0.412 | 0.702 | 0.63 | 54.80 | 47.93 | 58.84 | 1.07 | -1965. | 62074. | 291. | 0.686 |
| 190. | 0.25 | 40.25 | 1.120 | 1.035 | 0.085 | 0.08 | 56.63 | 57.41 | 47.14 | 0.83 | 5040. | 8729. | 298. | 0.686 |
| 191. | 0.26 | 39.91 | 1.135 | 0.994 | 0.141 | 0.12 | 56.00 | 56.85 | 49.96 | 0.89 | 3980. | 12208. | 295. | 0.686 |
| 192. | 0.25 | 39.70 | 1.128 | 0.940 | 0.188 | 0.17 | 56.05 | 56.70 | 52.80 | 0.94 | 3116. | 15675. | 295. | 0.686 |

Table D.8 (cont.): Present Air-Water Flow Data: $D_3/D_1$ = 0.52, Horizontal Branch ($\Phi$ = 90°).

| RUN # | VsL1 (m/s) | VsG1 (m/s) | m1 (kg/s) | m2 (kg/s) | m3 (kg/s) | m3/m1 (-) | x1 (%) | x2 (%) | x3 (%) | x3/x1 (-) | p12 (Pa) | p13 (Pa) | T1 (K) | p1 (MPa) |
|---|---|---|---|---|---|---|---|---|---|---|---|---|---|---|
| 193. | 0.25 | 39.98 | 1.125 | 0.817 | 0.308 | 0.27 | 56.23 | 56.26 | 56.16 | 1.00 | 1849. | 5082. | 297. | 0.686 |
| 116. | 0.50 | 5.04 | 1.058 | 0.604 | 0.454 | 0.43 | 7.41 | 0.03 | 17.23 | 2.32 | -999. | 10507. | 302. | 0.686 |
| 114. | 0.50 | 4.98 | 1.057 | 0.391 | 0.666 | 0.63 | 7.34 | 0.09 | 11.61 | 1.58 | -1197. | 14394. | 303. | 0.690 |
| 184. | 0.51 | 4.93 | 1.078 | 0.239 | 0.839 | 0.78 | 7.12 | 1.29 | 8.77 | 1.23 | -877. | 14849. | 302. | 0.686 |
| 226. | 0.50 | 5.14 | 1.059 | 1.002 | 0.057 | 0.05 | 7.53 | 7.21 | 13.09 | 1.74 | -650. | 720. | 303. | 0.686 |
| 224. | 0.50 | 5.14 | 1.059 | 1.038 | 0.021 | 0.02 | 7.53 | 7.55 | 6.19 | 0.82 | 979. | 574. | 303. | 0.686 |
| 1083. | 0.50 | 10.01 | 1.141 | 1.102 | 0.039 | 0.03 | 13.77 | 13.25 | 28.51 | 2.07 | -582. | -209. | 299. | 0.686 |
| 1084. | 0.50 | 10.01 | 1.141 | 1.079 | 0.062 | 0.05 | 13.77 | 12.48 | 36.28 | 2.63 | -687. | 199. | 299. | 0.686 |
| 1085. | 0.50 | 10.01 | 1.141 | 1.056 | 0.085 | 0.07 | 13.77 | 11.71 | 39.26 | 2.85 | -646. | 879. | 299. | 0.686 |
| 1086. | 0.50 | 10.01 | 1.141 | 1.025 | 0.116 | 0.10 | 13.77 | 10.65 | 41.28 | 3.00 | -575. | 1497. | 299. | 0.686 |
| 1087. | 0.50 | 10.01 | 1.141 | 0.990 | 0.152 | 0.13 | 13.77 | 9.54 | 41.44 | 3.01 | -643. | 2421. | 299. | 0.686 |
| 1088. | 0.50 | 10.01 | 1.136 | 0.939 | 0.197 | 0.17 | 13.76 | 8.01 | 41.20 | 2.99 | -627. | 3947. | 301. | 0.686 |
| 1089. | 0.50 | 10.01 | 1.136 | 0.909 | 0.227 | 0.20 | 13.76 | 6.83 | 41.52 | 3.02 | -768. | 4887. | 301. | 0.686 |
| 1090. | 0.50 | 10.05 | 1.136 | 0.851 | 0.285 | 0.25 | 13.76 | 5.11 | 39.62 | 2.88 | -742. | 7815. | 302. | 0.686 |
| 1091. | 0.50 | 10.11 | 1.145 | 0.783 | 0.362 | 0.32 | 13.78 | 2.57 | 38.04 | 2.76 | -636. | 12391. | 301. | 0.686 |
| 1092. | 0.50 | 10.11 | 1.145 | 0.725 | 0.421 | 0.37 | 13.78 | 0.08 | 37.39 | 2.71 | -596. | 16706. | 301. | 0.686 |
| 104. | 0.49 | 20.12 | 1.284 | 0.325 | 0.959 | 0.75 | 24.96 | 3.16 | 34.47 | 1.38 | 3435. | 55627. | 295. | 0.686 |
| 105. | 0.49 | 19.80 | 1.284 | 0.475 | 0.808 | 0.63 | 24.56 | 9.56 | 33.38 | 1.36 | 2590. | 39856. | 295. | 0.686 |
| 106. | 0.49 | 19.80 | 1.284 | 0.681 | 0.603 | 0.47 | 24.56 | 12.41 | 38.30 | 1.56 | -2094. | 25150. | 295. | 0.686 |
| 180. | 0.51 | 20.06 | 1.309 | 1.249 | 0.061 | 0.05 | 24.24 | 24.37 | 21.52 | 0.89 | 1623. | 3030. | 297. | 0.686 |
| 181. | 0.51 | 20.12 | 1.304 | 1.158 | 0.146 | 0.11 | 24.16 | 22.89 | 34.27 | 1.42 | 681. | 3577. | 300. | 0.686 |
| 182. | 0.50 | 20.10 | 1.299 | 1.059 | 0.240 | 0.18 | 24.23 | 21.32 | 37.09 | 1.53 | 75. | 10490. | 300. | 0.686 |
| 183. | 0.51 | 20.33 | 1.317 | 0.967 | 0.351 | 0.27 | 24.00 | 18.57 | 38.97 | 1.62 | -284. | 20000. | 302. | 0.686 |
| 98. | 0.52 | 39.14 | 1.657 | 0.935 | 0.722 | 0.44 | 38.12 | 31.99 | 46.06 | 1.21 | -2434. | 61310. | 291. | 0.686 |
| 99. | 0.51 | 39.63 | 1.634 | 0.975 | 0.659 | 0.40 | 38.90 | 34.60 | 45.25 | 1.16 | -2220. | 46752. | 293. | 0.686 |
| 174. | 0.51 | 40.77 | 1.639 | 0.779 | 0.860 | 0.52 | 39.48 | 39.20 | 39.73 | 1.01 | 1346. | 31170. | 296. | 0.686 |
| 175. | 0.51 | 40.55 | 1.642 | 0.991 | 0.651 | 0.40 | 39.20 | 38.32 | 40.54 | 1.03 | 0. | 34332. | 296. | 0.686 |
| 176. | 0.51 | 40.62 | 1.645 | 1.169 | 0.476 | 0.29 | 39.05 | 38.68 | 39.96 | 1.02 | 1001. | 19668. | 297. | 0.686 |
| 177. | 0.52 | 40.34 | 1.651 | 1.389 | 0.261 | 0.16 | 38.78 | 39.95 | 32.56 | 0.84 | 3550. | 17682. | 296. | 0.686 |
| 178. | 0.53 | 40.57 | 1.684 | 1.533 | 0.151 | 0.09 | 38.37 | 39.28 | 29.10 | 0.76 | 5639. | 10951. | 295. | 0.686 |

Table D.8 (cont.): Present Air-Water Flow Data: $D_3/D_1$ = 0.52, Horizontal Branch ($\Phi$ = 90°).

| RUN # | VsL1 (m/s) | VsG1 (m/s) | m1 (kg/s) | m2 (kg/s) | m3 (kg/s) | m3/m1 (-) | x1 (%) | x2 (%) | x3 (%) | x3/x1 (-) | p12 (Pa) | p13 (Pa) | T1 (K) | p1 (MPa) |
|---|---|---|---|---|---|---|---|---|---|---|---|---|---|---|
| 179. | 0.53 | 40.13 | 1.671 | 1.594 | 0.077 | 0.05 | 38.25 | 39.24 | 17.82 | 0.47 | 7052. | 8277. | 295. | 0.686 |
| 229. | 0.51 | 39.99 | 1.610 | 1.569 | 0.042 | 0.03 | 38.50 | 39.07 | 17.19 | 0.45 | 5570. | 6660. | 303. | 0.686 |
| 228. | 0.51 | 39.99 | 1.610 | 1.582 | 0.028 | 0.02 | 38.50 | 38.94 | 13.71 | 0.36 | 6250. | 6160. | 303. | 0.686 |
| 227. | 0.51 | 39.99 | 1.610 | 1.592 | 0.019 | 0.01 | 38.50 | 38.87 | 6.93 | 0.18 | 6650. | 5950. | 303. | 0.686 |
| 350. | 1.00 | 1.00 | 1.979 | 1.836 | 0.143 | 0.07 | 0.83 | 0.83 | 0.85 | 1.03 | -513. | 957. | 287. | 0.686 |
| 351. | 1.00 | 1.00 | 1.979 | 1.706 | 0.273 | 0.14 | 0.83 | 0.75 | 1.29 | 1.56 | -727. | 2248. | 287. | 0.686 |
| 352. | 1.00 | 1.00 | 1.979 | 1.593 | 0.386 | 0.20 | 0.83 | 0.69 | 1.41 | 1.70 | -891. | 2745. | 287. | 0.686 |
| 353. | 1.00 | 1.00 | 1.979 | 1.398 | 0.580 | 0.29 | 0.83 | 0.64 | 1.29 | 1.56 | -1355. | 4147. | 287. | 0.686 |
| 354. | 1.00 | 1.00 | 1.979 | 1.205 | 0.774 | 0.39 | 0.83 | 0.33 | 1.61 | 1.94 | -1453. | 6780. | 287. | 0.686 |
| 355. | 1.00 | 1.00 | 1.979 | 0.806 | 1.173 | 0.59 | 0.83 | 0.18 | 1.28 | 1.54 | -1706. | 10120. | 287. | 0.686 |
| 356. | 1.00 | 1.00 | 1.979 | 0.060 | 1.919 | 0.97 | 0.83 | 0.87 | 0.83 | 1.00 | -1462. | 17630. | 287. | 0.686 |
| 349. | 1.00 | 1.00 | 1.979 | 1.941 | 0.038 | 0.02 | 0.83 | 0.84 | 0.39 | 0.47 | 286. | 493. | 287. | 0.686 |
| 358. | 1.00 | 2.57 | 1.994 | 1.954 | 0.040 | 0.02 | 2.09 | 2.11 | 1.04 | 0.50 | 14. | 845. | 290. | 0.686 |
| 359. | 1.00 | 2.57 | 1.994 | 1.895 | 0.099 | 0.05 | 2.09 | 2.00 | 3.65 | 1.75 | -490. | 898. | 290. | 0.686 |
| 360. | 1.00 | 2.57 | 1.994 | 1.788 | 0.206 | 0.10 | 2.09 | 1.88 | 3.87 | 1.86 | -526. | 1925. | 290. | 0.686 |
| 361. | 1.00 | 2.57 | 1.994 | 1.694 | 0.301 | 0.15 | 2.09 | 1.27 | 6.69 | 3.21 | -651. | 3030. | 290. | 0.686 |
| 362. | 1.00 | 2.57 | 1.994 | 1.489 | 0.505 | 0.25 | 2.09 | 0.80 | 5.88 | 2.82 | -855. | 5872. | 290. | 0.686 |
| 363. | 1.00 | 2.57 | 1.994 | 1.138 | 0.856 | 0.43 | 2.09 | 0.43 | 4.28 | 2.05 | -1410. | 10780. | 290. | 0.686 |
| 364. | 1.00 | 2.57 | 1.994 | 0.290 | 1.704 | 0.85 | 2.09 | 0.78 | 2.31 | 1.11 | -1510. | 23510. | 290. | 0.686 |
| 26. | 0.96 | 4.87 | 1.965 | 0.002 | 1.963 | 1.00 | 3.93 | 9.09 | 3.92 | 1.00 | -915. | 37928. | 298. | 0.690 |
| 27. | 0.93 | 4.87 | 1.898 | 0.672 | 1.226 | 0.65 | 4.07 | 0.10 | 6.24 | 1.53 | -1127. | 26303. | 298. | 0.690 |
| 31. | 1.00 | 5.16 | 2.043 | 1.476 | 0.567 | 0.28 | 3.80 | 0.61 | 12.13 | 3.19 | -909. | 13758. | 312. | 0.686 |
| 32. | 0.99 | 5.10 | 2.017 | 1.096 | 0.921 | 0.46 | 3.84 | 0.26 | 8.10 | 2.11 | -1895. | 21517. | 311. | 0.690 |
| 156. | 0.99 | 5.12 | 2.018 | 1.586 | 0.432 | 0.21 | 3.86 | 1.69 | 11.83 | 3.06 | -380. | 7817. | 309. | 0.686 |
| 157. | 0.99 | 5.08 | 2.018 | 1.785 | 0.233 | 0.12 | 3.89 | 3.20 | 9.18 | 2.36 | 238. | 3699. | 304. | 0.686 |
| 158. | 1.01 | 5.05 | 2.056 | 1.736 | 0.320 | 0.16 | 3.82 | 2.58 | 10.55 | 2.76 | 53. | 5164. | 304. | 0.690 |
| 159. | 1.04 | 5.08 | 2.118 | 1.990 | 0.128 | 0.06 | 3.70 | 3.49 | 6.97 | 1.88 | 375. | 2361. | 306. | 0.690 |
| 46. | 1.07 | 9.90 | 2.244 | 1.838 | 0.405 | 0.18 | 6.98 | 5.22 | 14.96 | 2.14 | 693. | 12702. | 299. | 0.690 |
| 47. | 1.03 | 9.77 | 2.171 | 1.661 | 0.510 | 0.23 | 7.22 | 4.01 | 17.64 | 2.44 | -38. | 17947. | 293. | 0.686 |
| 48. | 1.05 | 9.92 | 2.222 | 1.549 | 0.674 | 0.30 | 7.16 | 2.66 | 17.49 | 2.44 | -324. | 28022. | 293. | 0.686 |

Table D.8 (cont.): Present Air-Water Flow Data: $D_3/D_1$ = 0.52, Horizontal Branch ($\Phi$ = 90°).

| RUN # | VsL1 (m/s) | VsG1 (m/s) | m1 (kg/s) | m2 (kg/s) | m3 (kg/s) | m3/m1 (-) | x1 (%) | x2 (%) | x3 (%) | x3/x1 (-) | p12 (Pa) | p13 (Pa) | T1 (K) | p1 (MPa) |
|---|---|---|---|---|---|---|---|---|---|---|---|---|---|---|
| 165. | 1.00 | 10.10 | 2.120 | 1.953 | 0.167 | 0.08 | 7.31 | 7.16 | 9.10 | 1.24 | 1129. | 3912. | 306. | 0.686 |
| 166. | 1.02 | 10.15 | 2.146 | 1.824 | 0.322 | 0.15 | 7.26 | 6.09 | 13.92 | 1.92 | 672. | 8178. | 306. | 0.686 |
| 41. | 1.00 | 20.09 | 2.270 | 1.178 | 1.092 | 0.48 | 14.00 | 3.62 | 25.20 | 1.80 | -2076. | 54580. | 297. | 0.686 |
| 42. | 1.00 | 19.99 | 2.269 | 1.450 | 0.818 | 0.36 | 13.94 | 6.74 | 26.69 | 1.92 | -686. | 69332. | 297. | 0.686 |
| 44. | 0.93 | 19.73 | 2.133 | 1.859 | 0.274 | 0.13 | 14.62 | 13.09 | 25.00 | 1.71 | 1724. | 12895. | 299. | 0.690 |
| 167. | 0.99 | 20.35 | 2.258 | 2.121 | 0.137 | 0.06 | 14.16 | 14.26 | 12.63 | 0.89 | 3391. | 5806. | 299. | 0.686 |
| 168. | 0.99 | 20.07 | 2.255 | 2.016 | 0.239 | 0.11 | 13.98 | 13.31 | 19.67 | 1.41 | 2323. | 9311. | 299. | 0.686 |
| 36. | 1.02 | 39.44 | 2.618 | 2.295 | 0.323 | 0.12 | 23.99 | 24.04 | 23.58 | 0.98 | 4150. | 21464. | 295. | 0.686 |
| 37. | 1.01 | 40.22 | 2.612 | 1.655 | 0.956 | 0.37 | 24.28 | 19.93 | 31.81 | 1.31 | -1827. | 63528. | 298. | 0.686 |
| 38. | 1.05 | 40.23 | 2.681 | 1.882 | 0.799 | 0.30 | 23.48 | 21.56 | 28.01 | 1.19 | 647. | 42782. | 298. | 0.681 |
| 102. | 1.00 | 39.76 | 2.597 | 1.612 | 0.985 | 0.38 | 24.69 | 21.05 | 30.65 | 1.24 | -1566. | 67694. | 293. | 0.690 |
| 103. | 1.01 | 39.91 | 2.612 | 1.797 | 0.815 | 0.31 | 24.64 | 22.26 | 29.89 | 1.21 | -509. | 40128. | 293. | 0.690 |
| 169. | 1.02 | 39.16 | 2.605 | 2.383 | 0.223 | 0.09 | 23.62 | 24.55 | 13.61 | 0.58 | 4580. | 11247. | 299. | 0.686 |
| 170. | 1.00 | 39.10 | 2.579 | 2.276 | 0.304 | 0.12 | 23.82 | 24.65 | 17.57 | 0.74 | 4078. | 16122. | 299. | 0.686 |
| 171. | 1.00 | 39.33 | 2.583 | 2.147 | 0.436 | 0.17 | 23.92 | 24.70 | 20.11 | 0.84 | 2674. | 24861. | 299. | 0.686 |
| 172. | 1.00 | 39.10 | 2.579 | 1.593 | 0.986 | 0.38 | 23.82 | 22.09 | 26.61 | 1.12 | -1029. | 51546. | 299. | 0.686 |
| 173. | 1.00 | 39.13 | 2.580 | 1.499 | 1.081 | 0.42 | 23.83 | 22.43 | 25.78 | 1.08 | -1338. | 41288. | 299. | 0.686 |
| 342. | 1.98 | 1.00 | 3.896 | 3.717 | 0.178 | 0.05 | 0.42 | 0.42 | 0.46 | 1.10 | 363. | 2514. | 287. | 0.686 |
| 343. | 1.98 | 1.00 | 3.896 | 3.501 | 0.395 | 0.10 | 0.42 | 0.39 | 0.71 | 1.71 | 67. | 3500. | 287. | 0.686 |
| 344. | 1.98 | 1.00 | 3.896 | 3.336 | 0.560 | 0.14 | 0.42 | 0.35 | 0.85 | 2.04 | -641. | 5142. | 287. | 0.686 |
| 345. | 1.98 | 1.00 | 3.896 | 2.973 | 0.923 | 0.24 | 0.42 | 0.30 | 0.80 | 1.90 | -866. | 9056. | 287. | 0.686 |
| 346. | 1.98 | 1.00 | 3.896 | 2.642 | 1.254 | 0.32 | 0.42 | 0.15 | 0.98 | 2.33 | -1561. | 12422 | 287. | 0.686 |
| 347. | 1.98 | 1.00 | 3.896 | 2.094 | 1.801 | 0.46 | 0.42 | 0.09 | 0.80 | 1.91 | -2041. | 20714. | 287. | 0.686 |
| 287. | 1.99 | 2.52 | 3.934 | 3.845 | 0.089 | 0.02 | 1.05 | 1.06 | 0.47 | 0.45 | 998. | 2466. | 287. | 0.686 |
| 288. | 1.99 | 2.52 | 3.934 | 3.758 | 0.176 | 0.04 | 1.05 | 1.06 | 0.91 | 0.87 | 1138. | 3161. | 287. | 0.686 |
| 289. | 1.99 | 2.52 | 3.934 | 3.621 | 0.312 | 0.08 | 1.05 | 1.02 | 1.38 | 1.31 | 2383. | 4163. | 287. | 0.686 |
| 290. | 1.99 | 2.52 | 3.934 | 3.459 | 0.475 | 0.12 | 1.05 | 0.98 | 1.58 | 1.50 | -40. | 6710. | 287. | 0.686 |
| 291. | 1.99 | 2.52 | 3.934 | 3.179 | 0.755 | 0.19 | 1.05 | 0.83 | 1.99 | 1.89 | -811. | 9487. | 287. | 0.686 |
| 292. | 1.99 | 2.52 | 3.934 | 3.025 | 0.909 | 0.23 | 1.05 | 0.68 | 2.27 | 2.16 | -1088. | 12361. | 287. | 0.686 |
| 293. | 1.99 | 2.52 | 3.934 | 2.748 | 1.186 | 0.30 | 1.05 | 0.51 | 2.31 | 2.20 | -1712. | 17020. | 287. | 0.686 |

Table D.8 (cont.): Present Air-Water Flow Data: $D_3/D_1$ = 0.52, Horizontal Branch ($\Phi$ = 90°).

| RUN # | VsL1 (m/s) | VsG1 (m/s) | m1 (kg/s) | m2 (kg/s) | m3 (kg/s) | m3/m1 (-) | x1 (%) | x2 (%) | x3 (%) | x3/x1 (-) | p12 (Pa) | p13 (Pa) | T1 (K) | p1 (MPa) |
|---|---|---|---|---|---|---|---|---|---|---|---|---|---|---|
| 294. | 1.99 | 2.52 | 3.934 | 2.272 | 1.661 | 0.42 | 1.05 | 0.35 | 2.01 | 1.92 | -2708. | 26048. | 287. | 0.686 |
| 295. | 1.99 | 2.52 | 3.934 | 1.913 | 2.021 | 0.51 | 1.05 | 0.03 | 2.01 | 1.92 | -2937. | 34306. | 287. | 0.686 |
| 18. | 1.88 | 5.12 | 3.761 | 2.775 | 0.986 | 0.26 | 2.07 | 0.80 | 5.65 | 2.73 | 585. | 23537. | 309. | 0.686 |
| 19. | 1.98 | 5.26 | 3.965 | 3.652 | 0.313 | 0.08 | 2.00 | 1.83 | 4.04 | 2.02 | 915. | 7280. | 311. | 0.686 |
| 20. | 1.99 | 5.26 | 3.984 | 3.394 | 0.591 | 0.15 | 1.99 | 1.46 | 5.04 | 2.53 | 1630. | 12550. | 311. | 0.686 |
| 23. | 1.92 | 5.00 | 3.826 | 0.979 | 2.848 | 0.74 | 2.01 | 0.55 | 2.51 | 1.25 | -2850. | 44700. | 306. | 0.686 |
| 24. | 1.95 | 4.97 | 3.898 | 2.091 | 1.807 | 0.46 | 1.97 | 0.48 | 3.69 | 1.87 | -3020. | 27700. | 306. | 0.690 |
| 160. | 2.02 | 5.13 | 4.027 | 3.814 | 0.213 | 0.05 | 1.94 | 1.88 | 3.12 | 1.60 | 2280. | 4840. | 308. | 0.686 |
| 161. | 2.03 | 5.13 | 4.046 | 3.630 | 0.416 | 0.10 | 1.93 | 1.79 | 3.16 | 1.63 | 943. | 7830. | 308. | 0.686 |
| 162. | 2.04 | 4.94 | 4.074 | 3.074 | 1.000 | 0.25 | 1.86 | 0.88 | 4.87 | 2.62 | -370. | 21000. | 307. | 0.686 |
| 365. | 2.03 | 4.98 | 4.061 | 4.002 | 0.059 | 0.01 | 1.99 | 2.00 | 0.71 | 0.36 | 2774. | 3640. | 290. | 0.686 |
| 366. | 2.03 | 4.98 | 4.061 | 3.868 | 0.193 | 0.05 | 1.99 | 2.01 | 1.54 | 0.78 | 2230. | 5880. | 290. | 0.686 |
| 367. | 2.03 | 4.98 | 4.061 | 3.790 | 0.270 | 0.07 | 1.99 | 1.99 | 1.89 | 0.95 | 2140. | 5760. | 290. | 0.686 |
| 368. | 2.03 | 4.98 | 4.061 | 3.703 | 0.358 | 0.09 | 1.99 | 1.97 | 2.16 | 1.09 | 1840. | 6890. | 290. | 0.686 |
| 369. | 2.03 | 4.98 | 4.061 | 3.261 | 0.799 | 0.20 | 1.99 | 1.43 | 4.27 | 2.15 | 200. | 2500. | 290. | 0.686 |
| 370. | 2.03 | 4.98 | 4.061 | 2.847 | 1.214 | 0.30 | 1.99 | 0.88 | 4.58 | 2.30 | -1163. | 26377. | 290. | 0.686 |
| 371. | 2.03 | 4.98 | 4.061 | 2.519 | 1.542 | 0.38 | 1.99 | 0.74 | 4.03 | 2.03 | -3084. | 35999. | 290. | 0.686 |
| 49. | 1.99 | 10.02 | 4.064 | 3.731 | 0.333 | 0.08 | 3.91 | 3.79 | 5.30 | 1.35 | 3700. | 10900. | 296. | 0.686 |
| 50. | 1.98 | 10.08 | 4.039 | 3.524 | 0.515 | 0.13 | 3.96 | 3.49 | 7.16 | 1.81 | 2400. | 15800. | 296. | 0.686 |
| 51. | 2.01 | 10.23 | 4.102 | 3.033 | 1.068 | 0.26 | 3.88 | 2.06 | 9.03 | 2.33 | -120. | 22300. | 302. | 0.686 |
| 52. | 2.00 | 10.29 | 4.080 | 3.324 | 0.756 | 0.19 | 3.92 | 3.00 | 7.96 | 2.03 | 1330. | 24100. | 302. | 0.686 |
| 53. | 2.03 | 10.32 | 4.130 | 2.937 | 1.193 | 0.29 | 3.87 | 1.64 | 9.37 | 2.42 | -800. | 27300. | 303. | 0.686 |
| 54. | 2.01 | 9.94 | 4.084 | 1.903 | 2.181 | 0.53 | 3.76 | 0.07 | 6.98 | 1.86 | -4600. | 57700. | 304. | 0.686 |
| 55. | 2.03 | 10.15 | 4.131 | 2.966 | 1.165 | 0.28 | 3.80 | 1.30 | 10.17 | 2.68 | -530. | 24400. | 304. | 0.686 |
| 163. | 2.01 | 10.06 | 4.100 | 3.898 | 0.202 | 0.05 | 3.84 | 3.81 | 4.51 | 1.17 | 4847. | 7282. | 300. | 0.686 |
| 164. | 2.01 | 10.14 | 4.099 | 3.516 | 0.583 | 0.14 | 3.82 | 3.44 | 6.12 | 1.60 | 2973. | 15617. | 304. | 0.686 |
| 12. | 1.94 | 9.10 | 3.985 | 2.953 | 1.032 | 0.26 | 4.58 | 2.30 | 11.11 | 2.43 | 9700. | 24700. | 308. | 0.902 |
| 14. | 1.99 | 9.66 | 4.089 | 3.157 | 0.932 | 0.23 | 4.65 | 3.18 | 9.66 | 2.08 | 440. | 32400. | 308. | 0.886 |
| 244. | 2.01 | 20.14 | 4.253 | 4.120 | 0.133 | 0.03 | 7.59 | 7.76 | 2.41 | 0.32 | 8329. | 9245. | 293. | 0.686 |
| 245. | 2.01 | 20.14 | 4.253 | 4.052 | 0.201 | 0.05 | 7.59 | 7.83 | 2.90 | 0.38 | 7952. | 10404. | 293. | 0.686 |

Table D.8 (cont.): Present Air-Water Flow Data: $D_3/D_1$ = 0.52, Horizontal Branch ($\Phi$ = 90°).

| RUN # | VsL1 (m/s) | VsG1 (m/s) | m1 (kg/s) | m2 (kg/s) | m3 (kg/s) | m3/m1 (-) | x1 (%) | x2 (%) | x3 (%) | x3/x1 (-) | p12 (Pa) | p13 (Pa) | T1 (K) | p1 (MPa) |
|---|---|---|---|---|---|---|---|---|---|---|---|---|---|---|
| 246. | 2.01 | 20.14 | 4.253 | 4.014 | 0.239 | 0.06 | 7.59 | 7.87 | 3.01 | 0.40 | 7657. | 11159. | 293. | 0.686 |
| 247. | 2.01 | 20.14 | 4.253 | 3.850 | 0.403 | 0.09 | 7.59 | 7.95 | 4.18 | 0.55 | 7207. | 15328. | 293. | 0.686 |
| 248. | 2.01 | 20.14 | 4.253 | 3.773 | 0.480 | 0.11 | 7.59 | 7.81 | 5.84 | 0.77 | 6195. | 17497. | 293. | 0.686 |
| 382. | 1.99 | 19.82 | 4.222 | 4.141 | 0.082 | 0.02 | 7.69 | 7.81 | 1.49 | 0.19 | 8509. | 8690. | 287. | 0.686 |
| 383. | 1.99 | 19.82 | 4.222 | 4.094 | 0.128 | 0.03 | 7.69 | 7.86 | 2.19 | 0.29 | 8420. | 9436. | 287. | 0.686 |
| 384. | 1.99 | 19.82 | 4.222 | 4.043 | 0.180 | 0.04 | 7.69 | 7.91 | 2.66 | 0.35 | 8187. | 10416. | 287. | 0.686 |
| 385. | 2.00 | 19.93 | 4.243 | 4.006 | 0.237 | 0.06 | 7.69 | 7.96 | 3.16 | 0.41 | 7780. | 11670. | 287. | 0.686 |
| 386. | 2.01 | 20.09 | 4.257 | 3.933 | 0.324 | 0.08 | 7.67 | 7.95 | 4.36 | 0.57 | 6894. | 12844. | 289. | 0.686 |
| 387. | 2.01 | 20.09 | 4.257 | 3.861 | 0.395 | 0.09 | 7.67 | 7.94 | 5.09 | 0.66 | 6468. | 14822. | 289. | 0.686 |
| 388. | 2.01 | 20.09 | 4.257 | 3.773 | 0.484 | 0.11 | 7.67 | 7.91 | 5.82 | 0.76 | 5840. | 17175. | 289. | 0.686 |
| 389. | 2.01 | 20.09 | 4.257 | 3.636 | 0.621 | 0.15 | 7.67 | 7.84 | 6.72 | 0.88 | 5161. | 21640. | 289. | 0.686 |
| 390. | 2.01 | 20.09 | 4.257 | 3.543 | 0.714 | 0.17 | 7.67 | 7.50 | 8.55 | 1.11 | 4158. | 27756. | 289. | 0.686 |
| 391. | 2.01 | 20.09 | 4.257 | 3.467 | 0.789 | 0.19 | 7.67 | 7.31 | 9.28 | 1.21 | 3504. | 33135. | 289. | 0.686 |
| 392. | 2.01 | 20.09 | 4.257 | 3.356 | 0.901 | 0.21 | 7.67 | 7.09 | 9.83 | 1.28 | 2683. | 39316. | 289. | 0.686 |
| 393. | 2.01 | 20.09 | 4.257 | 3.130 | 1.126 | 0.26 | 7.67 | 5.74 | 13.05 | 1.70 | 1149. | 57396. | 289. | 0.686 |
| 394. | 2.01 | 20.09 | 4.257 | 3.012 | 1.244 | 0.29 | 7.67 | 5.25 | 13.54 | 1.76 | 273. | 74212. | 289. | 0.686 |
| 395. | 2.01 | 20.09 | 4.257 | 2.906 | 1.350 | 0.32 | 7.67 | 4.88 | 13.68 | 1.78 | 34. | 87608. | 289. | 0.686 |
| 396. | 2.01 | 20.09 | 4.257 | 2.797 | 1.459 | 0.34 | 7.67 | 4.15 | 14.42 | 1.88 | -284. | 115944. | 289. | 0.686 |
| 397. | 2.01 | 20.09 | 4.257 | 2.664 | 1.593 | 0.37 | 7.67 | 3.39 | 14.83 | 1.93 | -505. | 143688. | 289. | 0.686 |
| 274. | 2.52 | 4.98 | 5.005 | 4.909 | 0.096 | 0.02 | 1.59 | 1.61 | 0.86 | 0.54 | 4471. | 5093. | 293. | 0.686 |
| 275. | 2.52 | 4.98 | 5.005 | 4.721 | 0.284 | 0.06 | 1.59 | 1.60 | 1.57 | 0.98 | 3590. | 6912. | 293. | 0.686 |
| 276. | 2.52 | 4.98 | 5.005 | 4.595 | 0.410 | 0.08 | 1.59 | 1.57 | 1.89 | 1.19 | 3119. | 9121. | 293. | 0.686 |
| 277. | 2.52 | 4.98 | 5.005 | 4.382 | 0.623 | 0.12 | 1.59 | 1.42 | 2.83 | 1.78 | 2140. | 8105. | 293. | 0.686 |
| 278. | 2.52 | 4.98 | 5.005 | 4.058 | 0.947 | 0.19 | 1.59 | 1.11 | 3.68 | 2.31 | 1057. | 20752. | 293. | 0.686 |
| 279. | 2.52 | 4.98 | 5.005 | 3.816 | 1.189 | 0.24 | 1.59 | 0.89 | 3.84 | 2.41 | -360. | 27228. | 293. | 0.686 |
| 280. | 2.52 | 4.98 | 5.005 | 3.578 | 1.427 | 0.29 | 1.59 | 0.58 | 4.15 | 2.60 | -2062. | 34758. | 293. | 0.686 |
| 281. | 2.52 | 4.98 | 5.005 | 3.199 | 1.806 | 0.36 | 1.59 | 0.46 | 3.60 | 2.26 | -3842. | 25964. | 293. | 0.686 |
| 282. | 2.52 | 4.98 | 5.005 | 2.741 | 2.264 | 0.45 | 1.59 | 0.31 | 3.14 | 1.97 | -4466. | 34102. | 293. | 0.686 |
| 264. | 2.53 | 10.09 | 5.109 | 5.049 | 0.060 | 0.01 | 3.21 | 3.24 | 0.70 | 0.22 | 7525. | 7114. | 289. | 0.686 |
| 265. | 2.53 | 10.09 | 5.109 | 4.941 | 0.168 | 0.03 | 3.21 | 3.25 | 1.91 | 0.60 | 6749. | 8530. | 289. | 0.686 |

Table D.8 (cont.): Present Air-Water Flow Data: $D_3/D_1$ = 0.52, Horizontal Branch ($\Phi$ = 90°).

| RUN # | VsL1 (m/s) | VsG1 (m/s) | m1 (kg/s) | m2 (kg/s) | m3 (kg/s) | m3/m1 (-) | x1 (%) | x2 (%) | x3 (%) | x3/x1 (-) | p12 (Pa) | p13 (Pa) | T1 (K) | p1 (MPa) |
|---|---|---|---|---|---|---|---|---|---|---|---|---|---|---|
| 266. | 2.53 | 10.09 | 5.109 | 4.778 | 0.331 | 0.06 | 3.21 | 3.27 | 2.34 | 0.73 | 6050. | 11273. | 289. | 0.686 |
| 267. | 2.53 | 10.09 | 5.109 | 4.629 | 0.480 | 0.09 | 3.21 | 3.18 | 3.52 | 1.10 | 5068. | 13865. | 289. | 0.686 |
| 268. | 2.53 | 10.09 | 5.109 | 4.480 | 0.629 | 0.12 | 3.21 | 3.02 | 4.54 | 1.41 | 4202. | 18095. | 289. | 0.686 |
| 269. | 2.53 | 10.09 | 5.109 | 4.343 | 0.766 | 0.15 | 3.21 | 2.80 | 5.55 | 1.73 | 3010. | 22476. | 289. | 0.686 |
| 270. | 2.53 | 10.09 | 5.109 | 4.180 | 0.929 | 0.18 | 3.21 | 2.52 | 6.33 | 1.97 | 1636. | 29899. | 289. | 0.686 |
| 271. | 2.53 | 10.09 | 5.109 | 4.078 | 1.031 | 0.20 | 3.21 | 2.22 | 7.14 | 2.23 | 1097. | 35121. | 289. | 0.686 |
| 272. | 2.53 | 10.09 | 5.109 | 3.999 | 1.110 | 0.22 | 3.21 | 1.87 | 8.03 | 2.50 | 209. | 21262. | 289. | 0.686 |
| 77. | 3.99 | 4.91 | 7.894 | 7.397 | 0.497 | 0.06 | 0.99 | 0.99 | 1.02 | 1.03 | 7000. | 15600. | 300. | 0.696 |
| 78. | 4.09 | 5.12 | 8.094 | 7.148 | 0.946 | 0.12 | 0.96 | 0.88 | 1.55 | 1.61 | 4130. | 24700. | 309. | 0.686 |
| 79. | 3.99 | 5.03 | 7.881 | 6.416 | 1.465 | 0.19 | 0.98 | 0.68 | 2.29 | 2.33 | -570. | 23100. | 305. | 0.686 |
| 80. | 4.05 | 5.08 | 8.013 | 5.662 | 2.351 | 0.29 | 0.97 | 0.47 | 2.18 | 2.25 | -4100. | 39000. | 305. | 0.681 |
| 81. | 4.05 | 5.09 | 8.002 | 4.635 | 3.367 | 0.42 | 0.99 | 0.52 | 1.64 | 1.65 | -6000. | 62300. | 301. | 0.686 |
| 250. | 3.99 | 5.20 | 7.889 | 7.716 | 0.172 | 0.02 | 1.00 | 1.00 | 0.93 | 0.93 | 8310. | 10236. | 309. | 0.686 |
| 252. | 3.99 | 5.20 | 7.888 | 7.428 | 0.460 | 0.06 | 1.00 | 1.00 | 1.05 | 1.05 | 7067. | 13709. | 309. | 0.686 |
| 251. | 3.99 | 5.20 | 7.889 | 7.280 | 0.609 | 0.08 | 1.00 | 0.99 | 1.10 | 1.10 | 6575. | 0. | 309. | 0.686 |
| 119. | 4.07 | 9.64 | 8.106 | 7.593 | 0.513 | 0.06 | 1.80 | 1.73 | 2.86 | 1.59 | 9870. | 23000. | 310. | 0.686 |
| 121. | 4.07 | 9.66 | 8.106 | 6.944 | 1.163 | 0.14 | 1.80 | 1.49 | 3.65 | 2.03 | 4400. | 22700. | 311. | 0.686 |
| 120. | 4.07 | 9.64 | 8.106 | 7.219 | 0.887 | 0.11 | 1.80 | 1.63 | 3.20 | 1.78 | 6400. | 33400. | 310. | 0.686 |
| 123. | 4.07 | 9.51 | 8.108 | 6.354 | 1.754 | 0.22 | 1.82 | 1.18 | 4.14 | 2.28 | -3100. | 43000. | 303. | 0.686 |
| 124. | 4.09 | 9.54 | 8.157 | 5.949 | 2.209 | 0.27 | 1.81 | 1.06 | 3.84 | 2.12 | -5800. | 56700. | 304. | 0.686 |
| 1144. | 5.75 | 5.55 | 11.344 | 11.225 | 0.119 | 0.01 | 0.76 | 0.76 | 0.98 | 1.29 | 13042. | 12638. | 303. | 0.686 |
| 1145. | 5.75 | 5.55 | 11.344 | 11.070 | 0.274 | 0.02 | 0.76 | 0.75 | 1.23 | 1.62 | 11929. | 15371. | 303. | 0.686 |
| 1146. | 5.75 | 5.55 | 11.344 | 10.960 | 0.384 | 0.03 | 0.76 | 0.74 | 1.29 | 1.69 | 10635. | 17263. | 303. | 0.686 |
| 1147. | 5.75 | 5.55 | 11.344 | 10.831 | 0.513 | 0.05 | 0.76 | 0.73 | 1.31 | 1.73 | 9374. | 19207. | 303. | 0.686 |
| 1148. | 5.75 | 5.55 | 11.344 | 10.705 | 0.639 | 0.06 | 0.76 | 0.72 | 1.46 | 1.92 | 7463. | 22460. | 303. | 0.686 |
| 1149. | 5.75 | 5.55 | 11.344 | 10.650 | 0.694 | 0.06 | 0.76 | 0.71 | 1.58 | 2.09 | 7179. | 23014. | 303. | 0.686 |
| 1150. | 5.75 | 5.55 | 11.344 | 10.469 | 0.874 | 0.08 | 0.76 | 0.68 | 1.72 | 2.27 | 5155. | 27792. | 303. | 0.686 |
| 1151. | 5.75 | 5.55 | 11.344 | 10.290 | 1.053 | 0.09 | 0.76 | 0.65 | 1.82 | 2.40 | 3108. | 33521. | 303. | 0.686 |
| 1152. | 5.75 | 5.55 | 11.344 | 10.077 | 1.267 | 0.11 | 0.76 | 0.62 | 1.90 | 2.50 | 761. | 39048. | 303. | 0.686 |
| 1154. | 5.75 | 5.55 | 11.344 | 10.538 | 0.806 | 0.07 | 0.76 | 0.71 | 1.37 | 1.81 | 5861. | 24219. | 303. | 0.686 |

Table D.8 (cont.): Present Air-Water Flow Data: $D_3/D_1$ = 0.52, Horizontal Branch ($\Phi$ = 90°).

| RUN # | VsL1 (m/s) | VsG1 (m/s) | m1 (kg/s) | m2 (kg/s) | m3 (kg/s) | m3/m1 (-) | x1 (%) | x2 (%) | x3 (%) | x3/x1 (-) | p12 (Pa) | p13 (Pa) | T1 (K) | p1 (MPa) |
|---|---|---|---|---|---|---|---|---|---|---|---|---|---|---|
| 1168. | 6.00 | 4.98 | 11.817 | 8.260 | 3.556 | 0.30 | 0.65 | 0.47 | 1.06 | 1.64 | -10772. | 116716. | 305. | 0.686 |
| 1169. | 6.00 | 4.98 | 11.817 | 9.100 | 2.717 | 0.23 | 0.65 | 0.49 | 1.17 | 1.80 | -7629. | 82692. | 305. | 0.686 |
| 1170. | 6.00 | 4.98 | 11.817 | 9.459 | 2.358 | 0.20 | 0.65 | 0.50 | 1.23 | 1.90 | -5998. | 70404. | 305. | 0.686 |
| 1171. | 6.00 | 4.98 | 11.817 | 9.838 | 1.978 | 0.17 | 0.65 | 0.51 | 1.37 | 2.10 | -4451. | 61448. | 305. | 0.686 |
| 1172. | 5.96 | 4.91 | 11.750 | 10.519 | 1.231 | 0.10 | 0.66 | 0.56 | 1.55 | 2.34 | 376. | 39119. | 296. | 0.686 |
| 1173. | 5.96 | 4.95 | 11.750 | 10.321 | 1.430 | 0.12 | 0.66 | 0.55 | 1.45 | 2.18 | -387. | 43048. | 298. | 0.686 |
| 1062. | 0.05 | 29.79 | 0.584 | 0.533 | 0.051 | 0.09 | 82.40 | 85.36 | 51.34 | 0.62 | -1293. | 600. | 291. | 0.686 |
| 1063. | 0.05 | 29.49 | 0.578 | 0.497 | 0.081 | 0.14 | 83.19 | 87.07 | 59.46 | 0.71 | -1581. | 1417. | 288. | 0.686 |
| 1064. | 0.05 | 29.69 | 0.578 | 0.463 | 0.115 | 0.20 | 83.19 | 88.68 | 61.09 | 0.73 | -1916. | 2634. | 290. | 0.686 |
| 1065. | 0.05 | 29.69 | 0.578 | 0.426 | 0.152 | 0.26 | 83.19 | 90.44 | 62.83 | 0.76 | -2349. | 4620. | 290. | 0.686 |
| 1066. | 0.05 | 29.74 | 0.577 | 0.402 | 0.175 | 0.30 | 83.16 | 91.56 | 63.85 | 0.77 | -2406. | 6164. | 291. | 0.686 |
| 1067. | 0.05 | 30.10 | 0.576 | 0.372 | 0.204 | 0.35 | 83.14 | 92.97 | 65.23 | 0.78 | -2749. | 8970. | 295. | 0.686 |
| 1068. | 0.05 | 30.10 | 0.576 | 0.319 | 0.258 | 0.45 | 83.14 | 94.68 | 68.89 | 0.83 | -3177. | 14786. | 295. | 0.686 |
| 1069. | 0.05 | 29.83 | 0.584 | 0.276 | 0.309 | 0.53 | 82.42 | 95.32 | 70.90 | 0.86 | -3471. | 20966. | 291. | 0.686 |
| 1070. | 0.05 | 30.14 | 0.578 | 0.193 | 0.384 | 0.67 | 83.37 | 99.86 | 75.06 | 0.90 | -3576. | 33928. | 294. | 0.686 |
| 1071. | 0.05 | 29.85 | 0.571 | 0.096 | 0.476 | 0.83 | 83.18 | 100.44 | 79.71 | 0.96 | -3753. | 59631. | 295. | 0.686 |
| 1072. | 0.05 | 29.99 | 0.570 | 0.038 | 0.532 | 0.93 | 83.16 | 98.68 | 82.05 | 0.99 | -3380. | 74394. | 297. | 0.686 |
| 1118. | 1.00 | 5.03 | 2.004 | 1.849 | 0.156 | 0.08 | 2.20 | 1.53 | 10.13 | 4.61 | -291. | 1666. | 307. | 0.392 |
| 1119. | 1.00 | 4.94 | 2.004 | 1.804 | 0.200 | 0.10 | 2.21 | 1.28 | 10.59 | 4.80 | -352. | 2012. | 300. | 0.392 |
| 1120. | 1.00 | 4.99 | 2.004 | 1.784 | 0.220 | 0.11 | 2.21 | 1.08 | 11.35 | 5.15 | -452. | 2228. | 303. | 0.392 |
| 1121. | 1.00 | 4.99 | 2.004 | 1.763 | 0.241 | 0.12 | 2.21 | 0.86 | 12.10 | 5.48 | -667. | 2598. | 303. | 0.392 |
| 1122. | 1.00 | 4.99 | 2.004 | 1.721 | 0.283 | 0.14 | 2.21 | 0.69 | 11.42 | 5.18 | -375. | 3448. | 303. | 0.392 |
| 1123. | 1.00 | 5.09 | 2.004 | 1.663 | 0.341 | 0.17 | 2.21 | 0.51 | 10.47 | 4.75 | -798. | 4693. | 309. | 0.392 |
| 1124. | 1.00 | 5.09 | 2.004 | 1.600 | 0.403 | 0.20 | 2.21 | 0.25 | 9.95 | 4.51 | -872. | 5573. | 309. | 0.392 |
| 1126. | 1.00 | 4.99 | 2.058 | 1.989 | 0.070 | 0.03 | 4.76 | 4.47 | 13.08 | 2.75 | -575. | -103. | 308. | 0.882 |
| 1127. | 1.00 | 5.05 | 2.058 | 1.942 | 0.115 | 0.06 | 4.77 | 4.02 | 17.35 | 3.64 | -487. | 107. | 311. | 0.882 |
| 1128. | 1.00 | 5.05 | 2.058 | 1.887 | 0.171 | 0.08 | 4.77 | 3.58 | 17.88 | 3.75 | -689. | 268. | 311. | 0.882 |
| 1129. | 1.00 | 5.05 | 2.058 | 1.825 | 0.232 | 0.11 | 4.77 | 3.13 | 17.67 | 3.71 | -664. | 2438. | 311. | 0.882 |
| 1130. | 1.00 | 5.05 | 2.058 | 1.758 | 0.299 | 0.15 | 4.77 | 2.59 | 17.59 | 3.69 | -823. | 3834. | 311. | 0.882 |
| 1131. | 1.00 | 5.05 | 2.056 | 1.697 | 0.360 | 0.17 | 4.71 | 2.09 | 17.06 | 3.62 | -996. | 4750. | 315. | 0.882 |

Table D.8 (cont.): Present Air-Water Flow Data: $D_3/D_1$ = 0.52, Horizontal Branch ($\Phi$ = 90°).

| RUN # | VsL1 (m/s) | VsG1 (m/s) | m1 (kg/s) | m2 (kg/s) | m3 (kg/s) | m3/m1 (-) | x1 (%) | x2 (%) | x3 (%) | x3/x1 (-) | p13 (Pa) | T1 (K) | p1 (MPa) |
|---|---|---|---|---|---|---|---|---|---|---|---|---|---|
| 405. | 0.10 | 20.06 | 0.524 | 0.518 | 0.006 | 0.01 | 62.02 | 61.59 | 100.00 | 1.61 | 793. | 290. | 0.686 |
| 406. | 0.10 | 20.01 | 0.524 | 0.501 | 0.024 | 0.04 | 61.63 | 60.47 | 86.30 | 1.40 | 1458. | 291. | 0.686 |
| 407. | 0.10 | 20.05 | 0.520 | 0.460 | 0.060 | 0.12 | 61.76 | 58.37 | 87.52 | 1.42 | 2889. | 293. | 0.686 |
| 408. | 0.10 | 19.95 | 0.519 | 0.412 | 0.107 | 0.21 | 61.65 | 54.65 | 88.55 | 1.44 | 6000. | 293. | 0.686 |
| 409. | 0.10 | 19.95 | 0.525 | 0.359 | 0.167 | 0.32 | 60.89 | 48.71 | 87.04 | 1.43 | 11344. | 293. | 0.686 |
| 410. | 0.10 | 19.95 | 0.525 | 0.274 | 0.251 | 0.48 | 60.89 | 37.80 | 86.08 | 1.41 | 24285. | 293. | 0.686 |
| 411. | 0.10 | 19.95 | 0.525 | 0.121 | 0.405 | 0.77 | 60.89 | 3.58 | 77.96 | 1.28 | 47476. | 293. | 0.686 |
| 412. | 0.10 | 39.52 | 0.831 | 0.426 | 0.406 | 0.49 | 75.95 | 69.65 | 82.55 | 1.09 | 56060. | 294. | 0.686 |
| 413. | 0.10 | 39.52 | 0.831 | 0.514 | 0.316 | 0.38 | 76.04 | 70.85 | 84.47 | 1.11 | 33755. | 294. | 0.686 |
| 414. | 0.10 | 39.52 | 0.831 | 0.671 | 0.160 | 0.19 | 75.95 | 73.75 | 85.15 | 1.12 | 18378. | 294. | 0.686 |
| 531. | 0.50 | 5.08 | 1.059 | 1.040 | 0.019 | 0.02 | 7.56 | 6.07 | 87.43 | 11.56 | 161. | 298. | 0.686 |
| 532. | 0.50 | 5.08 | 1.059 | 1.018 | 0.042 | 0.04 | 7.56 | 4.15 | 90.63 | 11.99 | 810. | 298. | 0.686 |
| 533. | 0.50 | 5.15 | 1.059 | 0.995 | 0.064 | 0.06 | 7.54 | 2.20 | 90.28 | 11.97 | 1466. | 303. | 0.686 |
| 534. | 0.50 | 5.15 | 1.059 | 0.967 | 0.092 | 0.09 | 7.54 | 0.35 | 83.27 | 11.04 | 2564. | 303. | 0.686 |
| 535. | 0.50 | 5.15 | 1.059 | 0.728 | 0.331 | 0.31 | 7.54 | 0.01 | 24.14 | 3.20 | 5914. | 303. | 0.686 |
| 536. | 0.50 | 5.15 | 1.059 | 0.451 | 0.608 | 0.57 | 7.54 | 0.11 | 13.06 | 1.73 | 10151. | 303. | 0.686 |
| 537. | 0.50 | 5.15 | 1.059 | 0.005 | 1.054 | 0.99 | 7.54 | 12.68 | 7.52 | 1.00 | 18405. | 303. | 0.686 |
| 560. | 0.50 | 40.07 | 1.626 | 1.626 | 0.001 | 0.00 | 39.77 | 39.75 | 100.00 | 2.51 | 5855. | 291. | 0.686 |
| 561. | 0.50 | 39.59 | 1.623 | 1.621 | 0.002 | 0.00 | 39.65 | 39.58 | 100.00 | 2.52 | 6562. | 289. | 0.686 |
| 562. | 0.50 | 39.59 | 1.623 | 1.616 | 0.007 | 0.00 | 39.65 | 39.61 | 49.51 | 1.25 | 6857. | 289. | 0.686 |
| 563. | 0.50 | 39.59 | 1.623 | 1.572 | 0.051 | 0.03 | 39.65 | 39.51 | 44.06 | 1.11 | 8346. | 289. | 0.686 |
| 564. | 0.50 | 39.59 | 1.623 | 1.528 | 0.095 | 0.06 | 39.65 | 38.75 | 54.05 | 1.36 | 10660. | 289. | 0.686 |
| 565. | 0.50 | 39.79 | 1.622 | 1.488 | 0.134 | 0.08 | 39.61 | 38.18 | 55.50 | 1.40 | 13389. | 291. | 0.686 |
| 566. | 0.50 | 39.79 | 1.622 | 1.452 | 0.170 | 0.10 | 39.61 | 37.80 | 55.05 | 1.39 | 15707. | 291. | 0.686 |
| 549. | 1.01 | 1.01 | 1.994 | 1.993 | 0.001 | 0.00 | 0.82 | 0.79 | 98.66 | 119.96 | 700. | 290. | 0.686 |
| 550. | 1.01 | 1.01 | 1.994 | 1.992 | 0.002 | 0.00 | 0.82 | 0.75 | 55.34 | 67.29 | 1031. | 290. | 0.686 |
| 551. | 1.01 | 1.01 | 1.994 | 1.909 | 0.085 | 0.04 | 0.82 | 0.70 | 3.49 | 4.25 | 1039. | 290. | 0.686 |
| 552. | 1.01 | 1.01 | 1.994 | 1.787 | 0.207 | 0.10 | 0.82 | 0.65 | 2.35 | 2.86 | 1626. | 290. | 0.686 |
| 553. | 1.03 | 1.00 | 2.031 | 1.742 | 0.289 | 0.14 | 0.80 | 0.52 | 2.50 | 3.12 | 2398. | 287. | 0.686 |
| 554. | 1.03 | 1.02 | 2.031 | 1.639 | 0.392 | 0.19 | 0.80 | 0.29 | 2.96 | 3.69 | 2509. | 293. | 0.686 |

Table D.9: Present Air-Water Flow Data: $D_3/D_1$ = 0.52, Upward Branch ($\Phi$ = 0°).

| RUN # | VsL1 (m/s) | VsG1 (m/s) | m1 (kg/s) | m2 (kg/s) | m3 (kg/s) | m3/m1 (-) | x1 (%) | x2 (%) | x3 (%) | x3/x1 (-) | p13 (Pa) | T1 (K) | p1 (MPa) |
|---|---|---|---|---|---|---|---|---|---|---|---|---|---|
| 555. | 1.03 | 1.02 | 2.031 | 1.443 | 0.589 | 0.29 | 0.80 | 0.19 | 2.31 | 2.88 | 4771. | 293. | 0.686 |
| 556. | 1.03 | 1.02 | 2.031 | 1.138 | 0.893 | 0.44 | 0.80 | 0.12 | 1.67 | 2.08 | 7103. | 293. | 0.686 |
| 557. | 1.03 | 1.00 | 2.031 | 0.535 | 1.496 | 0.74 | 0.79 | 0.09 | 1.04 | 1.32 | 14400. | 293. | 0.686 |
| 558. | 1.03 | 1.00 | 2.031 | 0.000 | 2.031 | 1.00 | 0.79 | 9.04 | 0.79 | 1.00 | 25914. | 293. | 0.686 |
| 519. | 1.00 | 2.51 | 2.007 | 2.007 | 0.001 | 0.00 | 2.05 | 2.02 | 98.40 | 47.94 | 268. | 286. | 0.686 |
| 520. | 1.00 | 2.51 | 2.007 | 2.005 | 0.003 | 0.00 | 2.05 | 1.93 | 99.60 | 48.52 | 241. | 286. | 0.686 |
| 521. | 1.00 | 2.55 | 2.000 | 1.968 | 0.032 | 0.02 | 2.05 | 1.68 | 25.27 | 12.33 | 36. | 292. | 0.686 |
| 522. | 1.00 | 2.60 | 2.000 | 1.913 | 0.087 | 0.04 | 2.05 | 1.10 | 23.02 | 11.23 | 82. | 298. | 0.686 |
| 523. | 0.99 | 2.60 | 1.984 | 1.829 | 0.155 | 0.08 | 2.07 | 0.58 | 19.53 | 9.45 | 1777. | 298. | 0.686 |
| 524. | 1.00 | 2.50 | 1.999 | 1.412 | 0.587 | 0.29 | 2.02 | 0.05 | 6.75 | 3.35 | 5752. | 291. | 0.686 |
| 525. | 1.00 | 2.50 | 1.999 | 0.183 | 1.816 | 0.91 | 2.02 | 0.01 | 2.22 | 1.10 | 25149. | 291. | 0.686 |
| 509. | 1.00 | 4.92 | 2.039 | 2.038 | 0.001 | 0.00 | 3.92 | 3.89 | 98.58 | 25.15 | 782. | 289. | 0.686 |
| 510. | 1.00 | 4.92 | 2.039 | 2.036 | 0.003 | 0.00 | 3.92 | 3.80 | 99.61 | 25.42 | 820. | 289. | 0.686 |
| 511. | 1.00 | 4.92 | 2.039 | 2.021 | 0.018 | 0.01 | 3.92 | 3.67 | 31.38 | 8.01 | 972. | 289. | 0.686 |
| 512. | 1.00 | 5.13 | 2.038 | 1.996 | 0.042 | 0.02 | 3.91 | 3.11 | 41.22 | 10.56 | 1450. | 303. | 0.686 |
| 513. | 1.00 | 5.13 | 2.038 | 1.977 | 0.061 | 0.03 | 3.91 | 2.42 | 51.77 | 13.26 | 1884. | 303. | 0.686 |
| 514. | 1.00 | 5.13 | 2.038 | 1.934 | 0.105 | 0.05 | 3.91 | 1.32 | 51.76 | 13.26 | 2541. | 303. | 0.686 |
| 515. | 1.00 | 4.99 | 2.044 | 1.678 | 0.365 | 0.18 | 4.04 | 0.49 | 20.33 | 5.04 | 6980. | 284. | 0.686 |
| 516. | 1.00 | 4.99 | 2.044 | 1.385 | 0.658 | 0.32 | 4.04 | 0.25 | 12.01 | 2.98 | 11753. | 284. | 0.686 |
| 517. | 1.00 | 4.99 | 2.044 | 0.664 | 1.380 | 0.68 | 4.04 | 0.30 | 5.83 | 1.44 | 27055. | 284. | 0.686 |
| 416. | 0.99 | 10.07 | 2.100 | 2.091 | 0.010 | 0.00 | 7.63 | 7.51 | 33.11 | 4.34 | 2085. | 295. | 0.686 |
| 417. | 0.99 | 10.17 | 2.102 | 2.071 | 0.031 | 0.01 | 7.71 | 7.48 | 23.19 | 3.01 | 2371. | 295. | 0.686 |
| 418. | 0.99 | 10.17 | 2.102 | 2.035 | 0.067 | 0.03 | 7.71 | 6.75 | 36.71 | 4.76 | 3141. | 295. | 0.686 |
| 419. | 0.99 | 10.17 | 2.102 | 2.005 | 0.097 | 0.05 | 7.71 | 5.85 | 46.02 | 5.97 | 3841. | 295. | 0.686 |
| 420. | 1.00 | 10.00 | 2.114 | 1.957 | 0.157 | 0.07 | 7.66 | 4.16 | 51.34 | 6.70 | 6619. | 290. | 0.686 |
| 421. | 1.00 | 9.96 | 2.113 | 1.931 | 0.182 | 0.09 | 7.61 | 3.41 | 52.21 | 6.86 | 8094. | 291. | 0.686 |
| 422. | 1.00 | 9.96 | 2.113 | 1.889 | 0.224 | 0.11 | 7.61 | 1.76 | 56.88 | 7.48 | 10712. | 291. | 0.686 |
| 423. | 1.00 | 9.96 | 2.113 | 1.729 | 0.384 | 0.18 | 7.61 | 0.68 | 38.79 | 5.10 | 20154. | 291. | 0.686 |
| 424. | 1.00 | 10.04 | 2.113 | 1.221 | 0.892 | 0.42 | 7.60 | 0.00 | 17.98 | 2.37 | 39080. | 294. | 0.686 |
| 446. | 1.03 | 20.01 | 2.332 | 1.823 | 0.510 | 0.22 | 13.62 | 2.07 | 54.93 | 4.03 | 51444. | 296. | 0.686 |

Table D.9 (cont.): Present Air-Water Flow Data: $D_3/D_1$ = 0.52, Upward Branch ($\Phi$ = 0°).

| RUN # | VsL1 (m/s) | VsG1 (m/s) | m1 (kg/s) | m2 (kg/s) | m3 (kg/s) | m3/m1 (-) | x1 (%) | x2 (%) | x3 (%) | x3/x1 (-) | p13 (Pa) | T1 (K) | p1 (MPa) |
|---|---|---|---|---|---|---|---|---|---|---|---|---|---|
| 447. | 1.03 | 20.01 | 2.332 | 1.984 | 0.348 | 0.15 | 13.62 | 5.63 | 59.12 | 4.34 | 32686. | 296. | 0.686 |
| 448. | 1.03 | 20.01 | 2.332 | 2.062 | 0.271 | 0.12 | 13.62 | 7.43 | 60.76 | 4.46 | 20674. | 296. | 0.686 |
| 449. | 1.03 | 19.95 | 2.337 | 2.337 | 0.000 | 0.00 | 13.78 | 13.77 | 96.25 | 6.98 | 3652. | 291. | 0.686 |
| 450. | 1.05 | 19.95 | 2.373 | 2.373 | 0.001 | 0.00 | 13.57 | 13.55 | 98.58 | 7.26 | 3724. | 291. | 0.686 |
| 451. | 1.05 | 19.95 | 2.373 | 2.371 | 0.003 | 0.00 | 13.57 | 13.47 | 99.65 | 7.34 | 3912. | 291. | 0.686 |
| 452. | 1.05 | 19.95 | 2.373 | 2.362 | 0.011 | 0.00 | 13.57 | 13.61 | 5.22 | 0.38 | 4090. | 291. | 0.686 |
| 453. | 1.05 | 19.95 | 2.373 | 2.350 | 0.023 | 0.01 | 13.57 | 13.40 | 31.28 | 2.31 | 4157. | 291. | 0.686 |
| 454. | 1.02 | 19.95 | 2.312 | 2.264 | 0.048 | 0.02 | 13.93 | 13.22 | 46.99 | 3.37 | 4636. | 291. | 0.686 |
| 455. | 1.02 | 19.95 | 2.312 | 2.225 | 0.087 | 0.04 | 13.93 | 12.32 | 55.00 | 3.95 | 6364. | 291. | 0.686 |
| 456. | 1.02 | 19.95 | 2.312 | 2.201 | 0.111 | 0.05 | 13.93 | 11.82 | 55.87 | 4.01 | 7577. | 291. | 0.686 |
| 457. | 1.02 | 19.95 | 2.312 | 2.165 | 0.147 | 0.06 | 13.93 | 10.89 | 58.75 | 4.22 | 9894. | 291. | 0.686 |
| 459. | 1.03 | 39.84 | 2.653 | 2.653 | 0.001 | 0.00 | 24.07 | 24.06 | 98.09 | 4.08 | 7091. | 293. | 0.686 |
| 460. | 1.03 | 39.84 | 2.653 | 2.635 | 0.018 | 0.01 | 24.07 | 24.18 | 8.82 | 0.37 | 7329. | 293. | 0.686 |
| 461. | 1.03 | 38.94 | 2.650 | 2.585 | 0.065 | 0.02 | 23.97 | 24.28 | 11.58 | 0.48 | 7996. | 288. | 0.686 |
| 462. | 1.03 | 38.94 | 2.650 | 2.547 | 0.103 | 0.04 | 23.97 | 24.13 | 20.11 | 0.84 | 9074. | 288. | 0.686 |
| 463. | 1.03 | 38.94 | 2.650 | 2.507 | 0.143 | 0.05 | 23.97 | 23.92 | 24.88 | 1.04 | 10549. | 288. | 0.686 |
| 464. | 1.03 | 38.94 | 2.650 | 2.471 | 0.179 | 0.07 | 23.97 | 23.64 | 28.50 | 1.19 | 12614. | 288. | 0.686 |
| 465. | 1.03 | 39.01 | 2.649 | 2.459 | 0.190 | 0.07 | 23.94 | 23.37 | 31.33 | 1.31 | 13619. | 289. | 0.686 |
| 466. | 1.03 | 39.01 | 2.649 | 2.417 | 0.232 | 0.09 | 23.94 | 22.63 | 37.60 | 1.57 | 18631. | 289. | 0.686 |
| 467. | 1.03 | 39.28 | 2.649 | 2.271 | 0.378 | 0.14 | 23.94 | 21.60 | 37.97 | 1.59 | 27628. | 291. | 0.686 |
| 468. | 1.03 | 39.28 | 2.649 | 2.071 | 0.578 | 0.22 | 23.94 | 19.98 | 38.09 | 1.59 | 59496. | 291. | 0.686 |
| 539. | 2.00 | 1.02 | 3.934 | 3.933 | 0.001 | 0.00 | 0.42 | 0.40 | 43.77 | 105.00 | 1649. | 292. | 0.686 |
| 540. | 2.00 | 1.02 | 3.934 | 3.889 | 0.045 | 0.01 | 0.42 | 0.39 | 2.71 | 6.49 | 1781. | 292. | 0.686 |
| 541. | 2.00 | 1.02 | 3.934 | 3.819 | 0.115 | 0.03 | 0.42 | 0.36 | 2.45 | 5.87 | 2063. | 292. | 0.686 |
| 542. | 2.00 | 1.02 | 3.934 | 3.644 | 0.290 | 0.07 | 0.42 | 0.33 | 1.47 | 3.54 | 3761. | 292. | 0.686 |
| 543. | 2.00 | 1.02 | 3.934 | 3.440 | 0.494 | 0.13 | 0.42 | 0.28 | 1.37 | 3.29 | 5959. | 292. | 0.686 |
| 544. | 2.00 | 1.02 | 3.934 | 2.061 | 1.873 | 0.48 | 0.42 | 0.11 | 0.76 | 1.81 | 33541. | 292. | 0.686 |
| 545. | 2.00 | 1.02 | 3.934 | 3.410 | 0.524 | 0.13 | 0.42 | 0.23 | 1.63 | 3.90 | 5519. | 292. | 0.686 |
| 546. | 2.00 | 1.02 | 3.934 | 2.948 | 0.986 | 0.25 | 0.42 | 0.17 | 1.16 | 2.78 | 10035. | 292. | 0.686 |
| 547. | 2.00 | 1.02 | 3.934 | 2.602 | 1.332 | 0.34 | 0.42 | 0.13 | 0.98 | 2.35 | 15397. | 292. | 0.686 |

Table D.9 (cont.): Present Air-Water Flow Data: $D_3/D_1$ = 0.52, Upward Branch ($\Phi$ = 0°).

| RUN # | VsL1 (m/s) | VsG1 (m/s) | m1 (kg/s) | m2 (kg/s) | m3 (kg/s) | m3/m1 (-) | x1 (%) | x2 (%) | x3 (%) | x3/x1 (-) | p13 (Pa) | T1 (K) | p1 (MPa) |
|---|---|---|---|---|---|---|---|---|---|---|---|---|---|
| 500. | 2.01 | 2.50 | 3.970 | 3.969 | 0.001 | 0.00 | 1.01 | 0.99 | 100.00 | 99.25 | 1838. | 294. | 0.686 |
| 501. | 2.01 | 2.49 | 3.970 | 3.958 | 0.012 | 0.00 | 1.01 | 0.97 | 13.28 | 13.11 | 1960. | 291. | 0.686 |
| 502. | 2.01 | 2.49 | 3.970 | 3.909 | 0.062 | 0.02 | 1.01 | 0.91 | 7.26 | 7.17 | 2297. | 291. | 0.686 |
| 503. | 2.01 | 2.49 | 3.970 | 3.848 | 0.122 | 0.03 | 1.01 | 0.84 | 6.54 | 6.46 | 2965. | 291. | 0.686 |
| 504. | 2.01 | 2.49 | 3.970 | 3.734 | 0.236 | 0.06 | 1.01 | 0.69 | 6.03 | 5.96 | 3998. | 291. | 0.686 |
| 505. | 2.01 | 2.49 | 3.970 | 3.618 | 0.352 | 0.09 | 1.01 | 0.39 | 7.44 | 7.35 | 5162. | 291. | 0.686 |
| 506. | 1.99 | 2.53 | 3.944 | 2.978 | 0.966 | 0.24 | 1.00 | 0.09 | 3.83 | 3.82 | 13008. | 301. | 0.686 |
| 507. | 1.99 | 2.53 | 3.944 | 1.801 | 2.143 | 0.54 | 1.00 | 0.04 | 1.87 | 1.87 | 36659. | 301. | 0.686 |
| 489. | 2.01 | 5.04 | 4.012 | 4.011 | 0.001 | 0.00 | 2.04 | 2.02 | 100.00 | 48.99 | 2970. | 289. | 0.686 |
| 490. | 2.01 | 5.02 | 4.012 | 3.970 | 0.042 | 0.01 | 2.03 | 1.97 | 7.72 | 3.80 | 3361. | 289. | 0.686 |
| 491. | 2.01 | 4.96 | 4.011 | 3.923 | 0.088 | 0.02 | 2.01 | 1.87 | 8.32 | 4.14 | 3800. | 289. | 0.686 |
| 492. | 2.01 | 5.04 | 4.012 | 3.895 | 0.117 | 0.03 | 2.04 | 1.73 | 12.40 | 6.07 | 4405. | 289. | 0.686 |
| 493. | 2.01 | 5.04 | 4.012 | 3.801 | 0.211 | 0.05 | 2.04 | 1.27 | 15.96 | 7.82 | 5791. | 289. | 0.686 |
| 494. | 2.00 | 5.03 | 4.001 | 3.764 | 0.237 | 0.06 | 2.02 | 0.91 | 19.68 | 9.72 | 6698. | 292. | 0.686 |
| 495. | 2.00 | 5.03 | 4.001 | 3.682 | 0.319 | 0.08 | 2.02 | 0.76 | 16.61 | 8.20 | 8155. | 292. | 0.686 |
| 496. | 2.00 | 5.05 | 4.001 | 3.516 | 0.485 | 0.12 | 2.02 | 0.47 | 13.31 | 6.58 | 11782. | 293. | 0.686 |
| 497. | 2.00 | 5.05 | 4.001 | 3.217 | 0.784 | 0.20 | 2.02 | 0.34 | 8.94 | 4.41 | 17123. | 293. | 0.686 |
| 498. | 2.00 | 5.05 | 4.001 | 2.459 | 1.542 | 0.39 | 2.02 | 0.20 | 4.93 | 2.44 | 36717. | 293. | 0.686 |
| 426. | 2.01 | 10.01 | 4.096 | 3.069 | 1.027 | 0.25 | 3.91 | 0.30 | 14.68 | 3.76 | 48736. | 294. | 0.686 |
| 427. | 2.01 | 10.01 | 4.096 | 4.089 | 0.008 | 0.00 | 3.91 | 3.90 | 8.87 | 2.27 | 5222. | 294. | 0.686 |
| 428. | 2.01 | 9.92 | 4.089 | 4.012 | 0.077 | 0.02 | 3.89 | 3.88 | 4.31 | 1.11 | 5665. | 293. | 0.686 |
| 429. | 2.01 | 9.99 | 4.102 | 3.984 | 0.118 | 0.03 | 3.88 | 3.81 | 6.08 | 1.57 | 6455. | 295. | 0.686 |
| 430. | 2.01 | 9.99 | 4.102 | 3.912 | 0.190 | 0.05 | 3.88 | 3.47 | 12.24 | 3.16 | 7503. | 295. | 0.686 |
| 431. | 2.01 | 9.99 | 4.102 | 3.845 | 0.257 | 0.06 | 3.88 | 3.05 | 16.34 | 4.21 | 9838. | 295. | 0.686 |
| 432. | 2.01 | 9.99 | 4.102 | 3.781 | 0.321 | 0.08 | 3.88 | 2.77 | 16.94 | 4.37 | 11962. | 295. | 0.686 |
| 433. | 2.01 | 9.92 | 4.103 | 3.717 | 0.386 | 0.09 | 3.90 | 2.30 | 19.38 | 4.96 | 15248. | 291. | 0.686 |
| 434. | 2.01 | 9.92 | 4.103 | 3.660 | 0.443 | 0.11 | 3.90 | 1.85 | 20.87 | 5.35 | 18267. | 291. | 0.686 |
| 436. | 2.00 | 20.13 | 4.239 | 4.227 | 0.012 | 0.00 | 7.59 | 7.59 | 6.71 | 0.88 | 7356. | 294. | 0.686 |
| 437. | 2.01 | 19.77 | 4.250 | 4.176 | 0.074 | 0.02 | 7.54 | 7.61 | 3.49 | 0.46 | 8703. | 290. | 0.686 |
| 438. | 2.01 | 19.77 | 4.250 | 4.110 | 0.140 | 0.03 | 7.54 | 7.62 | 4.95 | 0.66 | 9530. | 290. | 0.686 |

Table D.9 (cont.): Present Air-Water Flow Data: $D_3/D_1$ = 0.52, Upward Branch ($\Phi$ = 0°).

| RUN # | VsL1 (m/s) | VsG1 (m/s) | m1 (kg/s) | m2 (kg/s) | m3 (kg/s) | m3/m1 (-) | x1 (%) | x2 (%) | x3 (%) | x3/x1 (-) | p13 (Pa) | T1 (K) | p1 (MPa) |
|---|---|---|---|---|---|---|---|---|---|---|---|---|---|
| 439. | 2.01 | 19.42 | 4.265 | 3.999 | 0.266 | 0.06 | 7.56 | 7.35 | 10.62 | 1.41 | 11496. | 283. | 0.686 |
| 440. | 2.01 | 19.55 | 4.265 | 3.899 | 0.366 | 0.09 | 7.56 | 6.94 | 14.16 | 1.87 | 16845. | 285. | 0.686 |
| 441. | 2.01 | 19.55 | 4.265 | 3.838 | 0.427 | 0.10 | 7.56 | 6.49 | 17.13 | 2.27 | 20035. | 285. | 0.686 |
| 442. | 2.01 | 19.55 | 4.265 | 3.772 | 0.493 | 0.12 | 7.56 | 6.10 | 18.70 | 2.47 | 25221. | 285. | 0.686 |
| 443. | 2.01 | 19.90 | 4.266 | 3.644 | 0.622 | 0.15 | 7.58 | 5.23 | 21.33 | 2.81 | 33688. | 289. | 0.686 |
| 444. | 2.01 | 20.40 | 4.266 | 3.443 | 0.823 | 0.19 | 7.59 | 3.41 | 25.08 | 3.30 | 57044. | 296. | 0.686 |
| 481. | 4.02 | 4.96 | 7.941 | 7.912 | 0.029 | 0.00 | 1.02 | 1.01 | 1.17 | 1.16 | 8974. | 289. | 0.686 |
| 482. | 4.02 | 4.96 | 7.941 | 7.748 | 0.193 | 0.02 | 1.02 | 1.01 | 1.38 | 1.36 | 10619. | 289. | 0.686 |
| 483. | 4.02 | 4.96 | 7.941 | 7.512 | 0.428 | 0.05 | 1.02 | 0.98 | 1.56 | 1.54 | 14326. | 289. | 0.686 |
| 484. | 4.07 | 5.13 | 8.041 | 7.461 | 0.579 | 0.07 | 1.00 | 0.88 | 2.56 | 2.55 | 16312. | 299. | 0.686 |
| 485. | 4.07 | 5.13 | 8.041 | 7.205 | 0.836 | 0.10 | 1.00 | 0.81 | 2.64 | 2.63 | 21314. | 299. | 0.686 |
| 486. | 4.07 | 5.13 | 8.041 | 6.965 | 1.076 | 0.13 | 1.00 | 0.74 | 2.71 | 2.70 | 28045. | 299. | 0.686 |
| 487. | 4.07 | 5.13 | 8.041 | 6.248 | 1.792 | 0.22 | 1.00 | 0.52 | 2.68 | 2.67 | 58760. | 299. | 0.686 |
| 470. | 4.02 | 10.04 | 8.022 | 7.900 | 0.122 | 0.02 | 2.02 | 2.02 | 1.85 | 0.92 | 14029. | 291. | 0.686 |
| 471. | 4.02 | 10.04 | 8.022 | 7.801 | 0.221 | 0.03 | 2.02 | 2.00 | 2.63 | 1.30 | 16583. | 291. | 0.686 |
| 473. | 4.02 | 9.97 | 8.022 | 7.492 | 0.530 | 0.07 | 2.02 | 1.93 | 3.36 | 1.66 | 21972. | 289. | 0.686 |
| 474. | 4.02 | 9.97 | 8.022 | 7.246 | 0.776 | 0.10 | 2.02 | 1.81 | 3.99 | 1.98 | 29811. | 289. | 0.686 |
| 475. | 4.02 | 9.97 | 8.022 | 7.019 | 1.004 | 0.13 | 2.02 | 1.70 | 4.29 | 2.12 | 37396. | 289. | 0.686 |
| 476. | 4.02 | 9.97 | 8.022 | 6.865 | 1.157 | 0.14 | 2.02 | 1.63 | 4.35 | 2.15 | 42772. | 289. | 0.686 |
| 478. | 4.02 | 9.97 | 8.022 | 6.767 | 1.256 | 0.16 | 2.02 | 1.41 | 5.30 | 2.62 | 50448. | 289. | 0.686 |
| 479. | 4.02 | 9.97 | 8.022 | 6.612 | 1.410 | 0.18 | 2.02 | 1.27 | 5.53 | 2.74 | 63752. | 289. | 0.686 |

Table D.9 (cont.): Present Air-Water Flow Data: $D_3/D_1$ = 0.52, Upward Branch ($\Phi$ = 0°).

| RUN # | VsL1 (m/s) | VsG1 (m/s) | m1 (kg/s) | m2 (kg/s) | m3 (kg/s) | m3/m1 (-) | x1 (%) | x2 (%) | x3 (%) | x3/x1 (-) | p13 (Pa) | T1 (K) | p1 (MPa) |
|---|---|---|---|---|---|---|---|---|---|---|---|---|---|
| 718. | 0.10 | 4.93 | 0.275 | 0.145 | 0.129 | 0.47 | 29.17 | 54.87 | 0.26 | 0.01 | 417. | 289. | 0.686 |
| 719. | 0.10 | 4.97 | 0.275 | 0.128 | 0.147 | 0.53 | 29.35 | 62.01 | 0.93 | 0.03 | 552. | 289. | 0.686 |
| 720. | 0.10 | 4.97 | 0.275 | 0.104 | 0.171 | 0.62 | 29.35 | 73.73 | 2.43 | 0.08 | 647. | 289. | 0.686 |
| 721. | 0.10 | 4.97 | 0.275 | 0.019 | 0.256 | 0.93 | 29.35 | 47.47 | 28.01 | 0.95 | 890. | 289. | 0.686 |
| 722. | 0.10 | 4.97 | 0.275 | 0.067 | 0.208 | 0.76 | 29.35 | 98.53 | 7.01 | 0.24 | 1135. | 289. | 0.686 |
| 723. | 0.10 | 4.97 | 0.275 | 0.052 | 0.224 | 0.81 | 29.35 | 98.99 | 13.30 | 0.45 | 2416. | 289. | 0.686 |
| 724. | 0.10 | 4.97 | 0.275 | 0.042 | 0.234 | 0.85 | 29.35 | 99.88 | 16.76 | 0.57 | 3084. | 289. | 0.686 |
| 725. | 0.10 | 4.97 | 0.275 | 0.032 | 0.244 | 0.88 | 29.35 | 99.84 | 20.18 | 0.69 | 3600. | 289. | 0.686 |
| 726. | 0.10 | 4.97 | 0.275 | 0.011 | 0.264 | 0.96 | 29.35 | 99.54 | 26.47 | 0.90 | 4442. | 289. | 0.686 |
| 727. | 0.10 | 4.97 | 0.275 | 0.000 | 0.275 | 1.00 | 29.35 | 3.89 | 29.35 | 1.00 | 6414. | 289. | 0.686 |
| 731. | 0.50 | 5.08 | 1.060 | 0.727 | 0.333 | 0.31 | 7.60 | 11.04 | 0.11 | 0.01 | 1615. | 296. | 0.686 |
| 732. | 0.50 | 5.08 | 1.060 | 0.651 | 0.409 | 0.39 | 7.60 | 12.25 | 0.20 | 0.03 | 2133. | 296. | 0.686 |
| 733. | 0.50 | 5.08 | 1.060 | 0.579 | 0.481 | 0.45 | 7.60 | 13.44 | 0.59 | 0.08 | 2914. | 296. | 0.686 |
| 734. | 0.50 | 5.08 | 1.060 | 0.476 | 0.584 | 0.55 | 7.60 | 15.98 | 0.77 | 0.10 | 3421. | 296. | 0.686 |
| 735. | 0.50 | 5.08 | 1.060 | 0.413 | 0.647 | 0.61 | 7.60 | 17.69 | 1.16 | 0.15 | 4735. | 296. | 0.686 |
| 736. | 0.50 | 5.08 | 1.060 | 0.295 | 0.765 | 0.72 | 7.60 | 21.28 | 2.32 | 0.31 | 7095. | 296. | 0.686 |
| 737. | 0.50 | 5.08 | 1.060 | 0.189 | 0.871 | 0.82 | 7.60 | 27.00 | 3.39 | 0.45 | 10344. | 296. | 0.686 |
| 738. | 0.50 | 5.08 | 1.060 | 0.131 | 0.929 | 0.88 | 7.60 | 30.27 | 4.41 | 0.58 | 13180. | 296. | 0.686 |
| 739. | 0.50 | 5.08 | 1.060 | 0.073 | 0.987 | 0.93 | 7.60 | 24.07 | 6.39 | 0.84 | 18386. | 296. | 0.686 |
| 740. | 0.50 | 5.08 | 1.060 | 0.000 | 1.060 | 1.00 | 7.60 | 22.77 | 7.60 | 1.00 | 22922. | 296. | 0.686 |
| 1000. | 0.50 | 39.15 | 1.609 | 1.500 | 0.109 | 0.07 | 39.14 | 41.44 | 7.50 | 0.19 | 6731. | 292. | 0.686 |
| 1001. | 0.50 | 39.29 | 1.611 | 1.455 | 0.157 | 0.10 | 39.22 | 42.36 | 10.04 | 0.26 | 7761. | 292. | 0.686 |
| 1002. | 0.50 | 39.29 | 1.611 | 1.411 | 0.201 | 0.12 | 39.22 | 42.88 | 13.54 | 0.35 | 9315. | 292. | 0.686 |
| 1003. | 0.50 | 38.66 | 1.608 | 1.369 | 0.239 | 0.15 | 39.08 | 42.27 | 20.85 | 0.53 | 11316. | 289. | 0.686 |
| 1004. | 0.51 | 38.72 | 1.619 | 1.311 | 0.308 | 0.19 | 38.74 | 42.76 | 21.66 | 0.56 | 14952. | 290. | 0.686 |
| 1005. | 0.51 | 38.72 | 1.619 | 1.264 | 0.355 | 0.22 | 38.74 | 43.16 | 23.04 | 0.59 | 17446. | 290. | 0.686 |
| 1006. | 0.51 | 38.72 | 1.619 | 1.240 | 0.379 | 0.23 | 38.74 | 43.16 | 24.28 | 0.63 | 19945. | 290. | 0.686 |
| 1007. | 0.51 | 38.96 | 1.618 | 1.198 | 0.420 | 0.26 | 38.48 | 42.95 | 25.74 | 0.67 | 24598. | 294. | 0.686 |
| 1008. | 0.51 | 38.96 | 1.618 | 1.130 | 0.487 | 0.30 | 38.48 | 42.77 | 28.55 | 0.74 | 32792. | 294. | 0.686 |
| 1009. | 0.51 | 38.96 | 1.618 | 1.089 | 0.529 | 0.33 | 38.48 | 42.60 | 30.00 | 0.78 | 38738. | 294. | 0.686 |

Table D.10: Present Air-Water Flow Data: $D_3/D_1$ = 0.52, Downward Branch ($\Phi$ = 180°).

| RUN # | VsL1 (m/s) | VsG1 (m/s) | m1 (kg/s) | m2 (kg/s) | m3 (kg/s) | m3/m1 (-) | x1 (%) | x2 (%) | x3 (%) | x3/x1 (-) | p13 (Pa) | T1 (K) | p1 (MPa) |
|---|---|---|---|---|---|---|---|---|---|---|---|---|---|
| 1010. | 0.51 | 38.96 | 1.618 | 0.947 | 0.671 | 0.41 | 38.48 | 41.67 | 33.98 | 0.88 | 64896. | 294. | 0.686 |
| 693. | 1.00 | 5.03 | 2.047 | 1.842 | 0.205 | 0.10 | 3.98 | 4.42 | 0.08 | 0.02 | 2471. | 290. | 0.686 |
| 694. | 1.00 | 5.03 | 2.047 | 1.713 | 0.334 | 0.16 | 3.98 | 4.73 | 0.15 | 0.04 | 3269. | 290. | 0.686 |
| 695. | 1.00 | 5.08 | 2.047 | 1.570 | 0.477 | 0.23 | 3.98 | 5.11 | 0.29 | 0.07 | 4494. | 293. | 0.686 |
| 696. | 1.00 | 5.08 | 2.047 | 1.425 | 0.622 | 0.30 | 3.98 | 5.55 | 0.39 | 0.10 | 5750. | 293. | 0.686 |
| 697. | 1.00 | 5.08 | 2.047 | 1.268 | 0.778 | 0.38 | 3.98 | 6.11 | 0.51 | 0.13 | 7396. | 293. | 0.686 |
| 698. | 1.00 | 5.08 | 2.047 | 1.132 | 0.915 | 0.45 | 3.98 | 6.60 | 0.75 | 0.19 | 9968. | 293. | 0.686 |
| 699. | 1.00 | 5.08 | 2.047 | 0.995 | 1.052 | 0.51 | 3.98 | 6.80 | 1.32 | 0.33 | 13194. | 293. | 0.686 |
| 700. | 1.00 | 5.08 | 2.047 | 0.901 | 1.146 | 0.56 | 3.98 | 6.83 | 1.75 | 0.44 | 16825. | 293. | 0.686 |
| 701. | 1.00 | 5.08 | 2.047 | 0.703 | 1.343 | 0.66 | 3.98 | 6.84 | 2.49 | 0.62 | 25153. | 293. | 0.686 |
| 702. | 1.00 | 5.08 | 2.047 | 0.674 | 1.372 | 0.67 | 3.98 | 6.10 | 2.94 | 0.74 | 28520. | 293. | 0.686 |
| 703. | 1.00 | 5.08 | 2.047 | 0.437 | 1.610 | 0.79 | 3.98 | 2.00 | 4.52 | 1.13 | 55364. | 293. | 0.686 |
| 662. | 1.01 | 10.23 | 2.142 | 2.069 | 0.073 | 0.03 | 7.66 | 7.92 | 0.35 | 0.05 | 3693. | 293. | 0.686 |
| 663. | 1.01 | 10.23 | 2.142 | 2.008 | 0.134 | 0.06 | 7.66 | 8.13 | 0.62 | 0.08 | 4106. | 293. | 0.686 |
| 664. | 1.01 | 10.12 | 2.140 | 1.916 | 0.224 | 0.10 | 7.58 | 8.37 | 0.90 | 0.12 | 4820. | 293. | 0.686 |
| 665. | 1.01 | 10.21 | 2.140 | 1.792 | 0.349 | 0.16 | 7.60 | 8.88 | 1.03 | 0.14 | 5789. | 295. | 0.686 |
| 666. | 1.01 | 10.21 | 2.140 | 1.596 | 0.544 | 0.25 | 7.60 | 9.73 | 1.35 | 0.18 | 8177. | 295. | 0.686 |
| 667. | 1.01 | 10.25 | 2.140 | 1.485 | 0.655 | 0.31 | 7.60 | 10.25 | 1.58 | 0.21 | 9987. | 296. | 0.686 |
| 668. | 1.01 | 10.25 | 2.140 | 1.371 | 0.769 | 0.36 | 7.60 | 10.77 | 1.93 | 0.25 | 13340. | 296. | 0.686 |
| 669. | 1.01 | 10.25 | 2.140 | 1.180 | 0.960 | 0.45 | 7.60 | 11.19 | 3.18 | 0.42 | 20371. | 296. | 0.686 |
| 670. | 1.01 | 10.25 | 2.140 | 0.824 | 1.316 | 0.62 | 7.60 | 9.20 | 6.60 | 0.87 | 53548. | 296. | 0.686 |
| 916. | 0.99 | 10.20 | 2.099 | 0.996 | 1.104 | 0.53 | 7.61 | 8.85 | 6.48 | 0.85 | 33281. | 300. | 0.686 |
| 915. | 0.99 | 10.11 | 2.100 | 0.773 | 1.326 | 0.63 | 7.62 | 6.14 | 8.48 | 1.11 | 60944. | 297. | 0.686 |
| 914. | 0.99 | 10.04 | 2.100 | 0.657 | 1.442 | 0.69 | 7.62 | 3.07 | 9.69 | 1.27 | 81980. | 295. | 0.686 |
| 925. | 1.00 | 19.63 | 2.268 | 2.061 | 0.207 | 0.09 | 13.92 | 14.99 | 3.30 | 0.24 | 6781. | 292. | 0.686 |
| 924. | 1.00 | 19.63 | 2.268 | 1.980 | 0.288 | 0.13 | 13.92 | 15.33 | 4.27 | 0.31 | 7987. | 292. | 0.686 |
| 923. | 1.00 | 19.63 | 2.268 | 1.809 | 0.459 | 0.20 | 13.92 | 15.79 | 6.57 | 0.47 | 10820. | 292. | 0.686 |
| 922. | 1.00 | 19.63 | 2.268 | 1.725 | 0.543 | 0.24 | 13.92 | 15.73 | 8.17 | 0.59 | 14611. | 292. | 0.686 |
| 921. | 0.98 | 19.64 | 2.234 | 1.651 | 0.583 | 0.26 | 13.76 | 15.42 | 9.08 | 0.66 | 17004. | 300. | 0.686 |
| 920. | 0.98 | 19.66 | 2.235 | 1.482 | 0.753 | 0.34 | 13.77 | 14.21 | 12.91 | 0.94 | 28291. | 300. | 0.686 |

Table D.10 (cont.): Present Air-Water Flow Data: $D_3/D_1$ = 0.52, Downward Branch ($\Phi$ = 180°).

| RUN # | VsL1 (m/s) | VsG1 (m/s) | m1 (kg/s) | m2 (kg/s) | m3 (kg/s) | m3/m1 (-) | x1 (%) | x2 (%) | x3 (%) | x3/x1 (-) | p13 (Pa) | T1 (K) | p1 (MPa) |
|---|---|---|---|---|---|---|---|---|---|---|---|---|---|
| 919. | 0.98 | 19.66 | 2.235 | 1.364 | 0.871 | 0.39 | 13.77 | 14.19 | 13.12 | 0.95 | 38976. | 300. | 0.686 |
| 918. | 0.98 | 19.66 | 2.235 | 1.221 | 1.014 | 0.45 | 13.77 | 13.18 | 14.49 | 1.05 | 55312. | 300. | 0.686 |
| 917. | 0.98 | 19.66 | 2.235 | 1.074 | 1.160 | 0.52 | 13.77 | 10.98 | 16.36 | 1.19 | 84004. | 300. | 0.686 |
| 971. | 1.01 | 40.14 | 2.618 | 2.500 | 0.118 | 0.05 | 24.58 | 25.00 | 15.85 | 0.64 | 7475. | 293. | 0.686 |
| 972. | 1.00 | 39.85 | 2.602 | 2.435 | 0.167 | 0.06 | 24.72 | 25.03 | 20.23 | 0.82 | 9394. | 291. | 0.686 |
| 973. | 1.00 | 39.71 | 2.600 | 2.394 | 0.206 | 0.08 | 24.66 | 24.86 | 22.36 | 0.91 | 10918. | 291. | 0.686 |
| 974. | 1.00 | 39.85 | 2.600 | 2.328 | 0.271 | 0.10 | 24.66 | 24.81 | 23.32 | 0.95 | 14978. | 292. | 0.686 |
| 975. | 1.00 | 39.85 | 2.600 | 2.282 | 0.317 | 0.12 | 24.66 | 24.60 | 25.08 | 1.02 | 18894. | 292. | 0.686 |
| 976. | 1.00 | 39.77 | 2.594 | 2.218 | 0.376 | 0.14 | 24.50 | 24.04 | 27.19 | 1.11 | 22711. | 294. | 0.686 |
| 977. | 1.00 | 39.50 | 2.592 | 2.112 | 0.480 | 0.19 | 24.43 | 23.66 | 27.80 | 1.14 | 34221. | 293. | 0.686 |
| 978. | 1.00 | 39.50 | 2.592 | 2.064 | 0.528 | 0.20 | 24.43 | 23.52 | 27.98 | 1.15 | 41168. | 293. | 0.686 |
| 996. | 1.00 | 40.07 | 2.598 | 2.070 | 0.528 | 0.20 | 24.73 | 23.98 | 27.67 | 1.12 | 42004. | 293. | 0.686 |
| 997. | 1.00 | 40.07 | 2.598 | 1.994 | 0.604 | 0.23 | 24.73 | 23.44 | 28.98 | 1.17 | 52840. | 293. | 0.686 |
| 998. | 1.00 | 39.13 | 2.595 | 1.889 | 0.706 | 0.27 | 24.51 | 22.37 | 30.23 | 1.23 | 70616. | 289. | 0.686 |
| 681. | 2.04 | 5.00 | 4.074 | 3.827 | 0.247 | 0.06 | 2.01 | 2.13 | 0.17 | 0.08 | 4320. | 287. | 0.686 |
| 682. | 2.03 | 5.00 | 4.050 | 3.579 | 0.470 | 0.12 | 2.02 | 2.25 | 0.26 | 0.13 | 6183. | 287. | 0.686 |
| 683. | 2.03 | 5.00 | 4.050 | 3.364 | 0.685 | 0.17 | 2.02 | 2.37 | 0.33 | 0.16 | 8469. | 287. | 0.686 |
| 684. | 2.03 | 5.00 | 4.050 | 3.093 | 0.956 | 0.24 | 2.02 | 2.49 | 0.50 | 0.25 | 12749. | 287. | 0.686 |
| 685. | 2.03 | 5.02 | 4.049 | 2.991 | 1.058 | 0.26 | 2.00 | 2.50 | 0.60 | 0.30 | 15669. | 291. | 0.686 |
| 686. | 2.03 | 5.02 | 4.049 | 2.931 | 1.118 | 0.28 | 2.00 | 2.50 | 0.69 | 0.35 | 17758. | 291. | 0.686 |
| 687. | 2.03 | 5.04 | 4.049 | 2.698 | 1.351 | 0.33 | 2.01 | 2.31 | 1.41 | 0.70 | 26816. | 291. | 0.686 |
| 688. | 2.03 | 5.04 | 4.049 | 2.514 | 1.535 | 0.38 | 2.01 | 2.15 | 1.77 | 0.88 | 35889. | 291. | 0.686 |
| 902. | 2.01 | 4.96 | 4.010 | 1.861 | 2.149 | 0.54 | 1.98 | 1.91 | 2.05 | 1.03 | 54072. | 293. | 0.686 |
| 901. | 1.95 | 5.02 | 3.888 | 1.436 | 2.452 | 0.63 | 2.05 | 1.75 | 2.22 | 1.08 | 66188. | 296. | 0.686 |
| 900. | 1.94 | 5.08 | 3.886 | 1.221 | 2.666 | 0.69 | 2.05 | 1.23 | 2.42 | 1.18 | 86368. | 300. | 0.686 |
| 673. | 1.97 | 9.95 | 4.017 | 3.927 | 0.090 | 0.02 | 4.06 | 4.14 | 0.38 | 0.09 | 6764. | 287. | 0.686 |
| 674. | 1.97 | 10.23 | 4.017 | 3.779 | 0.238 | 0.06 | 4.06 | 4.24 | 1.18 | 0.29 | 8209. | 295. | 0.686 |
| 675. | 1.97 | 10.23 | 4.017 | 3.673 | 0.343 | 0.09 | 4.06 | 4.30 | 1.39 | 0.34 | 9663. | 295. | 0.686 |
| 913. | 1.97 | 10.01 | 4.011 | 2.153 | 1.858 | 0.46 | 3.92 | 2.04 | 6.10 | 1.56 | 95956. | 299. | 0.686 |
| 912. | 1.97 | 10.01 | 4.011 | 3.517 | 0.494 | 0.12 | 3.92 | 4.22 | 1.80 | 0.46 | 10605. | 299. | 0.686 |

Table D.10 (cont.): Present Air-Water Flow Data: $D_3/D_1$ = 0.52, Downward Branch ($\Phi$ = 180°).

| RUN # | VsL1 (m/s) | VsG1 (m/s) | m1 (kg/s) | m2 (kg/s) | m3 (kg/s) | m3/m1 (-) | x1 (%) | x2 (%) | x3 (%) | x3/x1 (-) | p13 (Pa) | T1 (K) | p1 (MPa) |
|---|---|---|---|---|---|---|---|---|---|---|---|---|---|
| 911. | 1.97 | 10.01 | 4.011 | 3.311 | 0.700 | 0.17 | 3.92 | 4.25 | 2.38 | 0.61 | 15163. | 299. | 0.686 |
| 910. | 1.97 | 10.01 | 4.011 | 3.051 | 0.960 | 0.24 | 3.92 | 4.18 | 3.08 | 0.79 | 22948. | 299. | 0.686 |
| 909. | 1.88 | 10.01 | 3.847 | 2.797 | 1.050 | 0.27 | 4.09 | 4.28 | 3.57 | 0.87 | 27012. | 299. | 0.686 |
| 908. | 1.97 | 10.07 | 4.012 | 2.831 | 1.181 | 0.29 | 3.96 | 3.57 | 4.88 | 1.23 | 40822. | 298. | 0.686 |
| 907. | 1.95 | 9.94 | 3.979 | 2.587 | 1.392 | 0.35 | 3.95 | 3.26 | 5.23 | 1.32 | 54112. | 297. | 0.686 |
| 928. | 2.03 | 19.77 | 4.290 | 4.083 | 0.207 | 0.05 | 7.52 | 7.77 | 2.53 | 0.34 | 10649. | 288. | 0.686 |
| 929. | 2.03 | 19.77 | 4.290 | 4.014 | 0.276 | 0.06 | 7.52 | 7.79 | 3.58 | 0.48 | 12217. | 288. | 0.686 |
| 930. | 2.03 | 20.08 | 4.290 | 3.875 | 0.415 | 0.10 | 7.50 | 7.88 | 4.03 | 0.54 | 15069. | 293. | 0.686 |
| 931. | 2.05 | 20.08 | 4.333 | 3.790 | 0.543 | 0.13 | 7.43 | 7.80 | 4.84 | 0.65 | 18617. | 293. | 0.686 |
| 932. | 2.02 | 20.08 | 4.271 | 3.648 | 0.623 | 0.15 | 7.54 | 7.93 | 5.24 | 0.70 | 21004. | 293. | 0.686 |
| 933. | 2.02 | 20.08 | 4.271 | 3.532 | 0.739 | 0.17 | 7.54 | 7.85 | 6.06 | 0.80 | 25634. | 293. | 0.686 |
| 934. | 2.02 | 20.08 | 4.271 | 3.410 | 0.861 | 0.20 | 7.54 | 7.68 | 6.98 | 0.93 | 33054. | 293. | 0.686 |
| 935. | 2.08 | 19.57 | 4.389 | 3.193 | 1.196 | 0.27 | 7.35 | 7.31 | 7.46 | 1.01 | 99328. | 285. | 0.686 |
| 706. | 4.00 | 4.97 | 7.915 | 7.763 | 0.151 | 0.02 | 1.01 | 1.02 | 0.43 | 0.43 | 10526. | 293. | 0.686 |
| 707. | 4.00 | 4.92 | 7.915 | 7.681 | 0.234 | 0.03 | 1.01 | 1.02 | 0.43 | 0.42 | 11275. | 290. | 0.686 |
| 708. | 4.00 | 4.92 | 7.915 | 7.528 | 0.386 | 0.05 | 1.01 | 1.03 | 0.56 | 0.56 | 13172. | 290. | 0.686 |
| 709. | 4.00 | 4.92 | 7.915 | 7.360 | 0.555 | 0.07 | 1.01 | 1.04 | 0.63 | 0.63 | 15619. | 290. | 0.686 |
| 710. | 4.00 | 4.95 | 7.915 | 7.102 | 0.813 | 0.10 | 1.01 | 1.04 | 0.69 | 0.68 | 20027. | 292. | 0.686 |
| 711. | 4.00 | 4.95 | 7.915 | 6.855 | 1.060 | 0.13 | 1.01 | 1.04 | 0.76 | 0.75 | 26385. | 292. | 0.686 |
| 712. | 4.00 | 5.01 | 7.914 | 6.699 | 1.216 | 0.15 | 1.00 | 0.98 | 1.14 | 1.13 | 30981. | 296. | 0.686 |
| 713. | 4.00 | 5.01 | 7.914 | 6.543 | 1.372 | 0.17 | 1.00 | 0.96 | 1.24 | 1.23 | 37652. | 296. | 0.686 |
| 906. | 3.94 | 5.03 | 7.793 | 6.380 | 1.413 | 0.18 | 1.02 | 0.99 | 1.15 | 1.13 | 32599. | 297. | 0.686 |
| 905. | 3.96 | 5.02 | 7.835 | 5.679 | 2.156 | 0.28 | 1.01 | 0.87 | 1.40 | 1.38 | 61924. | 297. | 0.686 |
| 904. | 3.93 | 5.02 | 7.770 | 5.200 | 2.570 | 0.33 | 1.01 | 0.81 | 1.42 | 1.41 | 84576. | 301. | 0.686 |
| 903. | 3.95 | 5.02 | 7.812 | 4.569 | 3.243 | 0.42 | 1.00 | 0.65 | 1.49 | 1.49 | 110880. | 301. | 0.686 |

Table D.10 (cont.): Present Air-Water Flow Data: $D_3/D_1$ = 0.52, Downward Branch ($\Phi$ = 180°).

| RUN # | VsL1 (m/s) | VsG1 (m/s) | m1 (kg/s) | m2 (kg/s) | m3 (kg/s) | m3/m1 (-) | x1 (%) | x2 (%) | x3 (%) | x3/x1 (-) | p13 (Pa) | T1 (K) | p1 (MPa) |
|---|---|---|---|---|---|---|---|---|---|---|---|---|---|
| 871. | 0.05 | 9.26 | 0.197 | 0.140 | 0.056 | 0.29 | 48.86 | 38.20 | 75.39 | 1.54 | 85180. | 291. | 0.441 |
| 872. | 0.05 | 9.12 | 0.194 | 0.161 | 0.033 | 0.17 | 49.41 | 42.42 | 83.31 | 1.69 | 25930. | 291. | 0.448 |
| 873. | 0.05 | 9.12 | 0.194 | 0.145 | 0.050 | 0.26 | 49.41 | 44.06 | 64.90 | 1.31 | 166670. | 291. | 0.448 |
| 900. | 0.05 | 9.75 | 0.203 | 0.198 | 0.005 | 0.02 | 56.07 | 55.03 | 97.75 | 1.74 | 800. | 291. | 0.495 |
| 901. | 0.05 | 9.66 | 0.205 | 0.195 | 0.010 | 0.05 | 55.41 | 53.45 | 93.61 | 1.69 | 4130. | 291. | 0.500 |
| 902. | 0.05 | 9.72 | 0.214 | 0.198 | 0.016 | 0.07 | 53.03 | 50.25 | 87.50 | 1.65 | 9920. | 291. | 0.497 |
| 903. | 0.05 | 9.93 | 0.209 | 0.182 | 0.027 | 0.13 | 54.46 | 50.51 | 81.62 | 1.50 | 27260. | 291. | 0.486 |
| 904. | 0.05 | 9.87 | 0.208 | 0.172 | 0.035 | 0.17 | 55.95 | 50.74 | 81.22 | 1.45 | 25930. | 291. | 0.500 |
| 905. | 0.05 | 9.97 | 0.208 | 0.136 | 0.072 | 0.34 | 55.95 | 45.69 | 75.44 | 1.35 | 150860. | 291. | 0.495 |
| 984. | 0.05 | 10.40 | 0.215 | 0.205 | 0.011 | 0.05 | 53.30 | 51.35 | 91.12 | 1.71 | 3400. | 299. | 0.482 |
| 985. | 0.05 | 10.27 | 0.215 | 0.170 | 0.046 | 0.21 | 53.30 | 46.00 | 80.38 | 1.51 | 48640. | 299. | 0.488 |
| 867. | 0.05 | 9.28 | 0.166 | 0.158 | 0.008 | 0.05 | 41.41 | 38.64 | 97.80 | 2.36 | 4050. | 291. | 0.315 |
| 868. | 0.05 | 9.89 | 0.167 | 0.152 | 0.015 | 0.09 | 41.73 | 37.58 | 84.12 | 2.02 | 13550. | 291. | 0.299 |
| 869. | 0.05 | 9.93 | 0.167 | 0.145 | 0.022 | 0.13 | 41.73 | 35.55 | 82.49 | 1.98 | 32620. | 291. | 0.298 |
| 870. | 0.05 | 9.93 | 0.167 | 0.131 | 0.036 | 0.22 | 41.73 | 32.23 | 75.99 | 1.82 | 56790. | 291. | 0.298 |
| 725. | 0.05 | 9.92 | 0.154 | 0.141 | 0.012 | 0.08 | 30.49 | 25.52 | 87.19 | 2.86 | 16440. | 291. | 0.201 |
| 726. | 0.05 | 9.68 | 0.154 | 0.130 | 0.024 | 0.16 | 30.49 | 22.81 | 71.99 | 2.36 | 38640. | 291. | 0.206 |
| 727. | 0.05 | 9.68 | 0.154 | 0.125 | 0.029 | 0.19 | 30.49 | 21.13 | 71.11 | 2.33 | 45800. | 291. | 0.206 |
| 746. | 0.06 | 2.04 | 0.121 | 0.114 | 0.007 | 0.06 | 11.04 | 9.81 | 30.47 | 2.76 | 1065. | 294. | 0.282 |
| 747. | 0.06 | 1.93 | 0.122 | 0.102 | 0.020 | 0.17 | 10.80 | 9.39 | 17.90 | 1.66 | 4790. | 294. | 0.294 |
| 748. | 0.06 | 1.97 | 0.134 | 0.121 | 0.013 | 0.10 | 9.87 | 7.37 | 33.33 | 3.38 | 2520. | 294. | 0.287 |
| 703. | 0.06 | 2.28 | 0.118 | 0.084 | 0.034 | 0.29 | 7.94 | 8.44 | 6.71 | 0.84 | 7541. | 293. | 0.176 |
| 704. | 0.06 | 2.28 | 0.118 | 0.054 | 0.064 | 0.54 | 7.94 | 11.29 | 5.13 | 0.65 | 19257. | 293. | 0.176 |
| 705. | 0.06 | 2.14 | 0.122 | 0.000 | 0.122 | 1.00 | 7.61 | 0.0 | 3.47 | 0.46 | 30370. | 293. | 0.186 |
| 690. | 0.05 | 2.00 | 0.118 | 0.090 | 0.029 | 0.24 | 18.90 | 17.69 | 22.70 | 1.20 | 10730. | 293. | 0.480 |
| 691. | 0.06 | 2.14 | 0.132 | 0.003 | 0.134 | 1.00 | 17.11 | 0.0 | 15.73 | 0.92 | 71480. | 293. | 0.451 |
| 692. | 0.06 | 2.12 | 0.136 | 0.002 | 0.138 | 1.00 | 16.68 | 0.0 | 11.50 | 0.69 | 51850. | 293. | 0.456 |
| 693. | 0.05 | 1.95 | 0.129 | 0.026 | 0.103 | 0.80 | 17.26 | 46.40 | 9.97 | 0.58 | 19630. | 293. | 0.490 |
| 694. | 0.05 | 1.95 | 0.129 | 0.114 | 0.015 | 0.12 | 17.26 | 16.16 | 25.63 | 1.49 | 1972. | 293. | 0.490 |
| 913. | 0.06 | 2.03 | 0.141 | 0.104 | 0.037 | 0.26 | 16.35 | 16.01 | 17.29 | 1.06 | 9360. | 291. | 0.482 |

Table D.11: Present Air-Water Flow Data: $D_3/D_1$ = 0.2, Horizontal Branch ($\Phi$ = 90°).

| RUN # | VsL1 (m/s) | VsG1 (m/s) | m1 (kg/s) | m2 (kg/s) | m3 (kg/s) | m3/m1 (-) | x1 (%) | x2 (%) | x3 (%) | x3/x1 (-) | p13 (Pa) | T1 (K) | p1 (MPa) |
|---|---|---|---|---|---|---|---|---|---|---|---|---|---|
| 914. | 0.06 | 2.18 | 0.148 | 0.058 | 0.091 | 0.61 | 15.29 | 21.04 | 11.63 | 0.76 | 36530. | 291. | 0.443 |
| 757. | 0.06 | 20.35 | 0.339 | 0.335 | 0.004 | 0.01 | 67.50 | 67.27 | 88.59 | 1.31 | 1103. | 294. | 0.482 |
| 758. | 0.06 | 20.85 | 0.341 | 0.330 | 0.012 | 0.03 | 66.93 | 67.70 | 45.30 | 0.68 | 3615. | 294. | 0.470 |
| 759. | 0.06 | 20.85 | 0.341 | 0.326 | 0.016 | 0.05 | 66.93 | 67.76 | 49.91 | 0.75 | 7300. | 294. | 0.470 |
| 760. | 0.06 | 20.85 | 0.350 | 0.328 | 0.021 | 0.06 | 65.30 | 66.11 | 53.02 | 0.81 | 13310. | 294. | 0.470 |
| 761. | 0.06 | 20.85 | 0.350 | 0.322 | 0.028 | 0.08 | 65.30 | 65.77 | 59.87 | 0.92 | 22660. | 294. | 0.470 |
| 762. | 0.06 | 20.43 | 0.350 | 0.317 | 0.033 | 0.09 | 65.30 | 65.67 | 61.78 | 0.95 | 20000. | 294. | 0.480 |
| 763. | 0.06 | 20.64 | 0.350 | 0.308 | 0.042 | 0.12 | 65.30 | 65.50 | 63.90 | 0.98 | 33830. | 294. | 0.475 |
| 764. | 0.06 | 20.85 | 0.350 | 0.302 | 0.048 | 0.14 | 65.30 | 65.26 | 65.56 | 1.00 | 49390. | 294. | 0.470 |
| 765. | 0.06 | 21.07 | 0.354 | 0.296 | 0.058 | 0.16 | 64.49 | 64.23 | 65.82 | 1.02 | 83210. | 294. | 0.465 |
| 766. | 0.06 | 20.72 | 0.353 | 0.288 | 0.064 | 0.18 | 64.82 | 64.10 | 68.06 | 1.05 | 116420. | 294. | 0.473 |
| 767. | 0.06 | 19.90 | 0.347 | 0.272 | 0.075 | 0.22 | 65.83 | 64.37 | 71.13 | 1.08 | 190860. | 294. | 0.493 |
| 911. | 0.06 | 20.61 | 0.341 | 0.329 | 0.012 | 0.04 | 67.45 | 68.24 | 45.93 | 0.68 | 2810. | 291. | 0.474 |
| 912. | 0.06 | 19.56 | 0.341 | 0.310 | 0.031 | 0.09 | 67.45 | 67.88 | 63.21 | 0.94 | 30520. | 291. | 0.500 |
| 731. | 0.06 | 19.92 | 0.204 | 0.194 | 0.010 | 0.05 | 45.09 | 43.90 | 68.74 | 1.52 | 8550. | 291. | 0.196 |
| 732. | 0.06 | 19.92 | 0.204 | 0.190 | 0.014 | 0.07 | 45.09 | 43.50 | 66.38 | 1.47 | 16401. | 291. | 0.196 |
| 733. | 0.06 | 19.34 | 0.216 | 0.194 | 0.022 | 0.10 | 43.27 | 40.67 | 66.29 | 1.53 | 30250. | 291. | 0.205 |
| 734. | 0.06 | 17.24 | 0.214 | 0.186 | 0.027 | 0.13 | 43.66 | 39.37 | 72.73 | 1.67 | 38150. | 291. | 0.230 |
| 850. | 0.05 | 2.57 | 0.132 | 0.001 | 0.131 | 0.99 | 20.43 | 72.04 | 20.06 | 0.98 | 94690. | 291. | 0.446 |
| 851. | 0.06 | 2.72 | 0.136 | 0.033 | 0.103 | 0.76 | 20.00 | 35.10 | 15.19 | 0.76 | 39390. | 291. | 0.426 |
| 852. | 0.05 | 2.51 | 0.127 | 0.056 | 0.071 | 0.56 | 21.11 | 27.64 | 15.98 | 0.76 | 18150. | 291. | 0.456 |
| 853. | 0.05 | 2.37 | 0.127 | 0.115 | 0.013 | 0.10 | 21.11 | 19.24 | 38.06 | 1.80 | 3130. | 291. | 0.482 |
| 854. | 0.06 | 2.35 | 0.135 | 0.112 | 0.023 | 0.17 | 19.29 | 17.25 | 29.03 | 1.50 | 6180. | 291. | 0.470 |
| 855. | 0.05 | 2.26 | 0.133 | 0.064 | 0.069 | 0.52 | 19.59 | 22.62 | 16.77 | 0.86 | 30850. | 291. | 0.490 |
| 856. | 0.05 | 2.35 | 0.134 | 0.097 | 0.037 | 0.28 | 20.31 | 19.10 | 23.51 | 1.16 | 12530. | 291. | 0.492 |
| 1009. | 0.05 | 2.53 | 0.129 | 0.095 | 0.034 | 0.26 | 21.95 | 19.20 | 29.65 | 1.35 | 14200. | 297. | 0.486 |
| 1010. | 0.05 | 2.53 | 0.129 | 0.111 | 0.018 | 0.14 | 22.02 | 19.26 | 38.82 | 1.76 | 5810. | 297. | 0.487 |
| 1011. | 0.06 | 2.49 | 0.137 | 0.087 | 0.050 | 0.36 | 20.50 | 20.28 | 20.87 | 1.02 | 20100. | 297. | 0.490 |
| 1012. | 0.05 | 2.50 | 0.134 | 0.105 | 0.029 | 0.22 | 20.97 | 18.80 | 28.87 | 1.38 | 9960. | 297. | 0.488 |
| 1013. | 0.05 | 2.50 | 0.134 | 0.059 | 0.075 | 0.56 | 20.97 | 25.31 | 17.56 | 0.84 | 37280. | 297. | 0.488 |

Table D.11 (cont.): Present Air-Water Flow Data: $D_3/D_1$ = 0.2, Horizontal Branch ($\Phi$ = 90°).

| RUN # | VsL1 (m/s) | VsG1 (m/s) | m1 (kg/s) | m2 (kg/s) | m3 (kg/s) | m3/m1 (-) | x1 (%) | x2 (%) | x3 (%) | x3/x1 (-) | p13 (Pa) | T1 (K) | p1 (MPa) |
|---|---|---|---|---|---|---|---|---|---|---|---|---|---|
| 1014. | 0.05 | 2.52 | 0.134 | 0.038 | 0.096 | 0.72 | 20.97 | 32.45 | 16.41 | 0.78 | 31970. | 297. | 0.483 |
| 1015. | 0.06 | 2.52 | 0.142 | 0.026 | 0.116 | 0.82 | 19.79 | 32.03 | 17.10 | 0.86 | 50620. | 297. | 0.483 |
| 1016. | 0.06 | 2.49 | 0.147 | 0.004 | 0.142 | 0.97 | 19.15 | 15.66 | 19.26 | 1.01 | 97780. | 297. | 0.490 |
| 1004. | 0.05 | 7.20 | 0.178 | 0.106 | 0.072 | 0.41 | 45.95 | 27.75 | 72.56 | 1.58 | 183210. | 297. | 0.492 |
| 1005. | 0.05 | 7.20 | 0.176 | 0.123 | 0.053 | 0.30 | 46.55 | 32.93 | 78.43 | 1.68 | 64200. | 297. | 0.492 |
| 1006. | 0.05 | 7.19 | 0.176 | 0.135 | 0.041 | 0.23 | 46.55 | 35.63 | 82.78 | 1.78 | 36670. | 297. | 0.493 |
| 1007. | 0.05 | 7.22 | 0.176 | 0.152 | 0.024 | 0.14 | 46.55 | 39.93 | 88.41 | 1.90 | 10990. | 297. | 0.491 |
| 1008. | 0.05 | 7.20 | 0.181 | 0.164 | 0.017 | 0.09 | 45.09 | 40.31 | 91.62 | 2.03 | 10780. | 297. | 0.492 |
| 894. | 0.10 | 10.13 | 0.309 | 0.234 | 0.075 | 0.24 | 37.21 | 27.31 | 68.19 | 1.83 | 185180. | 291. | 0.482 |
| 895. | 0.10 | 9.71 | 0.304 | 0.249 | 0.054 | 0.18 | 37.85 | 29.90 | 74.41 | 1.97 | 76540. | 291. | 0.503 |
| 896. | 0.10 | 11.94 | 0.305 | 0.268 | 0.038 | 0.12 | 37.62 | 32.23 | 76.03 | 2.02 | 29260. | 291. | 0.409 |
| 897. | 0.10 | 9.93 | 0.307 | 0.282 | 0.025 | 0.08 | 37.00 | 33.30 | 78.11 | 2.11 | 23690. | 291. | 0.486 |
| 898. | 0.10 | 9.71 | 0.302 | 0.282 | 0.020 | 0.07 | 37.58 | 34.54 | 79.88 | 2.13 | 16570. | 291. | 0.497 |
| 899. | 0.10 | 9.85 | 0.302 | 0.297 | 0.005 | 0.02 | 37.58 | 36.55 | 96.10 | 2.56 | 2540. | 291. | 0.490 |
| 982. | 0.10 | 9.96 | 0.311 | 0.288 | 0.023 | 0.07 | 36.91 | 33.54 | 79.31 | 2.15 | 20160. | 291. | 0.490 |
| 983. | 0.09 | 9.96 | 0.299 | 0.288 | 0.011 | 0.04 | 38.34 | 36.40 | 89.28 | 2.33 | 3770. | 291. | 0.490 |
| 990. | 0.10 | 2.53 | 0.227 | 0.000 | 0.228 | 1.00 | 12.01 | 555.61 | 10.88 | 0.91 | 177280. | 309. | 0.487 |
| 991. | 0.10 | 2.51 | 0.224 | 0.056 | 0.168 | 0.75 | 12.19 | 18.99 | 9.92 | 0.81 | 53090. | 309. | 0.490 |
| 992. | 0.10 | 2.44 | 0.221 | 0.095 | 0.126 | 0.57 | 12.37 | 14.81 | 10.54 | 0.85 | 32960. | 309. | 0.505 |
| 993. | 0.10 | 2.43 | 0.220 | 0.125 | 0.095 | 0.43 | 12.41 | 12.45 | 12.36 | 1.00 | 20370. | 309. | 0.507 |
| 994. | 0.10 | 2.43 | 0.220 | 0.153 | 0.067 | 0.30 | 12.41 | 10.99 | 15.68 | 1.26 | 23900. | 309. | 0.507 |
| 995. | 0.10 | 2.51 | 0.220 | 0.189 | 0.031 | 0.14 | 12.41 | 10.08 | 26.59 | 2.14 | 10290. | 309. | 0.490 |
| 996. | 0.10 | 2.50 | 0.220 | 0.199 | 0.021 | 0.09 | 12.41 | 10.37 | 32.15 | 2.59 | 5370. | 309. | 0.493 |
| 874. | 0.10 | 5.15 | 0.259 | 0.172 | 0.087 | 0.34 | 22.05 | 8.10 | 49.60 | 2.25 | 192590. | 291. | 0.472 |
| 875. | 0.10 | 4.96 | 0.259 | 0.200 | 0.059 | 0.23 | 22.05 | 12.18 | 55.21 | 2.50 | 53090. | 291. | 0.490 |
| 876. | 0.10 | 4.96 | 0.257 | 0.213 | 0.044 | 0.17 | 22.23 | 14.30 | 60.32 | 2.71 | 32720. | 291. | 0.490 |
| 877. | 0.10 | 4.96 | 0.259 | 0.229 | 0.031 | 0.12 | 22.06 | 16.27 | 65.36 | 2.96 | 13830. | 291. | 0.490 |
| 878. | 0.10 | 4.89 | 0.255 | 0.238 | 0.017 | 0.07 | 22.40 | 18.21 | 82.53 | 3.68 | 9350. | 291. | 0.496 |
| 879. | 0.10 | 4.95 | 0.253 | 0.242 | 0.011 | 0.04 | 22.60 | 19.56 | 90.38 | 4.00 | 510. | 291. | 0.490 |
| 988. | 0.11 | 5.19 | 0.267 | 0.244 | 0.024 | 0.09 | 21.11 | 16.42 | 69.52 | 3.29 | 21370. | 309. | 0.490 |

Table D.11 (cont.): Present Air-Water Flow Data: $D_3/D_1$ = 0.2, Horizontal Branch ($\Phi$ = 90°).

| RUN # | VsL1 (m/s) | VsG1 (m/s) | m1 (kg/s) | m2 (kg/s) | m3 (kg/s) | m3/m1 (-) | x1 (%) | x2 (%) | x3 (%) | x3/x1 (-) | p13 (Pa) | T1 (K) | p1 (MPa) |
|---|---|---|---|---|---|---|---|---|---|---|---|---|---|
| 989. | 0.11 | 5.27 | 0.267 | 0.210 | 0.057 | 0.21 | 21.11 | 11.62 | 56.14 | 2.66 | 57040. | 309. | 0.483 |
| 890. | 0.16 | 29.57 | 0.450 | 0.437 | 0.013 | 0.03 | 30.60 | 30.73 | 26.29 | 0.86 | 5080. | 291. | 0.198 |
| 891. | 0.16 | 29.72 | 0.450 | 0.432 | 0.019 | 0.04 | 30.60 | 30.59 | 30.87 | 1.01 | 12570. | 291. | 0.197 |
| 892. | 0.16 | 29.72 | 0.447 | 0.425 | 0.022 | 0.05 | 30.82 | 30.71 | 32.95 | 1.07 | 19630. | 291. | 0.197 |
| 893. | 0.16 | 29.90 | 0.444 | 0.411 | 0.033 | 0.07 | 30.90 | 30.18 | 39.99 | 1.29 | 40620. | 291. | 0.195 |
| 997. | 0.10 | 7.50 | 0.275 | 0.267 | 0.008 | 0.03 | 29.62 | 27.74 | 93.63 | 3.16 | 2230. | 309. | 0.490 |
| 998. | 0.10 | 7.53 | 0.275 | 0.265 | 0.010 | 0.04 | 29.62 | 27.23 | 93.35 | 3.15 | 4050. | 309. | 0.488 |
| 999. | 0.10 | 7.56 | 0.275 | 0.258 | 0.017 | 0.06 | 29.62 | 25.73 | 88.20 | 2.98 | 12460. | 309. | 0.486 |
| 1000. | 0.10 | 7.60 | 0.270 | 0.251 | 0.019 | 0.07 | 30.14 | 25.62 | 89.30 | 2.96 | 17850. | 309. | 0.483 |
| 1001. | 0.11 | 7.26 | 0.290 | 0.248 | 0.042 | 0.15 | 28.13 | 20.32 | 73.82 | 2.62 | 36540. | 297. | 0.488 |
| 1002. | 0.10 | 7.23 | 0.275 | 0.214 | 0.062 | 0.22 | 29.67 | 19.18 | 66.01 | 2.23 | 76540. | 297. | 0.490 |
| 1003. | 0.10 | 7.29 | 0.278 | 0.200 | 0.079 | 0.28 | 29.35 | 16.33 | 62.29 | 2.12 | 186670. | 297. | 0.486 |
| 906. | 0.25 | 10.50 | 0.611 | 0.531 | 0.080 | 0.13 | 19.00 | 13.53 | 55.46 | 2.92 | 153700. | 291. | 0.470 |
| 907. | 0.25 | 10.07 | 0.598 | 0.549 | 0.048 | 0.08 | 19.43 | 15.62 | 62.70 | 3.23 | 39380. | 291. | 0.490 |
| 908. | 0.25 | 10.04 | 0.614 | 0.581 | 0.033 | 0.05 | 18.85 | 16.29 | 63.45 | 3.37 | 35660. | 291. | 0.490 |
| 909. | 0.25 | 9.86 | 0.602 | 0.581 | 0.021 | 0.03 | 19.23 | 17.51 | 66.86 | 3.48 | 14670. | 291. | 0.499 |
| 910. | 0.25 | 10.04 | 0.604 | 0.591 | 0.013 | 0.02 | 19.17 | 17.90 | 78.18 | 4.08 | 7550. | 291. | 0.490 |
| 941. | 0.25 | 10.42 | 0.613 | 0.603 | 0.010 | 0.02 | 18.85 | 17.95 | 71.87 | 3.81 | 3590. | 298. | 0.483 |
| 942. | 0.25 | 10.48 | 0.613 | 0.579 | 0.034 | 0.05 | 18.85 | 16.19 | 64.79 | 3.44 | 35900. | 298. | 0.480 |
| 943. | 0.25 | 10.70 | 0.613 | 0.564 | 0.049 | 0.08 | 18.85 | 15.06 | 62.35 | 3.31 | 39010. | 298. | 0.470 |
| 944. | 0.26 | 10.70 | 0.622 | 0.560 | 0.062 | 0.10 | 18.57 | 14.06 | 59.32 | 3.19 | 68280. | 298. | 0.470 |
| 960. | 0.25 | 10.06 | 0.600 | 0.579 | 0.021 | 0.03 | 19.18 | 17.39 | 68.82 | 3.59 | 17660. | 291. | 0.486 |
| 961. | 0.25 | 10.44 | 0.600 | 0.542 | 0.058 | 0.10 | 19.24 | 14.64 | 62.11 | 3.23 | 68520. | 291. | 0.470 |
| 980. | 0.25 | 10.16 | 0.607 | 0.597 | 0.010 | 0.02 | 18.93 | 17.88 | 83.84 | 4.43 | 1570. | 291. | 0.480 |
| 981. | 0.25 | 9.86 | 0.607 | 0.581 | 0.026 | 0.04 | 18.93 | 16.68 | 69.37 | 3.67 | 21590. | 291. | 0.495 |
| 885. | 0.25 | 2.45 | 0.520 | 0.440 | 0.080 | 0.15 | 5.44 | 1.76 | 25.85 | 4.75 | 41110. | 291. | 0.490 |
| 886. | 0.26 | 2.39 | 0.533 | 0.477 | 0.056 | 0.10 | 5.25 | 2.72 | 26.93 | 5.13 | 34660. | 291. | 0.497 |
| 887. | 0.26 | 2.42 | 0.530 | 0.497 | 0.033 | 0.06 | 5.29 | 3.51 | 32.26 | 6.10 | 13340. | 291. | 0.492 |
| 888. | 0.26 | 2.47 | 0.535 | 0.512 | 0.023 | 0.04 | 5.23 | 3.90 | 34.16 | 6.53 | 7970. | 291. | 0.482 |
| 889. | 0.26 | 2.43 | 0.535 | 0.520 | 0.015 | 0.03 | 5.23 | 4.29 | 37.07 | 7.09 | 3640. | 291. | 0.490 |

Table D.11 (cont.): Present Air-Water Flow Data: $D_3/D_1$ = 0.2, Horizontal Branch ($\Phi$ = 90°).

| RUN # | VsL1 (m/s) | VsG1 (m/s) | m1 (kg/s) | m2 (kg/s) | m3 (kg/s) | m3/m1 (-) | x1 (%) | x2 (%) | x3 (%) | x3/x1 (-) | p13 (Pa) | T1 (K) | p1 (MPa) |
|---|---|---|---|---|---|---|---|---|---|---|---|---|---|
| 978. | 0.25 | 2.52 | 0.510 | 0.490 | 0.021 | 0.04 | 5.59 | 4.00 | 43.27 | 7.75 | 9090. | 291. | 0.480 |
| 979. | 0.25 | 2.58 | 0.510 | 0.453 | 0.057 | 0.11 | 5.59 | 2.65 | 28.72 | 5.14 | 23460. | 291. | 0.470 |
| 791. | 0.26 | 4.91 | 0.557 | 0.548 | 0.008 | 0.02 | 9.50 | 8.48 | 76.22 | 8.02 | 4957. | 299. | 0.470 |
| 792. | 0.26 | 5.03 | 0.557 | 0.544 | 0.012 | 0.02 | 9.50 | 8.19 | 68.45 | 7.20 | 5998. | 299. | 0.459 |
| 793. | 0.26 | 5.02 | 0.557 | 0.539 | 0.017 | 0.03 | 9.50 | 7.82 | 62.48 | 6.57 | 9737. | 299. | 0.460 |
| 794. | 0.26 | 4.75 | 0.557 | 0.524 | 0.032 | 0.06 | 9.50 | 6.92 | 51.34 | 5.40 | 25643. | 299. | 0.486 |
| 795. | 0.26 | 5.08 | 0.557 | 0.508 | 0.048 | 0.09 | 9.50 | 6.20 | 44.15 | 4.65 | 30860. | 299. | 0.455 |
| 796. | 0.25 | 5.30 | 0.547 | 0.481 | 0.066 | 0.12 | 9.67 | 5.32 | 41.06 | 4.25 | 59500. | 299. | 0.436 |
| 797. | 0.24 | 4.84 | 0.531 | 0.438 | 0.094 | 0.18 | 9.95 | 4.13 | 37.19 | 3.74 | 99880. | 299. | 0.477 |
| 798. | 0.24 | 4.81 | 0.531 | 0.427 | 0.104 | 0.20 | 9.95 | 3.64 | 35.92 | 3.61 | 143950. | 299. | 0.480 |
| 880. | 0.25 | 5.02 | 0.544 | 0.531 | 0.013 | 0.02 | 10.50 | 9.02 | 69.79 | 6.65 | 6180. | 291. | 0.483 |
| 881. | 0.25 | 5.02 | 0.544 | 0.516 | 0.028 | 0.05 | 10.50 | 8.08 | 55.03 | 5.24 | 20720. | 291. | 0.483 |
| 882. | 0.25 | 5.02 | 0.550 | 0.505 | 0.045 | 0.08 | 10.38 | 7.05 | 47.28 | 4.56 | 25930. | 291. | 0.483 |
| 883. | 0.25 | 4.95 | 0.542 | 0.477 | 0.065 | 0.12 | 10.54 | 6.08 | 43.16 | 4.09 | 49880. | 291. | 0.490 |
| 884. | 0.25 | 5.03 | 0.542 | 0.431 | 0.111 | 0.20 | 10.54 | 3.91 | 36.39 | 3.45 | 158020. | 291. | 0.482 |
| 976. | 0.25 | 5.02 | 0.549 | 0.510 | 0.039 | 0.07 | 10.44 | 7.43 | 50.31 | 4.82 | 19140. | 291. | 0.485 |
| 977. | 0.24 | 4.97 | 0.536 | 0.523 | 0.013 | 0.02 | 10.69 | 9.16 | 74.90 | 7.00 | 5330. | 291. | 0.490 |
| 683. | 0.51 | 10.80 | 1.110 | 1.092 | 0.018 | 0.02 | 10.39 | 10.00 | 33.89 | 3.26 | 4255. | 298. | 0.465 |
| 684. | 0.51 | 11.16 | 1.114 | 1.079 | 0.035 | 0.03 | 10.36 | 9.54 | 36.02 | 3.48 | 20420. | 298. | 0.450 |
| 685. | 0.52 | 11.65 | 1.141 | 1.074 | 0.068 | 0.06 | 10.11 | 8.53 | 35.25 | 3.49 | 48150. | 298. | 0.431 |
| 776. | 0.52 | 10.47 | 1.132 | 1.059 | 0.073 | 0.06 | 9.90 | 8.11 | 35.98 | 3.64 | 50250. | 301. | 0.470 |
| 779. | 0.52 | 10.32 | 1.123 | 1.109 | 0.014 | 0.01 | 10.03 | 9.85 | 23.34 | 2.33 | 3149. | 295. | 0.470 |
| 780. | 0.51 | 10.06 | 1.104 | 1.082 | 0.023 | 0.02 | 10.19 | 9.74 | 31.77 | 3.12 | 7200. | 295. | 0.482 |
| 781. | 0.52 | 10.28 | 1.126 | 1.093 | 0.033 | 0.03 | 10.00 | 9.32 | 32.54 | 3.25 | 16446. | 295. | 0.472 |
| 782. | 0.52 | 10.17 | 1.123 | 1.069 | 0.054 | 0.05 | 10.03 | 8.74 | 35.63 | 3.55 | 24940. | 295. | 0.477 |
| 783. | 0.52 | 10.32 | 1.137 | 1.040 | 0.097 | 0.09 | 9.90 | 7.35 | 37.35 | 3.77 | 114690. | 295. | 0.470 |
| 932. | 0.50 | 10.07 | 1.086 | 1.038 | 0.048 | 0.04 | 10.55 | 9.09 | 41.93 | 3.97 | 24200. | 298. | 0.495 |
| 933. | 0.51 | 10.39 | 1.106 | 1.082 | 0.025 | 0.02 | 10.36 | 9.73 | 37.70 | 3.64 | 12040. | 298. | 0.480 |
| 962. | 0.51 | 10.32 | 1.118 | 1.034 | 0.083 | 0.07 | 10.30 | 7.89 | 40.13 | 3.90 | 85560. | 301. | 0.490 |
| 963. | 0.51 | 10.30 | 1.118 | 1.077 | 0.041 | 0.04 | 10.30 | 9.17 | 39.94 | 3.88 | 16300. | 301. | 0.491 |

Table D.11 (cont.): Present Air-Water Flow Data: $D_3/D_1$ = 0.2, Horizontal Branch ($\Phi$ = 90°).

| RUN # | VsL1 (m/s) | VsG1 (m/s) | m1 (kg/s) | m2 (kg/s) | m3 (kg/s) | m3/m1 (-) | x1 (%) | x2 (%) | x3 (%) | x3/x1 (-) | p13 (Pa) | T1 (K) | p1 (MPa) |
|---|---|---|---|---|---|---|---|---|---|---|---|---|---|
| 679. | 0.51 | 20.74 | 1.214 | 1.131 | 0.084 | 0.07 | 18.45 | 16.72 | 41.82 | 2.27 | 99140. | 298. | 0.470 |
| 680. | 0.51 | 20.74 | 1.214 | 1.145 | 0.070 | 0.06 | 18.45 | 17.12 | 40.21 | 2.18 | 53700. | 298. | 0.470 |
| 681. | 0.51 | 21.66 | 1.221 | 1.187 | 0.034 | 0.03 | 18.35 | 17.94 | 33.04 | 1.80 | 7012. | 298. | 0.450 |
| 682. | 0.50 | 21.42 | 1.211 | 1.192 | 0.019 | 0.02 | 18.49 | 18.28 | 31.41 | 1.70 | 3915. | 298. | 0.455 |
| 775. | 0.53 | 20.21 | 1.258 | 1.193 | 0.065 | 0.05 | 17.54 | 16.25 | 41.02 | 2.34 | 50370. | 301. | 0.480 |
| 930. | 0.50 | 20.82 | 1.212 | 1.133 | 0.079 | 0.07 | 18.94 | 17.22 | 43.69 | 2.31 | 95060. | 298. | 0.480 |
| 931. | 0.50 | 20.39 | 1.209 | 1.148 | 0.061 | 0.05 | 18.99 | 17.83 | 40.66 | 2.14 | 45060. | 298. | 0.490 |
| 934. | 0.50 | 20.44 | 1.202 | 1.174 | 0.028 | 0.02 | 19.16 | 18.80 | 34.28 | 1.79 | 12590. | 298. | 0.490 |
| 940. | 0.49 | 20.69 | 1.184 | 1.161 | 0.023 | 0.02 | 19.57 | 19.29 | 33.54 | 1.71 | 8160. | 298. | 0.487 |
| 968. | 0.49 | 19.82 | 1.186 | 1.133 | 0.053 | 0.04 | 18.75 | 17.19 | 51.87 | 2.77 | 47410. | 293. | 0.480 |
| 969. | 0.48 | 19.57 | 1.163 | 1.135 | 0.028 | 0.02 | 19.11 | 18.39 | 48.69 | 2.55 | 8640. | 293. | 0.486 |
| 807. | 0.52 | 2.61 | 1.047 | 1.023 | 0.024 | 0.02 | 2.64 | 2.17 | 22.49 | 8.50 | 5892. | 297. | 0.460 |
| 808. | 0.52 | 2.53 | 1.043 | 0.997 | 0.046 | 0.04 | 2.66 | 1.82 | 20.97 | 7.89 | 16365. | 297. | 0.475 |
| 809. | 0.52 | 2.58 | 1.043 | 0.984 | 0.059 | 0.06 | 2.66 | 1.56 | 21.07 | 7.93 | 30660. | 297. | 0.465 |
| 810. | 0.53 | 2.65 | 1.061 | 0.979 | 0.082 | 0.08 | 2.61 | 1.14 | 20.24 | 7.75 | 32470. | 297. | 0.454 |
| 811. | 0.53 | 2.61 | 1.061 | 0.917 | 0.144 | 0.14 | 2.61 | 0.51 | 15.96 | 6.11 | 74200. | 297. | 0.460 |
| 915. | 0.50 | 2.41 | 1.000 | 0.963 | 0.037 | 0.04 | 2.84 | 2.03 | 24.08 | 8.48 | 13160. | 291. | 0.501 |
| 916. | 0.50 | 2.39 | 1.000 | 0.903 | 0.096 | 0.10 | 2.84 | 0.92 | 20.84 | 7.33 | 41110. | 291. | 0.504 |
| 972. | 0.50 | 2.52 | 1.010 | 0.906 | 0.104 | 0.10 | 2.89 | 0.91 | 20.13 | 6.96 | 52840. | 291. | 0.492 |
| 973. | 0.51 | 2.62 | 1.033 | 0.998 | 0.036 | 0.03 | 2.83 | 2.02 | 25.29 | 8.95 | 13010. | 295. | 0.480 |
| 800. | 0.50 | 5.16 | 1.035 | 1.015 | 0.020 | 0.02 | 5.36 | 4.86 | 31.28 | 5.83 | 5986. | 299. | 0.470 |
| 801. | 0.50 | 5.10 | 1.035 | 1.009 | 0.026 | 0.03 | 5.36 | 4.64 | 33.33 | 6.22 | 9958. | 299. | 0.475 |
| 802. | 0.50 | 5.08 | 1.034 | 0.981 | 0.053 | 0.05 | 5.33 | 3.88 | 32.01 | 6.01 | 21235. | 303. | 0.480 |
| 803. | 0.50 | 5.08 | 1.034 | 0.950 | 0.085 | 0.08 | 5.33 | 3.05 | 30.75 | 5.77 | 55190. | 303. | 0.480 |
| 804. | 0.51 | 5.13 | 1.059 | 0.948 | 0.111 | 0.11 | 5.20 | 2.26 | 30.21 | 5.81 | 110740. | 303. | 0.475 |
| 805. | 0.52 | 5.30 | 1.075 | 0.952 | 0.123 | 0.11 | 5.13 | 1.92 | 29.91 | 5.83 | 188150. | 303. | 0.460 |
| 917. | 0.50 | 4.85 | 1.041 | 1.009 | 0.032 | 0.03 | 5.47 | 4.57 | 34.39 | 6.28 | 15810. | 291. | 0.499 |
| 918. | 0.52 | 5.09 | 1.070 | 0.985 | 0.085 | 0.08 | 5.32 | 3.15 | 30.33 | 5.70 | 54320. | 291. | 0.476 |
| 970. | 0.50 | 5.06 | 1.037 | 1.009 | 0.028 | 0.03 | 5.58 | 4.82 | 32.78 | 5.87 | 12600. | 291. | 0.486 |
| 971. | 0.50 | 5.01 | 1.044 | 0.962 | 0.082 | 0.08 | 5.55 | 3.40 | 30.78 | 5.55 | 48400. | 291. | 0.491 |

Table D.11 (cont.): Present Air-Water Flow Data: $D_3/D_1$ = 0.2, Horizontal Branch ($\Phi$ = 90°).

| RUN # | VsL1 (m/s) | VsG1 (m/s) | m1 (kg/s) | m2 (kg/s) | m3 (kg/s) | m3/m1 (-) | x1 (%) | x2 (%) | x3 (%) | x3/x1 (-) | p13 (Pa) | T1 (K) | p1 (MPa) |
|---|---|---|---|---|---|---|---|---|---|---|---|---|---|
| 769. | 0.99 | 9.97 | 2.057 | 2.016 | 0.042 | 0.02 | 5.41 | 5.24 | 13.27 | 2.46 | 10970. | 301. | 0.490 |
| 770. | 0.99 | 9.60 | 2.054 | 2.022 | 0.032 | 0.02 | 5.41 | 5.27 | 14.27 | 2.64 | 7813. | 301. | 0.509 |
| 771. | 0.98 | 10.00 | 2.037 | 1.955 | 0.082 | 0.04 | 5.41 | 4.94 | 16.71 | 3.09 | 25930. | 301. | 0.485 |
| 772. | 0.99 | 10.10 | 2.044 | 1.977 | 0.066 | 0.03 | 5.40 | 5.03 | 16.28 | 3.02 | 15062. | 301. | 0.480 |
| 773. | 0.99 | 10.32 | 2.053 | 1.939 | 0.114 | 0.06 | 5.37 | 4.55 | 19.33 | 3.60 | 63580. | 301. | 0.470 |
| 925. | 1.00 | 10.10 | 2.083 | 1.931 | 0.152 | 0.07 | 5.58 | 4.49 | 19.42 | 3.48 | 119630. | 291. | 0.489 |
| 926. | 1.00 | 10.10 | 2.083 | 1.972 | 0.111 | 0.05 | 5.58 | 4.86 | 18.37 | 3.29 | 50980. | 291. | 0.489 |
| 936. | 0.99 | 10.33 | 2.055 | 2.003 | 0.052 | 0.03 | 5.64 | 5.44 | 13.33 | 2.36 | 15910. | 298. | 0.488 |
| 937. | 0.99 | 10.39 | 2.055 | 2.020 | 0.035 | 0.02 | 5.64 | 5.51 | 12.65 | 2.24 | 6880. | 298. | 0.485 |
| 964. | 1.00 | 10.50 | 2.082 | 1.995 | 0.087 | 0.04 | 5.53 | 5.15 | 14.28 | 2.58 | 39990. | 301. | 0.482 |
| 965. | 1.00 | 10.50 | 2.082 | 2.023 | 0.058 | 0.03 | 5.53 | 5.29 | 13.91 | 2.52 | 18830. | 301. | 0.482 |
| 927. | 1.01 | 20.28 | 2.201 | 2.089 | 0.112 | 0.05 | 10.45 | 10.09 | 17.26 | 1.65 | 51000. | 291. | 0.482 |
| 928. | 1.00 | 20.24 | 2.196 | 2.085 | 0.111 | 0.05 | 10.52 | 10.16 | 17.28 | 1.64 | 50900. | 291. | 0.485 |
| 929. | 1.00 | 20.24 | 2.194 | 2.058 | 0.136 | 0.06 | 10.53 | 9.93 | 19.63 | 1.86 | 112000. | 291. | 0.485 |
| 935. | 0.98 | 20.36 | 2.157 | 2.100 | 0.057 | 0.03 | 10.67 | 10.63 | 12.20 | 1.14 | 16300. | 298. | 0.492 |
| 938. | 0.98 | 20.33 | 2.146 | 2.108 | 0.038 | 0.02 | 10.77 | 10.76 | 11.79 | 1.09 | 5800. | 298. | 0.495 |
| 939. | 0.98 | 20.57 | 2.146 | 2.092 | 0.055 | 0.03 | 10.79 | 10.71 | 13.70 | 1.27 | 14500. | 298. | 0.490 |
| 966. | 0.99 | 20.14 | 2.157 | 2.116 | 0.042 | 0.02 | 10.31 | 10.08 | 21.68 | 2.10 | 15300. | 301. | 0.485 |
| 967. | 0.99 | 20.36 | 2.167 | 2.080 | 0.086 | 0.04 | 10.26 | 9.50 | 28.64 | 2.79 | 58800. | 301. | 0.480 |
| 774. | 1.00 | 19.72 | 2.172 | 2.050 | 0.122 | 0.06 | 10.16 | 9.77 | 16.77 | 1.65 | 64500. | 301. | 0.492 |
| 686. | 0.99 | 22.74 | 2.167 | 2.045 | 0.121 | 0.06 | 10.33 | 9.90 | 17.63 | 1.71 | 103400. | 298. | 0.428 |
| 687. | 0.99 | 22.74 | 2.167 | 2.055 | 0.111 | 0.05 | 10.33 | 10.05 | 15.54 | 1.50 | 71000. | 298. | 0.428 |
| 688. | 0.99 | 22.74 | 2.167 | 2.096 | 0.070 | 0.03 | 10.33 | 10.25 | 12.58 | 1.22 | 23300. | 298. | 0.428 |
| 689. | 0.99 | 22.74 | 2.167 | 2.105 | 0.061 | 0.03 | 10.33 | 10.30 | 11.40 | 1.10 | 15700. | 298. | 0.428 |
| 813. | 1.00 | 2.57 | 1.990 | 1.937 | 0.053 | 0.03 | 1.37 | 1.18 | 8.32 | 6.09 | 10360. | 311. | 0.480 |
| 814. | 1.02 | 2.65 | 2.017 | 1.932 | 0.085 | 0.04 | 1.35 | 1.01 | 9.07 | 6.73 | 23828. | 311. | 0.465 |
| 815. | 1.02 | 2.69 | 2.033 | 1.912 | 0.121 | 0.06 | 1.34 | 0.88 | 8.57 | 6.41 | 30370. | 311. | 0.460 |
| 816. | 1.02 | 2.58 | 2.033 | 1.816 | 0.217 | 0.11 | 1.34 | 0.55 | 7.96 | 5.93 | 71110. | 311. | 0.480 |
| 817. | 1.00 | 2.53 | 1.986 | 1.719 | 0.267 | 0.13 | 1.37 | 0.42 | 7.50 | 5.46 | 125310. | 311. | 0.490 |
| 818. | 1.01 | 2.56 | 1.995 | 1.682 | 0.314 | 0.16 | 1.37 | 0.39 | 6.59 | 4.81 | 200250. | 311. | 0.485 |

Table D.11 (cont.): Present Air-Water Flow Data: $D_3/D_1$ = 0.2, Horizontal Branch ($\Phi$ = 90°).

| RUN # | VsL1 (m/s) | VsG1 (m/s) | m1 (kg/s) | m2 (kg/s) | m3 (kg/s) | m3/m1 (-) | x1 (%) | x2 (%) | x3 (%) | x3/x1 (-) | p13 (Pa) | T1 (K) | p1 (MPa) |
|---|---|---|---|---|---|---|---|---|---|---|---|---|---|
| 974. | 1.02 | 2.53 | 2.024 | 1.959 | 0.065 | 0.03 | 1.44 | 1.11 | 11.44 | 7.93 | 22040. | 291. | 0.490 |
| 975. | 1.01 | 2.49 | 1.999 | 1.861 | 0.138 | 0.07 | 1.46 | 0.78 | 10.67 | 7.30 | 38150. | 291. | 0.498 |
| 785. | 1.00 | 33.98 | 2.357 | 2.302 | 0.055 | 0.02 | 16.56 | 16.66 | 12.36 | 0.75 | 15100. | 295. | 0.495 |
| 786. | 1.01 | 34.32 | 2.360 | 2.287 | 0.073 | 0.03 | 16.54 | 16.71 | 11.29 | 0.68 | 24600. | 295. | 0.490 |
| 787. | 1.01 | 34.88 | 2.369 | 2.266 | 0.103 | 0.04 | 16.48 | 16.64 | 13.06 | 0.79 | 33900. | 295. | 0.482 |
| 788. | 1.01 | 34.60 | 2.365 | 2.263 | 0.102 | 0.04 | 16.51 | 16.48 | 17.18 | 1.04 | 60100. | 295. | 0.486 |
| 789. | 1.01 | 36.13 | 2.377 | 2.226 | 0.151 | 0.06 | 16.43 | 16.42 | 16.50 | 1.00 | 139300. | 295. | 0.465 |
| 919. | 1.00 | 4.87 | 2.020 | 1.964 | 0.056 | 0.03 | 2.82 | 2.50 | 14.01 | 4.96 | 17500. | 291. | 0.498 |
| 920. | 0.98 | 4.85 | 1.972 | 1.935 | 0.037 | 0.02 | 2.89 | 2.73 | 11.54 | 3.99 | 7150. | 291. | 0.500 |
| 921. | 0.98 | 4.85 | 1.976 | 1.930 | 0.046 | 0.02 | 2.88 | 2.63 | 13.62 | 4.72 | 11830. | 291. | 0.500 |
| 922. | 0.99 | 4.87 | 1.992 | 1.914 | 0.078 | 0.04 | 2.86 | 2.38 | 14.77 | 5.16 | 33060. | 291. | 0.497 |
| 923. | 0.99 | 4.94 | 2.004 | 1.890 | 0.114 | 0.06 | 2.84 | 1.99 | 17.06 | 6.00 | 47280. | 291. | 0.490 |
| 924. | 1.01 | 5.13 | 2.035 | 1.867 | 0.169 | 0.08 | 2.80 | 1.44 | 17.83 | 6.37 | 160620. | 291. | 0.472 |
| 713. | 0.06 | 5.22 | 0.169 | 0.161 | 0.008 | 0.05 | 33.23 | 30.06 | 96.56 | 2.91 | 3743. | 293. | 0.461 |
| 714. | 0.06 | 5.20 | 0.169 | 0.156 | 0.013 | 0.08 | 33.23 | 28.57 | 89.30 | 2.69 | 7782. | 293. | 0.463 |
| 715. | 0.06 | 5.11 | 0.169 | 0.145 | 0.024 | 0.14 | 33.16 | 26.74 | 71.49 | 2.16 | 21071. | 293. | 0.468 |
| 716. | 0.06 | 5.20 | 0.169 | 0.129 | 0.040 | 0.24 | 33.16 | 22.94 | 65.76 | 1.98 | 29380. | 293. | 0.461 |
| 717. | 0.06 | 5.51 | 0.177 | 0.132 | 0.045 | 0.25 | 31.81 | 21.22 | 62.90 | 1.98 | 47650. | 293. | 0.436 |
| 718. | 0.06 | 5.39 | 0.177 | 0.116 | 0.061 | 0.35 | 31.81 | 17.24 | 59.40 | 1.87 | 87650. | 293. | 0.446 |
| 719. | 0.06 | 5.15 | 0.171 | 0.087 | 0.084 | 0.49 | 32.81 | 20.99 | 44.98 | 1.37 | 163580. | 293. | 0.466 |
| 720. | 0.06 | 5.03 | 0.171 | 0.058 | 0.113 | 0.66 | 32.73 | 29.16 | 34.57 | 1.06 | 183210. | 293. | 0.475 |
| 721. | 0.06 | 4.98 | 0.171 | 0.057 | 0.114 | 0.66 | 32.73 | 29.87 | 34.17 | 1.04 | 200250. | 293. | 0.480 |
| 857. | 0.06 | 4.96 | 0.172 | 0.156 | 0.016 | 0.09 | 33.57 | 28.32 | 84.57 | 2.52 | 10410. | 291. | 0.494 |
| 858. | 0.06 | 5.24 | 0.175 | 0.153 | 0.022 | 0.13 | 33.20 | 26.47 | 80.25 | 2.42 | 15900. | 291. | 0.470 |
| 859. | 0.06 | 5.17 | 0.170 | 0.159 | 0.011 | 0.06 | 33.63 | 29.59 | 94.34 | 2.81 | 5090. | 291. | 0.470 |
| 860. | 0.05 | 5.00 | 0.163 | 0.118 | 0.045 | 0.28 | 35.07 | 22.86 | 66.69 | 1.90 | 38390. | 291. | 0.486 |
| 861. | 0.05 | 5.02 | 0.159 | 0.043 | 0.116 | 0.73 | 35.96 | 29.34 | 38.41 | 1.07 | 185430. | 291. | 0.483 |
| 986. | 0.05 | 5.08 | 0.158 | 0.101 | 0.057 | 0.36 | 35.63 | 21.93 | 59.98 | 1.68 | 58520. | 299. | 0.484 |
| 987. | 0.05 | 4.97 | 0.158 | 0.129 | 0.029 | 0.19 | 35.63 | 26.21 | 76.79 | 2.16 | 16300. | 299. | 0.495 |
| 750. | 0.06 | 5.10 | 0.153 | 0.150 | 0.004 | 0.02 | 22.74 | 21.25 | 85.88 | 3.78 | 4900. | 294. | 0.294 |

Table D.11 (cont.): Present Air-Water Flow Data: $D_3/D_1$ = 0.2, Horizontal Branch ($\Phi$ = 90°).

| RUN # | VsL1 (m/s) | VsG1 (m/s) | m1 (kg/s) | m2 (kg/s) | m3 (kg/s) | m3/m1 (-) | x1 (%) | x2 (%) | x3 (%) | x3/x1 (-) | p13 (Pa) | T1 (K) | p1 (MPa) |
|---|---|---|---|---|---|---|---|---|---|---|---|---|---|
| 751. | 0.06 | 5.03 | 0.154 | 0.149 | 0.006 | 0.04 | 22.63 | 20.25 | 86.80 | 3.84 | 5650. | 294. | 0.298 |
| 752. | 0.06 | 5.18 | 0.161 | 0.152 | 0.009 | 0.06 | 21.72 | 18.13 | 81.88 | 3.77 | 7220. | 294. | 0.289 |
| 753. | 0.06 | 5.10 | 0.161 | 0.143 | 0.018 | 0.11 | 21.72 | 16.43 | 64.75 | 2.98 | 17640. | 294. | 0.294 |
| 754. | 0.06 | 5.10 | 0.161 | 0.135 | 0.025 | 0.16 | 21.72 | 14.86 | 58.25 | 2.68 | 30460. | 294. | 0.294 |
| 755. | 0.06 | 5.37 | 0.161 | 0.122 | 0.038 | 0.24 | 21.72 | 12.19 | 51.95 | 2.39 | 45560. | 294. | 0.279 |
| 862. | 0.05 | 4.76 | 0.132 | 0.045 | 0.088 | 0.66 | 26.04 | 24.21 | 26.97 | 1.04 | 117280. | 291. | 0.308 |
| 863. | 0.04 | 4.90 | 0.118 | 0.061 | 0.057 | 0.48 | 29.14 | 26.57 | 31.87 | 1.09 | 57040. | 291. | 0.299 |
| 864. | 0.05 | 5.13 | 0.136 | 0.122 | 0.014 | 0.10 | 25.33 | 19.84 | 73.46 | 2.90 | 12670. | 291. | 0.286 |
| 865. | 0.04 | 4.99 | 0.118 | 0.091 | 0.027 | 0.23 | 29.14 | 21.33 | 55.56 | 1.91 | 32620. | 291. | 0.294 |
| 866. | 0.05 | 4.76 | 0.131 | 0.122 | 0.009 | 0.07 | 26.42 | 22.16 | 87.15 | 3.30 | 4760. | 291. | 0.308 |
| 696. | 0.06 | 5.33 | 0.146 | 0.142 | 0.004 | 0.03 | 16.35 | 14.71 | 72.99 | 4.47 | 5900. | 293. | 0.192 |
| 697. | 0.06 | 5.50 | 0.146 | 0.133 | 0.014 | 0.09 | 16.35 | 12.26 | 56.21 | 3.44 | 14471. | 293. | 0.186 |
| 698. | 0.06 | 5.30 | 0.143 | 0.126 | 0.018 | 0.12 | 16.66 | 11.38 | 54.50 | 3.27 | 30860. | 293. | 0.193 |
| 699. | 0.06 | 4.04 | 0.133 | 0.017 | 0.116 | 0.87 | 17.80 | 70.75 | 10.14 | 0.57 | 77650. | 293 | 0.250 |
| 707. | 0.06 | 4.76 | 0.135 | 0.107 | 0.028 | 0.21 | 16.85 | 13.63 | 29.03 | 1.72 | 22313. | 293. | 0.204 |
| 708. | 0.06 | 4.60 | 0.135 | 0.092 | 0.043 | 0.32 | 16.79 | 14.38 | 21.96 | 1.31 | 37880. | 293. | 0.210 |
| 709. | 0.06 | 4.65 | 0.137 | 0.088 | 0.049 | 0.36 | 16.62 | 14.96 | 19.62 | 1.18 | 34940. | 293. | 0.209 |
| 711. | 0.06 | 4.40 | 0.135 | 0.128 | 0.008 | 0.06 | 16.56 | 14.71 | 47.20 | 2.85 | 5078. | 293. | 0.218 |
| 737. | 0.06 | 5.34 | 0.148 | 0.102 | 0.046 | 0.31 | 16.53 | 11.60 | 27.45 | 1.66 | 53210. | 294. | 0.196 |

Table D.11 (cont.): Present Air-Water Flow Data: $D_3/D_1$ = 0.2, Horizontal Branch ($\Phi$ = 90°).

| RUN # | VsL1 (m/s) | VsG1 (m/s) | m1 (kg/s) | m2 (kg/s) | m3 (kg/s) | m3/m1 (-) | x1 (%) | x2 (%) | x3 (%) | x3/x1 (-) | p13 (Pa) | T1 (K) | p1 (MPa) |
|---|---|---|---|---|---|---|---|---|---|---|---|---|---|
| 2112. | 0.10 | 5.04 | 0.299 | 0.296 | 0.003 | 0.01 | 34.09 | 33.47 | 97.70 | 2.87 | -361. | 297. | 0.877 |
| 2113. | 0.10 | 5.01 | 0.296 | 0.287 | 0.009 | 0.03 | 34.05 | 32.10 | 99.22 | 2.91 | 660. | 299. | 0.877 |
| 2114. | 0.10 | 4.89 | 0.291 | 0.274 | 0.017 | 0.06 | 34.13 | 30.17 | 99.60 | 2.92 | 3504. | 299. | 0.887 |
| 2115. | 0.10 | 5.04 | 0.298 | 0.251 | 0.048 | 0.16 | 33.64 | 21.08 | 99.86 | 2.97 | 23612. | 302. | 0.877 |
| 2116. | 0.10 | 4.98 | 0.300 | 0.164 | 0.137 | 0.46 | 33.39 | 5.93 | 80.37 | 2.41 | 209088. | 302. | 0.887 |
| 2117. | 0.11 | 5.07 | 0.308 | 0.190 | 0.118 | 0.38 | 33.15 | 4.04 | 93.08 | 2.81 | 161748. | 302. | 0.887 |
| 2118. | 0.11 | 5.16 | 0.308 | 0.222 | 0.086 | 0.28 | 33.15 | 7.22 | 99.92 | 3.01 | 80132. | 302. | 0.872 |
| 2119. | 0.11 | 5.16 | 0.308 | 0.252 | 0.056 | 0.18 | 33.15 | 18.48 | 99.88 | 3.01 | 33000. | 302. | 0.872 |
| 2102. | 0.11 | 10.22 | 0.425 | 0.422 | 0.003 | 0.01 | 49.44 | 49.13 | 97.87 | 1.98 | -722. | 287. | 0.862 |
| 2103. | 0.11 | 10.34 | 0.427 | 0.419 | 0.008 | 0.02 | 50.56 | 49.69 | 95.46 | 1.89 | 612. | 290. | 0.882 |
| 2104. | 0.11 | 10.52 | 0.427 | 0.413 | 0.014 | 0.03 | 50.56 | 48.95 | 97.79 | 1.93 | 3215. | 290. | 0.867 |
| 2105. | 0.10 | 10.45 | 0.419 | 0.389 | 0.030 | 0.07 | 51.14 | 47.45 | 98.39 | 1.92 | 9684. | 291. | 0.872 |
| 2106. | 0.10 | 10.12 | 0.413 | 0.371 | 0.043 | 0.10 | 50.54 | 45.03 | 98.64 | 1.95 | 18104. | 291. | 0.877 |
| 2107. | 0.11 | 10.12 | 0.415 | 0.359 | 0.056 | 0.13 | 50.37 | 42.88 | 98.57 | 1.96 | 31450. | 291. | 0.877 |
| 2108. | 0.11 | 10.16 | 0.415 | 0.343 | 0.072 | 0.17 | 50.36 | 40.18 | 98.66 | 1.96 | 56120. | 292. | 0.877 |
| 2109. | 0.11 | 10.01 | 0.424 | 0.337 | 0.087 | 0.21 | 48.79 | 35.91 | 98.71 | 2.02 | 84116. | 292. | 0.882 |
| 2110. | 0.11 | 10.06 | 0.429 | 0.313 | 0.116 | 0.27 | 47.93 | 29.11 | 98.51 | 2.06 | 157180. | 295. | 0.882 |
| 2111. | 0.11 | 10.06 | 0.422 | 0.292 | 0.129 | 0.31 | 48.78 | 26.83 | 98.45 | 2.02 | 206432. | 295. | 0.882 |
| 2144. | 0.10 | 19.91 | 0.616 | 0.487 | 0.129 | 0.21 | 68.21 | 62.75 | 88.79 | 1.30 | 232980. | 286. | 0.882 |
| 2145. | 0.10 | 20.02 | 0.616 | 0.502 | 0.115 | 0.19 | 68.21 | 63.64 | 88.16 | 1.29 | 170180. | 286. | 0.877 |
| 2146. | 0.10 | 20.02 | 0.618 | 0.549 | 0.069 | 0.11 | 68.06 | 65.78 | 86.28 | 1.27 | 65068. | 286. | 0.877 |
| 2147. | 0.10 | 20.16 | 0.617 | 0.578 | 0.038 | 0.06 | 68.11 | 67.10 | 83.35 | 1.22 | 20290. | 290. | 0.882 |
| 2148. | 0.10 | 20.16 | 0.621 | 0.606 | 0.014 | 0.02 | 67.68 | 67.46 | 77.22 | 1.14 | 3660. | 290. | 0.882 |
| 2149. | 0.10 | 20.16 | 0.622 | 0.621 | 0.001 | 0.00 | 67.50 | 67.63 | 0.50 | 0.01 | 252. | 290. | 0.882 |
| 2150. | 0.10 | 20.18 | 0.424 | 0.358 | 0.066 | 0.16 | 53.88 | 47.75 | 87.12 | 1.62 | 122064. | 296. | 0.490 |
| 2151. | 0.10 | 20.18 | 0.423 | 0.369 | 0.054 | 0.13 | 54.05 | 49.35 | 86.19 | 1.59 | 63100. | 296. | 0.490 |
| 2152. | 0.10 | 19.77 | 0.422 | 0.390 | 0.032 | 0.08 | 54.09 | 51.47 | 85.58 | 1.58 | 20429. | 296. | 0.500 |
| 2120. | 0.25 | 5.13 | 0.599 | 0.596 | 0.003 | 0.01 | 17.52 | 17.08 | 99.97 | 5.71 | 182. | 295. | 0.882 |
| 2121. | 0.25 | 5.13 | 0.592 | 0.583 | 0.009 | 0.02 | 17.72 | 16.39 | 99.79 | 5.63 | 629. | 295. | 0.882 |
| 2122. | 0.25 | 4.97 | 0.596 | 0.577 | 0.019 | 0.03 | 17.09 | 14.38 | 99.79 | 5.84 | 4300. | 295. | 0.882 |

Table D.12: Present Air-Water Flow Data: $D_3/D_1$ = 0.2, Upward Branch ($\Phi$ = 0°).

| RUN # | VsL1 (m/s) | VsG1 (m/s) | m1 (kg/s) | m2 (kg/s) | m3 (kg/s) | m3/m1 (-) | x1 (%) | x2 (%) | x3 (%) | x3/x1 (-) | p13 (Pa) | T1 (K) | p1 (MPa) |
|---|---|---|---|---|---|---|---|---|---|---|---|---|---|
| 2123. | 0.25 | 4.94 | 0.596 | 0.556 | 0.040 | 0.07 | 17.09 | 11.19 | 99.75 | 5.84 | 16639. | 295. | 0.887 |
| 2124. | 0.25 | 5.10 | 0.590 | 0.535 | 0.055 | 0.09 | 17.45 | 9.02 | 99.67 | 5.71 | 31190. | 299. | 0.882 |
| 2125. | 0.25 | 5.19 | 0.596 | 0.521 | 0.074 | 0.12 | 17.23 | 5.45 | 99.72 | 5.79 | 63836. | 302. | 0.872 |
| 2126. | 0.25 | 5.09 | 0.597 | 0.497 | 0.100 | 0.17 | 17.04 | 0.47 | 99.91 | 5.86 | 104980. | 302. | 0.882 |
| 2127. | 0.25 | 5.15 | 0.590 | 0.470 | 0.120 | 0.20 | 17.46 | 2.21 | 94.39 | 5.41 | 174800. | 302. | 0.882 |
| 2128. | 0.25 | 5.21 | 0.590 | 0.463 | 0.128 | 0.22 | 17.46 | 2.12 | 88.33 | 5.06 | 197600. | 302. | 0.872 |
| 2129. | 0.25 | 5.21 | 0.590 | 0.463 | 0.128 | 0.22 | 17.46 | 1.71 | 86.86 | 4.97 | 207250. | 302. | 0.872 |
| 2091. | 0.25 | 10.06 | 0.702 | 0.700 | 0.002 | 0.00 | 30.01 | 29.86 | 96.92 | 3.23 | -97. | 288. | 0.882 |
| 2092. | 0.25 | 10.06 | 0.702 | 0.698 | 0.004 | 0.01 | 30.01 | 29.66 | 92.77 | 3.09 | 164. | 288. | 0.882 |
| 2093. | 0.25 | 9.97 | 0.697 | 0.677 | 0.020 | 0.03 | 29.97 | 28.14 | 93.16 | 3.11 | 4705. | 288. | 0.882 |
| 2094. | 0.26 | 10.06 | 0.714 | 0.675 | 0.039 | 0.06 | 29.49 | 25.49 | 98.09 | 3.33 | 15544. | 288. | 0.882 |
| 2095. | 0.26 | 10.25 | 0.722 | 0.674 | 0.048 | 0.07 | 28.92 | 24.13 | 96.52 | 3.34 | 25830. | 297. | 0.882 |
| 2096. | 0.26 | 10.25 | 0.722 | 0.659 | 0.063 | 0.09 | 28.92 | 22.60 | 95.10 | 3.29 | 46780. | 297. | 0.882 |
| 2097. | 0.26 | 10.25 | 0.722 | 0.649 | 0.072 | 0.10 | 28.92 | 21.46 | 96.03 | 3.32 | 67492. | 297. | 0.882 |
| 2098. | 0.26 | 10.25 | 0.722 | 0.637 | 0.084 | 0.12 | 28.92 | 20.19 | 94.74 | 3.28 | 86604. | 297. | 0.882 |
| 2099. | 0.26 | 10.25 | 0.722 | 0.620 | 0.101 | 0.14 | 28.92 | 18.34 | 93.60 | 3.24 | 120960. | 297. | 0.882 |
| 2100. | 0.25 | 10.31 | 0.699 | 0.577 | 0.122 | 0.17 | 29.70 | 16.30 | 93.22 | 3.14 | 186072. | 297. | 0.872 |
| 2101. | 0.25 | 10.31 | 0.699 | 0.568 | 0.131 | 0.19 | 29.70 | 14.82 | 94.04 | 3.17 | 212576. | 297. | 0.872 |
| 2033. | 0.50 | 7.44 | 1.135 | 1.131 | 0.004 | 0.00 | 13.74 | 13.53 | 71.28 | 5.19 | 1. | 288. | 0.882 |
| 2034. | 0.50 | 5.01 | 1.083 | 1.074 | 0.008 | 0.01 | 9.56 | 8.99 | 81.26 | 8.50 | 462. | 291. | 0.877 |
| 2035. | 0.50 | 5.01 | 1.083 | 1.068 | 0.014 | 0.01 | 9.56 | 8.52 | 86.64 | 9.07 | 2189. | 291. | 0.877 |
| 2036. | 0.50 | 5.01 | 1.083 | 1.050 | 0.033 | 0.03 | 9.56 | 7.02 | 90.19 | 9.44 | 10151. | 291. | 0.877 |
| 2037. | 0.50 | 5.01 | 1.083 | 1.038 | 0.044 | 0.04 | 9.56 | 5.92 | 94.64 | 9.90 | 20800. | 291. | 0.877 |
| 2038. | 0.50 | 5.01 | 1.083 | 1.007 | 0.076 | 0.07 | 9.56 | 3.55 | 89.05 | 9.32 | 66748. | 291. | 0.877 |
| 2039. | 0.50 | 5.01 | 1.083 | 0.974 | 0.109 | 0.10 | 9.56 | 0.47 | 91.06 | 9.53 | 130290. | 291. | 0.877 |
| 2040. | 0.50 | 5.01 | 1.083 | 0.954 | 0.129 | 0.12 | 9.56 | 0.97 | 87.13 | 9.12 | 187480. | 291. | 0.877 |
| 2041. | 0.50 | 5.04 | 1.083 | 0.942 | 0.141 | 0.13 | 9.56 | 1.16 | 81.44 | 8.52 | 210904. | 291. | 0.872 |
| 2130. | 0.50 | 5.14 | 1.038 | 1.036 | 0.002 | 0.00 | 5.61 | 5.44 | 99.74 | 17.78 | 99. | 296. | 0.490 |
| 2131. | 0.50 | 5.13 | 1.040 | 1.026 | 0.014 | 0.01 | 5.59 | 4.66 | 73.31 | 13.11 | 3111. | 296. | 0.490 |
| 2132. | 0.52 | 5.10 | 1.067 | 1.027 | 0.039 | 0.04 | 5.42 | 2.36 | 85.29 | 15.75 | 29760. | 296. | 0.490 |

Table D.12 (cont.): Present Air-Water Flow Data: $D_3/D_1$ = 0.2, Upward Branch ($\Phi$ = 0°).

| RUN # | VsL1 (m/s) | VsG1 (m/s) | m1 (kg/s) | m2 (kg/s) | m3 (kg/s) | m3/m1 (-) | x1 (%) | x2 (%) | x3 (%) | x3/x1 (-) | p13 (Pa) | T1 (K) | p1 (MPa) |
|---|---|---|---|---|---|---|---|---|---|---|---|---|---|
| 2133. | 0.51 | 5.07 | 1.056 | 0.992 | 0.064 | 0.06 | 5.44 | 0.65 | 79.81 | 14.67 | 68896. | 296. | 0.490 |
| 2134. | 0.51 | 4.78 | 1.055 | 0.947 | 0.108 | 0.10 | 5.39 | 0.42 | 48.91 | 9.07 | 104008. | 296. | 0.515 |
| 2000. | 0.53 | 10.01 | 1.249 | 1.228 | 0.021 | 0.02 | 16.66 | 15.82 | 66.38 | 3.98 | 3073. | 289. | 0.877 |
| 2001. | 0.53 | 10.01 | 1.249 | 1.202 | 0.047 | 0.04 | 16.66 | 14.33 | 76.36 | 4.58 | 23865. | 289. | 0.877 |
| 2002. | 0.53 | 10.01 | 1.249 | 1.184 | 0.065 | 0.05 | 16.66 | 13.27 | 78.60 | 4.72 | 42492. | 289. | 0.877 |
| 2003. | 0.53 | 10.01 | 1.249 | 1.169 | 0.080 | 0.06 | 16.66 | 12.50 | 77.67 | 4.66 | 65728. | 289. | 0.877 |
| 2004. | 0.53 | 10.01 | 1.249 | 1.145 | 0.104 | 0.08 | 16.66 | 11.01 | 79.11 | 4.75 | 120828. | 289. | 0.877 |
| 2005. | 0.53 | 10.01 | 1.249 | 1.125 | 0.124 | 0.10 | 16.66 | 9.47 | 81.85 | 4.91 | 184788. | 289. | 0.877 |
| 2006. | 0.53 | 10.01 | 1.249 | 1.115 | 0.134 | 0.11 | 16.66 | 8.77 | 82.49 | 4.95 | 224800. | 289. | 0.877 |
| 2042. | 0.51 | 20.01 | 1.407 | 1.400 | 0.007 | 0.00 | 29.06 | 29.02 | 37.26 | 1.28 | 363. | 294. | 0.877 |
| 2043. | 0.50 | 19.90 | 1.380 | 1.360 | 0.021 | 0.01 | 29.62 | 29.21 | 56.90 | 1.92 | 3490. | 294. | 0.882 |
| 2044. | 0.50 | 19.90 | 1.380 | 1.298 | 0.083 | 0.06 | 29.62 | 27.21 | 67.35 | 2.27 | 59652. | 294. | 0.882 |
| 2045. | 0.50 | 19.90 | 1.380 | 1.294 | 0.086 | 0.06 | 29.62 | 26.13 | 82.04 | 2.77 | 108112. | 294. | 0.882 |
| 2046. | 0.50 | 19.90 | 1.380 | 1.252 | 0.128 | 0.09 | 29.62 | 25.87 | 66.31 | 2.24 | 158400. | 294. | 0.882 |
| 2047. | 0.50 | 19.90 | 1.380 | 1.246 | 0.134 | 0.10 | 29.62 | 25.47 | 68.18 | 2.30 | 188504. | 294. | 0.882 |
| 2048. | 0.50 | 19.90 | 1.380 | 1.235 | 0.146 | 0.11 | 29.62 | 25.16 | 67.36 | 2.27 | 206880. | 294. | 0.882 |
| 2135. | 1.00 | 2.51 | 2.012 | 2.007 | 0.004 | 0.00 | 2.58 | 2.50 | 42.27 | 16.35 | 176. | 292. | 0.882 |
| 2136. | 1.00 | 2.56 | 2.013 | 1.947 | 0.067 | 0.03 | 2.63 | 1.50 | 35.55 | 13.51 | 13912. | 292. | 0.882 |
| 2137. | 1.00 | 2.59 | 2.012 | 1.895 | 0.117 | 0.06 | 2.63 | 1.02 | 28.69 | 10.91 | 32800. | 298. | 0.887 |
| 2138. | 1.00 | 2.59 | 2.014 | 1.637 | 0.377 | 0.19 | 2.59 | 0.47 | 11.74 | 4.54 | 128640. | 298. | 0.872 |
| 2139. | 1.00 | 2.59 | 2.014 | 1.717 | 0.297 | 0.15 | 2.59 | 0.68 | 13.62 | 5.27 | 79956. | 298. | 0.872 |
| 2140. | 1.01 | 2.58 | 2.026 | 1.878 | 0.148 | 0.07 | 2.56 | 0.61 | 27.35 | 10.70 | 55700. | 298. | 0.872 |
| 2141. | 1.00 | 2.59 | 2.006 | 1.545 | 0.460 | 0.23 | 2.57 | 0.49 | 9.56 | 3.71 | 95600. | 303. | 0.882 |
| 2142. | 1.00 | 2.59 | 2.006 | 1.461 | 0.544 | 0.27 | 2.57 | 0.45 | 8.26 | 3.21 | 228760. | 303. | 0.882 |
| 2143. | 1.00 | 2.59 | 2.006 | 1.461 | 0.544 | 0.27 | 2.57 | 0.45 | 8.26 | 3.21 | 241550. | 303. | 0.882 |
| 2015. | 1.00 | 5.16 | 2.061 | 2.057 | 0.003 | 0.00 | 5.14 | 5.01 | 86.86 | 16.90 | 350. | 291. | 0.872 |
| 2016. | 1.00 | 5.09 | 2.066 | 2.054 | 0.012 | 0.01 | 5.08 | 4.90 | 37.08 | 7.30 | 1035. | 291. | 0.877 |
| 2017. | 1.00 | 5.09 | 2.066 | 2.047 | 0.019 | 0.01 | 5.08 | 4.68 | 48.05 | 9.45 | 7685. | 291. | 0.877 |
| 2018. | 1.00 | 5.11 | 2.066 | 2.023 | 0.043 | 0.02 | 5.07 | 3.98 | 56.78 | 11.19 | 10934. | 293. | 0.877 |
| 2019. | 1.00 | 5.13 | 2.065 | 2.002 | 0.063 | 0.03 | 5.04 | 3.15 | 64.86 | 12.88 | 30628. | 296. | 0.877 |

Table D.12 (cont.): Present Air-Water Flow Data: $D_3/D_1$ = 0.2, Upward Branch ($\Phi$ = 0°).

| RUN # | VsL1 (m/s) | VsG1 (m/s) | m1 (kg/s) | m2 (kg/s) | m3 (kg/s) | m3/m1 (-) | x1 (%) | x2 (%) | x3 (%) | x3/x1 (-) | p13 (Pa) | T1 (K) | p1 (MPa) |
|---|---|---|---|---|---|---|---|---|---|---|---|---|---|
| 2020. | 0.99 | 5.13 | 2.039 | 1.960 | 0.079 | 0.04 | 5.10 | 2.39 | 72.02 | 14.12 | 55968. | 296. | 0.877 |
| 2021. | 0.99 | 5.13 | 2.039 | 1.925 | 0.114 | 0.06 | 5.10 | 1.31 | 68.92 | 13.51 | 121560. | 296. | 0.877 |
| 2022. | 0.99 | 5.13 | 2.039 | 1.899 | 0.140 | 0.07 | 5.10 | 0.75 | 64.27 | 12.60 | 175156. | 296. | 0.877 |
| 2023. | 0.99 | 5.13 | 2.039 | 1.858 | 0.181 | 0.09 | 5.10 | 0.69 | 50.32 | 9.87 | 209104. | 296. | 0.877 |
| 2024. | 0.99 | 5.13 | 2.039 | 1.859 | 0.180 | 0.09 | 5.10 | 0.61 | 51.53 | 10.10 | 223224. | 296. | 0.877 |
| 2007. | 1.00 | 9.95 | 2.160 | 2.151 | 0.009 | 0.00 | 9.41 | 9.33 | 27.70 | 2.94 | 1587. | 294. | 0.877 |
| 2008. | 1.02 | 9.95 | 2.209 | 2.194 | 0.015 | 0.01 | 9.21 | 9.08 | 27.76 | 3.02 | 1600. | 294. | 0.877 |
| 2009. | 1.00 | 9.95 | 2.162 | 2.123 | 0.039 | 0.02 | 9.40 | 8.66 | 49.93 | 5.31 | 9951. | 294. | 0.877 |
| 2010. | 1.00 | 9.95 | 2.162 | 2.091 | 0.071 | 0.03 | 9.40 | 7.86 | 54.69 | 5.82 | 36000. | 294. | 0.877 |
| 2011. | 1.00 | 9.95 | 2.162 | 2.065 | 0.097 | 0.04 | 9.40 | 7.16 | 57.14 | 6.08 | 70936. | 294. | 0.877 |
| 2012. | 1.01 | 10.17 | 2.182 | 2.053 | 0.130 | 0.06 | 9.52 | 6.34 | 59.86 | 6.29 | 194710. | 294. | 0.877 |
| 2013. | 0.99 | 9.99 | 2.155 | 2.007 | 0.148 | 0.07 | 9.65 | 5.76 | 62.50 | 6.48 | 205536. | 290. | 0.882 |
| 2014. | 0.99 | 9.99 | 2.155 | 1.994 | 0.161 | 0.07 | 9.65 | 5.70 | 58.63 | 6.07 | 230944. | 290. | 0.882 |
| 2049. | 1.00 | 19.68 | 2.371 | 2.368 | 0.002 | 0.00 | 17.35 | 17.26 | 99.96 | 5.76 | 1168. | 289. | 0.882 |
| 2050. | 1.00 | 19.68 | 2.371 | 2.359 | 0.012 | 0.00 | 17.35 | 17.26 | 34.99 | 2.02 | -1701. | 289. | 0.882 |
| 2051. | 1.00 | 19.68 | 2.371 | 2.324 | 0.047 | 0.02 | 17.35 | 16.53 | 57.85 | 3.33 | 17020. | 289. | 0.882 |
| 2052. | 1.00 | 19.68 | 2.371 | 2.303 | 0.068 | 0.03 | 17.35 | 16.07 | 60.95 | 3.51 | 35480. | 289. | 0.882 |
| 2053. | 1.00 | 19.68 | 2.371 | 2.289 | 0.082 | 0.03 | 17.35 | 15.75 | 62.18 | 3.58 | 53644. | 289. | 0.882 |
| 2054. | 1.00 | 19.68 | 2.371 | 2.259 | 0.112 | 0.05 | 17.35 | 15.48 | 55.16 | 3.18 | 87160. | 289. | 0.882 |
| 2055. | 1.00 | 19.68 | 2.371 | 2.245 | 0.126 | 0.05 | 17.35 | 14.87 | 61.39 | 3.54 | 150804. | 289. | 0.882 |
| 2056. | 1.00 | 19.68 | 2.371 | 2.225 | 0.145 | 0.06 | 17.35 | 14.44 | 61.80 | 3.56 | 204472. | 289. | 0.882 |
| 2057. | 1.00 | 19.68 | 2.371 | 2.219 | 0.151 | 0.06 | 17.35 | 14.31 | 61.86 | 3.57 | 221240. | 289. | 0.882 |
| 2025. | 0.99 | 19.94 | 2.169 | 2.163 | 0.006 | 0.00 | 10.42 | 10.35 | 37.45 | 3.59 | 3598. | 296. | 0.490 |
| 2026. | 1.00 | 19.94 | 2.185 | 2.175 | 0.010 | 0.00 | 10.35 | 10.23 | 35.99 | 3.48 | 1515. | 296. | 0.490 |
| 2027. | 1.00 | 19.94 | 2.185 | 2.164 | 0.021 | 0.01 | 10.35 | 9.92 | 55.12 | 5.33 | 7309. | 296. | 0.490 |
| 2028. | 1.00 | 19.94 | 2.183 | 2.149 | 0.034 | 0.02 | 10.36 | 9.62 | 56.89 | 5.49 | 16971. | 296. | 0.490 |
| 2029. | 1.00 | 19.94 | 2.185 | 2.136 | 0.049 | 0.02 | 10.35 | 9.26 | 58.33 | 5.64 | 33400. | 296. | 0.490 |
| 2030. | 1.00 | 19.94 | 2.185 | 2.130 | 0.055 | 0.03 | 10.35 | 9.10 | 58.65 | 5.67 | 48240. | 296. | 0.490 |
| 2031. | 1.00 | 19.94 | 2.185 | 2.122 | 0.063 | 0.03 | 10.35 | 8.89 | 59.42 | 5.74 | 65304. | 296. | 0.490 |
| 2032. | 1.00 | 19.94 | 2.185 | 2.108 | 0.076 | 0.03 | 10.35 | 8.48 | 61.77 | 5.97 | 107724. | 296. | 0.490 |

Table D.12 (cont.): Present Air-Water Flow Data: $D_3/D_1$ = 0.2, Upward Branch ($\Phi$ = 0°).

| RUN # | VsL1 (m/s) | VsG1 (m/s) | m1 (kg/s) | m2 (kg/s) | m3 (kg/s) | m3/m1 (-) | x1 (%) | x2 (%) | x3 (%) | x3/x1 (-) | p13 (Pa) | T1 (K) | p1 (MPa) |
|---|---|---|---|---|---|---|---|---|---|---|---|---|---|
| 2073. | 1.98 | 5.03 | 3.990 | 3.989 | 0.001 | 0.00 | 2.62 | 2.58 | 98.59 | 37.65 | 869. | 290. | 0.880 |
| 2074. | 1.98 | 5.03 | 3.990 | 3.971 | 0.019 | 0.00 | 2.62 | 2.56 | 14.22 | 5.43 | 2179. | 290. | 0.880 |
| 2075. | 1.98 | 5.03 | 3.990 | 3.932 | 0.058 | 0.01 | 2.62 | 2.31 | 23.32 | 8.90 | 8855. | 290. | 0.880 |
| 2076. | 1.98 | 5.03 | 3.990 | 3.890 | 0.101 | 0.03 | 2.62 | 1.96 | 28.07 | 10.72 | 34480. | 290. | 0.880 |
| 2077. | 2.00 | 5.07 | 4.023 | 3.883 | 0.140 | 0.03 | 2.62 | 1.55 | 32.13 | 12.27 | 76676. | 290. | 0.880 |
| 2078. | 2.00 | 5.07 | 4.023 | 3.840 | 0.183 | 0.05 | 2.62 | 1.27 | 30.99 | 11.83 | 138520. | 290. | 0.880 |
| 2079. | 2.00 | 5.07 | 4.023 | 3.795 | 0.228 | 0.06 | 2.62 | 1.16 | 26.87 | 10.26 | 205260. | 290. | 0.880 |
| 2080. | 2.00 | 5.07 | 4.023 | 3.762 | 0.260 | 0.06 | 2.62 | 1.08 | 24.80 | 9.47 | 246776. | 290. | 0.880 |
| 2066. | 2.00 | 10.16 | 4.137 | 4.126 | 0.011 | 0.00 | 5.16 | 5.12 | 17.20 | 3.33 | 2955. | 287. | 0.880 |
| 2067. | 2.00 | 10.16 | 4.137 | 4.105 | 0.032 | 0.01 | 5.16 | 5.09 | 14.20 | 2.75 | 5716. | 287. | 0.880 |
| 2068. | 2.00 | 10.16 | 4.137 | 4.053 | 0.084 | 0.02 | 5.16 | 4.90 | 17.71 | 3.43 | 14840. | 287. | 0.880 |
| 2069. | 2.04 | 10.04 | 4.201 | 4.066 | 0.135 | 0.03 | 4.95 | 4.46 | 19.67 | 3.97 | 39828. | 291. | 0.880 |
| 2070. | 2.04 | 10.04 | 4.201 | 4.026 | 0.175 | 0.04 | 4.95 | 4.22 | 21.73 | 4.39 | 75164. | 291. | 0.880 |
| 2071. | 2.04 | 10.04 | 4.201 | 3.961 | 0.240 | 0.06 | 4.95 | 3.95 | 21.59 | 4.36 | 158980. | 291. | 0.880 |
| 2072. | 2.06 | 9.56 | 4.228 | 3.734 | 0.494 | 0.12 | 4.68 | 0.56 | 44.31 | 9.47 | 274200. | 291. | 0.880 |
| 2081. | 2.00 | 20.17 | 4.338 | 4.328 | 0.010 | 0.00 | 9.69 | 9.70 | 8.11 | 0.84 | 2904. | 289. | 0.880 |
| 2082. | 2.00 | 20.17 | 4.338 | 4.316 | 0.022 | 0.01 | 9.69 | 9.68 | 11.82 | 1.22 | 4322. | 289. | 0.880 |
| 2083. | 2.00 | 20.17 | 4.338 | 4.290 | 0.048 | 0.01 | 9.69 | 9.56 | 21.58 | 2.23 | 6836. | 289. | 0.880 |
| 2084. | 2.00 | 20.17 | 4.338 | 4.252 | 0.086 | 0.02 | 9.69 | 9.49 | 19.86 | 2.05 | 21300. | 289. | 0.880 |
| 2085. | 2.03 | 20.20 | 4.385 | 4.275 | 0.110 | 0.03 | 9.51 | 9.23 | 20.34 | 2.14 | 35784. | 292. | 0.880 |
| 2085. | 2.03 | 20.20 | 4.385 | 4.275 | 0.110 | 0.03 | 9.51 | 9.23 | 20.34 | 2.14 | 35784. | 292. | 0.880 |
| 2086. | 2.03 | 20.20 | 4.385 | 4.234 | 0.151 | 0.03 | 9.51 | 8.98 | 24.50 | 2.58 | 77556. | 292. | 0.880 |
| 2087. | 2.03 | 20.20 | 4.385 | 4.194 | 0.191 | 0.04 | 9.51 | 8.76 | 26.00 | 2.73 | 137984. | 292. | 0.880 |
| 2088. | 2.03 | 20.20 | 4.385 | 4.181 | 0.204 | 0.05 | 9.51 | 8.63 | 27.47 | 2.89 | 172920. | 292. | 0.880 |
| 2089. | 2.03 | 20.20 | 4.385 | 4.164 | 0.220 | 0.05 | 9.51 | 8.63 | 26.22 | 2.76 | 194720. | 292. | 0.880 |
| 2090. | 2.03 | 20.20 | 4.385 | 4.139 | 0.245 | 0.06 | 9.51 | 8.55 | 25.63 | 2.69 | 242776. | 292. | 0.880 |
| 2058. | 4.02 | 4.96 | 7.963 | 7.956 | 0.007 | 0.00 | 1.29 | 1.29 | 3.38 | 2.61 | 2120. | 290. | 0.880 |
| 2059. | 4.02 | 4.96 | 7.963 | 7.936 | 0.028 | 0.00 | 1.29 | 1.29 | 2.12 | 1.64 | 4352. | 290. | 0.880 |
| 2060. | 4.02 | 4.96 | 7.963 | 7.882 | 0.082 | 0.01 | 1.29 | 1.28 | 2.37 | 1.83 | 8526. | 290. | 0.880 |
| 2061. | 4.02 | 4.96 | 7.963 | 7.771 | 0.192 | 0.02 | 1.29 | 1.23 | 3.69 | 2.85 | 24029. | 290. | 0.880 |

Table D.12 (cont.): Present Air-Water Flow Data: $D_3/D_1$ = 0.2, Upward Branch ($\Phi$ = 0°).

| RUN # | VsL1 (m/s) | VsG1 (m/s) | m1 (kg/s) | m2 (kg/s) | m3 (kg/s) | m3/m1 (-) | x1 (%) | x2 (%) | x3 (%) | x3/x1 (-) | p13 (Pa) | T1 (K) | p1 (MPa) |
|---|---|---|---|---|---|---|---|---|---|---|---|---|---|
| 2062. | 4.02 | 4.96 | 7.963 | 7.688 | 0.275 | 0.03 | 1.29 | 1.22 | 3.27 | 2.53 | 47404. | 290. | 0.880 |
| 2063. | 4.02 | 4.96 | 7.963 | 7.518 | 0.445 | 0.06 | 1.29 | 1.18 | 3.15 | 2.44 | 120940. | 290. | 0.880 |
| 2064. | 4.02 | 4.96 | 7.963 | 7.420 | 0.543 | 0.07 | 1.29 | 1.13 | 3.59 | 2.77 | 203360. | 290. | 0.880 |
| 2065. | 4.02 | 4.96 | 7.963 | 7.516 | 0.447 | 0.06 | 1.29 | 1.08 | 4.80 | 3.71 | 272856. | 290. | 0.880 |

Table D.12 (cont.): Present Air-Water Flow Data: $D_3/D_1$ = 0.2, Upward Branch ($\Phi$ = 0°).

| RUN # | VsL1 (m/s) | VsG1 (m/s) | m1 (kg/s) | m2 (kg/s) | m3 (kg/s) | m3/m1 (-) | x1 (%) | x2 (%) | x3 (%) | x3/x1 (-) | p13 (Pa) | T1 (K) | p1 (MPa) |
|---|---|---|---|---|---|---|---|---|---|---|---|---|---|
| 2188. | 0.10 | 5.01 | 0.298 | 0.183 | 0.115 | 0.39 | 34.17 | 54.89 | 1.19 | 0.03 | 4952. | 296. | 0.877 |
| 2189. | 0.10 | 5.01 | 0.298 | 0.165 | 0.132 | 0.45 | 34.17 | 60.78 | 0.98 | 0.03 | 6480. | 296. | 0.877 |
| 2190. | 0.10 | 5.01 | 0.298 | 0.147 | 0.151 | 0.51 | 34.15 | 65.57 | 3.70 | 0.11 | 14480. | 296. | 0.877 |
| 2191. | 0.10 | 5.09 | 0.298 | 0.115 | 0.183 | 0.62 | 34.20 | 79.51 | 5.89 | 0.17 | 26450. | 298. | 0.872 |
| 2192. | 0.10 | 5.09 | 0.295 | 0.091 | 0.204 | 0.69 | 34.53 | 92.47 | 8.62 | 0.25 | 43032. | 298. | 0.872 |
| 2193. | 0.10 | 5.09 | 0.295 | 0.078 | 0.217 | 0.74 | 34.53 | 101.15 | 10.59 | 0.31 | 61816. | 298. | 0.872 |
| 2194. | 0.10 | 5.09 | 0.295 | 0.067 | 0.228 | 0.77 | 34.53 | 105.90 | 13.62 | 0.39 | 89576. | 298. | 0.872 |
| 2195. | 0.10 | 5.09 | 0.295 | 0.044 | 0.251 | 0.85 | 34.53 | 142.04 | 15.64 | 0.45 | 123232. | 298. | 0.872 |
| 2196. | 0.10 | 5.09 | 0.295 | 0.039 | 0.256 | 0.87 | 34.53 | 123.84 | 20.85 | 0.60 | 210552. | 298. | 0.872 |
| 2179. | 0.10 | 9.98 | 0.409 | 0.320 | 0.089 | 0.22 | 52.06 | 65.75 | 2.60 | 0.05 | 4197. | 283. | 0.882 |
| 2180. | 0.10 | 10.02 | 0.405 | 0.278 | 0.128 | 0.32 | 51.65 | 72.71 | 5.87 | 0.11 | 13364. | 289. | 0.882 |
| 2181. | 0.10 | 10.02 | 0.405 | 0.231 | 0.174 | 0.43 | 51.65 | 84.76 | 7.64 | 0.15 | 31540. | 289. | 0.882 |
| 2182. | 0.10 | 10.04 | 0.405 | 0.208 | 0.197 | 0.49 | 51.63 | 88.77 | 12.51 | 0.24 | 63956. | 290. | 0.882 |
| 2183. | 0.10 | 10.04 | 0.405 | 0.216 | 0.189 | 0.47 | 51.63 | 89.19 | 8.82 | 0.17 | 40072. | 290. | 0.882 |
| 2184. | 0.10 | 10.09 | 0.405 | 0.188 | 0.217 | 0.54 | 51.63 | 94.95 | 14.06 | 0.27 | 89452. | 290. | 0.877 |
| 2185. | 0.10 | 10.09 | 0.405 | 0.163 | 0.242 | 0.60 | 51.63 | 104.11 | 16.34 | 0.32 | 124560. | 290. | 0.877 |
| 2186. | 0.10 | 10.09 | 0.405 | 0.147 | 0.258 | 0.64 | 51.63 | 104.55 | 21.43 | 0.42 | 195720. | 290. | 0.877 |
| 2187. | 0.10 | 10.09 | 0.405 | 0.146 | 0.259 | 0.64 | 51.63 | 104.59 | 21.83 | 0.42 | 212760. | 290. | 0.877 |
| 2170. | 0.10 | 19.94 | 0.608 | 0.567 | 0.041 | 0.07 | 67.76 | 72.32 | 5.27 | 0.08 | 2500. | 292. | 0.882 |
| 2171. | 0.10 | 19.94 | 0.608 | 0.500 | 0.108 | 0.18 | 67.76 | 78.74 | 16.72 | 0.25 | 26500. | 292. | 0.882 |
| 2172. | 0.10 | 20.02 | 0.615 | 0.542 | 0.073 | 0.12 | 68.12 | 75.94 | 10.36 | 0.15 | 8830. | 287. | 0.877 |
| 2173. | 0.10 | 19.94 | 0.608 | 0.468 | 0.140 | 0.23 | 67.76 | 80.37 | 25.49 | 0.38 | 65260. | 292. | 0.882 |
| 2174. | 0.10 | 20.02 | 0.615 | 0.455 | 0.160 | 0.26 | 68.12 | 83.02 | 25.78 | 0.38 | 85740. | 287. | 0.877 |
| 2175. | 0.10 | 20.02 | 0.615 | 0.421 | 0.194 | 0.32 | 68.12 | 82.85 | 36.10 | 0.53 | 115216. | 287. | 0.877 |
| 2176. | 0.10 | 20.02 | 0.615 | 0.430 | 0.185 | 0.30 | 68.12 | 84.49 | 30.19 | 0.44 | 139732. | 287. | 0.877 |
| 2177. | 0.10 | 20.02 | 0.615 | 0.418 | 0.197 | 0.32 | 68.12 | 84.94 | 32.42 | 0.48 | 202728. | 287. | 0.877 |
| 2178. | 0.10 | 20.18 | 0.612 | 0.421 | 0.191 | 0.31 | 67.96 | 85.06 | 30.26 | 0.45 | 167600. | 291. | 0.877 |
| 2325. | 0.10 | 19.98 | 0.426 | 0.373 | 0.053 | 0.12 | 54.79 | 62.12 | 3.38 | 0.06 | 3673. | 287. | 0.490 |
| 2326. | 0.10 | 19.98 | 0.424 | 0.343 | 0.080 | 0.19 | 55.16 | 66.53 | 6.48 | 0.12 | 11030. | 287. | 0.490 |
| 2327. | 0.10 | 19.98 | 0.424 | 0.324 | 0.099 | 0.23 | 55.16 | 69.65 | 7.76 | 0.14 | 21800. | 287. | 0.490 |

Table D.13: Present Air-Water Flow Data: $D_3/D_1$ = 0.2, Downward Branch ($\Phi$ = 180°).

| RUN # | VsL1 (m/s) | VsG1 (m/s) | m1 (kg/s) | m2 (kg/s) | m3 (kg/s) | m3/m1 (-) | x1 (%) | x2 (%) | x3 (%) | x3/x1 (-) | p13 (Pa) | T1 (K) | p1 (MPa) |
|---|---|---|---|---|---|---|---|---|---|---|---|---|---|
| 2328. | 0.10 | 19.98 | 0.424 | 0.299 | 0.125 | 0.29 | 55.16 | 73.39 | 11.54 | 0.21 | 46170. | 287. | 0.490 |
| 2329. | 0.10 | 19.98 | 0.428 | 0.280 | 0.148 | 0.35 | 54.57 | 76.26 | 13.71 | 0.25 | 81336. | 287. | 0.490 |
| 2330. | 0.10 | 19.98 | 0.428 | 0.263 | 0.165 | 0.39 | 54.57 | 78.69 | 16.27 | 0.30 | 118540. | 287. | 0.490 |
| 2331. | 0.10 | 48.71 | 0.423 | 0.410 | 0.014 | 0.03 | 54.59 | 56.42 | 0.01 | 0.00 | 2859. | 290. | 0.201 |
| 2332. | 0.10 | 49.93 | 0.423 | 0.393 | 0.030 | 0.07 | 54.59 | 58.38 | 5.20 | 0.10 | 4510. | 290. | 0.196 |
| 2333. | 0.10 | 49.93 | 0.423 | 0.385 | 0.038 | 0.09 | 54.59 | 59.47 | 5.73 | 0.10 | 6470. | 290. | 0.196 |
| 2334. | 0.10 | 49.93 | 0.423 | 0.376 | 0.048 | 0.11 | 54.59 | 60.37 | 9.12 | 0.17 | 14880. | 290. | 0.196 |
| 2335. | 0.10 | 49.93 | 0.423 | 0.363 | 0.060 | 0.14 | 54.59 | 61.89 | 10.62 | 0.19 | 24600. | 290. | 0.196 |
| 2336. | 0.10 | 49.93 | 0.423 | 0.362 | 0.061 | 0.14 | 54.59 | 61.81 | 11.72 | 0.21 | 29600. | 290. | 0.196 |
| 2331. | 0.10 | 48.71 | 0.423 | 0.410 | 0.014 | 0.03 | 54.59 | 56.42 | 0.01 | 0.00 | 2859. | 290. | 0.201 |
| 2332. | 0.10 | 49.93 | 0.423 | 0.393 | 0.030 | 0.07 | 54.59 | 58.38 | 5.20 | 0.10 | 4510. | 290. | 0.196 |
| 2333. | 0.10 | 49.93 | 0.423 | 0.385 | 0.038 | 0.09 | 54.59 | 59.47 | 5.73 | 0.10 | 6470. | 290. | 0.196 |
| 2334. | 0.10 | 49.93 | 0.423 | 0.376 | 0.048 | 0.11 | 54.59 | 60.37 | 9.12 | 0.17 | 14880. | 290. | 0.196 |
| 2335. | 0.10 | 49.93 | 0.423 | 0.363 | 0.060 | 0.14 | 54.59 | 61.89 | 10.62 | 0.19 | 24600. | 290. | 0.196 |
| 2336. | 0.10 | 49.93 | 0.423 | 0.362 | 0.061 | 0.14 | 54.59 | 61.81 | 11.72 | 0.21 | 29600. | 290. | 0.196 |
| 2304. | 0.25 | 4.98 | 0.595 | 0.520 | 0.075 | 0.13 | 17.38 | 19.87 | 0.00 | 0.00 | 1490. | 291. | 0.882 |
| 2305. | 0.25 | 5.01 | 0.595 | 0.369 | 0.226 | 0.38 | 17.38 | 27.84 | 0.27 | 0.02 | 10000. | 291. | 0.877 |
| 2306. | 0.25 | 5.01 | 0.595 | 0.305 | 0.289 | 0.49 | 17.38 | 33.08 | 0.83 | 0.05 | 21900. | 291. | 0.877 |
| 2307. | 0.25 | 5.01 | 0.595 | 0.242 | 0.352 | 0.59 | 17.38 | 40.37 | 1.59 | 0.09 | 43690. | 291. | 0.877 |
| 2308. | 0.25 | 5.01 | 0.595 | 0.204 | 0.391 | 0.66 | 17.38 | 44.59 | 3.20 | 0.18 | 81712. | 291. | 0.877 |
| 2309. | 0.25 | 5.00 | 0.595 | 0.131 | 0.464 | 0.78 | 17.44 | 59.61 | 5.48 | 0.31 | 164630. | 291. | 0.882 |
| 2310. | 0.25 | 5.00 | 0.595 | 0.101 | 0.494 | 0.83 | 17.44 | 71.64 | 6.30 | 0.36 | 219900. | 291. | 0.882 |
| 2197. | 0.25 | 10.22 | 0.701 | 0.527 | 0.175 | 0.25 | 29.96 | 39.60 | 0.89 | 0.03 | 9121. | 292. | 0.877 |
| 2198. | 0.25 | 10.05 | 0.694 | 0.428 | 0.265 | 0.38 | 29.41 | 46.15 | 2.37 | 0.08 | 32359. | 296. | 0.877 |
| 2199. | 0.25 | 10.05 | 0.694 | 0.496 | 0.198 | 0.29 | 29.41 | 40.42 | 1.82 | 0.06 | 17090. | 296. | 0.877 |
| 2200. | 0.25 | 9.88 | 0.692 | 0.368 | 0.324 | 0.47 | 29.15 | 51.66 | 3.58 | 0.12 | 62360. | 296. | 0.882 |
| 2201. | 0.25 | 9.97 | 0.690 | 0.316 | 0.374 | 0.54 | 29.32 | 59.09 | 4.19 | 0.14 | 92888. | 296. | 0.877 |
| 2202. | 0.25 | 9.83 | 0.690 | 0.306 | 0.384 | 0.56 | 29.31 | 59.36 | 5.32 | 0.18 | 126250. | 292. | 0.877 |
| 2203. | 0.25 | 9.83 | 0.684 | 0.270 | 0.414 | 0.61 | 29.56 | 65.42 | 6.18 | 0.21 | 164696. | 292. | 0.877 |
| 2204. | 0.25 | 9.83 | 0.684 | 0.229 | 0.455 | 0.66 | 29.56 | 74.68 | 6.80 | 0.23 | 210616. | 292. | 0.877 |

Table D.13 (cont.): Present Air-Water Flow Data: $D_3/D_1$ = 0.2, Downward Branch ($\Phi$ = 180°).

| RUN # | VsL1 (m/s) | VsG1 (m/s) | m1 (kg/s) | m2 (kg/s) | m3 (kg/s) | m3/m1 (-) | x1 (%) | x2 (%) | x3 (%) | x3/x1 (-) | p13 (Pa) | T1 (K) | p1 (MPa) |
|---|---|---|---|---|---|---|---|---|---|---|---|---|---|
| 2205. | 0.25 | 9.83 | 0.684 | 0.225 | 0.459 | 0.67 | 29.56 | 74.14 | 7.77 | 0.26 | 270248. | 292. | 0.877 |
| 2337. | 0.25 | 9.97 | 0.701 | 0.243 | 0.458 | 0.65 | 29.93 | 71.73 | 7.76 | 0.26 | 269100. | 287. | 0.882 |
| 2338. | 0.25 | 9.97 | 0.701 | 0.303 | 0.398 | 0.57 | 29.93 | 61.68 | 5.69 | 0.19 | 138020. | 287. | 0.882 |
| 2339. | 0.25 | 9.97 | 0.701 | 0.376 | 0.325 | 0.46 | 29.93 | 52.62 | 3.64 | 0.12 | 69040. | 287. | 0.882 |
| 2340. | 0.25 | 9.97 | 0.701 | 0.434 | 0.267 | 0.38 | 29.93 | 47.10 | 2.07 | 0.07 | 33490. | 287. | 0.882 |
| 2341. | 0.25 | 9.97 | 0.701 | 0.495 | 0.206 | 0.29 | 29.93 | 41.94 | 1.11 | 0.04 | 15260. | 287. | 0.882 |
| 2342. | 0.25 | 9.97 | 0.701 | 0.557 | 0.144 | 0.21 | 29.93 | 37.60 | 0.30 | 0.01 | 6860. | 287. | 0.882 |
| 2311. | 0.50 | 9.97 | 1.186 | 1.045 | 0.141 | 0.12 | 17.44 | 19.79 | 0.04 | 0.00 | 6930. | 291. | 0.882 |
| 2312. | 0.50 | 9.97 | 1.186 | 0.972 | 0.214 | 0.18 | 17.44 | 21.20 | 0.37 | 0.02 | 13300. | 291. | 0.882 |
| 2313. | 0.50 | 9.97 | 1.186 | 0.887 | 0.300 | 0.25 | 17.44 | 23.08 | 0.77 | 0.04 | 26240. | 291. | 0.882 |
| 2314. | 0.50 | 9.97 | 1.186 | 0.803 | 0.383 | 0.32 | 17.44 | 25.16 | 1.28 | 0.07 | 56700. | 291. | 0.882 |
| 2315. | 0.50 | 9.97 | 1.186 | 0.714 | 0.472 | 0.40 | 17.44 | 27.64 | 2.00 | 0.11 | 108140. | 291. | 0.882 |
| 2316. | 0.50 | 10.02 | 1.187 | 0.684 | 0.503 | 0.42 | 17.52 | 28.41 | 2.72 | 0.16 | 145400. | 291. | 0.882 |
| 2317. | 0.50 | 10.02 | 1.183 | 0.606 | 0.577 | 0.49 | 17.59 | 30.71 | 3.82 | 0.22 | 266100. | 291. | 0.882 |
| 2221. | 0.50 | 20.14 | 1.393 | 1.364 | 0.029 | 0.02 | 29.91 | 30.55 | 0.00 | 0.00 | 3068. | 292. | 0.882 |
| 2222. | 0.50 | 20.14 | 1.393 | 1.319 | 0.074 | 0.05 | 29.91 | 31.46 | 2.27 | 0.08 | 6150. | 292. | 0.882 |
| 2223. | 0.50 | 20.14 | 1.393 | 1.255 | 0.138 | 0.10 | 29.91 | 32.69 | 4.50 | 0.15 | 18529. | 292. | 0.882 |
| 2224. | 0.50 | 20.14 | 1.393 | 1.223 | 0.170 | 0.12 | 29.91 | 33.25 | 5.88 | 0.20 | 28000. | 292. | 0.882 |
| 2225. | 0.50 | 20.14 | 1.393 | 1.154 | 0.239 | 0.17 | 29.91 | 34.38 | 8.29 | 0.28 | 69968. | 292. | 0.882 |
| 2226. | 0.50 | 20.14 | 1.393 | 1.130 | 0.263 | 0.19 | 29.91 | 34.66 | 9.44 | 0.32 | 95780. | 292. | 0.882 |
| 2227. | 0.50 | 20.14 | 1.393 | 1.114 | 0.279 | 0.20 | 29.91 | 34.81 | 10.30 | 0.34 | 121250. | 292. | 0.882 |
| 2228. | 0.50 | 20.14 | 1.393 | 1.091 | 0.302 | 0.22 | 29.91 | 35.10 | 11.15 | 0.37 | 158240. | 292. | 0.882 |
| 2229. | 0.50 | 20.14 | 1.393 | 1.054 | 0.339 | 0.24 | 29.91 | 35.60 | 12.17 | 0.41 | 225100. | 292. | 0.882 |
| 2230. | 0.50 | 20.14 | 1.393 | 1.039 | 0.354 | 0.25 | 29.91 | 35.71 | 12.86 | 0.43 | 273400. | 292. | 0.882 |
| 2318. | 1.00 | 2.49 | 2.017 | 1.869 | 0.149 | 0.07 | 2.58 | 2.79 | 0.01 | 0.00 | 5347. | 289. | 0.882 |
| 2319. | 1.00 | 2.49 | 2.017 | 1.590 | 0.427 | 0.21 | 2.58 | 3.28 | 0.00 | 0.00 | 23960. | 289. | 0.882 |
| 2320. | 1.00 | 2.49 | 2.017 | 1.248 | 0.769 | 0.38 | 2.58 | 4.15 | 0.05 | 0.02 | 76924. | 289. | 0.882 |
| 2321. | 1.01 | 2.49 | 2.030 | 1.161 | 0.869 | 0.43 | 2.57 | 4.35 | 0.18 | 0.07 | 119860. | 289. | 0.882 |
| 2322. | 1.01 | 2.49 | 2.030 | 1.023 | 1.007 | 0.50 | 2.57 | 4.71 | 0.39 | 0.15 | 201000. | 289. | 0.882 |
| 2323. | 1.01 | 2.49 | 2.030 | 0.958 | 1.072 | 0.53 | 2.57 | 4.93 | 0.46 | 0.18 | 240280. | 289. | 0.882 |

Table D.13 (cont.): Present Air-Water Flow Data: $D_3/D_1$ = 0.2, Downward Branch ($\Phi$ = 180°).

| RUN # | VsL1 (m/s) | VsG1 (m/s) | m1 (kg/s) | m2 (kg/s) | m3 (kg/s) | m3/m1 (-) | x1 (%) | x2 (%) | x3 (%) | x3/x1 (-) | p13 (Pa) | T1 (K) | p1 (MPa) |
|---|---|---|---|---|---|---|---|---|---|---|---|---|---|
| 2324. | 1.01 | 2.49 | 2.030 | 0.957 | 1.073 | 0.53 | 2.57 | 4.87 | 0.51 | 0.20 | 275600. | 289. | 0.882 |
| 2296. | 1.00 | 4.98 | 2.068 | 1.905 | 0.163 | 0.08 | 5.00 | 5.42 | 0.01 | 0.00 | 8670. | 291. | 0.882 |
| 2297. | 1.00 | 4.98 | 2.068 | 1.672 | 0.397 | 0.19 | 5.00 | 6.18 | 0.03 | 0.01 | 28190. | 291. | 0.882 |
| 2298. | 1.00 | 4.98 | 2.068 | 1.547 | 0.522 | 0.25 | 5.00 | 6.59 | 0.27 | 0.05 | 55400. | 291. | 0.882 |
| 2299. | 1.02 | 4.89 | 2.092 | 1.495 | 0.597 | 0.29 | 4.86 | 6.63 | 0.40 | 0.08 | 81740. | 291. | 0.882 |
| 2300. | 1.03 | 4.89 | 2.116 | 1.355 | 0.761 | 0.36 | 4.80 | 7.17 | 0.58 | 0.12 | 157300. | 291. | 0.882 |
| 2301. | 1.05 | 4.89 | 2.165 | 1.324 | 0.840 | 0.39 | 4.69 | 7.07 | 0.95 | 0.20 | 218000. | 291. | 0.882 |
| 2302. | 1.05 | 4.89 | 2.165 | 1.232 | 0.933 | 0.43 | 4.69 | 7.57 | 0.89 | 0.19 | 250800. | 291. | 0.882 |
| 2303. | 1.05 | 4.89 | 2.165 | 1.232 | 0.933 | 0.43 | 4.69 | 7.56 | 0.90 | 0.19 | 258780. | 291. | 0.882 |
| 2239. | 1.00 | 9.97 | 2.174 | 2.137 | 0.037 | 0.02 | 9.62 | 9.79 | 0.03 | 0.00 | 4290. | 288. | 0.882 |
| 2240. | 1.00 | 9.97 | 2.174 | 2.033 | 0.142 | 0.07 | 9.62 | 10.27 | 0.27 | 0.03 | 10600. | 288. | 0.882 |
| 2241. | 1.03 | 9.97 | 2.224 | 1.953 | 0.271 | 0.12 | 9.40 | 10.60 | 0.81 | 0.09 | 25320. | 288. | 0.882 |
| 2242. | 1.03 | 9.97 | 2.224 | 2.015 | 0.209 | 0.09 | 9.40 | 10.32 | 0.55 | 0.06 | 17460. | 288. | 0.882 |
| 2243. | 0.99 | 10.11 | 2.149 | 1.797 | 0.352 | 0.16 | 9.73 | 11.35 | 1.48 | 0.15 | 46080. | 292. | 0.882 |
| 2244. | 0.99 | 10.06 | 2.149 | 1.746 | 0.403 | 0.19 | 9.72 | 11.60 | 1.54 | 0.16 | 62144. | 291. | 0.882 |
| 2245. | 0.99 | 10.06 | 2.149 | 1.703 | 0.446 | 0.21 | 9.72 | 11.81 | 1.73 | 0.18 | 75220. | 291. | 0.882 |
| 2246. | 0.99 | 10.06 | 2.149 | 1.650 | 0.498 | 0.23 | 9.72 | 12.13 | 1.75 | 0.18 | 107500. | 291. | 0.882 |
| 2247. | 0.99 | 10.06 | 2.149 | 1.618 | 0.531 | 0.25 | 9.72 | 12.27 | 1.92 | 0.20 | 129200. | 291. | 0.882 |
| 2248. | 0.99 | 10.06 | 2.149 | 1.581 | 0.567 | 0.26 | 9.72 | 12.43 | 2.15 | 0.22 | 172280. | 291. | 0.882 |
| 2249. | 1.03 | 10.06 | 2.224 | 1.566 | 0.658 | 0.30 | 9.39 | 12.22 | 2.65 | 0.28 | 278790. | 291. | 0.882 |
| 2250. | 1.03 | 10.06 | 2.224 | 1.626 | 0.598 | 0.27 | 9.39 | 11.91 | 2.53 | 0.27 | 213500. | 291. | 0.882 |
| 2272. | 1.00 | 19.95 | 2.379 | 2.347 | 0.032 | 0.01 | 17.40 | 17.63 | 0.32 | 0.02 | 4400. | 291. | 0.882 |
| 2273. | 1.00 | 19.95 | 2.379 | 2.294 | 0.086 | 0.04 | 17.40 | 18.00 | 1.40 | 0.08 | 7996. | 291. | 0.882 |
| 2274. | 1.00 | 19.95 | 2.379 | 2.261 | 0.118 | 0.05 | 17.40 | 18.21 | 2.03 | 0.12 | 12770. | 291. | 0.882 |
| 2275. | 1.00 | 19.95 | 2.379 | 2.218 | 0.161 | 0.07 | 17.40 | 18.46 | 2.86 | 0.16 | 20790. | 291. | 0.882 |
| 2276. | 1.00 | 19.95 | 2.379 | 2.107 | 0.273 | 0.11 | 17.40 | 19.07 | 4.55 | 0.26 | 54472. | 291. | 0.882 |
| 2277. | 1.00 | 19.95 | 2.379 | 2.054 | 0.326 | 0.14 | 17.40 | 19.33 | 5.28 | 0.30 | 90300. | 291. | 0.882 |
| 2278. | 0.99 | 20.02 | 2.357 | 2.003 | 0.354 | 0.15 | 17.69 | 19.79 | 5.81 | 0.33 | 128500. | 290. | 0.882 |
| 2279. | 0.99 | 20.02 | 2.357 | 1.951 | 0.405 | 0.17 | 17.69 | 19.98 | 6.66 | 0.38 | 189600. | 290. | 0.882 |
| 2280. | 0.99 | 20.02 | 2.357 | 1.907 | 0.450 | 0.19 | 17.69 | 20.09 | 7.51 | 0.42 | 302840. | 290. | 0.882 |

Table D.13 (cont.): Present Air-Water Flow Data: $D_3/D_1$ = 0.2, Downward Branch ($\Phi$ = 180°).

| RUN # | VsL1 (m/s) | VsG1 (m/s) | m1 (kg/s) | m2 (kg/s) | m3 (kg/s) | m3/m1 (-) | x1 (%) | x2 (%) | x3 (%) | x3/x1 (-) | p13 (Pa) | T1 (K) | p1 (MPa) |
|---|---|---|---|---|---|---|---|---|---|---|---|---|---|
| 2281. | 1.01 | 19.95 | 2.208 | 2.152 | 0.056 | 0.03 | 10.45 | 10.72 | 0.18 | 0.02 | 5410. | 290. | 0.490 |
| 2282. | 1.01 | 19.95 | 2.208 | 2.061 | 0.147 | 0.07 | 10.45 | 11.14 | 0.88 | 0.08 | 14400. | 290. | 0.490 |
| 2283. | 1.01 | 19.95 | 2.208 | 2.012 | 0.196 | 0.09 | 10.45 | 11.34 | 1.33 | 0.13 | 24910. | 290. | 0.490 |
| 2284. | 1.01 | 19.95 | 2.208 | 1.925 | 0.284 | 0.13 | 10.45 | 11.66 | 2.25 | 0.22 | 55164. | 290. | 0.490 |
| 2285. | 1.01 | 19.95 | 2.208 | 1.869 | 0.340 | 0.15 | 10.45 | 11.99 | 2.00 | 0.19 | 88980. | 290. | 0.490 |
| 2286. | 1.01 | 19.95 | 2.208 | 1.837 | 0.371 | 0.17 | 10.45 | 12.06 | 2.50 | 0.24 | 130992. | 290. | 0.490 |
| 2287. | 1.01 | 19.95 | 2.208 | 1.821 | 0.388 | 0.18 | 10.45 | 12.16 | 2.42 | 0.23 | 164656. | 290. | 0.490 |
| 2349. | 1.02 | 28.74 | 2.591 | 2.511 | 0.080 | 0.03 | 23.19 | 23.84 | 2.50 | 0.11 | 10800. | 289. | 0.882 |
| 2350. | 1.04 | 27.71 | 2.606 | 2.344 | 0.262 | 0.10 | 22.22 | 23.80 | 8.07 | 0.36 | 89600. | 289. | 0.882 |
| 2351. | 1.04 | 27.71 | 2.606 | 2.302 | 0.304 | 0.12 | 22.22 | 23.88 | 9.70 | 0.44 | 161128. | 289. | 0.882 |
| 2352. | 1.04 | 27.71 | 2.606 | 2.201 | 0.406 | 0.16 | 22.22 | 24.48 | 10.00 | 0.45 | 291100. | 289. | 0.882 |
| 2288. | 2.00 | 4.96 | 4.021 | 3.858 | 0.163 | 0.04 | 2.57 | 2.68 | 0.06 | 0.02 | 11710. | 290. | 0.882 |
| 2289. | 2.00 | 4.96 | 4.021 | 3.752 | 0.269 | 0.07 | 2.57 | 2.74 | 0.15 | 0.06 | 21120. | 290. | 0.882 |
| 2290. | 2.00 | 4.96 | 4.021 | 3.557 | 0.464 | 0.12 | 2.57 | 2.86 | 0.39 | 0.15 | 54160. | 290. | 0.882 |
| 2291. | 2.00 | 4.96 | 4.021 | 3.377 | 0.643 | 0.16 | 2.57 | 2.97 | 0.47 | 0.18 | 102224. | 290. | 0.882 |
| 2292. | 2.00 | 4.96 | 4.021 | 3.257 | 0.763 | 0.19 | 2.57 | 2.97 | 0.86 | 0.34 | 149600. | 290. | 0.882 |
| 2293. | 2.00 | 4.96 | 4.021 | 3.182 | 0.838 | 0.21 | 2.57 | 3.06 | 0.71 | 0.28 | 208192. | 290. | 0.882 |
| 2294. | 2.00 | 4.96 | 4.021 | 3.062 | 0.959 | 0.24 | 2.57 | 3.12 | 0.81 | 0.32 | 274380. | 290. | 0.882 |
| 2295. | 2.00 | 4.96 | 4.021 | 3.087 | 0.933 | 0.23 | 2.57 | 3.08 | 0.90 | 0.35 | 279840. | 290. | 0.882 |
| 2263. | 2.00 | 10.09 | 4.126 | 4.057 | 0.068 | 0.02 | 5.04 | 5.12 | 0.15 | 0.03 | 8199. | 293. | 0.882 |
| 2264. | 2.00 | 10.09 | 4.126 | 3.968 | 0.158 | 0.04 | 5.04 | 5.20 | 1.14 | 0.23 | 17326. | 293. | 0.882 |
| 2265. | 2.00 | 10.09 | 4.126 | 3.914 | 0.211 | 0.05 | 5.04 | 5.23 | 1.56 | 0.31 | 24500. | 293. | 0.882 |
| 2266. | 2.00 | 9.96 | 4.124 | 3.867 | 0.257 | 0.06 | 5.01 | 5.22 | 1.87 | 0.37 | 32827. | 291. | 0.882 |
| 2267. | 2.00 | 10.07 | 4.126 | 3.757 | 0.370 | 0.09 | 5.06 | 5.36 | 2.08 | 0.41 | 70132. | 291. | 0.882 |
| 2268. | 2.00 | 10.07 | 4.126 | 3.652 | 0.474 | 0.11 | 5.06 | 5.40 | 2.51 | 0.50 | 116860. | 291. | 0.882 |
| 2269. | 2.00 | 9.96 | 4.124 | 3.589 | 0.535 | 0.13 | 5.01 | 5.34 | 2.80 | 0.56 | 188824. | 291. | 0.882 |
| 2270. | 2.00 | 10.03 | 4.126 | 3.513 | 0.613 | 0.15 | 5.04 | 5.40 | 3.02 | 0.60 | 272850. | 291. | 0.882 |
| 2271. | 1.99 | 9.96 | 4.112 | 3.498 | 0.614 | 0.15 | 5.03 | 5.37 | 3.10 | 0.62 | 291824. | 291. | 0.882 |
| 2251. | 2.00 | 19.92 | 4.312 | 4.298 | 0.014 | 0.00 | 9.15 | 9.18 | 0.07 | 0.01 | 5999. | 305. | 0.882 |
| 2252. | 2.00 | 19.92 | 4.312 | 4.269 | 0.043 | 0.01 | 9.15 | 9.23 | 0.70 | 0.08 | 7570. | 305. | 0.882 |

Table D.13 (cont.): Present Air-Water Flow Data: $D_3/D_1$ = 0.2, Downward Branch ($\Phi$ = 180°).

| RUN # | VsL1 (m/s) | VsG1 (m/s) | m1 (kg/s) | m2 (kg/s) | m3 (kg/s) | m3/m1 (-) | x1 (%) | x2 (%) | x3 (%) | x3/x1 (-) | p13 (Pa) | T1 (K) | p1 (MPa) |
|---|---|---|---|---|---|---|---|---|---|---|---|---|---|
| 2253. | 2.00 | 19.92 | 4.312 | 4.239 | 0.073 | 0.02 | 9.15 | 9.28 | 1.72 | 0.19 | 11026. | 305. | 0.882 |
| 2254. | 2.00 | 19.95 | 4.333 | 4.231 | 0.102 | 0.02 | 9.59 | 9.76 | 2.35 | 0.24 | 16027. | 290. | 0.882 |
| 2255. | 2.00 | 19.95 | 4.333 | 4.191 | 0.142 | 0.03 | 9.59 | 9.77 | 4.21 | 0.44 | 21620. | 290. | 0.882 |
| 2256. | 2.00 | 19.95 | 4.333 | 4.140 | 0.193 | 0.04 | 9.59 | 9.84 | 4.29 | 0.45 | 34748. | 290. | 0.882 |
| 2257. | 2.00 | 19.95 | 4.333 | 4.084 | 0.249 | 0.06 | 9.59 | 9.90 | 4.57 | 0.48 | 54750. | 290. | 0.882 |
| 2258. | 2.00 | 19.95 | 4.333 | 4.039 | 0.294 | 0.07 | 9.59 | 9.88 | 5.58 | 0.58 | 77856. | 290. | 0.882 |
| 2259. | 2.00 | 19.95 | 4.333 | 4.006 | 0.327 | 0.08 | 9.59 | 9.91 | 5.72 | 0.60 | 102324. | 290. | 0.882 |
| 2260. | 2.00 | 19.95 | 4.333 | 3.981 | 0.352 | 0.08 | 9.59 | 9.96 | 5.40 | 0.56 | 122300. | 290. | 0.882 |
| 2261. | 2.00 | 19.85 | 4.331 | 3.946 | 0.385 | 0.09 | 9.54 | 9.88 | 6.07 | 0.64 | 164992. | 290. | 0.882 |
| 2262. | 2.00 | 19.85 | 4.331 | 3.861 | 0.470 | 0.11 | 9.54 | 9.89 | 6.73 | 0.70 | 293592. | 290. | 0.882 |
| 2231. | 4.02 | 5.11 | 7.966 | 7.106 | 0.860 | 0.11 | 1.33 | 1.36 | 1.05 | 0.79 | 281550. | 291. | 0.882 |
| 2232. | 4.02 | 4.98 | 7.964 | 7.122 | 0.841 | 0.11 | 1.30 | 1.33 | 1.07 | 0.82 | 253800. | 290. | 0.882 |
| 2233. | 4.02 | 4.98 | 7.964 | 7.200 | 0.764 | 0.10 | 1.30 | 1.34 | 0.98 | 0.75 | 191680. | 290. | 0.882 |
| 2234. | 4.02 | 5.08 | 7.966 | 7.320 | 0.646 | 0.08 | 1.33 | 1.36 | 0.94 | 0.71 | 143140. | 290. | 0.882 |
| 2235. | 4.02 | 5.08 | 7.966 | 7.501 | 0.465 | 0.06 | 1.33 | 1.37 | 0.64 | 0.48 | 81656. | 290. | 0.882 |
| 2236. | 4.02 | 5.08 | 7.966 | 7.603 | 0.363 | 0.05 | 1.33 | 1.37 | 0.41 | 0.31 | 54760. | 290. | 0.882 |
| 2237. | 4.02 | 5.08 | 7.966 | 7.757 | 0.209 | 0.03 | 1.33 | 1.35 | 0.48 | 0.36 | 36156. | 290. | 0.882 |
| 2238. | 4.02 | 5.08 | 7.966 | 7.856 | 0.110 | 0.01 | 1.33 | 1.35 | 0.09 | 0.07 | 12800. | 290. | 0.882 |
| 2345. | 3.83 | 9.86 | 7.716 | 7.477 | 0.238 | 0.03 | 2.81 | 2.84 | 1.66 | 0.59 | 41980. | 284. | 0.911 |
| 2346. | 3.83 | 9.86 | 7.716 | 7.321 | 0.395 | 0.05 | 2.81 | 2.83 | 2.33 | 0.83 | 103900. | 284. | 0.911 |
| 2347. | 3.83 | 9.86 | 7.716 | 7.201 | 0.515 | 0.07 | 2.81 | 2.77 | 3.26 | 1.16 | 186500. | 284. | 0.911 |
| 2348. | 4.07 | 9.92 | 8.169 | 7.543 | 0.626 | 0.08 | 2.55 | 2.49 | 3.32 | 1.30 | 287168. | 288. | 0.882 |
| 2343. | 3.55 | 9.97 | 7.170 | 7.086 | 0.085 | 0.01 | 3.06 | 3.08 | 1.34 | 0.44 | 14180. | 284. | 0.911 |
| 2344. | 3.55 | 9.97 | 7.170 | 7.053 | 0.118 | 0.02 | 3.06 | 3.08 | 1.43 | 0.47 | 16800. | 284. | 0.911 |
| 2355. | 5.18 | 2.47 | 10.199 | 9.008 | 1.191 | 0.12 | 0.50 | 0.55 | 0.16 | 0.31 | 326056. | 290. | 0.882 |
| 2354. | 5.61 | 4.15 | 11.060 | 10.101 | 0.959 | 0.09 | 0.79 | 0.79 | 0.77 | 0.98 | 291400. | 287. | 0.882 |
| 2353. | 4.81 | 7.85 | 9.590 | 8.870 | 0.720 | 0.08 | 1.78 | 1.73 | 2.40 | 1.35 | 298450. | 287. | 0.911 |

Table D.13 (cont.): Present Air-Water Flow Data: $D_3/D_1$ = 0.2, Downward Branch ($\Phi$ = 180°).

| RUN # | VsL1 (m/s) | VsG1 (m/s) | m1 (kg/s) | m2 (kg/s) | m3 (kg/s) | m3/m1 (-) | x1 (%) | x2 (%) | x3 (%) | x3/x1 (-) | p13 (Pa) | T1 (K) | p1 (MPa) |
|---|---|---|---|---|---|---|---|---|---|---|---|---|---|
| 362. | 0.06 | 1.00 | 0.130 | 0.096 | 0.034 | 0.26 | 15.44 | 16.41 | 12.71 | 0.82 | 37400. | 300. | 0.884 |
| 363. | 0.06 | 1.00 | 0.130 | 0.022 | 0.108 | 0.83 | 15.44 | 37.81 | 10.80 | 0.70 | 452800. | 300. | 0.878 |
| 364. | 0.06 | 1.01 | 0.134 | 0.067 | 0.067 | 0.50 | 15.00 | 20.55 | 9.42 | 0.63 | 117200. | 300. | 0.874 |
| 529. | 0.05 | 1.06 | 0.128 | 0.101 | 0.027 | 0.21 | 16.55 | 17.20 | 14.13 | 0.85 | 21800. | 300. | 0.876 |
| 530. | 0.05 | 1.06 | 0.128 | 0.091 | 0.037 | 0.29 | 16.55 | 18.34 | 12.15 | 0.73 | 32400. | 300. | 0.876 |
| 531. | 0.05 | 1.06 | 0.128 | 0.075 | 0.053 | 0.42 | 16.55 | 20.53 | 10.98 | 0.66 | 66300. | 300. | 0.876 |
| 532. | 0.05 | 1.06 | 0.128 | 0.046 | 0.082 | 0.64 | 16.55 | 28.90 | 9.57 | 0.58 | 166000. | 300. | 0.876 |
| 533. | 0.05 | 1.06 | 0.128 | 0.030 | 0.098 | 0.77 | 16.55 | 39.57 | 9.53 | 0.58 | 293600. | 300. | 0.876 |
| 534. | 0.05 | 1.06 | 0.128 | 0.016 | 0.112 | 0.88 | 16.55 | 62.09 | 10.14 | 0.61 | 455600. | 300. | 0.876 |
| 221. | 0.05 | 2.62 | 0.148 | 0.145 | 0.003 | 0.02 | 35.33 | 33.97 | 93.06 | 2.63 | 10900. | 300. | 0.875 |
| 222. | 0.05 | 2.52 | 0.150 | 0.145 | 0.005 | 0.03 | 34.07 | 32.05 | 94.83 | 2.78 | 15600. | 300. | 0.890 |
| 223. | 0.05 | 2.56 | 0.156 | 0.150 | 0.006 | 0.04 | 33.10 | 30.61 | 95.38 | 2.88 | 19900. | 300. | 0.883 |
| 224. | 0.05 | 2.57 | 0.156 | 0.148 | 0.008 | 0.05 | 33.14 | 29.82 | 95.76 | 2.89 | 28600. | 300. | 0.881 |
| 225. | 0.05 | 2.55 | 0.156 | 0.147 | 0.009 | 0.06 | 33.14 | 29.34 | 92.16 | 2.78 | 35800. | 300. | 0.888 |
| 226. | 0.05 | 2.56 | 0.156 | 0.144 | 0.012 | 0.08 | 33.14 | 28.64 | 88.28 | 2.66 | 47600. | 300. | 0.884 |
| 227. | 0.05 | 2.59 | 0.156 | 0.142 | 0.014 | 0.09 | 33.14 | 27.90 | 87.55 | 2.64 | 63100. | 300. | 0.875 |
| 228. | 0.06 | 2.62 | 0.163 | 0.147 | 0.016 | 0.10 | 32.29 | 26.78 | 83.06 | 2.57 | 88100. | 300. | 0.879 |
| 229. | 0.06 | 2.63 | 0.163 | 0.145 | 0.017 | 0.11 | 32.29 | 26.30 | 82.53 | 2.56 | 108800. | 300. | 0.874 |
| 230. | 0.06 | 2.44 | 0.160 | 0.143 | 0.017 | 0.11 | 31.32 | 26.01 | 75.16 | 2.40 | 161900. | 300. | 0.901 |
| 231. | 0.06 | 2.69 | 0.163 | 0.150 | 0.013 | 0.08 | 32.54 | 27.78 | 85.45 | 2.63 | 79400. | 300. | 0.865 |
| 232. | 0.06 | 2.69 | 0.163 | 0.147 | 0.016 | 0.10 | 32.54 | 27.55 | 78.96 | 2.43 | 101200. | 300. | 0.865 |
| 233. | 0.06 | 2.69 | 0.163 | 0.146 | 0.017 | 0.11 | 32.54 | 27.12 | 78.49 | 2.41 | 123500. | 300. | 0.865 |
| 234. | 0.06 | 2.51 | 0.161 | 0.143 | 0.018 | 0.11 | 31.57 | 26.66 | 69.75 | 2.21 | 186100. | 300. | 0.886 |
| 235. | 0.06 | 2.45 | 0.160 | 0.126 | 0.034 | 0.21 | 31.32 | 29.08 | 39.58 | 1.26 | 236100. | 300. | 0.898 |
| 236. | 0.06 | 2.50 | 0.160 | 0.133 | 0.027 | 0.17 | 31.32 | 27.44 | 50.52 | 1.61 | 200300. | 300. | 0.878 |
| 237. | 0.06 | 2.65 | 0.163 | 0.134 | 0.028 | 0.17 | 32.41 | 28.57 | 50.56 | 1.56 | 224900. | 300. | 0.873 |
| 238. | 0.06 | 2.67 | 0.163 | 0.126 | 0.037 | 0.22 | 32.41 | 29.20 | 43.55 | 1.34 | 321400. | 300. | 0.866 |
| 239. | 0.06 | 2.49 | 0.161 | 0.120 | 0.041 | 0.25 | 31.49 | 28.74 | 39.62 | 1.26 | 374800. | 300. | 0.892 |
| 240. | 0.06 | 2.49 | 0.161 | 0.119 | 0.042 | 0.26 | 31.57 | 28.68 | 39.85 | 1.26 | 417600. | 300. | 0.892 |
| 170. | 0.05 | 2.63 | 0.134 | 0.129 | 0.004 | 0.03 | 21.99 | 21.37 | 39.87 | 1.81 | 7200. | 300. | 0.490 |

Table D.14: Present Air-Water Flow Data: $D_3/D_1$ = 0.084, Horizontal Branch ($\Phi$ = 90°).

| RUN # | VsL1 (m/s) | VsG1 (m/s) | m1 (kg/s) | m2 (kg/s) | m3 (kg/s) | m3/m1 (-) | x1 (%) | x2 (%) | x3 (%) | x3/x1 (-) | p13 (Pa) | T1 (K) | p1 (MPa) |
|---|---|---|---|---|---|---|---|---|---|---|---|---|---|
| 171. | 0.05 | 2.63 | 0.134 | 0.127 | 0.007 | 0.05 | 21.99 | 20.94 | 41.84 | 1.90 | 12300. | 300. | 0.490 |
| 172. | 0.05 | 2.63 | 0.134 | 0.124 | 0.010 | 0.07 | 21.99 | 20.78 | 36.94 | 1.68 | 19600. | 300. | 0.490 |
| 173. | 0.05 | 2.63 | 0.134 | 0.122 | 0.012 | 0.09 | 21.99 | 20.59 | 36.15 | 1.64 | 28500. | 300. | 0.490 |
| 174. | 0.05 | 2.63 | 0.134 | 0.120 | 0.014 | 0.11 | 21.99 | 20.88 | 31.37 | 1.43 | 38400. | 300. | 0.490 |
| 175. | 0.06 | 2.63 | 0.141 | 0.125 | 0.016 | 0.11 | 20.79 | 19.49 | 30.93 | 1.49 | 49200. | 300. | 0.490 |
| 176. | 0.06 | 2.64 | 0.141 | 0.122 | 0.020 | 0.14 | 20.79 | 19.48 | 28.90 | 1.39 | 67900. | 300. | 0.488 |
| 177. | 0.06 | 2.64 | 0.141 | 0.115 | 0.027 | 0.19 | 20.79 | 19.75 | 25.26 | 1.21 | 125800. | 300. | 0.488 |
| 178. | 0.06 | 2.64 | 0.141 | 0.111 | 0.030 | 0.21 | 20.79 | 19.83 | 24.31 | 1.17 | 181600. | 300. | 0.488 |
| 179. | 0.06 | 2.58 | 0.141 | 0.108 | 0.034 | 0.24 | 20.79 | 20.01 | 23.28 | 1.12 | 214100. | 300. | 0.500 |
| 180. | 0.06 | 2.58 | 0.150 | 0.115 | 0.036 | 0.24 | 19.55 | 18.71 | 22.25 | 1.14 | 247100. | 300. | 0.500 |
| 181. | 0.06 | 2.61 | 0.145 | 0.110 | 0.036 | 0.24 | 20.26 | 19.27 | 23.33 | 1.15 | 268500. | 300. | 0.494 |
| 549. | 0.05 | 2.48 | 0.130 | 0.120 | 0.010 | 0.07 | 21.00 | 19.34 | 41.88 | 1.99 | 15600. | 300. | 0.482 |
| 550. | 0.05 | 2.48 | 0.130 | 0.116 | 0.014 | 0.11 | 21.00 | 19.18 | 36.10 | 1.72 | 37000. | 300. | 0.482 |
| 551. | 0.05 | 2.48 | 0.130 | 0.107 | 0.023 | 0.18 | 21.00 | 19.52 | 27.86 | 1.33 | 79200. | 300. | 0.482 |
| 552. | 0.05 | 2.48 | 0.130 | 0.099 | 0.031 | 0.24 | 21.00 | 19.82 | 24.82 | 1.18 | 136000. | 300. | 0.482 |
| 366. | 0.05 | 2.43 | 0.154 | 0.142 | 0.012 | 0.08 | 32.05 | 29.30 | 64.92 | 2.03 | 28600. | 300. | 0.887 |
| 367. | 0.06 | 2.48 | 0.162 | 0.127 | 0.035 | 0.22 | 30.82 | 26.18 | 47.50 | 1.54 | 241300. | 300. | 0.882 |
| 368. | 0.06 | 2.42 | 0.161 | 0.141 | 0.020 | 0.12 | 30.30 | 27.39 | 51.11 | 1.69 | 63100. | 300. | 0.882 |
| 384. | 0.05 | 2.50 | 0.150 | 0.101 | 0.049 | 0.33 | 33.24 | 33.73 | 32.25 | 0.97 | 455600. | 300. | 0.874 |
| 385. | 0.05 | 2.47 | 0.150 | 0.111 | 0.039 | 0.26 | 33.24 | 31.42 | 38.51 | 1.16 | 331200. | 300. | 0.885 |
| 386. | 0.05 | 2.56 | 0.151 | 0.116 | 0.035 | 0.23 | 33.55 | 31.41 | 40.64 | 1.21 | 258200. | 300. | 0.867 |
| 524. | 0.06 | 2.50 | 0.161 | 0.151 | 0.010 | 0.06 | 30.88 | 27.46 | 82.19 | 2.66 | 31600. | 300. | 0.868 |
| 525. | 0.06 | 2.50 | 0.161 | 0.152 | 0.008 | 0.05 | 30.88 | 28.14 | 80.24 | 2.60 | 23100. | 300. | 0.868 |
| 526. | 0.06 | 2.50 | 0.161 | 0.155 | 0.006 | 0.04 | 30.88 | 28.73 | 88.14 | 2.85 | 14700. | 300. | 0.868 |
| 527. | 0.06 | 2.50 | 0.161 | 0.156 | 0.005 | 0.03 | 30.88 | 29.06 | 88.69 | 2.87 | 12500. | 300. | 0.868 |
| 49. | 0.05 | 5.06 | 0.204 | 0.198 | 0.007 | 0.03 | 49.98 | 48.33 | 97.31 | 1.95 | 16800. | 300. | 0.884 |
| 50. | 0.06 | 5.06 | 0.214 | 0.205 | 0.009 | 0.04 | 47.71 | 45.53 | 97.53 | 2.04 | 30100. | 300. | 0.884 |
| 51. | 0.06 | 5.12 | 0.213 | 0.201 | 0.012 | 0.06 | 48.36 | 45.39 | 97.95 | 2.03 | 49300. | 300. | 0.882 |
| 52. | 0.06 | 5.12 | 0.212 | 0.198 | 0.014 | 0.07 | 48.56 | 45.05 | 97.65 | 2.01 | 66400. | 300. | 0.882 |
| 53. | 0.06 | 5.11 | 0.215 | 0.198 | 0.017 | 0.08 | 47.93 | 43.58 | 97.85 | 2.04 | 90700. | 300. | 0.884 |

Table D.14 (cont.): Present Air-Water Flow Data: $D_3/D_1$ = 0.084, Horizontal Branch ($\Phi$ = 90°).

| RUN # | VsL1 (m/s) | VsG1 (m/s) | m1 (kg/s) | m2 (kg/s) | m3 (kg/s) | m3/m1 (-) | x1 (%) | x2 (%) | x3 (%) | x3/x1 (-) | p13 (Pa) | T1 (K) | p1 (MPa) |
|---|---|---|---|---|---|---|---|---|---|---|---|---|---|
| 89. | 0.05 | 10.54 | 0.313 | 0.295 | 0.019 | 0.06 | 67.71 | 66.62 | 84.68 | 1.25 | 133500. | 300. | 0.882 |
| 90. | 0.05 | 10.54 | 0.313 | 0.294 | 0.020 | 0.06 | 67.71 | 66.49 | 85.75 | 1.27 | 168800. | 300. | 0.882 |
| 91. | 0.05 | 10.64 | 0.313 | 0.291 | 0.022 | 0.07 | 67.71 | 66.35 | 85.81 | 1.27 | 236200. | 300. | 0.874 |
| 92. | 0.05 | 10.53 | 0.313 | 0.291 | 0.022 | 0.07 | 67.71 | 66.36 | 85.44 | 1.26 | 287200. | 300. | 0.883 |
| 122. | 0.05 | 9.87 | 0.214 | 0.210 | 0.004 | 0.02 | 52.69 | 51.83 | 94.49 | 1.79 | 16000. | 300. | 0.500 |
| 123. | 0.05 | 10.09 | 0.221 | 0.215 | 0.006 | 0.03 | 51.36 | 50.43 | 87.48 | 1.70 | 20100. | 300. | 0.492 |
| 124. | 0.05 | 10.09 | 0.221 | 0.214 | 0.006 | 0.03 | 51.36 | 50.27 | 87.69 | 1.71 | 26600. | 300. | 0.492 |
| 125. | 0.06 | 10.09 | 0.230 | 0.223 | 0.007 | 0.03 | 49.28 | 48.10 | 87.61 | 1.78 | 36000. | 300. | 0.492 |
| 126. | 0.06 | 10.09 | 0.230 | 0.221 | 0.009 | 0.04 | 49.28 | 47.66 | 89.59 | 1.82 | 50600. | 300. | 0.492 |
| 127. | 0.06 | 10.10 | 0.230 | 0.220 | 0.010 | 0.04 | 49.30 | 47.46 | 89.56 | 1.82 | 69200. | 300. | 0.492 |
| 128. | 0.06 | 10.18 | 0.230 | 0.219 | 0.011 | 0.05 | 49.30 | 47.22 | 89.93 | 1.82 | 89000. | 300. | 0.488 |
| 129. | 0.06 | 10.14 | 0.230 | 0.218 | 0.012 | 0.05 | 49.30 | 46.98 | 89.89 | 1.82 | 115100. | 300. | 0.490 |
| 130. | 0.06 | 10.14 | 0.230 | 0.217 | 0.013 | 0.06 | 49.30 | 46.77 | 90.10 | 1.83 | 152400. | 300. | 0.490 |
| 131. | 0.06 | 10.14 | 0.230 | 0.216 | 0.014 | 0.06 | 49.30 | 46.65 | 89.14 | 1.81 | 196000. | 300. | 0.490 |
| 132. | 0.06 | 10.06 | 0.230 | 0.215 | 0.015 | 0.07 | 49.30 | 46.51 | 89.45 | 1.81 | 231800. | 300. | 0.494 |
| 133. | 0.06 | 10.10 | 0.230 | 0.215 | 0.015 | 0.07 | 49.30 | 46.47 | 89.94 | 1.82 | 244400. | 300. | 0.492 |
| 281. | 0.10 | 0.99 | 0.210 | 0.175 | 0.035 | 0.17 | 9.54 | 9.66 | 8.93 | 0.94 | 24200. | 300. | 0.887 |
| 282. | 0.10 | 0.99 | 0.210 | 0.166 | 0.044 | 0.21 | 9.54 | 9.89 | 8.18 | 0.86 | 36500. | 300. | 0.882 |
| 283. | 0.10 | 1.00 | 0.217 | 0.167 | 0.049 | 0.23 | 9.23 | 9.62 | 7.91 | 0.86 | 46500. | 300. | 0.875 |
| 284. | 0.10 | 1.01 | 0.219 | 0.161 | 0.058 | 0.26 | 9.12 | 9.47 | 8.14 | 0.89 | 71500. | 300. | 0.868 |
| 285. | 0.10 | 1.01 | 0.219 | 0.148 | 0.071 | 0.32 | 9.12 | 9.40 | 8.53 | 0.94 | 101800. | 300. | 0.866 |
| 286. | 0.10 | 0.99 | 0.219 | 0.133 | 0.087 | 0.40 | 9.12 | 9.96 | 7.82 | 0.86 | 171700. | 300. | 0.882 |
| 287. | 0.11 | 1.01 | 0.229 | 0.138 | 0.091 | 0.40 | 8.67 | 8.57 | 8.82 | 1.02 | 217700. | 300. | 0.862 |
| 288. | 0.10 | 1.00 | 0.215 | 0.115 | 0.100 | 0.47 | 9.26 | 9.94 | 8.47 | 0.92 | 318500. | 300. | 0.874 |
| 289. | 0.10 | 0.98 | 0.215 | 0.097 | 0.118 | 0.55 | 9.21 | 10.14 | 8.46 | 0.92 | 473700. | 300. | 0.887 |
| 352. | 0.10 | 1.01 | 0.214 | 0.172 | 0.042 | 0.19 | 9.43 | 9.47 | 9.28 | 0.98 | 31600. | 300. | 0.874 |
| 353. | 0.10 | 1.02 | 0.214 | 0.073 | 0.141 | 0.66 | 9.43 | 16.41 | 5.84 | 0.62 | 464900. | 300. | 0.870 |
| 354. | 0.10 | 1.00 | 0.209 | 0.136 | 0.073 | 0.35 | 9.67 | 10.40 | 8.31 | 0.86 | 103700. | 300. | 0.882 |
| 378. | 0.10 | 1.03 | 0.216 | 0.189 | 0.027 | 0.13 | 9.57 | 8.95 | 13.92 | 1.45 | 25200. | 300. | 0.882 |
| 379. | 0.10 | 1.04 | 0.223 | 0.172 | 0.051 | 0.23 | 9.30 | 8.84 | 10.84 | 1.17 | 58000. | 300. | 0.870 |

Table D.14 (cont.): Present Air-Water Flow Data: $D_3/D_1$ = 0.084, Horizontal Branch ($\Phi$ = 90°).

| RUN # | VsL1 (m/s) | VsG1 (m/s) | m1 (kg/s) | m2 (kg/s) | m3 (kg/s) | m3/m1 (-) | x1 (%) | x2 (%) | x3 (%) | x3/x1 (-) | p13 (Pa) | T1 (K) | p1 (MPa) |
|---|---|---|---|---|---|---|---|---|---|---|---|---|---|
| 380. | 0.10 | 1.04 | 0.216 | 0.154 | 0.062 | 0.29 | 9.59 | 9.09 | 10.83 | 1.13 | 108100. | 300. | 0.872 |
| 381. | 0.10 | 1.05 | 0.220 | 0.150 | 0.070 | 0.32 | 9.40 | 8.32 | 11.73 | 1.25 | 166700. | 300. | 0.864 |
| 382. | 0.10 | 1.04 | 0.220 | 0.103 | 0.118 | 0.53 | 9.40 | 9.46 | 9.36 | 0.99 | 447400. | 300. | 0.872 |
| 536. | 0.10 | 1.11 | 0.221 | 0.195 | 0.026 | 0.12 | 10.00 | 9.12 | 16.59 | 1.66 | 25700. | 300. | 0.876 |
| 537. | 0.10 | 1.11 | 0.221 | 0.178 | 0.043 | 0.19 | 10.00 | 9.43 | 12.33 | 1.23 | 39800. | 300. | 0.876 |
| 538. | 0.10 | 1.11 | 0.221 | 0.173 | 0.049 | 0.22 | 10.00 | 8.82 | 14.16 | 1.42 | 85300. | 300. | 0.876 |
| 539. | 0.10 | 1.11 | 0.221 | 0.123 | 0.098 | 0.44 | 10.00 | 11.30 | 8.35 | 0.84 | 214300. | 300. | 0.876 |
| 540. | 0.10 | 1.11 | 0.221 | 0.115 | 0.106 | 0.48 | 10.00 | 9.73 | 10.29 | 1.03 | 440800. | 300. | 0.876 |
| 243. | 0.11 | 2.59 | 0.259 | 0.254 | 0.005 | 0.02 | 20.13 | 18.76 | 85.21 | 4.23 | 13700. | 300. | 0.882 |
| 244. | 0.10 | 2.60 | 0.246 | 0.240 | 0.006 | 0.02 | 21.20 | 19.61 | 86.20 | 4.07 | 16700. | 300. | 0.880 |
| 245. | 0.10 | 2.59 | 0.246 | 0.239 | 0.007 | 0.03 | 21.20 | 19.28 | 86.49 | 4.08 | 20300. | 300. | 0.884 |
| 246. | 0.10 | 2.59 | 0.246 | 0.238 | 0.009 | 0.03 | 21.20 | 18.89 | 85.61 | 4.04 | 29100. | 300. | 0.884 |
| 247. | 0.10 | 2.61 | 0.251 | 0.234 | 0.018 | 0.07 | 20.68 | 16.61 | 74.79 | 3.62 | 87000. | 300. | 0.872 |
| 248. | 0.11 | 2.66 | 0.260 | 0.238 | 0.022 | 0.08 | 20.25 | 15.75 | 69.44 | 3.43 | 125300. | 300. | 0.867 |
| 249. | 0.11 | 2.64 | 0.260 | 0.234 | 0.025 | 0.10 | 20.25 | 15.58 | 63.34 | 3.13 | 208100. | 300. | 0.872 |
| 250. | 0.10 | 2.53 | 0.242 | 0.210 | 0.032 | 0.13 | 21.08 | 15.42 | 57.86 | 2.74 | 401000. | 300. | 0.884 |
| 251. | 0.10 | 2.53 | 0.242 | 0.209 | 0.033 | 0.14 | 21.08 | 15.28 | 57.93 | 2.75 | 463000. | 300. | 0.884 |
| 253. | 0.10 | 2.58 | 0.252 | 0.220 | 0.031 | 0.12 | 20.41 | 16.61 | 47.13 | 2.31 | 302100. | 300. | 0.872 |
| 254. | 0.10 | 2.50 | 0.251 | 0.225 | 0.025 | 0.10 | 20.06 | 16.27 | 53.74 | 2.68 | 186400. | 300. | 0.883 |
| 255. | 0.10 | 2.50 | 0.251 | 0.231 | 0.020 | 0.08 | 20.06 | 16.74 | 58.04 | 2.89 | 123900. | 300. | 0.883 |
| 349. | 0.10 | 2.51 | 0.245 | 0.234 | 0.010 | 0.04 | 20.72 | 18.10 | 79.43 | 3.83 | 33700. | 300. | 0.884 |
| 350. | 0.10 | 2.57 | 0.253 | 0.218 | 0.035 | 0.14 | 20.22 | 14.90 | 52.97 | 2.62 | 436300. | 300. | 0.874 |
| 351. | 0.10 | 2.57 | 0.253 | 0.231 | 0.022 | 0.09 | 20.22 | 16.11 | 62.71 | 3.10 | 137700. | 300. | 0.874 |
| 183. | 0.10 | 2.62 | 0.229 | 0.224 | 0.004 | 0.02 | 12.89 | 11.86 | 65.45 | 5.08 | 15300. | 300. | 0.494 |
| 184. | 0.10 | 2.65 | 0.229 | 0.223 | 0.006 | 0.03 | 12.89 | 11.50 | 62.48 | 4.85 | 22700. | 300. | 0.488 |
| 185. | 0.10 | 2.65 | 0.229 | 0.223 | 0.006 | 0.03 | 12.89 | 11.50 | 62.48 | 4.85 | 22700. | 300. | 0.488 |
| 186. | 0.10 | 2.64 | 0.229 | 0.218 | 0.011 | 0.05 | 12.89 | 10.74 | 56.13 | 4.36 | 53300. | 300. | 0.490 |
| 187. | 0.10 | 2.64 | 0.229 | 0.215 | 0.014 | 0.06 | 12.89 | 10.45 | 50.51 | 3.92 | 75200. | 300. | 0.490 |
| 188. | 0.10 | 2.66 | 0.229 | 0.212 | 0.017 | 0.08 | 12.89 | 10.08 | 47.06 | 3.65 | 108800. | 300. | 0.486 |
| 189. | 0.10 | 2.63 | 0.229 | 0.209 | 0.020 | 0.09 | 12.89 | 9.95 | 43.94 | 3.41 | 143300. | 300. | 0.492 |

Table D.14 (cont.): Present Air-Water Flow Data: $D_3/D_1$ = 0.084, Horizontal Branch ($\Phi$ = 90°).

| RUN # | VsL1 (m/s) | VsG1 (m/s) | m1 (kg/s) | m2 (kg/s) | m3 (kg/s) | m3/m1 (-) | x1 (%) | x2 (%) | x3 (%) | x3/x1 (-) | p13 (Pa) | T1 (K) | p1 (MPa) |
|---|---|---|---|---|---|---|---|---|---|---|---|---|---|
| 190. | 0.10 | 2.62 | 0.229 | 0.206 | 0.023 | 0.10 | 12.85 | 9.42 | 43.57 | 3.39 | 210100. | 300. | 0.491 |
| 191. | 0.10 | 2.62 | 0.229 | 0.207 | 0.022 | 0.10 | 12.85 | 9.60 | 43.01 | 3.35 | 261000. | 300. | 0.491 |
| 59. | 0.10 | 5.09 | 0.293 | 0.288 | 0.006 | 0.02 | 35.13 | 33.96 | 94.67 | 2.69 | 10000. | 300. | 0.887 |
| 60. | 0.10 | 5.11 | 0.297 | 0.287 | 0.010 | 0.03 | 34.70 | 32.64 | 95.72 | 2.76 | 19400. | 300. | 0.884 |
| 61. | 0.10 | 5.11 | 0.297 | 0.285 | 0.012 | 0.04 | 34.70 | 32.01 | 96.19 | 2.77 | 39000. | 300. | 0.884 |
| 62. | 0.10 | 5.11 | 0.297 | 0.283 | 0.014 | 0.05 | 34.70 | 31.63 | 96.08 | 2.77 | 41900. | 300. | 0.884 |
| 63. | 0.10 | 5.11 | 0.297 | 0.281 | 0.016 | 0.05 | 34.70 | 31.15 | 95.91 | 2.76 | 61800. | 300. | 0.884 |
| 64. | 0.10 | 5.21 | 0.306 | 0.290 | 0.015 | 0.05 | 34.16 | 30.91 | 95.37 | 2.79 | 78600. | 300. | 0.878 |
| 65. | 0.10 | 5.18 | 0.303 | 0.286 | 0.017 | 0.05 | 34.51 | 30.99 | 95.43 | 2.77 | 104800. | 300. | 0.884 |
| 66. | 0.10 | 5.20 | 0.307 | 0.288 | 0.018 | 0.06 | 34.09 | 30.30 | 94.63 | 2.78 | 142300. | 300. | 0.880 |
| 67. | 0.11 | 5.18 | 0.317 | 0.298 | 0.020 | 0.06 | 32.95 | 28.93 | 94.31 | 2.86 | 173200. | 300. | 0.884 |
| 68. | 0.11 | 5.18 | 0.317 | 0.297 | 0.021 | 0.06 | 32.95 | 28.74 | 93.82 | 2.85 | 270600. | 300. | 0.883 |
| 69. | 0.11 | 5.18 | 0.317 | 0.294 | 0.023 | 0.07 | 32.95 | 28.23 | 93.13 | 2.83 | 426100. | 300. | 0.883 |
| 193. | 0.10 | 5.13 | 0.254 | 0.251 | 0.003 | 0.01 | 22.36 | 21.61 | 86.02 | 3.85 | 13400. | 300. | 0.485 |
| 194. | 0.10 | 5.14 | 0.254 | 0.250 | 0.004 | 0.02 | 22.36 | 21.22 | 89.75 | 4.01 | 20800. | 300. | 0.484 |
| 195. | 0.10 | 5.06 | 0.254 | 0.249 | 0.005 | 0.02 | 22.36 | 20.94 | 89.83 | 4.02 | 26600. | 300. | 0.492 |
| 196. | 0.10 | 5.11 | 0.254 | 0.248 | 0.006 | 0.02 | 22.36 | 20.64 | 91.06 | 4.07 | 34000. | 300. | 0.487 |
| 197. | 0.10 | 5.06 | 0.254 | 0.246 | 0.008 | 0.03 | 22.36 | 20.20 | 91.36 | 4.09 | 49200. | 300. | 0.492 |
| 198. | 0.10 | 5.13 | 0.261 | 0.252 | 0.009 | 0.03 | 21.94 | 19.43 | 92.29 | 4.21 | 65200. | 300. | 0.488 |
| 199. | 0.10 | 5.11 | 0.260 | 0.249 | 0.011 | 0.04 | 22.09 | 19.15 | 91.79 | 4.16 | 85600. | 300. | 0.492 |
| 200. | 0.10 | 5.11 | 0.260 | 0.249 | 0.011 | 0.04 | 22.09 | 18.91 | 91.50 | 4.14 | 100200. | 300. | 0.492 |
| 201. | 0.10 | 5.11 | 0.260 | 0.247 | 0.013 | 0.05 | 22.09 | 18.58 | 91.16 | 4.13 | 126900. | 300. | 0.492 |
| 202. | 0.10 | 5.12 | 0.260 | 0.246 | 0.014 | 0.05 | 22.12 | 18.33 | 90.28 | 4.08 | 162600. | 300. | 0.492 |
| 203. | 0.10 | 5.15 | 0.260 | 0.246 | 0.014 | 0.05 | 22.12 | 18.21 | 89.71 | 4.06 | 191300. | 300. | 0.489 |
| 204. | 0.10 | 5.15 | 0.260 | 0.245 | 0.015 | 0.06 | 22.12 | 18.03 | 89.35 | 4.04 | 223000. | 300. | 0.489 |
| 205. | 0.10 | 5.11 | 0.260 | 0.245 | 0.015 | 0.06 | 22.12 | 17.99 | 88.98 | 4.02 | 244600. | 300. | 0.493 |
| 109. | 0.10 | 7.74 | 0.354 | 0.348 | 0.006 | 0.02 | 43.89 | 43.08 | 87.62 | 2.00 | 15600. | 300. | 0.880 |
| 110. | 0.10 | 7.71 | 0.354 | 0.346 | 0.008 | 0.02 | 43.86 | 42.80 | 88.17 | 2.01 | 26500. | 300. | 0.882 |
| 111. | 0.10 | 7.71 | 0.354 | 0.345 | 0.009 | 0.03 | 43.86 | 42.63 | 89.08 | 2.03 | 34800. | 300. | 0.882 |
| 112. | 0.10 | 7.82 | 0.350 | 0.338 | 0.012 | 0.03 | 44.59 | 43.02 | 89.85 | 2.02 | 50700. | 300. | 0.874 |

Table D.14 (cont.): Present Air-Water Flow Data: $D_3/D_1$ = 0.084, Horizontal Branch ($\Phi$ = 90°).

| RUN # | VsL1 (m/s) | VsG1 (m/s) | m1 (kg/s) | m2 (kg/s) | m3 (kg/s) | m3/m1 (-) | x1 (%) | x2 (%) | x3 (%) | x3/x1 (-) | p13 (Pa) | T1 (K) | p1 (MPa) |
|---|---|---|---|---|---|---|---|---|---|---|---|---|---|
| 113. | 0.10 | 7.55 | 0.346 | 0.332 | 0.015 | 0.04 | 44.00 | 41.95 | 90.63 | 2.06 | 74000. | 300. | 0.884 |
| 114. | 0.10 | 7.57 | 0.349 | 0.332 | 0.017 | 0.05 | 43.66 | 41.25 | 91.62 | 2.10 | 98200. | 300. | 0.882 |
| 115. | 0.10 | 7.68 | 0.356 | 0.337 | 0.019 | 0.05 | 43.18 | 40.41 | 92.09 | 2.13 | 140700. | 300. | 0.878 |
| 116. | 0.10 | 7.31 | 0.337 | 0.318 | 0.020 | 0.06 | 44.12 | 41.16 | 91.11 | 2.07 | 185600. | 300. | 0.892 |
| 117. | 0.10 | 7.42 | 0.346 | 0.325 | 0.022 | 0.06 | 43.23 | 39.98 | 91.42 | 2.11 | 244700. | 300. | 0.885 |
| 118. | 0.10 | 7.42 | 0.346 | 0.324 | 0.023 | 0.07 | 43.23 | 39.84 | 91.07 | 2.11 | 291000. | 300. | 0.884 |
| 119. | 0.10 | 7.42 | 0.346 | 0.322 | 0.024 | 0.07 | 43.23 | 39.61 | 91.57 | 2.12 | 367600. | 300. | 0.884 |
| 120. | 0.10 | 7.42 | 0.346 | 0.321 | 0.025 | 0.07 | 43.23 | 39.47 | 91.20 | 2.11 | 429800. | 300. | 0.884 |
| 146. | 0.10 | 8.04 | 0.294 | 0.290 | 0.004 | 0.02 | 30.54 | 29.63 | 89.65 | 2.94 | 16800. | 300. | 0.490 |
| 147. | 0.10 | 8.09 | 0.294 | 0.289 | 0.006 | 0.02 | 30.54 | 29.37 | 90.19 | 2.95 | 26600. | 300. | 0.487 |
| 148. | 0.10 | 8.09 | 0.290 | 0.283 | 0.007 | 0.02 | 31.02 | 29.62 | 88.75 | 2.86 | 36400. | 300. | 0.487 |
| 149. | 0.10 | 8.04 | 0.290 | 0.282 | 0.008 | 0.03 | 31.02 | 29.31 | 89.40 | 2.88 | 52400. | 300. | 0.490 |
| 150. | 0.10 | 8.04 | 0.290 | 0.280 | 0.010 | 0.03 | 31.02 | 28.94 | 89.79 | 2.89 | 74600. | 300. | 0.490 |
| 151. | 0.10 | 8.07 | 0.290 | 0.279 | 0.011 | 0.04 | 31.02 | 28.67 | 90.35 | 2.91 | 97400. | 300. | 0.488 |
| 152. | 0.10 | 8.07 | 0.290 | 0.278 | 0.012 | 0.04 | 31.02 | 28.42 | 89.97 | 2.90 | 121800. | 300. | 0.488 |
| 153. | 0.10 | 7.95 | 0.290 | 0.276 | 0.014 | 0.05 | 30.97 | 27.96 | 90.99 | 2.94 | 173500. | 300. | 0.494 |
| 154. | 0.10 | 7.95 | 0.290 | 0.275 | 0.014 | 0.05 | 30.97 | 27.81 | 91.09 | 2.94 | 200400. | 300. | 0.494 |
| 155. | 0.10 | 7.95 | 0.290 | 0.275 | 0.015 | 0.05 | 30.97 | 27.71 | 91.24 | 2.95 | 229100. | 300. | 0.494 |
| 156. | 0.10 | 7.95 | 0.290 | 0.275 | 0.015 | 0.05 | 30.97 | 27.71 | 90.66 | 2.93 | 243800. | 300. | 0.494 |
| 71. | 0.10 | 10.58 | 0.405 | 0.400 | 0.004 | 0.01 | 52.04 | 52.05 | 51.39 | 0.99 | 16600. | 300. | 0.872 |
| 72. | 0.10 | 10.23 | 0.398 | 0.386 | 0.012 | 0.03 | 51.93 | 51.82 | 55.59 | 1.07 | 25900. | 300. | 0.885 |
| 73. | 0.10 | 10.27 | 0.406 | 0.395 | 0.011 | 0.03 | 50.90 | 50.20 | 76.17 | 1.50 | 35000. | 300. | 0.882 |
| 74. | 0.10 | 10.10 | 0.403 | 0.390 | 0.013 | 0.03 | 50.48 | 49.50 | 79.45 | 1.57 | 54500. | 300. | 0.882 |
| 75. | 0.10 | 10.08 | 0.403 | 0.387 | 0.016 | 0.04 | 50.51 | 49.27 | 80.85 | 1.60 | 89200. | 300. | 0.884 |
| 76. | 0.11 | 10.11 | 0.411 | 0.394 | 0.018 | 0.04 | 49.67 | 48.18 | 82.34 | 1.66 | 119700. | 300. | 0.886 |
| 77. | 0.11 | 10.36 | 0.416 | 0.395 | 0.021 | 0.05 | 50.22 | 48.55 | 82.13 | 1.64 | 164800. | 300. | 0.883 |
| 78. | 0.11 | 10.18 | 0.411 | 0.389 | 0.022 | 0.05 | 49.67 | 47.77 | 82.57 | 1.66 | 218400. | 300. | 0.880 |
| 79. | 0.11 | 10.36 | 0.423 | 0.399 | 0.024 | 0.06 | 49.34 | 47.34 | 82.63 | 1.67 | 256000. | 300. | 0.883 |
| 80. | 0.11 | 10.36 | 0.423 | 0.399 | 0.025 | 0.06 | 49.34 | 47.27 | 83.02 | 1.68 | 336000. | 300. | 0.883 |
| 81. | 0.11 | 10.38 | 0.416 | 0.391 | 0.025 | 0.06 | 50.22 | 48.14 | 83.12 | 1.66 | 388200. | 300. | 0.882 |

Table D.14 (cont.): Present Air-Water Flow Data: $D_3/D_1$ = 0.084, Horizontal Branch ($\Phi$ = 90°).

| RUN # | VsL1 (m/s) | VsG1 (m/s) | m1 (kg/s) | m2 (kg/s) | m3 (kg/s) | m3/m1 (-) | x1 (%) | x2 (%) | x3 (%) | x3/x1 (-) | p13 (Pa) | T1 (K) | p1 (MPa) |
|---|---|---|---|---|---|---|---|---|---|---|---|---|---|
| 481. | 0.26 | 10.08 | 0.705 | 0.694 | 0.012 | 0.02 | 28.59 | 28.02 | 62.76 | 2.19 | 26800. | 300. | 0.877 |
| 482. | 0.25 | 10.25 | 0.703 | 0.686 | 0.017 | 0.02 | 29.20 | 28.36 | 63.77 | 2.18 | 60200. | 300. | 0.877 |
| 483. | 0.25 | 10.25 | 0.703 | 0.682 | 0.020 | 0.03 | 29.20 | 28.01 | 68.97 | 2.36 | 101800. | 300. | 0.877 |
| 484. | 0.25 | 10.37 | 0.703 | 0.677 | 0.025 | 0.04 | 29.20 | 27.61 | 71.68 | 2.45 | 175400. | 300. | 0.867 |
| 485. | 0.25 | 10.46 | 0.705 | 0.678 | 0.026 | 0.04 | 29.38 | 27.78 | 70.51 | 2.40 | 253800. | 300. | 0.867 |
| 486. | 0.24 | 9.91 | 0.676 | 0.649 | 0.027 | 0.04 | 29.67 | 27.93 | 71.27 | 2.40 | 406400. | 300. | 0.886 |
| 487. | 0.24 | 10.22 | 0.679 | 0.652 | 0.027 | 0.04 | 30.04 | 28.34 | 70.90 | 2.36 | 448300. | 300. | 0.875 |
| 339. | 0.25 | 10.09 | 0.604 | 0.598 | 0.007 | 0.01 | 18.51 | 18.12 | 52.29 | 2.82 | 12100. | 300. | 0.486 |
| 340. | 0.25 | 10.05 | 0.604 | 0.595 | 0.010 | 0.02 | 18.51 | 17.93 | 54.04 | 2.92 | 29700. | 300. | 0.488 |
| 341. | 0.25 | 10.11 | 0.604 | 0.594 | 0.011 | 0.02 | 18.51 | 17.80 | 56.69 | 3.06 | 45500. | 300. | 0.485 |
| 342. | 0.25 | 10.11 | 0.604 | 0.592 | 0.013 | 0.02 | 18.51 | 17.59 | 60.94 | 3.29 | 70500. | 300. | 0.485 |
| 343. | 0.25 | 10.17 | 0.604 | 0.590 | 0.015 | 0.02 | 18.51 | 17.41 | 62.53 | 3.38 | 109700. | 300. | 0.482 |
| 344. | 0.25 | 10.00 | 0.600 | 0.584 | 0.017 | 0.03 | 18.64 | 17.33 | 64.71 | 3.47 | 156500. | 300. | 0.490 |
| 345. | 0.25 | 10.00 | 0.600 | 0.582 | 0.018 | 0.03 | 18.64 | 17.21 | 64.50 | 3.46 | 210900. | 300. | 0.490 |
| 346. | 0.25 | 10.00 | 0.600 | 0.582 | 0.019 | 0.03 | 18.64 | 17.17 | 64.76 | 3.47 | 249300. | 300. | 0.490 |
| 717. | 0.50 | 5.03 | 1.091 | 1.084 | 0.007 | 0.01 | 9.53 | 9.52 | 11.51 | 1.21 | 5802. | 292. | 0.882 |
| 718. | 0.50 | 5.03 | 1.091 | 1.078 | 0.013 | 0.01 | 9.53 | 9.47 | 14.94 | 1.57 | 20804. | 292. | 0.882 |
| 719. | 0.50 | 5.03 | 1.091 | 1.063 | 0.028 | 0.03 | 9.53 | 9.39 | 15.13 | 1.59 | 141856. | 292. | 0.882 |
| 720. | 0.50 | 5.03 | 1.091 | 1.057 | 0.034 | 0.03 | 9.53 | 9.37 | 14.43 | 1.51 | 238572. | 292. | 0.882 |
| 721. | 0.50 | 5.03 | 1.091 | 1.052 | 0.039 | 0.04 | 9.53 | 9.36 | 14.24 | 1.49 | 436840. | 292. | 0.882 |
| 711. | 0.51 | 5.01 | 1.056 | 1.048 | 0.008 | 0.01 | 5.46 | 5.42 | 10.12 | 1.86 | 5885. | 292. | 0.490 |
| 712. | 0.51 | 5.01 | 1.056 | 1.045 | 0.011 | 0.01 | 5.46 | 5.33 | 17.85 | 3.27 | 14504. | 292. | 0.490 |
| 713. | 0.51 | 5.01 | 1.056 | 1.043 | 0.013 | 0.01 | 5.46 | 5.27 | 20.47 | 3.75 | 19000. | 292. | 0.490 |
| 714. | 0.51 | 5.01 | 1.056 | 1.042 | 0.014 | 0.01 | 5.46 | 5.25 | 20.71 | 3.80 | 27824. | 292. | 0.490 |
| 715. | 0.51 | 5.01 | 1.056 | 1.039 | 0.017 | 0.02 | 5.46 | 5.23 | 19.61 | 3.59 | 170480. | 292. | 0.490 |
| 716. | 0.51 | 5.01 | 1.056 | 1.029 | 0.027 | 0.03 | 5.46 | 5.10 | 18.99 | 3.48 | 246880. | 292. | 0.490 |
| 464. | 0.51 | 9.88 | 1.201 | 1.187 | 0.015 | 0.01 | 16.66 | 16.41 | 37.19 | 2.23 | 25340. | 299. | 0.885 |
| 465. | 0.51 | 9.88 | 1.201 | 1.175 | 0.027 | 0.02 | 16.66 | 16.02 | 44.88 | 2.69 | 108160. | 299. | 0.885 |
| 466. | 0.52 | 9.99 | 1.221 | 1.182 | 0.039 | 0.03 | 16.49 | 15.52 | 45.93 | 2.78 | 431720. | 299. | 0.880 |
| 457. | 0.51 | 19.74 | 1.409 | 1.393 | 0.016 | 0.01 | 28.74 | 28.74 | 29.22 | 1.02 | 26700. | 295. | 0.884 |

Table D.14 (cont.): Present Air-Water Flow Data: $D_3/D_1$ = 0.084, Horizontal Branch ($\Phi$ = 90°).

| RUN # | VsL1 (m/s) | VsG1 (m/s) | m1 (kg/s) | m2 (kg/s) | m3 (kg/s) | m3/m1 (-) | x1 (%) | x2 (%) | x3 (%) | x3/x1 (-) | p13 (Pa) | T1 (K) | p1 (MPa) |
|---|---|---|---|---|---|---|---|---|---|---|---|---|---|
| 458. | 0.51 | 20.01 | 1.409 | 1.387 | 0.022 | 0.02 | 28.74 | 28.77 | 26.84 | 0.93 | 34980. | 299. | 0.884 |
| 459. | 0.51 | 20.01 | 1.409 | 1.382 | 0.027 | 0.02 | 28.74 | 28.76 | 27.98 | 0.97 | 63880. | 299. | 0.884 |
| 460. | 0.51 | 20.01 | 1.409 | 1.371 | 0.038 | 0.03 | 28.74 | 28.58 | 34.45 | 1.20 | 189400. | 299. | 0.884 |
| 461. | 0.51 | 20.01 | 1.409 | 1.362 | 0.047 | 0.03 | 28.74 | 28.53 | 34.89 | 1.21 | 369480. | 299. | 0.884 |
| 462. | 0.51 | 20.01 | 1.409 | 1.361 | 0.048 | 0.03 | 28.74 | 28.50 | 35.63 | 1.24 | 479000. | 299. | 0.884 |

Table D.14 (cont.): Present Air-Water Flow Data: $D_3/D_1$ = 0.084, Horizontal Branch ($\Phi$ = 90°).

| RUN # | VsL1 (m/s) | VsG1 (m/s) | m1 (kg/s) | m2 (kg/s) | m3 (kg/s) | m3/m1 (-) | x1 (%) | x2 (%) | x3 (%) | x3/x1 (-) | p13 (Pa) | T1 (K) | p1 (MPa) |
|---|---|---|---|---|---|---|---|---|---|---|---|---|---|
| 703. | 0.26 | 4.94 | 0.605 | 0.602 | 0.003 | 0.00 | 16.77 | 16.39 | 99.60 | 5.94 | 6838. | 291. | 0.872 |
| 704. | 0.26 | 4.94 | 0.605 | 0.593 | 0.012 | 0.02 | 16.77 | 15.04 | 99.86 | 5.96 | 352600. | 291. | 0.872 |
| 705. | 0.26 | 4.94 | 0.605 | 0.592 | 0.013 | 0.02 | 16.77 | 14.90 | 99.80 | 5.95 | 389856. | 291. | 0.872 |
| 606. | 0.25 | 5.02 | 0.547 | 0.547 | 0.001 | 0.00 | 10.23 | 10.15 | 78.83 | 7.71 | 213. | 301. | 0.490 |
| 607. | 0.25 | 5.02 | 0.547 | 0.546 | 0.001 | 0.00 | 10.23 | 10.06 | 79.85 | 7.81 | 341. | 301. | 0.490 |
| 608. | 0.25 | 5.02 | 0.547 | 0.545 | 0.002 | 0.00 | 10.23 | 9.90 | 86.30 | 8.44 | 6004. | 301. | 0.490 |
| 609. | 0.25 | 5.02 | 0.547 | 0.544 | 0.004 | 0.01 | 10.23 | 9.74 | 81.40 | 7.96 | 48620. | 301. | 0.490 |
| 610. | 0.25 | 5.02 | 0.547 | 0.543 | 0.005 | 0.01 | 10.23 | 9.60 | 84.41 | 8.25 | 142196. | 301. | 0.490 |
| 611. | 0.25 | 5.02 | 0.547 | 0.542 | 0.005 | 0.01 | 10.23 | 9.52 | 84.70 | 8.28 | 199668. | 301. | 0.490 |
| 612. | 0.25 | 5.02 | 0.547 | 0.542 | 0.005 | 0.01 | 10.23 | 9.52 | 84.09 | 8.22 | 221628. | 301. | 0.490 |
| 535. | 0.25 | 9.95 | 0.698 | 0.684 | 0.013 | 0.02 | 28.69 | 27.42 | 93.80 | 3.27 | 483720. | 301. | 0.884 |
| 536. | 0.25 | 9.95 | 0.698 | 0.684 | 0.014 | 0.02 | 28.69 | 27.43 | 91.89 | 3.20 | 484000. | 301. | 0.884 |
| 537. | 0.25 | 9.95 | 0.698 | 0.685 | 0.012 | 0.02 | 28.69 | 27.55 | 91.64 | 3.19 | 289144. | 301. | 0.884 |
| 538. | 0.25 | 9.95 | 0.698 | 0.693 | 0.004 | 0.01 | 28.69 | 28.33 | 87.17 | 3.04 | 69904. | 301. | 0.884 |
| 539. | 0.25 | 9.95 | 0.698 | 0.695 | 0.003 | 0.00 | 28.69 | 28.43 | 100.00 | 3.49 | 23639. | 301. | 0.884 |
| 696. | 0.26 | 19.87 | 0.923 | 0.920 | 0.003 | 0.00 | 44.09 | 44.11 | 37.52 | 0.85 | 891. | 295. | 0.882 |
| 697. | 0.26 | 19.87 | 0.923 | 0.917 | 0.006 | 0.01 | 44.09 | 44.02 | 54.35 | 1.23 | 8895. | 295. | 0.882 |
| 698. | 0.26 | 19.87 | 0.923 | 0.914 | 0.009 | 0.01 | 44.09 | 44.07 | 46.14 | 1.05 | 56272. | 295. | 0.882 |
| 699. | 0.26 | 19.87 | 0.923 | 0.910 | 0.012 | 0.01 | 44.09 | 43.98 | 51.88 | 1.18 | 184892. | 295. | 0.882 |
| 700. | 0.26 | 19.87 | 0.923 | 0.907 | 0.015 | 0.02 | 44.09 | 43.89 | 55.90 | 1.27 | 333768. | 295. | 0.882 |
| 701. | 0.26 | 19.87 | 0.923 | 0.907 | 0.016 | 0.02 | 44.09 | 43.86 | 56.90 | 1.29 | 408128. | 295. | 0.882 |
| 702. | 0.26 | 19.87 | 0.923 | 0.906 | 0.017 | 0.02 | 44.09 | 43.82 | 58.65 | 1.33 | 472416. | 295. | 0.882 |
| 598. | 0.50 | 2.50 | 1.038 | 1.035 | 0.004 | 0.00 | 4.90 | 4.74 | 53.30 | 10.87 | 4540. | 297. | 0.882 |
| 599. | 0.50 | 2.50 | 1.038 | 1.033 | 0.006 | 0.01 | 4.90 | 4.68 | 45.40 | 9.26 | 6041. | 297. | 0.882 |
| 600. | 0.50 | 2.50 | 1.038 | 1.031 | 0.007 | 0.01 | 4.90 | 4.62 | 47.35 | 9.66 | 22995. | 297. | 0.882 |
| 601. | 0.50 | 2.50 | 1.038 | 1.028 | 0.010 | 0.01 | 4.90 | 4.47 | 48.83 | 9.96 | 59512. | 297. | 0.882 |
| 602. | 0.50 | 2.50 | 1.038 | 1.024 | 0.014 | 0.01 | 4.90 | 4.32 | 47.44 | 9.68 | 199612. | 297. | 0.882 |
| 603. | 0.50 | 2.50 | 1.038 | 1.019 | 0.019 | 0.02 | 4.90 | 3.97 | 53.75 | 10.96 | 237292. | 297. | 0.882 |
| 604. | 0.50 | 2.50 | 1.038 | 1.015 | 0.023 | 0.02 | 4.90 | 3.94 | 47.91 | 9.77 | 393368. | 297. | 0.882 |
| 605. | 0.50 | 2.50 | 1.038 | 1.016 | 0.022 | 0.02 | 4.90 | 3.96 | 48.87 | 9.97 | 456456. | 297. | 0.882 |

Table D.15: Present Air-Water Flow Data: $D_3/D_1$ = 0.084, Upward Branch ($\Phi$ = 0°).

| RUN # | VsL1 (m/s) | VsG1 (m/s) | m1 (kg/s) | m2 (kg/s) | m3 (kg/s) | m3/m1 (-) | x1 (%) | x2 (%) | x3 (%) | x3/x1 (-) | p13 (Pa) | T1 (K) | p1 (MPa) |
|---|---|---|---|---|---|---|---|---|---|---|---|---|---|
| 598. | 0.50 | 2.50 | 1.038 | 1.035 | 0.004 | 0.00 | 4.90 | 4.74 | 53.30 | 10.87 | 4540. | 297. | 0.882 |
| 599. | 0.50 | 2.50 | 1.038 | 1.033 | 0.006 | 0.01 | 4.90 | 4.68 | 45.40 | 9.26 | 6041. | 297. | 0.882 |
| 600. | 0.50 | 2.50 | 1.038 | 1.031 | 0.007 | 0.01 | 4.90 | 4.62 | 47.35 | 9.66 | 22995. | 297. | 0.882 |
| 601. | 0.50 | 2.50 | 1.038 | 1.028 | 0.010 | 0.01 | 4.90 | 4.47 | 48.83 | 9.96 | 59512. | 297. | 0.882 |
| 602. | 0.50 | 2.50 | 1.038 | 1.024 | 0.014 | 0.01 | 4.90 | 4.32 | 47.44 | 9.68 | 199612. | 297. | 0.882 |
| 603. | 0.50 | 2.50 | 1.038 | 1.019 | 0.019 | 0.02 | 4.90 | 3.97 | 53.75 | 10.96 | 237292. | 297. | 0.882 |
| 604. | 0.50 | 2.50 | 1.038 | 1.015 | 0.023 | 0.02 | 4.90 | 3.94 | 47.91 | 9.77 | 393368. | 297. | 0.882 |
| 605. | 0.50 | 2.50 | 1.038 | 1.016 | 0.022 | 0.02 | 4.90 | 3.96 | 48.87 | 9.97 | 456456. | 297. | 0.882 |
| 515. | 0.51 | 2.56 | 1.042 | 1.042 | 0.000 | 0.00 | 4.82 | 4.78 | 100.00 | 20.76 | 336. | 305. | 0.872 |
| 516. | 0.51 | 2.52 | 1.042 | 1.035 | 0.007 | 0.01 | 4.82 | 4.54 | 44.04 | 9.14 | 1464. | 305. | 0.887 |
| 517. | 0.51 | 2.55 | 1.042 | 1.039 | 0.003 | 0.00 | 4.82 | 4.68 | 48.50 | 10.07 | 619. | 305. | 0.878 |
| 518. | 0.50 | 2.48 | 1.029 | 1.020 | 0.010 | 0.01 | 4.86 | 4.59 | 33.30 | 6.86 | 33173. | 300. | 0.882 |
| 519. | 0.50 | 2.48 | 1.029 | 1.013 | 0.016 | 0.02 | 4.86 | 4.43 | 31.60 | 6.51 | 129576. | 300. | 0.882 |
| 520. | 0.50 | 2.48 | 1.029 | 0.993 | 0.036 | 0.04 | 4.86 | 4.19 | 23.23 | 4.78 | 302776. | 300. | 0.882 |
| 521. | 0.50 | 2.48 | 1.029 | 0.983 | 0.046 | 0.04 | 4.86 | 4.16 | 19.76 | 4.07 | 428840. | 300. | 0.882 |
| 522. | 0.50 | 2.48 | 1.029 | 0.979 | 0.050 | 0.05 | 4.86 | 4.26 | 16.64 | 3.43 | 4993. | 300. | 0.882 |
| 540. | 0.50 | 9.97 | 1.177 | 1.172 | 0.005 | 0.00 | 17.35 | 17.24 | 41.90 | 2.41 | 12817. | 293. | 0.877 |
| 541. | 0.50 | 10.05 | 1.177 | 1.171 | 0.006 | 0.01 | 17.33 | 17.17 | 46.51 | 2.68 | 21677. | 296. | 0.877 |
| 542. | 0.50 | 10.05 | 1.177 | 1.170 | 0.007 | 0.01 | 17.33 | 17.17 | 43.28 | 2.50 | 37389. | 296. | 0.877 |
| 543. | 0.50 | 10.05 | 1.177 | 1.167 | 0.009 | 0.01 | 17.33 | 17.09 | 46.92 | 2.71 | 105700. | 296. | 0.877 |
| 544. | 0.50 | 10.05 | 1.177 | 1.164 | 0.013 | 0.01 | 17.33 | 16.97 | 50.10 | 2.89 | 181028. | 296. | 0.877 |
| 545. | 0.50 | 10.05 | 1.177 | 1.161 | 0.016 | 0.01 | 17.33 | 16.79 | 57.40 | 3.31 | 363240. | 296. | 0.877 |
| 546. | 0.50 | 10.05 | 1.177 | 1.161 | 0.016 | 0.01 | 17.33 | 16.76 | 58.25 | 3.36 | 419120. | 296. | 0.877 |
| 547. | 0.50 | 10.05 | 1.177 | 1.160 | 0.017 | 0.01 | 17.33 | 16.71 | 60.00 | 3.46 | 428408. | 296. | 0.877 |
| 574. | 0.50 | 20.08 | 1.395 | 1.394 | 0.002 | 0.00 | 29.59 | 29.56 | 50.22 | 1.70 | 5287. | 292. | 0.877 |
| 575. | 0.50 | 20.08 | 1.395 | 1.391 | 0.004 | 0.00 | 29.59 | 29.58 | 33.80 | 1.14 | 6007. | 292. | 0.877 |
| 576. | 0.50 | 20.08 | 1.395 | 1.389 | 0.007 | 0.00 | 29.59 | 29.56 | 36.15 | 1.22 | 9463. | 292. | 0.877 |
| 577. | 0.50 | 20.08 | 1.395 | 1.388 | 0.008 | 0.01 | 29.59 | 29.55 | 36.64 | 1.24 | 20270. | 292. | 0.877 |
| 578. | 0.50 | 20.08 | 1.395 | 1.384 | 0.012 | 0.01 | 29.59 | 29.49 | 41.11 | 1.39 | 74308. | 292. | 0.877 |
| 579. | 0.50 | 20.08 | 1.395 | 1.381 | 0.014 | 0.01 | 29.59 | 29.47 | 41.35 | 1.40 | 188252. | 292. | 0.877 |

Table D.15 (cont.): Present Air-Water Flow Data: $D_3/D_1$ = 0.084, Upward Branch ($\Phi$ = 0°).

| RUN # | VsL1 (m/s) | VsG1 (m/s) | m1 (kg/s) | m2 (kg/s) | m3 (kg/s) | m3/m1 (-) | x1 (%) | x2 (%) | x3 (%) | x3/x1 (-) | p13 (Pa) | T1 (K) | p1 (MPa) |
|---|---|---|---|---|---|---|---|---|---|---|---|---|---|
| 580. | 0.50 | 20.08 | 1.395 | 1.378 | 0.017 | 0.01 | 29.59 | 29.42 | 43.83 | 1.48 | 336568. | 292. | 0.877 |
| 581. | 0.50 | 20.08 | 1.395 | 1.378 | 0.018 | 0.01 | 29.59 | 29.38 | 45.78 | 1.55 | 405560. | 292. | 0.877 |
| 582. | 0.50 | 20.08 | 1.395 | 1.375 | 0.020 | 0.01 | 29.59 | 29.26 | 52.49 | 1.77 | 420688. | 292. | 0.877 |
| 591. | 1.00 | 2.49 | 2.010 | 1.995 | 0.015 | 0.01 | 2.55 | 2.48 | 11.90 | 4.67 | 10893. | 292. | 0.877 |
| 592. | 1.00 | 2.49 | 2.010 | 1.992 | 0.018 | 0.01 | 2.55 | 2.43 | 15.41 | 6.04 | 17143. | 292. | 0.877 |
| 593. | 1.00 | 2.49 | 2.010 | 1.983 | 0.027 | 0.01 | 2.55 | 2.43 | 11.19 | 4.39 | 37600. | 292. | 0.877 |
| 594. | 1.00 | 2.49 | 2.010 | 1.968 | 0.042 | 0.02 | 2.55 | 2.37 | 10.91 | 4.28 | 122180. | 292. | 0.877 |
| 595. | 1.00 | 2.49 | 2.010 | 1.952 | 0.058 | 0.03 | 2.55 | 2.36 | 8.83 | 3.46 | 229444. | 292. | 0.877 |
| 596. | 1.00 | 2.49 | 2.010 | 1.945 | 0.065 | 0.03 | 2.55 | 2.32 | 9.30 | 3.65 | 410672. | 292. | 0.877 |
| 597. | 1.00 | 2.49 | 2.010 | 1.940 | 0.070 | 0.04 | 2.55 | 2.32 | 9.02 | 3.54 | 434824. | 292. | 0.877 |
| 523. | 1.00 | 2.67 | 2.011 | 2.000 | 0.011 | 0.01 | 2.56 | 2.49 | 16.44 | 6.42 | 7134. | 311. | 0.877 |
| 524. | 1.00 | 2.49 | 2.009 | 1.994 | 0.015 | 0.01 | 2.46 | 2.34 | 19.09 | 7.75 | 14032. | 306. | 0.887 |
| 525. | 1.00 | 2.49 | 2.009 | 1.987 | 0.022 | 0.01 | 2.46 | 2.33 | 14.13 | 5.74 | 36884. | 306. | 0.887 |
| 526. | 1.00 | 2.49 | 2.009 | 1.973 | 0.036 | 0.02 | 2.46 | 2.27 | 13.25 | 5.38 | 130148. | 306. | 0.887 |
| 527. | 1.00 | 2.64 | 2.010 | 1.966 | 0.044 | 0.02 | 2.53 | 2.28 | 13.71 | 5.41 | 166384. | 311. | 0.877 |
| 528. | 0.99 | 2.52 | 1.992 | 1.923 | 0.069 | 0.03 | 2.47 | 2.17 | 10.87 | 4.39 | 375728. | 311. | 0.887 |
| 529. | 0.99 | 2.52 | 1.992 | 1.921 | 0.071 | 0.04 | 2.47 | 2.18 | 10.36 | 4.19 | 437176. | 311. | 0.887 |
| 628. | 1.00 | 4.98 | 2.060 | 2.053 | 0.007 | 0.00 | 4.91 | 4.85 | 22.92 | 4.66 | 5507. | 297. | 0.882 |
| 629. | 1.00 | 4.98 | 2.060 | 2.050 | 0.010 | 0.00 | 4.91 | 4.81 | 26.30 | 5.35 | 11782. | 297. | 0.882 |
| 630. | 1.00 | 4.98 | 2.060 | 2.045 | 0.015 | 0.01 | 4.91 | 4.74 | 28.29 | 5.76 | 83092. | 297. | 0.882 |
| 631. | 1.00 | 4.98 | 2.060 | 2.038 | 0.022 | 0.01 | 4.91 | 4.64 | 30.12 | 6.13 | 235348. | 297. | 0.882 |
| 632. | 1.00 | 4.98 | 2.060 | 2.031 | 0.029 | 0.01 | 4.91 | 4.53 | 31.97 | 6.51 | 390112. | 297. | 0.882 |
| 633. | 1.00 | 4.98 | 2.060 | 2.029 | 0.031 | 0.01 | 4.91 | 4.51 | 31.81 | 6.48 | 416464. | 297. | 0.882 |
| 634. | 1.00 | 4.98 | 2.060 | 2.029 | 0.031 | 0.01 | 4.91 | 4.51 | 31.81 | 6.48 | 416400. | 297. | 0.882 |
| 621. | 1.00 | 4.96 | 2.024 | 2.021 | 0.003 | 0.00 | 2.85 | 2.83 | 17.88 | 6.28 | 4645. | 289. | 0.490 |
| 622. | 1.00 | 4.96 | 2.024 | 2.017 | 0.007 | 0.00 | 2.85 | 2.79 | 18.38 | 6.46 | 7639. | 289. | 0.490 |
| 623. | 1.00 | 4.96 | 2.024 | 2.010 | 0.014 | 0.01 | 2.85 | 2.74 | 17.82 | 6.26 | 17870. | 289. | 0.490 |
| 624. | 1.00 | 4.96 | 2.024 | 2.009 | 0.015 | 0.01 | 2.85 | 2.72 | 19.11 | 6.72 | 63864. | 289. | 0.490 |
| 625. | 1.00 | 4.96 | 2.024 | 2.007 | 0.017 | 0.01 | 2.85 | 2.69 | 21.18 | 7.44 | 132108. | 289. | 0.490 |
| 626. | 1.00 | 4.96 | 2.024 | 2.005 | 0.020 | 0.01 | 2.85 | 2.67 | 20.58 | 7.23 | 204408. | 289. | 0.490 |

Table D.15 (cont.): Present Air-Water Flow Data: $D_3/D_1$ = 0.084, Upward Branch ($\Phi$ = 0°).

| RUN # | VsL1 (m/s) | VsG1 (m/s) | m1 (kg/s) | m2 (kg/s) | m3 (kg/s) | m3/m1 (-) | x1 (%) | x2 (%) | x3 (%) | x3/x1 (-) | p13 (Pa) | T1 (K) | p1 (MPa) |
|---|---|---|---|---|---|---|---|---|---|---|---|---|---|
| 627. | 1.00 | 4.96 | 2.024 | 2.003 | 0.021 | 0.01 | 2.85 | 2.65 | 21.61 | 7.59 | 235580. | 289. | 0.490 |
| 548. | 1.00 | 5.03 | 2.064 | 2.062 | 0.002 | 0.00 | 4.99 | 4.96 | 37.15 | 7.44 | 6388. | 295. | 0.882 |
| 549. | 1.00 | 5.03 | 2.064 | 2.058 | 0.006 | 0.00 | 4.99 | 4.93 | 23.80 | 4.77 | 7221. | 295. | 0.882 |
| 550. | 1.00 | 5.03 | 2.064 | 2.055 | 0.009 | 0.00 | 4.99 | 4.87 | 31.29 | 6.27 | 15286. | 295. | 0.882 |
| 551. | 1.00 | 5.03 | 2.064 | 2.050 | 0.015 | 0.01 | 4.99 | 4.82 | 29.33 | 5.87 | 92916. | 295. | 0.882 |
| 552. | 1.00 | 5.03 | 2.064 | 2.048 | 0.016 | 0.01 | 4.99 | 4.80 | 29.52 | 5.91 | 135188. | 295. | 0.882 |
| 553. | 1.00 | 5.03 | 2.064 | 2.044 | 0.021 | 0.01 | 4.99 | 4.68 | 35.88 | 7.19 | 249648. | 295. | 0.882 |
| 554. | 1.00 | 5.03 | 2.064 | 2.040 | 0.025 | 0.01 | 4.99 | 4.66 | 32.28 | 6.47 | 404112. | 295. | 0.882 |
| 555. | 1.00 | 5.03 | 2.064 | 2.039 | 0.026 | 0.01 | 4.99 | 4.62 | 34.72 | 6.95 | 434632. | 295. | 0.882 |
| 556. | 1.00 | 5.03 | 2.064 | 2.041 | 0.023 | 0.01 | 4.99 | 4.63 | 36.75 | 7.36 | 526888. | 295. | 0.882 |
| 628. | 1.00 | 4.98 | 2.060 | 2.053 | 0.007 | 0.00 | 4.91 | 4.85 | 22.92 | 4.66 | 5507. | 297. | 0.882 |
| 629. | 1.00 | 4.98 | 2.060 | 2.050 | 0.010 | 0.00 | 4.91 | 4.81 | 26.30 | 5.35 | 11782. | 297. | 0.882 |
| 630. | 1.00 | 4.98 | 2.060 | 2.045 | 0.015 | 0.01 | 4.91 | 4.74 | 28.29 | 5.76 | 83092. | 297. | 0.882 |
| 631. | 1.00 | 4.98 | 2.060 | 2.038 | 0.022 | 0.01 | 4.91 | 4.64 | 30.12 | 6.13 | 235348. | 297. | 0.882 |
| 632. | 1.00 | 4.98 | 2.060 | 2.031 | 0.029 | 0.01 | 4.91 | 4.53 | 31.97 | 6.51 | 390112. | 297. | 0.882 |
| 633. | 1.00 | 4.98 | 2.060 | 2.029 | 0.031 | 0.01 | 4.91 | 4.51 | 31.81 | 6.48 | 416464. | 297. | 0.882 |
| 634. | 1.00 | 4.98 | 2.060 | 2.029 | 0.031 | 0.01 | 4.91 | 4.51 | 31.81 | 6.48 | 416400. | 297. | 0.882 |
| 621. | 1.00 | 4.96 | 2.024 | 2.024 | 0.000 | 0.00 | 2.85 | 2.82 | 99.98 | 35.14 | 4645. | 289. | 0.490 |
| 622. | 1.00 | 4.96 | 2.024 | 2.017 | 0.007 | 0.00 | 2.85 | 2.79 | 18.38 | 6.46 | 7639. | 289. | 0.490 |
| 623. | 1.00 | 4.96 | 2.024 | 2.010 | 0.014 | 0.01 | 2.85 | 2.74 | 17.82 | 6.26 | 17870. | 289. | 0.490 |
| 624. | 1.00 | 4.96 | 2.024 | 2.009 | 0.015 | 0.01 | 2.85 | 2.72 | 19.11 | 6.72 | 63864. | 289. | 0.490 |
| 625. | 1.00 | 4.96 | 2.024 | 2.007 | 0.017 | 0.01 | 2.85 | 2.69 | 21.18 | 7.44 | 132108. | 289. | 0.490 |
| 626. | 1.00 | 4.96 | 2.024 | 2.005 | 0.020 | 0.01 | 2.85 | 2.67 | 20.58 | 7.23 | 204408. | 289. | 0.490 |
| 627. | 1.00 | 4.96 | 2.024 | 2.003 | 0.021 | 0.01 | 2.85 | 2.65 | 21.61 | 7.59 | 235580. | 289. | 0.490 |
| 557. | 1.00 | 10.04 | 2.172 | 2.164 | 0.008 | 0.00 | 9.47 | 9.43 | 17.78 | 1.88 | 8105. | 295. | 0.882 |
| 558. | 1.00 | 10.04 | 2.172 | 2.161 | 0.011 | 0.01 | 9.47 | 9.41 | 19.55 | 2.06 | 12912. | 295. | 0.882 |
| 559. | 1.00 | 10.04 | 2.172 | 2.159 | 0.013 | 0.01 | 9.47 | 9.40 | 21.24 | 2.24 | 17531. | 295. | 0.882 |
| 560. | 1.00 | 10.04 | 2.172 | 2.152 | 0.020 | 0.01 | 9.47 | 9.40 | 16.67 | 1.76 | 106608. | 295. | 0.882 |
| 561. | 1.00 | 10.04 | 2.172 | 2.146 | 0.026 | 0.01 | 9.47 | 9.33 | 21.06 | 2.23 | 143376. | 295. | 0.882 |
| 562. | 1.00 | 10.04 | 2.172 | 2.145 | 0.027 | 0.01 | 9.47 | 9.32 | 20.84 | 2.20 | 273624. | 295. | 0.882 |

Table D.15 (cont.): Present Air-Water Flow Data: $D_3/D_1$ = 0.084, Upward Branch ($\Phi$ = 0°).

| RUN # | VsL1 (m/s) | VsG1 (m/s) | m1 (kg/s) | m2 (kg/s) | m3 (kg/s) | m3/m1 (-) | x1 (%) | x2 (%) | x3 (%) | x3/x1 (-) | p13 (Pa) | T1 (K) | p1 (MPa) |
|---|---|---|---|---|---|---|---|---|---|---|---|---|---|
| 563. | 1.00 | 10.04 | 2.172 | 2.143 | 0.029 | 0.01 | 9.47 | 9.28 | 23.40 | 2.47 | 417080. | 295. | 0.882 |
| 564. | 1.00 | 10.04 | 2.172 | 2.142 | 0.031 | 0.01 | 9.47 | 9.21 | 27.50 | 2.90 | 446776. | 295. | 0.882 |
| 565. | 1.00 | 10.04 | 2.172 | 2.141 | 0.032 | 0.01 | 9.47 | 9.21 | 26.61 | 2.81 | 450352. | 295. | 0.882 |
| 566. | 1.00 | 20.23 | 2.375 | 2.369 | 0.007 | 0.00 | 17.20 | 17.17 | 28.90 | 1.68 | 7757. | 299. | 0.882 |
| 567. | 1.00 | 20.23 | 2.375 | 2.366 | 0.009 | 0.00 | 17.20 | 17.15 | 31.59 | 1.84 | 14864. | 299. | 0.882 |
| 568. | 1.00 | 20.23 | 2.375 | 2.363 | 0.012 | 0.01 | 17.20 | 17.12 | 32.45 | 1.89 | 49064. | 299. | 0.882 |
| 569. | 1.00 | 20.23 | 2.375 | 2.359 | 0.016 | 0.01 | 17.20 | 17.06 | 37.35 | 2.17 | 118692. | 299. | 0.882 |
| 570. | 1.00 | 20.23 | 2.375 | 2.355 | 0.021 | 0.01 | 17.20 | 17.02 | 38.50 | 2.24 | 234252. | 299. | 0.882 |
| 571. | 1.00 | 20.23 | 2.375 | 2.352 | 0.023 | 0.01 | 17.20 | 16.98 | 39.85 | 2.32 | 375264. | 299. | 0.882 |
| 572. | 1.00 | 20.23 | 2.375 | 2.352 | 0.024 | 0.01 | 17.20 | 16.96 | 41.46 | 2.41 | 436408. | 299. | 0.882 |
| 573. | 1.00 | 20.23 | 2.375 | 2.351 | 0.025 | 0.01 | 17.20 | 16.98 | 38.26 | 2.22 | 233068. | 299. | 0.882 |
| 679. | 1.03 | 20.06 | 2.242 | 2.241 | 0.001 | 0.00 | 10.14 | 10.11 | 84.86 | 8.37 | 6645. | 296. | 0.490 |
| 680. | 1.03 | 20.06 | 2.242 | 2.235 | 0.007 | 0.00 | 10.14 | 10.10 | 24.15 | 2.38 | 12280. | 296. | 0.490 |
| 681. | 1.03 | 20.06 | 2.242 | 2.233 | 0.010 | 0.00 | 10.14 | 10.08 | 23.85 | 2.35 | 16512. | 296. | 0.490 |
| 682. | 1.03 | 20.06 | 2.242 | 2.231 | 0.012 | 0.01 | 10.14 | 10.06 | 26.53 | 2.62 | 26812. | 296. | 0.490 |
| 683. | 1.03 | 20.06 | 2.242 | 2.229 | 0.014 | 0.01 | 10.14 | 10.03 | 27.95 | 2.76 | 55356. | 296. | 0.490 |
| 684. | 1.03 | 20.06 | 2.242 | 2.226 | 0.017 | 0.01 | 10.14 | 10.03 | 25.40 | 2.50 | 144428. | 296. | 0.490 |
| 685. | 1.03 | 20.06 | 2.242 | 2.225 | 0.017 | 0.01 | 10.14 | 10.03 | 25.13 | 2.48 | 201276. | 296. | 0.490 |
| 686. | 1.03 | 20.06 | 2.242 | 2.225 | 0.018 | 0.01 | 10.14 | 10.03 | 24.15 | 2.38 | 237392. | 296. | 0.490 |
| 663. | 2.00 | 2.46 | 3.974 | 3.970 | 0.004 | 0.00 | 1.27 | 1.26 | 11.89 | 9.38 | 3511. | 295. | 0.882 |
| 664. | 2.00 | 2.46 | 3.974 | 3.950 | 0.024 | 0.01 | 1.27 | 1.23 | 7.63 | 6.02 | 18721. | 295. | 0.882 |
| 665. | 2.00 | 2.46 | 3.974 | 3.946 | 0.028 | 0.01 | 1.27 | 1.20 | 11.09 | 8.75 | 27095. | 295. | 0.882 |
| 666. | 2.00 | 2.46 | 3.974 | 3.931 | 0.043 | 0.01 | 1.27 | 1.20 | 7.07 | 5.57 | 120340. | 295. | 0.882 |
| 667. | 2.00 | 2.46 | 3.974 | 3.910 | 0.065 | 0.02 | 1.27 | 1.17 | 7.23 | 5.70 | 236580. | 295. | 0.882 |
| 668. | 2.00 | 2.46 | 3.974 | 3.910 | 0.064 | 0.02 | 1.27 | 1.15 | 8.60 | 6.78 | 237144. | 295. | 0.882 |
| 669. | 2.00 | 2.46 | 3.974 | 3.905 | 0.070 | 0.02 | 1.27 | 1.12 | 9.41 | 7.42 | 448136. | 295. | 0.882 |
| 670. | 2.00 | 2.46 | 3.974 | 3.903 | 0.071 | 0.02 | 1.27 | 1.13 | 8.62 | 6.79 | 463400. | 295. | 0.882 |
| 642. | 2.00 | 4.95 | 4.018 | 4.017 | 0.002 | 0.00 | 2.50 | 2.50 | 9.26 | 3.70 | 8346. | 297. | 0.882 |
| 643. | 2.00 | 4.95 | 4.018 | 4.011 | 0.007 | 0.00 | 2.50 | 2.50 | 7.11 | 2.84 | 9046. | 297. | 0.882 |
| 644. | 2.00 | 4.95 | 4.018 | 3.993 | 0.025 | 0.01 | 2.50 | 2.48 | 6.60 | 2.63 | 21514. | 297. | 0.882 |

Table D.15 (cont.): Present Air-Water Flow Data: $D_3/D_1$ = 0.084, Upward Branch ($\Phi$ = 0°).

| RUN # | VsL1 (m/s) | VsG1 (m/s) | m1 (kg/s) | m2 (kg/s) | m3 (kg/s) | m3/m1 (-) | x1 (%) | x2 (%) | x3 (%) | x3/x1 (-) | p13 (Pa) | T1 (K) | p1 (MPa) |
|---|---|---|---|---|---|---|---|---|---|---|---|---|---|
| 645. | 2.00 | 4.95 | 4.018 | 3.976 | 0.042 | 0.01 | 2.50 | 2.46 | 6.52 | 2.60 | 54924. | 297. | 0.882 |
| 646. | 2.00 | 4.95 | 4.018 | 3.948 | 0.070 | 0.02 | 2.50 | 2.45 | 5.33 | 2.13 | 235228. | 297. | 0.882 |
| 647. | 2.00 | 4.95 | 4.018 | 3.930 | 0.088 | 0.02 | 2.50 | 2.45 | 5.09 | 2.03 | 412688. | 297. | 0.882 |
| 648. | 2.00 | 4.95 | 4.018 | 3.933 | 0.085 | 0.02 | 2.50 | 2.42 | 6.20 | 2.47 | 481424. | 297. | 0.882 |
| 656. | 2.01 | 4.94 | 4.000 | 3.989 | 0.011 | 0.00 | 1.43 | 1.41 | 6.91 | 4.85 | 12842. | 291. | 0.490 |
| 657. | 2.01 | 4.94 | 4.000 | 3.973 | 0.027 | 0.01 | 1.43 | 1.39 | 6.72 | 4.72 | 28869. | 291. | 0.490 |
| 658. | 2.01 | 4.94 | 4.000 | 3.969 | 0.031 | 0.01 | 1.43 | 1.38 | 7.06 | 4.95 | 38210. | 291. | 0.490 |
| 659. | 2.01 | 4.94 | 4.000 | 3.962 | 0.038 | 0.01 | 1.43 | 1.37 | 7.19 | 5.05 | 72044. | 291. | 0.490 |
| 660. | 2.01 | 4.94 | 4.000 | 3.955 | 0.045 | 0.01 | 1.43 | 1.36 | 7.42 | 5.21 | 140772. | 291. | 0.490 |
| 661. | 2.01 | 4.94 | 4.000 | 3.953 | 0.047 | 0.01 | 1.43 | 1.35 | 7.38 | 5.18 | 214972. | 291. | 0.490 |
| 662. | 2.01 | 4.94 | 4.000 | 3.950 | 0.049 | 0.01 | 1.43 | 1.35 | 7.10 | 4.98 | 260368. | 291. | 0.490 |
| 649. | 2.00 | 9.97 | 4.118 | 4.100 | 0.018 | 0.00 | 4.86 | 4.86 | 5.31 | 1.09 | 14233. | 301. | 0.882 |
| 650. | 2.00 | 9.97 | 4.118 | 4.080 | 0.038 | 0.01 | 4.86 | 4.85 | 5.62 | 1.16 | 35393. | 301. | 0.882 |
| 651. | 2.00 | 9.97 | 4.118 | 4.072 | 0.045 | 0.01 | 4.86 | 4.84 | 6.35 | 1.31 | 63396. | 301. | 0.882 |
| 652. | 2.00 | 9.97 | 4.118 | 4.047 | 0.070 | 0.02 | 4.86 | 4.85 | 5.52 | 1.14 | 213504. | 301. | 0.882 |
| 653. | 2.00 | 9.97 | 4.118 | 4.039 | 0.079 | 0.02 | 4.86 | 4.84 | 6.02 | 1.24 | 414560. | 301. | 0.882 |
| 654. | 2.00 | 9.97 | 4.118 | 4.032 | 0.085 | 0.02 | 4.86 | 4.83 | 6.33 | 1.30 | 477888. | 301. | 0.882 |
| 655. | 2.00 | 9.97 | 4.118 | 4.031 | 0.086 | 0.02 | 4.86 | 4.83 | 6.35 | 1.31 | 482776. | 301. | 0.882 |
| 672. | 2.03 | 17.06 | 4.192 | 4.168 | 0.024 | 0.01 | 5.35 | 5.35 | 5.66 | 1.06 | 23104. | 296. | 0.568 |
| 673. | 2.03 | 17.06 | 4.192 | 4.157 | 0.035 | 0.01 | 5.35 | 5.35 | 5.31 | 0.99 | 38978. | 296. | 0.568 |
| 674. | 2.03 | 17.06 | 4.192 | 4.145 | 0.047 | 0.01 | 5.35 | 5.35 | 5.80 | 1.08 | 100252. | 296. | 0.568 |
| 675. | 2.03 | 17.06 | 4.192 | 4.134 | 0.057 | 0.01 | 5.35 | 5.34 | 6.09 | 1.14 | 187536. | 296. | 0.568 |
| 676. | 2.03 | 17.06 | 4.192 | 4.130 | 0.062 | 0.01 | 5.35 | 5.33 | 6.49 | 1.21 | 126684. | 296. | 0.568 |
| 677. | 2.03 | 17.06 | 4.192 | 4.127 | 0.065 | 0.02 | 5.35 | 5.33 | 6.43 | 1.20 | 310608. | 296. | 0.568 |
| 678. | 2.03 | 17.06 | 4.192 | 4.127 | 0.065 | 0.02 | 5.35 | 5.33 | 6.50 | 1.21 | 323040. | 296. | 0.568 |

Table D.15 (cont.): Present Air-Water Flow Data: $D_3/D_1$ = 0.084, Upward Branch ($\Phi$ = 0°).

| RUN # | VsL1 (m/s) | VsG1 (m/s) | m1 (kg/s) | m2 (kg/s) | m3 (kg/s) | m3/m1 (-) | x1 (%) | x2 (%) | x3 (%) | x3/x1 (-) | p13 (Pa) | T1 (K) | p1 (MPa) |
|---|---|---|---|---|---|---|---|---|---|---|---|---|---|
| 54. | 0.06 | 5.11 | 0.215 | 0.198 | 0.018 | 0.08 | 47.93 | 43.53 | 97.63 | 2.04 | 137500. | 300. | 0.884 |
| 55. | 0.06 | 5.11 | 0.215 | 0.195 | 0.020 | 0.09 | 47.93 | 42.79 | 97.27 | 2.03 | 192300. | 300. | 0.884 |
| 56. | 0.06 | 5.10 | 0.213 | 0.190 | 0.023 | 0.11 | 48.33 | 42.62 | 96.18 | 1.99 | 245700. | 300. | 0.884 |
| 57. | 0.06 | 5.10 | 0.213 | 0.189 | 0.024 | 0.11 | 48.33 | 42.17 | 96.44 | 2.00 | 386000. | 300. | 0.884 |
| 58. | 0.06 | 5.10 | 0.213 | 0.189 | 0.024 | 0.11 | 48.33 | 42.19 | 96.38 | 1.99 | 429200. | 300. | 0.884 |
| 28. | 0.05 | 5.12 | 0.164 | 0.161 | 0.003 | 0.02 | 35.22 | 33.95 | 94.61 | 2.69 | 11700. | 300. | 0.495 |
| 29. | 0.05 | 5.12 | 0.164 | 0.159 | 0.005 | 0.03 | 35.22 | 33.44 | 94.34 | 2.68 | 17700. | 300. | 0.495 |
| 30. | 0.05 | 5.12 | 0.164 | 0.158 | 0.006 | 0.04 | 35.30 | 33.10 | 94.62 | 2.68 | 25300. | 300. | 0.496 |
| 31. | 0.05 | 5.12 | 0.164 | 0.157 | 0.007 | 0.04 | 35.30 | 32.52 | 94.72 | 2.68 | 35300. | 300. | 0.496 |
| 32. | 0.05 | 5.12 | 0.164 | 0.156 | 0.008 | 0.05 | 35.30 | 32.04 | 95.31 | 2.70 | 48700. | 300. | 0.496 |
| 33. | 0.05 | 5.15 | 0.164 | 0.154 | 0.010 | 0.06 | 35.30 | 31.37 | 95.68 | 2.71 | 70000. | 300. | 0.493 |
| 34. | 0.05 | 5.17 | 0.164 | 0.152 | 0.012 | 0.07 | 35.22 | 30.48 | 96.18 | 2.73 | 102100. | 300. | 0.490 |
| 35. | 0.05 | 5.15 | 0.163 | 0.150 | 0.013 | 0.08 | 35.44 | 30.21 | 96.40 | 2.72 | 128600. | 300. | 0.492 |
| 36. | 0.05 | 5.12 | 0.163 | 0.149 | 0.014 | 0.08 | 35.44 | 29.84 | 95.98 | 2.71 | 286200. | 300. | 0.495 |
| 37. | 0.05 | 5.11 | 0.163 | 0.151 | 0.012 | 0.07 | 35.44 | 30.70 | 95.21 | 2.69 | 196600. | 300. | 0.496 |
| 38. | 0.05 | 5.14 | 0.163 | 0.151 | 0.012 | 0.08 | 35.44 | 30.52 | 95.21 | 2.69 | 235300. | 300. | 0.493 |
| 207. | 0.05 | 5.16 | 0.159 | 0.157 | 0.002 | 0.01 | 36.31 | 35.51 | 97.75 | 2.69 | 9300. | 300. | 0.490 |
| 208. | 0.05 | 5.16 | 0.159 | 0.155 | 0.003 | 0.02 | 36.31 | 34.93 | 98.61 | 2.72 | 14300. | 300. | 0.490 |
| 209. | 0.05 | 5.18 | 0.159 | 0.155 | 0.004 | 0.03 | 36.31 | 34.60 | 98.20 | 2.70 | 20000. | 300. | 0.488 |
| 210. | 0.05 | 5.18 | 0.159 | 0.154 | 0.005 | 0.03 | 36.31 | 34.21 | 98.24 | 2.71 | 28000. | 300. | 0.488 |
| 211. | 0.05 | 5.22 | 0.159 | 0.153 | 0.006 | 0.04 | 36.31 | 33.86 | 97.87 | 2.70 | 36000. | 300. | 0.484 |
| 212. | 0.06 | 5.22 | 0.175 | 0.168 | 0.008 | 0.04 | 32.93 | 30.06 | 95.49 | 2.90 | 49000. | 300. | 0.484 |
| 213. | 0.05 | 5.22 | 0.160 | 0.151 | 0.009 | 0.06 | 36.06 | 32.45 | 95.94 | 2.66 | 64600. | 300. | 0.484 |
| 214. | 0.05 | 5.22 | 0.160 | 0.150 | 0.010 | 0.07 | 36.06 | 31.87 | 96.21 | 2.67 | 80100. | 300. | 0.484 |
| 215. | 0.05 | 5.22 | 0.160 | 0.148 | 0.012 | 0.08 | 36.06 | 31.08 | 96.58 | 2.68 | 101000. | 300. | 0.484 |
| 216. | 0.05 | 5.22 | 0.160 | 0.147 | 0.013 | 0.08 | 36.06 | 30.70 | 96.66 | 2.68 | 133200. | 300. | 0.484 |
| 217. | 0.05 | 5.13 | 0.160 | 0.146 | 0.014 | 0.09 | 36.06 | 30.20 | 96.47 | 2.68 | 172200. | 300. | 0.493 |
| 218. | 0.05 | 5.13 | 0.160 | 0.145 | 0.015 | 0.09 | 36.06 | 30.03 | 95.49 | 2.65 | 197700. | 300. | 0.493 |
| 219. | 0.05 | 5.15 | 0.160 | 0.145 | 0.015 | 0.09 | 36.06 | 29.93 | 95.40 | 2.65 | 227500. | 300. | 0.491 |
| 94. | 0.06 | 7.64 | 0.270 | 0.265 | 0.005 | 0.02 | 56.40 | 55.75 | 92.07 | 1.63 | 14900. | 300. | 0.872 |

Table D.16 : Present Air-Water Flow Data: $D_3/D_1$ = 0.084, Downward Branch ($\Phi$ = 180°).

| RUN # | VsL1 (m/s) | VsG1 (m/s) | m1 (kg/s) | m2 (kg/s) | m3 (kg/s) | m3/m1 (-) | x1 (%) | x2 (%) | x3 (%) | x3/x1 (-) | p13 (Pa) | T1 (K) | p1 (MPa) |
|---|---|---|---|---|---|---|---|---|---|---|---|---|---|
| 95. | 0.06 | 7.64 | 0.270 | 0.263 | 0.006 | 0.02 | 56.40 | 55.54 | 92.85 | 1.65 | 20200. | 300. | 0.872 |
| 96. | 0.06 | 7.34 | 0.261 | 0.253 | 0.008 | 0.03 | 56.66 | 55.54 | 93.49 | 1.65 | 28400. | 300. | 0.882 |
| 97. | 0.06 | 7.36 | 0.261 | 0.252 | 0.009 | 0.03 | 56.66 | 55.32 | 93.84 | 1.66 | 35900. | 300. | 0.879 |
| 98. | 0.06 | 7.33 | 0.261 | 0.249 | 0.012 | 0.05 | 56.66 | 54.90 | 93.72 | 1.65 | 52000. | 300. | 0.883 |
| 99. | 0.06 | 7.28 | 0.260 | 0.246 | 0.014 | 0.05 | 56.49 | 54.40 | 93.94 | 1.66 | 67200. | 300. | 0.883 |
| 100. | 0.06 | 7.29 | 0.260 | 0.243 | 0.017 | 0.06 | 56.49 | 53.87 | 94.63 | 1.68 | 93000. | 300. | 0.882 |
| 101. | 0.06 | 7.40 | 0.264 | 0.247 | 0.017 | 0.06 | 56.55 | 53.91 | 94.60 | 1.67 | 122100. | 300. | 0.885 |
| 102. | 0.06 | 7.40 | 0.264 | 0.247 | 0.018 | 0.07 | 56.58 | 53.86 | 94.31 | 1.67 | 146700. | 300. | 0.886 |
| 103. | 0.06 | 7.40 | 0.264 | 0.245 | 0.020 | 0.07 | 56.60 | 53.58 | 94.31 | 1.67 | 186800. | 300. | 0.886 |
| 104. | 0.06 | 7.40 | 0.264 | 0.242 | 0.022 | 0.08 | 56.60 | 53.08 | 94.74 | 1.67 | 228400. | 300. | 0.886 |
| 105. | 0.07 | 7.44 | 0.279 | 0.256 | 0.023 | 0.08 | 53.64 | 49.94 | 94.27 | 1.76 | 281000. | 300. | 0.882 |
| 106. | 0.05 | 7.69 | 0.258 | 0.234 | 0.024 | 0.09 | 59.53 | 56.04 | 94.12 | 1.58 | 331400. | 300. | 0.874 |
| 107. | 0.05 | 7.69 | 0.258 | 0.233 | 0.024 | 0.09 | 59.53 | 55.93 | 94.17 | 1.58 | 398000. | 300. | 0.874 |
| 158. | 0.05 | 7.97 | 0.193 | 0.189 | 0.004 | 0.02 | 46.48 | 45.37 | 94.64 | 2.04 | 15500. | 300. | 0.493 |
| 159. | 0.05 | 7.97 | 0.193 | 0.188 | 0.005 | 0.03 | 46.48 | 45.18 | 93.55 | 2.01 | 22400. | 300. | 0.493 |
| 160. | 0.05 | 8.00 | 0.193 | 0.187 | 0.006 | 0.03 | 46.48 | 44.99 | 93.39 | 2.01 | 26900. | 300. | 0.491 |
| 161. | 0.06 | 8.00 | 0.199 | 0.192 | 0.006 | 0.03 | 45.12 | 43.49 | 93.56 | 2.07 | 35000. | 300. | 0.491 |
| 162. | 0.06 | 8.02 | 0.199 | 0.191 | 0.008 | 0.04 | 45.12 | 43.02 | 94.18 | 2.09 | 51600. | 300. | 0.490 |
| 163. | 0.06 | 8.02 | 0.199 | 0.189 | 0.010 | 0.05 | 45.10 | 42.53 | 94.95 | 2.11 | 74000. | 300. | 0.490 |
| 164. | 0.06 | 8.02 | 0.199 | 0.188 | 0.011 | 0.06 | 45.10 | 42.10 | 94.51 | 2.10 | 100160. | 300. | 0.490 |
| 165. | 0.06 | 8.02 | 0.199 | 0.186 | 0.013 | 0.06 | 45.10 | 41.75 | 94.17 | 2.09 | 139000. | 300. | 0.490 |
| 166. | 0.06 | 7.89 | 0.199 | 0.185 | 0.014 | 0.07 | 45.10 | 41.33 | 93.56 | 2.07 | 188300. | 300. | 0.498 |
| 167. | 0.06 | 7.86 | 0.199 | 0.184 | 0.015 | 0.07 | 45.10 | 41.29 | 93.45 | 2.07 | 210600. | 300. | 0.500 |
| 168. | 0.06 | 7.86 | 0.199 | 0.184 | 0.015 | 0.07 | 45.10 | 41.24 | 93.68 | 2.08 | 244100. | 300. | 0.500 |
| 83. | 0.05 | 10.57 | 0.317 | 0.310 | 0.007 | 0.02 | 67.12 | 66.80 | 80.97 | 1.21 | 16300. | 300. | 0.882 |
| 84. | 0.05 | 10.54 | 0.317 | 0.307 | 0.009 | 0.03 | 67.05 | 66.61 | 81.75 | 1.22 | 25200. | 300. | 0.882 |
| 85. | 0.05 | 10.50 | 0.317 | 0.306 | 0.010 | 0.03 | 67.05 | 66.52 | 82.51 | 1.23 | 34900. | 300. | 0.885 |
| 86. | 0.05 | 10.50 | 0.317 | 0.304 | 0.013 | 0.04 | 67.05 | 66.42 | 82.27 | 1.23 | 50100. | 300. | 0.885 |
| 87. | 0.05 | 10.54 | 0.317 | 0.302 | 0.014 | 0.05 | 67.05 | 66.29 | 82.85 | 1.24 | 73100. | 300. | 0.882 |
| 88. | 0.05 | 10.62 | 0.317 | 0.300 | 0.016 | 0.05 | 67.05 | 66.12 | 84.16 | 1.26 | 97000. | 300. | 0.875 |

Table D.16 (cont.): Present Air-Water Flow Data: $D_3/D_1$ = 0.084, Downward Branch ($\Phi$ = 180°).

| RUN # | VsL1 (m/s) | VsG1 (m/s) | m1 (kg/s) | m2 (kg/s) | m3 (kg/s) | m3/m1 (-) | x1 (%) | x2 (%) | x3 (%) | x3/x1 (-) | p13 (Pa) | T1 (K) | p1 (MPa) |
|---|---|---|---|---|---|---|---|---|---|---|---|---|---|
| 475. | 0.05 | 5.08 | 0.207 | 0.158 | 0.049 | 0.24 | 49.30 | 63.74 | 2.54 | 0.05 | 20000. | 301. | 0.882 |
| 476. | 0.05 | 5.08 | 0.207 | 0.145 | 0.061 | 0.30 | 49.30 | 68.06 | 4.93 | 0.10 | 56012. | 301. | 0.882 |
| 477. | 0.05 | 5.08 | 0.207 | 0.135 | 0.072 | 0.35 | 49.30 | 71.72 | 6.88 | 0.14 | 130662. | 301. | 0.882 |
| 478. | 0.05 | 5.08 | 0.207 | 0.128 | 0.079 | 0.38 | 49.30 | 74.61 | 8.33 | 0.17 | 224008. | 301. | 0.882 |
| 492. | 0.05 | 9.82 | 0.306 | 0.264 | 0.042 | 0.14 | 65.77 | 75.44 | 5.10 | 0.08 | 30360. | 295. | 0.884 |
| 493. | 0.05 | 9.82 | 0.306 | 0.252 | 0.054 | 0.18 | 65.77 | 78.24 | 7.57 | 0.12 | 82032. | 295. | 0.884 |
| 494. | 0.05 | 9.82 | 0.306 | 0.234 | 0.072 | 0.24 | 65.77 | 83.65 | 7.99 | 0.12 | 148040. | 295. | 0.884 |
| 495. | 0.05 | 9.82 | 0.306 | 0.233 | 0.073 | 0.24 | 65.77 | 83.58 | 9.25 | 0.14 | 217904. | 295. | 0.884 |
| 496. | 0.05 | 9.82 | 0.306 | 0.232 | 0.074 | 0.24 | 65.77 | 83.51 | 10.46 | 0.16 | 281572. | 295. | 0.884 |
| 469. | 0.10 | 5.03 | 0.297 | 0.213 | 0.084 | 0.28 | 34.05 | 47.17 | 0.82 | 0.02 | 40912. | 301. | 0.882 |
| 470. | 0.10 | 5.03 | 0.297 | 0.200 | 0.097 | 0.33 | 34.05 | 49.76 | 1.58 | 0.05 | 90772. | 301. | 0.882 |
| 471. | 0.10 | 5.03 | 0.297 | 0.189 | 0.108 | 0.36 | 34.05 | 52.13 | 2.34 | 0.07 | 160124. | 301. | 0.882 |
| 472. | 0.10 | 5.03 | 0.297 | 0.175 | 0.121 | 0.41 | 34.05 | 54.86 | 4.05 | 0.12 | 299373. | 301. | 0.882 |
| 473. | 0.10 | 5.03 | 0.297 | 0.168 | 0.128 | 0.43 | 34.05 | 56.67 | 4.39 | 0.13 | 425008. | 301. | 0.882 |
| 474. | 0.10 | 5.03 | 0.297 | 0.166 | 0.131 | 0.44 | 34.05 | 57.23 | 4.65 | 0.14 | 520000. | 301. | 0.882 |
| 486. | 0.10 | 10.03 | 0.400 | 0.337 | 0.064 | 0.16 | 51.04 | 60.40 | 1.73 | 0.03 | 33756. | 295. | 0.878 |
| 487. | 0.10 | 10.03 | 0.400 | 0.328 | 0.072 | 0.18 | 51.04 | 61.70 | 2.51 | 0.05 | 72816. | 295. | 0.878 |
| 488. | 0.10 | 10.03 | 0.400 | 0.318 | 0.082 | 0.21 | 51.04 | 63.33 | 3.45 | 0.07 | 137068. | 295. | 0.878 |
| 489. | 0.10 | 10.03 | 0.400 | 0.305 | 0.096 | 0.24 | 51.04 | 65.22 | 5.84 | 0.11 | 283484. | 295. | 0.878 |
| 490. | 0.10 | 10.03 | 0.400 | 0.296 | 0.104 | 0.26 | 51.04 | 66.90 | 5.96 | 0.12 | 399040. | 295. | 0.878 |
| 491. | 0.10 | 10.03 | 0.400 | 0.293 | 0.108 | 0.27 | 51.04 | 67.50 | 6.35 | 0.12 | 525000. | 295. | 0.878 |
| 458. | 0.25 | 4.63 | 0.545 | 0.416 | 0.128 | 0.24 | 9.55 | 12.45 | 0.13 | 0.01 | 42488. | 299. | 0.490 |
| 459. | 0.25 | 5.01 | 0.547 | 0.395 | 0.152 | 0.28 | 10.27 | 14.14 | 0.19 | 0.02 | 82108. | 299. | 0.490 |
| 460. | 0.25 | 5.01 | 0.547 | 0.370 | 0.177 | 0.32 | 10.27 | 15.06 | 0.27 | 0.03 | 159768. | 299. | 0.490 |
| 461. | 0.25 | 5.01 | 0.547 | 0.366 | 0.181 | 0.33 | 10.27 | 15.14 | 0.40 | 0.04 | 217632. | 299. | 0.490 |
| 462. | 0.25 | 5.01 | 0.547 | 0.343 | 0.204 | 0.37 | 10.27 | 16.07 | 0.53 | 0.05 | 337832. | 299. | 0.490 |
| 463. | 0.25 | 5.14 | 0.594 | 0.459 | 0.134 | 0.23 | 17.45 | 22.51 | 0.14 | 0.01 | 54812. | 299. | 0.880 |
| 464. | 0.25 | 5.14 | 0.594 | 0.426 | 0.167 | 0.28 | 17.45 | 24.09 | 0.54 | 0.03 | 111292. | 299. | 0.880 |
| 465. | 0.25 | 5.13 | 0.593 | 0.399 | 0.195 | 0.33 | 17.42 | 25.64 | 0.60 | 0.03 | 200652. | 299. | 0.880 |
| 466. | 0.25 | 5.13 | 0.593 | 0.373 | 0.220 | 0.37 | 17.42 | 27.37 | 0.58 | 0.03 | 298844. | 299. | 0.880 |

Table D.16 (cont.): Present Air-Water Flow Data: $D_3/D_1$ = 0.084, Downward Branch ($\Phi$ = 180°).

| RUN # | VsL1 (m/s) | VsG1 (m/s) | m1 (kg/s) | m2 (kg/s) | m3 (kg/s) | m3/m1 (-) | x1 (%) | x2 (%) | x3 (%) | x3/x1 (-) | p13 (Pa) | T1 (K) | p1 (MPa) |
|---|---|---|---|---|---|---|---|---|---|---|---|---|---|
| 135. | 0.10 | 10.04 | 0.307 | 0.302 | 0.005 | 0.02 | 36.89 | 36.16 | 78.94 | 2.14 | 17100. | 300. | 0.495 |
| 136. | 0.10 | 10.04 | 0.314 | 0.308 | 0.007 | 0.02 | 36.08 | 35.14 | 79.92 | 2.21 | 24900. | 300. | 0.495 |
| 137. | 0.10 | 10.04 | 0.314 | 0.306 | 0.008 | 0.03 | 36.08 | 34.94 | 79.33 | 2.20 | 35900. | 300. | 0.495 |
| 138. | 0.10 | 10.14 | 0.314 | 0.305 | 0.009 | 0.03 | 36.08 | 34.72 | 81.39 | 2.26 | 54400. | 300. | 0.490 |
| 139. | 0.10 | 10.14 | 0.314 | 0.303 | 0.011 | 0.04 | 36.08 | 34.41 | 81.81 | 2.27 | 77700. | 300. | 0.490 |
| 140. | 0.10 | 10.23 | 0.319 | 0.307 | 0.012 | 0.04 | 35.87 | 34.00 | 82.94 | 2.31 | 100800. | 300. | 0.490 |
| 141. | 0.10 | 10.23 | 0.311 | 0.298 | 0.013 | 0.04 | 36.77 | 34.71 | 83.21 | 2.26 | 129500. | 300. | 0.490 |
| 142. | 0.10 | 10.25 | 0.311 | 0.297 | 0.014 | 0.05 | 36.81 | 34.53 | 83.55 | 2.27 | 167600. | 300. | 0.490 |
| 143. | 0.10 | 10.25 | 0.319 | 0.304 | 0.015 | 0.05 | 35.91 | 33.55 | 83.62 | 2.33 | 199900. | 300. | 0.490 |
| 144. | 0.10 | 10.25 | 0.319 | 0.303 | 0.016 | 0.05 | 35.91 | 33.50 | 82.15 | 2.29 | 247600. | 300. | 0.490 |
| 354. | 0.18 | 1.06 | 0.367 | 0.346 | 0.021 | 0.06 | 5.81 | 4.46 | 28.40 | 4.89 | 21900. | 300. | 0.884 |
| 355. | 0.18 | 1.05 | 0.367 | 0.286 | 0.081 | 0.22 | 5.81 | 3.19 | 15.10 | 2.60 | 371700. | 300. | 0.887 |
| 356. | 0.18 | 1.05 | 0.367 | 0.330 | 0.037 | 0.10 | 5.81 | 3.31 | 28.06 | 4.83 | 122600. | 300. | 0.887 |
| 542. | 0.18 | 1.09 | 0.365 | 0.341 | 0.023 | 0.06 | 5.92 | 4.67 | 24.37 | 4.11 | 32000. | 300. | 0.870 |
| 543. | 0.18 | 1.09 | 0.365 | 0.332 | 0.032 | 0.09 | 5.92 | 4.28 | 22.94 | 3.87 | 50400. | 300. | 0.870 |
| 545. | 0.18 | 1.09 | 0.365 | 0.323 | 0.041 | 0.11 | 5.92 | 3.59 | 24.14 | 4.08 | 126700. | 300. | 0.870 |
| 546. | 0.18 | 1.10 | 0.365 | 0.299 | 0.066 | 0.18 | 5.98 | 2.73 | 20.61 | 3.45 | 292600. | 300. | 0.870 |
| 547. | 0.18 | 1.10 | 0.365 | 0.283 | 0.081 | 0.22 | 5.98 | 2.49 | 18.12 | 3.03 | 447000. | 300. | 0.870 |
| 291. | 0.18 | 2.55 | 0.395 | 0.387 | 0.008 | 0.02 | 12.98 | 12.03 | 61.25 | 4.72 | 16500. | 300. | 0.882 |
| 292. | 0.18 | 2.61 | 0.400 | 0.389 | 0.011 | 0.03 | 12.97 | 11.58 | 62.15 | 4.79 | 31800. | 300. | 0.872 |
| 293. | 0.18 | 2.59 | 0.400 | 0.387 | 0.014 | 0.03 | 12.97 | 11.28 | 61.10 | 4.71 | 44700. | 300. | 0.877 |
| 294. | 0.18 | 2.60 | 0.400 | 0.381 | 0.020 | 0.05 | 12.97 | 10.58 | 59.42 | 4.58 | 73700. | 300. | 0.875 |
| 295. | 0.18 | 2.60 | 0.400 | 0.377 | 0.023 | 0.06 | 12.97 | 10.27 | 56.99 | 4.39 | 101800. | 300. | 0.874 |
| 296. | 0.18 | 2.65 | 0.410 | 0.382 | 0.028 | 0.07 | 12.81 | 9.70 | 56.03 | 4.37 | 158100. | 300. | 0.867 |
| 297. | 0.17 | 2.53 | 0.393 | 0.361 | 0.032 | 0.08 | 13.04 | 9.88 | 48.37 | 3.71 | 230300. | 300. | 0.887 |
| 298. | 0.17 | 2.49 | 0.390 | 0.356 | 0.034 | 0.09 | 13.00 | 9.55 | 49.23 | 3.79 | 309400. | 300. | 0.891 |
| 299. | 0.17 | 2.55 | 0.393 | 0.357 | 0.037 | 0.09 | 13.04 | 9.39 | 48.33 | 3.71 | 476600. | 300. | 0.882 |
| 358. | 0.18 | 2.62 | 0.406 | 0.396 | 0.010 | 0.02 | 12.65 | 11.38 | 65.13 | 5.15 | 18800. | 300. | 0.857 |
| 359. | 0.17 | 2.48 | 0.386 | 0.348 | 0.038 | 0.10 | 12.97 | 9.24 | 47.45 | 3.66 | 468500. | 300. | 0.886 |
| 360. | 0.17 | 2.43 | 0.389 | 0.360 | 0.029 | 0.07 | 12.85 | 10.21 | 45.63 | 3.55 | 166300. | 300. | 0.901 |

Table D.16 (cont.): Present Air-Water Flow Data: $D_3/D_1$ = 0.084, Downward Branch ($\Phi$ = 180°).

| RUN # | VsL1 (m/s) | VsG1 (m/s) | m1 (kg/s) | m2 (kg/s) | m3 (kg/s) | m3/m1 (-) | x1 (%) | x2 (%) | x3 (%) | x3/x1 (-) | p13 (Pa) | T1 (K) | p1 (MPa) |
|---|---|---|---|---|---|---|---|---|---|---|---|---|---|
| 319. | 0.18 | 2.60 | 0.381 | 0.376 | 0.006 | 0.01 | 7.47 | 7.10 | 32.51 | 4.35 | 13700. | 300. | 0.480 |
| 320. | 0.18 | 2.57 | 0.381 | 0.372 | 0.009 | 0.02 | 7.47 | 6.63 | 40.89 | 5.47 | 29100. | 300. | 0.486 |
| 321. | 0.18 | 2.52 | 0.381 | 0.368 | 0.014 | 0.04 | 7.47 | 6.27 | 40.07 | 5.36 | 42400. | 300. | 0.495 |
| 323. | 0.18 | 2.52 | 0.381 | 0.365 | 0.016 | 0.04 | 7.47 | 5.95 | 41.47 | 5.55 | 70400. | 300. | 0.495 |
| 324. | 0.18 | 2.52 | 0.381 | 0.361 | 0.020 | 0.05 | 7.47 | 5.59 | 40.66 | 5.44 | 101600. | 300. | 0.495 |
| 325. | 0.18 | 2.52 | 0.381 | 0.357 | 0.024 | 0.06 | 7.47 | 5.19 | 41.11 | 5.50 | 166700. | 300. | 0.495 |
| 326. | 0.18 | 2.52 | 0.381 | 0.355 | 0.026 | 0.07 | 7.47 | 5.11 | 39.62 | 5.30 | 211200. | 300. | 0.495 |
| 327. | 0.18 | 2.57 | 0.381 | 0.355 | 0.027 | 0.07 | 7.47 | 5.07 | 39.50 | 5.29 | 244800. | 300. | 0.485 |
| 266. | 0.28 | 0.84 | 0.563 | 0.503 | 0.060 | 0.11 | 2.88 | 1.49 | 14.38 | 5.00 | 123200. | 300. | 0.847 |
| 267. | 0.26 | 0.81 | 0.532 | 0.498 | 0.033 | 0.06 | 3.05 | 2.44 | 12.09 | 3.97 | 22000. | 300. | 0.872 |
| 268. | 0.27 | 0.82 | 0.546 | 0.464 | 0.081 | 0.15 | 2.97 | 1.26 | 12.76 | 4.30 | 252100. | 300. | 0.862 |
| 269. | 0.28 | 0.83 | 0.563 | 0.447 | 0.116 | 0.21 | 2.88 | 1.00 | 10.11 | 3.52 | 436200. | 300. | 0.852 |
| 270. | 0.26 | 0.80 | 0.532 | 0.418 | 0.113 | 0.21 | 3.05 | 0.62 | 11.98 | 3.93 | 489900. | 300. | 0.887 |
| 258. | 0.26 | 1.42 | 0.543 | 0.520 | 0.024 | 0.04 | 5.17 | 4.21 | 25.94 | 5.02 | 36000. | 300. | 0.867 |
| 259. | 0.26 | 1.42 | 0.543 | 0.513 | 0.030 | 0.06 | 5.17 | 3.77 | 28.79 | 5.57 | 85600. | 300. | 0.867 |
| 260. | 0.26 | 1.44 | 0.543 | 0.501 | 0.043 | 0.08 | 5.17 | 3.25 | 27.57 | 5.33 | 157400. | 300. | 0.857 |
| 261. | 0.27 | 1.44 | 0.557 | 0.507 | 0.050 | 0.09 | 5.04 | 2.78 | 27.82 | 5.52 | 252200. | 300. | 0.857 |
| 262. | 0.28 | 1.52 | 0.574 | 0.523 | 0.051 | 0.09 | 5.12 | 2.67 | 30.30 | 5.92 | 369200. | 300. | 0.847 |
| 263. | 0.27 | 1.49 | 0.563 | 0.503 | 0.060 | 0.11 | 5.22 | 2.76 | 25.88 | 4.95 | 457600. | 300. | 0.867 |
| 264. | 0.27 | 1.44 | 0.555 | 0.492 | 0.063 | 0.11 | 5.30 | 2.78 | 25.09 | 4.74 | 492000. | 300. | 0.892 |
| 271. | 0.26 | 2.55 | 0.553 | 0.541 | 0.012 | 0.02 | 9.35 | 8.58 | 45.11 | 4.82 | 26800. | 300. | 0.887 |
| 272. | 0.26 | 2.63 | 0.553 | 0.537 | 0.015 | 0.03 | 9.35 | 8.30 | 45.99 | 4.92 | 31200. | 300. | 0.862 |
| 273. | 0.26 | 2.58 | 0.562 | 0.543 | 0.020 | 0.03 | 9.04 | 7.73 | 45.32 | 5.02 | 47900. | 300. | 0.862 |
| 274. | 0.26 | 2.52 | 0.562 | 0.537 | 0.025 | 0.04 | 9.04 | 7.37 | 45.22 | 5.00 | 83600. | 300. | 0.882 |
| 275. | 0.26 | 2.58 | 0.560 | 0.529 | 0.032 | 0.06 | 9.12 | 7.03 | 43.98 | 4.82 | 140300. | 300. | 0.867 |
| 276. | 0.26 | 2.67 | 0.566 | 0.531 | 0.035 | 0.06 | 9.28 | 7.16 | 41.06 | 4.43 | 248900. | 300. | 0.862 |
| 277. | 0.26 | 2.63 | 0.566 | 0.527 | 0.039 | 0.07 | 9.28 | 6.92 | 41.34 | 4.46 | 328700. | 300. | 0.875 |
| 278. | 0.26 | 2.60 | 0.565 | 0.525 | 0.040 | 0.07 | 9.10 | 6.72 | 40.36 | 4.43 | 408200. | 300. | 0.867 |
| 279. | 0.26 | 2.57 | 0.565 | 0.519 | 0.046 | 0.08 | 9.10 | 6.76 | 35.68 | 3.92 | 446100. | 300. | 0.875 |
| 375. | 0.25 | 2.58 | 0.544 | 0.527 | 0.017 | 0.03 | 9.40 | 8.25 | 45.60 | 4.85 | 36400. | 300. | 0.867 |

Table D.16 (cont.): Present Air-Water Flow Data: $D_3/D_1$ = 0.084, Downward Branch ($\Phi$ = 180°).

| RUN # | VsL1 (m/s) | VsG1 (m/s) | m1 (kg/s) | m2 (kg/s) | m3 (kg/s) | m3/m1 (-) | x1 (%) | x2 (%) | x3 (%) | x3/x1 (-) | p13 (Pa) | T1 (K) | p1 (MPa) |
|---|---|---|---|---|---|---|---|---|---|---|---|---|---|
| 376. | 0.25 | 2.58 | 0.544 | 0.501 | 0.042 | 0.08 | 9.40 | 6.75 | 40.87 | 4.35 | 305200. | 300. | 0.867 |
| 377. | 0.25 | 2.57 | 0.544 | 0.520 | 0.023 | 0.04 | 9.40 | 7.81 | 44.73 | 4.76 | 81200. | 300. | 0.872 |
| 301. | 0.26 | 2.54 | 0.529 | 0.517 | 0.012 | 0.02 | 5.31 | 4.64 | 34.80 | 6.55 | 22900. | 300. | 0.484 |
| 302. | 0.26 | 2.54 | 0.529 | 0.513 | 0.016 | 0.03 | 5.31 | 4.32 | 36.98 | 6.96 | 41300. | 300. | 0.484 |
| 303. | 0.26 | 2.54 | 0.529 | 0.511 | 0.018 | 0.03 | 5.31 | 4.17 | 37.99 | 7.15 | 56200. | 300. | 0.484 |
| 304. | 0.26 | 2.54 | 0.529 | 0.508 | 0.021 | 0.04 | 5.31 | 3.89 | 39.00 | 7.34 | 103200. | 300. | 0.484 |
| 305. | 0.26 | 2.49 | 0.529 | 0.503 | 0.026 | 0.05 | 5.31 | 3.56 | 38.89 | 7.32 | 187100. | 300. | 0.495 |
| 306. | 0.26 | 2.49 | 0.529 | 0.502 | 0.028 | 0.05 | 5.31 | 3.44 | 39.50 | 7.44 | 235300. | 300. | 0.495 |
| 475. | 0.25 | 5.22 | 0.601 | 0.590 | 0.011 | 0.02 | 17.28 | 16.36 | 64.96 | 3.76 | 35800. | 300. | 0.872 |
| 476. | 0.25 | 5.22 | 0.601 | 0.584 | 0.017 | 0.03 | 17.28 | 15.65 | 71.84 | 4.16 | 69400. | 300. | 0.872 |
| 477. | 0.25 | 5.22 | 0.601 | 0.575 | 0.026 | 0.04 | 17.28 | 14.65 | 74.67 | 4.32 | 195900. | 300. | 0.872 |
| 478. | 0.25 | 5.22 | 0.601 | 0.572 | 0.030 | 0.05 | 17.28 | 14.48 | 70.92 | 4.11 | 355400. | 300. | 0.872 |
| 479. | 0.25 | 5.22 | 0.601 | 0.571 | 0.031 | 0.05 | 17.28 | 14.51 | 68.62 | 3.97 | 436400. | 300. | 0.872 |
| 308. | 0.25 | 4.88 | 0.552 | 0.545 | 0.007 | 0.01 | 9.98 | 9.53 | 47.08 | 4.72 | 13300. | 300. | 0.495 |
| 309. | 0.25 | 4.88 | 0.552 | 0.542 | 0.010 | 0.02 | 9.98 | 9.19 | 52.42 | 5.25 | 32700. | 300. | 0.495 |
| 310. | 0.26 | 4.96 | 0.556 | 0.544 | 0.012 | 0.02 | 9.91 | 8.91 | 54.51 | 5.50 | 49600. | 300. | 0.487 |
| 313. | 0.26 | 4.99 | 0.556 | 0.541 | 0.015 | 0.03 | 9.91 | 8.59 | 57.58 | 5.81 | 85800. | 300. | 0.484 |
| 314. | 0.26 | 4.93 | 0.560 | 0.544 | 0.017 | 0.03 | 9.83 | 8.35 | 58.29 | 5.93 | 102800. | 300. | 0.490 |
| 315. | 0.26 | 4.96 | 0.560 | 0.542 | 0.018 | 0.03 | 9.83 | 8.18 | 59.30 | 6.03 | 151900. | 300. | 0.487 |
| 316. | 0.26 | 4.99 | 0.560 | 0.541 | 0.020 | 0.03 | 9.83 | 8.04 | 59.50 | 6.05 | 200000. | 300. | 0.484 |
| 317. | 0.26 | 5.02 | 0.560 | 0.540 | 0.020 | 0.04 | 9.83 | 7.99 | 58.71 | 5.97 | 229200. | 300. | 0.481 |
| 329. | 0.25 | 7.49 | 0.579 | 0.572 | 0.007 | 0.01 | 14.60 | 14.06 | 57.68 | 3.95 | 19400. | 300. | 0.495 |
| 330. | 0.25 | 7.59 | 0.579 | 0.569 | 0.010 | 0.02 | 14.60 | 13.88 | 56.78 | 3.89 | 32900. | 300. | 0.488 |
| 331. | 0.25 | 7.79 | 0.579 | 0.567 | 0.012 | 0.02 | 14.92 | 13.93 | 61.67 | 4.13 | 59600. | 300. | 0.486 |
| 332. | 0.25 | 7.79 | 0.579 | 0.565 | 0.014 | 0.02 | 14.92 | 13.73 | 63.90 | 4.28 | 83000. | 300. | 0.486 |
| 333. | 0.25 | 7.79 | 0.579 | 0.564 | 0.015 | 0.03 | 14.92 | 13.57 | 64.10 | 4.30 | 109900. | 300. | 0.486 |
| 334. | 0.25 | 7.79 | 0.579 | 0.562 | 0.017 | 0.03 | 14.92 | 13.45 | 64.05 | 4.29 | 144300. | 300. | 0.486 |
| 335. | 0.25 | 7.79 | 0.579 | 0.561 | 0.018 | 0.03 | 14.92 | 13.32 | 65.74 | 4.41 | 187700. | 300. | 0.486 |
| 336. | 0.25 | 7.80 | 0.583 | 0.565 | 0.018 | 0.03 | 14.81 | 13.21 | 64.55 | 4.36 | 220400. | 300. | 0.485 |
| 337. | 0.25 | 7.80 | 0.583 | 0.564 | 0.019 | 0.03 | 14.81 | 13.16 | 63.51 | 4.29 | 245000. | 300. | 0.485 |

Table D.16 (cont.): Present Air-Water Flow Data: $D_3/D_1$ = 0.084, Downward Branch ($\Phi$ = 180°).

| RUN # | VsL1 (m/s) | VsG1 (m/s) | m1 (kg/s) | m2 (kg/s) | m3 (kg/s) | m3/m1 (-) | x1 (%) | x2 (%) | x3 (%) | x3/x1 (-) | p13 (Pa) | T1 (K) | p1 (MPa) |
|---|---|---|---|---|---|---|---|---|---|---|---|---|---|
| 467. | 0.25 | 5.13 | 0.593 | 0.366 | 0.227 | 0.38 | 17.42 | 27.68 | 0.86 | 0.05 | 383652. | 299. | 0.880 |
| 468. | 0.25 | 5.13 | 0.593 | 0.350 | 0.244 | 0.41 | 17.42 | 28.89 | 0.96 | 0.06 | 590000. | 299. | 0.880 |
| 479. | 0.25 | 10.06 | 0.698 | 0.607 | 0.090 | 0.13 | 29.19 | 33.48 | 0.37 | 0.01 | 32020. | 299. | 0.884 |
| 480. | 0.25 | 10.06 | 0.698 | 0.586 | 0.112 | 0.16 | 29.19 | 34.63 | 0.62 | 0.02 | 52084. | 299. | 0.884 |
| 481. | 0.25 | 10.06 | 0.698 | 0.558 | 0.140 | 0.20 | 29.19 | 36.28 | 0.98 | 0.03 | 126768. | 299. | 0.884 |
| 482. | 0.25 | 10.06 | 0.698 | 0.530 | 0.168 | 0.24 | 29.19 | 38.15 | 0.95 | 0.03 | 243800. | 299. | 0.884 |
| 483. | 0.25 | 10.06 | 0.698 | 0.520 | 0.177 | 0.25 | 29.19 | 38.74 | 1.16 | 0.04 | 352492. | 299. | 0.884 |
| 484. | 0.25 | 10.06 | 0.698 | 0.510 | 0.187 | 0.27 | 29.19 | 39.46 | 1.20 | 0.04 | 434928. | 299. | 0.884 |
| 485. | 0.25 | 10.06 | 0.698 | 0.505 | 0.193 | 0.28 | 29.19 | 39.84 | 1.28 | 0.04 | 565000. | 299. | 0.884 |
| 373. | 0.50 | 2.54 | 1.030 | 0.872 | 0.159 | 0.15 | 4.93 | 5.83 | 0.02 | 0.00 | 59000. | 301. | 0.880 |
| 374. | 0.50 | 2.51 | 1.022 | 0.831 | 0.190 | 0.19 | 4.91 | 6.03 | 0.03 | 0.01 | 104300. | 301. | 0.880 |
| 375. | 0.50 | 2.51 | 1.022 | 0.784 | 0.238 | 0.23 | 4.91 | 6.39 | 0.04 | 0.01 | 177916. | 301. | 0.880 |
| 376. | 0.50 | 2.49 | 1.022 | 0.744 | 0.278 | 0.27 | 4.91 | 6.73 | 0.05 | 0.01 | 241510. | 301. | 0.885 |
| 377. | 0.50 | 2.50 | 1.030 | 0.718 | 0.312 | 0.30 | 4.91 | 7.01 | 0.09 | 0.02 | 306100. | 299. | 0.885 |
| 378. | 0.50 | 2.50 | 1.030 | 0.697 | 0.333 | 0.32 | 4.91 | 7.19 | 0.14 | 0.03 | 394400. | 299. | 0.885 |
| 379. | 0.50 | 2.50 | 1.030 | 0.626 | 0.404 | 0.39 | 4.91 | 7.95 | 0.21 | 0.04 | 491152. | 299. | 0.885 |
| 350. | 0.49 | 5.03 | 1.022 | 0.787 | 0.235 | 0.23 | 5.70 | 7.31 | 0.31 | 0.05 | 354400. | 288. | 0.487 |
| 351. | 0.50 | 4.99 | 1.035 | 0.808 | 0.227 | 0.22 | 5.66 | 7.19 | 0.18 | 0.03 | 248800. | 289. | 0.495 |
| 352. | 0.50 | 5.02 | 1.031 | 0.835 | 0.196 | 0.19 | 5.63 | 6.92 | 0.15 | 0.03 | 160000. | 290. | 0.490 |
| 358. | 0.50 | 5.05 | 1.045 | 0.953 | 0.093 | 0.09 | 5.55 | 6.09 | 0.04 | 0.01 | 20024. | 289. | 0.485 |
| 359. | 0.51 | 5.05 | 1.058 | 0.949 | 0.109 | 0.10 | 5.49 | 6.11 | 0.05 | 0.01 | 30850. | 289. | 0.485 |
| 360. | 0.51 | 5.05 | 1.058 | 0.916 | 0.142 | 0.13 | 5.49 | 6.33 | 0.07 | 0.01 | 58120. | 289. | 0.485 |
| 361. | 0.51 | 4.99 | 1.057 | 0.849 | 0.208 | 0.20 | 5.44 | 6.74 | 0.14 | 0.03 | 149972. | 294. | 0.495 |
| 362. | 0.51 | 4.99 | 1.057 | 0.819 | 0.238 | 0.23 | 5.44 | 6.96 | 0.24 | 0.04 | 295420. | 294. | 0.495 |
| 386. | 0.51 | 4.98 | 1.098 | 0.946 | 0.152 | 0.14 | 9.37 | 10.85 | 0.15 | 0.02 | 66872. | 291. | 0.878 |
| 387. | 0.50 | 4.96 | 1.090 | 0.875 | 0.215 | 0.20 | 9.44 | 11.71 | 0.20 | 0.02 | 145640. | 291. | 0.882 |
| 388. | 0.50 | 4.96 | 1.090 | 0.843 | 0.247 | 0.23 | 9.44 | 12.14 | 0.26 | 0.03 | 200868. | 291. | 0.882 |
| 389. | 0.50 | 4.96 | 1.090 | 0.804 | 0.287 | 0.26 | 9.44 | 12.66 | 0.40 | 0.04 | 396688. | 291. | 0.882 |
| 390. | 0.50 | 4.96 | 1.090 | 0.799 | 0.291 | 0.27 | 9.44 | 12.71 | 0.45 | 0.05 | 468280. | 291. | 0.882 |
| 391. | 0.50 | 4.96 | 1.090 | 0.786 | 0.304 | 0.28 | 9.44 | 12.93 | 0.42 | 0.04 | 495272. | 291. | 0.882 |

Table D.16 (cont.): Present Air-Water Flow Data: $D_3/D_1$ = 0.084, Downward Branch ($\Phi$ = 180°).

| RUN # | VsL1 (m/s) | VsG1 (m/s) | m1 (kg/s) | m2 (kg/s) | m3 (kg/s) | m3/m1 (-) | x1 (%) | x2 (%) | x3 (%) | x3/x1 (-) | p13 (Pa) | T1 (K) | p1 (MPa) |
|---|---|---|---|---|---|---|---|---|---|---|---|---|---|
| 392. | 0.50 | 10.07 | 1.177 | 1.076 | 0.101 | 0.09 | 17.58 | 19.19 | 0.39 | 0.02 | 41448. | 294. | 0.882 |
| 393. | 0.50 | 10.07 | 1.177 | 1.040 | 0.137 | 0.12 | 17.58 | 19.81 | 0.57 | 0.03 | 88304. | 294. | 0.882 |
| 394. | 0.50 | 10.07 | 1.177 | 1.009 | 0.168 | 0.14 | 17.58 | 20.39 | 0.65 | 0.04 | 143364. | 294. | 0.882 |
| 395. | 0.50 | 10.07 | 1.177 | 0.980 | 0.197 | 0.17 | 17.58 | 20.98 | 0.64 | 0.04 | 293560. | 294. | 0.882 |
| 396. | 0.50 | 10.10 | 1.189 | 0.965 | 0.223 | 0.19 | 17.61 | 21.53 | 0.68 | 0.04 | 394240. | 293. | 0.887 |
| 397. | 0.50 | 10.10 | 1.189 | 0.937 | 0.251 | 0.21 | 17.61 | 22.15 | 0.71 | 0.04 | 510856. | 293. | 0.887 |
| 398. | 0.50 | 10.10 | 1.189 | 0.937 | 0.252 | 0.21 | 17.61 | 22.14 | 0.73 | 0.04 | 522784. | 293. | 0.887 |
| 412. | 0.51 | 20.08 | 1.399 | 1.347 | 0.052 | 0.04 | 29.32 | 30.39 | 1.57 | 0.05 | 26800. | 295. | 0.880 |
| 413. | 0.51 | 20.08 | 1.399 | 1.314 | 0.085 | 0.06 | 29.32 | 31.08 | 2.01 | 0.07 | 80232. | 295. | 0.880 |
| 414. | 0.51 | 20.08 | 1.399 | 1.292 | 0.107 | 0.08 | 29.32 | 31.54 | 2.46 | 0.08 | 170560. | 295. | 0.880 |
| 415. | 0.51 | 20.08 | 1.399 | 1.281 | 0.118 | 0.08 | 29.32 | 31.77 | 2.71 | 0.09 | 287056. | 295. | 0.880 |
| 416. | 0.51 | 20.12 | 1.399 | 1.268 | 0.131 | 0.09 | 29.32 | 31.96 | 3.77 | 0.13 | 407272. | 295. | 0.878 |
| 417. | 0.51 | 20.12 | 1.399 | 1.264 | 0.135 | 0.10 | 29.32 | 32.02 | 3.95 | 0.13 | 530000. | 295. | 0.878 |
| 504. | 0.50 | 39.68 | 1.786 | 1.772 | 0.014 | 0.01 | 45.18 | 45.41 | 16.77 | 0.37 | 6952. | 297. | 0.882 |
| 505. | 0.50 | 39.68 | 1.786 | 1.767 | 0.019 | 0.01 | 45.18 | 45.39 | 25.67 | 0.57 | 30796. | 297. | 0.882 |
| 506. | 0.50 | 39.68 | 1.786 | 1.763 | 0.024 | 0.01 | 45.18 | 45.43 | 26.52 | 0.59 | 49976. | 297. | 0.882 |
| 507. | 0.50 | 39.68 | 1.786 | 1.759 | 0.027 | 0.02 | 45.18 | 45.45 | 27.39 | 0.61 | 72436. | 297. | 0.882 |
| 366. | 1.00 | 2.48 | 2.010 | 1.887 | 0.123 | 0.06 | 2.56 | 2.72 | 0.04 | 0.02 | 43360. | 293. | 0.888 |
| 367. | 1.00 | 2.48 | 2.010 | 1.857 | 0.153 | 0.08 | 2.56 | 2.77 | 0.05 | 0.02 | 65900. | 293. | 0.888 |
| 368. | 1.00 | 2.52 | 2.007 | 1.822 | 0.185 | 0.09 | 2.61 | 2.87 | 0.06 | 0.02 | 86172. | 293. | 0.888 |
| 369. | 1.00 | 2.51 | 2.007 | 1.785 | 0.222 | 0.11 | 2.59 | 2.91 | 0.06 | 0.02 | 162740. | 293. | 0.888 |
| 357. | 1.00 | 2.53 | 2.007 | 1.785 | 0.222 | 0.11 | 2.60 | 2.91 | 0.07 | 0.03 | 161740. | 293. | 0.880 |
| 370. | 1.01 | 2.54 | 2.027 | 1.724 | 0.303 | 0.15 | 2.57 | 3.01 | 0.08 | 0.03 | 276704. | 293. | 0.877 |
| 371. | 1.00 | 2.53 | 2.011 | 1.677 | 0.333 | 0.17 | 2.58 | 3.07 | 0.09 | 0.04 | 338476. | 295. | 0.882 |
| 372. | 1.00 | 2.53 | 2.011 | 1.556 | 0.454 | 0.23 | 2.58 | 3.30 | 0.09 | 0.03 | 269196. | 295. | 0.882 |
| 353. | 1.00 | 5.00 | 2.017 | 1.858 | 0.159 | 0.08 | 2.87 | 3.10 | 0.16 | 0.06 | 111120. | 290. | 0.490 |
| 354. | 1.00 | 5.00 | 2.017 | 1.820 | 0.196 | 0.10 | 2.87 | 3.15 | 0.22 | 0.08 | 207960. | 290. | 0.490 |
| 355. | 1.00 | 5.00 | 2.017 | 1.778 | 0.238 | 0.12 | 2.87 | 3.22 | 0.22 | 0.08 | 289232. | 290. | 0.490 |
| 356. | 1.00 | 5.00 | 2.017 | 1.766 | 0.250 | 0.12 | 2.87 | 3.23 | 0.29 | 0.10 | 361664. | 290. | 0.490 |
| 363. | 1.00 | 5.04 | 2.017 | 1.934 | 0.083 | 0.04 | 2.85 | 2.97 | 0.13 | 0.05 | 24080. | 294. | 0.490 |

Table D.16 (cont.): Present Air-Water Flow Data: $D_3/D_1$ = 0.084, Downward Branch ($\Phi$ = 180°).

| RUN # | VsL1 (m/s) | VsG1 (m/s) | m1 (kg/s) | m2 (kg/s) | m3 (kg/s) | m3/m1 (-) | x1 (%) | x2 (%) | x3 (%) | x3/x1 (-) | p13 (Pa) | T1 (K) | p1 (MPa) |
|---|---|---|---|---|---|---|---|---|---|---|---|---|---|
| 364. | 1.01 | 5.04 | 2.025 | 1.981 | 0.044 | 0.02 | 2.84 | 2.90 | 0.09 | 0.03 | 5668. | 294. | 0.490 |
| 365. | 1.01 | 5.04 | 2.025 | 1.810 | 0.215 | 0.11 | 2.84 | 3.15 | 0.21 | 0.07 | 251644. | 294. | 0.490 |
| 380. | 1.00 | 5.06 | 2.061 | 1.968 | 0.093 | 0.05 | 4.96 | 5.18 | 0.31 | 0.06 | 26576. | 299. | 0.882 |
| 381. | 1.00 | 5.06 | 2.061 | 1.937 | 0.124 | 0.06 | 4.96 | 5.26 | 0.30 | 0.06 | 60200. | 299. | 0.882 |
| 382. | 1.00 | 5.11 | 2.062 | 1.903 | 0.159 | 0.08 | 5.01 | 5.40 | 0.33 | 0.07 | 97296. | 299. | 0.882 |
| 383. | 1.00 | 5.11 | 2.062 | 1.839 | 0.223 | 0.11 | 5.01 | 5.56 | 0.40 | 0.08 | 224492. | 299. | 0.882 |
| 384. | 1.00 | 5.11 | 2.062 | 1.783 | 0.278 | 0.14 | 5.01 | 5.73 | 0.38 | 0.08 | 201988. | 299. | 0.882 |
| 385. | 1.00 | 5.11 | 2.062 | 1.749 | 0.313 | 0.15 | 5.01 | 5.84 | 0.35 | 0.07 | 245008. | 299. | 0.882 |
| 399. | 1.00 | 10.05 | 2.164 | 2.082 | 0.082 | 0.04 | 9.49 | 9.82 | 0.96 | 0.10 | 35320. | 295. | 0.880 |
| 400. | 1.00 | 10.05 | 2.164 | 2.068 | 0.096 | 0.04 | 9.49 | 9.88 | 1.05 | 0.11 | 52516. | 295. | 0.880 |
| 401. | 1.00 | 10.05 | 2.164 | 2.021 | 0.143 | 0.07 | 9.49 | 10.11 | 0.72 | 0.08 | 135448. | 295. | 0.880 |
| 402. | 1.00 | 10.05 | 2.164 | 1.988 | 0.177 | 0.08 | 9.49 | 10.26 | 0.74 | 0.08 | 217096. | 295. | 0.880 |
| 403. | 1.00 | 10.05 | 2.164 | 1.967 | 0.198 | 0.09 | 9.49 | 10.35 | 0.84 | 0.09 | 324776. | 295. | 0.880 |
| 404. | 1.00 | 10.05 | 2.164 | 1.954 | 0.210 | 0.10 | 9.49 | 10.41 | 0.89 | 0.09 | 401960. | 295. | 0.880 |
| 405. | 1.00 | 10.05 | 2.164 | 1.940 | 0.224 | 0.10 | 9.49 | 10.48 | 0.89 | 0.09 | 585000. | 295. | 0.880 |
| 406. | 1.00 | 20.68 | 2.383 | 2.343 | 0.039 | 0.02 | 17.63 | 17.89 | 1.90 | 0.11 | 16700. | 296. | 0.878 |
| 407. | 1.00 | 20.68 | 2.383 | 2.315 | 0.068 | 0.03 | 17.63 | 18.08 | 2.09 | 0.12 | 64780. | 296. | 0.878 |
| 408. | 1.00 | 20.68 | 2.383 | 2.285 | 0.098 | 0.04 | 17.63 | 18.27 | 2.58 | 0.15 | 154084. | 296. | 0.878 |
| 409. | 1.00 | 20.68 | 2.383 | 2.269 | 0.114 | 0.05 | 17.63 | 18.38 | 2.58 | 0.15 | 223104. | 296. | 0.878 |
| 410. | 1.00 | 20.33 | 2.383 | 2.259 | 0.124 | 0.05 | 17.63 | 18.38 | 3.84 | 0.22 | 371928. | 294. | 0.887 |
| 411. | 1.00 | 20.33 | 2.383 | 2.248 | 0.135 | 0.06 | 17.63 | 18.45 | 3.85 | 0.22 | 550000. | 294. | 0.887 |
| 508. | 0.99 | 39.56 | 2.747 | 2.726 | 0.022 | 0.01 | 29.28 | 29.47 | 6.28 | 0.21 | 8076. | 297. | 0.882 |
| 509. | 0.99 | 39.16 | 2.747 | 2.718 | 0.030 | 0.01 | 29.28 | 29.47 | 12.22 | 0.42 | 49028. | 297. | 0.891 |
| 510. | 0.99 | 39.16 | 2.747 | 2.701 | 0.047 | 0.02 | 29.28 | 29.64 | 8.75 | 0.30 | 67568. | 297. | 0.891 |
| 511. | 0.99 | 39.16 | 2.747 | 2.683 | 0.064 | 0.02 | 29.28 | 29.80 | 7.53 | 0.26 | 109228. | 297. | 0.891 |
| 512. | 0.99 | 39.16 | 2.747 | 2.675 | 0.072 | 0.03 | 29.28 | 29.86 | 8.04 | 0.27 | 155276. | 297. | 0.891 |
| 513. | 0.99 | 39.16 | 2.747 | 2.671 | 0.077 | 0.03 | 29.28 | 29.88 | 8.56 | 0.29 | 208916. | 297. | 0.891 |
| 514. | 0.99 | 39.16 | 2.747 | 2.665 | 0.082 | 0.03 | 29.28 | 29.94 | 8.18 | 0.28 | 249676. | 297. | 0.891 |
| 444. | 1.99 | 2.47 | 3.942 | 3.853 | 0.089 | 0.02 | 1.27 | 1.29 | 0.24 | 0.19 | 19192. | 302. | 0.892 |
| 445. | 1.99 | 2.55 | 3.944 | 3.790 | 0.154 | 0.04 | 1.31 | 1.35 | 0.29 | 0.22 | 94592. | 302. | 0.892 |

Table D.16 (cont.): Present Air-Water Flow Data: $D_3/D_1$ = 0.084, Downward Branch ($\Phi$ = 180°).

| RUN # | VsL1 (m/s) | VsG1 (m/s) | m1 (kg/s) | m2 (kg/s) | m3 (kg/s) | m3/m1 (-) | x1 (%) | x2 (%) | x3 (%) | x3/x1 (-) | p13 (Pa) | T1 (K) | p1 (MPa) |
|---|---|---|---|---|---|---|---|---|---|---|---|---|---|
| 446. | 2.02 | 2.57 | 4.001 | 3.792 | 0.209 | 0.05 | 1.29 | 1.34 | 0.28 | 0.21 | 159920. | 302. | 0.884 |
| 447. | 2.02 | 2.57 | 4.001 | 3.753 | 0.247 | 0.06 | 1.29 | 1.35 | 0.30 | 0.24 | 237832. | 302. | 0.884 |
| 448. | 2.02 | 2.57 | 4.001 | 3.724 | 0.276 | 0.07 | 1.29 | 1.36 | 0.31 | 0.24 | 304488. | 302. | 0.884 |
| 449. | 2.02 | 2.57 | 4.001 | 3.714 | 0.286 | 0.07 | 1.29 | 1.36 | 0.32 | 0.25 | 408708. | 302. | 0.884 |
| 450. | 2.02 | 2.57 | 4.001 | 3.680 | 0.321 | 0.08 | 1.29 | 1.37 | 0.34 | 0.26 | 655000. | 302. | 0.884 |
| 437. | 1.98 | 4.97 | 3.923 | 3.884 | 0.038 | 0.01 | 1.43 | 1.44 | 0.06 | 0.04 | 124800. | 297. | 0.490 |
| 438. | 1.98 | 4.97 | 3.923 | 3.834 | 0.089 | 0.02 | 1.43 | 1.45 | 0.53 | 0.37 | 42196. | 297. | 0.490 |
| 439. | 1.98 | 4.97 | 3.923 | 3.824 | 0.098 | 0.03 | 1.43 | 1.45 | 0.55 | 0.38 | 61700. | 297. | 0.490 |
| 440. | 1.98 | 4.97 | 3.923 | 3.794 | 0.129 | 0.03 | 1.43 | 1.46 | 0.55 | 0.38 | 108684. | 297. | 0.490 |
| 441. | 1.98 | 4.98 | 3.923 | 3.776 | 0.147 | 0.04 | 1.43 | 1.47 | 0.60 | 0.42 | 175756. | 297. | 0.490 |
| 442. | 1.98 | 4.98 | 3.923 | 3.755 | 0.167 | 0.04 | 1.43 | 1.47 | 0.59 | 0.41 | 244800. | 297. | 0.490 |
| 443. | 1.98 | 4.98 | 3.923 | 3.746 | 0.177 | 0.05 | 1.43 | 1.47 | 0.60 | 0.42 | 340588. | 297. | 0.490 |
| 431. | 1.98 | 5.03 | 3.985 | 3.918 | 0.067 | 0.02 | 2.50 | 2.53 | 0.75 | 0.30 | 25776. | 303. | 0.877 |
| 432. | 1.98 | 5.03 | 3.985 | 3.881 | 0.105 | 0.03 | 2.50 | 2.55 | 0.79 | 0.32 | 65996. | 303. | 0.877 |
| 433. | 1.98 | 5.03 | 3.985 | 3.842 | 0.144 | 0.04 | 2.50 | 2.56 | 0.86 | 0.34 | 153508. | 303. | 0.877 |
| 434. | 1.98 | 5.03 | 3.985 | 3.805 | 0.181 | 0.05 | 2.50 | 2.58 | 0.90 | 0.36 | 281304. | 303. | 0.877 |
| 435. | 1.98 | 5.03 | 3.985 | 3.793 | 0.192 | 0.05 | 2.50 | 2.58 | 0.93 | 0.37 | 365032. | 303. | 0.877 |
| 436. | 1.98 | 5.03 | 3.985 | 3.770 | 0.215 | 0.05 | 2.50 | 2.59 | 0.92 | 0.37 | 575000. | 303. | 0.877 |
| 418. | 2.00 | 10.01 | 4.122 | 4.070 | 0.052 | 0.01 | 4.95 | 5.00 | 1.38 | 0.28 | 22008. | 295. | 0.878 |
| 419. | 2.00 | 10.01 | 4.122 | 4.037 | 0.084 | 0.02 | 4.95 | 5.02 | 1.46 | 0.29 | 52920. | 295. | 0.878 |
| 420. | 2.00 | 10.01 | 4.122 | 4.020 | 0.102 | 0.02 | 4.95 | 5.03 | 1.68 | 0.34 | 113192. | 295. | 0.878 |
| 421. | 2.00 | 10.01 | 4.122 | 3.997 | 0.125 | 0.03 | 4.95 | 5.05 | 1.68 | 0.34 | 173824. | 295. | 0.878 |
| 422. | 2.00 | 10.01 | 4.122 | 3.975 | 0.146 | 0.04 | 4.95 | 5.07 | 1.72 | 0.35 | 283672. | 295. | 0.878 |
| 423. | 2.00 | 10.01 | 4.122 | 3.962 | 0.159 | 0.04 | 4.95 | 5.08 | 1.70 | 0.34 | 381948. | 295. | 0.878 |
| 424. | 2.00 | 10.01 | 4.122 | 3.957 | 0.164 | 0.04 | 4.95 | 5.08 | 1.81 | 0.37 | 550000. | 295. | 0.878 |
| 497. | 2.00 | 19.97 | 4.328 | 4.297 | 0.031 | 0.01 | 9.49 | 9.54 | 2.67 | 0.28 | 18440. | 293. | 0.880 |
| 498. | 2.00 | 19.97 | 4.328 | 4.275 | 0.053 | 0.01 | 9.49 | 9.56 | 3.37 | 0.35 | 39168. | 293. | 0.880 |
| 499. | 2.00 | 19.97 | 4.328 | 4.247 | 0.081 | 0.02 | 9.49 | 9.60 | 3.45 | 0.36 | 101384. | 293. | 0.880 |
| 500. | 2.00 | 19.97 | 4.328 | 4.226 | 0.102 | 0.02 | 9.49 | 9.62 | 4.20 | 0.44 | 188172. | 293. | 0.880 |
| 501. | 2.00 | 19.97 | 4.328 | 4.212 | 0.116 | 0.03 | 9.49 | 9.62 | 4.53 | 0.48 | 327120. | 293. | 0.880 |

Table D.16 (cont.): Present Air-Water Flow Data: $D_3/D_1$ = 0.084, Downward Branch ($\Phi$ = 180°).

| RUN # | VsL1 (m/s) | VsG1 (m/s) | m1 (kg/s) | m2 (kg/s) | m3 (kg/s) | m3/m1 (-) | x1 (%) | x2 (%) | x3 (%) | x3/x1 (-) | p13 (Pa) | T1 (K) | p1 (MPa) |
|---|---|---|---|---|---|---|---|---|---|---|---|---|---|
| 502. | 2.00 | 19.97 | 4.328 | 4.198 | 0.130 | 0.03 | 9.49 | 9.65 | 4.29 | 0.45 | 426176. | 293. | 0.880 |
| 503. | 2.00 | 19.97 | 4.328 | 4.197 | 0.131 | 0.03 | 9.49 | 9.64 | 4.46 | 0.47 | 530000. | 293. | 0.880 |
| 425. | 3.99 | 5.03 | 7.911 | 7.842 | 0.069 | 0.01 | 1.28 | 1.28 | 1.16 | 0.91 | 37576. | 300. | 0.882 |
| 426. | 3.99 | 5.03 | 7.911 | 7.822 | 0.089 | 0.01 | 1.28 | 1.28 | 1.24 | 0.97 | 66676. | 300. | 0.882 |
| 427. | 3.96 | 5.15 | 7.862 | 7.749 | 0.113 | 0.01 | 1.31 | 1.31 | 1.37 | 1.05 | 156092. | 303. | 0.882 |
| 428. | 3.96 | 5.15 | 7.862 | 7.693 | 0.169 | 0.02 | 1.31 | 1.31 | 1.29 | 0.99 | 320580. | 303. | 0.882 |
| 429. | 3.96 | 5.15 | 7.862 | 7.682 | 0.180 | 0.02 | 1.31 | 1.31 | 1.29 | 0.99 | 387724. | 303. | 0.882 |
| 430. | 3.96 | 5.15 | 7.862 | 7.662 | 0.200 | 0.03 | 1.31 | 1.31 | 1.24 | 0.95 | 555000. | 303. | 0.882 |

Table D.16 (cont.): Present Air-Water Flow Data: $D_3/D_1$ = 0.084, Downward Branch ($\Phi$ = 180°).